INVESTIGATION OF THE IMPACT OF CLIMATE CHANGE ON ROAD MAINTENANCE

By

MICHAEL ANYALA

A Thesis Submitted to the

University of Birmingham for the Degree of

DOCTOR OF PHILOSOPHY

School of Civil Engineering

College of Engineering and Physical Sciences

The University of Birmingham

May 2011

DEDICATION

This work is dedicated to my parents (RIP), wife, sister and brothers for their inspiration, motivation and support.

ABSTRACT

The performance of roads is known to progressively reduce as a result of separate and interactive effects of climate and traffic. Existing decision support tools such as HDM-4 which are widely used to investigate long-term road maintenance strategies utilise past climate data instead of future climate predictions. Uncertainties inherent in future climate predictions however imply that application of such tools could lead to outputs that are not robust in light of climate change.

The objectives of the study were threefold: firstly, to develop a rut depth prediction model that considered potential effects of future climate; secondly, to formulate a framework for quantification of uncertainties; and finally, to demonstrate the application of the tools developed using a case study.

The model was developed using data provided by the UK Highways Agency and UK Climate Impacts Programme. The methodology used was based on Bayesian regression. The developed model was found to perform better than the current asphalt surfacing rut depth model implemented in HDM-4 when future climate data was used.

It was concluded that probabilistic outputs from the tools developed including deterioration rates, pavement condition and discounted maintenance costs for each maintenance strategy, and future climate and socio-economic scenarios provide a useful decision making framework for considering alternative strategies for road maintenance on the basis of the level of climate change risks that can be tolerated.

ACKNOWLEDGEMENT

The author would like to thank his supervisors Prof. C.J. Baker and Dr. J.B. Odoki for their support, guidance, and insightful contribution to the development of this thesis.

I am grateful to the Highways Agency and the UK Climate Impacts Programme for providing the data used in this research. Sincere appreciation is also extended to all those who in one way or another contributed to this work.

TABLE OF CONTENTS

LIST OF FIGURES

LIST OF TABLES

ACCRONYMS AND ABBREVIATIONS

ANOVA	Analysis of Variance
DBM	Dense Bitumen Macadam
DIC	Deviance Information Criteria
DMRB	Design Manual for Roads and Bridges
dTIMS	Deighton Total Infrastructure Management System
GDP	Growth Domestic Product
GHG	Greenhouse Gas
HAAFM	Highways Agency Adaptation Framework Model
HAPMS	Highways Agency Pavement Management System
HATRIS	Highway Agency Traffic Information System
HDM-4	Highway Development and Management System
HRA	Hot Rolled Asphalt
IPCC	Intergovernmental Panel on Climate Change
MCMC	Markov Chain Monte Carlo
MEPDG	Mechanistic Empirical Pavement Design Guide
NRTF	National Road Traffic Forecasts
NTM	National Transport Model
RAC	Road Agency Costs
RM-ANOVA	Repeated Measure Analysis of Variance
SP	Softening Point of Asphalt Mix Binder in ^{o}C
TPM	Transition Probability Matrix
TRACS	Traffic Speed Condition Survey
TRL	Transport Research Laboratory
TSCS	Thin Surface Course System
UKCIP	UK Climate Impact Programme
UKCP09	The 2009 UK Climate Projections
UNFCCC	United Nations Framework Convention for Climate Change
VOC	Vehicle Operating Costs
WiLCO	Whole Life Cost Optimisation System
WinBUGS	Windows version of Bayesian Inference Using Gibbs Sampling

LIST OF NOTATIONS

Notation	Description	Unit
Model Structure and Equations		
ε	Error term in rut depth model structures	[-]
f(TPmax)	Functional form for modelling the effects of hot dry summers	[^{o}C]
ρ_0 to ρ_3	Model coefficient for HDM-4 plastic deformation model	[-]
η^1, η^2	Model coefficients for voids in mix model	[-]
ΔRUT	Annual incremental plastic deformation within the asphalt layers of the pavement	[mm]
ΔSP	Annual increase in asphalt binder softening point	[^{o}C]
ΔVIM(%)	Percentage annual rate of change in asphalt Voids in Mix (VIM)	[%]
AGE	Age of asphalt surfacing	[Years]
AXL	Average load on an axle of a commercial vehicle	[Tonnes]
CDS	Construction Defect indicator for asphalt surfacing	[-]
F	Average Annual Daily Traffic	[-]
G	Road section gradient	[-]
H_0, H_1	Rut depth model structure binary constants that take values of 0 or 1 as defined in section 4.4.3.3.	[-]
HS	Asphalt surfacing thickness	[mm]
P	Proportion of commercial vehicles on heavily loaded lane	[%]
SAXL	Standard single axle load	[Tonnes]
sh	Average speed of heavy vehicles	[km/h]
SP	Asphalt binder softening point	[^{o}C]
SPD	Design or initial asphalt binder softening point	[^{o}C]

Model Structure and Equations (Continued)

T_{air}	Maximum air temperature	[^{o}C]
TPmax	Maximum pavement temperature at 20mm below the asphalt surface	[^{o}C]
$T_{s(max)}$	Maximum pavement surface temperature	[^{o}C]
VIM	Voids in Mix	[%]
VIMD	Initial or design asphalt Voids in Mix	[%]
W	Structural wear factor for commercial vehicles	[-]
YE4	Annual number of equivalent standard axles	[msa]
α	Significance level	[-]
$\alpha 1$, $\alpha 2$	Model coefficients for binder softening point model	[-]
β_0	The intercept constant in the linear rut depth model structure	[-]
β_1 to β_6	Model coefficients for improved and alternative rut depth model structures	[-]

Bayesian Regression, Hypothesis Tests and Other Statistics

ϕ	Vector of rut depth model coefficients	[-]
φ	A constrained set of rut depth model coefficients and statistical parameters.	[-]
Λ	The transpose of the vector of the precision of the model coefficients	[-]
λ	Transformation variable in the Box Cox power transformation algorithm	[-]
μ	Mean	[-]
σ	Standard deviation	[-]
γ	Location parameter in a statistical model	[-]
ϕ_μ	Transpose of the vector of the mean of model coefficients	[-]
R_B^2	Bayesian version R-squared	[-]

Bayesian Regression, Hypothesis Tests and Other Statistics (Continued)

DF	Degrees of freedom	[-]
$G(\omega, \vartheta)$	Gamma distribution with shape parameter ω and scale parameter ϑ	[-]
GM	Geometric mean of a data sample	[-]
Ha	Alternative hypothesis	[-]
Ho	Null hypothesis	[-]
k	Shape parameter in a statistical model	[-]
M	Transpose of the vector of hyperparameters of the Bayesian hierarchical model	[-]
N	Number of Monte-Carlo simulations	[-]
$N(\mu, \tau)$	Normal distribution with mean μ and precision τ	[-]
$P[\phi/\Delta RUT]$	Combined posterior distribution of elements of the model coefficient vector ϕ given observed rut depth data	[-]
$P[\phi]$	Prior distribution of rut depth model coefficients	[-]
$P[\Delta RUT /\phi]$	Likelihood of the observed data given model parameters ϕ	[-]
P0	Probability of posterior estimate of model coefficient being greater than zero	[-]
p-value	The estimated probability of rejecting the null hypothesis (Ho) when it is true	[-]
S^2	Sample variance	[-]
SD	Posterior standard deviation	[-]

CHAPTER 1 INTRODUCTION

1.1 Background

Road transport is vital for general economic development and consequently significant resources are devoted to road construction and maintenance. The resultant road network normally has an asset value that is a significant proportion of the national wealth of a country (Robinson et al., 1988). Several researchers including McElvaney and Snaith (2002) and Powel et al. (1984) argue that the ability of roads to carry load and serve the road users is progressively reduced as a result of separate and interactive effects of climate and traffic. For example, according to TRL (2003) the combination of high temperature extremes and traffic can lead to rutting of asphalt surfacing. Furthermore, potholes on asphalt roads can develop as a consequence of rain water seeping through cracks caused by traffic, when the water freezes; it expands as ice pushing the road surfacing layer upwards and when it melts voids are left below the asphalt surfacing which then rupture under the stress of vehicles and turns into potholes (Lincolnshire County Council, 2011). These problems can be addressed by more frequent resurfacing and reconstruction of road pavements but at significant costs to road agencies.

Since roads typically have design lives in the range of 20 to 40 years (DMRB HD26/06, 2006), prior knowledge of expected consequences of future climate by road managers and engineers could ensure timely implementation of appropriate maintenance strategies which could in the long-term result in costs savings and a road network that is more robust to the consequences of climate change. Investigation of appropriate maintenance strategies is

possible using predictive tools such as the Highway Development and Management system (HDM-4) (Kerali et al., 2000). To that end, it is important that the deterioration models used in such tools correctly consider key factors such as climate and traffic that affect the performance of roads.

1.2 Problem Definition

Road pavement deterioration models used in current decision support systems such as HDM-4 have been formulated on the basis of a static climate assumption using past observations without considering the implication of climate change and uncertainties inherent in climate predictions as well as road pavement performance. The use of such tools in evaluating road pavement maintenance needs, maintenance strategies and other road management policies in the face of uncertainties in future climate and socio-economic scenarios is therefore likely to result in outputs that under or overstate the relative contribution of future climate to the rate of road pavement deterioration.

1.3 Aim and Objectives

1.3.1 Aim

The research was aimed at investigating tools and methods for use in assessing the impact of climate change on road pavement performance. The tools may be used by road managers, engineers and general practitioners to support road maintenance management decisions in the light of uncertainties that exist in future climate predictions.

1.3.2 Objectives

The objectives of the research were:

1. To develop an asphalt pavement surfacing rut depth prediction model that: can be used for assessing the impacts of future climate; embodies uncertainties inherent in the data used to develop the model; and can be used to support the investigation of strategies for adapting to unavoidable climate change.
2. To develop a framework that can be used for the quantification and propagation of uncertainties associated with climate impact assessment studies undertaken using the model in 1 above whilst accounting for uncertainties inherent in climate predictions, in other inputs to the impact model and in the coefficients of the model.
3. To demonstrate the application of the tools developed in objectives 1 and 2 in investigating the implication of future climate predictions on road pavement performance and maintenance costs under predefined road pavement maintenance strategies.

1.4 Research Scope

The focus of this study was on the development of asphalt surfacing rut depth deterioration model for use in investigating the consequences of future climate change on road pavement performance and maintenance needs since rutting is one of the most critical types of distresses that govern the overall pavement condition (DMRB HD26/06, 2006). Road network data used in the model development and case study were derived from trunk roads located in the United

Kingdom. Climate data used in the study were obtained from the 2009 version of climate projections for the United Kingdom (UKCP09).

The study did not however address issues associated with changes in components of road user costs such as vehicle operating costs and delays which may be directly or indirectly linked to changes in future climate and road pavement maintenance strategies. These issues were excluded because of the resource and time constraints that were available for this study.

1.5 Structure of the Thesis

The thesis is structured into eleven chapters as illustrated in Figure 1.1. The figure also highlights the interdependences between the chapters.

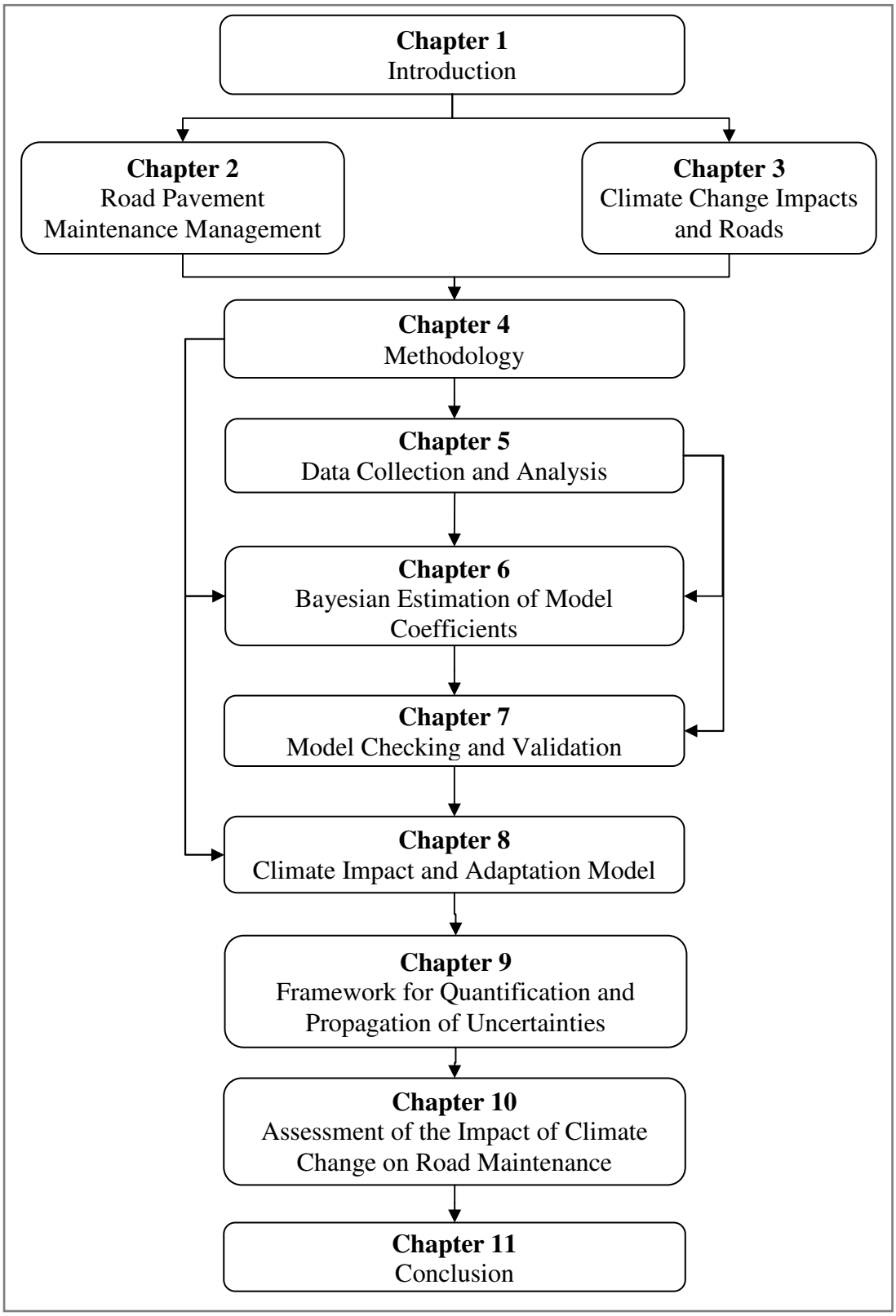

Figure 1.1: Structure of the thesis

Chapter 1 introduces the study and defines the research problem, aim and the objectives. The scope of the study and its benefits are also discussed.

Chapter 2 provides a review of the current road pavement maintenance practice in the United Kingdom with particular focus on data available for the development of road deterioration models, the mechanism of road pavement deterioration and existing methods and models for pavement deterioration modelling and prediction.

Chapter 3 discusses the current state of knowledge in approaches used for climate impact and adaptation assessments of infrastructure. Studies that have been undertaken within the United Kingdom and elsewhere to investigate the implication of climate change on roads are reviewed and research gaps highlighted.

Chapter 4 introduces the research gaps upon which this study was based and thereafter sets out the approach and modelling concepts used in the study.

Chapter 5 deals with discussions on the data used in the study and how they were collected, processed and the accuracy and reliability of the data. Graphical and statistical analyses of the evidence of the effects of recently observed climate events in collected rut depth data are discussed.

Chapter 6 discusses the estimation of the coefficients of the rut depth model using Bayesian regression and Markov Chain Monte-Carlo techniques. Detailed interpretation of the estimated model coefficients is provided including a discussion of how the model coefficients relate to theoretical expectations.

Chapter 7 is concerned with the checking and validation of the developed model to establish if the model is appropriate for use in performing predictions.

Chapter 8 sets out the analytical framework of a road pavement Climate Impact and Adaptation tool developed within a Microsoft Excel framework. A comparison is also made between outputs from the developed model and outputs from HDM-4.

Chapter 9 describes a framework within which the Climate Impact and Adaptation model discussed in Chapter 8 may be applied in climate impact and adaptation studies related to road pavement maintenance management.

Chapter 10 provides a detailed discussion of a case study aimed at demonstrating the application of the Climate Impact and Adaptation tool presented in Chapter 8 together with the uncertainty analysis framework set out in Chapter 9.

1.6 Benefits of the Research

The outcome of the study included a set of tools that can be used by road managers and engineers at the strategic and project levels of road management to forecast the performance of road asphalt pavements under defined scenarios of future climate and road maintenance strategies in the face of uncertainties that exist in climate change predictions as well as in the performance of the road pavement.

The tools developed can be applied to derive cumulative distributions of the costs of road pavement maintenance that can be attributed to climate change under predefined pavement

maintenance strategies. The outputs generated provide road managers with a framework for comparing several alternative road pavement maintenance strategies on the basis of the level of climate change risk that the particular road agency or organisation responsible for the management of the road network can tolerate.

The deliverables of the study can also be used to investigate alternative road pavement maintenance strategies for adapting to the potential consequences of climate change. It is anticipated that such maintenance policies could for example be characterised by the use of materials known to provide better resilience to the effects of climate change and the use of recycled materials for performing road pavement maintenance with a view to encouraging a sustainable approach to exploitation of materials for road construction and maintenance.

CHAPTER 2 ROAD PAVEMENT MAINTENANCE MANAGEMENT

2.1 Introduction

This chapter provides a review of current road pavement maintenance practice in the United Kingdom and in particular approaches for long-term road pavement performance prediction, pavement condition data that are available and the appropriateness of existing models in considering climate change.

Section 2.2 introduces the concept of road pavement performance prediction and modelling. This is followed by a consideration of the implication of sources of data for pavement deterioration modelling in section 2.3. Section 2.4 is concerned with the pavement deterioration mechanism on trunk roads in the United Kingdom. Section 2.5 reviews methods used for pavement deterioration modelling and a summary to the chapter is provided in section 2.6.

2.2 Modelling and Concepts of Pavement Performance Prediction

Pavement performance modelling and prediction is an essential part of pavement maintenance management at both the network and project levels of road management (Lytton, 1987). At the network level performance modelling and prediction using road management decision support tools is used to perform a number of function including: long-term estimates of maintenance and development needs for the whole road network often under various budgetary and economic scenarios; and prioritisation of road sections in need of maintenance, improvement or new construction under budget constraint (Robinson et al., 1998; Hass et al.,

1994). At the project level decision support tools are used to compare several maintenance and rehabilitation alternatives over the life cycle of the road amongst others (Kerali et al., 2000).

Examples of road management decision support tools used for pavement performance modelling includes: the Whole Life Cost Optimisation system (WiLCO) which was used by the UK Highways Agency to inform strategic planning decisions (Smith, 2011); the Highway Development and Management system (HDM-4) (Kerali et al., 2000); and the Deighton Total Infrastructure Management System (dTIMS) (Deighton Associates Limited, 2011) amongst others. Figure 2.1 adapted from Hass et al. (1994) illustrate the concept of pavement performance prediction.

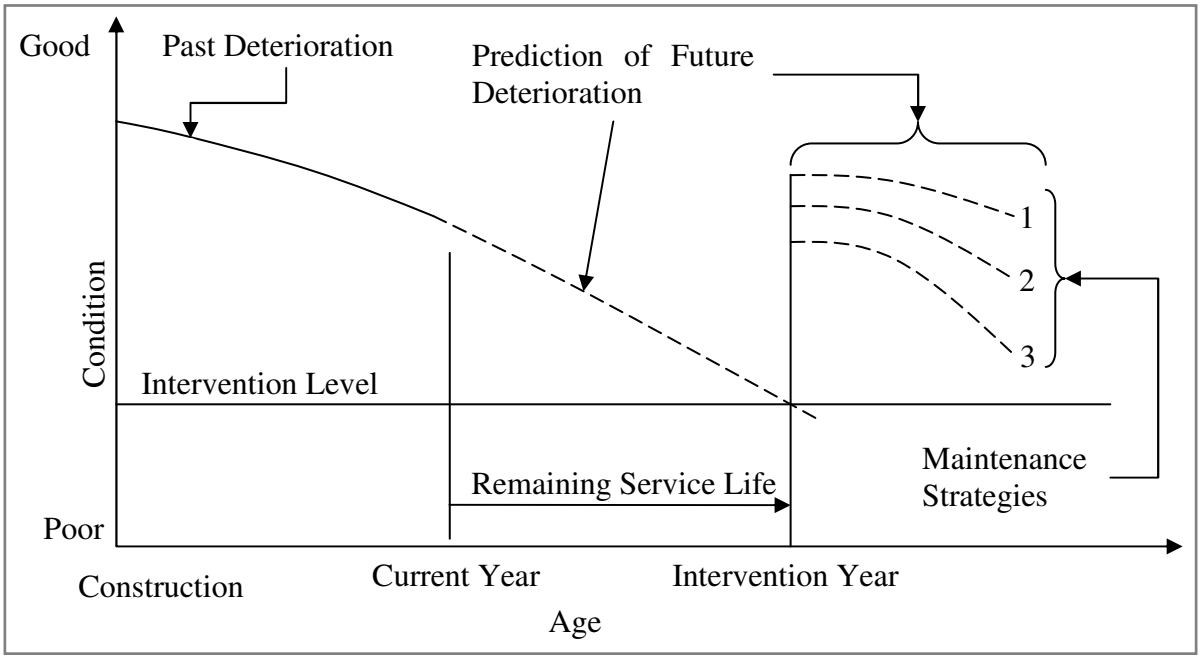

Figure 2.1: Concepts of Pavement Performance Prediction

From Figure 2.1 past deterioration trend is determined from collected inventory and condition data while prediction of future performance (deterioration) is performed using pavement

deterioration models embedded in road management decision support tools. Maintenance strategies refer to a set of pavement maintenance options corresponding to a combination of the following components: initial pavement condition, treatment types, intervention levels and road hierarchy (Mott MacDonald, 2006). According to Robinson et al. (1998), the choice of appropriate maintenance strategies is important in ensuring that roads are kept to a good standard in the long-term thereby ensuring continued use by traffic in an efficient and safe manner.

Road deterioration prediction models embedded in decision support tools are used to investigate appropriate pavement maintenance strategies. An important requirement of these models is that they must correctly consider the key factors such as traffic and climate that affect road pavement performance (Robinson et al., 1998). Bennett and Paterson (2000) argue that the reliability of the outputs obtained from these models is dependent upon two considerations:

- The accuracy of the data provided to the models; and
- The ability of the underlying models to simulate the real behaviour of the road network system for the conditions to which it is applied.

The implication of these two considerations is illustrated in Figure 2.2. Considering the accuracy of input data, for a given set of criteria for maintenance intervention and initial condition C_1, the road pavement will deteriorate and reach the set intervention threshold in a certain period of time between times T_1 and T_2. An incorrect initial condition, for example, C_2 instead of C_1 could result in a significantly different timing of maintenance works.

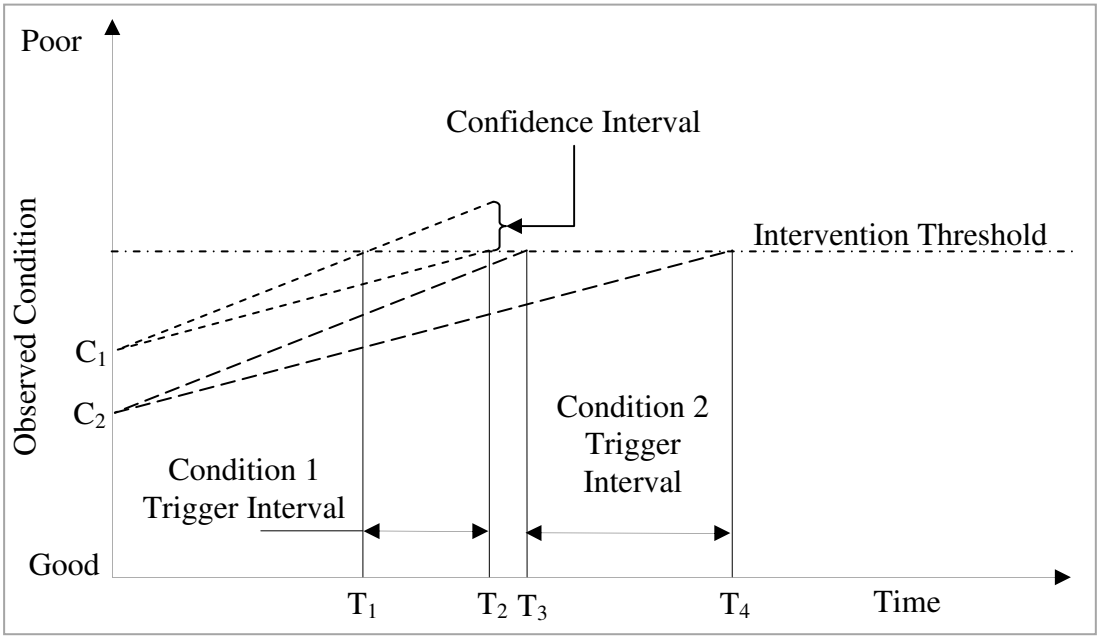

Figure 2.2: The Impact of Accuracy of Data on Road Deterioration Prediction

Figure 2.2 also highlights a second issue regarding the accuracy of the deterioration models. A confidence interval is associated to the mean distribution of the models and the greater into the future predictions are made, the greater the spread in the confidence interval and hence the uncertainty in the output of the analysis. In addition, the accuracy of the deterioration model also depends not only on the quality of the input data used in an analysis but also on the quality of the data used to develop the models in the first place (Bennett and Paterson, 2000). The next section therefore discusses pavement condition data available in the United Kingdom for use in the development of road deterioration models.

2.3 Data for Pavement Deterioration Modelling

Data used in the development of pavement deterioration models may be categorised as: data from experimental pavement sections and data from selected in-service road pavement sections (Archilla and Madanat, 2000).

2.3.1 Data from Experimental Pavement Sections

Data from experimental sites can be further categorised into:

- Data from purpose built pavement sections which are subjected to actual traffic and environmental conditions; and
- Data from purpose built pavement sections subjected to the effects of accelerated traffic loading and environmental (Sanders and Nunn, 2005).

An important advantage of experimental data is that key factors affecting pavement performance such as axle loads and pavement structure are carefully controlled thereby reducing uncertainties associated with model development (Archilla and Madanat, 2000). Furthermore, Haider et al. (2007) claim that experimental data provide a good basis upon which cause-and-effect relationships between the explanatory and response variables can be established. Prozzi and Madanat (2004) however suggests that data obtained from experimental sites do not provide a true reflection of the pavement deterioration process and are thus likely to result in models that are biased towards the effect of the controlled environments within which the tests were performed. Furthermore, such data are usually collected over a limited period of time, thus there is a likelihood of truncation bias if events (for example climate related) that occurred during the data collection period are used in the model development and events that occurred before and after are excluded. Similarly if the censoring of events is not properly accounted for then the resultant model may be prone to censoring bias (Prozzi and Madanat, 2000).

2.3.2 Data from In-service Road Sections

Data sourced from in-service road pavements are considered to be the most representative of actual deterioration process because they would have been collected from road sections that have been subjected to the effects of actual traffic and the environment (Hong and Prozzi, 2010).

In-service pavement data from trunk roads in England (United Kingdom) are collected using the Traffic Speed Condition Surveys (TRACS). A Summary description of the key pavement data types that are collected including comments on their reliability and accuracy is provided in Table 2.1 (DMRB HD 29/08, 2008). Other types of data collected using TRACS survey include texture depth and fretting.

The data available to this study were those collected annually from in-service pavements and stored in the Highways Agency Pavement Management system (HAPMS). These data types are discussed in the next section.

Table 2.1: Summary of Key Data Collected from In-Service Trunk Road Sections in England

Data Types	Description	Accuracy and Reliability
Rut Depth	• Reported as rut depth in millimetres at the nearside and offside wheel tracks. • Measurement is based on an algorithm that simulates placing a 2m straight edge across the measured profile.	• The measured data is highly comparable to manual measurements • The accuracy of the measured wheel track rut depth may be affected if the measuring vehicle drives off-line.
Cracking	• Reported as intensity of cracking in percentage.	• Measured intensity of cracking is not consistent with manual measurements performed by inspectors • The collected data is not suitable for developing time-series trends of deterioration.
Ride Quality	• Based on 3m, 10m an 30m Enhanced Longitudinal Profile Variance derived from measured longitudinal profile.	• Measurements can be affected by variations in road geometry, • Survey at slow vehicle speed leads to low values being reported. • Prior to June 2004 ride quality from TRACS was reported as Moving Average Longitudinal Variance.

With the exception of rut depth most condition data types measured on the UK Highways Agency road network using TRACS surveys embody a high degree of measurement uncertainty as noted in Table 2.1 and detailed in DMRB HD 29/08 (2008). Furthermore complete records of events such as maintenance interventions that influence the deterioration rate of road sections are not available because such data are not routinely updated (Highways Agency, 2009). As a consequence the estimation of the underlying rate of deterioration from available in-service data by filtering out events such as maintenance works is not straight forward.

Martin and Hoque (2006) developed a statistical methodology for estimating the underlying rates of deterioration from data collected from in-service pavements. They claim that their approach can be used to filter out the effects of maintenance works and outliers through statistical time-series analysis of data for a given road section using predefined rules. The latest underlying rate of road deterioration as illustrated Figure 2.3 is then used in the development of deterioration models. The approach was used to calibrate the HDM-4 deterioration models to reflect conditions in Australia (Hoque et al., 2008). Other statistical techniques for discerning the road pavement deterioration trends from data collected from in-service road sections have been proposed by Haider et al. (2007). These studies suggest that it is possible to use TRACS survey data in the development of pavement deterioration models.

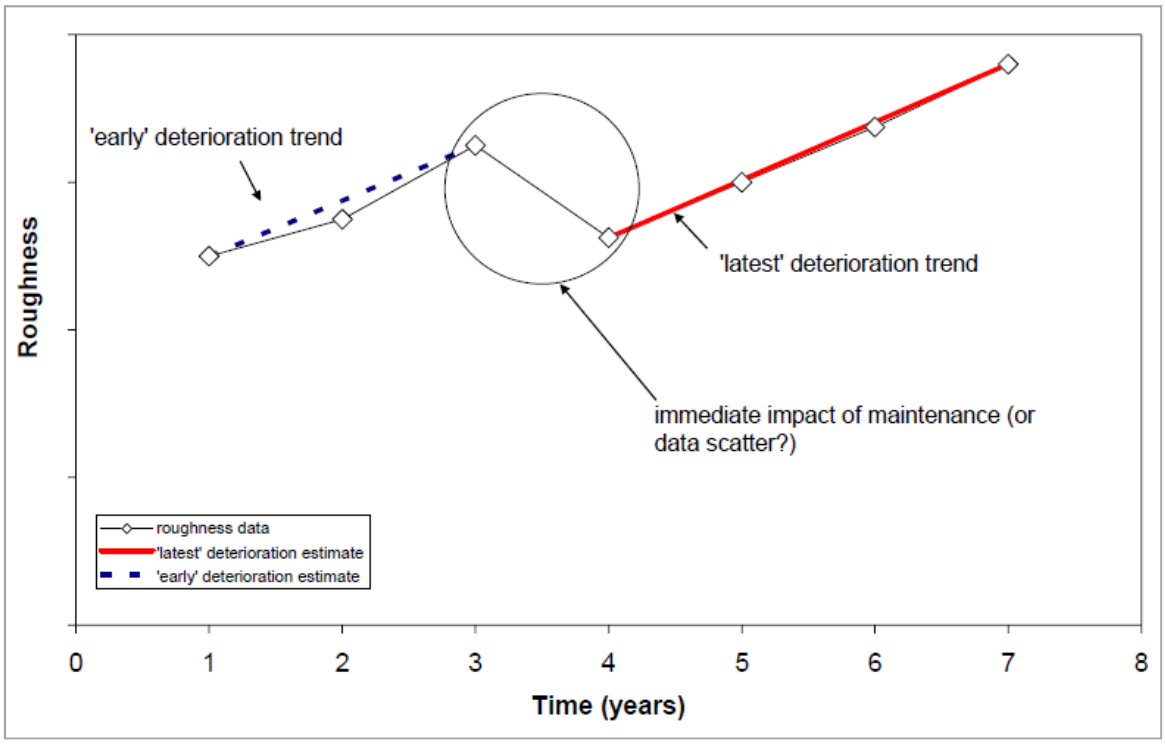

Figure 2.3: Estimation of the Underlying Rate of Deterioration from Historical Data (Source: Martin and Hoque (2006)).

2.4 Mechanism of Pavement Deterioration and Performance

2.4.1 Factors Affecting Pavement Deterioration and Performance

The deterioration and consequently performance of road pavements are influenced by the interaction between: climate factors with the pavement structure; the timings, methods and quality of road construction; traffic characteristics including axle loads, vehicle speeds, axle configuration, tyre types and pressure; and the maintenance policy (Hass et al., 2001). The interaction of these variables is illustrated in Figure 2.4.

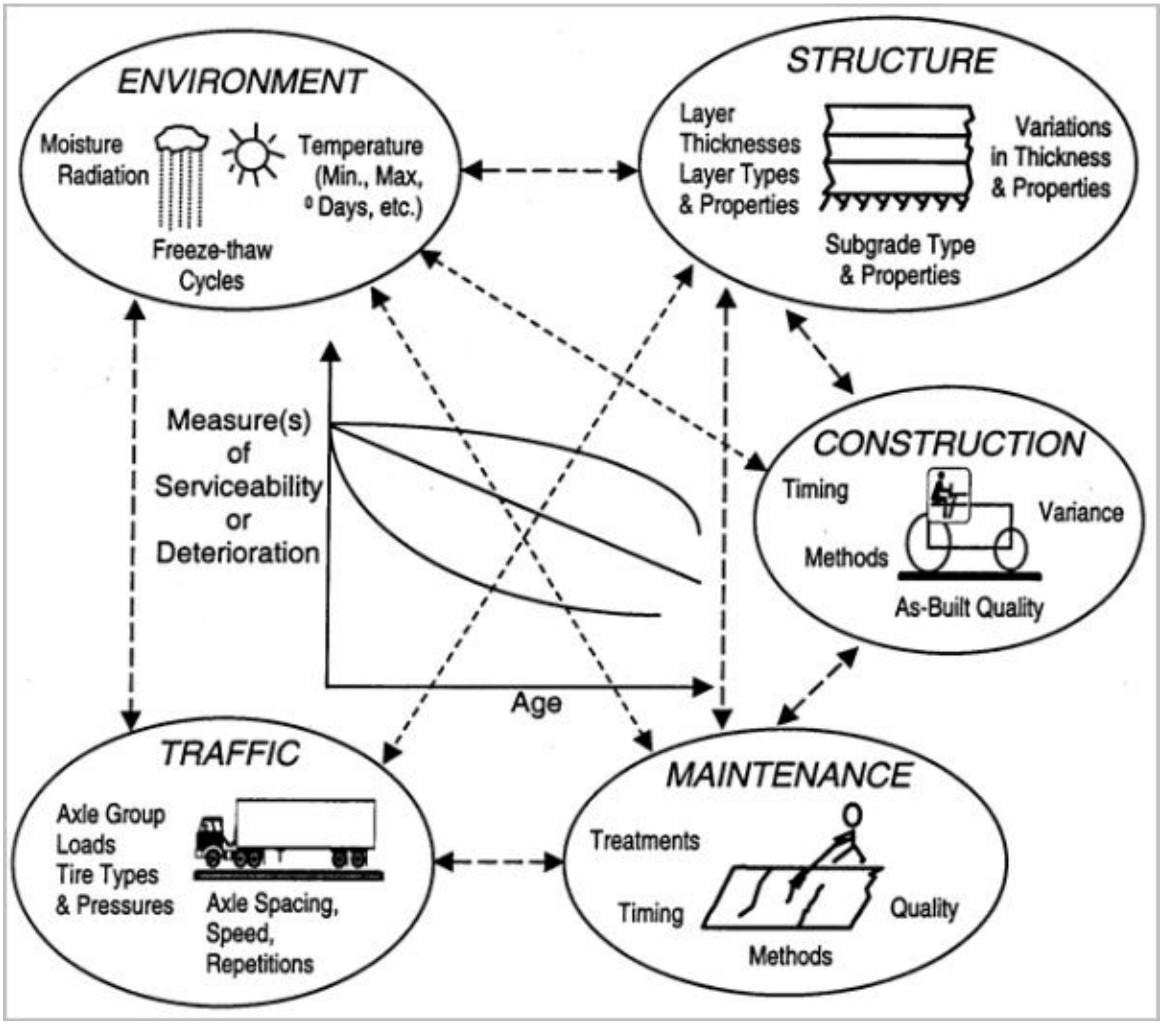

Figure 2.4: Factors Affecting Pavement Performance and Deterioration (Source: Haas et al., 2001)

It is theoretically possible but practically challenging to discern the relative and interactive effects of the factors that influence pavement deterioration and performance (Haas et al., 2001). This challenge has been attempted by several researchers (Prozzi and Madanat, 2001; Morosuik et al., 2004; Paterson, 1987; Hong and Prozzi, 2006) using modelling approaches reviewed in section 2.5. As a consequence, climate has been identified in such studies as an important factor in the initiation and progression of cracking and rutting of road pavements (Mills et al., 2007).

2.4.2 Modes of Pavement Deterioration

Cracking and rutting of road asphalt pavements are the two most critical types of distresses that govern the overall pavement condition. Fully flexible road pavements are traditionally designed to resist the structural rutting of the sub-grade and fatigue cracking of the road base (DMRB HD26/06, 2006; Yang et al., 2006). These two modes of deterioration are considered as structural modes of deterioration while distress such as rutting within the asphalt layers, ride quality and cracking originating from the surface of the road pavement are considered to be non-structural or surface deterioration (Merill et al., 2006). A study of the mechanisms of deterioration on trunk roads in Europe compared several modes of pavement distresses as shown in Figure 2.5 and concluded that rutting occurring on the asphalt layer of pavements is the most important (Merill et al., 2006). This study utilised data from UK trunk roads, to that end, the next section reviews the mode of rutting on such types of roads.

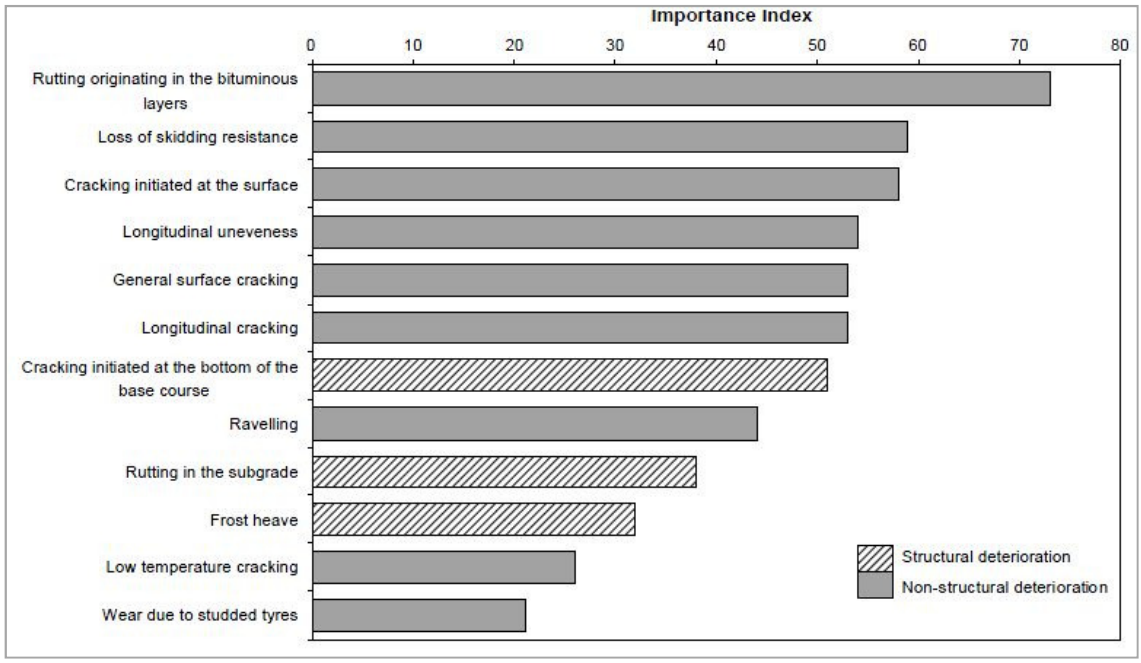

Figure 2.5: Importance of Perceived Modes of Deterioration in Fully Flexible Pavements (Source: Merill et al., 2006).

2.4.3 Modes of Rutting on Trunk Roads

A study by Nunn et al. (1997) investigated the relationship between rates of asphalt rutting observed on more than 40 sites covering experimental and in-service pavements located on trunk roads in England. Low rates of rutting were observed on sections with asphalt thickness greater than 180mm while road sections with thinner asphalt layers exhibited high rates of rutting due to failure of the sub grade as a consequence of excessive traffic induced stresses. The rates of rutting with asphalt layer thickness are depicted in Figure 2.6. Since trunk roads in the United Kingdom are usually constructed with thick asphalt layers, the researcher concluded the predominant mode of rut depth deterioration on such roads is limited to the asphalt layer.

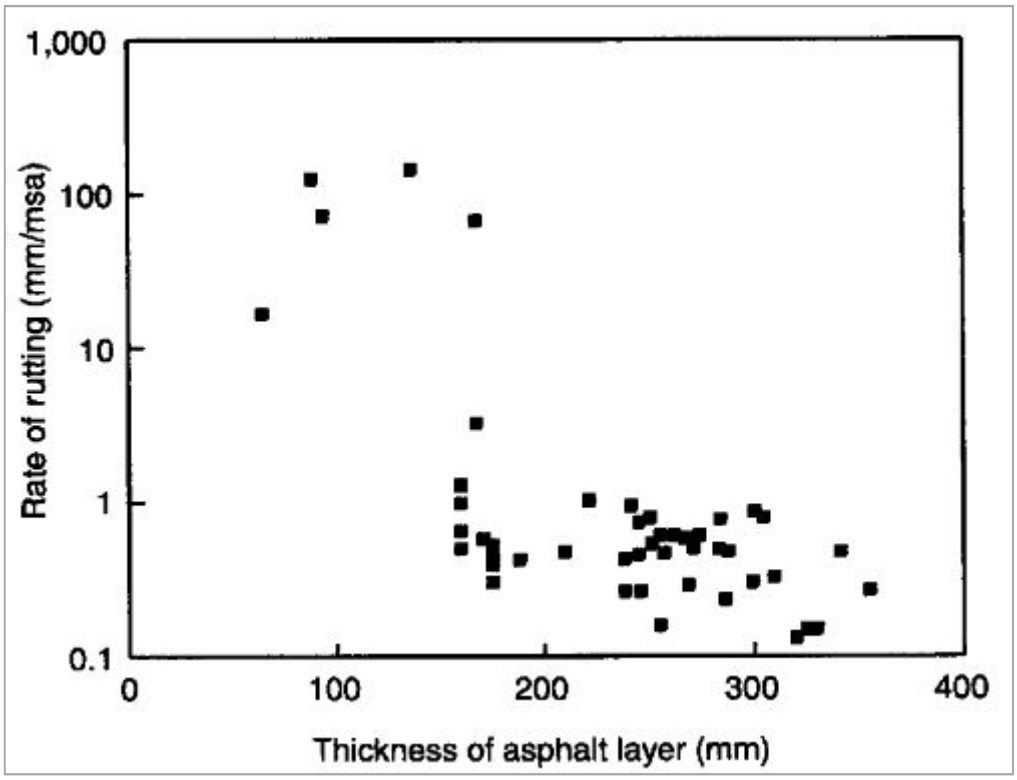

Figure 2.6: Rates of Asphalt Rutting with Thickness on Trunk Roads in England (Source: Nunn et al., 1997).

Another study reported by Weston et al. (2001) investigated the rut depth deterioration of a 360mm thick asphalt pavement layer depicted in Figure 2.7 using accelerated loading tests. Deformation was observed to be restricted to the surfacing and binder course layers which is consistent with findings by Nunn et al., (1997) and confirms that surface rutting is the dominant mechanism of rutting on trunk roads in England. To that end, the first objective of this study was limited to the development of asphalt surfacing rutting using data from trunk roads.

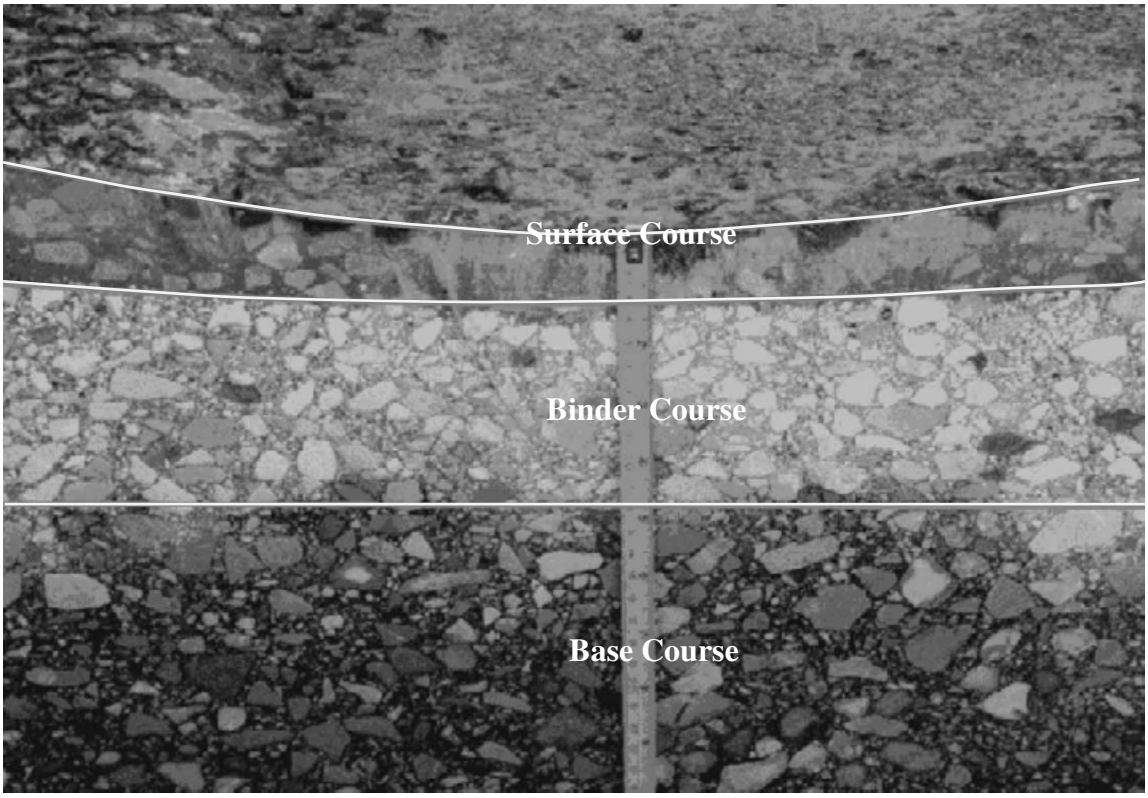

Figure 2.7: Deformation in Asphalt Layer following Accelerated Load Testing.

2.4.4 Mechanism of Asphalt Surface Rutting

Surface rutting is said to be a result of plastic flow of the asphalt and occurs when the stress induced by traffic exceeds the shear strength of the material, or are sufficient to induce creep (Paterson, 1987). TRL (1993) states that surface rutting occur as a combination of two or more of the following scenarios:

- Very heavy axle loads;
- High maximum temperatures;
- Channelized traffic;
- Stopping or slow moving traffic.

It is argued (Morosuik et al., 2004) that surface rutting may not occur following a combination of the above factors because the asphalt mix could have been designed to withstand such conditions. It is therefore suggested that models for predicting surface rutting should include not only the above factors but also the properties of asphalt materials (Morosuik et al., 2004). Table 2.2 adapted from Sousa et al. (1991) provides a summary of asphalt material properties and their influence (increasing or decreasing) on rutting resistance of asphalt mixes.

Table 2.2: Implication of Material Properties and other Factors on Rutting

Material Properties/Factor	**Change in Material Properties**	**Resistance of Asphalt Mixture to Rutting**
Binder stiffness	Increase	Increase
Air void contents	Increase	Decrease
Voids in mineral aggregates	Increase	Decrease
Temperature	Increase	Decrease
State of stress/strain	Increase in tyre pressure	Decrease
Load repetition	Increase	Decrease

The mechanism asphalt surface rutting discussed in this section identified variables that are important for the development of asphalt surfacing deterioration models. The next section reviews existing deterioration models.

2.5 Deterioration Models

Pavement deterioration models reviewed in this section are discussed under the following headings: Probabilistic models; deterministic models; and Bayesian Models.

2.5.1 Probabilistic Models

Models categorised as probabilistic are used to predict future condition as a probability function of a range of possible conditions (Morosuik et al., 2004). Unlike deterministic models, a key advantage of probabilistic models is that they attempt to account for the uncertainties inherent in the variables used in the prediction of pavement performance. These variables include traffic, climatic conditions, pavement material properties and geometric variables (Hong and Wang, 2003).

The most common types of probabilistic pavement deterioration models are those based on Markov chains (Lytton, 1987; Yang et al., 2006; Costello et al., 2006; Li et al., 1996; Seyedshohadaie, 2010). Markov models for pavement deterioration are based on transition matrices. These matrices express the probability that a homogeneous group of pavement sections will move from one state of distress or condition band to another within a given time period (Ortiz-Garcia et al., 2006). The approach (Markov prediction models) is governed by three criteria:

- The number of states or condition bands in which a pavement can be found in a given time is finite;
- Transition from one state to another is dependent only on the present state; and
- The process of transition is stationary, implying that the probability of changing from one state to another does not depend on time.

(Isaacson and Madsen, 1976)

According to Li et al. (1996) and Lytton (1987), the assumption that the transition process of moving from one state to the next depends only on the present state implies that within a given planning horizon, changes in factors such as climate or traffic which are important for road pavement performance do not change the transition probabilities. Furthermore, variables known to be responsible for pavement deterioration and performance such as climate, traffic and material properties are not explicitly represented (Costello et al., 2006) making it difficult for the relative and combined effects of such variables to be discerned. This is a major disadvantage in studies such as climate impact and adaptations assessment of road maintenance options where it is important to explicitly consider future climate and socio-economic scenarios UKCIP (2000). Consequently, this modelling approach was not used in this study.

2.5.2 Deterministic Models

Deterministic models are used to predict condition as a precise value using mathematical functions based on observed or measured values. This group of models can be broken down further under three categories: empirical models; mechanistic models; and mechanistic-empirical models (Morosuik et al., 2004).

2.5.2.1 Empirical Deterioration Models

In empirical models, a dependent variable such as rut depth is related to one or more explanatory variables such as asphalt surfacing age or traffic loading. The models are developed based on statistical considerations only, without accounting for the true underlying factors responsible for pavement deterioration (Prozzi and Madanat, 2001). Therefore, such

models are only valid in the location in which they have been developed and are not transferable to other locations (Paterson, 1987).

The WiLCO decision support tool which was developed for use by the UK Highways Agency utilises an empirical model for rut depth prediction. The system assumes that rutting progresses at a rate of 1mm per year on UK trunk roads with asphalt surfacing (Smith 2011). Such models are not appropriate for policy studies because the contribution to deterioration of climate, traffic, material properties and other variables are not known (Paterson, 1987). The use of such models for climate impact assessment is therefore not appropriate, since uncertainties associated with future climate predictions as well as changes in socio-economic scenarios are would not be accounted for (UKCIP, 2000).

2.5.2.2 Mechanistic Deterioration Models

Mechanistic models attempt to account for all the pavement materials properties and response functions believed to represent the actual behaviour of the pavement when subjected to the effects of traffic as well as the environment (Prozzi and Madanat, 2001; Paterson, 1987). Mechanistic models are very data intensive and rely on parameters which are difficult to quantify in practice (Morosuik et al., 2004). Given the complexity in developing such models, their application has been limited (Prozzi and Madanat, 2001).

2.5.2.3 Mechanistic – Empirical Deterioration Models

Mechanistic-empirical models utilise concepts from both mechanistic and empirical models. Mechanistic principles are used to determine the functional forms and variables important for describing distress of interest such as rut depth while empirical approaches are used to derive

and combine functional forms with observed data (Morosuik et al., 2004). Mechanistic-empirical models have an advantage over empirical models in that they can be used outside the area in which they were developed provided appropriate calibration is undertaken (Lytton, 1987).

Given the shortcomings associated with empirical and mechanistic models and the flexibility associated with the use of mechanistic-empirical models, Paterson (1987) proposed their use in the Highway Development and Management System (HDM-4). The functional form of asphalt surface rutting model used in HDM-4 is given in Equation 2.1 (Morosuik et al., 2004).

$$\Delta RDPD = K_{rpd} a_0 \times CDS^{a_1} \times YE4 \times sh^{a_2} \times HS^{a_3} \quad (2.1)$$

where: $\Delta RDPD$ = incremental increase in surface or plastic deformation within the asphalt layers of the pavement in mm; CDS is the Construction Defect indicator for asphalt surfacing ranging in value from 0.5 for brittle asphalt mix to 1.5 for soft asphalt mix; YE4= annual number of equivalent standard axles in millions/lane; sh= average speed of heavy vehicles in km/h; HS= thickness of asphalt layer in mm; and a_0 to a_3 are model coefficients which can be estimated using statistical methods such as Ordinary Least Squares (OLS). K_{rpd} = model calibration factor. A detailed description of the model is given in Morosuik et al. (2004).

The limitation of the incremental rut depth functional form given in Equation 2.1 is that it does not explicitly account for the asphalt material properties and pavement temperature which as noted in section 2.4 are important for describing surface rutting. According to Morosuik et al. (2004), this simplification was adopted because of perceived practical difficulties in obtaining values of material properties and pavement temperature from in-service road pavements. In addition a review by Mott MacDonald (2006) argued that HDM-4

models were developed using data from Australia and Japan, and to that end, cannot be directly used in the United Kingdom unless it is properly calibrated. Preliminary calibration of the HDM-4 models to UK conditions was performed by Odoki et al. (2006) based on expert knowledge of the deterioration of roads in the United Kingdom but detailed calibration using pavement performance data was recommended.

Other variations of mechanistic-empirical models have been proposed by Archilla and Madanat (2001), and Prozzi and Madanat (2004). These models were however developed using data obtained outside the UK and to that end require detail calibration (Mott MacDonald, 2006). The rut depth model used by the UK highways agency is empirical as noted in section 2.5.2.1.

Deterministic model coefficients such as those given in Equation 2.1 (a_0 to a_3) have traditionally been estimated using Ordinary Least Squares (OLS). The advantage of the OLS approach is that it is simple to use and does not require a lot of computational effort. The disadvantage is that it does not work well with data with small sample size and the approach ignores prior knowledge by experts (DelSole, 2007). An alternative approach is based on Bayesian regression.

2.5.3 Bayesian Deterioration Models

Bayesian inference can be used to estimate the distribution of the model coefficients of deterministic model forms such as Equation 2.1. The approach combines information from observed data with prior knowledge about the model coefficients (referred to as priors) to give updated distribution of the model coefficients (referred to as posterior), which is described using Bayes' theory as:

$$P(a/DATA) = \frac{P(DATA/a)P(a)}{\int P(DATA/a)P(a)da} \quad (2.2)$$

where P(a/DATA) = combined posterior distribution of model coefficients (a) given observed data (DATA); P(DATA/a) = the likelihood of the observed data given the model coefficients (a); and, P(a) = prior distribution of the model coefficients. The integral in the denominator denoted by $\int P(DATA/a)P(a)da$ calculates the total probability across the model parameter space resulting into a constant (Ntzoufras, 2009).

The main difference between estimation of model coefficients using ordinary least square and Bayesian approach is that the latter associates a probability distribution with the model. This probability distribution known as prior distribution quantifies uncertainties in the model coefficients before data becomes available and this uncertainty is then transferred to the posterior estimates of the model coefficients. The prior distribution can be elicited from experts with knowledge of the performance of the road network being modelled or from published literature. (DelSole, 2007).

Since the estimated model coefficients are presented using distributions, it is possible to perform predictions in a probabilistic manner using Monte-Carlo simulation. Furthermore, the approach also provides a framework for updating the estimates of model coefficients when new data becomes available (C-SHRP,1994).

An obstacle that has prevented the wide use of Bayesian analysis has been the difficulties associated with evaluating the combined posterior distribution to derive marginal distributions of the model coefficients. The development of computer programs such as the Windows

version of Bayesian Updating using Gibbs Sampling (WinBUGS) has made the process much easier (Jiang et al., 2009).

Hong and Prozzi (2006) used a Bayesian methodology to develop a pavement deterioration model. They concluded that due to the significant variability in the model coefficients the Bayesian approach provides a good framework for addressing the problem of heterogeneity which is inherent in pavement performance modelling. Furthermore, they noted that the Bayesian approach provides an effective and flexible alternative for model estimation and updating.

2.5.4 Summary Review of Deterioration Models

A summary of the advantages and disadvantages of the deterioration models and methods reviewed in section 2.5 is provided in Table 2.3.

Table 2.3: Advantages and Disadvantages of Deterioration Model Types

Models	Advantage	Disadvantage
Markov	• Encapsulates uncertainties in pavement deterioration; • Reflects performance trend regardless of whether it is actually non-linear or not.	• Physical factors that cause deterioration are not included in the model; • Development of transition probabilities is challenging if data is limited.
Empirical	• Easy to formulate and implement in road management decision support systems • Can be used to support all road management functions	• The models are not transferable to other places ; • May not account for the true underlying courses of deterioration; and • Does not take into account uncertainties associated with data used in the model development.
Mechanistic	• Formulated based on mechanistic principles that reflect the true behaviour of materials and factors affecting deterioration.	• Requires a lot of inputs and significant computing power; • Not feasible for use in long-term predictions. Predicts basic outputs such as stress, strains and deflections; • Applicable at the project level or for research purposes.

Table 2.2: Advantages and Disadvantages of Deterioration Model Types (Continued)

Models	Advantage	Disadvantage
Mechanistic-empirical	• Variables that explain the underlying rates of deterioration are included in the model; • The models can be used in a different location from which it was developed provided it has been calibrated; and • Can be used at both the project and network levels of road management.	• Model coefficients are often estimated using ordinary least squares which does not allow for uncertainties in data to be quantified; • Does not account for uncertainty associated with model inputs as well as the model functional form; and
Bayesian	• Has the ability to consider past experience; • Provides a framework for updating the model using new data; and • Quantifies uncertainties in model coefficients which can allow probabilistic predictions using Monte-Carlo simulation.	• Estimated model coefficients can be affected by wrong prior information; and • Many require large computing resources if predictions are made using Monte-Carlo simulation at the network level.

From the review of the various model types and the summary of the advantages and disadvantages given in Table 2.3, it is apparent that mechanistic-empirical models together with the Bayesian regression approach provide an appropriate framework within which a model for use in climate impact assessment of road pavement maintenance can be developed.

2.6 Summary

This chapter highlighted the need for accurate prediction of future performance of road pavements to support decisions in managing roads in the United Kingdom at both the network and project levels. To that end the following key challenges were identified:

- Availability of appropriate data; and
- Availability of appropriate models for predicting pavement performance.

Asphalt surfacing rut depth was identified as an important mode of distress on UK trunk roads. Appropriate models for predicting the future performance of trunk roads on the basis of rut depth whilst explicitly quantifying the impacts associated with climate change are currently not available. It was concluded that the Bayesian method combined with mechanistic-empirical models provides an appropriate framework within which model(s) for assessing the impact of climate change on road pavement maintenance can be developed.

The next chapter investigates current understanding on the assessment of the impacts of climate change on roads through reviews of studies that have been undertaken in the United Kingdom and elsewhere.

CHAPTER 3 CLIMATE CHANGE IMPACTS AND ROADS

3.1 Introduction

This chapter focuses on climate change, its impacts on roads and the assessment of impacts associated with future climate prediction. The chapter is aimed at identifying the current state of knowledge with respect to climate impact assessments in the United Kingdom.

Section 3.2 provides definitions and relevant concepts related to climate change including a summary of the predicted climate change in the United Kingdom. Section 3.3 highlights current United Kingdom government policies on climate change adaptation. Section 3.4 reviews frameworks and methods for climate change impact and adaptation assessment. A review of studies performed within and outside the United Kingdom is provided in section 3.5. Section 3.6 outlines research gaps followed by a conclusion to the chapter in section 3.7.

3.2 Definitions and Concepts

3.2.1 Climate Change

The Intergovernmental Panel on Climate Change (IPCC) defines climate change as:

> 'A change in the state of the climate that can be identified by changes in the mean and/or the variability of its properties, and that persists for an extended period, typically decades or longer' (IPCC, 2007).

The United Nations Framework Convention on Climate Change (UNFCCC) however defines climate changes as:

> 'A change of climate which is attributed directly or indirectly to human activity that alters the composition of the global atmosphere and which in addition to natural variability is observed over comparable time periods' (IPCC, 2007).

The UNFCC definition makes a distinction between climate change that is attributable to human influences and climate variability due to natural causes. This is in contrast to the broader view by the IPCC that climate change can occur as a result of natural variability and human activity. The IPCC definition is adopted in this study.

An analysis of observed global surface temperature performed by Brohan et al. (2006) concluded that global warming has occurred in two phases, from the 1910s to the 1940s and more lately from the 1970s to present as depicted in Figure 3.1. It is apparent that global surface temperature has risen by about 0.6^{o}C since the beginning of the twentieth century with about 0.4^{o}C occurring since the 1970s. There is evidence to suggest that the rise in global surface temperature observed since the mid 20th was caused by increase in greenhouse gas (GHG) emissions due to human activity (Stott et al., 2000; Allen, 2005; Gillett et al., 2002; Hegerl et al., 2001; IPCC, 2007; Karl et al., 2006; Karoly and Wu, 2005; Stone and Allen, 2005; Stott et al., 2001; Tett et al., 2002; Zhang et al., 2006; Zwiers and Zhang, 2003).

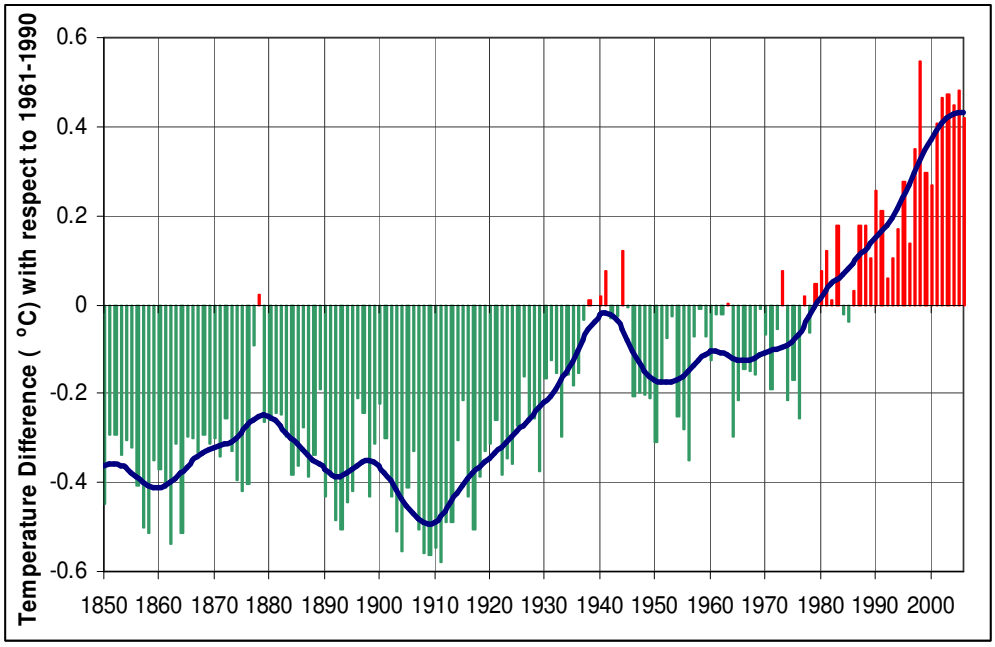

Figure 3.1: Global-average surface temperature (1850 to 2006).

3.2.2 Summary of Predicted Change in UK Climate

To facilitate the understanding of future climate the UK Climate Impacts Programme (UKCIP) has developed climate change projections for the United Kingdom. Table 3.1 adapted from Hulme et al. (2002) gives a general summary of expected climate change in the UK. The general trend is that summers are predicted to get hotter and drier while winters are expected to get wetter. The frequencies of extreme events are also expected to increase (Murphy et al., 2009). The latest version of climate projections for the United Kingdom are referred to as UKCP09 and are described in detail by Murphy et al., (2009).

Table 3.1: General summary of expected climate change in the UK

Climate Parameter	Expected Changes
Temperature	Annual warming by the end of the century of between 1°C and 5°C depending on emission scenario.
	Greater summer warming in the southeast than in the northwest.
	Increase in the number of very hot days.
	Decrease in the number of very cold days
Precipitation	Generally wetter winters for the whole of the UK, and increases in winter precipitation intensity.
	Substantially drier summers
Soil Moisture	Decreases in summer and autumn, especially in the southeast.
Sea level	Global average sea level will continue to rise for several centuries. According to the Intergovernmental Panel on Climate Change's 4th Assessment, global sea level will increase by the 2090s by between 20 and 60cm, depending on the emissions scenario.
	There will be significant regional differences in relative sea level rise around the UK.
	For some costal locations and some scenarios, storm surges will become more frequent.

Source: Hulme et al., (2002).

3.2.3 Climate Change Mitigation and Adaptation

Projections of future climate suggests that although mitigation of the effects of climate change through reducing man-made GHG emissions is vital to avoid the most dangerous effects of climate change on the society and infrastructure, some changes in climate is now inevitable as a result of past emissions (Defra, 2009). Therefore, in addition to reduction in GHG emissions, there is a need to adapt to minimise the consequences and maximise the opportunities associated with climate change (Murphy et al., 2009).

According to Defra (2009), mitigation is concerned with taking action to tackle the causes of climate change by reducing concentrations of GHGs in the atmosphere while adaptation deals with taking action to address the consequences of a changing climate resulting from increased levels of GHG emissions. The role of mitigation and adaptation strategies in addressing the impact of climate change on roads is illustrated in Figure 3.2.

The focus of this study is on adaptation to climate change. To that end, the greyed boxes in Figure 3.2 highlight components that are relevant to the review presented in this chapter. The next section sets out current United Kingdom government policy on climate change impact and adaptation.

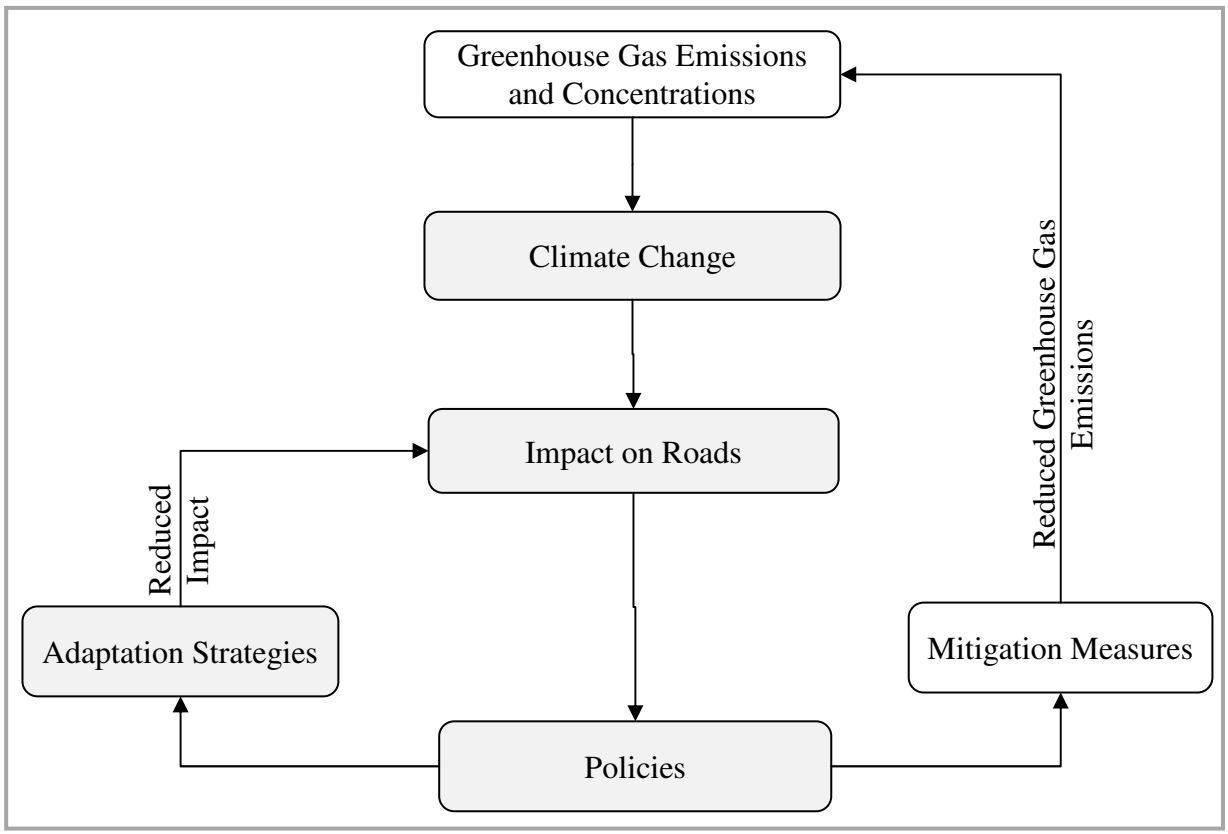

Figure 3.2: Role of Adaptation Strategies and Mitigation Measures in Dealing with Climate Change Impacts on Roads (Adapted from National Research Council, 2008)

3.3 UK Climate Change Adaptation Policies

3.3.1 The Climate Change Act

In recognition of the potential impact of climate change, the climate change act become law in November 2008. It is intended to enhance the ability of the United Kingdom to adapt to the impact of climate change. The key provisions of the act related to adaptation to climate change include the following:

- a requirement on the Government to report at least every five years on the risks to the UK of current and predicted climate;
- a requirement on the Government to publish a national adaptation programme for England setting out how the climate risks will be addressed;
- powers for the Government to require public bodies and statutory undertakers to carry out their own risk assessment and make adaptation plans to address those risks; and
- a recommendation for the formation of an Adaptation Sub-Committee of the Committee on Climate Change tasked with overseeing progress and providing advice to the Government on adapting to climate change and on risk assessments.

  (The National Archives, 2008)

3.3.2 The Nottingham Declaration

The Nottingham Declaration was launched in October 2000. It is a pledge that local authorities in England can sign as a formal commitment to their community to mitigate and adapt to climate change. The declaration is nationally recognised albeit not forming part of the

central government programme (Climate East Midlands, 2009). Components of the declaration which are relevant to climate change adaptation include commitments to:

- work with the central government to contribute, at a local level, to the delivery of the UK Climate Change Programme;
- develop plans with partners and local communities to progressively adapt to the impacts of climate change;
- undertaken risk assessments associated with climate change and adapt accordingly; and
- encourage all sectors in the local community to adapt to the impacts of climate change.

(Energy Saving Trusts, 2011)

3.4 Approaches for Climate Impact and Adaptation Assessments

A number of studies have been undertaken in the area of climate change impact and adaptation assessments but few have provided robust outputs for use by decision makers in the planning and design, construction, maintenance and operation of roads (Infrastructure Canada, 2006; National Research Council, 2008; Dessai and Hulme, 2004). This is partly because of the existence of persistent uncertainties in climate change projections augmented by the lack of data at the appropriate spatial and temporal resolution for use by road engineers and managers (Burton et al., 2002; Infrastructure Canada, 2006).

According to Parry and Carter (1998), the approach most commonly used for climate impact and adaptation assessments of infrastructure can be generally described as predictive. It

involves the formulation of future scenarios of world development. GHG emissions estimated to result from these future scenarios are then used in climate models to derive predictions of future climate which is in turn used in impact models to assess impacts and to investigate adaptation options on roads and other types of infrastructure (Parry and Carter, 1998). Subsequent sub-sections review approaches for climate impact and adaptation assessments that are available in the literature.

3.4.1 IPCC Approach

The Intergovernmental Panel on Climate Change (IPCC) approach to climate impact assessment detailed in Carter et al. (1994) and Parry and Carter (1998) comprise the following seven steps:

1. Definition of the problem including the area and scope of the study;
2. Selection of method of assessment that is most appropriate for the problem defined;
3. Testing methods/ sensitivity analysis;
4. Selection and application of climate change scenarios;
5. Assessing biophysical and socio-economic impacts;
6. Assessment of autonomous adjustments; and
7. Evaluation of adaptation strategies.

According to Dessai and Van der Sluijs (2007), the IPCC approach is heavily reliant on uncertain information from climate change scenarios (Step 4) which is then used to drive the investigation of impacts in Step 5 and subsequently to inform adaptation strategies in Step 7. Pittock et al. (2001) argue that to allow optimal and focused adaptation plans it is more appropriate to represent the outputs of such assessments in the form of cumulative

probabilities which, according to Pate-Cornell (1996) provides useful information in making risk management decisions under uncertainties and resource constraints.

3.4.2 UKCIP Approach

The UK Climate Impacts Programme (UKCIP) approach is based on a framework intended to support decision makers in taking account of risk and uncertainty associated with climate variability and climate change with the view of identifying optimal adaptation options (Willows and Connell, 2003). The framework has eight stages which are depicted in Figure 3.3

Unlike the IPCC approach, within the UKCIP framework the use of uncertain climate information is not explicitly included as a step. However in Step 3 (Assess Risks) three options (tiers) of risk assessments are available to decision-makers. Tier 1 refers to preliminary climate change risk assessments; Tier 2 is concerned with qualitative, semi-quantitative and generic quantitative risk analysis while Tier 3 deals with specific quantitative risk assessment. The detail and effort in the quantification of uncertainties increases from Tier 1 to 3. The basis upon which a particular risk assessment tier may be selected is also governed by the level of decision; the level of understanding of the decision marker on how climate change will affect his or her decision; and the purpose of the decision, whether it is a climate adaptation or a climate influenced decision (Willows and Connell, 2003; Dessai and Van der Sluijs, 2007).

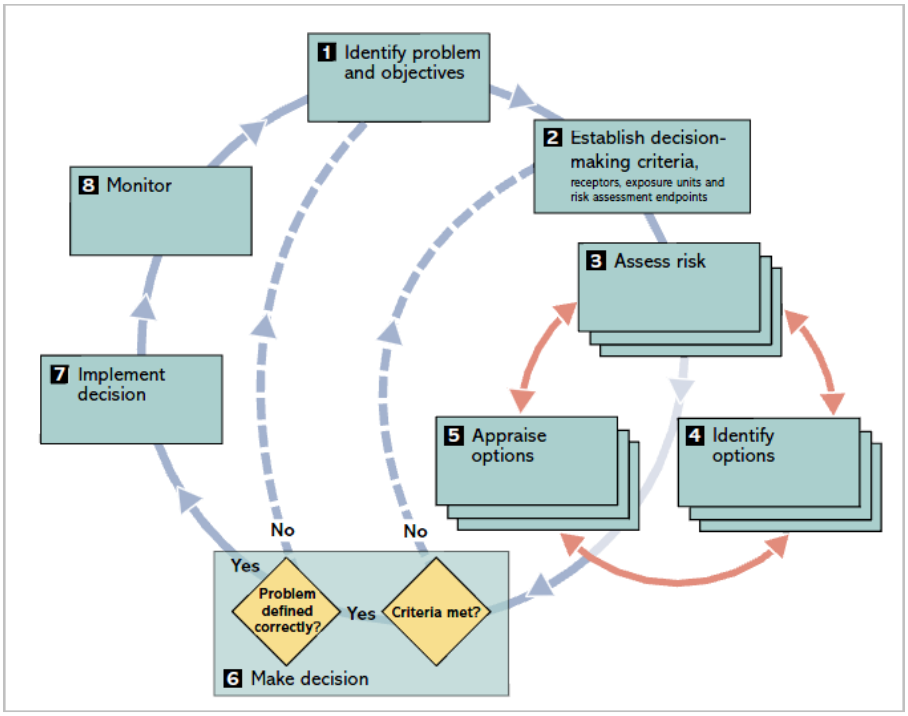

Figure 3.3: UKCIP Risk, Uncertainty and Decision Making Framework (Willows and Connell, 2003).

The UKCIP guideline also proposes a range of tools and techniques. Table 3.2 provides a summary of the tools and techniques used in the three tiers. Descriptions of these tools are given in Willows and Connell (2003) but comprehensive guidance on their application is not provided.

Quantitative methods listed in Table 3.2 such as statistical models, Monte-Carlo techniques, Bayesian methods and Markov chain modelling are also used in pavement deterioration modelling as discussed in section 2.5.

Table 3.2: Summary of Tools and Techniques

Tier 1 (Preliminary Climate Change Risk Assessment)	Tier 2 and 3 (Qualitative and Quantitative Risk)
• Checklists • Brainstorming • Problem Mapping Tools • Process Influence Diagrams • Consultation Exercises • Fault/Event Trees • Expert Judgement and Elicitation • Scenario Analysis • Climate Change Scenarios • Cross-Impact Analysis • Deliberate Imprecision • Pedigree Analysis	• Uncertainty Radial • Fault/Event Trees • Decision and Probability Trees • Expert Judgement and Elicitation • Scenario Analysis • Climate Change Scenarios • Cross-Impact Analysis • Monte Carlo Techniques • Modelling Tools: Process Response Models • Statistical Models • Development and use of Specific Sophisticated Modelling Tools • Climate Typing • Downscaling • Bayesian Methods • Markov Chain Modelling • Interval Analysis

Source (Willows and Connell, 2003)

3.4.3 Highways Agency Adaptation Strategy Model

The UK Highways Agency developed a seven stage framework referred to as the Highways Agency Adaptation Framework Model (HAAFM). The development of the framework was partially motivated by the requirements of the Climate Change Act discussed in section 3.3.1. The HAAFM (Figure 3.4) is aimed at providing a consistent approach for indentifying (Stage 2) and managing roads related activities that are projected to be affected by climate change (Stages 3 and 4) and to support decision makers in formulating adaptation options (Stage 5) (Highways Agency, 2009).

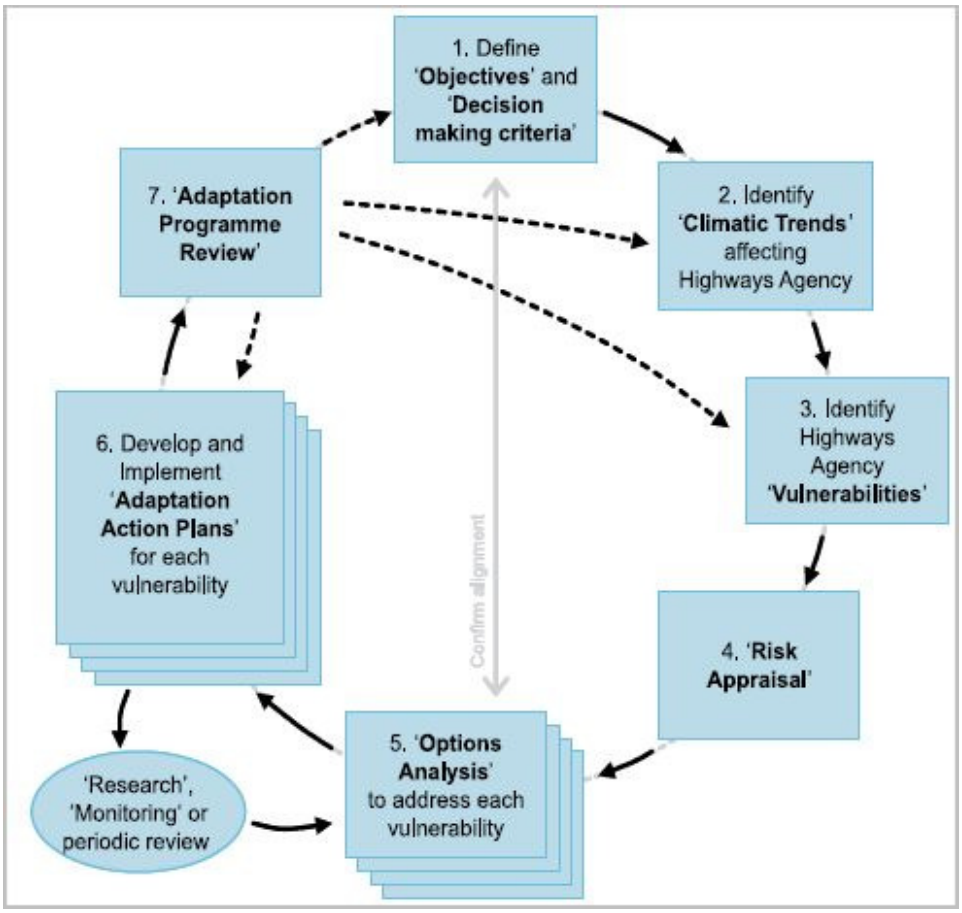

Figure 3.4: Highways Agency Adaptation Framework Model

The HAAFM makes use of UK climate projections and associated guidance on assessments of climate change vulnerability, risk, and adaptation options. According to the IPCC (2001), vulnerability is defined as the extent to which a system is susceptible to, or unable to cope with, adverse effects of climate change, including climate variability and extremes.

Stage 1 of the framework deals with defining the objectives and decision making criteria upon which the assessment is based. Stages 2 and 3 provide guidance to road managers in identifying the potential impact of climate change to the agency and the associated vulnerabilities. The vulnerabilities are ranked in Stage 4 based on scores associated to each of

the following primary criteria: uncertainty; rate of climate change; extent of disruption; and severity of disruption (Highways Agency, 2009).

The scoring associated to each of the above primary criteria is however derived using expert opinion augmented with subjective judgement. In Stages 5 and 6, the vulnerabilities are prioritised with the aim of obtaining time scales for action and to identify priority areas for adaptation actions (Highways Agency, 2009). Unlike the IPCC approach, the Highways Agency framework does not provide guidance on the tools and techniques available for climate impact and adaptation studies (Highways Agency, 2009; Willows and Connell, 2003).

3.5 Assessment of Impact of Climate Change on Roads

3.5.1 UK Studies

The UKCIP in association with Cambridgeshire County Council undertook a case study to estimate future climate-induced maintenance costs associated to summer road subsidence (Lorraine, 2005). The study used the UKCIP costing methodology detailed in Metroeconomica (2004). The approach comprised the following steps:

1. Identification and quantification of the climate change impact;
2. Identification and estimation of expenditure incurred to replace the asset damaged as a result of climate change; and
3. Calculation of the total costs of the impact.

(Lorraine, 2005)

The study assumed that desiccation and shrinkage of peat/clay soils which is common in the East of England would become more significant if hot dry periods such as that recorded in the summer of 2003 become more frequent. The costs of repairing the damage observed on the road network following the hot dry summer of 2003 was used as a basis for estimating predicted costs of climate change. The study concluded that summer road subsidence would result in an average annual climate change-induced maintenance costs of between £600,000 (for 2020s (2010 – 2039) low emission climate scenario) and £3,000,000 (for 2080s (2040 – 2069) high emissions climate scenario) compared to £46,000 incurred in 2003 to repair roads that were damaged as a consequence of the very hot dry summer (Lorraine, 2005). The study however did not account for the uncertainties associated with climate predictions as well as the future performance of the road network. Furthermore, a static socio-economic scenario was assumed to prevail throughout the analysis period. According to UKCIP (2000), future climate change is likely to take place in a world different from the current social and economic setting thus studies that assume a static climate are flawed.

Another study by the Scottish Executive (2005) identified the potential impacts of climate change on road users and road agencies on the trunk road network in Scotland. Their findings on the likely impacts of changes in temperature and precipitation on the management of the trunk road network is summarised in Table 3.3.

Table 3.3: Likely Impacts of Climate Variables on Scottish Trunk Road

Key Climate Variable(s)	Proposed measure of change of climate variable	Likely Impact
High Temperatures	Change in frequency and magnitude of extreme high temperatures, together with likely seasonal changes	Deformation of road surface due to high temperatures
High Intensity Storm	Change in frequency and magnitude of sub-daily intense rainfall	Road surface damage
High Intensity Storm	Change in frequency and magnitude of sub-daily intense rainfall	Surface water sheds slowly, risks to road users
Average Precipitation	Change in average amount of seasonal rainfall	Pavement deterioration in wet conditions

Source: Scottish Executive (2005).

The study was limited to investigating the vulnerabilities of the Scottish network to predicted change in climate. Selected recommendations included: a review of parameters for the design storm for surface water drainage; use of materials with appropriate stiffness to reduce the risks of pavement deformation at high temperatures; and review of the effects of high temperatures on pavement interventions (Scottish Executive, 2005).

Another study by the Transport Research Laboratory (TRL) investigated the potential implication of climate change on local roads in England (Willay et al., 2008). Excess water, soil moisture deficit and high temperatures were identified as the main climate parameters that will affect the performance of local asphalt roads in England. The findings of the study included a summary of potential impacts, risks and consequences associated with projected

changes in excess water, soil moisture deficit and high temperatures. Table 3.4 summarises the potential impacts on asphalt pavements associated with the three climate change variables.

Table 3.4: Summary of Climate-induced Pavement Deterioration and Consequences

Climate Change	Potential Impact on Asphalt Pavement
Excess water	• Binder stripping, particularly at asphalt layer interfaces; • Surface scouring; • Hydroplaning in water-filled ruts; • Accelerated polishing of surfacing; and • Weakening of sub base or subgrade materials in foundations.
Soil moisture deficit	• Subsidence; • Cracking.
High temperatures	• Increased rutting; • Fatting, resulting in reduced skid resistance; Binder softening, resulting in loss of surface integrity; • More rapid age hardening of binder, resulting in increased cracking; • Contribution to heat island effect.

Table 3.5 gives a summary of the potential risks and consequences associated with high temperatures. Details of risks and consequences for excess water and soil moisture deficit are given in (Willay et al., 2008).

Table 3.5: Summary of Climate-induced Pavement Deterioration and Consequences

Climate change	Pavement risks	Other risks	Consequences
• Increase in the average annual temperature; • increase in the frequency and temperature of high summer extremes; • increase in the frequency of extremely warm summer days; • Exposure of the pavement to ultra violet radiation	*Pavement structure* The risk to thick asphalt pavements is surface deformation and deterioration. Structural deformation is possible on pavements with thin asphalt. *Pavement condition* Cracked/damaged surfaces leave materials more exposed to high temperature. *Pavement design* Pavements that have evolved rather than being designed may not have the resistance to high temperature effects.	*Traffic flow* Roads with an excessive proportion of heavy goods vehicles or farm traffic.	• Rapid structural and surface deterioration; • Loss of skid resistance; • Potential benefits are a decrease in the incidences of frost and snow, reduced freeze–thaw damage and less damage as a result of frost heave; • The health and safety of the construction workers may need to be considered in relation to working in hotter summer conditions; and • Contributing to the increase in ambient temperature and the heat island effect.

Source: (Willay et al., 2008)

Arkell and Darch (2006) investigated the impact of climate change on London's transport network. They undertook a case study to assess infrastructure damage caused by flooding and concluded that significant improvement in the existing drainage infrastructure will be necessary to cope with forecasted increase in frequency of high intensity rainfall, in addition, they claimed that flood related delays during peak periods are estimated to costs £100,000 per hour. A case study to investigate the impact of hot summer of 2003 found no evidence of problems associated with London's road network (Arkell and Darch, 2006). The study did not however quantify road network maintenance needs associated with predicted change in climate and therefore possible road maintenance adaptation strategies were not investigated. They however identified the need for assessment of risks due to climate change on new infrastructure and called for the consideration of the implication of climate change throughout the life cycle of infrastructures (Arkell and Darch, 2006).

More recently the UK Department for Transport (DfT) published a climate change adaptation plan with the aim of embedding the consideration of climate change risks in the department's decision making process. The plan recognises the need to reduce vulnerability and to improve the resilience of transport infrastructure to the effects of climate change (DfT, 2010). It sets out the potential implication of future changes in climate on transport. A summary of these implications relevant to the road transport is summarised in Table 3.6 (DfT, 2010).

Table 3.6: Key Road Transport Climate Risks for the DfT

Climate Change	**Potential implications for transport**
Increased temperature	Deformation of road; Hardcore underpinning cracking; Passenger discomfort; Risk to passenger and workers' safety.
Increased rainfall	Flood damage to roads e.g. foundations, surfaces; Standing water reducing safety; Reduced visibility; Increased demand for car use; Risks to passenger and workers' safety.
Rising sea levels, increased coastal erosion and flooding	Permanent asset loss at coastal sites; Periodic flooding of coastal roads; Risk to workers' safety.
Increase in extreme weather -storms and storm surges	Operational constraints at exposed locations e.g. bridges for high sided vehicles, ports, airports; Flooding at coast inundating coastal roads.
Combined extremes in weather	Asset failure due to long, hot, dry periods followed by intense rain causing flash floods

Adapted from DfT (2010)

The DfT adaptation report (DfT, 2010) identified a number of challenges in adapting to the changing climate including addressing the problem of uncertainties, adapting existing policies and projects, determining what to adapt and when, human responses, design life of infrastructure, and opportunities and benefits. A description of these challenges is given in Table 3.7.

Table 3.7: Challenges in Climate Change Adaptation

Challenge	Description
Uncertainties	• Uncertainties are inherent in climate change predictions as well as future GHG emissions. There are also uncertainties in the way climate will affect the activities of the DfT, the performance of roads and the behaviour of road users.
Adapting existing polices and projects	• Especially challenging if the options for managing risk are geographically constrained or require significant additional investment. Some risks can be addressed through routine renewal and updated procedures when repairs or replacements are made.
What to adapt and when	• There is a need to understand what critical infrastructure is and what needs to be adapted first. • There is a need to prioritise action and investment to ensure that the degree of resilience provided is proportionate to the degree of threat.
Design life of infrastructure	• Road infrastructures are typically built with long life spans. Construction costs are usually significant with renewal and maintenance costs generally very high. • In addition some roads are managed by the private sector therefore investment is generally led by business cases for profit. To that end it is difficult for the private sector to consider the idea of adaptation because immediate benefits are not apparent. • Most transport infrastructure is built using a long design life based on a historical understanding of weather stresses. Retrofitting existing infrastructure before the end of its design life may prove costly.
Identification of opportunities and benefits	• It is easy to identify the negative impacts of climate change, the risks and uncertainties, threats and vulnerabilities. However, there could also be opportunities and benefits from the predicted change in climate.

Source: DfT (2010)

The DfT Climate Change Adaptation plan proposes generic options for adapting to the potential impacts of climate change on the transport system. These are summarised in Table

3.8. In addition to these generic adaptation options, the following research gaps are acknowledged in the adaptation plan:

- Identification of vulnerabilities of different transport sectors;
- Determination of probable risks of climate change; and
- Investigation of adaptation options or approaches that would seek to reduce uncertainty in determining preferred adaptation option.

(DfT, 2010).

Table 3.8: Generic Adaptation Options

Adaptation Option	Typical Actions
Business as usual	• Minimum action aimed at maintaining a safe and serviceable network. • Could include contingency plans, monitoring changes and routine asset repairs and/or replacements.
Future proof designs	• Updating design requirements including technical standards and specifications to provide additional capacity and/or functionality in the event of gradual climatic change.
Retro-fit solutions	• Modifications to existing assets and/or activities outside the normal renewal cycle. • Determination of where and when the road assets need to be maintained or replaced.
Develop contingency plans	• Pre-planned responses for when/if climate change risks are realised so immediate effects can be managed.
Update operating procedures	• Update existing operating procedures to take account of the impacts of climate change such as procedures for working in high temperatures.
Monitor	• Monitor the rate of climate change and/or subsequent effects on specific transport mode assets or operations to help determine the most appropriate adaptation measures and identify indicators of change and thresholds for adaptation.

Source: DfT (2010)

3.5.2 Other Studies

Perhaps one of the most detailed assessments of the impacts of climate change on road maintenance was the study undertaken in Australia by Austroads (2004) using the World Banks Highway Development and Management system (HDM-4). HDM-4 was used to assess the long-term impacts of climate change on the Australian National Highway network. The study compared pavement maintenance and rehabilitation costs for the year 2100 for a high emission scenario with current levels (Austroads, 2004).

The researchers suggested that significant variations in the change in pavement maintenance and rehabilitation costs across states in Australia is likely to occur as a consequence of climate variation and population and transport demand levels. Furthermore, a relatively small decrease of 0% to 3% in the required pavement maintenance and rehabilitation budget was estimated based on climate change factors only. It is claimed that this reduction in maintenance costs reflects the warmer and drier Australian climate which results in a reduced rate of pavement deterioration (Austroads, 2004). The findings of this study are however subject to three major limitations.

Firstly, the calibration of the HDM-4 models were not completed (Austroads, 2004). This implies a low confidence in the accuracy of the outputs from the model. Secondly, the effects of extreme weather events which are predicted to increase in Australia (IPCC, 2001) were not taken into account. Such extreme events are likely to cause severe damage to the road pavements and result in significant maintenance and rehabilitation costs (Willay et al, 2008). Thirdly, much uncertainty exists in the assessment of the impacts of climate change including uncertainties in the levels of future GHG emissions, uncertainties in future climate projections

and uncertainties in the inputs to impact models. These uncertainties were not accounted for in the study (Austroads, 2004). Furthermore, the HDM-4 outputs are deterministic which, implies that uncertainties inherent in the inputs to the model are not propagated to the outputs (Morosuik, 2004).

Another study by Mills et al. (2007) investigated the implication of climate change for pavement infrastructure in Southern Canada. Two sets of case studies were undertaken. The first utilised climate indicators (Table 3.9) important in three pavement deterioration process, thermal cracking, frost heave and thaw weakening and rutting. Time series analysis was undertaken to investigate how these climate indicators would change relative to a 1961 to 1990 baseline data on 17 sites in Canada.

Table 3.9: Climate and Deterioration Indicators

Climate Indicators	Deterioration Indicators	Application
Extreme minimum daily temperature	Thermal cracking	Choice of performance grade bituminous binders
7-day average maximum daily temperature	Rutting	Choice on performance grade bituminous binders
Freezing and thawing indices	Frost heave and thaw weakening	Establishing winter weight premiums and spring load restrictions

Source (Mills et al., 2007)

The second set of case studies used the Mechanistic Empirical Pavement Design Guide (MEPDG) software to assess the impact of climate change on long-term pavement performance. The findings suggested that climate change will increase the severity of rutting

and cracking (alligator and longitudinal), however traverse cracking is expected to become less of a problem (Mills et al., 2007).

The study by Mills et al. (2007) was however limited to conditions prevalent in Canada and findings may not be directly translated to conditions in other countries. In addition the outputs of the study were deterministic which meant that uncertainties inherent in the inputs to the models were not sufficiently explored to derive outputs that are robust.

The National Research Council (2008) investigated the potential impacts of climate change on transportation in the United States (U.S). The findings and recommendations of the study are summarised in Table 3.10.

Table 3.10: Summary of Findings and Recommendations on Impact of Climate Change on U.S. Transportation

Findings	Recommendations
Authorities in the public and private sector responsible for road and other infrastructure management continually make short and long-term investment decisions which have implications on the resilience of transportation systems to climate change.	Public and private infrastructure providers should include climate change in their long-term capital improvement plans, maintenance practices, operations and emergency plans.
The cost of redesigning and retrofitting roads to adapt to the potential impacts of climate change is significant.	Engineers should use probabilistic investment analyses and design approaches that incorporate techniques for trading off the cost of making the infrastructure more robust against the economic costs of failure.
Lack of sufficiently detailed information about expected climate changes and their timing.	Improved communication between road engineers and climate scientist with a view of deriving climate projections relevant to the purpose of road management.
There is a need for decision support tools for use for by decision makers in the road sector.	Ongoing and planned research activities that provide climate data and decision support tools should include the needs of transportation decision makers.
Increased use of technology would help infrastructure providers to monitor climate change events and receive advance warning of potential failures due to certain climate variables.	Research in the development of such monitoring technologies should be encouraged
Review, developing, and updating design standards for road infrastructure to address the impacts of climate change.	Research into improved design standards should undertaken as improved understanding on future climate becomes apparent. In the short-term infrastructure considered to be at high risk to climate change should be built or maintained to a higher standard to improve resilience to the impacts of climate change.

Source (National Research Council, 2008)

3.6 Gaps in Current Knowledge in Climate Change Impact and Adaptation Assessment of Roads

Following the review of literature on the need for further research in particular areas was apparent. The review showed that significant work has been done in:

- Formulating frameworks to support the assessment of climate change impacts and adaptation options;
- Identifying the projected climate change and their potential impacts on roads;
- Undertaking qualitative risk assessments; and
- Formulating generic options for adaptation.

There was however less focus on in the following areas:

- Development of quantitative methodologies for assessing impacts;
- Quantifying and propagating uncertainties; and
- Evaluating adaptation strategies or options.

The following sub-sections sets out the research gaps that were identified.

3.6.1 Data Collection

As noted in section 2.3.2, the quality of pavement cracking and ride quality data collected annually on UK Highways Agency trunk roads using TRACS surveys suggests that such data are not appropriate for use in the development of deterioration models. Consequently, there is a need for collection of more accurate and reliable pavement performance data to facilitate the development of cracking and ride quality prediction models which may be used in the

assessment of the impact of climate change on road pavement maintenance. This could for example be achieved by implementing a long term pavement performance monitoring programme across the UK road network similar to the LTPP programme in North America (US Department of Transportation, 2011).

3.6.2 Development of Pavement Deterioration Models for Climate Impact Assessment

The HDM-4 model was used by Austroads (2004) for climate impact studies. The models did not however account for the effects of extreme climate events and is deterministic (Morosuik et al., 2004), thus, not appropriate for uncertainty analysis. Furthermore existing deterioration models used in the United Kingdom discussed in section 2.5 were found not to be suitable for use in climate impact assessment studies. There is a need to develop improved road pavement deterioration prediction models capable of using future probabilistic climate predictions instead of past observations.

3.6.3 Quantification and Propagation of Uncertainties

Most studies including Austroads (2004), Lorraine (2005) and Mills et al. (2007) acknowledged the existence of uncertainties but analyses performed used deterministic tools or techniques. There is a need for probabilistic approaches and tools for use in managing uncertainties that are inherent in climate impact and adaptation assessments. Furthermore, methodologies for quantification of uncertainties inherent in projected climate data as well as in other inputs to road decision support tools and propagation of these uncertainties to the outputs of analyses with respect to road pavement maintenance were not available in literature

reviewed. Such a methodology would ensure that uncertainties are incorporated in the decision making process.

3.6.4 Increased use of Technology

A review by the National Research Council (2008) indentified the need for increased use of technology which would help infrastructure providers to monitor climate change events and receive advance warning of potential failures. Such technologies could be used to investigate thresholds for adaptation to the impacts of climate change.

3.6.5 Quantification of Indirect Impacts of Climate Change

Extreme climate events such as intense precipitation could have significant indirect impacts. Such indirect impacts include road accidents and delay to road users. It is therefore necessary to develop tools and techniques which can be used to quantify such impacts. Outputs from such tools could be used to inform decisions on climate change adaptation strategies.

3.7 Summary

This chapter was aimed at reviewing current state of knowledge in climate impact and adaptation studies. In the United Kingdom, summers are predicted to get hotter and drier while winters are expected to get wetter. The frequencies of extreme events are also expected to increase (Murphy et al., 2009).

Various approaches are used to investigate the impact of climate change on infrastructure. These approaches generally involve the formulation of future scenarios of world development. GHG emissions estimated to result from these future scenarios are then used in

climate models to derive predictions of future climate which is in turn used in impact models to assess impacts and to investigate adaptation options on roads and other infrastructures (Parry and Carter, 1998).

Studies on climate impact and adaptation for road infrastructure have generally been of a qualitative rather than quantitative nature. Potential impacts of projected climate change in the United Kingdom includes deformation of asphalt surfaces due to high temperatures, road surface damage due to high intensity rainfall and increased rate of pavement deterioration during wet conditions.

CHAPTER 4 METHODOLOGY

4.1 Overall Procedure

This Chapter presents the research methodology and modelling concepts. The methodology used is illustrated using the flow chart given as Figure 4.1. The methodology was structured into eight components: literature review, preliminary analysis, formulation of theoretical modelling concepts, data collection and processing, estimations of coefficients of the proposed model, development of a climate impact and adaptation assessment model, development of a framework for quantification and propagation of uncertainties, and a case study aimed at assessing the impact of climate change on road maintenance. Figure 4.1 also links the research objectives of this research with the research process. Subsequent sections in this Chapter provide a discussion of the approach adopted in undertaking each of the eight components shown Figure 4.1.

4.2 Literature Review

The review of the state of knowledge on road maintenance management and climate change issues discussed in Chapters 2 and 3 respectively identified gaps in knowledge in the assessment of the impact of climate change on road maintenance. These gaps in knowledge are summarised in sections 2.6 and 3.6. This study was however limited to the following gaps due to time and resource constraints: the need for an improved asphalt rut depth prediction model; the quantification of uncertainties in model coefficients; and development of a framework for quantification and propagation of uncertainties.

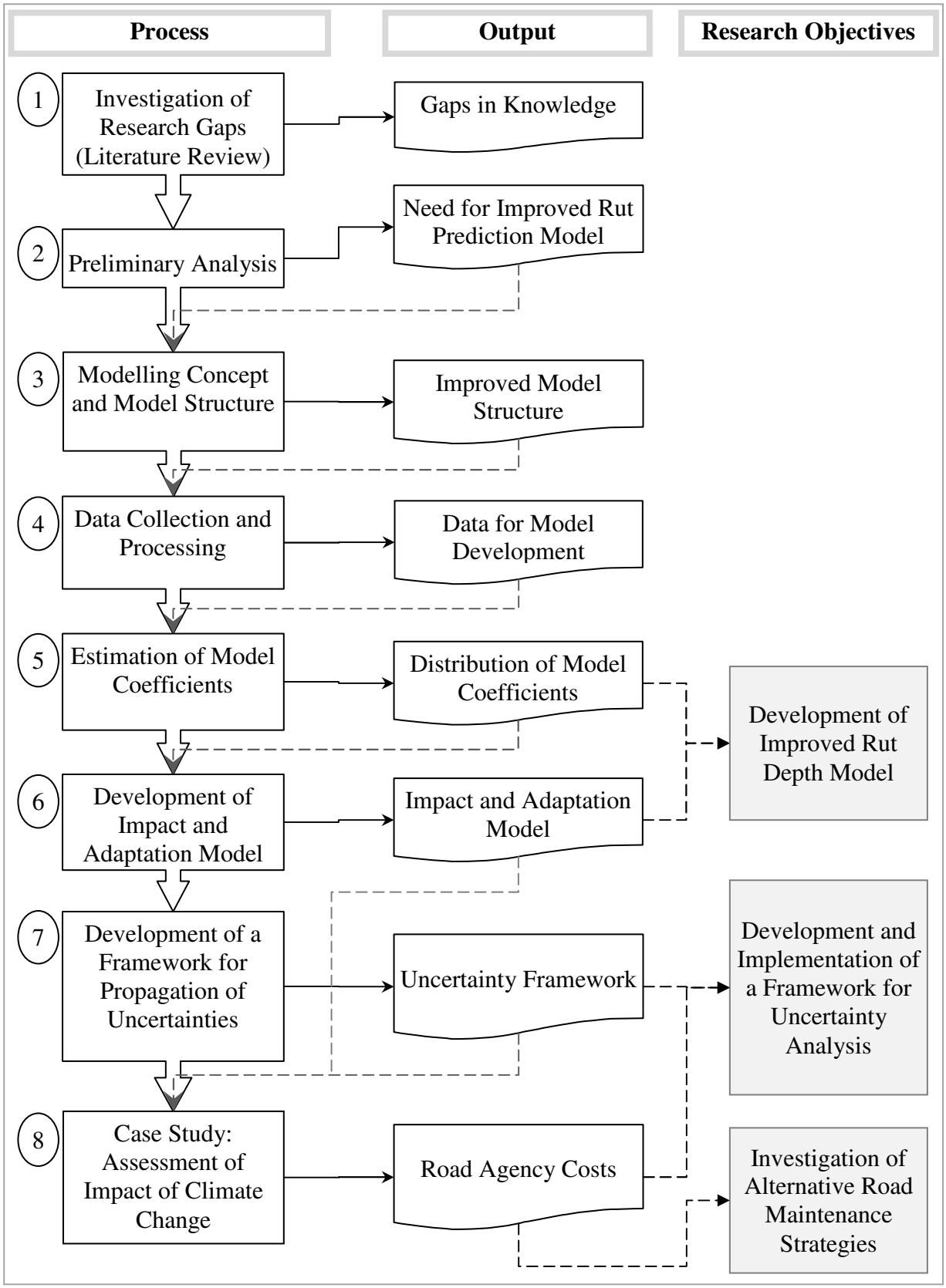

Figure 4.1: Outline of the Research Methodology

4.2.1 Need for Improved Asphalt Rut Depth Prediction Model

Current models for prediction of asphalt surface rut depth which have been implemented in decision support systems such as the Highway Development and Management System (HDM-4) assume a static climate based on averages of past climate records. The outputs of these models often form the basis for decisions on road management policies (Kerali et al., 2000). There is a need for asphalt rut depth prediction models with improved structures that explicitly account for the impacts associated with future climate predictions.

4.2.2 Estimation of Uncertainties in Model Coefficients

Previous studies undertaken to assess the impact of climate change on roads have used deterministic models such as those implemented in HDM-4 and given in Equation 2.1. The coefficients of such models are usually estimated as single values without consideration of inherent uncertainties. In this study, the uncertainties inherent in the coefficients of deterministic model structures were estimated using Bayesian regression resulting in probability distributions of model coefficients.

To that end, the resultant model can then be applied within a Monte-Carlo simulation framework to derive probabilistic outputs that encapsulate uncertainties in the model coefficients as well as those inherent in the inputs to the model. Such probabilistic outputs are important for characterising the risks and vulnerability of roads for a predefined road maintenance strategy and a given range of potential future climate and socio-economic scenarios.

4.2.3 Framework for Analysis of Uncertainties

Most studies reviewed including Austroads (2004), Lorraine (2005) and Mills et al. (2007) acknowledged the existence of uncertainties in climate change impact and adaptation assessments. These studies however, used deterministic tools or techniques in which the inputs to and coefficients of the impact models were represented using single values to estimate deterministic outputs. This approach fails to capture uncertainties and variability inherent in climate change data, other model inputs and model coefficients.

To facilitate good decisions on the choice road maintenance strategies that could improve the resilience of the road network in light of the variability and uncertainties associated with future climate predictions, it is important to understand the uncertainties in the impact model outputs and the divergence between these outputs for predefined alternative maintenance strategies (Lloyd and Ries, 2007). Furthermore, variability and uncertainties also exist in other inputs to as well as in coefficients of the impact model. To that end, need was identified for a framework for quantification and propagation of uncertainties in climate impact and adaptation assessment for a given road maintenance strategy.

The following sections discuss the approach and modelling concepts used to address the selected gaps in knowledge.

4.3 Preliminary Analysis

A preliminary analysis was undertaken to investigate if evidence of impacts of recently observed climate were discernible in road pavement performance data collected annually. The analysis was done on asphalt rutting data collected from the Highways Agency Area 6 road network located in the East of England. Figure 4.2 shows the study area and roads.

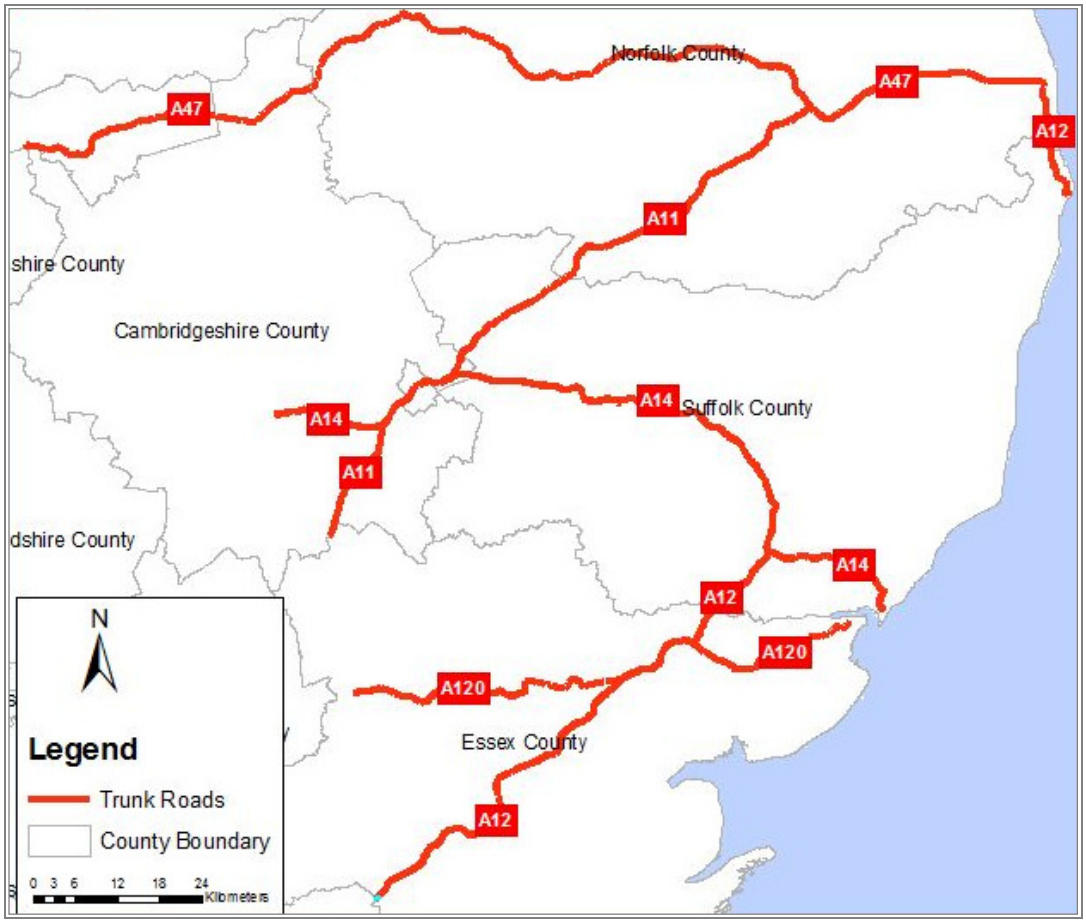

Figure 4.2: A map of the Study Area showing Trunk Roads in the East of England

The approach to the preliminary analysis was structured in three parts as follows: graphical comparison of annual incremental rut depths with climate variables; statistical time series comparison of annual incremental rut depth observed every year from 2003 to 2005; and investigation of frequency of observed and predicted climate scenario relevant to asphalt

surface rut depth progression. The approach to the analysis for each of the three parts is discussed in subsequent sections.

4.3.1 Graphical Comparison of Observed Climate and Rut Depth Data

Based on discussions in section 2.4 higher rates of asphalt surface rutting should be observed in years with very hot summers such as that recorded in 2003. This claim was investigated using scatter plots of annual incremental rut depth against temperature, precipitation and snow related climate variables defined in Table 4.1. Annual incremental rut depth on each sub-section of road was calculated as the change in average absolute rut depth on both wheel paths measured annually before and after the summer months of June, July and August of each year from 2002 to 2006. The approached used to calculate annual incremental rut depth is detailed in section 5.3.2.5.

Gridded climate variables defined in Table 4.1 at 5km x 5km spatial resolution covering the study area were associated to each road sub-section. Annual incremental rut depth and corresponding climate variables at each road sub-section were then plotted in a scatter diagram as illustrated in Figure 4.3. The figure shows a plot of annual incremental rut depth with mean daily maximum temperature during the summer. Higher rates of rutting are apparent in 2003 which had a very hot summer. A similar trend to Figure 4.3 was observed when sunshine duration was plotted instead of mean daily maximum temperature during the summer but not when precipitation and snow related climate variables were used. Plots of annual incremental rut depth against each of the climate variables given in Table 4.1 together with discussions of findings are provided in section 5.4.1.

Table 4.1: Definition of Observed Climate Variables

Category	Climate variable	Definition
Temperature Related Variables	Mean daily maximum temperature during the summer	Average of the daily highest air temperatures (°C)
	Sunshine duration	Duration of bright sunshine during the month (hours per day)
Precipitation Related Variables	Total precipitation	Total rainfall amount (mm) during the month
	Days of rain ≥10 mm	Number of days with greater than 10mm of rainfall
Snow Related Variables	Days of sleet or snow falling	Number of days with sleet or snow falling
	Days of snow lying	Number of days with greater than 50% of the ground covered by snow at 0900 hours

Source: (Met Office, 2009)

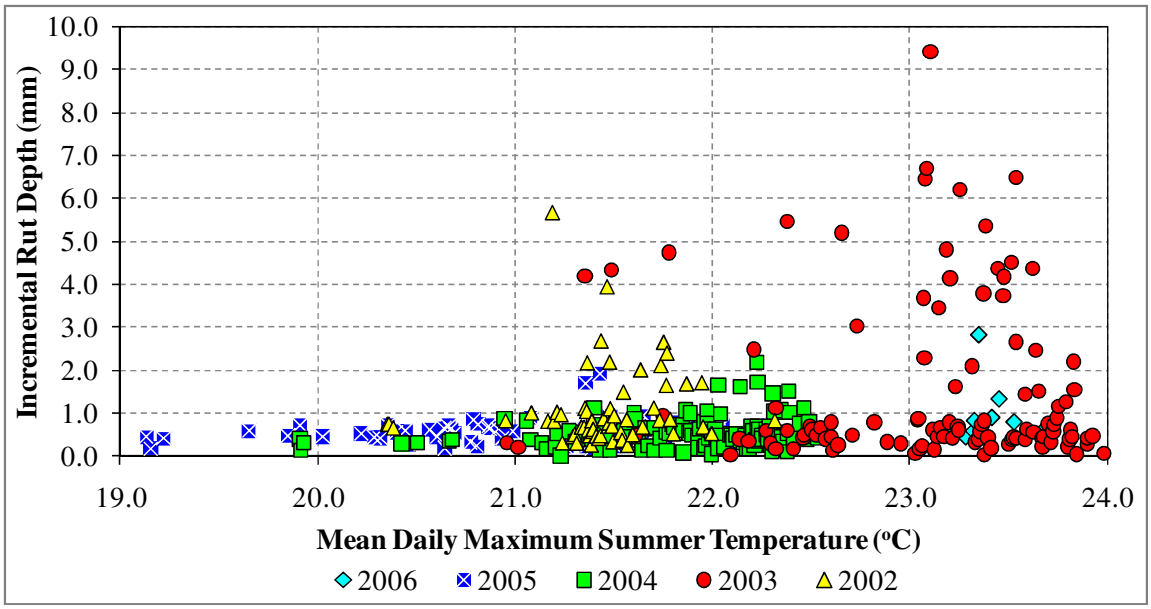

Figure 4.3: Recorded Annual Rates of Rutting and Mean Daily Maximum Summer Temperature.

4.3.2 Statistical Comparison of Annual Observed Rut Depth

The purpose of the statistical analysis was to investigate the following null hypothesis (Ho) and alternative hypothesis (Ha):

- Ho: for road sub-sections for which annual incremental rut depth data for at least three consecutive years including 2003 were available, there are no significant differences in the mean annual incremental rut depth due to the hot dry summer of 2003.
- Ha: for road sub-sections for which annual incremental rut depth data for at least three consecutive years including 2003 were available, there are significant differences in the mean annual incremental rut depth due to the hot dry summer of 2003.

The hypothesis tests used was the Repeated Measures one-way Analysis of Variance (RM-ANOVA) since for each road sub-section used in the analysis, annual incremental rut depth observations are repeated for a minimum of three consecutive years. Details of the concepts, approach and results of the analysis are given in section 5.4.2.

4.3.3 Frequency of Observed and Predicted Climate Scenario

An analysis of frequency of observed and predicted 2003-type hot dry summers was performed to determine if the increase in frequencies of such an event is likely to be significant given future climate projections. The frequency of the 2003-type summer within the UKCIP baseline period from 1961 to 1990 was determined by plotting anomalies of average monthly precipitation during the summer months with corresponding anomalies of mean daily maximum temperature during the summer months as illustrated in Figure 4.4.

Anomalies were calculated as the difference between values of climate variables observed in a given year and the corresponding values of the climate variable averaged over the UKCIP climate baseline period from 1961 to 1990. Temperature anomalies are expressed in degrees

Celsius while rainfall anomalies are expressed as a percentage of the average precipitation recorded over the baseline period.

The observed frequency of the 2003-type summer during the baseline period (1961 -1990) was compared with UKCP09 projections for the study area. For example, Figure 4.4 shows that over the 30 year baseline period (1961 -1990) observations in one year had below average rainfall with temperature anomalies similar to or greater than that recorded in 2003 hence the frequency of the 2003-type summer over the baseline period was 1 in 30 or 3%. Plots and results for future climate predictions including discussion on findings of the frequency of 2003-type summers are detailed in section 5.4.3.2.

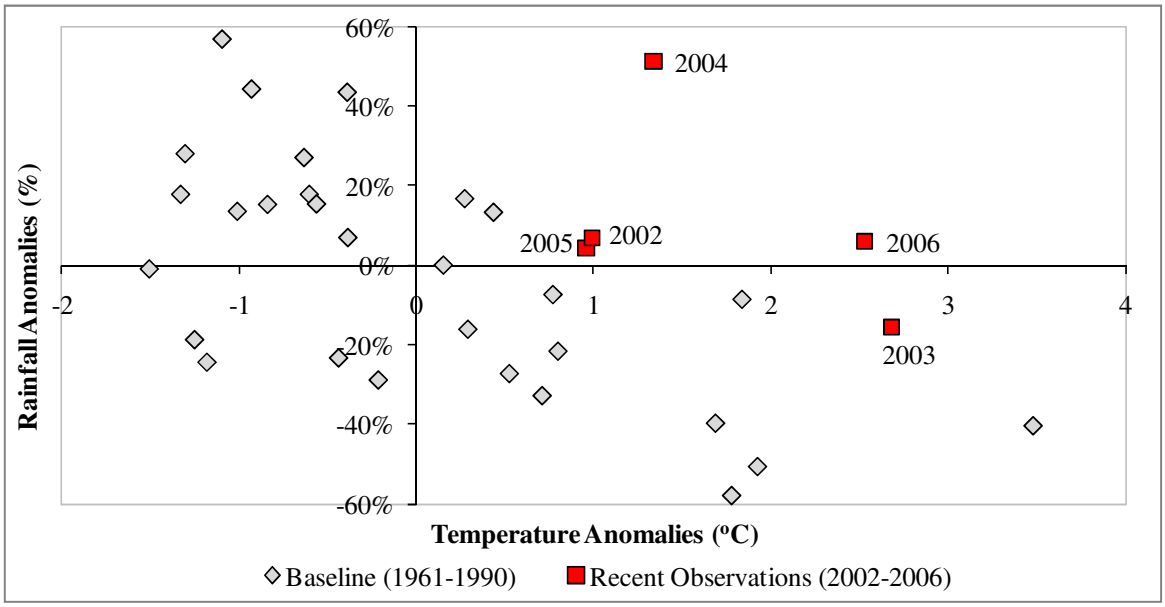

Figure 4.4: Comparison of Rainfall and Temperature Anomalies of Recent Observations (2002 to 2006) over the Baseline Period (1961 – 1990).Modelling Concept

4.4 Modelling Concept

The findings of the preliminary analysis detailed in section 5.4 confirmed the need for the development of a model for rut depth prediction that took into account the contribution of hot

dry summers such as that observed in 2003. This section sets out the concepts upon which the rut depth model structure was formulated.

4.4.1 Background

Findings of accelerated testing of the deformation behaviour of asphalt pavements undertaken in South Africa (Freeme, 1983) and the structure of the current HDM-4 rutting models formed the basis for the modelling concept. Figure 4.5 adopted from Morosuik et al (2004) after Freeme (1983) illustrates the deformation trend of asphalt surfacing materials under various scenarios. For example increase in temperature of asphalt pavements is known to result in higher rates of asphalt deformation. This observation is consistent with the results of the preliminary analysis shown in Figure 4.3. The rutting model implemented in HDM-4 does not however explicitly capture this effect.

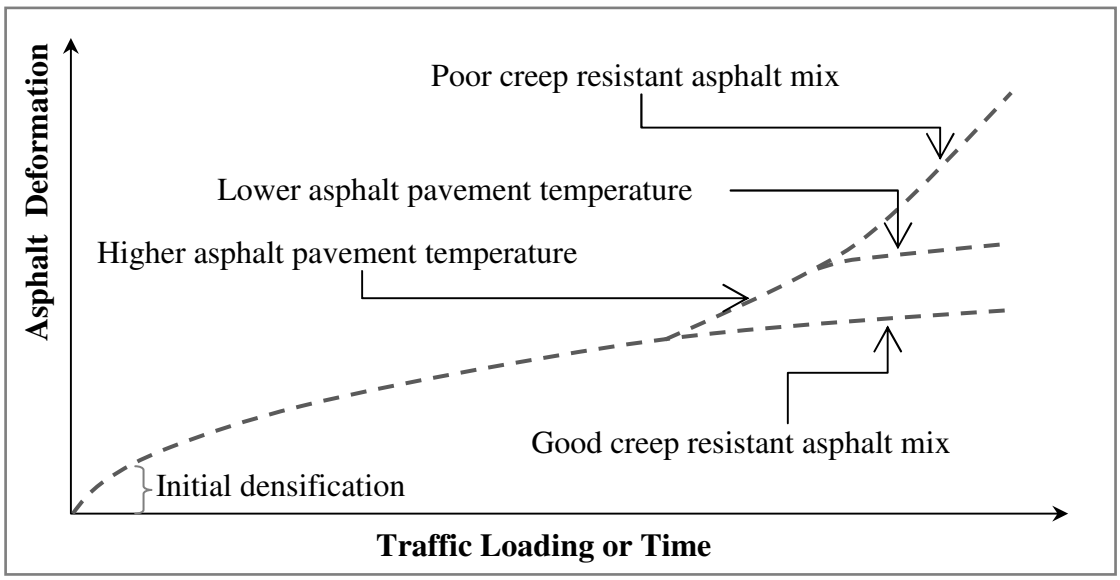

Figure 4.5: Relative Behaviour of Asphalt Material (adopted from Morosuik et al., 2004 after Freeme, 1983)

4.4.2 Current Model Structure

The current HDM-4 rutting model structure was used as a basis for developing an improved model. HDM-4 rutting model has four components: initial densification, wear from studded tyres, structural deformation, and plastic deformation. Each component is modelled separately. The models are detailed in Morosuik et al. (2004).

Initial densification is related to the level of compaction of the pavement layers during construction and traffic loading. The current HDM-4 initial densification model is used to account for the rapid initial increase in rutting on newly constructed pavements once it is opened to traffic.

In this study, initial densification is partially accounted for in the improved rutting model by new models for two asphalt mix properties. These material properties are Voids in Mix (VIM) and Softening Point (SP) of binder. The models for the material properties are discussed in section 4.4.3.2.

The wear from studded tyres component of the HDM-4 rut depth model is not applicable to the study area since it accounts for pavement rutting caused by vehicles using studded tyres and snow chains.

The HDM-4 model for structural deformation component of rutting is dependent on pavement strength, traffic loading and precipitation. The model is used to simulate deformation in the asphalt as well as foundation layers of road pavements. Studies by Nunn et al. (1997) and Weston et al. (2001) discussed in section 2.4 concluded that rutting on UK trunk roads is

restricted to the asphalt layer on roads with a minimum asphalt thickness of 180mm. This finding suggests that the problem of pavement deformation on UK asphalt trunk roads is restricted to surface deformation rather than structural deformation. Surface deformation is restricted to the asphalt surfacing layers of the pavement while structural deformation affects both the asphalt and foundation layers of the pavement. The current surface deformation model structure implemented in HDM-4 is given in Equation 4.1.

$$\Delta RUT_{imt} = \rho_0 \times CDS_m^{\rho_1} \times YE4_{it} \times sh_{it}^{\rho_2} \times HS_{imt}^{\rho_3} \quad (4.1)$$

where: ΔRUT_{imt}= incremental increase in plastic deformation within the asphalt layers of the pavement, in millimetres for road section i during year t; CDS_m is the Construction Defect indicator for asphalt surfacing type m ranging in value from 0.5 for a brittle asphalt mix to 1.5 for a soft asphalt mix; $YE4_{it}$= annual number of equivalent standard axles, in millions/lane on road section i during year t; sh_{it}= average speed of heavy vehicles on road section i, in kilometres per hour (km/h) during year t; HS_{imt}= thickness of asphalt layer on section i for asphalt surfacing m during year t, in millimetres; and ρ_0 to ρ_3 are model coefficients. A detailed description of the model is given in Morosuik et al. (2004).

According to TRL Road Note 31 (TRL, 1993), asphalt road sections prone to surface rutting are characterised by a combination of two or more of the following factors: frequent heavy axle loads, high maximum temperature, slow moving heavy traffic, channelled traffic and material with insufficient resistance to rutting. The existing surface rutting model structure given in Equation 4.1 does not account for the impacts of hot dry summers discussed in section 4.3. In addition other variables likely to contribute to surfacing rutting such as road

gradient, properties of asphalt mixes (TRL, 1993) are either omitted or not explicitly defined. Improvements proposed to the structure of the current model are discussed in the next section.

4.4.3 Improvements to Current Model Structure

This section discusses improvements that were made to current HDM-4 asphalt surfacing model, to ensure that they are appropriate for use for climate impact assessment studies.

4.4.3.1 Road Geometry

It is claimed that road sections with high gradient such as climbing lanes are prone to rutting because of increased loading time by slow moving heavy vehicles (TRL, 1993). To that end, a road geometric variable G which represents the gradient of a road section i during year t was introduced as shown in Equations 4.5, 4.6 and 4.7.

4.4.3.2 Asphalt Material Properties

As noted in section 4.4.2, the current HDM-4 surface rutting model structure makes use of a deterministic indicator (CDS) to model susceptibility of asphalt mixes to rutting. This approach however fails to capture the variations in asphalt material properties which may result as a consequence of aging and compaction due to traffic of the in-situ asphalt material.

NDLI (1995) evaluated several asphalt mix properties based on: ability to quantify changes in performance, obtainable without specialised equipment and availability in a typical application. Asphalt binder viscosity and voids in mix (VIM) were identified as the most appropriate for inclusion in the surface rutting model.

Binder viscosity has a strong influence on the stability of an asphalt mix at high road temperatures. Since it is not convenient to measure viscosity directly, the ring and ball Softening Point (SP) was instead adopted. SP is defined as the temperature at which bitumen attains a certain level of consistency (Morosuik et al., 2004). Asphalt mix with high voids content are more permeable and results in an increase in softening point with time because of age hardening (Daines, 1992). To that end, a model for SP based on the age (AGE_{imt}) of asphalt layer of road section i with material type m in year t was proposed (Equation 4.2).

$$SP_{imt} = \alpha 1_m \times Ln(AGE_{imt} + 0.0001) + \alpha 2_m \quad (4.2)$$

where SP_{imt} is the reclaimed binder softening point in degrees Celsius (^oC) on road section i with surfacing material m in year t. AGE_{imt} is the age in years since laying of the asphalt surfacing on road section i with material type m during year t. Model coefficient $\alpha 1_m$ is interpreted as the rate of change in softening point with time for asphalt surfacing type m. α_m^2 is the softening point in degrees Celsius at the end of the first year since the asphalt surfacing m was laid. $\alpha 2_m$ may be alternatively viewed as the softening point of the binder immediately after the initial densification phase of rutting. The constant 0.0001was included in the model structure to avoid numerical overflow when modelling newly re-surfaced road sections with the explanatory variable AGE_{imt} set to zero. The estimation of model coefficients α_m^1 and α_m^2 is discussed in Chapter 6.

Percentage VIM is an important asphalt mix property for the stability and consequently resistance to rutting. VIM is known to decrease with time due to the compaction effect of traffic (Nicholls et al., 2007; NDLI, 1995). The rate of decrease in VIM is higher in earlier years of a newly laid asphalt surfacing. The proposed model structure for VIM is given in Equation 4.3.

$$VIM_{imt} = \eta 1_m \times Ln(AGE_{imt} + 0.0001) + \eta 2_m \quad (4.3)$$

where VIM_{imt} is the Voids in Mix in percentage for an asphalt pavement surfacing for road section i of asphalt material type m in year t. $\eta 1_m$ and $\eta 2_m$ are model coefficients for asphalt surfacing material type m. η_m^2 is the voids in mix in percentage one year after laying the asphalt surfacing material. The estimated values of the model coefficients are given in Chapter 6.

The effect of material properties was included in the new rutting model structure as a ratio of VIM and SP as shown in equation 4.5.

4.4.3.3 Hot Dry Summer

Following the discussions in sections 4.3 and 5.4.1 on the impacts of hot dry summers on surface rutting of asphalt pavements, a function f(TPmax) was proposed. A generalised form of the function is illustrated in Figure 4.6 and Equation 4.4.

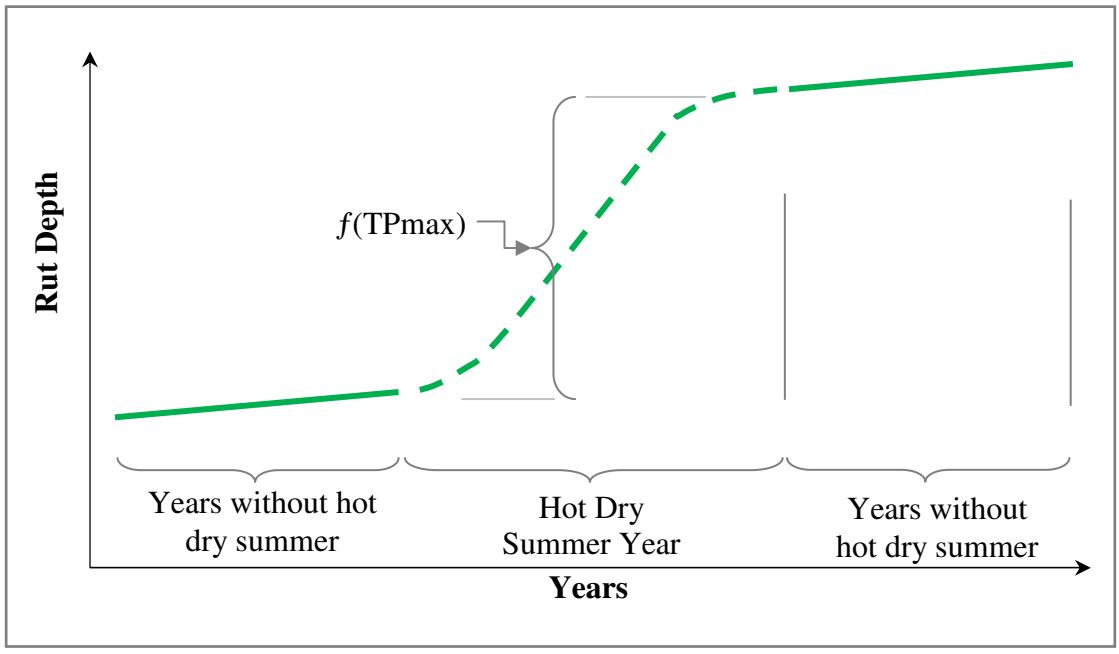

Figure 4.6: Illustration of a Function for Modelling Impacts of Hot Dry Summers

$$f(\text{TPmax}) = [\text{H}_0 + \beta_{6m} \times \text{TPmax}_{it} \times \text{H}_1] \quad (4.4)$$

where: TPmax is the maximum pavement temperature in degree Celsius (^{o}C) at 20mm below the asphalt surface during a hot dry summer year; β_{6m} is model coefficient for a given asphalt surfacing type m. The values of the model coefficients are estimated and discussed in Chapter 6. H_0 and H_1 are single digit binary constants. H_0 takes on a value of 0 during hot dry summer years otherwise a value of 1 is assumed. A value of 1 is assigned to H_1 during hot dry climate scenarios or 0 otherwise.

4.4.4 Improved Model Structure

The improved model structure was derived by modifying the existing model structure for surface rutting given in Equation 4.1 as discussed in section 4.4.3 to give Equation 4.5.

$$\Delta\text{RUT}_{imt} = \text{YE4}_{imt}^{\beta_{1m}} \times \text{sh}_{im}^{\beta_{2m}} \times \text{G}_{it}^{\beta_{3m}} \times \text{HS}_{imt}^{\beta_{4m}} \times \left(\frac{\text{VIM}_{imt}}{\text{SP}_{imt}}\right)^{\beta_{5m}} \times [\text{H}_0 + \beta_{6m} \times \text{TPmax}_{it} \times \text{H}_1] + \varepsilon_{imt} \quad (4.5)$$

where ΔRUT_{imt}= annual incremental increase in deformation within the asphalt layers of the pavement, in mm for road section i during time period t; YE4_{it}= annual number of equivalent standard axles, in millions/lane on road section i during year t; sh_{it}= average speed of heavy vehicles on section i, in km/h during year t; G_{it} gradient of road section i during year t; HS_{it}= thickness of asphalt layer on section i during year t, in mm; VIM_{imt} = Voids in Mix for road asphalt material type m on road section i during year t; SP_{imt}= Softening point of binder for road section i with material type m during year t.; TPmax_{imt} = maximum asphalt pavement temperature at 20mm below the surface in ^{o}C. TPmax is determined from mean daily

maximum temperature during summer months using Equations given in section 5.3.3.3; ε_{imt} = error term; β_{1m} to β_{6m} are model coefficients for each surface material type m.

4.4.5 Alternative Model Structures

The improved model structure given in Equation 4.5 was formulated from the current model structure implemented in HDM-4. In recognition of the uncertainties that may exist in deriving a suitable model using just a single model structure, two alternative model structures given as Equations 4.6 and 4.7 were proposed in addition to the improved model structure in Equation 4.5. The appropriateness of the three model structures is discussed in section 6.6.

In equation 4.6 the non-linear structure of the improved model structure is maintained but a simplified functional form for the hot dry summers f(TPmax) was adopted.

$$\Delta RUT_{imt} = YE4_{imt}^{\beta_{1m}} \times sh_{imt}^{\beta_{2m}} \times G_{it}^{\beta_{3m}} \times HS_{imt}^{\beta_{4m}} \times \left(\frac{VIM_{imt}}{SP_{imt}}\right)^{\beta_{5m}} \times TPmax_{it}^{\beta_{6m} \times H_1} + \varepsilon_{imt} \qquad (4.6)$$

The model structure given in Equation 4.7 is linear as opposed to the non-linear structures in Equations 4.5 and 4.6.

$$\Delta RUT_{imt} = \beta_{0m} + \beta_{1m} YE4_{imt} + \beta_{2m} sh_{im} + \beta_{3m} G_i + \beta_{4m} HS_{imt} + \beta_{5m} \left(\frac{VIM_{imt}}{SP_{imt}}\right) + \beta_{6m} TPmax_{it} \times H_1 + \varepsilon_{imt} \qquad (4.7)$$

In Equations 4.7, model coefficient β_{0m} for asphalt surfacing type m is a constant which represents the predicted annual incremental rut depth when all other model variables are equal to zero. All other model variables in Equations 4.6 and 4.7 and their coefficients have the same definition as in Equation 4.5.

4.5 Data Collection and Processing

4.5.1 Data Types and Sources

Data was collected for use in the estimation of model coefficients in Equations 4.5 to 4.7 and for validation of the models. The types of data, description, and sources are summarised in Table 4.2. The scope of the data collection was limited to the study area shown in Figure 4.2.

The processing of the data together with discussions on sample size, data quality and reliability are presented in Chapter 5.

Table 4.2: Data Types and Sources

Model Variables			Collected Data		
Model Notation	**Description**	**Units**	**Description**	**Units**	**Data Source**
ΔRUT	Annual Incremental Rut Depth	mm	Time series of absolute average left and right wheel track rutting values for trunk roads in the East of England (2001 to 2007)	mm	Highways Agency Pavement Management System (HAPMS)
TPmax	Maximum Asphalt Temperature at 20mm below the Pavement Surface	^{o}C	Time series of mean daily maximum temperature during summer for the UK (2001 to 2006) at 5x5km spatial resolution	^{o}C	UKCP09 gridded observed dataset
YE4	Number of Equivalent Standard Axles	millions/ lane	Equivalent Standard Axle Load Factor for Commercial/Heavy Vehicles	-	Highways Agency Design Manual for Roads and Bridges (DMRB HD 24/06, 2006)
			Average Annual Daily Traffic (commercial/heavy vehicles)	AADT	Highways Agency Pavement Management System (HAPMS)
sh	Average Speed of heavy vehicles	km/h	Average heavy vehicle speed	km/h	Highway Agency Traffic Information System Database (HATRIS)
HS	Total Thickness of Asphalt Surfacing	mm	Thickness of asphalt layers of in-service pavement	mm	Highways Agency Pavement Management System (HAPMS)
SP	Binder Softening Point	^{o}C	Binder softening point for asphalt surfacing	^{o}C	Nicholls et al. (2007), (Durability of TSCS); Harun and Morosuik (1995); UK Design Manual for Roads and Bridges (DMRB)
VIM	Voids in Mix	%	Voids in Mix (Air Voids) for asphalt mixes	%	

4.5.2 Hierarchical Data Structure

The analysed data was hierarchically structured into three levels as illustrated in Figure 4.7. Data collected during year t from each road pavement section i was categorised into three asphalt surfacing groups of Dense Bitumen Macadam (DBM), Hot Rolled Asphalt (HRA) and Thin Surface Course System (TSCS). Model coefficients were estimated at level 2 of the hierarchical structure for each surface group.

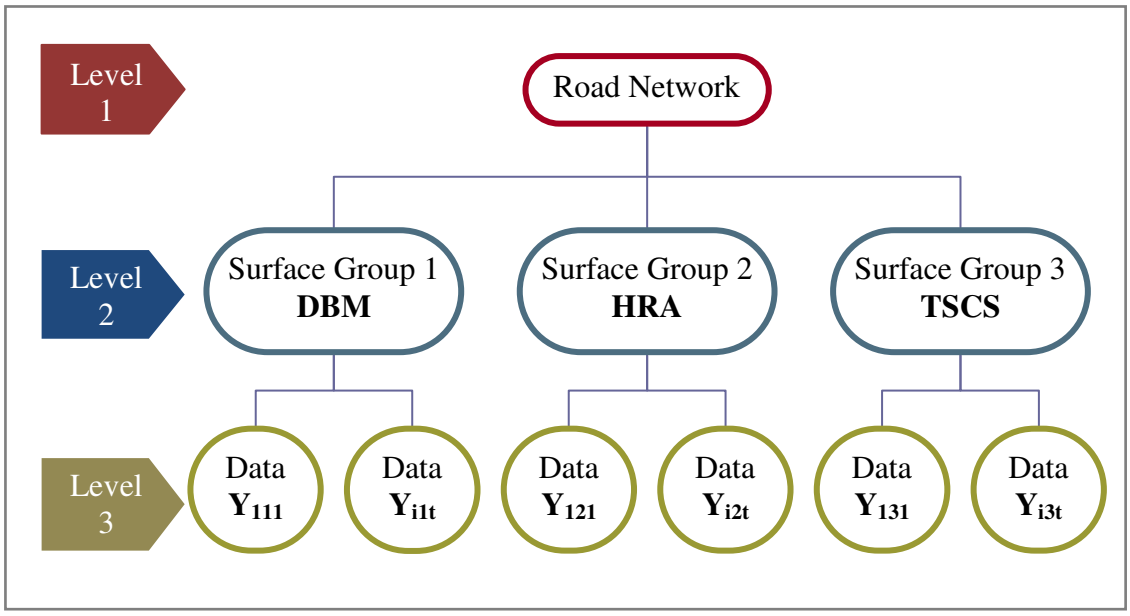

Figure 4.7: Illustration of Hierarchical Data Structure

where: Y_{imt} denotes data observed in road sub-section i with material surfacing type m during year t; DBM = Dense Bitumen Macadam; HRA = Hot Rolled Asphalt; TSCS = Thin Surface Course System.

The next section sets out a Bayesian approach to estimation of the model coefficients.

4.6 Estimation of Model Coefficient

4.6.1 Introduction

The model coefficients in Equations 4.5 to 4.7 were estimated using the Bayesian regression approach in combination with the Markov Chain Monte Carlo (MCMC) technique. The reasons for adopting this approach are as follows:

(i) Bayesian approach associates a probability distribution to model coefficients. This distributions initially known as prior distribution is used to quantify uncertainties in the model coefficients before more accurate data becomes available. It is also used to capture expert knowledge of the distribution of the model coefficients (DelSole, 2007).

(ii) The approach provides a framework for updating model parameters as new data becomes available. Given the prior probability $P[\phi]$ it is possible to determine the distribution of model coefficients when more accurate data is available using Bayes' theorem (Equation 4.8) in combination with MCMC.

(iii) It is relatively easy to model complex data structures such as the hierarchical data structure illustrated in Figure 4.7 within a Bayesian framework.

(iv) According to (Jiang et al., 2009) Bayesian estimation of model coefficients has not been widely used in the past largely due to difficulties associated with evaluating the combined posterior distribution to derive the marginal distribution of the model coefficients. Such evaluations has however been made relatively simpler through use of MCMC approaches and the high performance of modern computers.

The concept used in estimating the model coefficients is based on Bayes' theorem given in Equation 4.8.

$$P[\phi/\Delta RUT] = \frac{P[\Delta RUT/\phi]P[\phi]}{\int P[\Delta RUT/\phi]\, P[\phi]d\phi} \tag{4.8}$$

where: $P[\phi/\Delta RUT]$ = the combined posterior distribution of elements of the model parameters vector ϕ given observed data; $P[\Delta RUT/\phi]$ = the likelihood of the observed data given model parameters ϕ; and $P[\phi]$ = the prior distribution of the model parameters ϕ.

The integral in the denominator denoted as $\int P[\Delta RUT/\phi]\, P[\phi]d\phi$ calculates total probability across the model parameters space thus resulting in a constant. This implies that the posterior distribution can be written as proportional to the numerator of Equation 4.8 as follows.

$$P[\phi/\Delta RUT] \propto P[\Delta RUT/\phi]P[\phi] \tag{4.9}$$

The combined posterior distribution $P[\phi/\Delta RUT]$ was evaluated using the Bayesian statistical software WinBUGS. The WinBUGS programme has a built in Gibbs sampler, an algorithm used for generating random samples in combination with MCMC simulation (Ntzoufras, 2009).

The approach to the estimation of the model coefficient comprised five stages shown in Figure 4.8. These stages are discussed in subsequent sections.

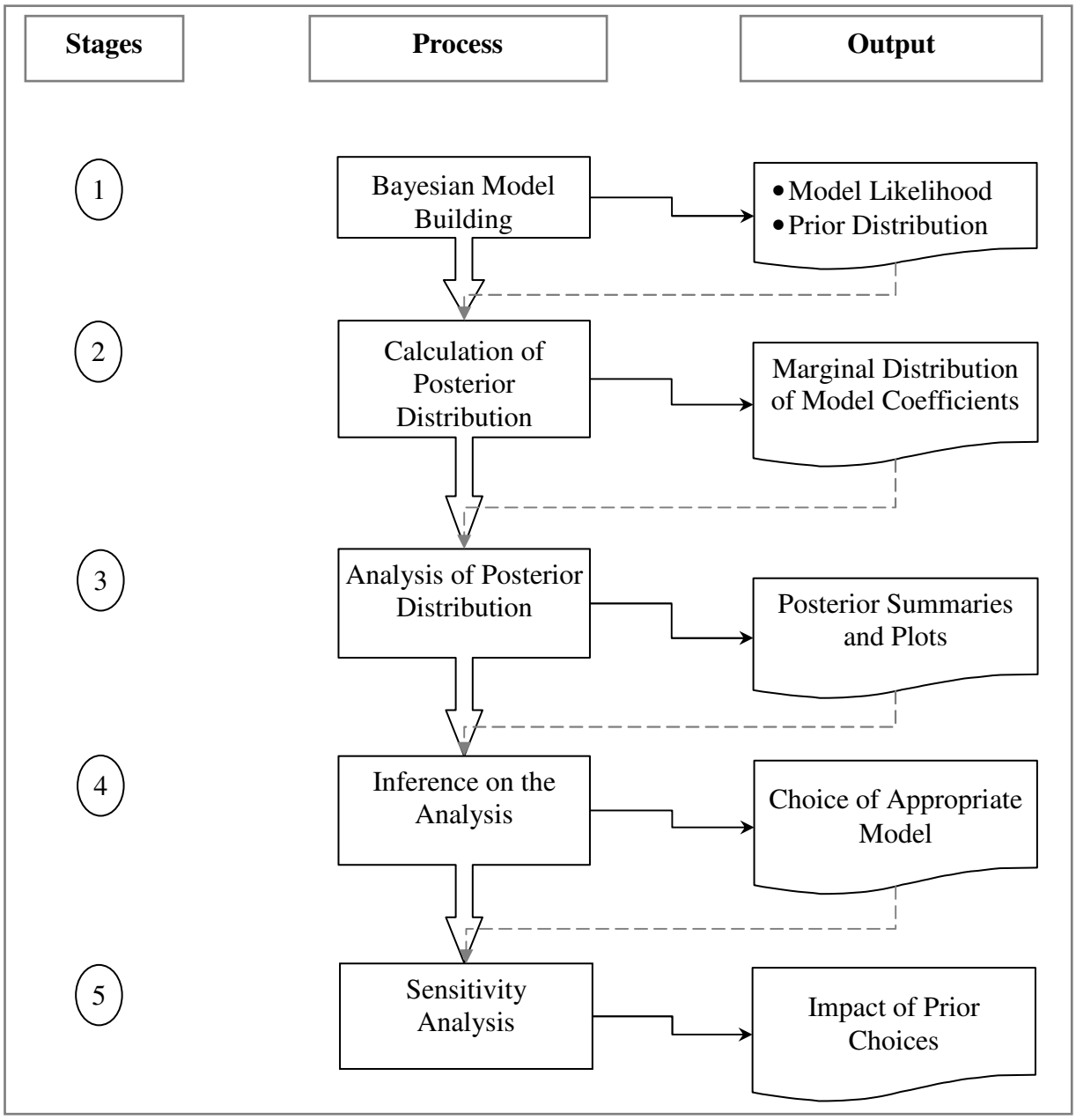

Figure 4.8: Stages for Bayesian Estimation of Model Coefficients

4.6.2 Bayesian Model Building

Model building was categorised into the following steps: definition of the likelihood distribution $P[\Delta RUT/\phi]$ for the annual incremental rut depth (ΔRUT) response variable given model parameters ϕ and specification of the prior distribution $P[\phi/\Delta RUT]$ for all the model parameters.

4.6.2.1 Likelihood Specification

The Annual Incremental Rut Depth (ΔRUT) observed on I numbers of road sub-sections across M asphalt surface groups over T years is stochastically denoted as:

$$\Delta RUT \sim D(F(x)) \tag{4.10}$$

F(x) embodies the statistical parameter vector of the assumed distribution D and is associated to the explanatory variables through a deterministic function h given in equations 4.5 to 4.7. F(x) is given as

$$F(x) = h\left(\varphi, YE4, sh, G, HS, \frac{VIM}{SP}, TPmax\right) \tag{4.11}$$

φ is a constrained set of model coefficients and statistical parameters used to specify the link function and the structure of the Bayesian model. The vector F(x) contains the actual set of model coefficients to be estimated. Considering data observed on a road sub-section i of asphalt surfacing group m in year t the set of model coefficients to be estimated $F(x_{imt})$ is given as

$$F(x_{imt}) = h\left(\varphi, YE4_{imt}, sh_{imt}, G_{it}, HS_{imt}, \frac{VIM_{imt}}{SP_{imt}}, TPmax_{it}\right) \tag{4.12}$$

Considering the complete study data set comprising a total of I road sub-sections across M asphalt surfacing groups recorded over T years, a general form of the likelihood function P[ΔRUT/ϕ] is specified as

$$P[\Delta RUT/\phi] = \prod_{i}^{I}\prod_{m}^{M}\prod_{t}^{T} P\left(\Delta RUT_{imt}/h\left(\varphi, YE4_{imt}, sh_{imt}, G_{it}, HS_{imt}, \frac{VIM_{imt}}{SP_{imt}}, TPmax_{it}\right)\right)$$

(4.13)

Equation 4.13 gives a general form of the likelihood P[ΔRUT/ϕ] which may be developed further based on the assumption of the underlying distribution of the response variable ΔRUT given section 6.3. If for example, D is assumed to be normally distributed, then the stochastic component of the likelihood would be given as

$$\Delta RUT \sim N(\mu_{imt}, \tau) \quad (4.14)$$

where μ_{imt} = Equations 4.5, 4.6 or 4.7; $F(x_{imt}) = (\mu_{imt}, \tau)$; $\varphi = (\tau, \beta_1, \beta_2, \beta_3, \beta_4, \beta_5, \beta_6)$ if model structures in Equations 4.5 and 4.6 are used or $\varphi = (\tau, \beta_0, \beta_1, \beta_2, \beta_3, \beta_4, \beta_5, \beta_6)$ for Equation 4.7 model structure. $h\left(\varphi, YE4, sh, G, HS, \frac{VIM}{SP}, TPmax, \right) = \binom{\mu}{\tau}$. The likelihood is given as

$$P[\Delta RUT/\phi] = \prod_{i}^{I}\prod_{m}^{M}\prod_{t}^{T} P\left(\Delta RUT_{imt}/\mu_{imt}, \tau\right)$$

(4.15)

4.6.2.2 Specification of the Prior Distribution

The prior distribution of the model coefficients were hierarchically structured in line with the data structure discussed in section 4.5.2. Considering the hierarchical data structure it is

possible within the Bayesian framework to estimate model coefficients at the Network Level (Level 1) or at the Surface Group Level (Level 2).

In the first approach, the pooled mean effect of the model coefficients denoted as ϕ_μ of all observations are estimated at level 1 (network level) of the data hierarchy. If as an example the distribution D of the response variable in Equation 4.10 is assumed to be normally distributed, then the stochastic part of the model is given as

$$\Delta RUT \sim N(\phi_\mu, \Lambda) \tag{4.16}$$

where N = normal distribution, $\phi_\mu = \{ \beta_{\mu 0}, \beta_{\mu 1}, \beta_{\mu 2}, \beta_{\mu 3}, \beta_{\mu 4}, \beta_{\mu 5}, \beta_{\mu 5}, \beta_{\mu 6}\}^T$ is the transpose of the vector of the mean of model coefficients for observations at the network level. $\Lambda = \{\tau_{\beta 0,} \tau_{\beta 1}, \tau_{\beta 2}, \tau_{\beta 3}, \tau_{\beta 4}, \tau_{\beta 5}, \tau_{\beta 5,} \tau_{\beta 6}\}^T$ denotes the precision of each model coefficient in ϕ

In the second approach, mean effects $\phi_{m\mu}$ is independently estimated for each asphalt surface group m. $\phi_{m\mu} = \{\beta_{0m\mu}, \beta 1m_\mu, \beta_{2m\mu}, \beta_{3m\mu}, \beta_{4m\mu}, \beta_{5m\mu}, \beta_{6m\mu}\}^T$ denotes the transpose of the vector of the mean of model coefficients within each asphalt surface group(level 2).

In practice the estimation of model coefficients using the second approach is desired since results in models describing the performance of each asphalt surfacing group. According to (Ntzoufras, 2009), if in the second approach the mean effect of the model coefficients $\phi_{m\mu}$ are estimated independently for each surface group, then large uncertainties are likely in the posterior estimates. To that end, it was assumed in this study that all expected means $\phi_{m\mu}$ of

the model coefficients of each asphalt surfacing group are observables from a population distribution with mean ϕ_μ , an overall network level average effect.

$$\phi_{m\mu} \sim N(\phi_\mu, M) \tag{4.17}$$

The prior distribution in this Bayesian model formulation is thus characterised by two levels as illustrated in Figure 4.9. The prior distribution for the first level is denoted by $P(\phi/\phi m)$ and for the second level is denoted by $P(\phi m/M)$. The prior distribution of the second level of the hierarchy $P(\phi m/M)$ is referred to as hyperprior and the corresponding parameters denoted by the transposed vector M are called hyperparameters of the prior parameters denoted by the transpose of the vector ϕm. Λ denotes the transpose of the vector of the precision of the prior parameters of the prior parameters given by vector ϕm. Precision is defined as the reciprocal of the variance.

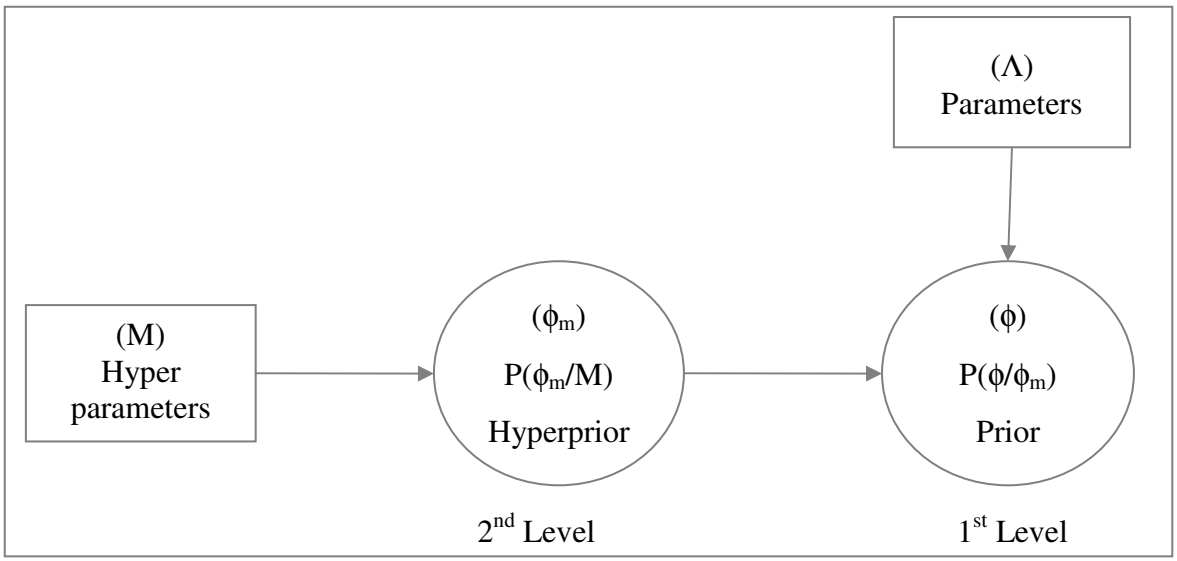

Figure 4.9: A Representation of the Hierarchical Prior Specification. Square Nodes denote Constant Parameters; Circular Nodes refer to Stochastic Components.

A generalised form of the prior distribution is given as

$$P[\phi] = \prod D(\phi) \prod D(\phi_m) \prod G(M)G(\Lambda) \quad (4.18)$$

The complete prior distributions for the model coefficients of the improved and alternative model structures given in Equations 4.6, 4.7 and 4.8 are specified in section 6.2.

4.6.3 Calculation of Posterior Distribution

From Bayes' theory the joint distribution of the model coefficients given the observed data P[ϕ/ΔRUT] is obtained by combining the likelihood P[ΔRUT/ϕ] with the prior P[ϕ]. The aim however is to summarise the marginal distribution of each model coefficients β_k given the data where k = 0 to 6. This can be achieved by integrating out all model coefficients except coefficient β_k of which the marginal distribution is desired as illustrated in Equation 4.19.

$$P(\beta_k/\Delta RUT) = \int P(\beta_0, \dots, \beta_{k-1}, \beta_{k+1}, \dots, \beta_p/\Delta RUT)\, d\beta_1, \dots, d\beta_{k-1}, d\beta_{k+1}, \dots, d\beta_p \quad (4.19)$$

Such integrations require computationally demanding methods such as multi-dimensional integration. MCMC methods however provide less complex alternatives for deriving the marginal distributions for each of the model coefficients from the joint posterior distribution (Congdon, 2003).

A Markov Chain is a stochastic process such as $\{\phi^{(1)}, \phi^{(2)}, ..., \phi^{(T)}\}$ in which $P(\phi^{(t+1)} | \phi^{(t)}, ..., \phi^{(1)}) = P(\phi^{(t+1)} | \phi^{(t)})$ which is interpreted as the distribution of ϕ at sequence t+1 given all preceding values depends only on the distribution $\phi^{(t)}$ of the previous sequence t. As $t \rightarrow \infty$ the

distribution of $\phi^{(t)}$ converges to its target distribution which is independent of the initial values of the chain $\phi^{(0)}$. More details are given in Gilks et al (1996).

The WINBUGS software which has an inbuilt Gibbs sampler was used to derive the marginal distributions. Gibbs sampling approach is a Markovian updating scheme described in detail in detail in Geman and Geman (1984), Casella and George (1992) and Smith and Roberts (1993).

The marginal distributions are achieved after a large number of iterations and when the Markov chain converges to a target distribution. Convergence is required for the sampled value to represent a random draw from the marginal distribution. This was achieved by running multiple Markov chains simultaneously. The first (B) iterations of each chain deemed to include random draws before convergence or "burn-in" were discarded. Convergence was considered achieved when the traces of the chains were found to be overlapping as illustrated in Figure 4.10.

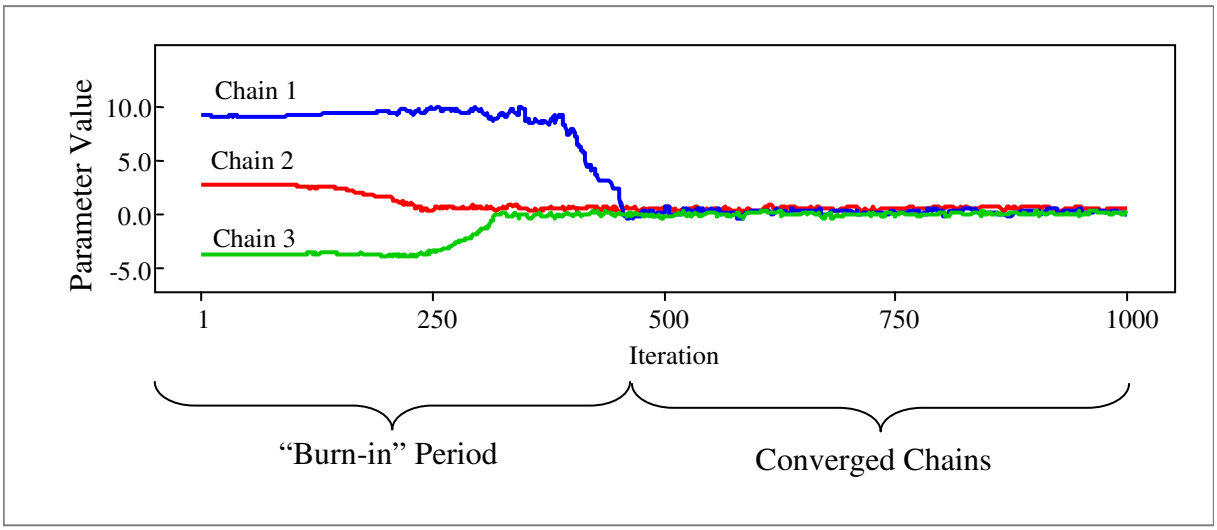

Figure 4.10: Illustration of Multiple Markov Chains.

4.6.4 Analysis of Posterior Distribution

After the "burn-in" period, the results for each model coefficient were obtained based on the converged chains illustrated in Figure 4.10. The WinBUGS software was used to perform the following analysis: plot posterior distribution for each model coefficient, and to obtain summaries of posterior distribution including mean, median, standard deviation, quartiles and correlations. The results are presented in section 6.5.

4.6.5 Inference

Inference regarding the results of the set of the model coefficients for each surfacing group was based on the following:

- The importance of each model coefficient to the prediction or description of the annual incremental rut depth response variable (ΔRUT);
- The association between the response variable ΔRUT and each model coefficients and
- The relative magnitude of the effect of each explanatory variable on ΔRUT.

4.6.6 Sensitivity Analysis

Sensitivity analysis was undertaken to investigate the robustness of the posterior distribution to selection of the prior distribution. The analysis was achieved by assessing changes in the posterior distribution over different prior distributions. In the case where informative priors were used, sensitivity analysis was focused on the structure of the prior distribution. When non-informative priors were used, it focused on how different prior parameters may influence the posterior inference. The results of the sensitivity analysis are discussed in 6.7.

4.7 Development of a Climate Impact and Adaptation Model

The developed rut depth model was used to formulate a Microsoft Excel based Climate Impact and Adaptation Model for use in investigating the impact climate change as well as road maintenance strategies for adapting to climate change.

The components of the model were categorised under: Inputs, Analysis and Outputs. The model framework is illustrated in Figure 4.11.

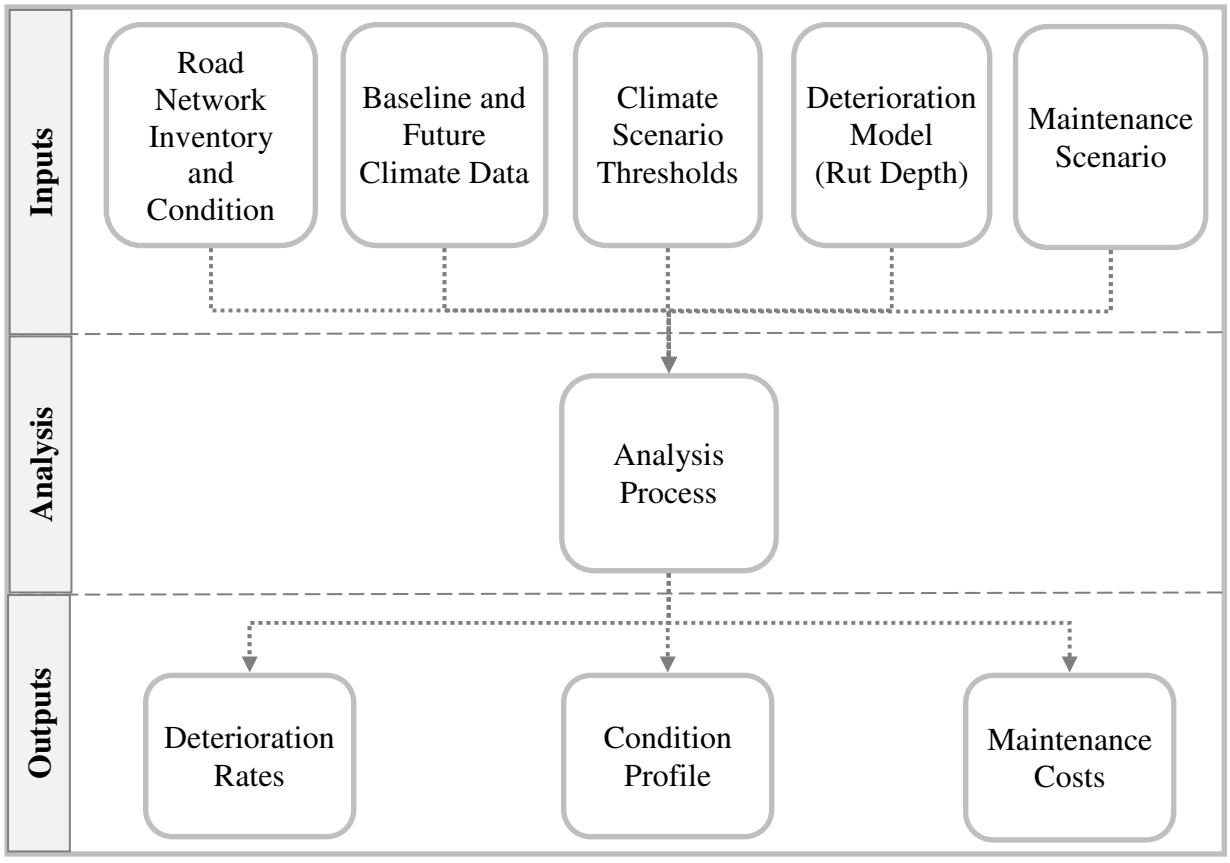

Figure 4.11: Climate Impact and Adaptation Model Framework.

Each component of the model illustrated in Figure 4.11 is discussed in Chapter 8.

4.8 A Framework for Quantification and Propagation of Uncertainties

The literature review identified the need for a framework to guide the analysis of uncertainties associated prediction of the impacts associated with predicted climate change on road maintenance.

A framework for quantification and propagation of uncertainties in climate impact assessment of road maintenance strategies was formulated based on an understanding of the inputs of the Climate Impact and Adaptation Model described in Chapter 8.

The framework is broken down into six components which are: definition/choice of scenarios; collation of independent input variables; quantification of uncertainties in model inputs; propagation of uncertainties using simulation; and representation, analysis and discussion of results. These components are explained in detail in Chapter 9.

4.9 Case Study

The application of the Climate Impact and Adaptation Assessment Model described in Chapter 8 together with the uncertainty framework described in Chapter 9 were demonstrated using a case study aimed at deriving rut depth deterioration rates, road condition over a 30-year period, and the discounted costs of maintaining the study road pavement on the basis of rut depth deterioration of the road. These outputs were investigated using predefined socio-economic, climate change and road maintenance scenarios.

4.9.1 Scope

The case study utilised data from the southbound section of the M11 motorway between junctions 4 and 6. The case study area (depicted in

Figure 10.1) was selected because of availability of data as well as its close proximity to the study area shown in Figure 4.2.

4.9.2 Maintenance Strategy and Analysis Scenarios

The analysis was performed for the Medium Emission UKCIP climate scenario over the following 30-year periods: Baseline (1961 – 1990), 2020s (2010 – 2039), 2030s (2020 – 2049), 2040s (2030 – 2059) and 2050s (2040 – 2069).

The analysis was performed for two road maintenance strategies: a Current Practice maintenance strategy and an Adaptation strategy. Detailed definition of these strategies is given in section 10.3.3.3 and the setup of the model under these two maintenance strategies is discussed in section 10.6.

A summary of the road pavement maintenance strategies, climate change scenarios analysed and the outputs of the analysis are given in Table 4.3. The outputs of the case study are discussed in section 10.8.

Table 4.3: Case Study Maintenance Strategy, Climate Scenario and Outputs

Maintenance Strategy	**Climate Scenario**	**Outputs**
Current Practice	Baseline (1961-1990)	• Rut depth deterioration rates in mm/year • Condition profile • Discounted maintenance costs
	Future Climate (2020s, 2030s, 2040s, 2050s)	• Rut depth deterioration rates in mm/year • Condition profile • Discounted maintenance costs
Adaptation Strategy	Baseline (1961-1990)	• Rut depth deterioration rates in mm/year • Condition profile • Discounted maintenance costs
	Future Climate (2020s, 2030s, 2040s, 2050s)	• Rut depth deterioration rates in mm/year • Condition profile • Discounted maintenance costs

4.10 Summary

This Chapter discussed the approach followed in undertaking the study. The methodology comprised the following eight major components: literature review, preliminary analysis, modelling concepts, data collection and processing, estimation of model coefficients,

development of Climate Impact and Adaptation Model, framework for quantification and propagation of uncertainties, and a case study.

A copy of a peer reviewed paper based on the methodology described in this chapter is given in Appendix A (Anyala et al., 2011). The next chapter focuses on data collection and processing.

CHAPTER 5 DATA COLLECTION AND ANALYSIS

5.1 Introduction

This chapter describes the data used in the study and how they were collected and processed. It is structured into four major sections. Section 5.2 introduces the study area. Section 5.3 gives a description of the types of data, their sources, accuracy and reliability. The section is also concerned with the processing of the collected data to formats and units suitable for model development and validation. Section 5.4 investigates the link between recently observed climate data and recorded annual incremental rut depth. Section 5.5 provides a summary of the processed data. The chapter is concluded in section 5.6.

5.2 The Study Area

The study was based on data relating to the United Kingdom Highways Agency Area 6 road network illustrated in Figure 5.1. The study area covers parts of the English counties of Cambridgeshire, Suffolk, Norfolk and Essex. A summary of the length of roads used in the study is given in Table 5.1.

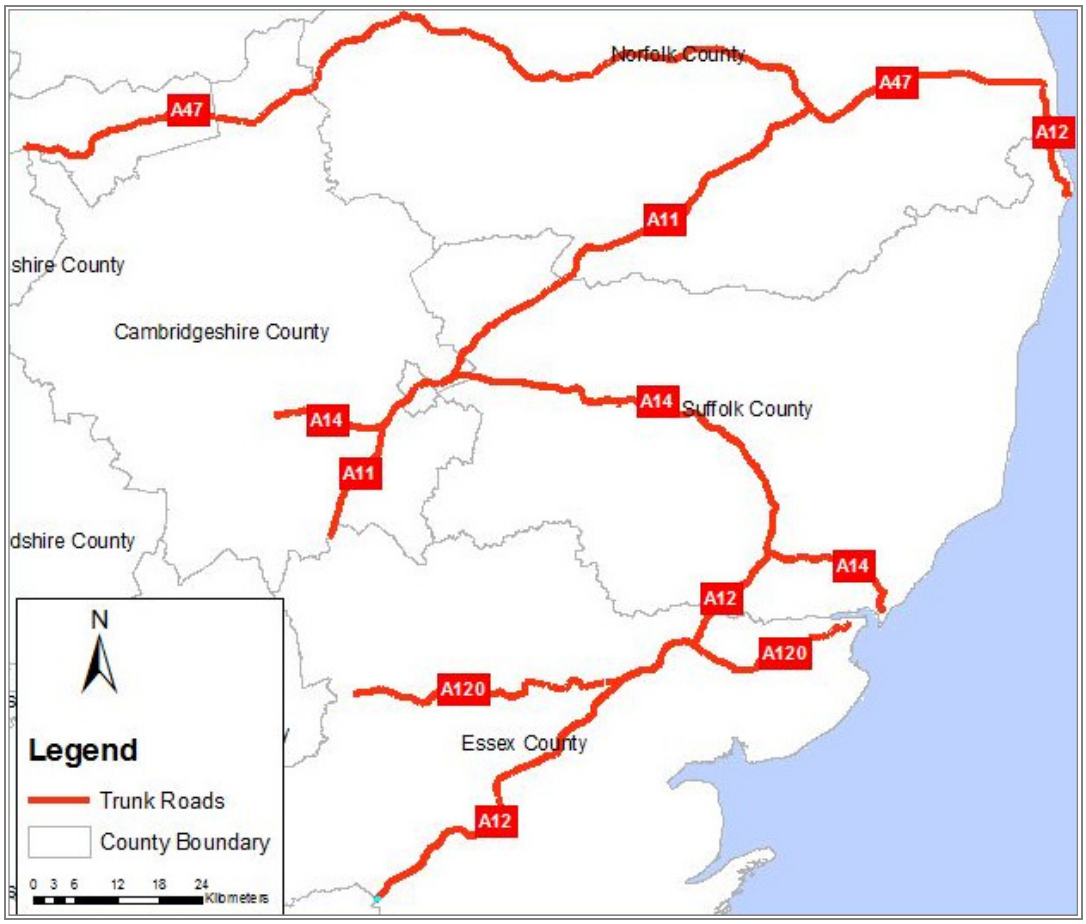

Figure 5.1: Highways Agency Area 6 Trunk Road Network

Table 5.1: Summary of Study Road Lengths

Road Number	Road Name	Carriageway Road Lengths (km)			
		Main Carriageway	Round - abouts	Slip Roads	Total
A11	A11 London - Norwich	161.814	2.233	29.778	193.825
A47	A47 Nuneaton - Great Yarmouth	240.754	5.023	34.257	280.034
A12	A12 Wanstead - Great Yarmouth	195.478	3.015	45.872	244.365
A120	A120 Puckeridge - Harwich	111.709	1.267	15.485	128.461
A14	A14 M6 - Harwich Haven (Felixstowe)	227.802	0.799	58.085	286.686

5.3 Data Description and Analysis

5.3.1 Data Types and Sources

The data required for the development of the improved rut depth models proposed in Chapter 4 are grouped under the following categories: asphalt surfacing rut depth, climate, traffic, road geometry and asphalt material properties. The methods used to collect the data, their sample sizes and accuracy are discussed in subsequent sections for each data group.

5.3.2 Asphalt Surfacing Rut Depth Data

5.3.2.1 Measurement of Rut Depth

Asphalt rut depth data is collected annually on Highways Agency trunk roads using Traffic-Speed Condition Survey (TRACS). The raw data collected by TRACS is processed using the Highways Agency's Machine Survey Pre-processor (MSP) software to generate TRACS Base Condition Data (BCD) which includes rut depths in the nearside and offside wheel-tracks calculated from measured transverse profile, over 10m lengths. MSP uses an algorithm that simulates placing a notional 2m straight edge on the recorded transverse profile, and measuring the largest deviation from the straight edge to the transverse profile as illustrated in Figure 5.2. The TRACS BCD is loaded into the Highways Agency Pavement Management System (HAPMS) (DMRB HD 29/08, 2008).

Rut depth is stored in HAPMS as average rut depth for each wheel-track over a 10m length. This information is then used by HAPMS to calculate the following length weighted average values:

- Left Rut using the left-track values only;
- Right Rut using the right wheel-track values only;
- Average Rut using both wheel-track values; and
- Maximum Rut using maximum wheel-track values from each 10m measurement section.

(DMRB HD 29/08, 2008).

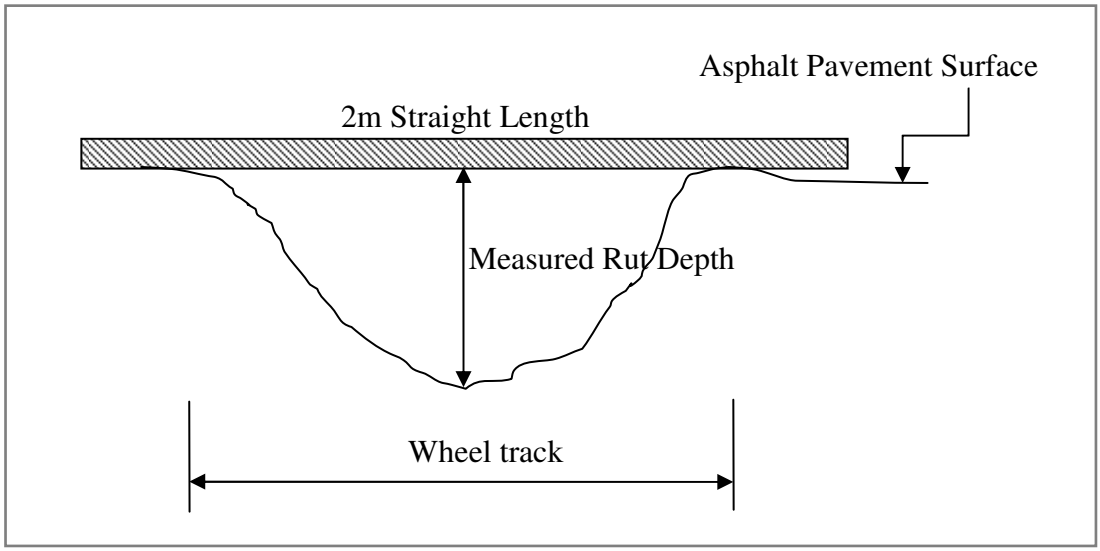

Figure 5.2: Illustration of Rut Depth Measurement

5.3.2.2 Sampled Rut Depth

Absolute rut depth samples were obtained from HAPMS for the following annual periods: 2001/2002, 2002/2003, 2003/2004, 2004/2005, 2005/2006, and 2006/2007. The severity and spatial coverage of the collected rut depth data are illustrated in maps generated using Global Information System (GIS) software. Figure 5.3 depicts the spatial coverage and severity of the 2001/2002 absolute rut depths data. Maps for the other annual periods are provided in Appendix B1.

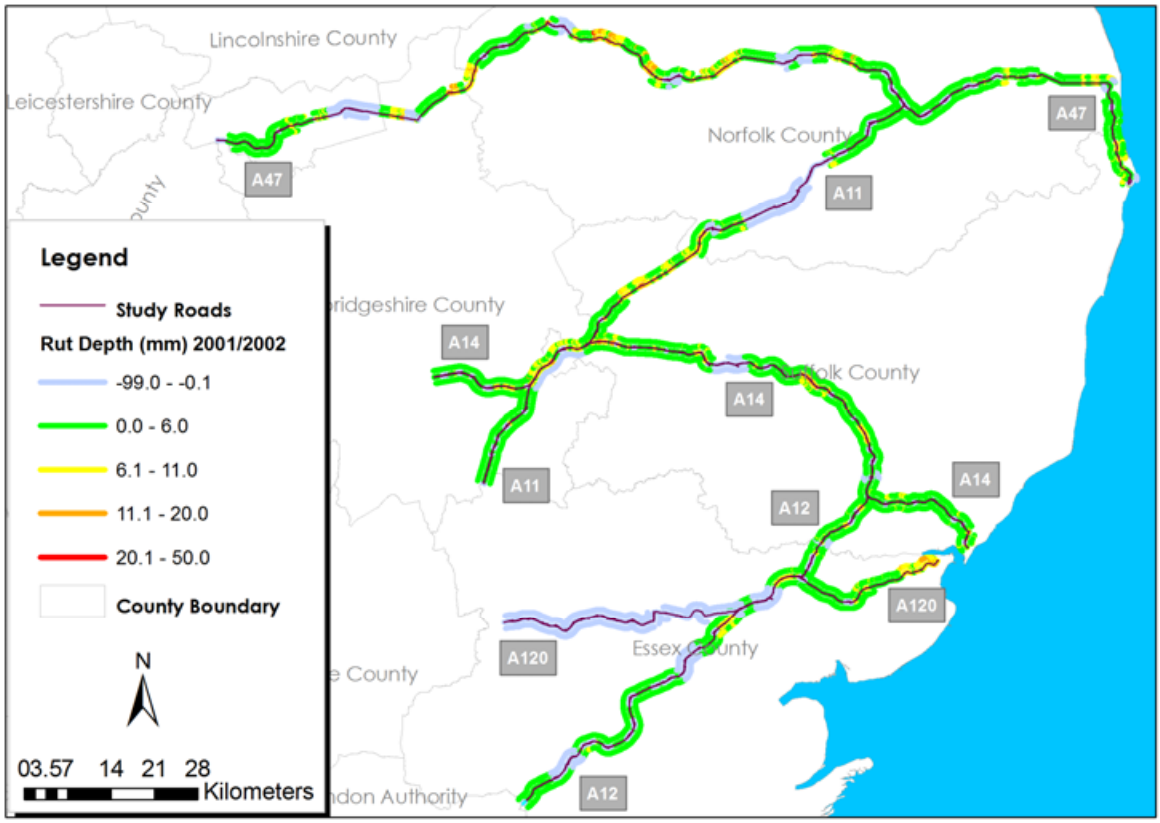

Figure 5.3: Spatial Representation of Sampled Rut Depth Measured in 2001/2002.

The values of rut depths displayed on the maps were banded into four ranges defined using thresholds given in Table 5.2. The negative rut depth range (-99 to -0.1) on the map legends denote missing data.

Table 5.2: Definition of Condition Bands for Rut Depth

Rut Depth Range (mm)	Definition	Description
0 – 6	Sound	No visible deterioration.
6.1 – 11	Some Deterioration	The deterioration is not serious and more detailed investigations are not needed.
11.1 – 20	Moderate Deterioration	The deterioration is becoming serious and needs to be investigated.
>20	Severe Deterioration	This condition is not expected to occur very frequently on trunk road network.

Source: Adopted from Design Manual for Roads and Bridges (DMRB HD 29/08, 2008)

Summary statistics of the collected absolute rut depth data showing sample sizes, measures of central tendency and measures of variability by annual survey period for the study road network is given in Table 5.3.

Table 5.3: Descriptive Statistics of Rut Depths Sampled on the Study Road Network.

Statistics	Survey Period					
	2001/ 2002	**2002/ 2003**	**2003/ 2004**	**2004/ 2005**	**2005/ 2006**	**2006/ 2007**
Sample Size	18,951	17,804	17,034	17,310	18,864	15,836
Mean	4.236	3.683	3.735	3.774	3.817	4.153
Standard Error	0.017	0.017	0.019	0.019	0.018	0.020
Median	3.628	3.113	3.083	3.076	3.102	3.453
Standard Deviation	2.389	2.296	2.424	2.551	2.503	2.569
Sample Variance	5.709	5.270	5.874	6.509	6.267	6.598
Kurtosis	5.239	6.314	6.061	6.420	6.274	6.574
Skewness	1.930	2.100	2.099	2.206	2.186	2.250
Range	24.147	22.159	21.966	22.929	22.651	22.321
Minimum	0.000	0.327	0.297	0.537	0.370	0.794
Maximum	24.147	22.486	22.263	23.466	23.021	23.115

Sample size in Table 5.3 denotes the total number of observed rut depth averaged over 100m road sub-sections on lanes 1 and 2 of the road carriageway. The low standard error suggests that the sample mean is a good estimate of the population mean. The median rut depth in each year is lower than the mean value indicating that the distribution of rut depths on the network is skewed to the right. The skewness of the rut depth data in all years in which samples were obtained are positive confirming the former assertion that the distribution of the absolute rut depths on the road network is skewed with a longer right-hand tail. Summary statistics of collected absolute rut depth by road type is presented in Appendix B2.

5.3.2.3 Reliability of Absolute Rut Depth Data

TRACS is recognised as a reliable and repeatable method for collecting rut depth values that are comparable to measurements made manually using a two metre straight edge (DMRB HD29/08, 2008; Halcrow, 2005). The setup of the survey vehicle is managed through a detailed and rigorous quality assurance regime supervised by an independent auditor. The TRACS survey vehicles are also subjected to accreditation and consistency testing before being given a certificate to commence surveys. In addition regular repeat surveys are carried out to check the consistency of the measured data. Measurements made using accredited survey vehicles are also compared with surveys undertaken by an independent survey vehicle (DMRB HD29/08, 2008).

5.3.2.4 Accuracy of Absolute Rut Depth Data

The major sources of errors in TRACS rut depth measurement are: errors due to incorrect setup of the survey vehicle and errors emanating from circumstances associated with the survey. The setup of the TRACS vehicle is managed through accreditation tests described in the previous section. Errors in rut depth measurement due to circumstances associated with the survey are possible under the following scenarios:

a) During conditions which prohibits the sensors mounted on the survey vehicle to provide reliable results such as presence of surface water;
b) Driving the survey vehicles offline either to the nearside or offside; and
c) Features such as lane edge markings which may be included in the transverse profile measurement leading to nearside rut depths that are much higher than those actually present on the road surface.

Error in measured absolute rut depth which may have resulted from scenarios (a) and (b) above are difficult to discern from sampled data due to lack of information on the prevailing circumstances during the survey. Regarding scenario (c) DMRB HD28/04 (2008) recommends that comparison should be made between the Left and Right rut depths obtained from HAPMS to check that there are no excessive differences which could have been caused by including the edge line in the measured Left rut depth.

Comparison of Left and Right rut depth data was performed using the paired student's t-test using random samples of 100 pairs of length weighted left and right wheel track rut depths taken from the available road network data sample in each of the six annual survey periods.

The null hypothesis Ho and the alternative hypothesis Ha were:

- Ho: in given year, there is no significant difference between mean values of the absolute Left wheel track rut depth and corresponding mean absolute rut depth measured on the Right wheel track; and
- Ha: in a given year, there is a significant difference in mean absolute rut depths measured on the Left wheel track compared to corresponding measurements on the Right wheel track.

The paired students t-test assumes that the differences between the paired data are normally distributed (MacDonald, 2009). A plot of the histogram of the difference between the paired Left and Right wheel track rut depth shown in Figure 5.4 suggests that this assumption is valid.

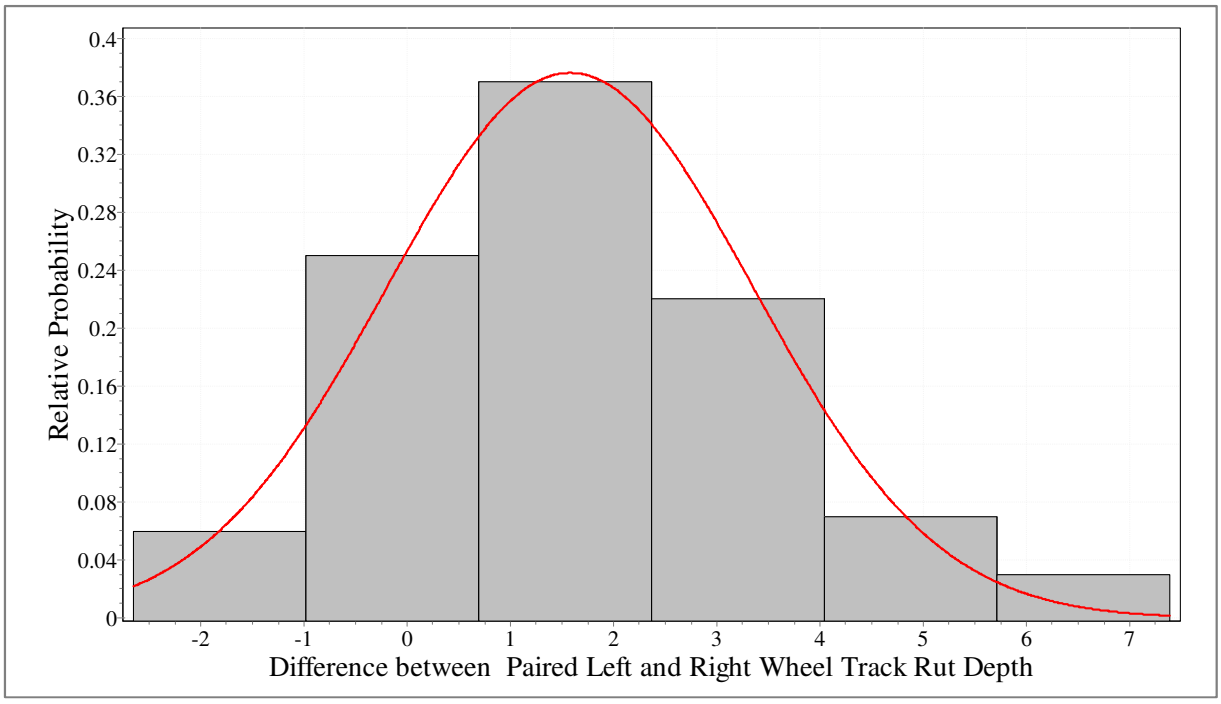

Figure 5.4: Histogram of the Difference between Left and Right Absolute Rut Depth in mm.

The results of the paired t-test is presented in Table 5.4 at $\alpha = 0.05$ level of significance or 95% confidence level. If the probability (p) that the null hypothesis is true is greater than α then Ho should be accepted however, if the probability (p) is less than α, then Ho should be rejected.

Table 5.4: Results of Paired Students t test for Left and Right Wheel Track Rut Depth

Parameter	**2001/ 2002**	**2002/ 2003**	**2003/ 2004**	**2004/ 2005**	**2005/ 2006**	**2006/ 2007**
t Statistics	1.295	-1.835	-0.198	0.052	-1.827	1.949
T Critical Two-tail	1.984	1.984	1.984	1.984	1.984	1.984
p(T<=t) two-tail	0.198	0.070	0.844	0.958	0.071	0.054
Decision	Accept Ho since p>0.05	Accept Ho since p>0.05	Accept Ho since p>0.05	Accept Ho since p>0.05	Accept Ho since p>0.05	Accept Ho since p>0.05

The results given in Table 5.4 suggest that the paired Left and Right rut depth data are consistent. The absolute rut depth data was analysed as discussed in the next section to derive annual incremental rut depth which is the response variable for the models proposed in Chapter 4 and developed in Chapter 6.

5.3.2.5 Estimation of Underlying Rates of Deterioration

The underlying rates of rut depth deterioration on the study road network in the form of annual incremental rut depth are required for estimating the coefficients of the models proposed in Chapter 4. The approach used comprised checking consistency of rut depth time series data, and calculation of annual incremental rut depth.

5.3.2.5.1 Consistency of Time Series Data

The consistency of rut depth time series data was checked on each road sub-section to identify and eliminate sub-sections in a given year with negative rates of deterioration which have resulted as a consequence of maintenance activities. For a given road sub-section, data was analysed to indentify annual time series of absolute rut depths showing increasing deterioration trend. The approach is illustrated in Figure 5.5 using data from a road sub-section on the study road network. Data denoted in Figure 5.5 as invalid were omitted from the analysis.

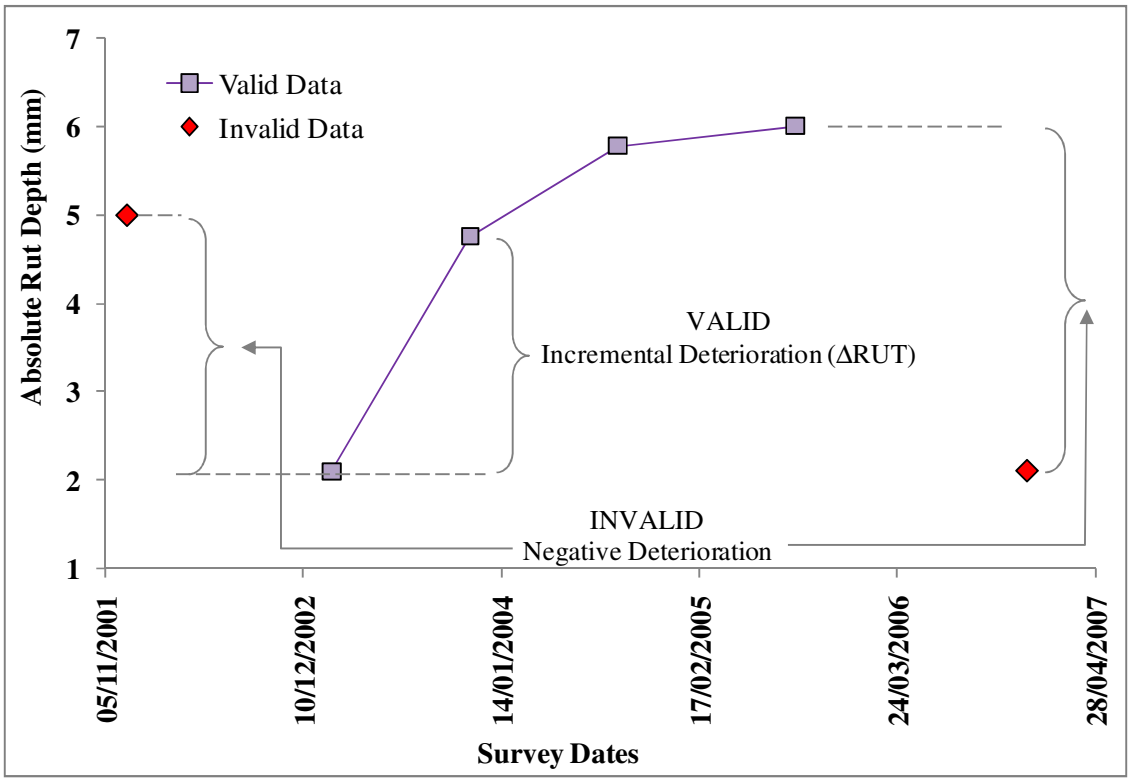

Figure 5.5: Illustration of invalid data and valid annual incremental rutting

5.3.2.5.2 Calculation of Annual Incremental Rut Depth

Annual incremental rut depths were calculated for each road sub-section as the change in average absolute rutting on both wheel paths measured before and after summer months of each year. The approach to the calculation is shown in Figure 5.6.

MEASURED RUT (mm)[1]	SURVEY DATE[2]	INTERVAL (Months)[3]	CORECTION FACTOR[4]	YEAR[5]	ΔRUT UNADJUSTED (mm)[6]	ΔRUT ADJUSTED (mm)[7]
4.998	18-Dec-01					
		13.611	0.882	2002	INVALID	INVALID
2.101	05-Feb-03					
		9.173	1.308	2003	[4.755 - 2.101] = 2.654	[2.654 * 1.308] = 3.472
4.755	11-Nov-03					
		9.830	1.221	2004	[5.777 - 4.755] = 1.022	[1.022 * 1.221] = 1.248
5.777	05-Sep-04					
		11.803	1.017	2005	[6.003 - 5.777] = 0.226	[0.226 * 1.017] = 0.230
6.003	30-Aug-05					
		15.452	0.777	2006	INVALID	INVALID
2.101	13-Dec-06					
		13.447	0.892	2007	[2.334 - 2.101] = 0.233	[0.233 * 0.892] = 0.208
2.334	26-Jan-08					

Figure 5.6: Illustration of the Calculation of Annual Incremental Rut Depth for a Road Subsection.

The definition of each of the columns in Figure 5.6 is as follows:

1. Measured rut depth is the average of the absolute left and right wheel track rut depths on a given road sub-section;
2. Survey date is the date on which the absolute rut depth data was collected;
3. Interval represents the time difference in months between dates of measurement of subsequent absolute rut depth values on each road sub-section;
4. The correction factor is the ratio of number of months in a year (12) and the interval;
5. Year refers to calendar year to which the annual incremental rut depth is associated;
6. ΔRUT Unadjusted refers to the difference between absolute rut depth values measured in consecutive years;

7. ΔRUT Adjusted was obtained by multiplying the correction factor in (4) with the unadjusted incremental rut depths to derive an annual incremental rut depth for a given road sub-section in a given year.

5.3.3 Observed Climate Data

5.3.3.1 Data Source

Monthly gridded datasets of observed climate variables shown in Table 5.5 were obtained from UKCP09 gridded observed dataset. These observations were derived from a network of weather stations located in the United Kingdom using a methodology detailed in Perry and Hollis (2005).

Table 5.5: Monthly Gridded Observed Climate Variables

Climate variable	Definition	Availability	
		From	To
Mean daily maximum temperature	Average of the daily highest air temperatures (°C)	1914	2006
Sunshine duration	Duration of bright sunshine during the month (hours per day)	1929	2006
Total precipitation	Total rainfall amount (mm) during the month	1914	2006
Days of rain ≥10 mm	Number of days with ≥10mm rainfall	1961	2006
Days of sleet or snow falling	Number of days with sleet or snow falling	1971	2000
Days of snow lying	Number of days with greater than 50% of the ground covered by snow at 0900 hours	1971	2006

Source: Met Office (2009)

5.3.3.2 Sampled Climate Data

Time series data samples from 1961 to 2006 at 5km by 5km spatial resolution covering the study area were obtained for each climate variable defined in Table 5.1 (Met Office, 2009).

The spatial representation of the data is illustrated in Figure 5.7 using mean daily maximum summer temperature for 2003.

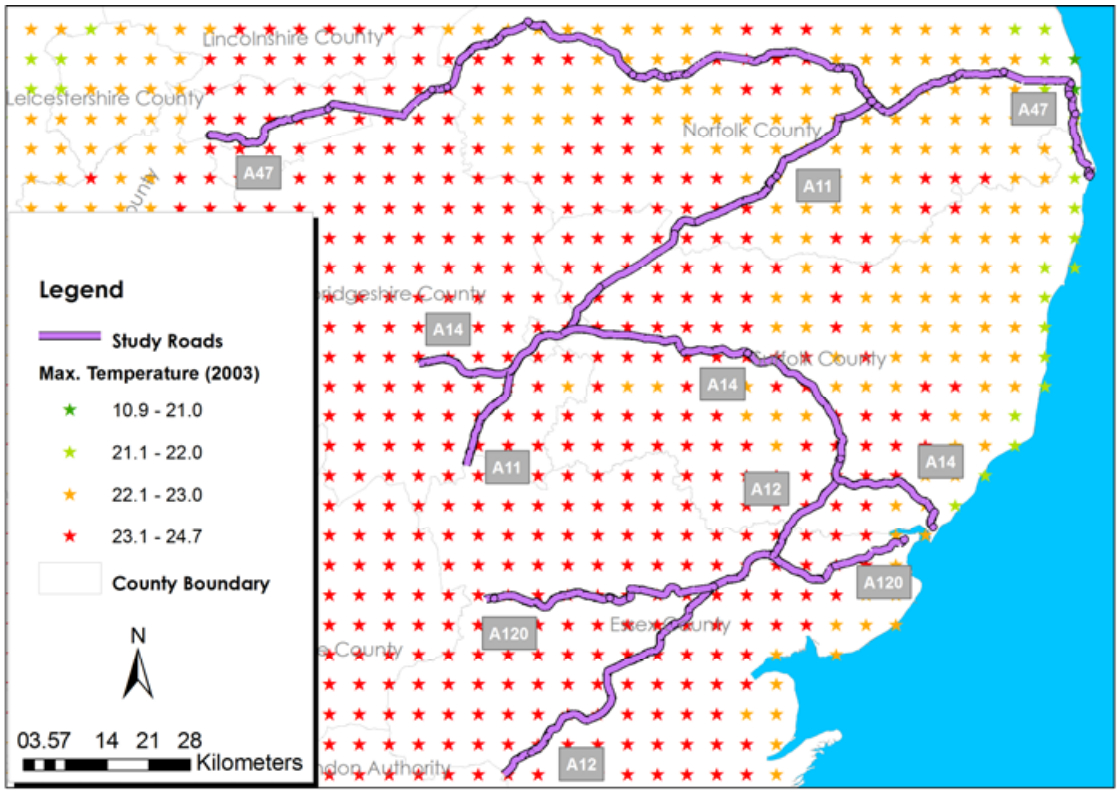

Figure 5.7: Gridded 2003 Mean Daily Maximum Summer Temperature.

The gridded climate data were transformed to the study road sub-sections by averaging all values closest to each road sub-sections using ArcGIS software (ERSI, 2009). A spatial representation of the transformed 2003 mean daily maximum temperature during the summer on the road sections is shown in Figure 5.8.

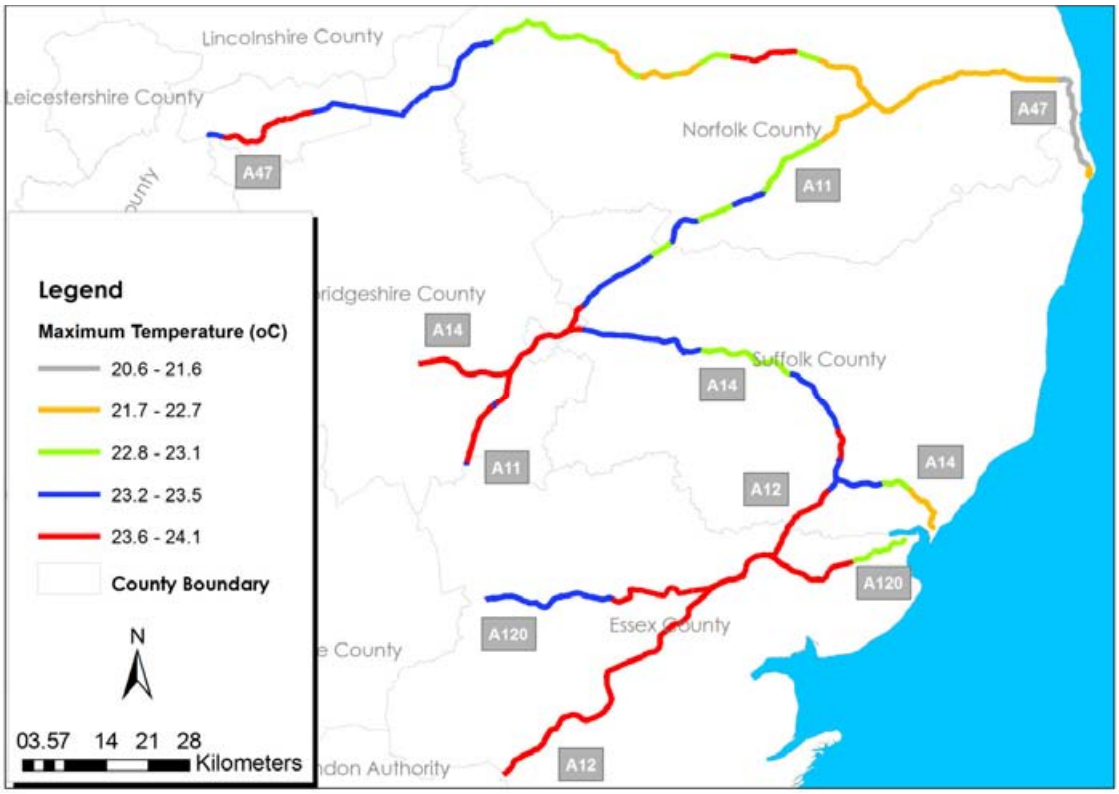

Figure 5.8: Study Road Section Mean Maximum Monthly 2003 Summer Temperature.

Descriptive statistics for the sampled climate data from 2001 to 2006 are given in Table 5.6. Annual mean plots of days with rainfall greater than 10mm during the summer, number of days with snow lying and maximum summer temperature are shown in Figure 5.9. It is apparent from Table 5.6 and Figure 5.9 that the summer of 2003 was the hottest and driest over the period from 2001 to 2006, while 2005 was the year with the highest number of days with snow lying. Box plots summarising the distribution of the all the climate variables considered in the study are given in Appendix B3.

Table 5.6: Climate Data Summary Statistics

Climate Variable	Parameter	2001	2002	2003	2004	2005	2006
Maximum Temperature	Mean	21.63	21.58	23.22	21.89	21.49	23.04
	Standard Deviation	0.49	0.33	0.59	0.49	0.64	0.72
	Minimum	19.70	20.35	20.96	19.91	19.13	20.19
	Maximum	22.36	22.32	24.06	22.61	22.43	24.20
Days with Rainfall greater than 10mm	Mean	1.75	1.20	1.18	2.14	1.65	1.57
	Standard Deviation	0.46	0.40	0.43	0.47	0.41	0.60
	Minimum	0.81	0.41	0.32	1.12	0.99	0.43
	Maximum	3.26	2.60	2.36	3.32	2.95	2.66
Precipitation	Mean	63.04	53.11	42.52	75.67	52.55	53.43
	Standard Deviation	7.25	9.64	8.44	9.35	7.65	12.09
	Minimum	48.03	29.53	27.20	55.48	34.52	31.28
	Maximum	83.42	89.19	70.46	105.50	71.73	81.21
Number of Days with Snow Lying	Mean	2.44	1.55	2.90	3.41	4.15	0.47
	Standard Deviation	0.90	1.26	0.94	0.57	0.64	0.35
	Minimum	0.69	0.00	1.04	2.46	2.97	0.00
	Maximum	4.59	3.96	5.53	5.68	5.58	1.52
Sunshine Duration	Mean	6.62	5.62	7.01	6.25	5.95	7.42
	Standard Deviation	0.49	0.27	0.51	0.47	0.31	0.36
	Minimum	5.75	4.97	6.24	5.55	5.36	6.72
	Maximum	7.61	6.49	7.92	7.16	6.72	7.90

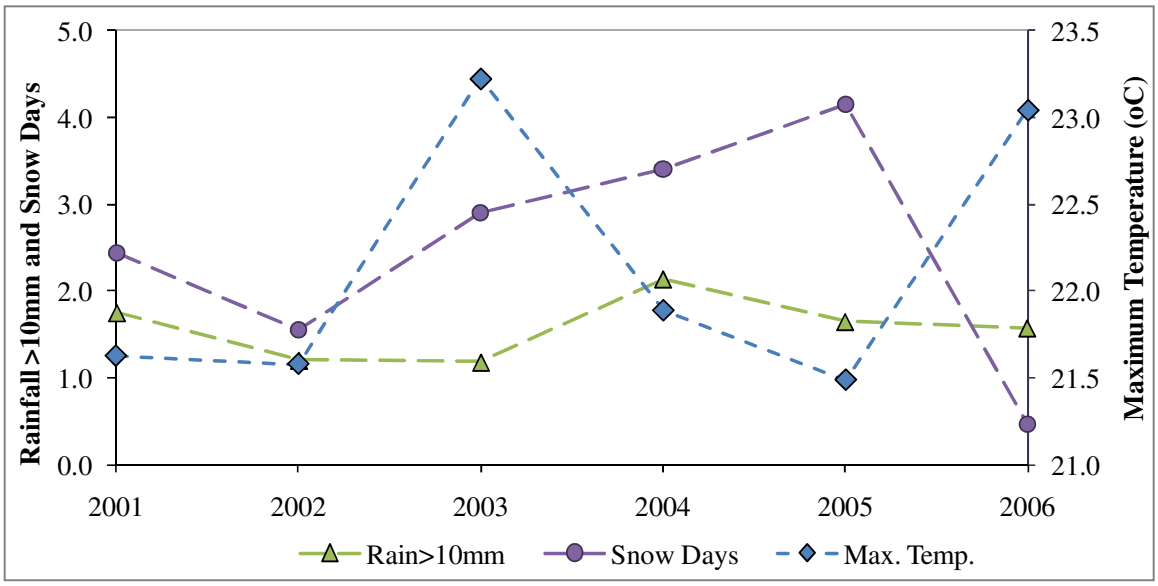

Figure 5.9: Mean Plots of Number of Days with Rainfall greater than 10mm, Snow Days and Mean Daily Maximum Summer Temperature.

5.3.3.3 Pavement Temperature

The climate variable TPmax given in the proposed rut depth model structures in Equations 4.5, 4.6 and 4.7 is defined as the asphalt temperature at 20mm below the pavement surface. The UKCP09 gridded observed datasets however gives air temperature measured at 1.5m above ground level.

Several models for calculating pavement temperature from air temperature based on the energy balance concept have been developed (Hermansson, 2000; Hermansson, 2001; Solaimanian and Kennedy, 1993; Robinson, 1985). Most of these models however require a large amount of input data. Consequently, a generalised model based on latitude of the road section, maximum air temperature and the depth below the pavement surface was used. The model is given in Equation 5.1 (Asphalt Institute, 2003).

$$TP_{max} = \left(T_{s(max)} + 17.8\right)(1 - 2.48 \times 10^{-3}d + 1.085 \times 10^{-5}d^2 - 2.441 \times 10^{-8}d^3) - 17.8 \quad (5.1)$$

where TPmax is the pavement temperature at depth (d) of 20mm in ^{o}C, $T_{s(max)}$ is the maximum pavement surface temperature in ^{o}C and is derived from maximum air temperature T_{air} in ^{o}C using Equation 5.2. Latitude is the geographical latitude of the road section (Asphalt Institute, 2003).

$$T_{s(max)} = T_{air(max)} - 0.001618 \times \text{Latitude}^2 + 0.2289 \times \text{Latitude} + 24.4 \quad (5.2)$$

5.3.3.4 Observed Climate Data Accuracy

The gridded climate data used in the study were based on records from weather stations. The data were collated and developed to a gridded format using the method set out in Perry and Hollis (2005). The observations made at weather stations were subjected to a rigorous quality control procedure with substitutions made for data that were missing or of poor quality. This information was then used to produce observed climate data for the UK at 5km by 5km spatial resolution (Perry and Hollis, 2005).

The gridded data were verified using actual observations made at stations that were not used in the gridding process. The verification stations were randomly selected. Table 5.10 shows the Root Mean Square Error (RMSE) derived following the verification process for each monthly climate variable (Perry and Hollis, 2005). The RMSE values are low for most values except the total precipitation climate variable, this suggest that the approach adopted to derive the gridded datasets was robust.

Table 5.7: Monthly Gridded Observed Climate Variables

Climate Variable	RMSE at Verification Stations
Mean daily maximum temperature	0.66
Sunshine duration	0.33
Total precipitation	16
Days of rain ≥10 mm	0.78
Days of snow lying	1.1

RMSE = Root Mean Square Error

Source (Perry and Hollis, 2005)

5.3.4 Heavy Vehicle Speed

Heavy vehicle speed (sh) is one of the explanatory variables of the proposed improved rut depth models given in Equations 4.5 to 4.7 in Chapter 4. Heavy vehicle speed data for each road sub-section was required for estimating the model coefficients for the heavy vehicle speed variable. Subsequent sections discuss the source of sample speed data, the scope of the sample obtained and the accuracy of the data.

5.3.4.1 Data Source and Measurement

Vehicle speed data was obtained from Highways Agency Traffic Information System Database (HATRIS). The data was collected using speed measuring equipment based on vehicle detectors located at several stations on the study road network. The speed collection equipment uses pairs of inductive loops which are installed in the road surface and connected to a detector unit fastened to convenient road furniture (DMRB TA22/81). The system distinguishes heavy vehicles from light vehicles using predefined vehicle lengths. Speed measurements were performed every hour for 24 hours and reported in miles per hour (HATRIS, 2011).

5.3.4.2 Sampled Heavy Vehicle Speed

Sampled heavy vehicle speed data comprised annual average spot speed values from 2001 to 2006 for speed measurement sites located on the study road sections. Figure 5.10 shows the location of the speed measurement sites within the study road network.

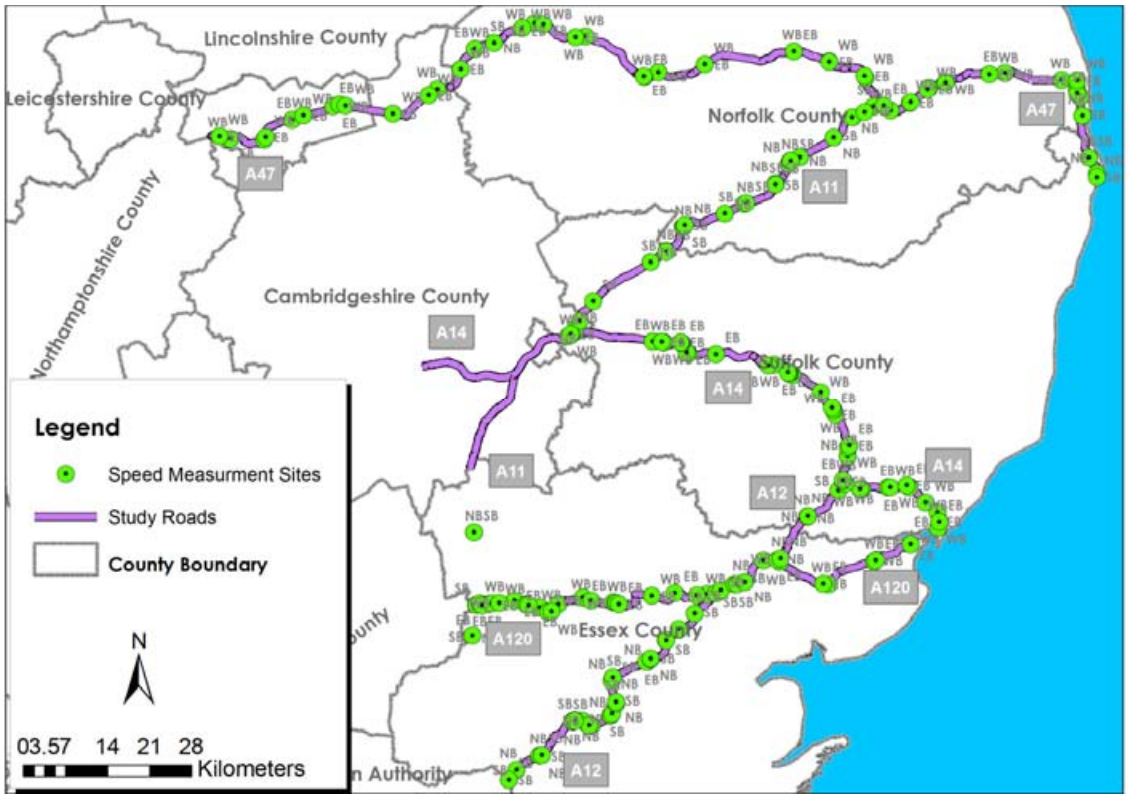

Figure 5.10: Highways Agency Vehicle Speed Measurement Sites within the Study Road Network (EB = East Bound, WB = West Bound, NB = North Bound, SB = South Bound)

The summary statistics of the sampled heavy vehicle speed data by road and year in which the data was collected together with the number of locations at which speed measurements were made is given in Table 5.8.

Table 5.8: Summary of Heavy Vehicle Speed Data Sample

	Road Name	Number of Sites Speed Measured	Mean Speed (km/h)	Minimum Speed (km/h)	Maximum Speed (km/h)	Skewness	Kurtosis
2001	A11	34	83.22	32.9	101.3	1.51	-1.42
	A12	79	78.62	18.0	108.9	0.00	-0.84
	A120	53	85.54	53.3	104.6	-0.82	-0.57
	A14	64	83.92	37.9	107.0	0.75	-1.16
	A47	65	80.96	53.4	104.8	-1.11	-0.10
2002	A11	34	82.09	32.9	101.3	1.68	-1.36
	A12	79	78.13	18.0	114.2	0.06	-0.81
	A120	53	85.57	53.3	104.6	-0.82	-0.58
	A14	64	83.18	37.9	105.0	0.62	-1.14
	A47	65	80.17	53.4	102.7	-1.03	-0.06
2003	A11	34	82.97	32.9	101.3	1.86	-1.48
	A12	79	78.08	18.0	109.1	-0.09	-0.79
	A120	53	85.20	53.3	104.6	-0.76	-0.57
	A14	64	83.17	37.9	107.3	0.70	-1.15
	A47	65	81.33	53.4	109.3	-0.79	-0.04
2004	A11	34	84.03	32.9	101.3	1.85	-1.55
	A12	79	78.01	18.0	108.9	0.10	-0.88
	A120	53	85.07	53.3	104.6	-0.71	-0.61
	A14	64	83.04	37.9	106.7	0.67	-1.14
	A47	65	80.62	53.4	102.7	-1.00	-0.16
2005	A11	34	83.66	32.9	101.5	2.65	-1.65
	A12	79	77.59	16.0	109.1	1.04	-1.08
	A120	53	85.13	54.4	104.6	-0.88	-0.55
	A14	64	83.71	37.1	104.1	0.57	-1.13
	A47	65	80.07	55.4	102.7	-1.15	0.04
2006	A11	34	83.38	32.9	100.8	0.92	-1.35
	A12	79	78.60	15.6	109.2	0.25	-0.92
	A120	53	85.89	52.6	104.6	-0.87	-0.54
	A14	64	84.10	37.2	104.4	0.22	-1.03
	A47	65	81.00	54.4	102.7	-1.20	-0.15

The distribution of average annual heavy vehicle speeds measurements on all sites on the study road network is shown in Figure 5.11.

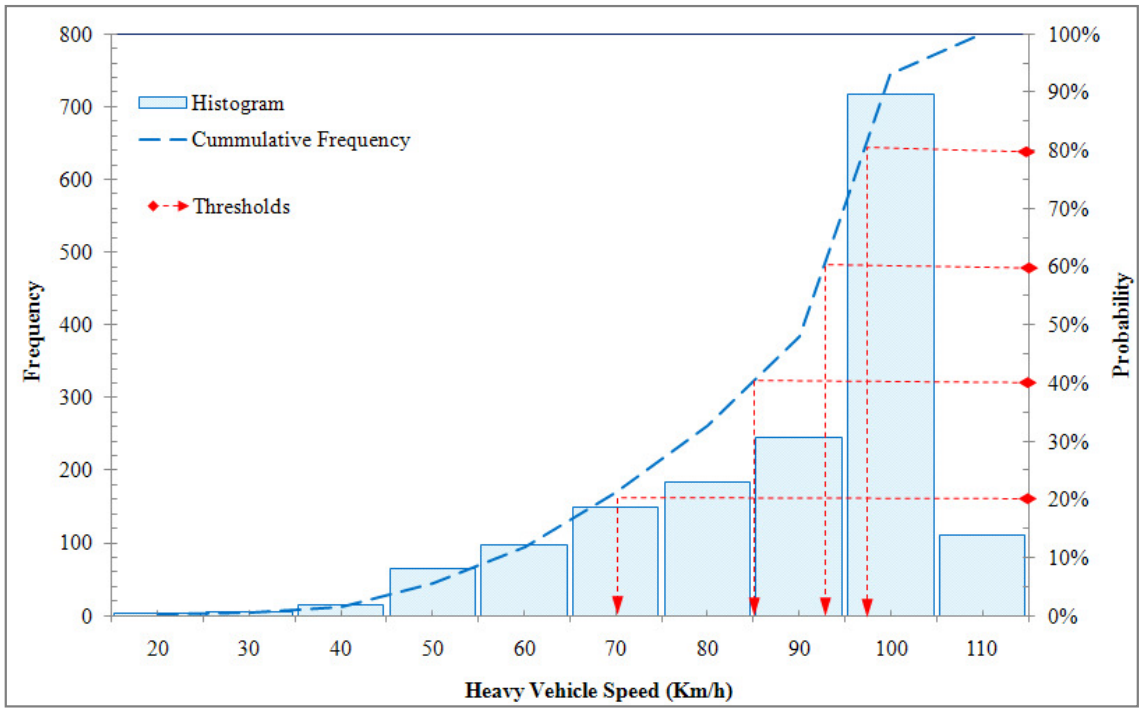

Figure 5.11: Average Annual Heavy Vehicle Speed Distribution on the Study Road Network

The spot speeds measured at locations shown in Figure 5.10,and summarised in Table 5.8 and Figure 5.11 were transformed to speeds along the study road sections using a Geographic Information System (ArcGIS). Each road section on the study network was assigned heavy vehicle speed measurements made at sites closest to that road section provided the following conditions were satisfied: the measurement site is located on the same traffic flow direction as the road section, and both the speed measurement sites and road sections are located on the same road link. A spatial illustration of average heavy vehicle speed at road sections in 5 bands is given in Figure 5.12. The 5 bands were based on threshold values corresponding to the 20^{th}, 40^{th}, 60^{th}, and 80^{th} percentile heavy vehicle speeds as illustrated in Figure 5.11. Similar maps for road section speeds averaged over each year from 2001 to 2006 are given in Appendix B4.

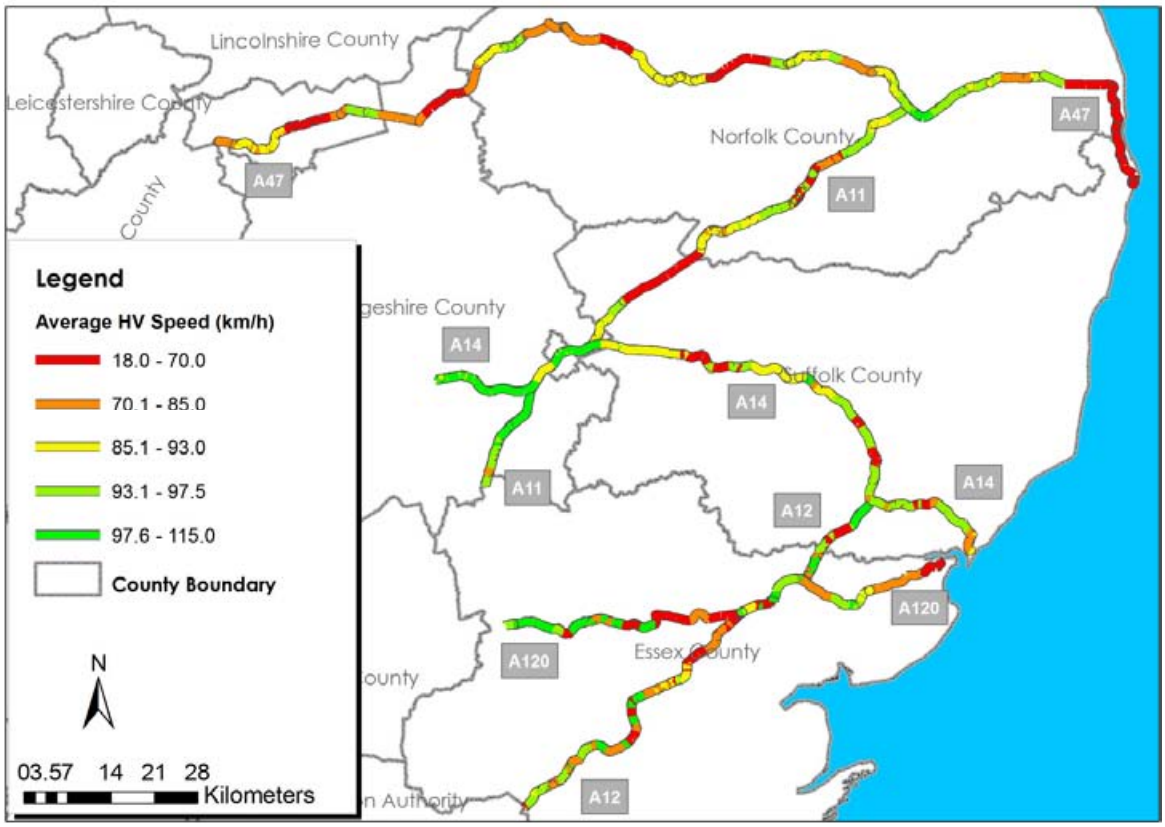

Figure 5.12: Spatial Representation of Average Speed of Heavy Vehicles.

5.3.4.3 Reliability and Accuracy of Vehicle Speed Data

Vehicle speeds vary in time and space. To account for the time variability of heavy vehicle speeds, data obtained comprised measurements at each site on the study network over a 24 hour period, on different days of the week, on several months and in different years from 2001 to 2006. Spatial variability was accounted for by the location of the speed measurement sites (Figure 5.10) and the number of measurement sites on the project roads (Table 5.8). Errors in the measurement speeds using vehicle detectors are possible from the way in which the recording device is set up, and the way the data are processed prior to loading to the HATRIS database (DMRB TA22/81, 1981).

Given that repeated measurement of speeds were made every year (from 2001 to 2006) at fixed locations on the study road network, it is reasonable to assume that the annual average heavy vehicle speed at each speed measurement site located on a given road, for example A47, in a particular year, for example 2003, is not significantly different from speeds observed at the same location in other years from 2001 to 2006. Significant differences in the speeds observed at each site in the different years for which data was collected could be as a result of errors in the data obtained or other unknown factors such as change in speed limit regulations or significant growth in traffic leading to incidences of congestion. To that end, the heavy vehicle speed samples grouped by road and year were assessed for consistency using one-way Analysis of Variance (ANOVA) statistical tests.

One-way ANOVA is parametric tests, therefore assumptions of normality and homocesdasticity or homogeneity of variance across data sets should be observed. To achieve normality, the data set summarised in Table 5.8 was transformed using the Box Cox power transformation algorithm (Box and Cox, 1964 and Osborne, 2010) of the form given in Equation 5.3.

$$\mathrm{sh}(\lambda) = \begin{cases} \frac{\mathrm{Sh}^{\lambda}-1}{\lambda * \mathrm{GM}^{\lambda-1}}; \text{if } \lambda \neq 0 \\ \mathrm{GM} * \mathrm{LOG}(\mathrm{Sh}); \text{if } \lambda = 0 \end{cases} \tag{5.3}$$

where sh is heavy vehicle speed, GM is the geometric mean of the data sample and λ is the transformation variable that minimises the sum of squares of residuals. The values of λ and GM were determined for each data set on a particular road using a statistics software and are summarised in Appendix B5. Descriptive statistics including skewness and excess kurtosis for the transformed data is presented in Appendix B5.

Homogeneity of variance was investigated by calculating Levene's statistics. The results of the tests are summarised in Table 5.9. The assumption of equal variances between the heavy vehicle speed measured on sites or sections on each road from 2001 to 2006 is valid since the p-values of the Levene's statistics for each set of data are greater than the 0.05 rejection level for all groups of data.

Table 5.9: Levene Tests Results for Homogeneity of Variance of Heavy Vehicle Speed Data

Parameter	**A11 (2001 – 2006)**	**A12 (2001 – 2006)**	**A120 (2001 – 2006)**	**A14 (2001 – 2006)**	**A47 (2001 – 2006)**
Levene Statistic	0.223	0.088	0.205	0.222	0.185
Significance (p-value)	0.952	0.994	0.960	0.953	0.968

Following the validation of the normality and homocesdasticity assumptions, it is possible to proceed with ANOVA hypothesis test. The null hypothesis Ho was:

Ho: $\mu_{sh2001} = \mu_{sh2002} = \mu_{sh2003} = \mu_{sh2004} = \mu_{sh2005} = \mu_{sh2006}$

This is stated as in a given year from 2001 to 2006, there is no significant difference in mean heavy vehicle speed (sh) observed on particular site or road section on the study road network compared to heavy vehicle speed observed on the same site or road section in other years from 2001 to 2006.

The alternative hypothesis Ha is stated as, in a given year from 2001 to 2006, there is a significant difference in heavy vehicle speed (sh) observed on particular site or road section on the study road network compared to heavy vehicle speed observed on the same site or road section in other years from 2001 to 2006.

A statistical significance level of $\alpha = 0.05$ or the 95% confidence level was used to determine if the null hypothesis should be rejected. If as illustrated in Figure 5.13 the probability (p) that the null hypothesis is true determined from the F distribution is greater than $\alpha = 0.05$ then Ho should be accepted and Ha rejected. If the probability (p) is less than α, then Ho should be rejected and Ha accepted. Alternatively, if the calculated F statistics is less than the critical value of F, then Ho should be accepted, otherwise Ha should be accepted.

The results of the ANOVA test summarised in Table 5.10 indicates that Ho should be accepted which suggests that the sampled heavy speed data are consistent across the years (2001 to 2006) in which the data were sampled.

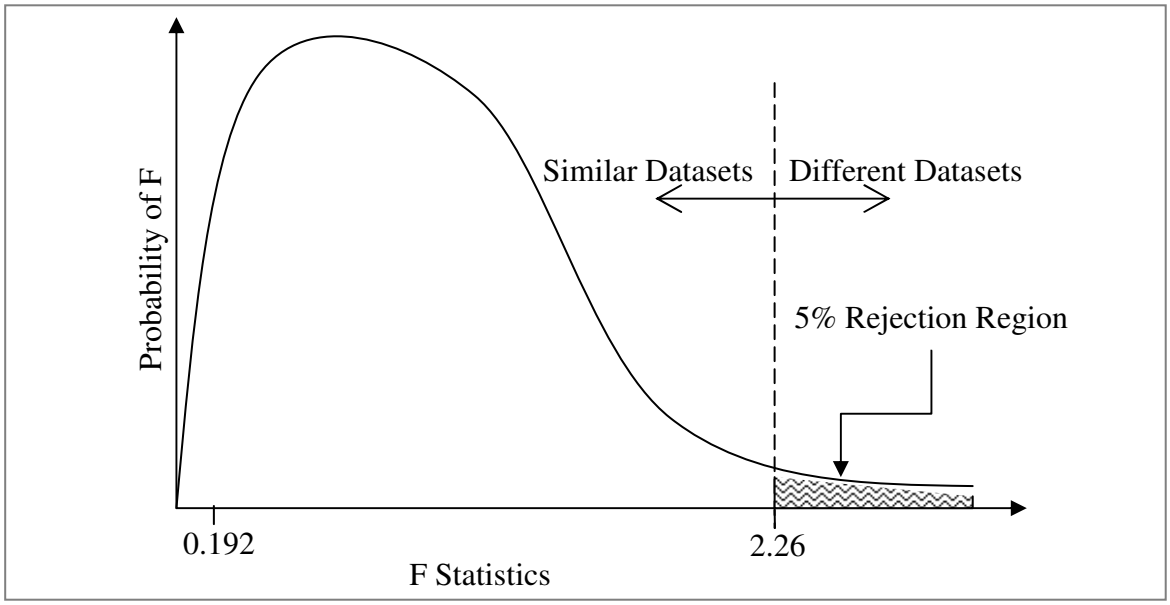

Figure 5.13: Interpretation of ANOVA results

Table 5.10: ANOVA results for Heavy Vehicle Speed Data

Road	Data Groupings	Sum of Squares	DF	Mean Square	F Statistics	Significance (p-value)	F Critical
A11	Between Years	196.506	5	39.301	0.192	0.965	2.26
	Within Years	40,559.48	198	204.846			
A12	Between Years	434.333	5	86.867	0.207	0.96	2.23
	Within Years	196,476.05	468	419.821			
A120	Between Years	197.197	5	39.439	0.176	0.972	2.24
	Within Years	70,028.78	312	224.451			
A14	Between Years	124.427	5	24.885	0.115	0.989	2.24
	Within Years	81,461.00	378	215.505			
A47	Between Years	44.959	5	8.992	0.048	0.999	2.24
	Within Years	72,502.40	384	188.808			

1. DF is the degree of freedom given as n-1, where n is number of years for which data samples were obtained (6 datasets Between Years from 2001 to 2006), and the total number of observations within each data set (Within Years).
2. The F statistics and significance values were calculated using SPSS software.
3. The critical F values corresponding to the degrees of freedom were obtained from the F table.

5.3.5 Traffic Loading

The implication of traffic loading on rutting was represented in the proposed model structures given in Chapter 4 using the annual number of equivalent standard axles (YE4) in millions per lane. YE4 on each road sub-section on the study road network was calculated using Equation 5.4 from traffic flow data and information obtained from HAPMS and DMRB.

$$YE4_{it} = \sum_{k=1}^{K} \frac{365 * F_{ikt} * W_k * GF_t * P_i}{10^6} \quad (5.4)$$

where F_{ikt} is the Average Annual Daily Traffic (AADT) of commercial vehicles class *k* in one direction on road section *i* during year *t*, W_k is the structural wear factor of commercial vehicle class *k*, GF is a traffic growth factor for adjusting existing traffic flow data to a desired year *t* and P_i is the proportion of commercial vehicles on heavily loaded lane of road section *i*.

5.3.5.1 Traffic Flow Data

The AADT of commercial vehicles (F) on each section of the study road network was obtained from HAPMS. Traffic flow data is measured using the same vehicle detector equipment used for speed measurement. The traffic flow data on the study road network is presented using a map of the study road network in Figure 5.14. It is apparent from the map that the A14 and A12 routes are subjected to the highest traffic flow. This perhaps is because these roads provide access to the largest container port in the UK located at Felixstowe.

The traffic flow data were categorised into the following three commercial vehicle classes: Other Goods Vehicle 1 (OGV1), Other Goods Vehicle 2 (OGV2), and Public Service Vehicles (PSV) in accordance with guidance given in the Design Manual for Roads and Bridges (DMRB HD 24/06, 2006).

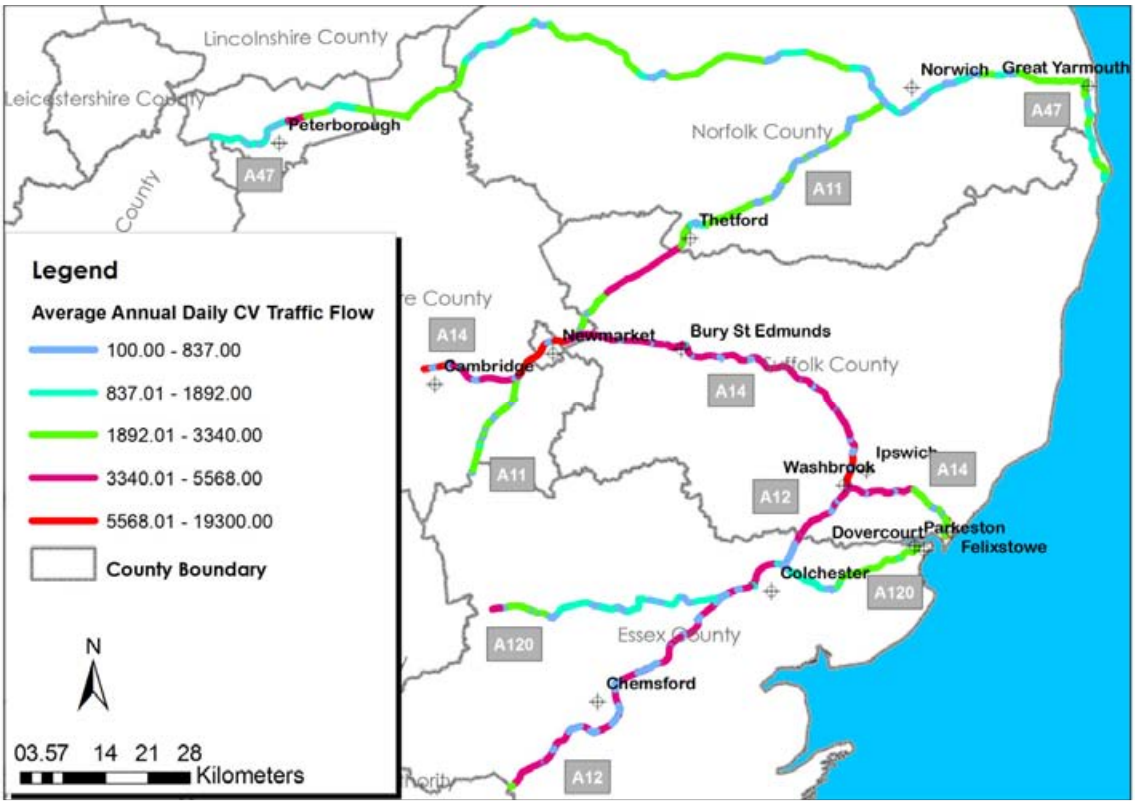

Figure 5.14: Spatial Representation of Commercial Vehicle Average Annual Daily Flow

5.3.5.2 Wear Factors

Wear factors are a measure of road pavement structural wear in the UK. The factors were formulated on the basis that the structural wear of road pavement is proportional to the 4th power of the axle load in accordance with Equation 5.5 (DMRB HD 24/06, 2006).

$$W_k = \sum_{i=1}^{I_k} PV_{ki} \sum_{j=1}^{J_k} \left(\frac{AXL_{kij}}{SAXL_j}\right)^4 \quad (5.5)$$

where W_k is the wear factor for commercial vehicle category k, I_k is the number of subgroups i of vehicles within a particular commercial vehicle category, PV_{ki} is the percentage of vehicles in subgroup i of category k, J_k is the number of axles per vehicle of type k, AXL_{kij} is the average load in tonnes on axle j of load range i in vehicle category k, and $SAXL_j$ is the

standard single axle load of axle load group type j taken as 8 tonnes in the UK according to DMRB HD 24/06 (2006).

Data used to determine the wear factors were collected from 12 sites located throughout the UK trunk road network and are recommended for use in the UK including within the study road network (Atkinson et al., 2006, DMRB HD24/06, 2006). The wear factors adopted for this study are given in Table 5.11 for the three commercial vehicle categories.

Table 5.11: Wear Factors by Commercial Vehicle Class

Commercial Vehicle Category (k)	**CV Classification by weight and Axles**	**Wear Factors**
Buses and Coaches **(PSV)**	Greater than 3.5 tonnes gross weight	0.6
Other Goods Vehicle 1 **(OGV 1)**	2 axles rigid	0.6
	3 axles rigid	
Other Goods Vehicles 2 **(OGV 2)**	3 axles articulated	3.0
	4 axles rigid	
	4 or more axles articulated	

Adopted from DMRB HD 24/04 (2006).

5.3.5.3 Traffic Growth Factors

The commercial vehicle traffic flow discussed in section 5.3.5.1 were collected on particular years on each road section, traffic growth rates obtained from DMRB HD24/06 (2006) were applied to derive flows in periods corresponding to years 2001 to 2006 for which rut depth and climate data were available. The growth rates are based on National Road Traffic Forecasts (NRTF) (DMRB HD24/06, 2006).

5.3.5.4 Number of Equivalent Standard Axle Loads

The annual number of equivalent standard axle loads (YE4) on each road section was calculated using Equation 5.4 for each year from 2001 to 2006. Average YE4 values over the period from 2001 to 2006 for each section of road are spatially illustrated in Figure 5.15. Descriptive statistics summarising the distribution of YE4 values by road link are given in Appendix B6.

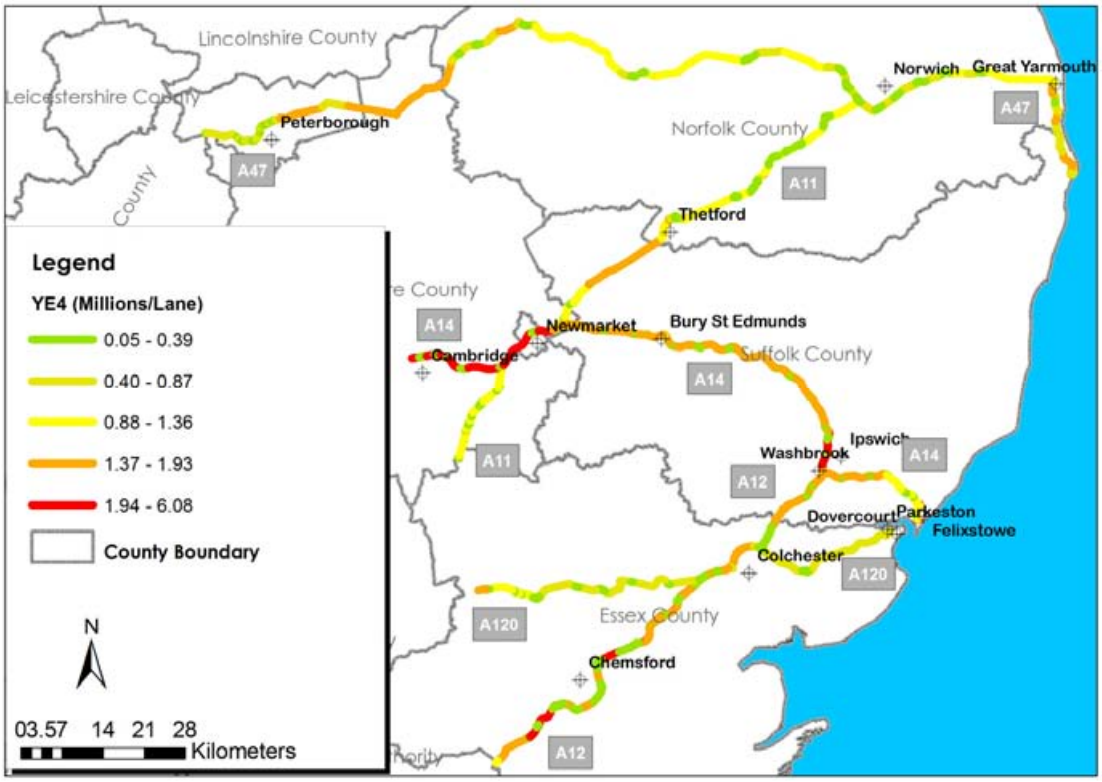

Figure 5.15: Spatial Representation of Average Equivalent Standard Axle Loads in Millions per lane

5.3.6 Road Gradient

The effect of road geometry on rutting is represented in the proposed model structures discussed in Chapter 4 using the gradient of road sub-sections.

5.3.6.1 Sampled Road Gradient Data

Road gradient data is collected on the study road network as part of the TRACS survey. The survey vehicle records road gradient at 5m intervals in percentages. The collected data is processed and stored on the HAPMS against each road sub-section. The sampled gradient data is illustrated in Figure 5.16.

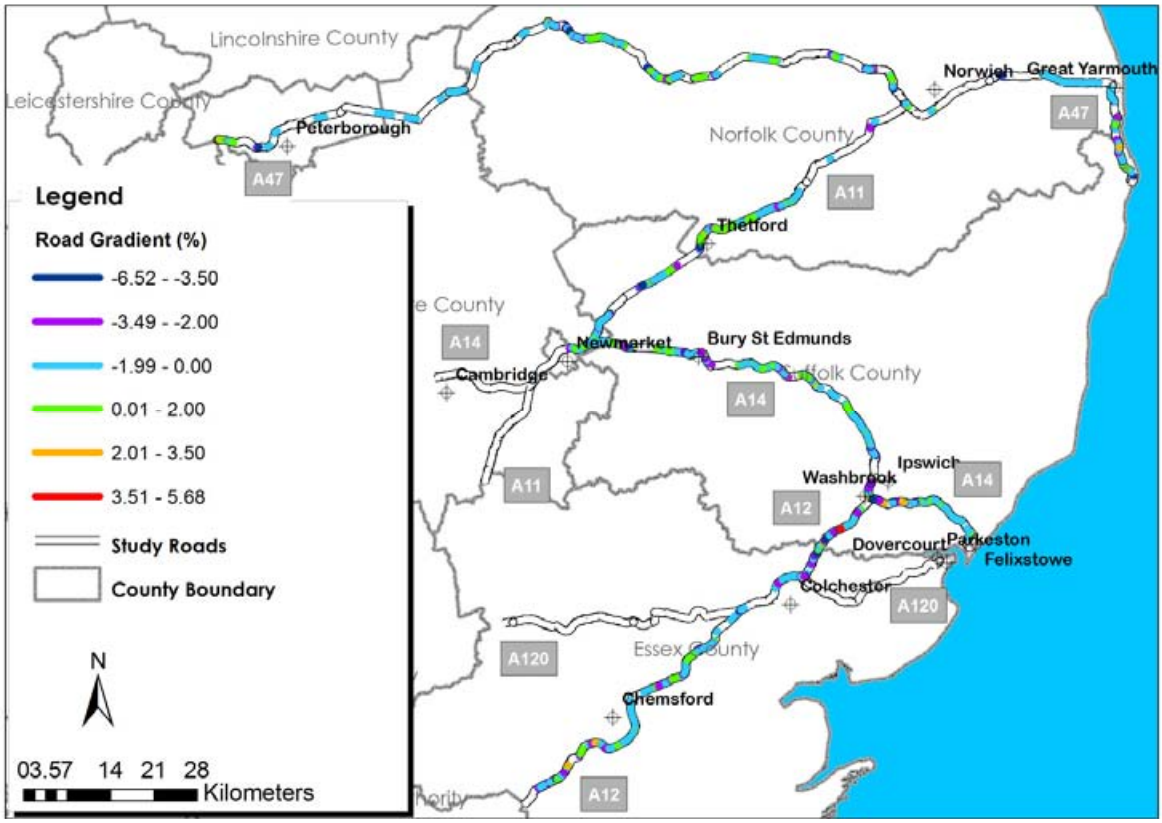

Figure 5.16: Spatial Representation of Road Gradient

5.3.6.2 Accuracy and Reliability of Gradient Data

The TRACS survey process is subjected to rigorous accreditation and acceptance testing as described in section 5.3.2.3. Gaps in the collected data are however possible in cases where the data are found to unreliable prior to loading in HAPMS or when the survey vehicle is forced to drive off lane due to obstructions such as road works. Road sections with missing

gradient data were not used in the study. Uncoloured sections of the study road in Figure 5.16 indicate road sections for which gradient data were missing.

5.3.7 Asphalt Surfacing Thickness

Asphalt surfacing thickness (HS) was included as an explanatory variable in the improved rut depth prediction model structures given as Equations 4.5, 4.6 and 4.7. As noted in section 2.4, rutting on trunk roads in England is limited to the asphalt layer. The data necessary for determining the model coefficient of this variable was elicited for each road sub-section on the study road network from HAPMS. Annual time series of asphalt thickness in millimetres on road sub-sections on the study road network from 2001 to 2006 were determined by examining the following:

- The pavement structure comprising pavement layers and material type;
- Pavement maintenance history including treatment type (e.g. overlay);
- The date the treatment was applied; and
- The thickness of each layer.

The pavement structure on each road sub-section comprised one of the following types:

- Fully Flexible (FF) pavement;
- Flexible Composite (FC) pavement; and
- Rigid pavement.

These pavement types are illustrated in Figure 5.17. Total Asphalt thickness was obtained on Fully Flexible and Flexible Composite pavement sub-sections shown in Figure 5.18. The

figure provides a spatial representation of the pavement types on the study road network together with the surfacing material type on each road sub-section.

The most predominant asphalt surfacing types on the study road network are Dense Bituminous Macadam (DBM), Hot Rolled Asphalt (HRA) and Thin Surface Course System (TSCS). These are the three asphalt surfacing types that were considered in the development of the rut depth prediction model. Other surfacing types on the study road network included Pavement Quality Concrete (PQC) and Porous Asphalt.

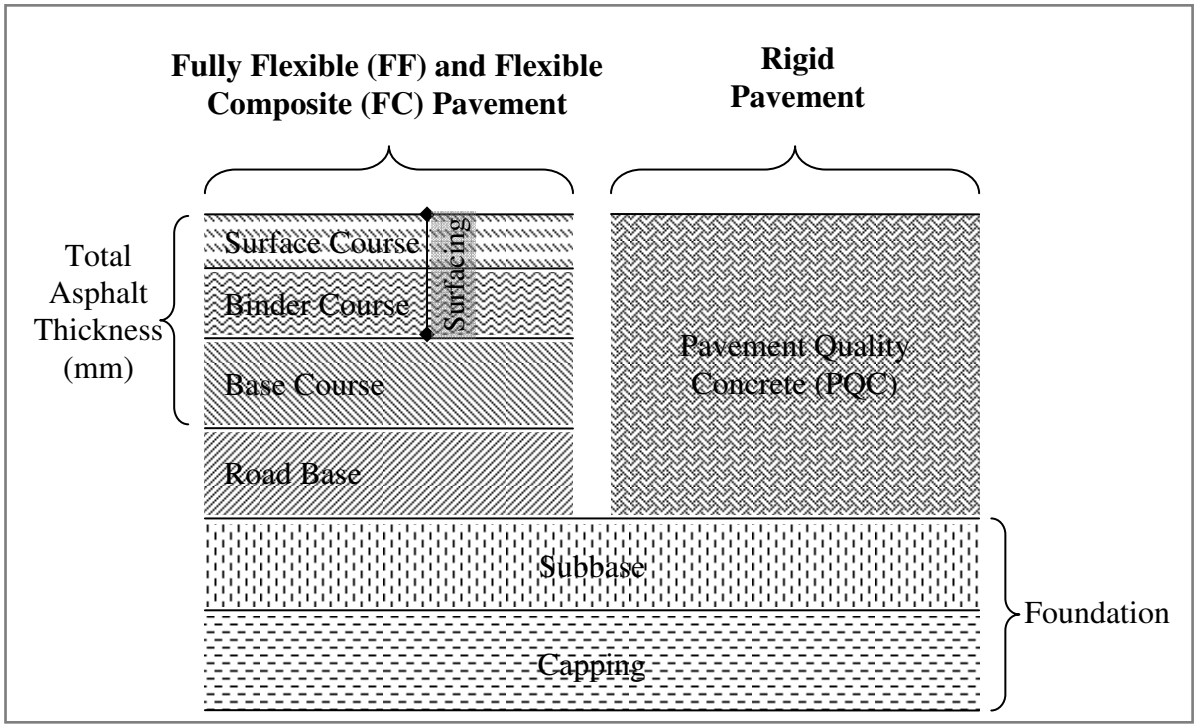

Figure 5.17: Pavement Types on the Study Road Network

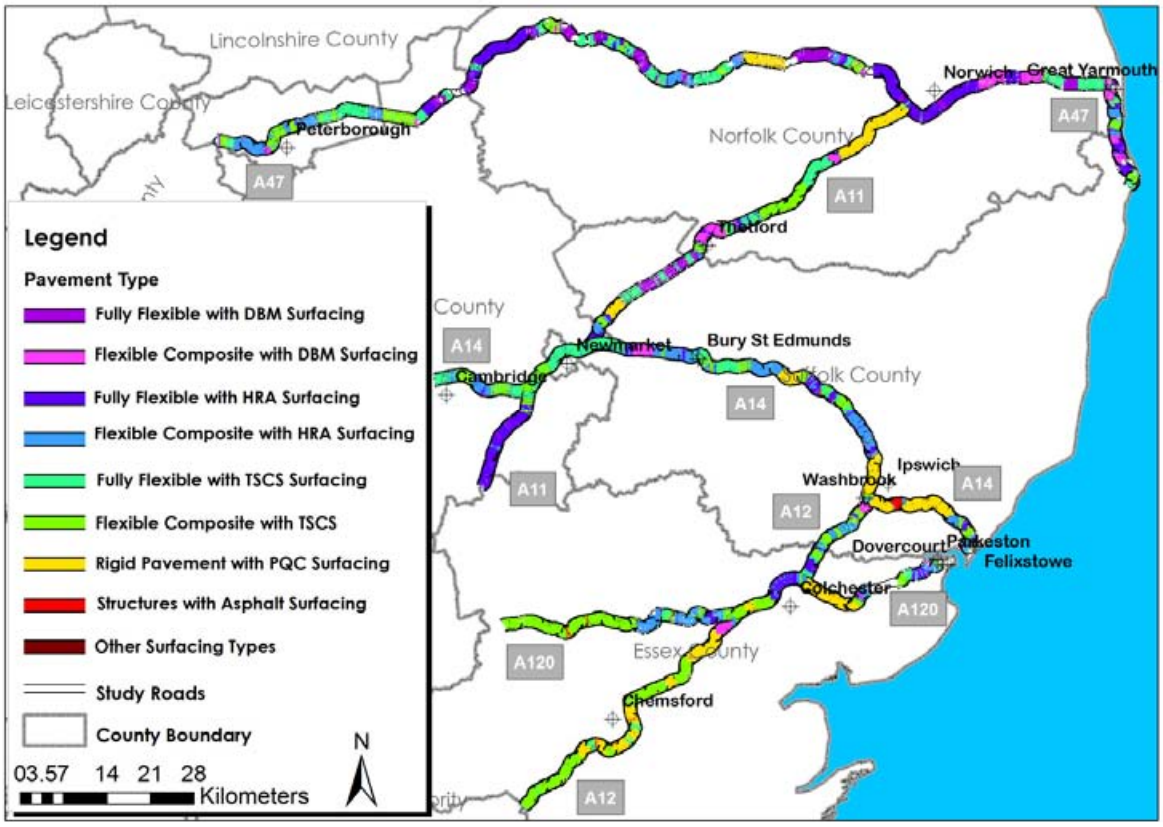

Figure 5.18: Pavement and Surfacing Types on the Study Road Network

5.3.8 Asphalt Material Properties

The effect of properties of asphalt surfacing material was represented in the improved model structures given in Equations 4.5, 4.6 and 4.7 using binder Softening Point (SP) and Voids in Mix (VIM). SP is the temperature in degrees Celsius at which bitumen attains a certain consistency while VIM is the proportion in percentage air voids in the asphalt mix.

It was assumed in Chapter 4 that for in-service roads with asphalt surfacing, SP and VIM vary with the surfacing age. Required data were obtained from trial studies and are presented in subsequent sections.

5.3.8.1 Binder Softening Point

Softening point data obtained is categorised as Thin Surface Course Systems (TSCS) data and other asphalt (HRA and DBM) data.

5.3.8.1.1 Thin Surface Course Systems Binder Softening Point

Softening Point data for TSCS was obtained from results of six years of performance monitoring of various types of in-service TSCS materials (Nicholls et al., 2002; Nicholls and Carswell, 2004; Nicholls et al., 2007). The data is detailed in Appendix B7 and summarised in Figure 5.19. SP were determined from cores taken from the trial road sections located on trunk roads in the United Kingdom. A total of 62 data points were recorded over the six years of monitoring.

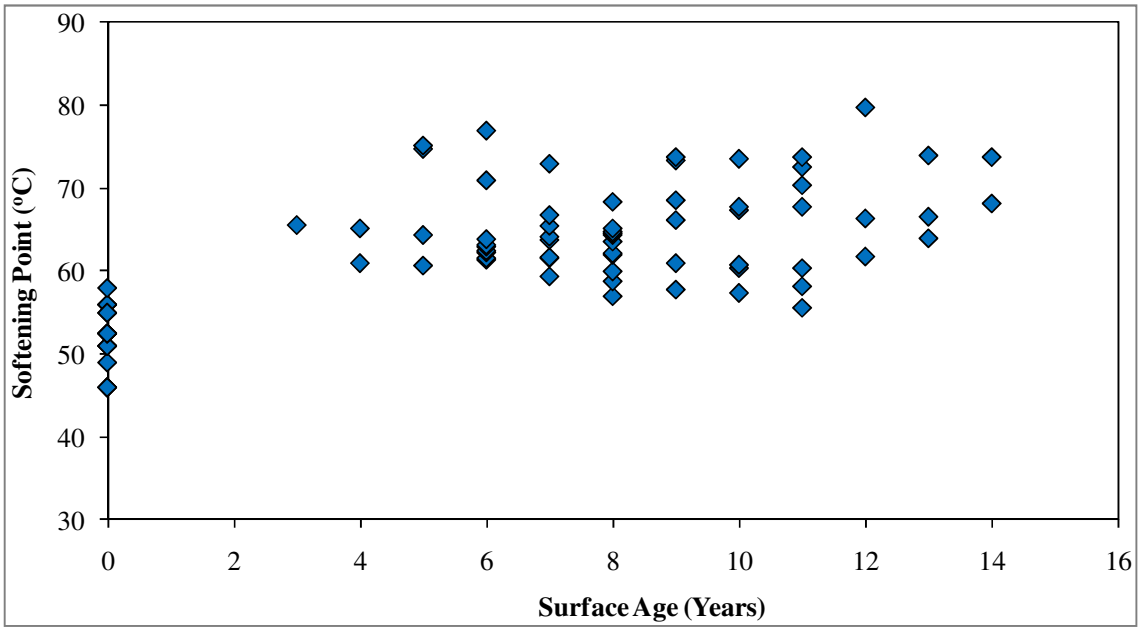

Figure 5.19: Summary of In-service TSCS Binder Softening Point with Age

Typical design specification for binder softening point for TSCS is given in Table 5.12. The design/initial values together with softening point data presented in Figure 5.19 were used to derive representative binder softening point values for each study road sub-sections with TSCS surfacing using the approach set out in section 5.3.8.1.3.

Table 5.12: Typical Initial/Design Values for TSCS Softening Point

Type of TSCS	**Typical Range of Initial/Design Softening Point (^{o}C)**
Paver – Laid Surface Dressing Systems (PLSD)	41 – 51
Thin Asphalt Concrete (TAC)	43 – 65
Thin Stone Mastic Asphalt (TSMA)	58 - 70

Source (Nicholls et al., 2002).

5.3.8.1.2 Other Asphalt Surfacing Materials

Softening Point data for Dense Bitumen Macadam (DBM) and Hot Rolled Asphalt (HRA) surfacing were derived from results several studies undertaken in the UK (Chaddock and Pledge, 1994; Daines, 1992; Nunn et al., 1997). The data are given in Appendix B7 and summarised in Figure 5.20.

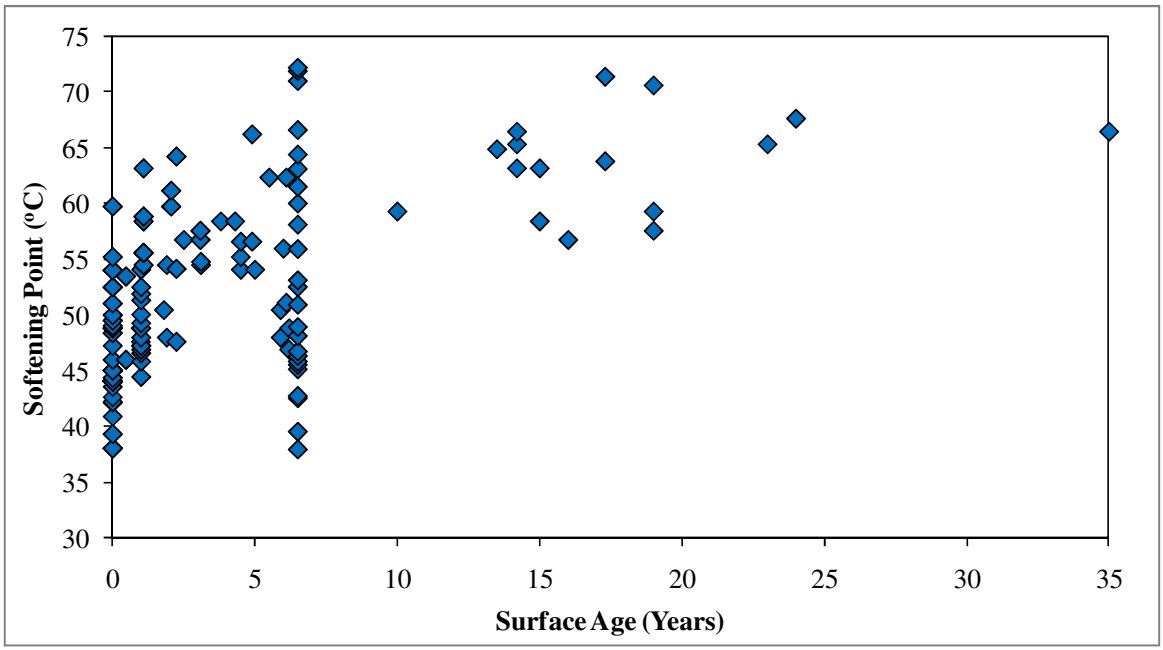

Figure 5.20: Summary of In-service Asphalt Binder Softening Point with Asphalt Surface Age

Typical design specification for binder softening point for HRA and DBM is given in Table 5.13. The design/initial values together with softening point data presented in Figure 5.20 were used to derive representative binder softening point values for each study road sub-sections with HRA or DBM surfacing using the approach set out in section 5.3.8.1.3.

Table 5.13: Typical Initial or Design Values for HRA and DBM Softening Point

Type	**Typical Range of Design Softening Point (^{o}C)**
Hot Rolled Asphalt (HRA)	41 – 64
Dense Bitumen Macadam (DBM)	33 – 51

Source (Hunter, 1994; Hunter 2000)

5.3.8.1.3 Associating Binder Softening Point Data to Study Road Sections

The binder softening point data recorded on trial sections were analysed to determine annual increase in softening point with age of the surfacing relative to the observed initial softening point values. The derived annualised changed in softening point values are given in Appendix B7 and are summarised in Figure 5.21 and Figure 5.22 for TSCS and other asphalt surfacing types (DBM, and HRA) respectively.

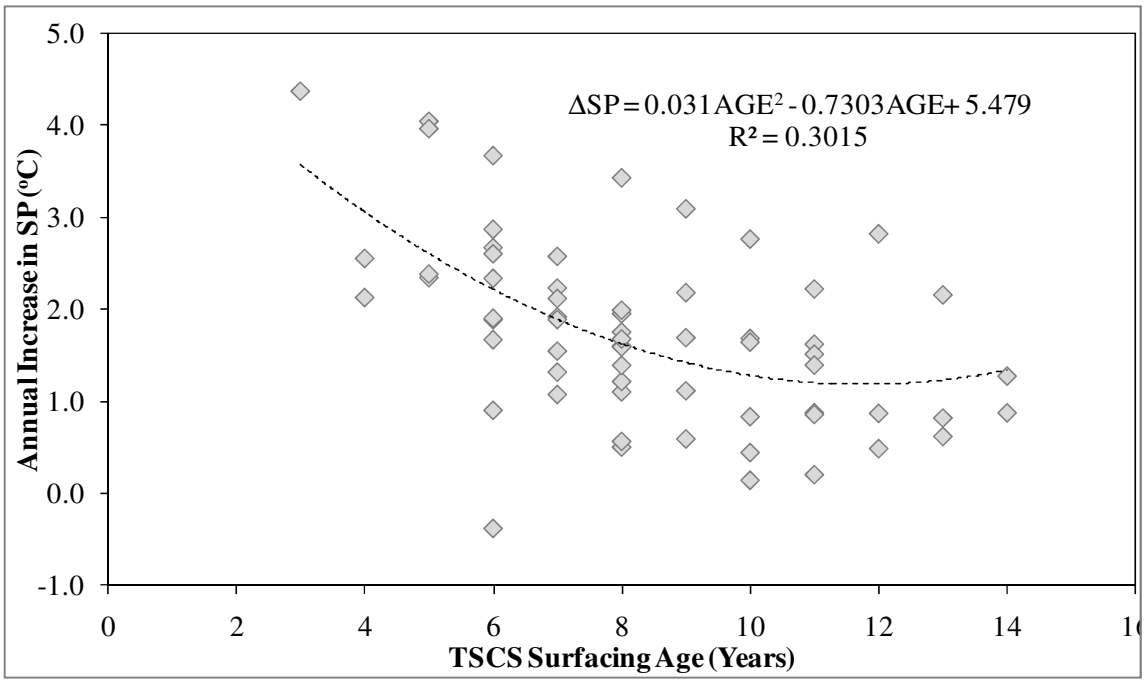

Figure 5.21: TSCS Annual Rate of Change of Binder Softening Point with Surfacing Age

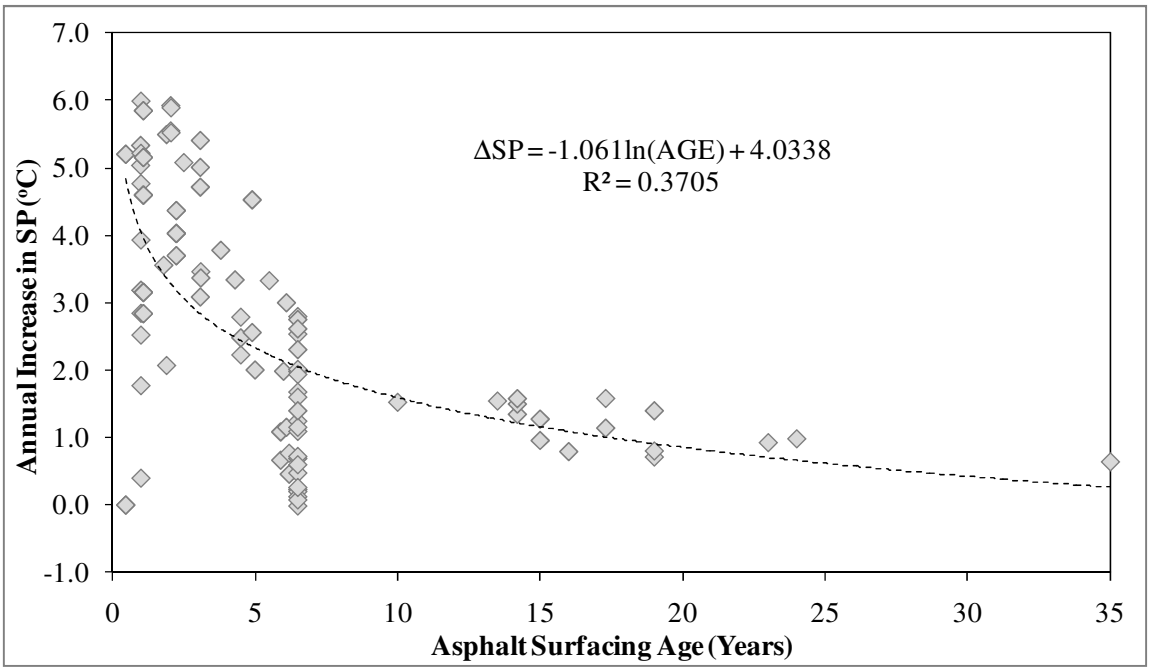

Figure 5.22: Combined HRA and DBM Annual Rate of Change of Binder Softening Point with Surfacing Age

It is apparent from the scatter plots in Figure 5.21 and Figure 5.22 that the annualised softening point values generally decrease with age of asphalt surfacing albeit with low correlation coefficients (R = 0.30 and 0.37 respectively). This correlation is not adequate to justify associating the observed binder softening point data to the study road sub-sections using a regression equation.

Instead, the annual increase in SP data was grouped into three surface age ranges and data in each group were fitted to statistical models. The fitted statistical models are given in Table 5.14 and Table 5.15 for TSCS and other surfacing types, respectively. The fit of the data to the statistical models was assessed using the Kolmogorov – Smirnov (K-S) tests. The results of the K-S test also given in Table 5.14 and Table 5.15 shows that the assumed statistical models are appropriate for describing the datasets since, the probability (P-value) of the K-S statistic is higher than critical values at the 0.05 confidence level.

Table 5.14: Distributions of Annual Rate of Change of TSCS Binder Softening Point

Surface Age (Years)	Sample Size	Fitted Distribution		Kolmogorov-Smirnov Tests		
		Type	Parameters	Statistics	P-Value	Critical Value at 0.05 Level
0 – 6	16	Normal	$\mu = 2.640, \sigma = 0.946$	0.176	0.639	0.327
7 – 9	25	Normal	$\mu = 1.666, \sigma = 0.676$	0.083	0.990	0.264
>9	21	Log Normal	$\mu = -0.023, \sigma = 0.770$	0.169	0.532	0.287

Where μ = Mean and σ = Standard Deviation

Table 5.15: Distributions of Annual Rate of Change of HRA and DBM Binder Softening Point

Surface Age (Years)	Sample Size	Fitted Distribution		Kolmogorov-Smirnov Tests		
		Type	Parameters	Statistics	P-Value	Critical Value at 0.05 Level
0 – 1.9	37	Normal	$\mu = 4.833, \sigma = 2.613$	0.112	0.700	0.218
2 – 6.2	33	Normal	$\mu = 3.438, \sigma = 1.563$	0.079	0.945	0.231
>6.2	40	Log Normal	$\mu = 1.290, \sigma = 0.0.201, \gamma = -2.477$	0.071	0.980	0.210

Where μ = Mean, σ = Standard Deviation and γ = Location Parameter

The observed SP data was associated to the study road sub-sections using Equation 5.6.

$$SP_{imG} = SPD_m + \sum_{g=1}^{G} \Delta SP_{mg} \quad (5.6)$$

where SP_{imG} = absolute binder softening point in ^oC for study road sub-section i with asphalt surfacing type m of age G, SPD_m is the design or initial binder softening point for surface type m taken from Table 5.12 or Table 5.13, ΔSP is the observed annual increase in softening point for surface type m in year g obtained through random sampling from statistical distributions given in Table 5.14 and Table 5.15.

5.3.8.2 Voids in Mix Data

Void in Mix (VIM) is defined as the total volume of air between binder coated aggregate particles of a compacted asphalt mixture (Hunter, 2000). VIM data by asphalt surfacing type and age was obtained from studies undertaken by Harun and Morosuik (1995) on six sites. A summary of the mean percentage voids in mix obtained after taking several cores from each site is given in Figure 5.23.

Typical initial/design values of VIM for TSCS, HRA and DBM are given in Table 5.16. The initial/design values together with VIM data from in-service roads and presented in Figure 5.23 were used to associate representative VIM values to each study road sub-sections as discussed in subsequent paragraphs.

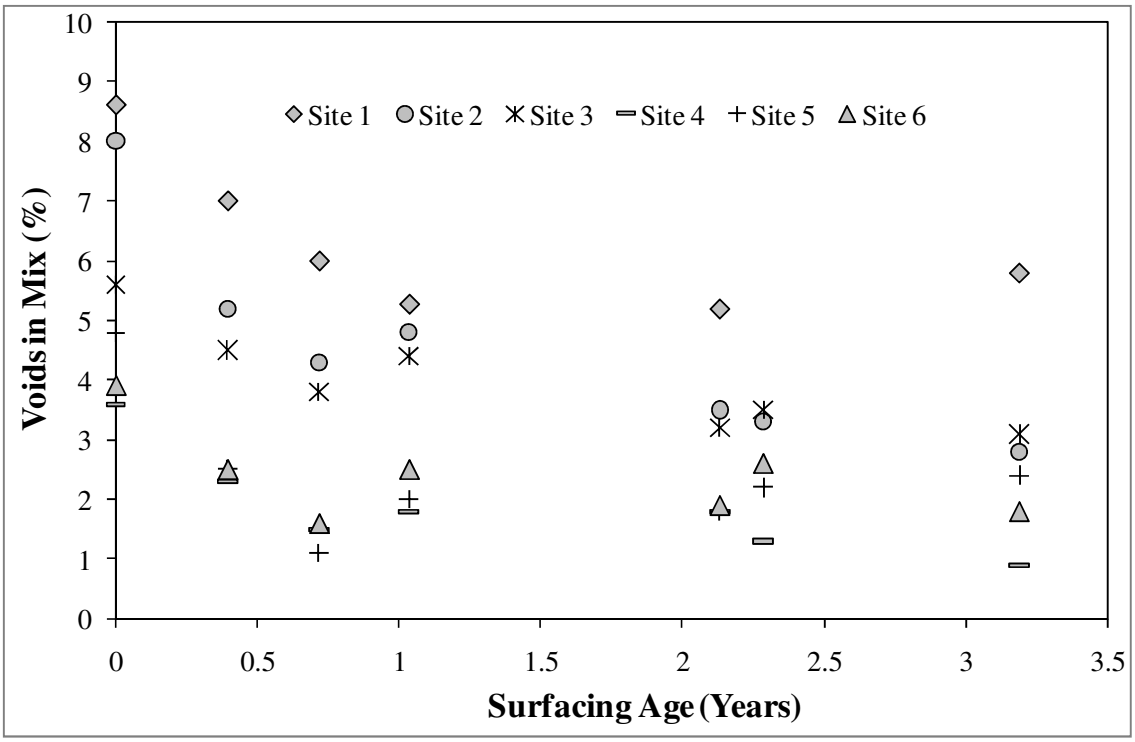

Figure 5.23: In-service Voids in Mix by Asphalt Surfacing Age

Table 5.16: Typical Initial/ Design Values for Voids in Mix

Description of Surfacing Material		Typical Voids In Mix (%)	
		Range	Mean
Thin Surface Course System[1]	Paver – Laid Surface Dressing Systems (PLSD)	-	6.9
	Thin Asphalt Concrete (TAC)	4.6 - 9.0	7.3
	Thin Stone Mastic Asphalt (TSMA)	2.5 – 6.2	4.0
Hot Rolled Asphalt[2]		-	3
Dense Bitumen Macadam[2]		-	8

1. Source: Nicholls et al., 2002.
2. Source: Hunter, 1994.

The observed VIM data (summarised in Figure 5.23) was analysed to determine the percentage annual rate of change in VIM relative to the initial voids in mix at year zero. The results of this analysis are illustrated in Figure 5.24. The data suggests that the percentage annual rate of change in VIM generally increases with increase in surfacing age. A correlation coefficient of 0.197 was achieved using the logarithmic relationship shown in Figure 5.24. The low correlation together with the high variability in the percentage annual change in VIM suggests that using the logarithmic relationship for deriving VIM on study road sections could produce outputs that are not representative of in-service pavement performance.

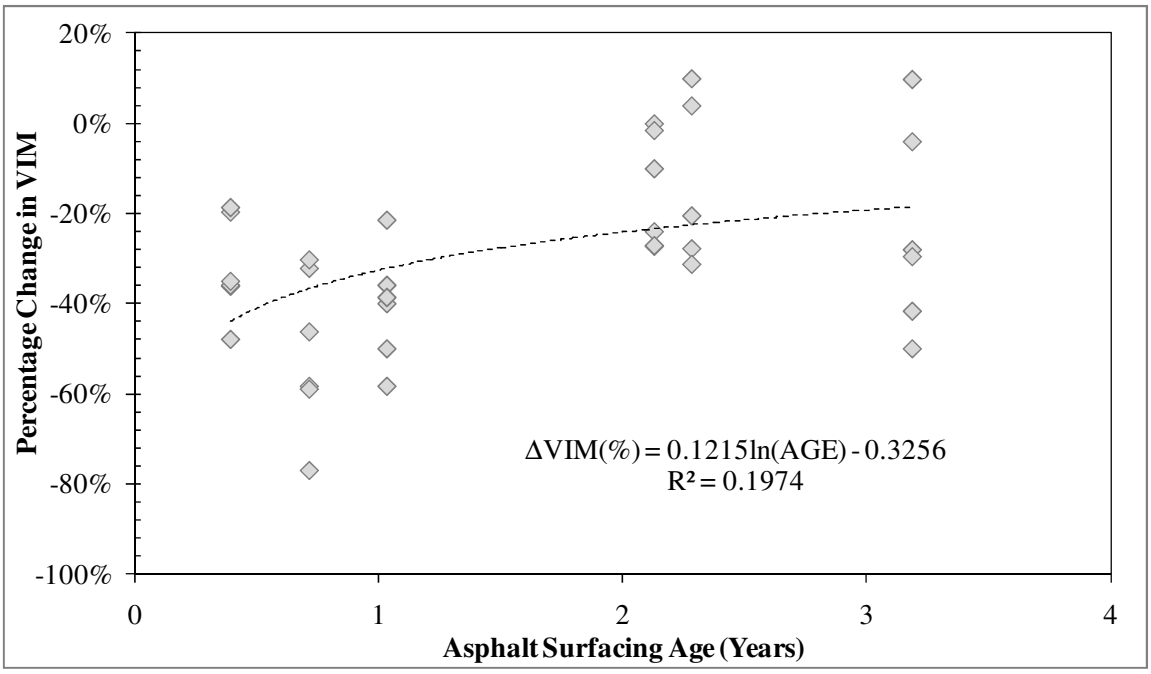

Figure 5.24: Percentage Annual Rate of Change of Voids in Mix with Asphalt Surfacing Age

In order to incorporate the variability of the observed percentage change in VIM to the study road sub-sections, the data was arranged into two surface age groups (less than 1 year old and greater than 1 year old). Statistical models were then fitted to the two groups of data. The assumed models together with the results of the Kolmogorov – Sminorvov (K-S) goodness of fit tests are given in Table 5.17. The results of the K-S test shows that the assumed statistical models are appropriate for describing the datasets since the p-value of the K-S statistics is higher than the critical values.

Table 5.17: Distributions of Annual Rate of Change of Voids in Mix

Age (Years)	Sample Size	Fitted Distribution		Kolmogorov-Smirnov Tests		
		Type	Parameters	Statistics	P-Value	Critical Value at 0.05 Level
0 – 1	18	Log Normal	μ = -0.450, σ = 0.170 k = -0.505	0.115	0.950	0.309
>1	17	Generalised Extreme Value	μ = -0.248, σ = 0.174, k = -0.191	0.150	0.789	0.318

Where μ = Mean, σ = Standard Deviation, and k = Shape Parameter

The observed VIM data was associated to the study road sub-sections using Equation 5.7.

$$VIM_{imG} = VIMD_m\left(1 + \sum_{g=1}^{G} \Delta VIM(\%)_g\right) \quad (5.7)$$

where VIM_{imG} = Voids in Mix for study road sub-section *i* with asphalt surfacing type *m* of age *G*, $VIMD_m$ is the initial Voids in Mix for surface type *m* assumed equivalent to the typical initial/design Voids in Mix given in Table 5.19, $\Delta VIM(\%)_g$ is the observed percentage annual rate of change in *VIM* in year *g* obtained through random sampling from statistical distributions given in Table 5.17.

5.4 Preliminary Analysis of Climate Data and Annual Incremental Rut Depth

The preliminary analysis was aimed at comparing the annual incremental rut depths discussed in section 5.3.2.5.2 with the climate data presented in section 5.3.3. The objectives of this comparison were three fold:

- Firstly, to assess if the impact of the hot dry summer of 2003 was evident in the annual incremental rut depth data;
- Secondly, to show that the annual increment rut depths observed in 2003 were significantly different from observations in other years; and
- Finally, to investigate the frequency of the 2003-type hot dry summer within the baseline period from 1961 to 1990 and in future climate predictions.

The approach to the analysis was structured in three parts:

- Graphical comparison of annual incremental rut depths with climate variables;
- Analysis of Variance (ANOVA) comparison of incremental rut depths observed in 2003 with observations in other years; and
- Investigation of the frequency of observed and predicted climate scenario relevant to rut depth.

5.4.1 Graphical Comparison of Rut Depth and Climate Data

Based on discussions in section 2.4 higher rates of rutting should be observed in years with very hot summers such as that recorded in 2003. This claim was investigated using scatter plots of annual incremental rut depth against temperature, precipitation and snow related climate variables. Plots of precipitation and snow related climate variables with annual incremental rut depths were aimed at demonstrating that the trends of the resultant scatter plots were not consistent with the trend of plots of annual incremental rut depth and the temperature related variables.

The climate variables comprised:

- Mean daily maximum summer temperature;
- Rainfall intensity during the summer given as the average number of days during summer months with rainfall greater than 10mm;
- Number of days with snow lying during the year; and

- Average sunshine duration during summer months, mean monthly rainfall during the summer.

Scatter plots of annual incremental rut depths on road sections from 2002 to 2006 and corresponding climate variables are given in the Figures below. The comparisons of maximum summer temperature and summer sunshine duration with annual incremental rutting (Figure 5.25 and Figure 5.28) indicates a trend of increasing rates of rutting with increase in the values of these climate variables. The scatter plot for rainfall and incremental rut depth (Figure 5.29) shows higher rates of rutting with decreasing mean summer monthly rainfall. These observations suggest that the impact of the combination of hot and dry summers such as that recorded in 2003 are evident in asphalt rut depth data collected annually by the Highways Agency. Trends similar to those illustrated in Figure 5.25, Figure 5.28 and Figure 5.29 were not discernible when the number of days with snow lying and rainfall intensity were plotted with annual incremental rut depths (Figure 5.27 and Figure 5.26).

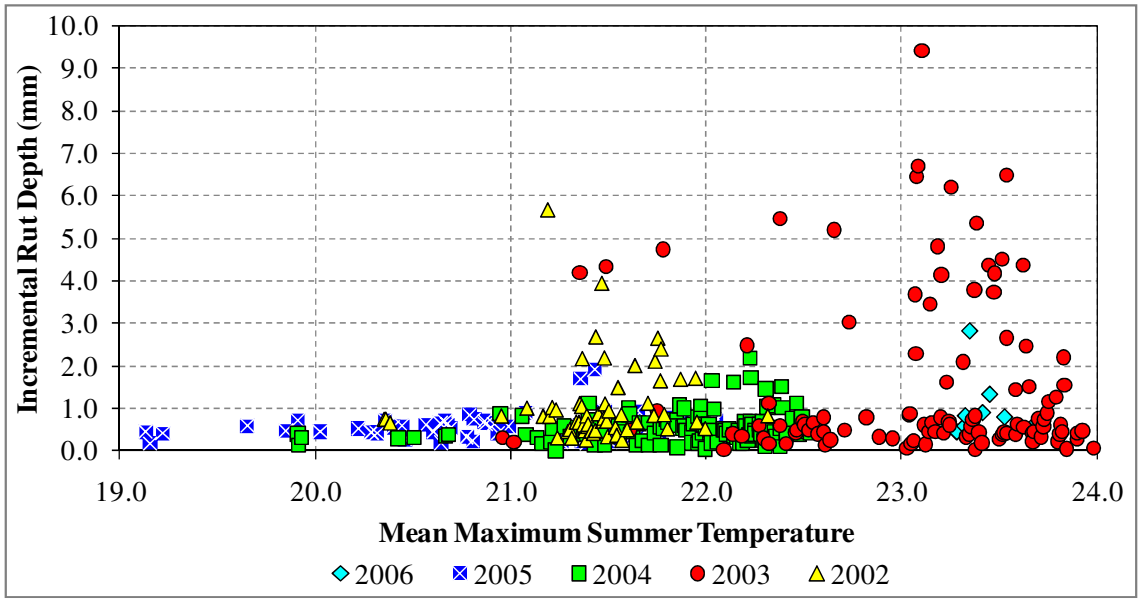

Figure 5.25: Comparison of Annual Incremental Rut Depth on Road Sections with corresponding Mean Summer Temperature

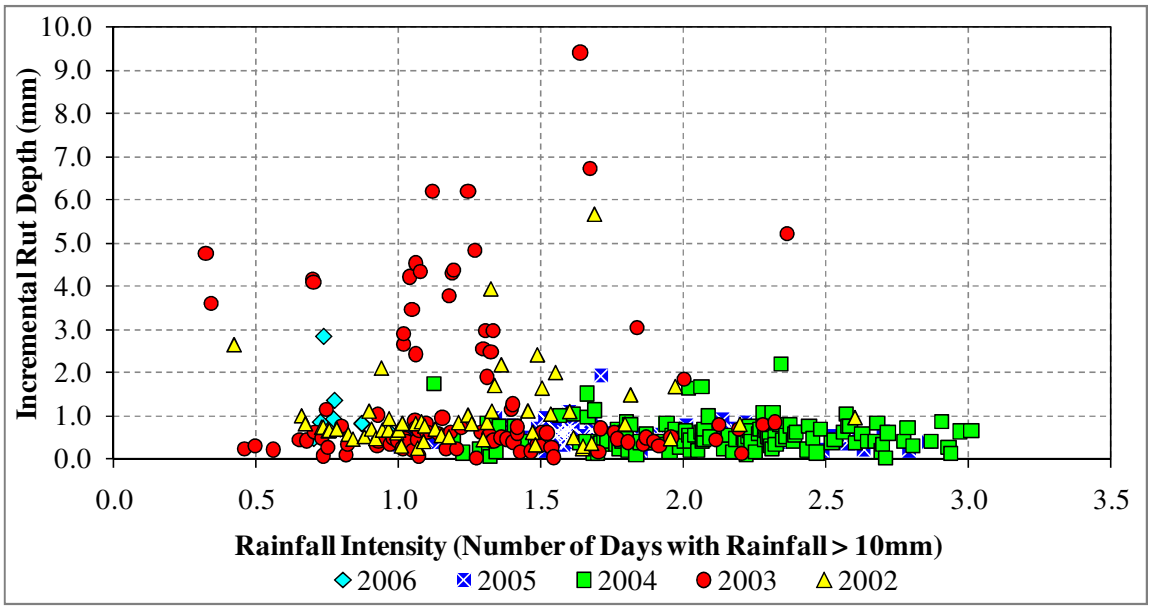

Figure 5.26: Comparison of Annual Incremental Rut Depth on Road sections with corresponding Rainfall Intensity

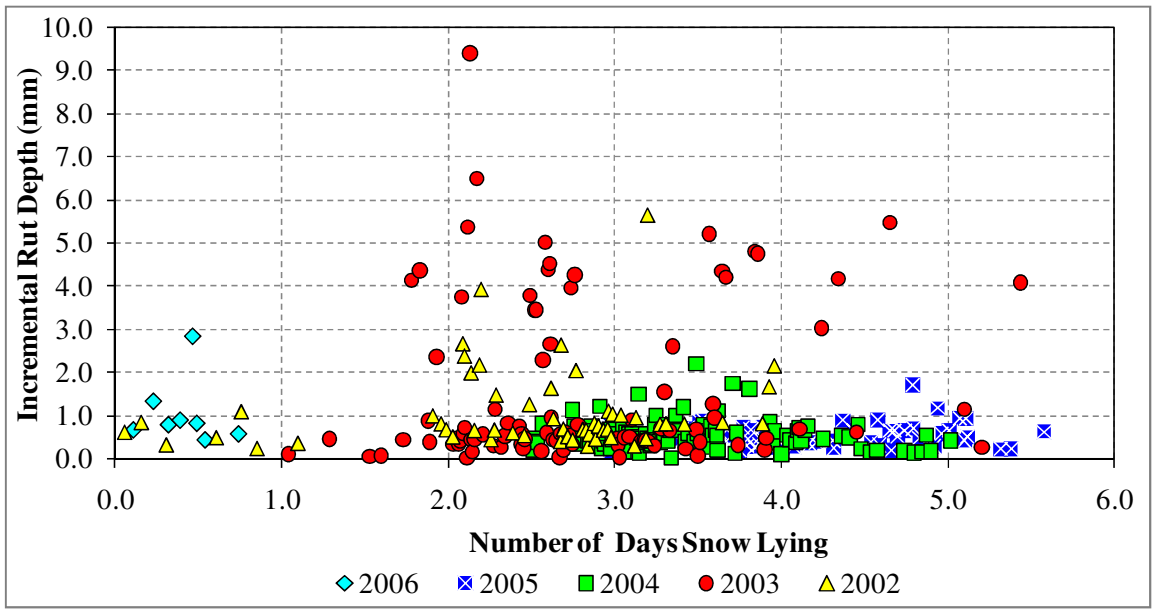

Figure 5.27: Comparison of Annual Incremental Rut Depth on Road Sections with corresponding Number of Days Snow Lying

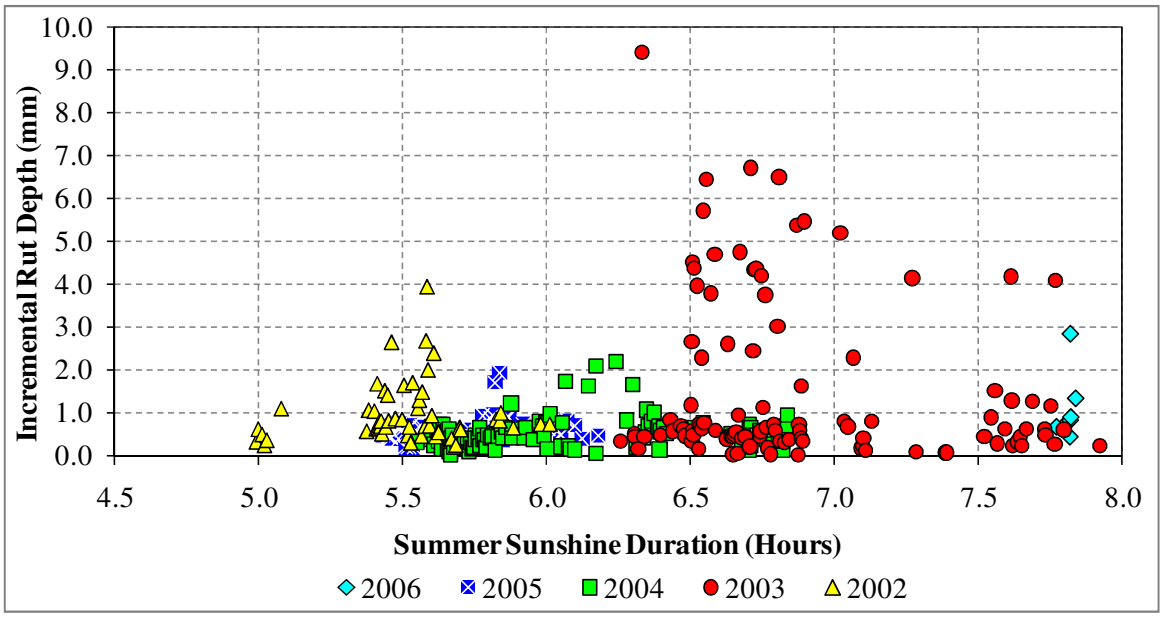

Figure 5.28: Comparison of Annual Incremental Rut Depth at Road Sections with corresponding Summer Sunshine Duration

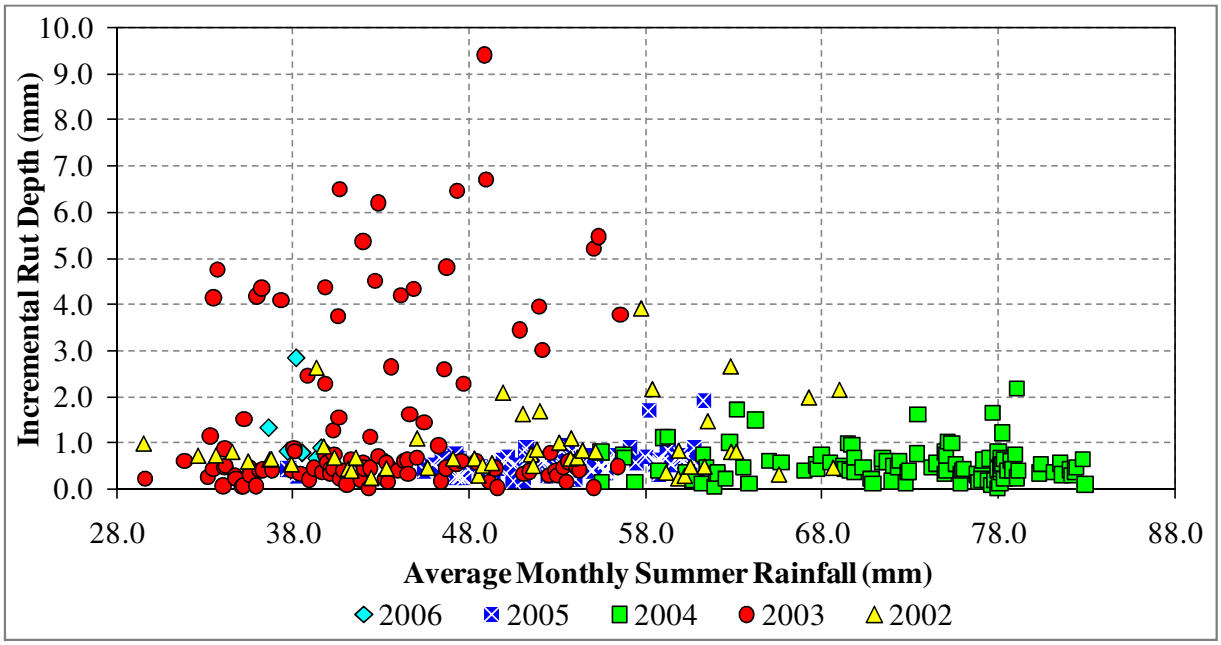

Figure 5.29: Comparison of Annual Incremental Rut Depth at Road Sections with corresponding Mean Monthly Summer Rainfall

5.4.2 Statistical Implication of Climate on Incremental Rut Depth

Following the graphical comparisons of annual incremental rutting rates with climate variables in the previous section, higher annual incremental rut depth rates were noted in the year 2003 which was characterised by a hot and dry summer. This section considers the statistical significance of this observation.

The analysis was done for 177 road sub-section samples obtained by filtering available data and selecting only those road sub-sections with valid annual incremental rut depth data in consecutive years including 2003. The observed climate in each year was represented using the concept of rainfall and temperature anomalies. Temperature and rainfall anomalies were calculated as the average difference between the mean maximum summer temperature and rainfall observed in a given year and the corresponding average maximum summer temperature and rainfall over the UKCIP climate baseline period from 1961 to 1990. Temperature anomalies are expressed in degrees Celsius while rainfall anomalies are expressed as a percentage of the baseline average rainfall. For a given geographical location or road section within the study area, a positive rainfall anomaly in a particular year indicates a wetter summer compared to the baseline period, while a negative anomaly indicates a dry summer. Similar inferences apply to temperature anomalies.

The filtered data is illustrated in Table 5.18 using 10 randomly selected road sub-section samples. Descriptive statistics of annual incremental rut depths for all 177 road sub-sections is given in Table 5.19.

Table 5.18: Sample Road Sections for Statistical Analysis

Section Label	Chainage		Pavement Type	Annual Incremental Rut Depth (mm)		
	Start (m)	End (m)		2005 [1°C, 4%]	2004 [1.3°C, 51%]	2003 [2.7°C, -15%]
2600A47/345	500	600	[HRA][FC]	0.74	0.144	3.809
2600A47/345	400	500	[HRA][FC]	0.41	0.437	4.356
0500A47/365	1100	1147	[TSCS(G)][FF]	0.258	0.072	0.121
0500A47/812	500	600	[TSCS(G)][FF]	0.295	0.401	0.252
2600A47/486	0	100	[HRA][FF]	0.643	0.188	0.271
2600A47/423	1400	1500	[DBM][FF]	1.127	0.225	0.669
2600A47/582	1000	1100	[HRA][FF]	0.629	0.117	0.438
2600A47/563	900	1000	[DBM][FF]	0.189	0.008	0.028
0535A47/715	500	600	[HRA][FF]	0.866	0.442	3.148
2600A47/325	0	100	[HRA][FF]	0.968	0.705	2.151

Notes to Table 5.18:

1. HRA = Hot Rolled Asphalt surfacing
2. DBM = Dense Bituminous Macadam surfacing
3. TSCS = Thin Surface Course System surfacing
4. FF = Fully Flexible pavement
5. FC = Flexible Composite pavement
6. [HRA][FC] = Hot Rolled Asphalt surfacing on a Flexible Composite pavement
7. [1°C, 4%] = A temperature anomaly of 1°C and a rainfall anomaly of 4%

Table 5.19: Descriptive Statistics of Annual Incremental Rut Depth Data Sample

Statistics	Data Set		
	2005 [1°C, 4%]	2004 [1.3°C, 51%]	2003 [2.7°C, -15%]
Mean	0.615	0.492	3.413
Standard Error	0.031	0.034	0.253
Median	0.564	0.378	2.359
Mode	0.410	0.144	0.438
Standard Deviation	0.419	0.454	3.360
Sample Variance	0.175	0.206	11.290
Excess Kurtosis	1.303	7.169	0.450
Skewness	0.959	2.097	1.113
Minimum	0.007	0.003	0.011
Maximum	2.334	3.186	14.170
Sample Size	177	177	177

The hypothesis tests used was the parametric Repeated Measures one-way Analysis of Variance (RM-ANOVA) since the annual incremental rut depth observations are repeated for each road subsection in all three data samples presented in Table 5.18 and Table 5.19.

The null hypothesis Ho is given as follows:

Ho: There are no significant differences in the mean annual incremental rut depth due to the hot dry summer of 2003 compared to observations in 2004 and 2005.

The alternative hypothesis Ha is stated as:

Ha: The mean of annual incremental rut depths observed in 2004 and 2005 significantly differ from that observed in 2003.

A step by step discussion of the calculations for the one-way RM-ANOVA with respect to this study is given in Appendix B8. The results of the tests revealed that at a 0.05 significance level, there are significant differences between paired samples 2005-2003 and 2004-2003. This implies that the most significant difference is between annual incremental rut depth samples observed in 2003 and the other two measured in 2004 and 2005. The null hypothesis Ho for the RM-ANOVA is therefore rejected in favour of the alternative hypothesis Ha that the mean of annual incremental rut depths observed in 2004 and 2005 differ from that recorded in 2003 due to the hot dry summer recorded in that year.

5.4.3 Frequency of Observed and Predicted Hot Dry Summer Years

Graphical comparisons and statistical analysis presented in the previous sections concluded that it is likely that the rates of asphalt surface rutting within the study area was generally higher in 2003 than in other years due to the effects of the hot dry summer recorded in that year. It is therefore important to ascertain if the frequency of such climate events are expected to increase within the study area compared to observations over the UKCIP climate baseline period from 1961 to 1990.

5.4.3.1 Frequency of Observed Hot Dry Summers

Mean maximum summer temperature anomalies were plotted against Average summer monthly rainfall anomalies for each year over the 30-Year baseline period from 1961 to 1990. Rainfall anomalies were computed as the difference between average monthly summer rainfall in a given year and the corresponding average over the baseline period. Temperature anomalies are defined as the difference between the average maximum summer temperature in a given year and the maximum summer temperature average over the UKCIP climate baseline period.

The plot of rainfall and temperature anomalies for the baseline period including plots of recent observations from 2002 to 2003 is presented in Figure 5.30. 1 in 30 years over the baseline period had a 2003 type hot dry summer.

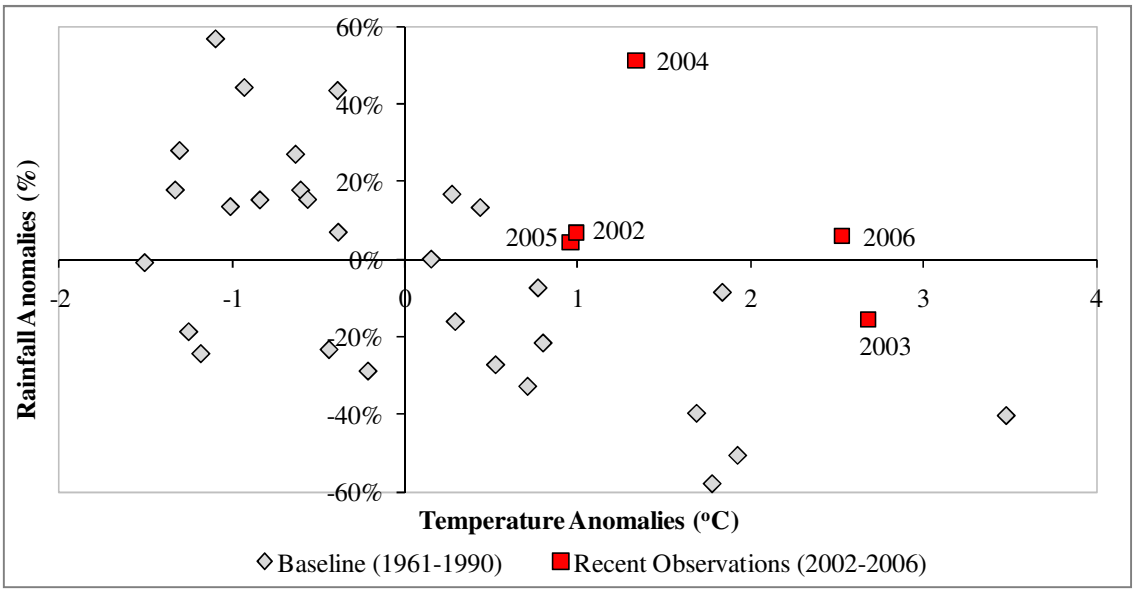

Figure 5.30: Comparison of Baseline (1961-1990) Rainfall and Temperature Anomalies with Recent Observations (2002-2006)

5.4.3.2 Frequency of Predicted Hot Dry Summers

Probabilistic predictions of summer rainfall and temperature anomalies for the study area were obtained from UKCP09 climate projections (Murphy et al., 2009) for three emission scenarios (High, Medium and Low) and four 30-year time slices (2020s[2011-2040], 2030s[2021-2050s], 2040s[2031-2060], 2050s[2041-2070]).

Scatter plots comparing random samples of predicted and recently observed rainfall and temperature anomalies are given in the Figures below. The frequencies of predicted 2003-type hot dry summers is summarised in Table 5.20.

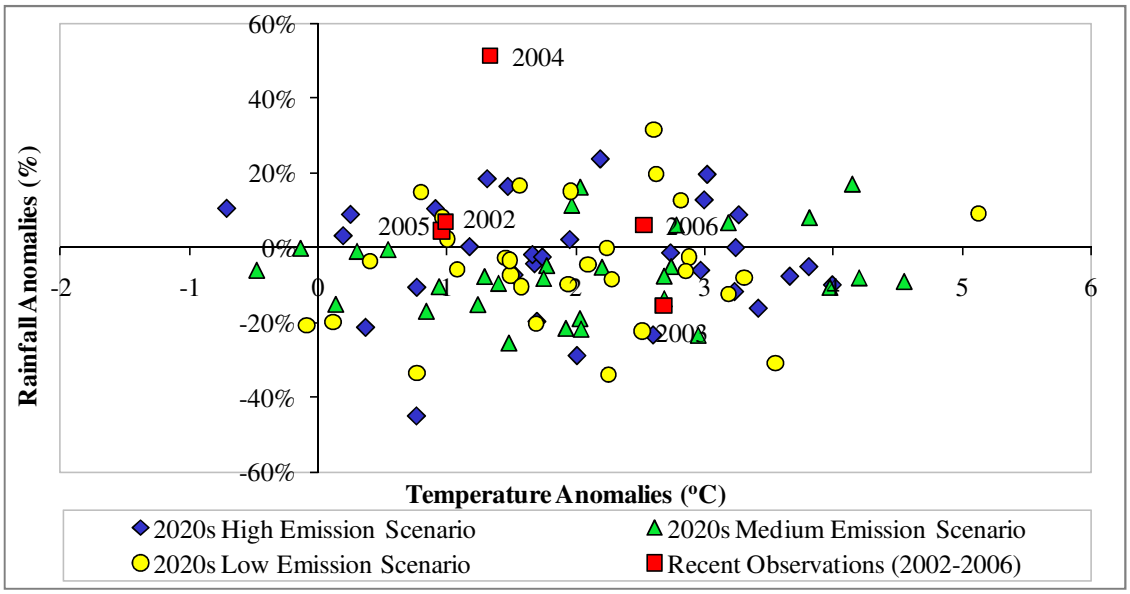

Figure 5.31: Summer Temperature and Rainfall Anomalies of Recent Observations (2002-2006) and UKCP09 Predictions for 2020s (2011-2040)

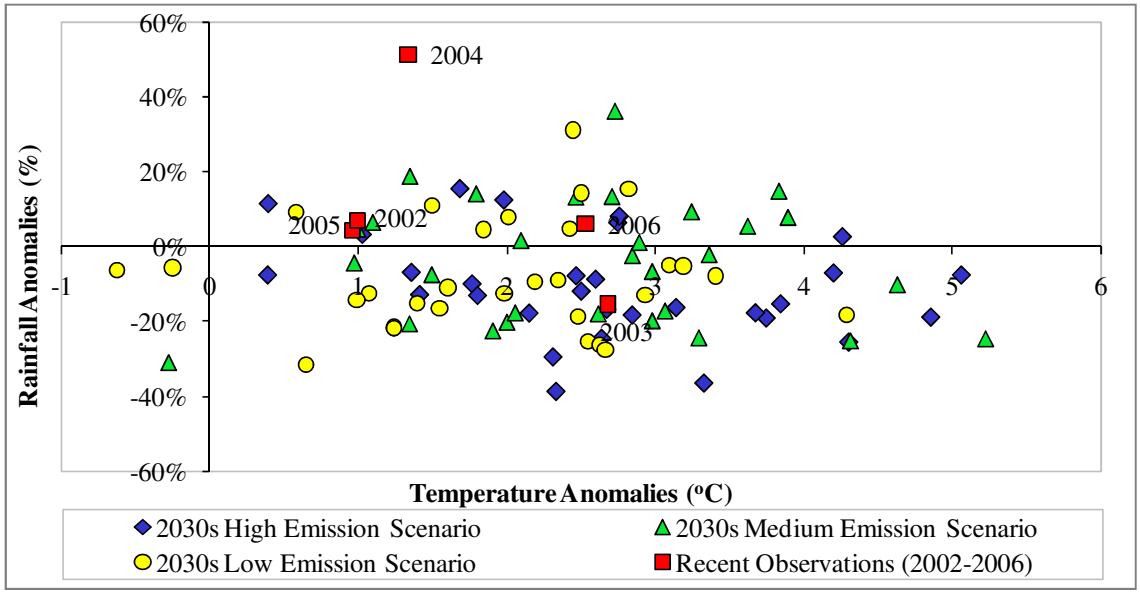

Figure 5.32: Summer Temperature and Rainfall Anomalies of Recent Observations (2002-2006) and UKCP09 Predictions for 2030s (2021-2050)

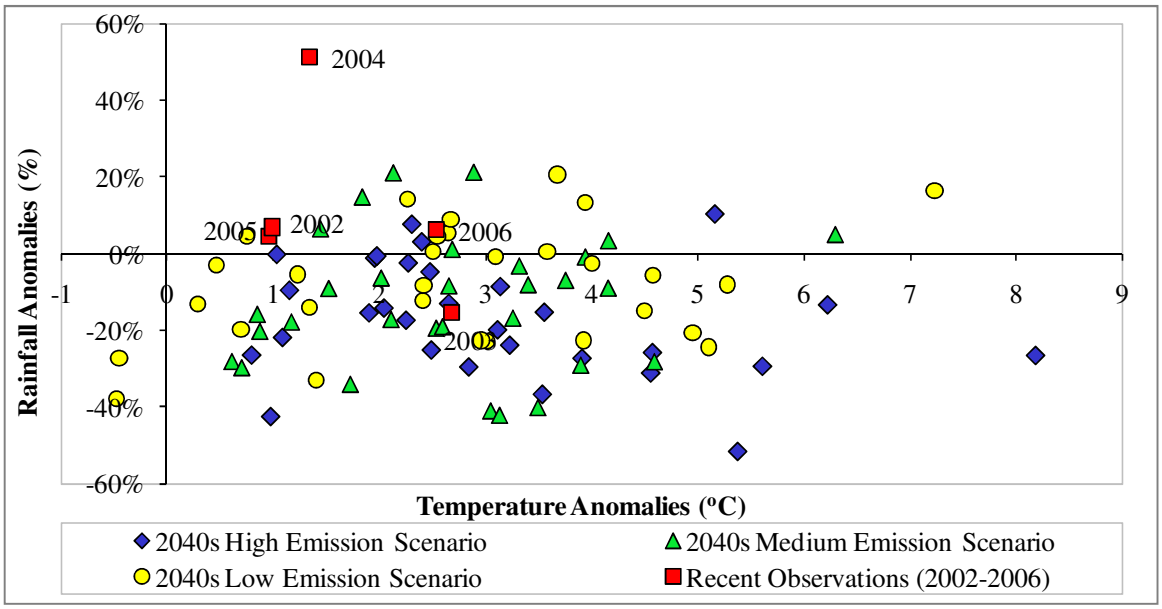

Figure 5.33: Summer Temperature and Rainfall Anomalies of Recent Observations (2002-2006) and UKCP09 Predictions for 2040s (2031-2060)

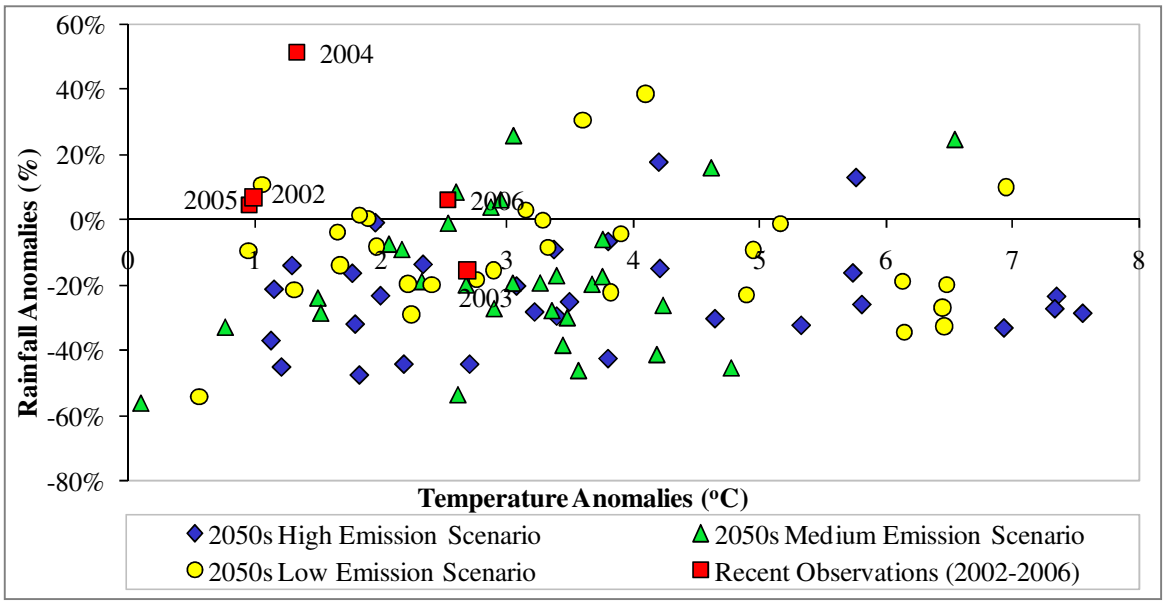

Figure 5.34: Summer Temperature and Rainfall Anomalies of Recent Observations (2002-2006) and UKCP09 Predictions for 2050s (2041-2070)

From the summary in Table 5.20, 3% of the years within the baseline period (1961 to 1990) had a 2003-type hot dry summer. This proportion is predicted to increase to a value in the

range of 17% to 27% during the 2020s and to a value in the range of 33% to 47% by the 2040s.

Table 5.20: Summary of Frequency of Observed and Predicted Hot Dry Summers

Time Slice	Observed	UKCP Emission Scenarios		
		Low	Medium	High
Baseline(1961-1990)	3%	-	-	-
2020s(2011-2040)	-	17%	23%	27%
2030s(2021-2050)	-	23%	33%	40%
2040s(2031-2060)	-	33%	40%	47%
2050s(2041-2070)	-	47%	53%	57%

5.5 Summary of Processed Data

Data suitable for use in the development of the rut depth models were available for a total of 3,006 road sub-sections. About two third of these road sub-sections and associated data were randomly selected for use in the estimation of the coefficients of the rut depth model structures discussed in section 4.4.3. The remaining one third was used for model validation.

A summary of the data used in Chapter 6 for the estimation of the model coefficients is given in Table 5.21, while data for model checking and validation are summarised in Table 7.1.

Table 5.21: Summary of Data for Estimation of Model Coefficients

Asphalt Surfacing Group	Number of Sub-Sections	Year	Statistics	Length	Annual Incremental Rut Depth	Annual Axle Loading	Heavy Vehicle Speed	Gradient	Asphalt Thickness	Voids in Mix	Surfacing Age	Softening Point	Asphalt Temperature
				-	ΔRUT	YE4	sh	G	HS	VIM	AGE	SP	TPmax
				m	mm	msa	km/h	-	mm	%	Years	°C	°C
Dense Bituminous Macadam (DBM)	108	2002	Mean	99.7	1.4	0.8	82.5	1.0	196.9	1.4	18.5	74.8	38.0
			Min.	75.0	0.0	0.6	48.9	0.0	95.0	0.9	3.0	51.1	37.1
			Max.	100.0	8.4	1.3	95.0	3.0	320.0	5.3	35.8	78.0	38.6
	149	2003	Mean	99.0	5.5	0.8	80.0	1.0	256.6	1.3	19.4	75.5	39.6
			Min.	52.0	0.0	0.2	49.5	0.0	96.0	0.9	5.7	60.7	37.7
			Max.	100.0	24.8	1.7	95.9	5.0	561.0	3.1	36.8	78.0	40.7
	250	2004	Mean	99.3	3.2	0.8	81.4	1.0	238.2	1.3	18.7	75.1	38.6
			Min.	50.0	0.0	0.2	49.4	0.0	95.0	0.9	5.0	58.2	36.7
			Max.	100.0	10.8	1.9	98.6	4.2	528.0	3.7	37.8	78.0	39.3
	328	2005	Mean	99.0	1.0	0.8	76.6	1.0	235.8	1.3	21.8	76.0	37.8
			Min.	52.0	0.0	0.2	47.8	0.0	95.0	0.9	6.0	61.4	35.9
			Max.	100.0	5.4	1.4	95.7	4.2	561.0	3.6	38.8	78.0	38.7
	1	2006	Mean	100.0	1.0	1.6	102.9	0.5	414.0	1.0	12.3	73.6	40.2
			Min.	100.0	1.0	1.6	102.9	0.5	414.0	1.0	12.3	73.6	40.2
			Max.	100.0	1.0	1.6	102.9	0.5	414.0	1.0	12.3	73.6	40.2
Hot Rolled Asphalt (HRA)	109	2002	Mean	98.4	1.1	0.8	81.4	1.1	257.7	1.2	13.6	77.1	38.2
			Min.	66.0	0.0	0.5	49.4	0.0	150.0	0.9	3.6	63.4	37.1
			Max.	100.0	4.8	1.1	97.4	4.0	550.0	2.1	34.8	78.0	38.7
	90	2003	Mean	97.5	3.1	1.1	86.9	1.2	270.4	1.2	16.1	77.5	39.7
			Min.	57.0	0.0	0.2	49.5	0.0	124.0	0.9	4.7	69.6	38.3
			Max.	100.0	16.4	2.2	107.3	4.1	441.0	1.8	28.8	78.0	40.7
	456	2004	Mean	98.4	1.8	1.5	84.4	1.3	261.3	1.2	15.3	76.7	38.7
			Min.	50.0	0.0	0.2	18.0	0.0	40.0	0.9	5.1	64.9	36.7
			Max.	100.0	22.9	2.8	106.7	6.4	587.0	1.9	36.8	78.0	39.3
	212	2005	Mean	98.3	0.7	0.8	80.5	1.3	262.5	1.2	18.9	77.7	37.7
			Min.	57.0	0.0	0.2	48.7	0.0	140.0	0.9	2.5	55.5	36.0
			Max.	100.0	3.9	1.2	98.1	5.4	550.0	2.5	37.8	78.0	38.8
	28	2006	Mean	99.0	2.8	1.6	98.2	0.9	418.5	1.2	12.3	77.8	40.2
			Min.	73.0	0.1	1.6	97.3	0.0	400.0	0.9	12.3	73.7	40.1
			Max.	100.0	9.6	1.6	102.9	3.5	445.0	1.5	12.3	78.0	40.3

Table 5.25: Summary of Data for Estimation of Model Coefficients (continued)

Asphalt Surfacing Group	Number of Sub-Sections	Year	Statistics	Length	Annual Incremental Rut Depth	Annual Axle Loading	Heavy Vehicle Speed	Gradient	Asphalt Thickness	Voids in Mix	Surfacing Age	Softening Point	Asphalt Temperature
				-	ΔRUT	YE4	sh	G	HS	VIM	AGE	SP	TPmax
				m	mm	msa	km/h	-	mm	%	Years	°C	°C
Thin Surface Course System (TSCS)	7	2002	Mean	100.0	2.1	1.0	73.0	1.1	143.1	3.4	4.0	66.1	38.0
			Min.	100.0	0.8	0.7	64.0	0.1	30.0	2.5	3.8	55.8	37.1
			Max.	100.0	3.4	1.3	80.8	3.5	214.0	4.4	4.9	78.0	38.5
	9	2003	Mean	100.0	3.7	0.5	65.1	1.5	280.4	2.6	7.7	72.3	38.6
			Min.	100.0	0.2	0.4	40.8	0.5	30.0	1.2	0.2	53.4	38.2
			Max.	100.0	12.0	0.6	92.8	3.0	360.0	5.4	15.0	80.0	39.3
	123	2004	Mean	99.3	1.2	1.3	80.0	1.4	210.6	4.1	3.2	65.7	38.7
			Min.	59.0	0.0	0.4	18.0	0.0	30.0	1.1	0.3	50.8	36.7
			Max.	100.0	5.8	2.2	98.9	4.1	454.0	7.6	16.0	80.0	39.4
	124	2005	Mean	99.7	0.6	0.9	86.6	1.0	221.2	3.5	4.6	67.7	37.8
			Min.	84.0	0.0	0.4	40.8	0.0	30.0	1.0	0.3	50.5	35.9
			Max.	100.0	2.8	1.4	96.3	3.9	360.0	6.5	38.8	80.0	38.4

5.6 Summary

This chapter provided a comprehensive description of the data used in the study. Processed data suitable for model validation were available for a total of 3, 006 road sub-sections. These road sub-sections together with the data associated to them were randomly divided into two groups by sampling without replacement such that the first group had about two thirds of the data and the second group had one third. Data in the first group were used in Chapter 6 for estimating the coefficients of the models given in Equations 4.5, 4.6 and 4.7. Data in the second group were used in Chapter 7 for checking and validating the models.

A comparison of observed annual incremental rut depths with climate data including mean daily maximum summer temperature, average monthly summer precipitation and sunshine hours indicated that high rates of asphalt surface rutting occurred in 2003 which had a hot dry summer. Similar trends in the rates of rutting were not discernible following comparison with the number of days with snow lying and rainfall intensity.

CHAPTER 6 BAYESIAN ESTIMATION OF MODEL COEFFICIENTS

6.1 Introduction

This Chapter discusses the Bayesian estimation of the coefficients of the rut depth prediction models proposed in Chapter 4 using data presented in section 5.5. The concepts and methodology used for the estimation of the model coefficients were discussed in section 4.6.

This Chapter is structured into eight major sections. Section 6.2 is concerned with the definition of prior distribution of model coefficients. Section 6.3 sets out the assumptions of the model likelihood for the observed annual incremental rut depth response variable. Section 6.4 focuses on the estimation of model coefficients using the Windows version of the Bayesian inference Using Gibbs Sampling (WinBUGS) software (Lunn et al., 2000). The results of the estimated model coefficients are presented in section 6.5 and discussed in section 6.6. Section 6.7 is concerned with the investigation of the robustness of the estimated model coefficients to choice of the structure and variance of the prior distribution of the model coefficients. The effect of including a climate variable in the improved rut depth model structure is investigated in section 6.8. Section 6.9 provides a summary to the chapter.

6.2 Specification of Prior Knowledge of Model Coefficients

The prior distribution of the model coefficients were defined using information elicited from previous research. The specification was achieved by defining the prior mean and variance. The prior mean provides a point estimate of the model coefficient while the variance indicates

the uncertainties in the estimate. If it is acknowledged from previous studies that the estimate of the prior mean of a particular model coefficient is accurate, then a low variance was specified, while high uncertainty concerning the prior mean were expressed using large variance. Prior distributions with large variances are referred to as low information or vague priors because they have little influence on the posterior estimates. Such prior distributions were adopted for model coefficients where prior information was not available.

The data collected was hierarchically structured as illustrated in Figure 4.7 in Chapter 4 into: Level 1 (Network Level) and Level 2 (Asphalt Surface Group Level). Level 1 of the hierarchy comprise all data within the study road network while at Level 2 data is categorised into the following three asphalt surfacing groups:

- Dense Bituminous Macadam (DBM),
- Hot Rolled Asphalt (HRA) , and
- Thin Surface Course System (TSCS).

These asphalt surfacing groups were defined in section 5.3.7. Within the Bayesian framework, prior distributions are assigned to level 1 statistical parameters of the hierarchical model (Ntzoufras, 2009). The prior distributions at level 2 (Asphalt Surface Group level) are known as hyper priors and are stochastically linked to level 1 prior distributions as illustrated in Equation 4.17 and Figure 4.9 in Chapter 4.

6.2.1 Prior Distribution for Rut Depth Model Coefficients

Building on from the formulation of prior distribution given in section 4.6.2.2, the model coefficients ϕ at the network level (level 1) were assumed to be normally distributed with

mean ϕ_μ and precision Λ respectively, where $\phi = \{ \beta_0, \beta_1, \beta_2, \beta_3, \beta_4, \beta_5, \beta_6\}^T$ is the transpose of the vector of the model coefficients, $\phi_\mu = \{ \beta_{\mu 0}, \beta_{\mu 1}, \beta_{\mu 2}, \beta_{\mu 3}, \beta_{\mu 4}, \beta_{\mu 5}, \beta_{\mu 6}\}^T$ is the transpose of the mean of the vector of the model coefficients at the network level and $\Lambda = \{\tau_{\beta 0}, \tau_{\beta 1}, \tau_{\beta 2}, \tau_{\beta 3}, \tau_{\beta 4}, \tau_{\beta 5}, \tau_{\beta 6}\}^T$ is the transpose of the precision of the model coefficients at the network level.

Concerning the prior values for the elements of the vector ϕ_μ, a vague prior mean was assumed for the linear regression model coefficient $\beta_{\mu 0}$ due to lack of prior information. The mean model coefficient for traffic loading variable (YE4) $\beta_{\mu 1}$ is expected to be positive since an increase in the number of equivalent standard axles would normally result in higher rates of asphalt surface rutting. According to Morosuik et al. (2004), model coefficient for traffic loading for the existing rut depth model discussed in Chapter 4 section 4.4.2 has a value of 1. Therefore a prior mean of $\beta_{\mu 1} = 1$ was adopted.

The mean model coefficient $\beta_{\mu 2}$ for the speed of heavy vehicles (sh) is expected to be negative since the rate of heavy vehicle loading is theoretically inversely proposal to speed. A prior value of $\beta_{\mu 2} = -0.78$ based on the existing HDM-4 plastic deformation rut depth model given in Morosuik et al. (2004) was assumed.

Road sections with steeper gradients (G) are expected to be more susceptible to rutting due to increased loading rates by heavy vehicles, a positive value of 0.5 was therefore assumed as the prior mean ($\beta_{\mu 3}$) of the model coefficient.

A vague or diffused prior mean $\beta_{\mu 5} = 0$ was assumed for asphalt material properties due to lack of prior information on the best estimate for the model coefficient for material properties. The prior mean coefficient for asphalt thickness $\beta_{\mu 4}$ was taken as 0.71 in line with the existing HDM-4 rut depth model (Morosuik et al., 2004). A non-informative prior mean of 0 was assumed for the climate variable model coefficient $\beta_{\mu 6}$. The prior mean of the vector ϕ is thus given as $\phi_{\mu} = \{0, 1, -0.78, 0.5, 0.71, 0, 0\}^{T}$.

The precision Λ_j of the elements of vector ϕ are assumed to have a gamma distribution denoted as

$$\Lambda_j \sim G(\omega, \vartheta) \tag{6.1}$$

where $G(\omega, \vartheta)$ = gamma distribution with shape and scale parameters denoted as ω and ϑ respectively. j = 1 to 7 denotes the elements (β_0, β_1, β_2, β_3, β_4, β_5, β_6) of the vector ϕ. Low information prior of 10^{-3} was assigned to both the shape and scale parameters of the gamma distribution.

6.2.2 Priors for the Error Term

The error term ε_{imt} in the proposed model structures in equations 4.5, 4.6 and 4.7 in Chapter 4 where assumed to be normally and independently distributed with a prior mean of 0. Equation 6.2 illustrates the prior distribution of the error term.

$$\varepsilon_{imt} \sim N(0, \tau_{\varepsilon}) \tag{6.2}$$

where N(.,.) denotes a normal distribution and τ_ε is the precision of the distribution of the error term. Precision is defined within the Bayesian statistics framework as the reciprocal of the variance (Congdon, 2003).

The precision of the error term τ_ε is usually represented by a low information gamma prior distribution because much uncertainty exist about the error term before the study (Hong and Prozzi, 2006; Ntzoufras, 2009). Equation 6.3 illustrates the prior distribution of the precision of the error term τ_ε.

$$\tau_\varepsilon \sim G(c, d) \tag{6.3}$$

where G(*c, d*) is the gamma distribution with *c,* and *d* as shape and scale parameters respectively. Low information priors of 10^{-3} were assigned to both the shape and scale parameters since much is not known about the distribution of the error term prior to the study.

6.2.3 Priors for the Softening Point and Voids in Mix Models

The priors for model coefficients α_1 and α_2 for the binder Softening Point model structure given in Equation 4.2, and the η_1 and η_1 for the Voids in Mix model structure given in Equation 4.3 were assumed to be normally distributed with means of 0 and a precisions of 10^{-3} since much is not known about their distribution prior to the study.

6.2.4 Summary of Prior Distribution

The prior distributions discussed in sections 6.2.1, 6.2.2 and 6.2.3 are summarised in Table 6.1.

Table 6.1: Summary of Prior Distributions

Proposed Model Variables	Model Coefficient	Prior Distribution	Data Source
Linear regression model coefficient β_0 in Equation 4.7.	β_0	N(0, 0.001)	Low information prior
Traffic Loading (YE4)	β_1	N(1, 0.001)	Morosuik (et al., 2004)
Heavy Vehicle Speed (sh)	β_2	N(-0.78, 0.001)	
Road Gradient (G)	β_3	N(0, 0.001)	Low information prior
Asphalt Surfacing Thickness (HS)	β_4	N(0.71, 0.001)	Morosuik et al. (2004)
Softening Point (SP) Model Coefficients	α_1	N(0, 0.001)	Low information priors
	α_2	N(0, 0.001)	
Voids in Mix (VIM) Coefficients	η_1	N(0, 0.001)	
	η_2	N(0, 0.001)	
Asphalt Material Properties (VIM/SP)	β_5	N(0, 0.001)	
Climate Variables	β_6	N(0, 0.001)	
Precision of Model Coefficients and error term (Λ, τ_ε)	-	G(0.001,0.001)	

Notes to Table 6.1

1. N(*a, b*) = Normal distribution with mean *a* and precision *b*. Precision (*b*) is defined as the reciprocal of the variance, hence a precision of 0.001 is equivalent to variance of 1000;
2. G(*c, d*) = Gamma distribution with parameters *c* and *d*;
3. $\Lambda = \{\tau_{\beta 0}, \tau_{\beta 1}, \tau_{\beta 2}, \tau_{\beta 3}, \tau_{\beta 4}, \tau_{\beta 5}, \tau_{\beta 6}\}^T$ is the transpose of the precision of the model coefficients.

6.3 Model Likelihoods

The observed annual incremental rut depth response variable is assumed to be independent and identically distributed. The likelihood is the joint distribution of the data and contains available information provided by the annual incremental rut depth sample. The distribution of the annual incremental rut depth data sample ΔRUT_{imt} observed on road section i of asphalt surface group m in year t can be stochastically represented using Equation 6.4.

$$\Delta RUT_{imt} \sim D(F(x)) \quad (6.4)$$

where F(x) is a deterministic function including explanatory variables and model coefficients. The deterministic function referred to are the following three proposed rut depth model structures:

- Model Structure 1 given as Equation 4.5;
- Model Structure 2 given as Equation 4.6; and
- Model Structure 3 given as Equation 4.7.

D in Equation 6.4 is the underlying statistical distribution of the data. Since the distribution (D) of the observed data is not known prior to the study, the following four distributions were investigated:

- Normal distribution;
- Student's t distribution;
- Double Exponential or Laplace distribution; and
- Lognormal distribution;

The first three distributions (Normal, Student's t, and Double Exponential) are symmetrical as illustrated in Figure 6.1. Considering these three distribution forms, the normal distribution is often assumed in pavement deterioration modelling (Hong and Prozzi, 2006; Paterson, 1987) its major drawback however is that it has a thin tail therefore extreme observations may be ignored. The Students t distribution with low degrees of freedom and the Double Exponential distributions have heavier tails which may capture extreme values if they exist in the data. A comparison of the three distributions is depicted in Figure 6.1. Unlike the Normal, Student's t,

and Double Exponential distributions, the probability densities of the Lognormal distributions is skewed and may therefore be more appropriate for describing asymmetric data.

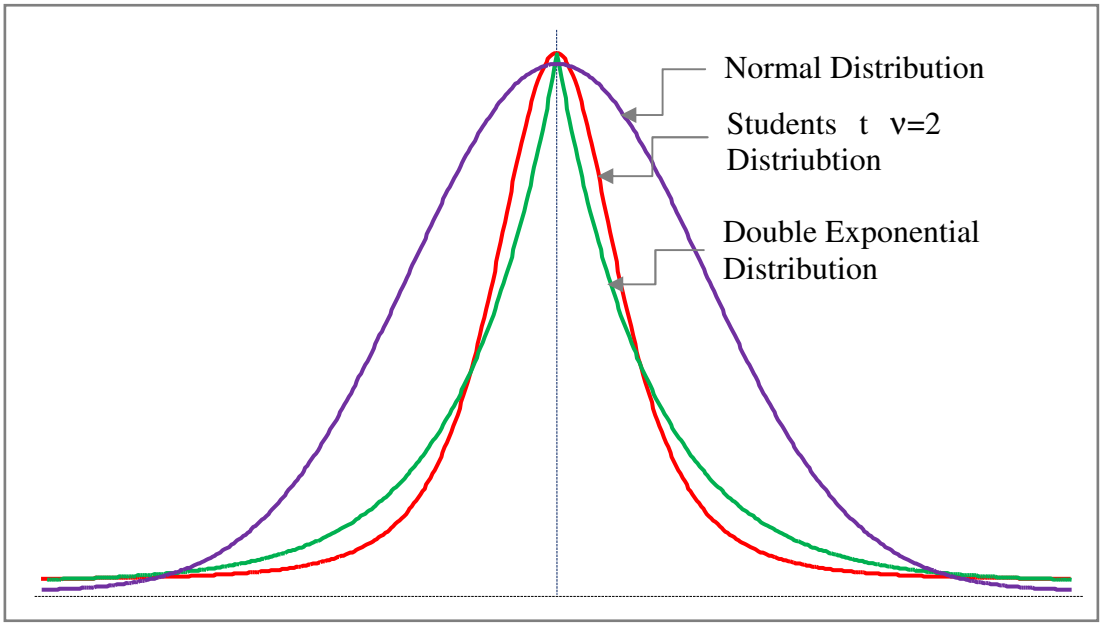

Figure 6.1: Comparison of Probability Densities of Double Exponential, Normal and Students t (with 2 degrees of freedom (ν=2)) Distributions

A normal likelihood was assumed for the softening point and voids in mix models proposed in Equations 4.2 and 4.3.

6.4 Estimation of Model Coefficients using WinBUGS

The likelihood functions described in section 6.3 were combined with the prior density using Bayes' theory to give the joint posterior distribution. Analytically, the joint posterior distribution is derived as a product of the likelihood and the prior distribution density. The posterior distribution expresses the current state of knowledge about the model coefficients given the observed data and prior knowledge of the model coefficients. The aim however is to derive the marginal distribution of each model coefficient β_0 to β_6 given the data from the joint posterior distribution. This was achieved using a Markov Chain Monte Carlo (MCMC)

technique by implementing Bayesian models described in section 6.4.1 in the WinBUGS software.

The WinBUGS software which has an inbuilt Gibbs sampler was used to derive the marginal distributions of each model coefficient. Gibbs sampling approach is a Markovian updating scheme. The concept of computing the marginal distributions from the joint posterior distribution using a Markovian updating scheme was introduced in section 4.6.3 and is described in detail in Geman and Geman (1984), Casella and George (1992) and Smith and Roberts (1993).

6.4.1 Naming Convention for Bayesian Models

The four assumptions of the likelihood of the underlying distribution of the data were combined with the prior distributions discussed in section 6.2 for each of the three deterministic rut depth model structures described in section 6.3. This combination resulted in 12 Bayesian models as summarised in Table 6.2.

Table 6.2: Naming Convention for Bayesian Models

Model Name	Description
Model 1D	Based on Model Structure 1 and Double Exponential likelihood assumption
Model 1L	Based on Model Structure 1 and Lognormal likelihood assumption
Model 1N	Based on Model Structure 1 and Normal likelihood assumption
Model 1S	Based on Model Structure 1 and Students t likelihood assumption
Model 2D	Based on Model Structure 2 and Double Exponential likelihood assumption
Model 2L	Based on Model Structure 2 and Lognormal likelihood assumption
Model 2N	Based on Model Structure 2 and Normal likelihood assumption
Model 2S	Based on Model Structure 2 and Students t likelihood assumption
Model 3D	Based on Model Structure 3 and Double Exponential likelihood assumption
Model 3L	Based on Model Structure 3 and Lognormal likelihood assumption
Model 3N	Based on Model Structure 3 and Normal likelihood assumption
Model 3S	Based on Model Structure 3 and Students t likelihood assumption

6.4.2 Implementation in WinBUGS Software

To facilitate the estimation of the model coefficients, the 12 Bayesian models summarised in Table 6.2 were implemented in the WinBUGS which is a programming language based software. The Software is used to generate random variables from the joint posterior distribution of the parameters of the Bayesian models with the aim of deriving the marginal distributions of the model coefficients β_0 to β_6. Details on the use of WinBUGS and on writing model codes in the BUGS language are given in (Lunn et al., 2000).

WinBUGS model codes were written for each of the 12 models given in Table 6.2. A typical model code for Bayesian Model 1N is given in Appendix C1.

6.4.3 Convergence Diagnostics

Convergence is required for the sampled value to represent a random draw from the marginal distribution of the model coefficients. The marginal distributions of each model coefficient β_0 to β_6 were derived after a large number of iterations and when the Markov chain converges to a target distribution.

Convergence diagnostics was performed by simultaneously running three Markov chains. Convergence was considered achieved when the traces of the chains were found to be overlapping. The iterations for each chain deemed to include random draws before convergence was achieved also known as "burn-in" iterations were discarded. Samples of converged chains are illustrated using selected trace plots of iterations against generated values for the traffic loading model coefficient β_1. The trace plots are depicted in Figure 6.2 to Figure 6.4.

Considering Figure 6.2, the first 50,000 iterations were discarded and the next 50,000 with the three chains overlapping were recorded. In addition, the generated values of the model coefficient (β_1) uniformly range between 0.3 and 0.7 without periodic irregularities indicating that convergence was achieved. Similar inference on convergence was applied to the random posterior samples shown in Figure 6.3 and 6.4 and to trace plots of all model coefficients β_0 to β_6.

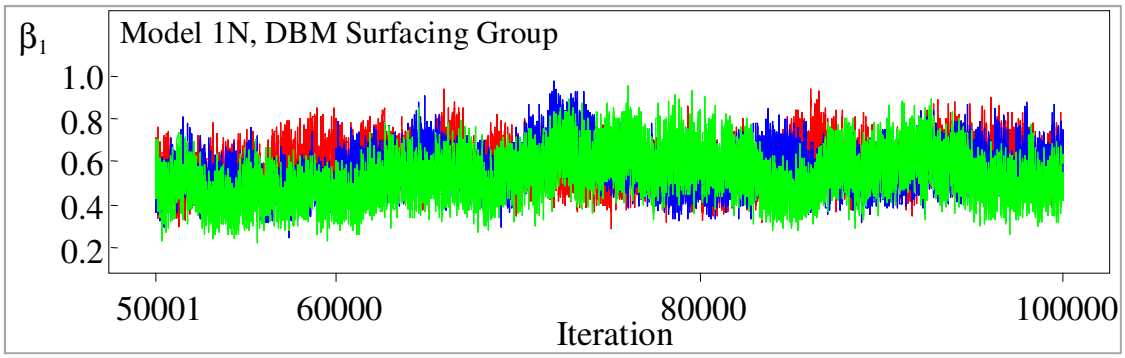

Figure 6.2: Overlapping Multiple Chains for Model 1N illustrating convergence of model coefficient β_1 for DBM surfacing group.

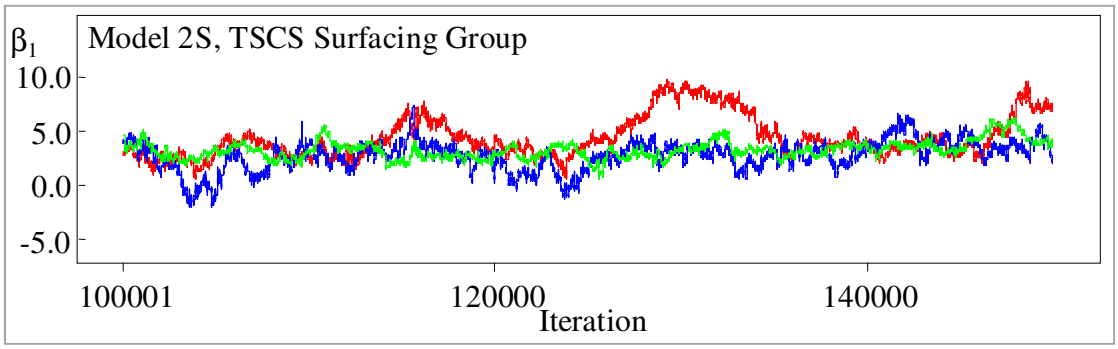

Figure 6.3: Overlapping Multiple Chains for Model 2S illustrating convergence of model coefficient β_1 for TSCS surfacing group.

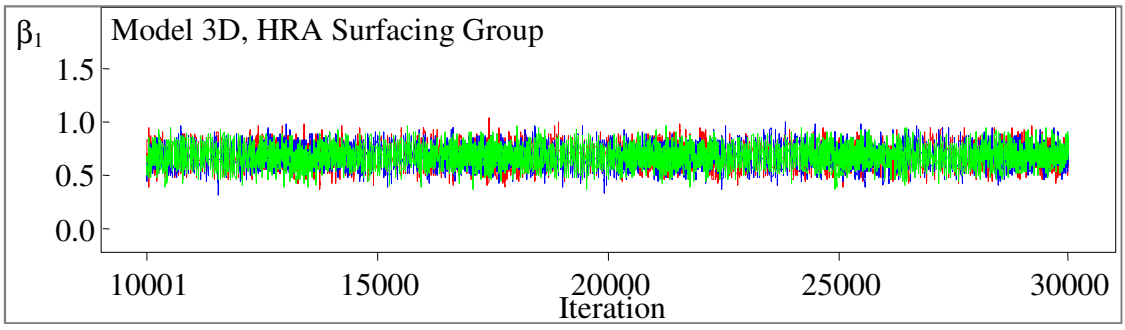

Figure 6.4: Overlapping Multiple Chains for Model 3D illustrating convergence of model coefficient β_1 for HRA surfacing group.

The number of iterations recorded after the "burn-in" period was determined by monitoring the Monte Carlo error (MC error), which measures the variability of each estimate due to the simulation. The MC error reduces with the number of iterations and is required to be low for

the estimated model coefficients to be calculated with precision (Lunn et al., 2000). To that end, the iterations after the "burn-in" period were stopped when the MC error for all model coefficients were less than 5% of the corresponding posterior standard deviation (Spiegelhalter et al., 2003).

The posterior statistics of each model coefficients were derived from iterations recorded after the "burn-in" period. The results are presented in the next section.

6.5 Estimated Model Coefficients

The results of the estimated model coefficients are provided for the improved rut depth models as well as for the proposed models for Softening Point (SP) and Voids in Mix (VIM).

6.5.1 Model Coefficients for Improved Rut Depth Models

The results of the estimated model coefficients for the improved rut depth models are presented as summary statistics of the marginal distributions of the model coefficients, the target distribution of each model coefficient, and plots of 95% posterior credible intervals of the model coefficients.

6.5.1.1 Posterior Summary Statistics

Table 6.3 gives summary statistics of the estimated model coefficients by asphalt surfacing group for Model 1L based on model structure 1 given in Equation 4.5 in Chapter 4, and a lognormal likelihood of the observed data. Tables of summary statistics for the remaining Bayesian models in Table 6.2 are given in Appendices C2 to C4.

The tables provide posterior estimates of the statistics of the model coefficients including mean, median, 2.5% and 97.5% posterior percentiles and the probability (P0) that the estimated model coefficients are greater than 0. The 2.5% and 97.5% percentile values of each estimated model coefficient define the limits of the 95% posterior credible.

Table 6.3: Summary Statistics for Estimated Model Coefficient for Model 1L (based on Model Structure 1 and Lognormal Likelihood)

Surfacing Group[1]	**Model Coefficient**	**Mean**	**SD[2]**	**MC Error**	**2.5 %**	**Median**	**97.5 %**	**P0[3]**	**Start[4]**	**Sample[5]**
DBM	β_1	0.26	0.11	3.7E-03	0.10	0.25	0.50	1.00	50,001	150,000
	β_2	-0.48	0.26	1.0E-02	-1.02	-0.46	-0.04	0.00	50,001	150,000
	β_3	0.04	0.03	4.7E-04	0.00	0.04	0.10	0.98	50,001	150,000
	β_4	0.29	0.11	4.3E-03	0.13	0.28	0.53	1.00	50,001	150,000
	β_5	-0.05	0.06	2.2E-03	-0.17	-0.04	0.08	0.20	50,001	150,000
	β_6	0.04	0.02	5.7E-04	0.03	0.04	0.09	1.00	50,001	150,000
HRA	β_1	0.65	0.47	1.7E-02	0.28	0.50	2.23	1.00	50,001	150,000
	β_2	-0.05	0.08	2.9E-03	-0.21	-0.05	0.09	0.18	50,001	150,000
	β_3	0.01	0.01	2.7E-04	0.00	0.01	0.05	1.00	50,001	150,000
	β_4	0.06	0.07	2.5E-03	-0.06	0.06	0.21	0.85	50,001	150,000
	β_5	0.14	0.19	7.3E-03	-0.06	0.10	0.71	0.84	50,001	150,000
	β_6	0.02	0.00	6.7E-05	0.02	0.02	0.03	1.00	50,001	150,000
TSCS	β_1	1.30	0.56	1.2E-02	0.39	1.26	2.53	1.00	50,001	150,000
	β_2	-0.81	0.30	1.0E-02	-1.47	-0.77	-0.31	0.00	50,001	150,000
	β_3	0.02	0.15	1.5E-03	-0.25	0.00	0.37	0.51	50,001	150,000
	β_4	0.41	0.22	7.9E-03	0.04	0.38	0.89	0.99	50,001	150,000
	β_5	0.23	0.23	7.3E-03	-0.19	0.22	0.70	0.83	50,001	150,000
	β_6	0.34	0.45	9.0E-03	0.05	0.24	1.25	1.00	50,001	150,000

Notes to Table 6.3.

1. DBM = Dense Bituminous Macadam, HRA = Hot Rolled Asphalt, and TSCS = Thin Surface Course System;
2. SD = Posterior Standard Deviation;
3. P0 = Probability of posterior estimate of model coefficient being greater than zero;
4. Start = The number of iterations that the generated sample started after the burn-in period.
5. Sample = The total number of iterations or generated posterior sample size.

The distribution of the estimated model coefficients by asphalt surfacing group for Model 1L (based on Model Structure 1 and Lognormal likelihood) is given in Figure 6.5. The estimated distributions of model coefficients for the remaining Bayesian models listed in Table 6.2 are provided in Appendices C2 to C3.

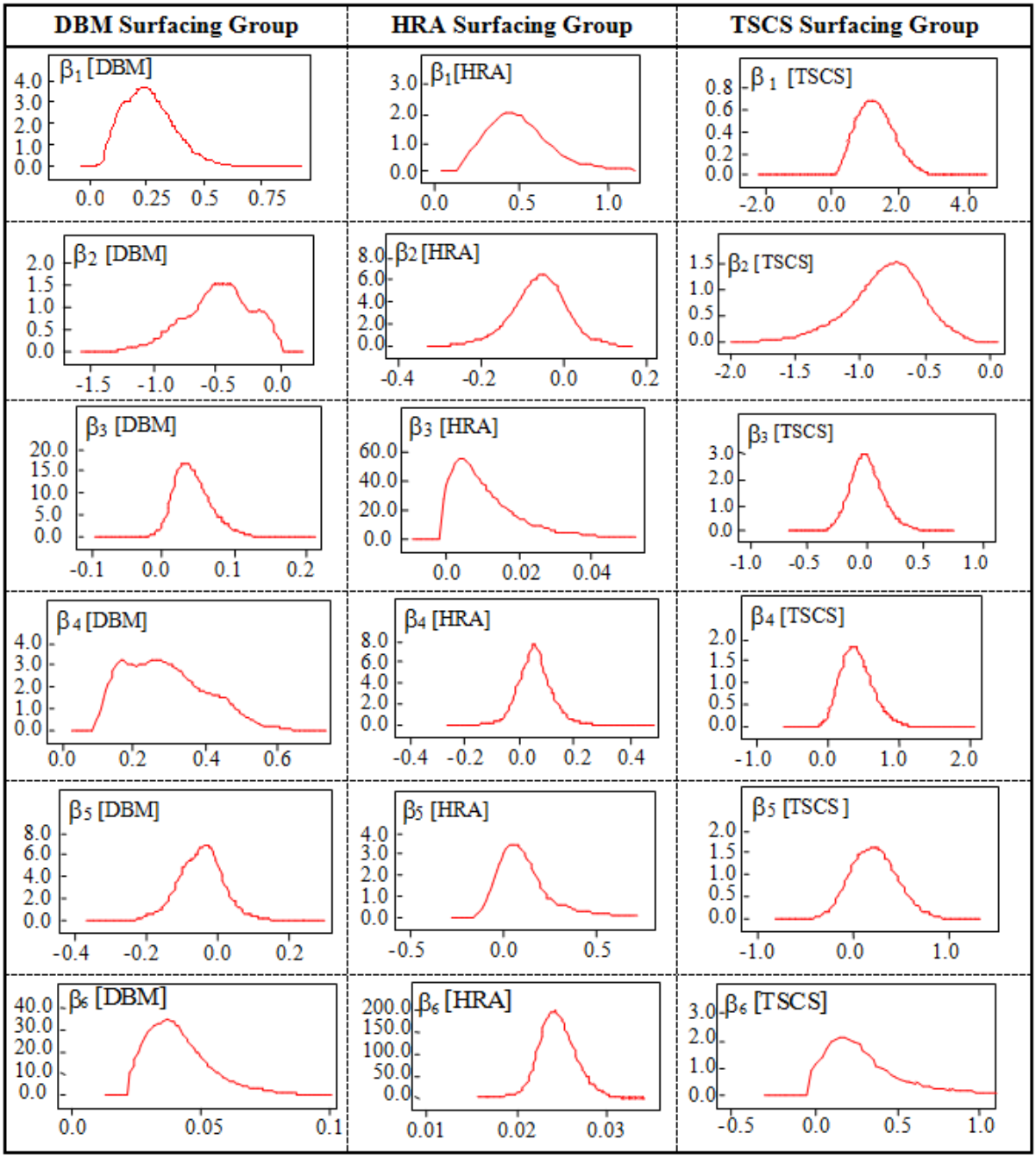

Figure 6.5: Estimated Distribution of Model Coefficients for Model 1L (Model Structure 1 and Lognormal Likelihood).

Considering the estimated distribution of the model coefficients in Figure 6.5 the horizontal axis denotes the range of values of the estimated model coefficients while the vertical axis denotes the posterior density.

6.5.1.2 Posterior Credible Intervals for Model Coefficients

A summary of the 95% posterior credible intervals for each model coefficient and Bayesian model types set out in Table 6.2 are given in Figure 6.6 to Figure 6.11 for model structure 1 (based on Equation 4.5 in Chapter 4), Figure 6.12 to Figure 6.17 for model structure 2 (based on Equation 4.6 in Chapter 4), and Figure 6.18 to Figure 6.24 for model structure 3 (based on Equation 4.7 in Chapter 4).

The vertical whisker lines in the figures represent the 95% credible intervals of the posterior estimate of the model coefficients for each surface group and model type. The ending of the whisker lines represent the 2.5% and 97.5% posterior percentiles of the values of the model coefficients. The diamond mark within the vertical whisker lines represents the estimated mean value of the model coefficient. The horizontal reference line in the figures corresponds to a model coefficient of zero. For example, considering Figure 6.6, the mean value of the model coefficient β_1 for the HRA surfacing group under Bayesian Model 1D is 6.6 with a 2.5% and 97.5% percentile values of 3.8 and 11.3 respectively.

A relatively large credible interval suggests greater uncertainty in the estimate of the mean value of the model coefficient. For example, considering the estimate for maximum temperature coefficient β_6 in Figure 6.11, larger uncertainty exists in the estimation of β_6 using Bayesian Model 1S (with a student's t likelihood) compared to estimates based on

Model 1D (Double Exponential Likelihood), Model 1L (Lognormal Likelihood), and Model 1N (Normal Likelihood).

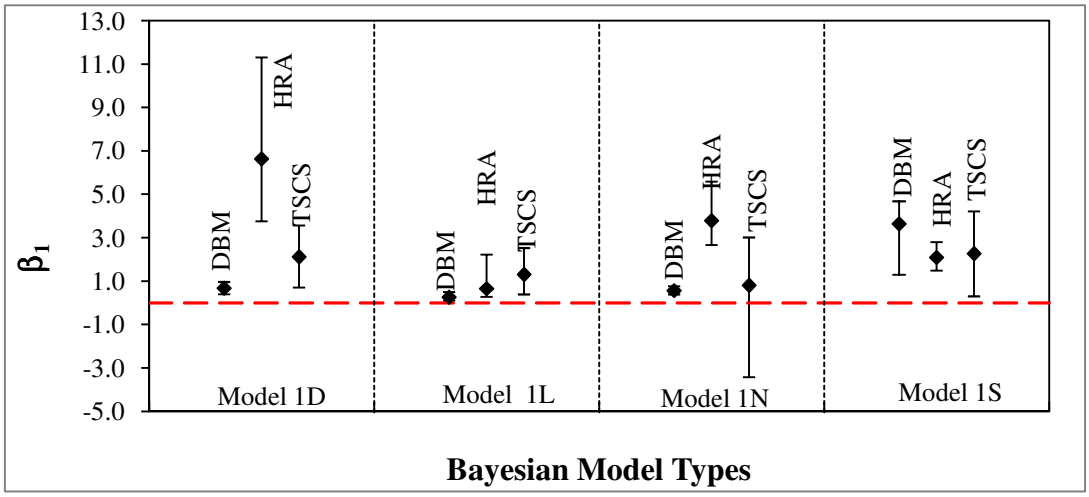

Figure 6.6: 95% Posterior Credible Interval of Model Coefficient β_1 in Model Structure 1.

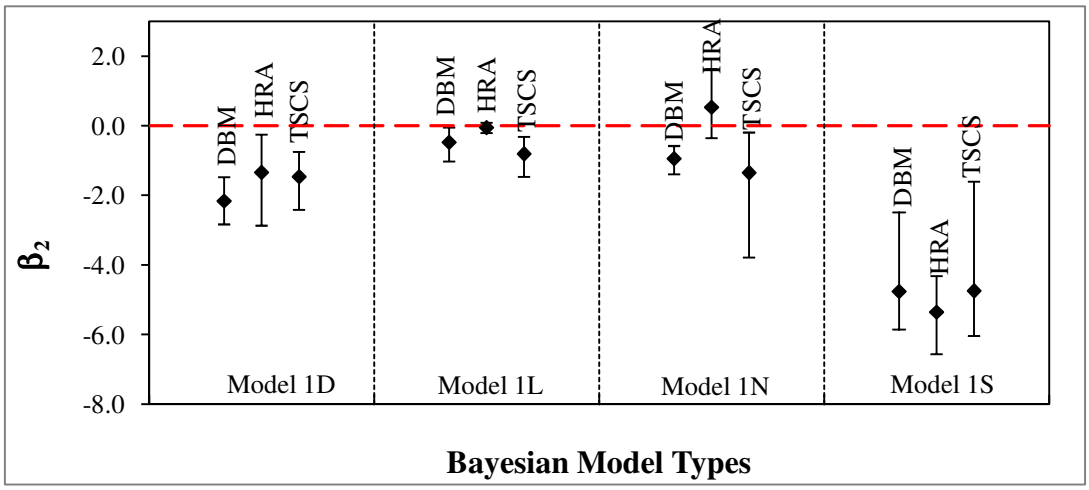

Figure 6.7: 95% Posterior Credible Interval of Model Coefficient β_2 in Model Structure 1.

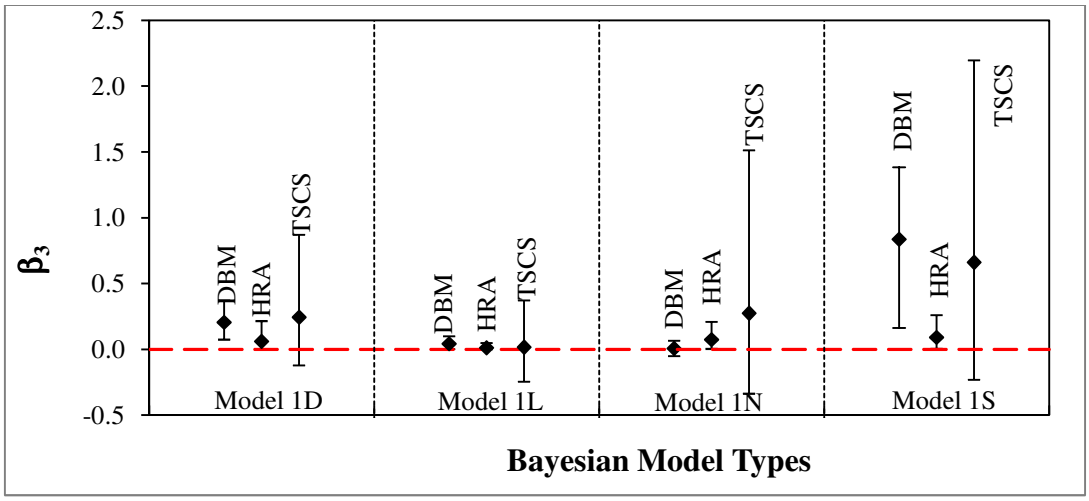

Figure 6.8: 95% Posterior Credible Interval of Model Coefficient β_3 in Model Structure 1.

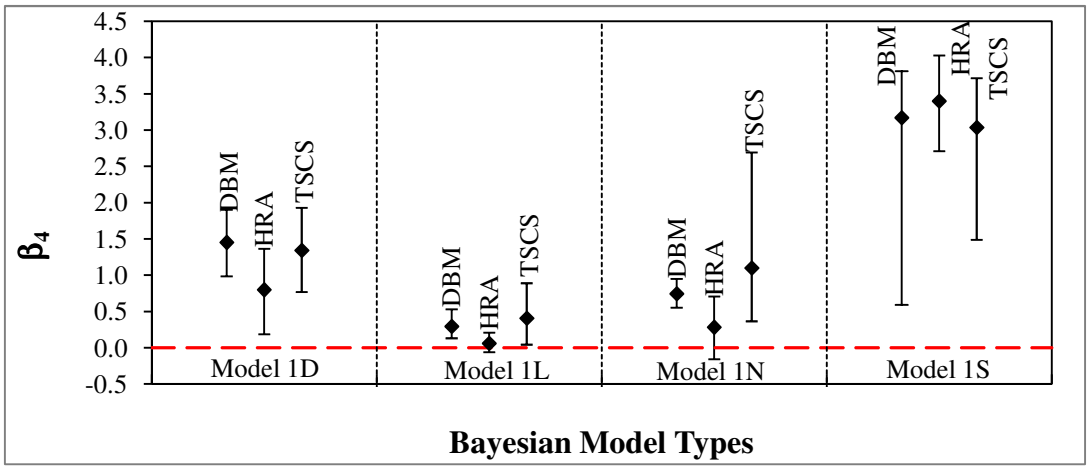

Figure 6.9: 95% Posterior Credible Interval of Model Coefficient β_4 in Model Structure 1.

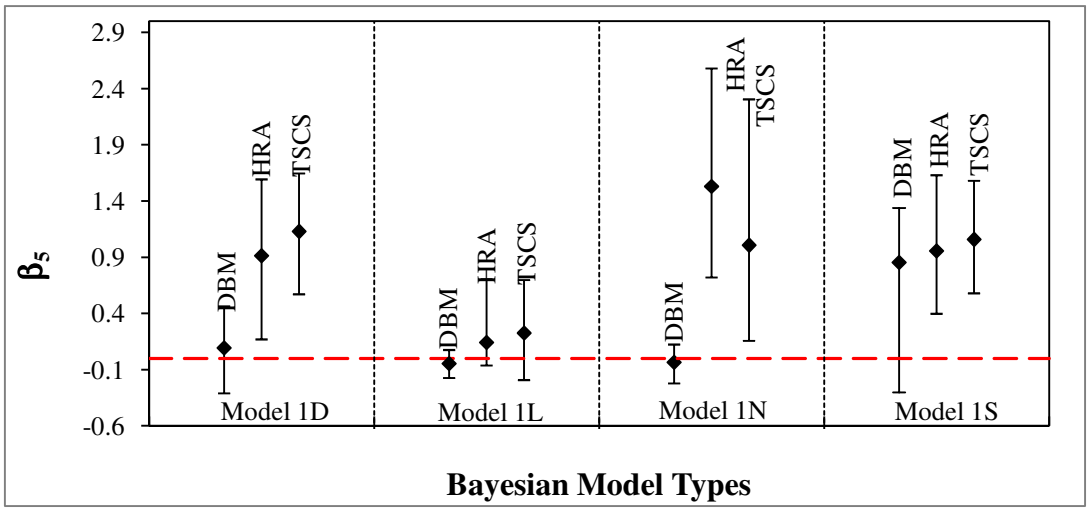

Figure 6.10: 95% Posterior Credible Interval of Model Coefficient β_5 in Model Structure 1.

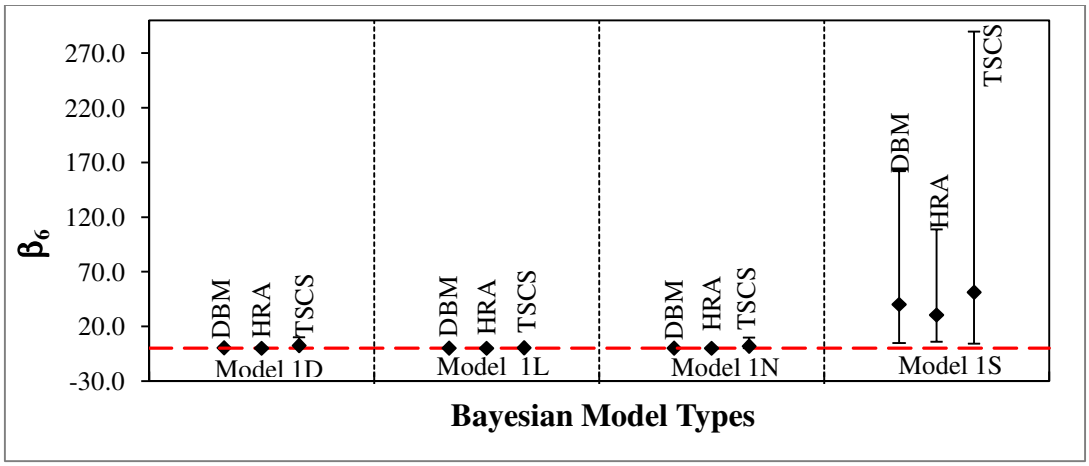

Figure 6.11: 95% Posterior Credible Interval of Model Coefficient β_6 in Model Structure 1.

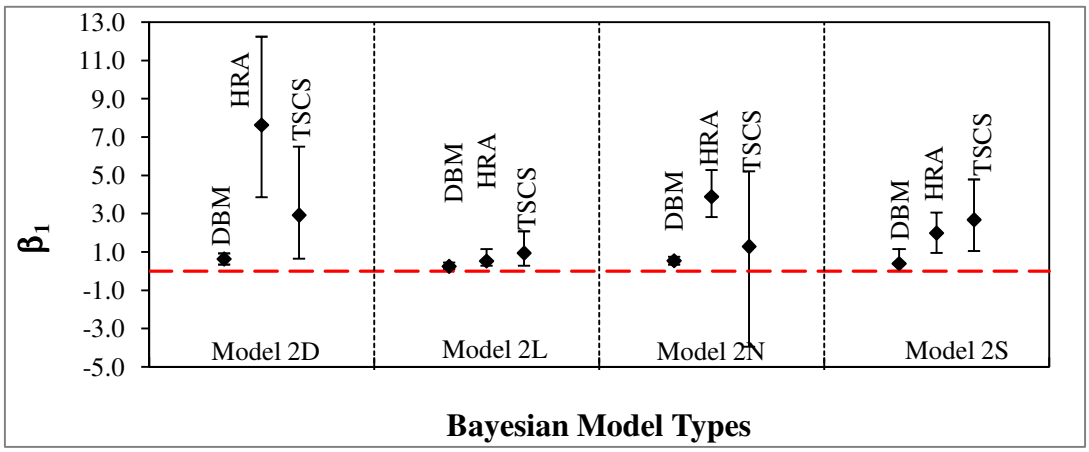

Figure 6.12: 95% Posterior Credible Interval of Model Coefficient β_1 in Model Structure 2.

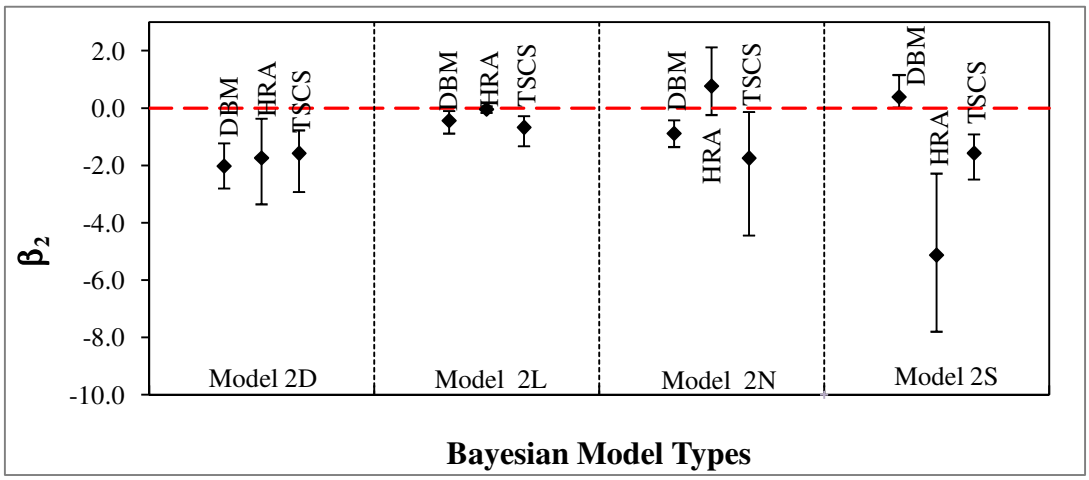

Figure 6.13: 95% Posterior Credible Interval of Model Coefficient β_2 in Model Structure 2.

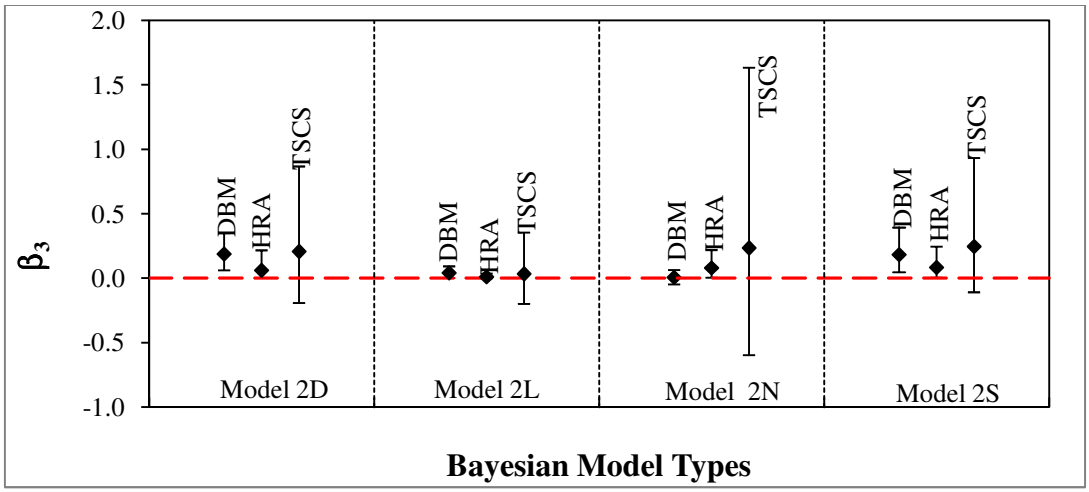

Figure 6.14: 95% Posterior Credible Interval of Model Coefficient β_3 in Model Structure 2.

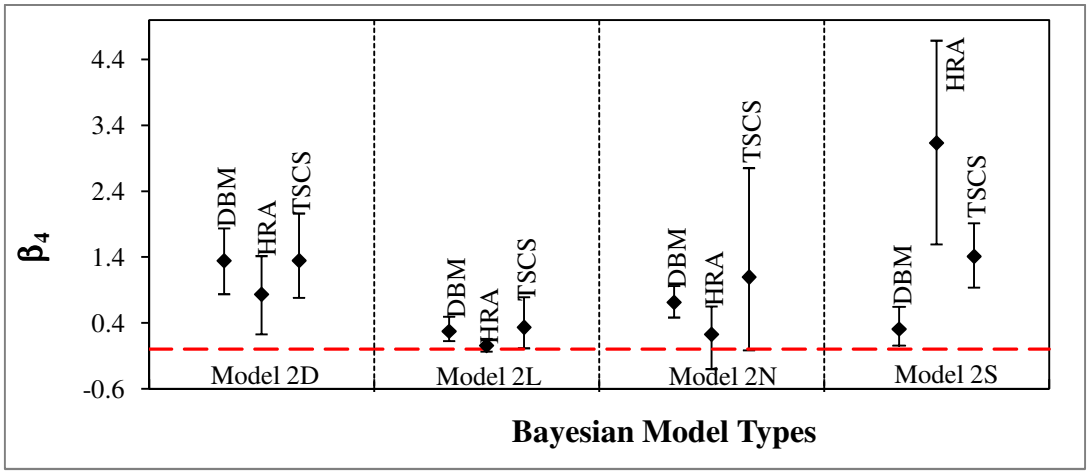

Figure 6.15: 95% Posterior Credible Interval of Model Coefficient β_4 in Model Structure 2.

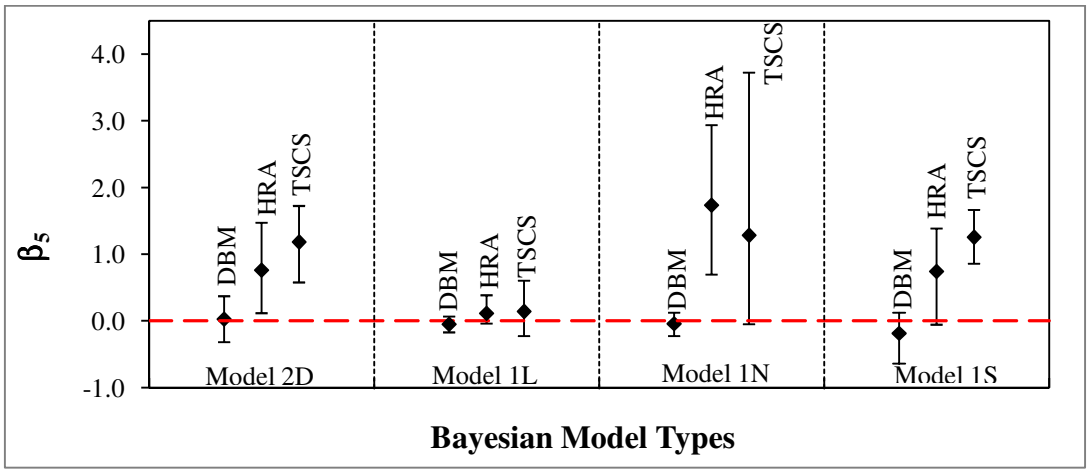

Figure 6.16: 95% Posterior Credible Interval of Model Coefficient β_5 in Model Structure 2.

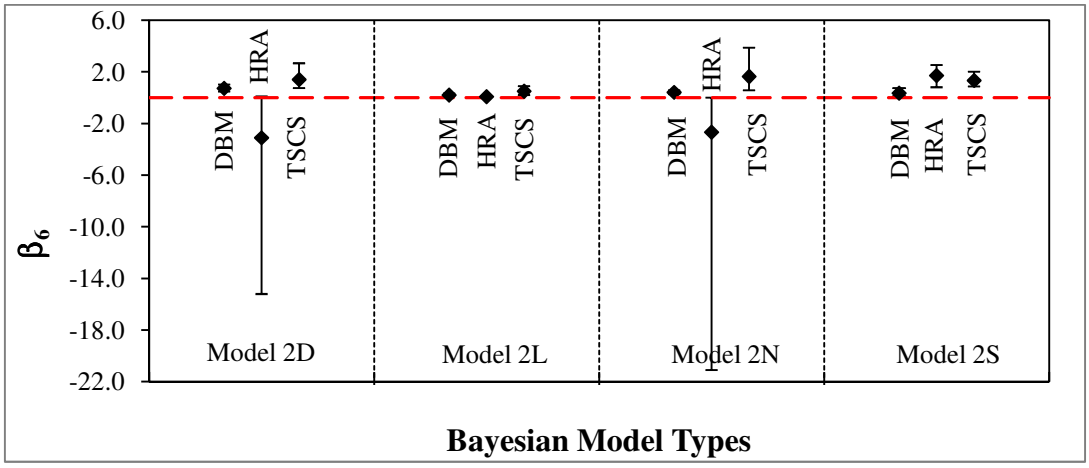

Figure 6.17: 95% Posterior Credible Interval of Model Coefficient β_6 in Model Structure 2.

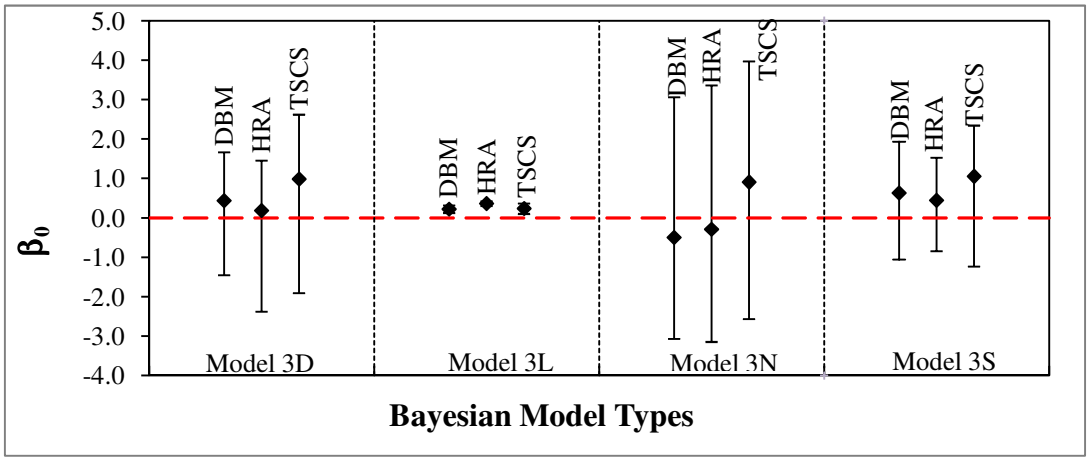

Figure 6.18: 95% Posterior Credible Interval of Model Coefficient β_0 in Model Structure 3.

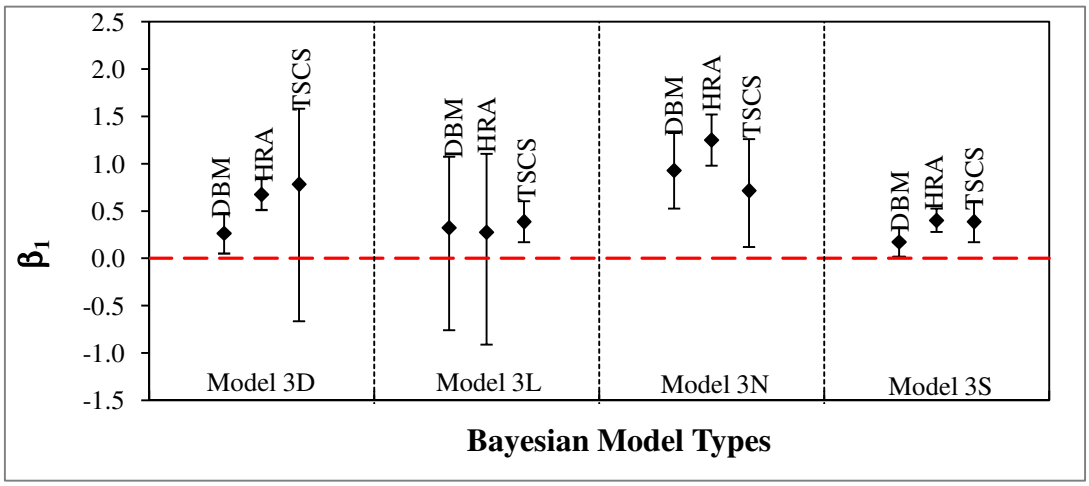

Figure 6.19: 95% Posterior Credible Interval of Model Coefficient β_1 in Model Structure 3.

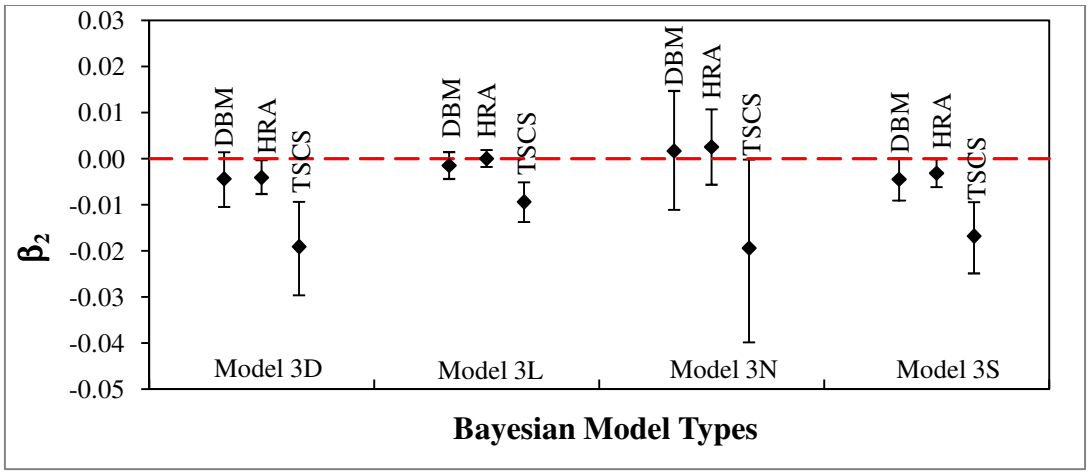

Figure 6.20: 95% Posterior Credible Interval of Model Coefficient β_2 in Model Structure 3.

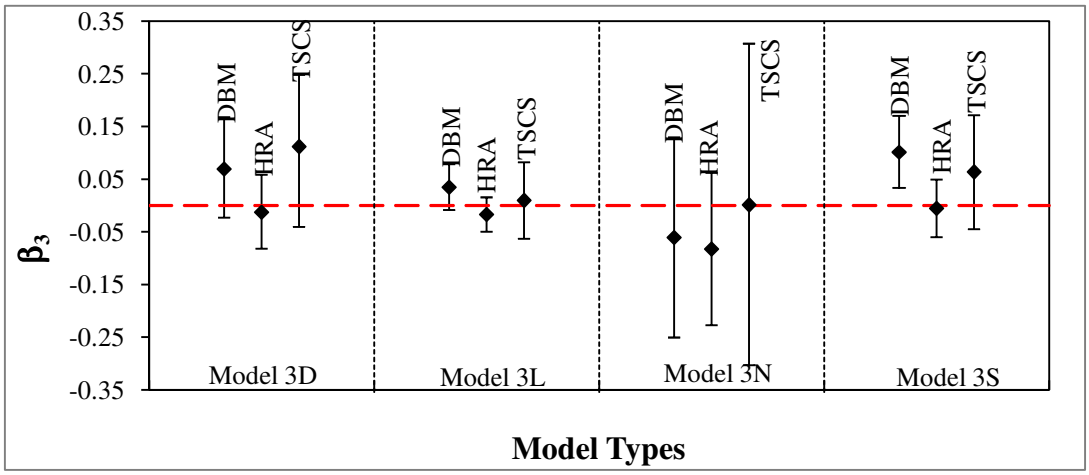

Figure 6.21: 95% Posterior Credible Interval of Model Coefficient β_3 in Model Structure 3.

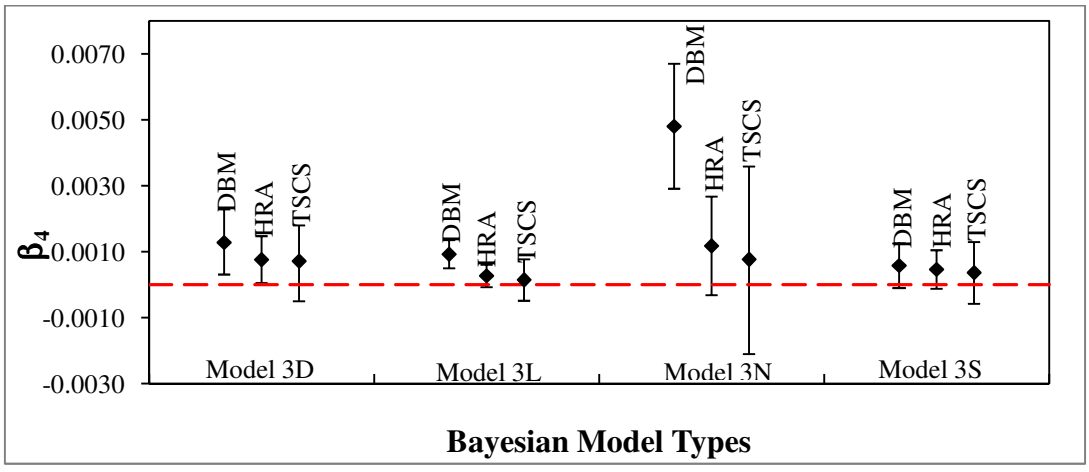

Figure 6.22: 95% Posterior Credible Interval of Model Coefficient β_4 in Model Structure 3.

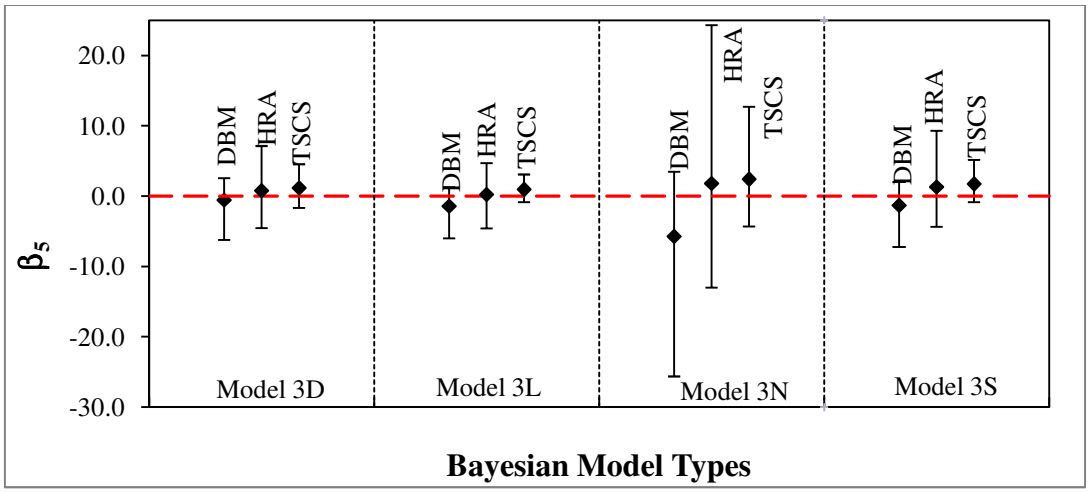

Figure 6.23: 95% Posterior Credible Interval of Model Coefficient β_5 in Model Structure 3.

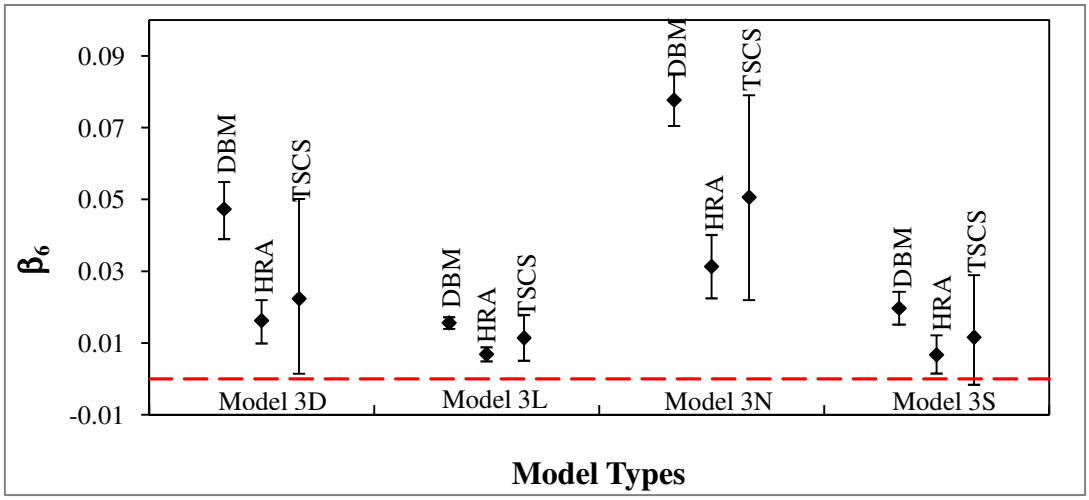

Figure 6.24: 95% Posterior Credible Interval of Model Coefficient β_6 in Model Structure 3.

6.5.2 Model Coefficients for Softening Point and Void in Mix Models

Table 6.4 provides summary statistics of the posterior estimates of the model coefficients for the proposed binder Softening Point (SP) and Voids in Mix (VIM) models. The proposed SP and VIM models are given in Equations 4.2 and 4.3 in Chapter 4.

Table 6.4: Summary Statistics for the Softening Point and Voids in Mix Models

Surfacing Group	Node	Mean	SD	MC Error	2.50%	Median	97.50%	Start	Sample
DBM	α_1	6.31	0.22	3.2E-03	5.88	6.31	6.73	100001	300000
	α_2	57.15	0.64	9.5E-03	55.89	57.15	58.40	100001	300000
	η_1	-0.52	0.03	4.6E-04	-0.58	-0.52	-0.45	100001	300000
	η_2	2.83	0.10	1.4E-03	2.65	2.83	3.02	100001	300000
HRA	α_1	2.52	0.19	2.2E-03	2.15	2.52	2.89	100001	300000
	α_2	70.50	0.50	5.7E-03	69.52	70.50	71.49	100001	300000
	η_1	-0.07	0.03	3.3E-04	-0.12	-0.07	-0.02	100001	300000
	$\eta_{2\iota}$	1.39	0.07	8.8E-04	1.24	1.39	1.54	100001	300000
TSCS	α_1	5.06	0.22	7.7E-04	4.63	5.06	5.48	100001	300000
	α_2	61.49	0.30	1.1E-03	60.90	61.49	62.08	100001	300000
	η_1	-1.30	0.03	1.2E-04	-1.37	-1.30	-1.24	100001	300000
	η_2	5.11	0.05	1.7E-04	5.02	5.11	5.19	100001	300000

The distribution of the estimated model coefficients by asphalt surfacing group for SP and VIM models are given Figure 6.25. Discussion of the results is provided in section 6.6.

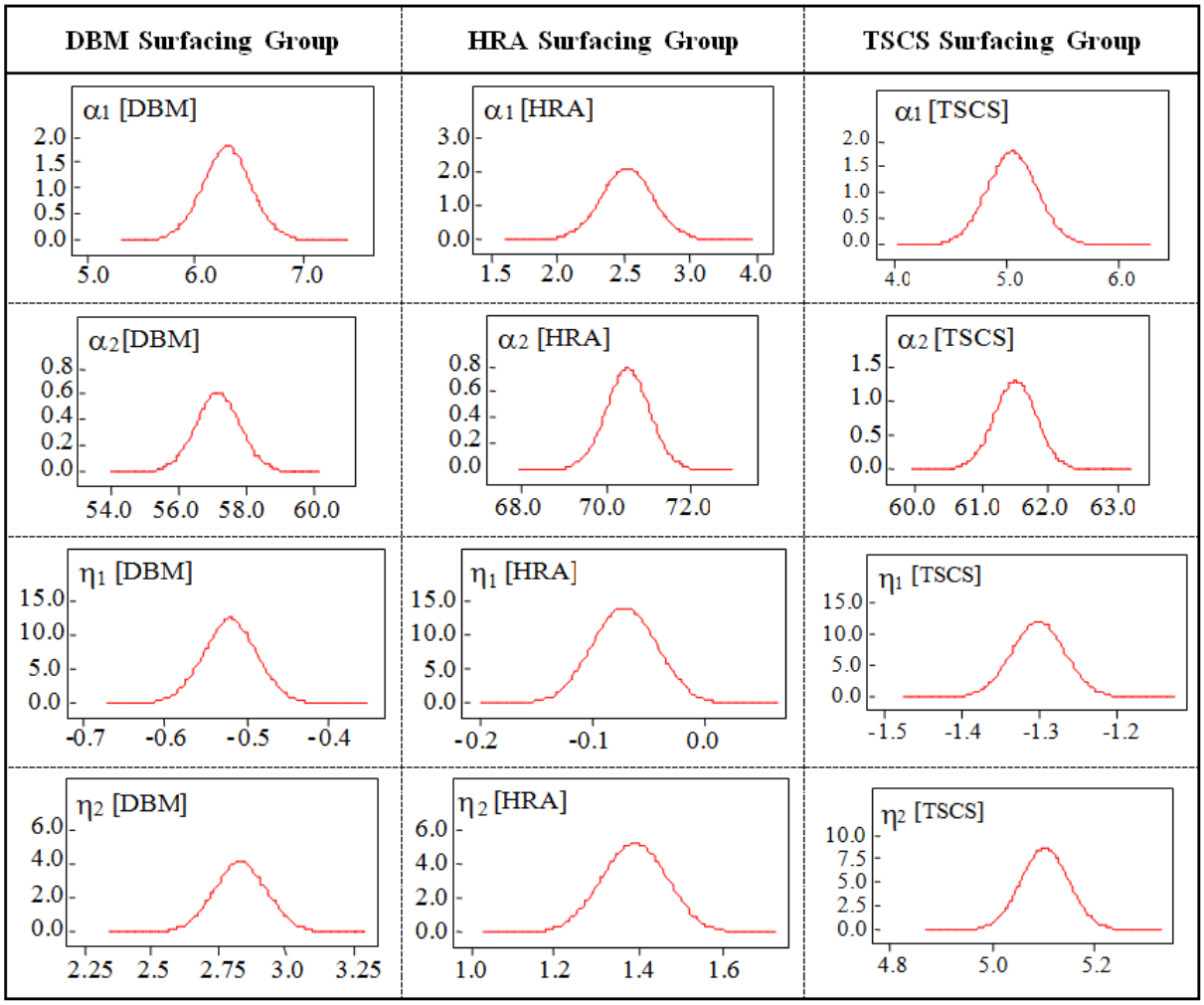

Figure 6.25: Estimated Distribution of Model Coefficients for VIM and SP models.

6.6 Interpretation of Estimated Model Coefficients

Inference regarding the results of the estimated model coefficients of each pavement surfacing type given the data used in the study is discussed for each annual incremental rut depth model structure based on the following criteria:

- The importance of the each explanatory variable comprising axle loading (YE4), speed of heavy vehicles (sh), road pavement gradient (G), asphalt thickness (HS),

asphalt material properties (VIM/SP) and maximum summer temperature (TPmax) to the prediction or description the annual incremental rut depth response variable (ΔRUT);

- The association (whether positive, negative or other) between ΔRUT and the explanatory variables given the estimated model coefficients;
- Bayesian model comparison using Deviance Information Criteria (DIC) which is a measure based on a trade off between the fit of the observed data to the model and the complexity of the model; and
- The relative magnitude of the effect of each of explanatory variable on ΔRUT.

6.6.1 Importance of Model Coefficients

Considering the importance of each model coefficient, the posterior distributions of the model coefficients given in section 6.5.1.1 together with plots of 95% credible interval given in section 6.5.1.2 were examined to assess whether they are scattered around zero or not. Posterior distributions of model coefficients far away from zero suggest a significant contribution of that variable to the prediction of annual incremental rut depth (ΔRUT).

For example, considering Figure 6.26, the posterior distribution of model coefficient for β_3 associated with road gradient (G) is scattered around zero. This suggests that road gradient (G) variable is less significant in predicting annual incremental rut depth for TSCS under the lognormal likelihood assumption. The model coefficient β_6 for maximum temperature is however important for describing annual incremental rut depth since posterior distribution is scattered away from zero.

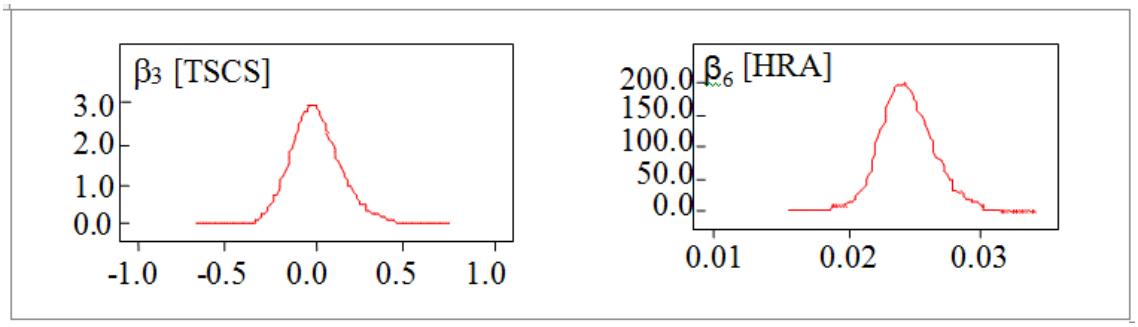

Figure 6.26: Posterior Model Coefficient Distribution β_3 and β_6 for Gradient and Maximum Temperature Variables based on Bayesian Model 1L.

The assessment of importance associated with the estimated model coefficients are initially presented for the three rut depth model structures followed by consideration model coefficients for the binder softening point and voids in mix models.

6.6.1.1 Rut Depth Model Structure 1

The assessment of the importance of the estimated model coefficients for annual rut depth model structure 1 (based on Equation 4.5 in Chapter 4) is summarised in Table 6.5 by the three asphalt surfacing groups (DBM, HRA and TSCS) and four Bayesian model types (Model 1D based on Double Exponential Likelihood), 1L (Lognormal Likelihood), 1N (Normal Likelihood) and 1S (Students t Likelihood).

Table 6.5: Importance of Explanatory Variables for Model Structure 1

Explanatory Variable	Model Coefficient	Model 1D			Model 1L			Model 1N			Model 1S		
		DBM	HRA	TSCS	DBM	HRA	TSCS	DBM	HRA	TSCS	DBM	HRA	TSCS
Traffic Loading (YE4)	β_1	✓	✓	✓	✓	✓	✓	✓	✓	✓	✓	✓	✓
Heavy Vehicle Speed (sh)	β_2	✓	✓	✓	✓	✓	✓	✓	✓	✓	✓	✓	✓
Gradient (G)	β_3	✓	✓	✓	✓	✓	×	×	✓	✓	✓	✓	✓
Asphalt Thickness (HS)	β_4	✓	✓	✓	✓	✓	✓	✓	✓	✓	✓	✓	✓
Material Properties (VIM/SP)	β_5	×	✓	✓	✓	✓	✓	×	✓	×	✓	✓	✓
Maximum Temperature (TPmax)	β_6	✓	×	✓	✓	✓	✓	✓	✓	✓	✓	✓	✓

Notes to Table 6.5

1. × = posterior distribution of the model coefficient is scattered around zero
2. ✓ = posterior distribution of the model coefficient is not scattered around zero.

The posterior estimates of the coefficient for axle loading (YE4), heavy vehicle speed (sh), and asphalt surfacing thickness (HS) are scattered away from zero for all four likelihood assumptions and three asphalt surfacing type. From the summary in Table 6.5 , 11 out of 12 or 92% of the estimates of the model coefficients for the maximum temperature variable (TPmax) are also scattered away from zero. Gradient (G) with 83% (10 out of 12) of the estimated model coefficients scattered away from zero and asphalt material properties (VIM/SP) with 75% (9 out of 12) of the estimated model coefficients scattered away from zero are also important variables for the prediction of annual incremental rut depth. All six explanatory variables are therefore important for the prediction of annual incremental rut depth under Model Structure 1 (Equation 4.5 in Chapter 4).

6.6.1.2 Rut Depth Model Structure 2

The assessment of the importance of the estimated model coefficients for annual rut depth model structure 2 (based on Equation 4.6 in Chapter 4) is summarised in Table 6.6.

Table 6.6: Importance of Explanatory Variables for Model Structure 2

Variable	Model Coefficient	Model 2D			Model 2L			Model 2N			Model 2S		
		DBM	HRA	TSCS	DBM	HRA	TSCS	DBM	HRA	TSCS	DBM	HRA	TSCS
Traffic Loading (YE4)	β_1	✓	✓	✓	✓	✓	✓	✓	✓	✓	✓	✓	✓
Heavy Vehicle Speed (sh)	β_2	✓	✓	✓	✓	✓	✓	✓	✓	✓	✓	✓	✓
Gradient (G)	β_3	✓	✓	✓	✓	✓	×	×	✓	×	✓	✓	✓
Asphalt Thickness (HS)	β_4	✓	✓	✓	✓	✓	✓	✓	✓	✓	✓	✓	✓
Material Properties (VIM/SP)	β_5	×	✓	✓	✓	✓	✓	×	✓	✓	✓	✓	✓
Maximum Temperature (TPmax)	β_6	✓	✓	✓	✓	✓	✓	✓	✓	✓	✓	✓	✓

Notes to Table 6.6

1. × = posterior distribution of the model coefficient is scattered around zero
2. ✓ = posterior distribution of the model coefficient is not scattered around zero.

The posterior estimates of the coefficient for axle loading (YE4), heavy vehicle speed (sh), asphalt surfacing thickness (HS), and maximum temperature (TPmax) are scattered away from zero for all four likelihood assumptions and are therefore important for the prediction of rut depth. Gradient (G) and asphalt material properties (VIM/SP) are also important variables for the prediction of annual incremental rut depth since 75% (9 out of 12) and 83% (10 out of 12) respectively of the estimated model coefficients are scattered away from zero. All six explanatory variables are therefore important for the prediction of annual incremental rut depth using rut depth Model Structure 2.

6.6.1.3 Rut Depth Model Structure 3

The assessment of the importance of the estimated model coefficients for annual incremental rut depth model structure 3 (based on Equation 4.7 in Chapter 4) is summarised in. Table 6.7.

Table 6.7: Importance of Explanatory Variables for Model Structure 3

Variable	Model Coefficient	Model 1D			Model 1L			Model 1N			Model 1S		
		DBM	HRA	TSCS	DBM	HRA	TSCS	DBM	HRA	TSCS	DBM	HRA	TSCS
Not Applicable	β_0	✓	×	✓	✓	✓	✓	×	×	×	✓	✓	✓
Traffic Loading (YE4)	β_1	✓	✓	✓	✓	✓	✓	✓	✓	✓	✓	✓	✓
Heavy Vehicle Speed (sh)	β_2	✓	✓	✓	✓	×	✓	✓	✓	✓	✓	✓	✓
Gradient (G)	β_3	✓	×	✓	✓	✓	×	✓	✓	×	✓	×	✓
Asphalt Thickness (HS)	β_4	✓	✓	✓	✓	✓	×	✓	✓	×	✓	✓	✓
Material Properties (VIM/SP)	β_5	×	×	✓	✓	×	✓	✓	×	×	×	✓	✓
Maximum Temperature (TPmax)	β_6	✓	✓	✓	✓	✓	✓	✓	✓	✓	✓	✓	✓

Notes to Table 6.7

1. × = posterior distribution of the model coefficient is scattered around zero
2. ✓ = posterior distribution of the model coefficient is not scattered around zero.

The constant term β_0 in model structure 3 corresponds to the expected value of the response variable ΔRUT when the observed values of all explanatory variables are equal to zero. β_0 is not important for the prediction of annual incremental rut depth (ΔRUT) for all three asphalt surfacing groups if a normal likelihood is assumed in the estimation of the model coefficients. From the summary in Table 6.7 β_0 was scattered away from zero for 8 out of the 12 (67%) estimates of the model coefficients.

The posterior estimates of the coefficient for axle loading (YE4) and maximum temperature (TPmax) are scattered away from zero for all four likelihood assumptions and the three asphalt surfacing types and are therefore important for the prediction of rut depth. 11 out of 12 (92%) of the posterior model coefficients for heavy vehicle speed variable (sh) are important for describing ΔRUT. 83% (10 out of 12) of the estimated model coefficients for asphalt surfacing thickness variable (HS) are scattered away from zero, while 75% (9 out of 12) estimated model coefficients for Gradient (G) also important for predicting ΔRUT.

The material properties variable (VIM/SP) is the least important to the description of ΔRUT with only 6 out of the 12 estimated posterior distributions scattered away from zero.

6.6.1.4 Softening Point and Voids in Mix Models

The distribution of estimated model coefficients for Softening Point (SP) and Voids in Mix (VIM) are given in Figure 6.25. The estimated model coefficients α_1, α_2 for SP model and η_1, η_2 for VIM model are all scattered away from zero and are therefore important for predicting asphalt binder softening point and asphalt voids in mix.

6.6.2 Association of Model Coefficients

The association of the model coefficients (whether positive or negative) to the prediction of annual incremental rut depth is identified based on the signs of the posterior summaries of means and relative locations (2.5% and 97.5% percentiles) given in Table 6.3 and summary statistics in Appendices C2, C3 and C4 augmented with 95% posterior credible interval plots given in Figure 6.6 to Figure 6.24.

If all of the 95% posterior credible interval for a model coefficient are positive or negative then the corresponding association is assumed. If the sign of the 2.5% percentile value is negative and that of the 97.5% percentile value is positive or the 95% posterior credible interval lies in both the positive and negative regions, the association is investigated by calculating the posterior probability:

$$P0 = f(\beta_{jm} > 0 / \Delta RUT_{OBS}) \quad (6.5)$$

where j = (0, ..., n), n = the number of model coefficients, and m = asphalt surfacing groups DBM, HRA and TSCS and ΔRUT_{OBS} = is the observed annual incremental rut depths.

When the value of P0 is close to 0.5 then there is no clear positive or negative association. Positive association is concluded for high values of P0 while negative association is concluded for low values P0.

For example, considering the credible interval for model coefficient β_2 and asphalt surfacing groups DBM, HRA and TSCS given in Figure 6.27, the association of the model coefficient for DBM and TSCS are negative since their 95% credible interval lie below the zero horizontal reference line. The 95% credible interval for HRA lies in both the negative and positive zones with probability P0 (given in Table 6.3) of 0.18. In this case, a negative association is concluded for the model coefficient β_2 for HRA since P0 is low.

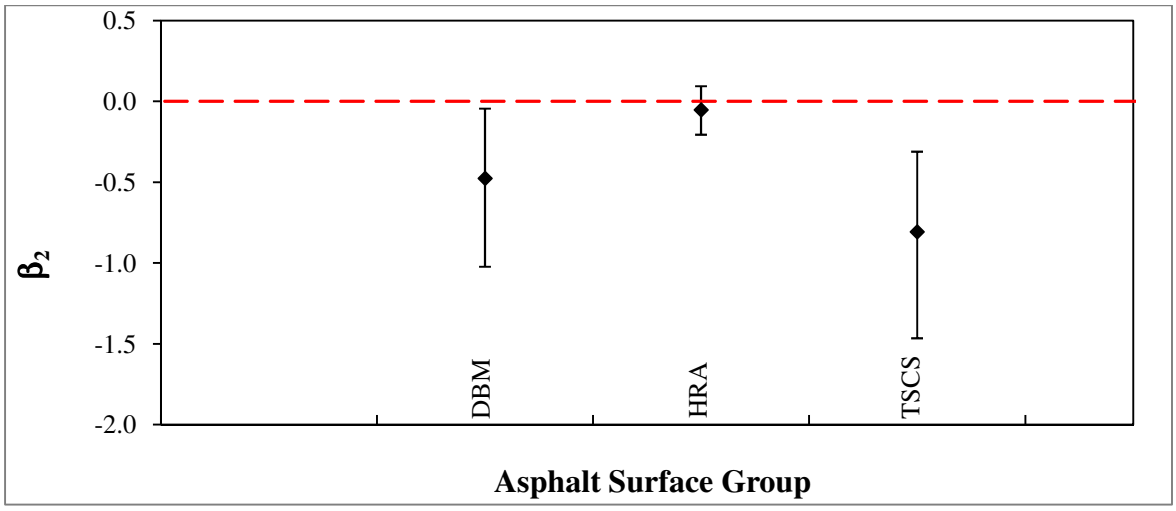

Figure 6.27: 95% Posterior Credible Interval for Model Coefficient β_2 based on Bayesian Model 1L

The association of each estimated model coefficient was compared with the expected association of each explanatory variable to determine whether they are consistent on not. The expected association of the coefficient of the explanatory variables is given as follows:

- Axle loading (YE4) coefficient (β_1) is expected to have a positive (+) association since increased axle loads should result in increased annual rates of asphalt surface rutting;
- Heavy vehicle speed (sh) coefficient (β_2) is expected to have a negative (-) association since vehicle speeds are inversely proportional to rates of loading and consequently asphalt surface rutting;
- The model coefficient for gradient (G) is expected to be positive since asphalt road sections with high gradient are known to be prone to rutting (TRL, 1993);
- Asphalt thickness (HS) is expected to have positive model coefficients based on the existing HDM-4 asphalt plastic deformation model structure (Morosuik et al., 2004);
- Both positive and negative associations are possible for the asphalt surfacing material properties (VIM/SP) since the asphalt Voids in Mix (VIM) and binder Softening Point (SP) vary at different rates with asphalt surfacing age;
- Maximum summer temperature (TPmax) is expected to result in increased rates of asphalt surface rutting, its coefficient is therefore expected to have a positive association;
- Asphalt binder SP is expected to increase with ageing of the surfacing, to that end the model coefficient α_1 associated with the asphalt surfacing age variable (AGE) is expected to be positive. In addition model coefficient α_2 which may be interpreted as the softening point in degrees Celsius at the end of the first year since the asphalt surfacing was laid is expected to be positive; and
- Asphalt VIM is expected to decrease with age of the surfacing, to that end the model coefficient η_1 associated with the asphalt surfacing age variable (AGE) is expected to be negative. In addition model coefficient η_2 which may be interpreted as the voids in

mix in percentage one year after laying the asphalt surfacing material is expected to be positive.

The association of the estimated model coefficients are discussed in subsequent subsection for each of the three proposed annual incremental rut depth model structures as well as the VIM and SP model structures.

6.6.2.1 Rut Depth Model Structure 1

The association (negative, positive or other) of estimated model coefficient for rut depth model structure 1(Equation 4.5 in Chapter 4) by asphalt surfacing group and Bayesian model types is summarised in Table 6.8.

All model coefficients estimated using Bayesian Models, 1D (Double Exponential likelihood), 1L (Lognormal likelihood) and 1S (Students t likelihood) have associations that are consistent with theoretical expectations. The model coefficient for heavy vehicle speed under the HRA surfacing group estimated using Model 1N (Normal likelihood) gives a positive sign, which is inconsistent with theoretical expectation. The inconsistency suggests that under model structure 1, the normal likelihood is not suited for describing the observed annual incremental rut depth.

Table 6.8: Summary of Association of Model Coefficients for Model Structure 1

Explanatory Variable	Model Coefficient	Expected[1]	Model 1D			Model 1L			Model 1N			Model 1S		
			DBM	HRA	TSCS	DBM	HRA	TSCS	DBM	HRA	TSCS	DBM	HRA	TSCS
Traffic Axle Loading (YE4)	β_1	(+)	(+)	(+)	(+)	(+)	(+)	(+)	(+)	(+)	(+)	(+)	(+)	(+)
Heavy Vehicle Speed (Sh)	β_2	(-)	(-)	(-)	(-)	(-)	(-)	(-)	(-)	(+)	(-)	(-)	(-)	(-)
Gradient (G)	β_3	(+)	(+)	(+)	(+)	(+)	(+)	(+)	(+)	(+)	(+)	(+)	(+)	(+)
Asphalt Thickness (HS)	β_4	(+)	(+)	(+)	(+)	(+)	(+)	(+)	(+)	(+)	(+)	(+)	(+)	(+)
Material Properties (VIM/SP)	β_5	(+) or (-)	(+)	(+)	(+)	(-)	(+)	(+)	(-)	(+)	(+)	(+)	(+)	(+)
Maximum Temperature (TPmax)	β_6	(+)	(+)	(+)	(+)	(+)	(+)	(+)	(+)	(+)	(+)	(+)	(+)	(+)

1. The expected sign of model coefficients for the each explanatory variable;
2. Model 1D, 1L, 1N and 1S are Bayesian models assuming Double Exponential, Lognormal, Normal and Students t distributions respectively.

6.6.2.2 Rut Depth Model Structure 2

The association (negative, positive or other) of estimated model coefficient for rut depth model structure 2(Equation 4.6 in Chapter 4) by asphalt surfacing group and Bayesian model types is summarised in Table 6.9.

The model coefficient for heavy vehicle speed and maximum temperature under the HRA surfacing group estimated using Model 2N (Normal likelihood) gives signs, which are inconsistent with theoretical expectation. In addition estimates using Model 2D for HRA surfacing group and Model 2L for DBM surfacing group results in negative coefficient for

maximum temperature which is not consistent with expected association. The observed inconsistencies suggest if model structure 2 is assumed, then the double exponential, lognormal and normal likelihoods are not suited for describing the observed annual incremental rut depth. All model coefficients estimated using Bayesian Model 2S (Students t likelihood) have associations that are consistent with theoretical expectations.

Table 6.9: Summary of Association of Model Coefficients for Model Structure

Explanatory Variable	Model Coefficient	Expected[1]	Model 2D			Model 2L			Model 2N			Model 2S		
			DBM	HRA	TSCS	DBM	HRA	TSCS	DBM	HRA	TSCS	DBM	HRA	TSCS
Traffic Axle Loading (YE4)	β_1	(+)	(+)	(+)	(+)	(+)	(+)	(+)	(+)	(+)	(+)	(+)	(+)	(+)
Heavy Vehicle Speed (Sh)	β_2	(-)	(-)	(-)	(-)	(-)	(-)	(-)	(-)	(+)	(-)	(-)	(-)	(-)
Gradient (G)	β_3	(+)	(+)	(+)	(+)	(+)	(+)	(+)	(+)	(+)	(+)	(+)	(+)	(+)
Asphalt Thickness (HS)	β_4	(+)	(+)	(+)	(+)	(+)	(+)	(+)	(+)	(+)	(+)	(+)	(+)	(+)
Material Properties (VIM/SP)	β_5	(+) or (-)	(+)	(+)	(+)	(+)	(+)	(+)	(-)	(+)	(+)	(-)	(+)	(+)
Maximum Temperature (TPmax)	β_6	(+)	(+)	(-)	(+)	(-)	(+)	(+)	(+)	(-)	(+)	(+)	(+)	(+)

1. The expected sign of model coefficients for the each explanatory variable;
2. Model 2D, 2L, 2N and 2S are Bayesian models assuming Double Exponential, Lognormal, Normal and Students t distributions respectively and model structure 2 (Equation 4.6).

6.6.2.3 Rut Depth Model Structure 3

The association (negative, positive or other) of estimated model coefficient for rut depth model structure 3 (Equation 4.7 in Chapter 4) by asphalt surfacing group and Bayesian model types is summarised in Table 6.10.

Table 6.10: Summary of Association of Model Coefficients for Model Structure 3

Explanatory Variable	Model Coefficient	Expected[1]	Model 3D			Model 3L			Model 3N			Model 3S		
			DBM	HRA	TSCS	DBM	HRA	TSCS	DBM	HRA	TSCS	DBM	HRA	TSCS
Not Applicable	β_0	(+) or (-)	(+)	(+)	(+)	(+)	(+)	(+)	(-)	(-)	(+)	(+)	(+)	(+)
Traffic Axle Loading (YE4)	β_1	(+)	(+)	(+)	(+)	(+)	(+)	(+)	(+)	(+)	(+)	(+)	(+)	(+)
Heavy Vehicle Speed (Sh)	β_2	(-)	(-)	(-)	(-)	(-)	(+/-)	(-)	(+)	(+)	(-)	(-)	(-)	(-)
Gradient (G)	β_3	(+)	(+)	(-)	(+)	(+)	(-)	(+)	(-)	(-)	(+/-)	(+)	(-)	(+)
Asphalt Thickness (HS)	β_4	(+)	(+)	(+)	(+)	(+)	(+)	(+)	(+)	(+)	(+)	(+)	(+)	(+)
Material Properties (VIM/SP)	β_5	(+) or (-)	(+/-)	(+)	(+)	(-)	(+)	(+)	(-)	(+)	(+)	(-)	(+)	(+)
Maximum Temperature (TPmax)	β_6	(+)	(+)	(+)	(+)	(+)	(+)	(+)	(+)	(+)	(+)	(+)	(+)	(+)

1. The expected sign of model coefficients for the each explanatory variable;
2. Model 3D, 3L, 3N and 3S are Bayesian models assuming Double Exponential, Lognormal, Normal and Students t distributions respectively and model structure 3 (Equation 4.7).

From Table 6.10 none of the Bayesian models (3D, 3L, 3N or 3S) provided model estimates of coefficients for model structure 3 that are consistent with theoretical expectations for all three asphalt surfacing types. This suggests that given the data used in the study the linear regression structure adopted for this model structure is not appropriate for describing annual incremental rut depths. Model structure 3 was introduced in Chapter 4 as Equation 4.7 and is reproduced hereunder as Equation 6.6

$$\Delta RUT_{imt} = \beta_{0m} + \beta_{1m} YE4_{imt} + \beta_{2m} sh_{im} + \beta_{3m} G_i + \beta_{4m} HS_{imt} + \beta_{5m} \left(\frac{VIM_{imt}}{SP_{imt}}\right) + \beta_{6m} TPmax_{it} \times H_1 \quad (6.6)$$

Equation 6.6 may not be suitable because the development of asphalt surface rutting is likely to be due to a synergy of two or more of the six explanatory variables. To that end, multiplicative structures adopted for model structures 1 (Equation 4.5 in Chapter 4) and 2 (Equation 4.6 in Chapter 4) are more suited.

6.6.2.4 VIM and SP Model Structures

The association (negative, positive or other) of estimated model coefficient for SP and VIM model structures (Equations 4.2 and 4.3 in Chapter 4) by asphalt surfacing group are summarised in Table 6.11.

Table 6.11: Summary of Association of Model Coefficients for SP and VIM Models

Models	Explanatory Variable	Model Coefficient	Expected[1]	DBM	HRA	TSCS
Softening Point Model	Asphalt Surfacing Age (AGE)	α_1	(+)	(+)	(+)	(+)
	-	α_2	(+)	(+)	(+)	(+)
Voids in Mix Model	Asphalt Surfacing Age (AGE)	η_1	(-)	(-)	(-)	(-)
	-	η_2	(+)	(+)	(+)	(+)

1. The expected sign of model coefficients for the SP and VIM models;
2. Model coefficient α_2 is synonymous to the softening point in degrees Celsius at the end of the first year since the asphalt surfacing was laid;
3. Model coefficient η_2 is synonymous to the voids in mix in percentage one year after the asphalt surfacing material is laid.

6.6.3 Bayesian Model Comparison using Deviance Information Criteria

Model comparison was limited to Bayesian models identified in the previous section (section 6.6.2) as having coefficients with associations (negative, positive or other) that are consistent with theoretical expectations for all three asphalt surfacing groups. These models are:

- Model 1D based on Model Structure 1 and Double Exponential likelihood
- Model 1L based on Model Structure 1 and Lognormal likelihood
- Model 1S based on Model Structure 1 and Students t likelihood
- Model 2S based on Model Structure 2 and Students t likelihood

Deviance Information Criteria (DIC) is a measure for Bayesian model comparison based on a trade off between the fit of the observed data to the model and the complexity of the model. The concepts of DIC are detailed in Spiegelhalter et al. (2002). DIC values for each of the above Bayesian model were calculated using the WinBUGS software. The model with the smallest DIC is estimated to be the model that would best replicate the dataset which has the same structure as that used to estimate the model coefficients. The DIC for the four Bayesian models are given in Table 6.12.

Bayesian Model 1L which assumed a lognormal likelihood and model structure 1 (based on Equation 4.5 in Chapter 4) has the lowest DIC value and thus provides the best fit to the observed data. Discussions in subsequent sections and Chapters refer to model coefficients estimated using Model 1L.

Table 6.12: Model Comparison using DIC

Bayesian Models	Dbar	Dhat	pD	DIC
Model 1D	7326.37	7313.36	13.015	7339.39
Model 1L	5974.5	5984.15	-9.655	5964.84
Model 1S	6718.25	7351.22	-632.97	6085.28
Model 2S	6705.31	6866.37	-161.061	6544.25

Note to Table 6.12

1. Dbar is the posterior mean of the deviance. Deviance is defined as -2*log(P[ΔRUT /ϕ]). P[ΔRUT /ϕ] is the likelihood of the observed data given model coefficients ϕ.

2. ϕ is a vector of the model coefficients for the annual incremental rut depth models.

3. Dhat is a point estimate of the deviance.

4. pD is the effective number of parameters, and is given by pD = Dbar - Dhat. Thus pD is the posterior mean of the deviance minus the deviance of the posterior means.

5. DIC is the Deviance Information Criteria and is given by DIC = Dbar + pD = Dhat + 2 * pD. The model with the smallest DIC is estimated to be the model that would best replicate the dataset of the same structure as that used to estimate the model coefficients.

6.6.4 Magnitude of the Effect of Explanatory Variables

The relative magnitude of the effect of the explanatory variables was investigated through sensitivity analysis using the posterior means of model coefficients for DBM, HRA and TSCS surfacing groups given in Table 6.3. This was achieved by changing values of each explanatory variable at a time from a plausible base value by 10% and 20% and 30% respectively and then calculating the percentage change in the expected value of ΔRUT using equation 4.5 (Model Structure 1) and model coefficients derived from Bayesian Model 1L. The results are depicted in Figure 6.28 for HRA surfacing group and in Appendix C5 for DBM and TSCS surfacing groups. The relative magnitude of the effect of the explanatory

variables given the estimated model coefficients is discernible by comparing the slopes of the plots of the variables. Variables with steeper slopes have higher effects on the prediction of annual incremental rut depth.

The magnitude of the effect of the explanatory variables is highly dependent on the estimated model coefficients. Considering Figure 6.28, the most sensitive variables in descending order are axle loading, asphalt material properties, heavy vehicle speeds, asphalt thickness, maximum temperature and road gradient. The modest sensitivity of the climate variable does not suggest that it is not important for the prediction of annual incremental rut depth. The effect of including the climate variable in the model structure is considered in section 6.8.

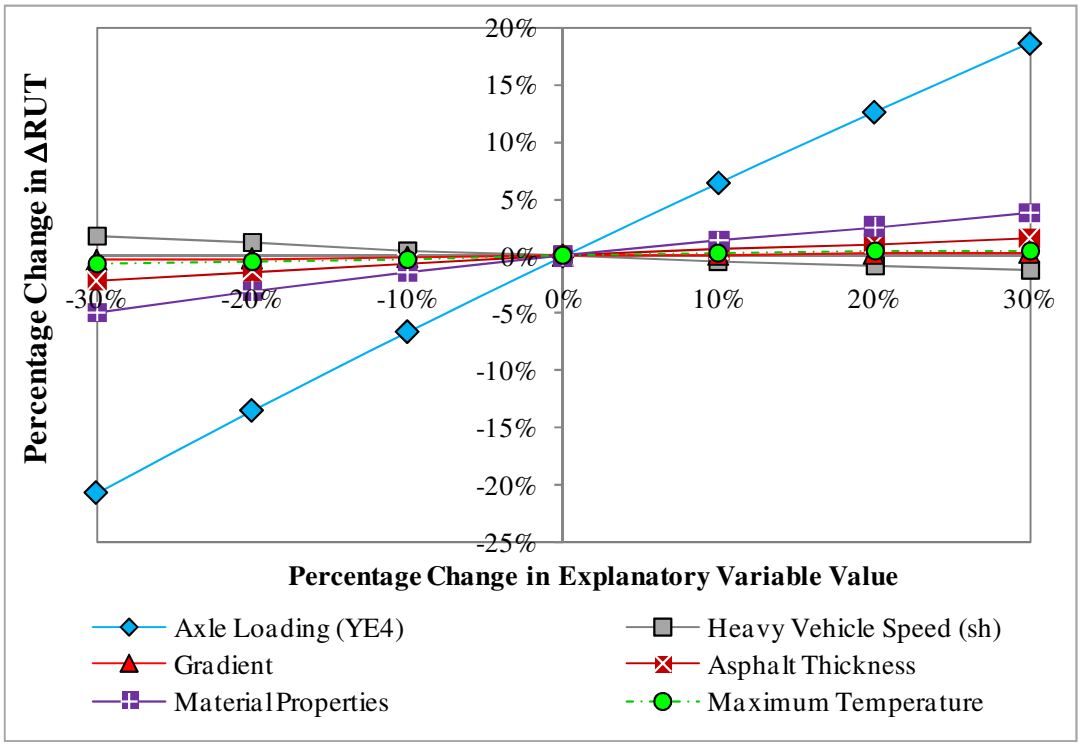

Figure 6.28: Relative Magnitude of the Effect of Explanatory Variables Based on HRA Model Coefficients and Bayesian Model 1L

6.7 Sensitivity of Prior Distributions

The model coefficients for the rut depth models were estimated based on the assumption that they are a priori normally distributed as given in Table 6.1. To that end, sensitivity analysis using Bayesian Model 1L was aimed at investigating the robustness of the posterior distribution and consequently the estimated model coefficients to the structure and parameters of the prior distribution. Separate sensitivity analyses were performed for informative priors and low information priors.

6.7.1 Sensitivity of Informative Priors

In cases where informative priors were used, sensitivity analysis was focused on the structure of the prior distribution. Informative priors were specified in Table 6.1 to the following three model coefficients: β_1 (axle loading), β_2 (heavy vehicle speed) and β_4 (asphalt surfacing thickness). Alternative prior distribution structures in addition to the normal distribution assumption in Table 6.1 were selected on the basis that they can be described by mean and variance parameters. To that end, the following alternative prior distributions were selected:

- double exponential distribution;
- logistic distribution, and;
- Student's t distribution with a degree of freedom (v) of 2.

The same values for mean and variance specified in Table 6.1 for the normal distribution were used in the alternate prior distribution structures. Sensitivities of posterior estimates of model coefficients β_1 and β_4 for TSCS and HRA surfacing groups are summarised in Figure 6.29

and Figure 6.30 respectively. Plots for other surfacing groups and for model coefficient β_2 are provided in Appendix C6.

Considering Figure 6.29 and Figure 6.30, the vertical whisker lines corresponding to each prior distribution structure are the 95% posterior credible interval of the model coefficients. The ends of the whisker lines represent the 2.5% and 97.5% percentile posterior values of the model coefficients. The squared mark between the vertical whisker lines corresponds to the posterior mean of the model coefficients. The horizontal reference line corresponds to the average of the posterior means estimated using all the four prior distribution structures.

Considering Figure 6.29 the posterior mean of β_1 TSCS ranged from 1.302 (Normal and Double Exponential prior structures) to 1.362 (Logistic prior structure). Similarly from Figure 6.30 the posterior mean of β_4 HRA ranged from 0.059 (Normal prior) to 0.097 (Students t prior). The results show that the estimated model coefficients are robust to the structure of the prior distribution.

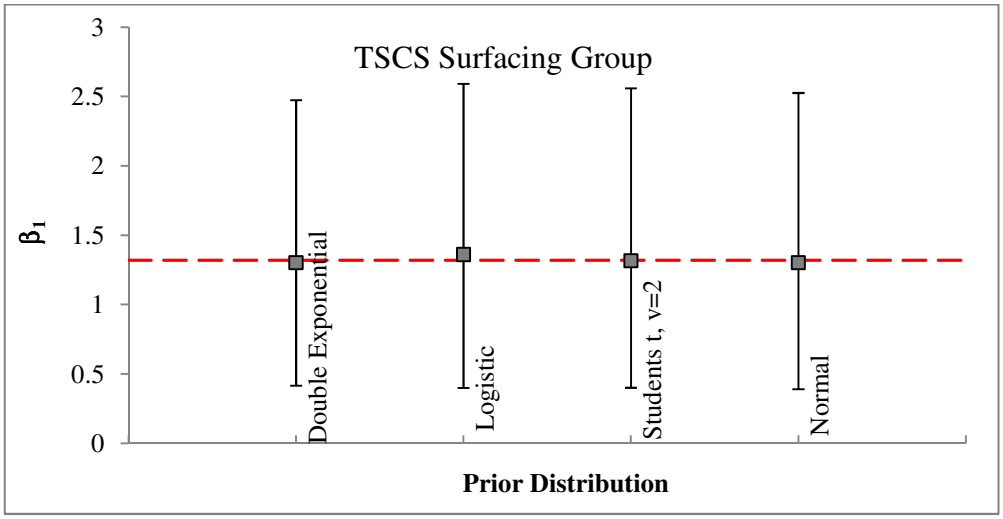

Figure 6.29: Sensitivity of TSCS Model Coefficient β_1 to Structure of Prior Distribution.

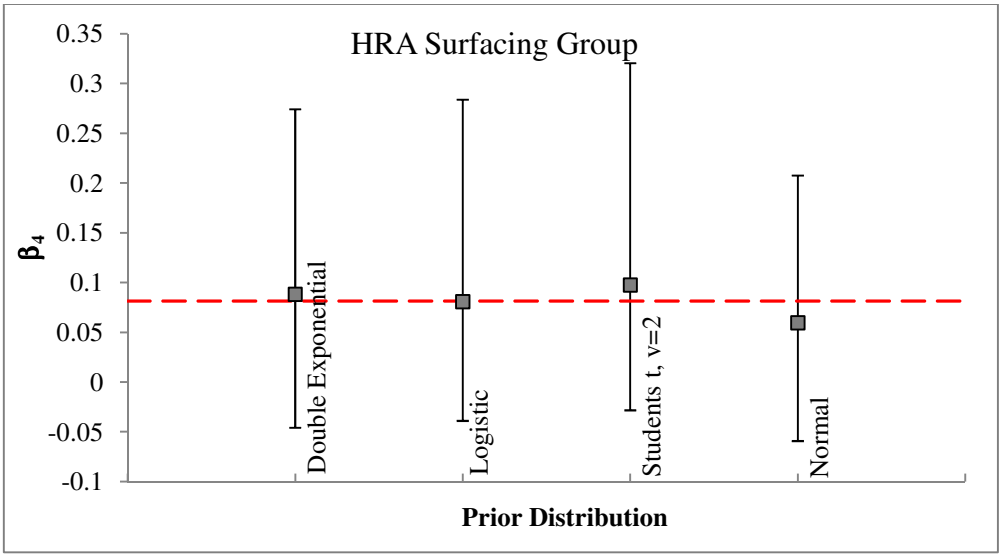

Figure 6.30: Sensitivity of HRA Model Coefficient β_4 to Structure of Prior Distribution.

6.7.2 Sensitivity of Variance of Prior Distribution

When low information or vague priors were used, sensitivity analysis was focused on how different prior variance parameters may influence the posterior inference. In order to reflect uncertainty in the variability of the prior distribution of the model coefficients large variance (1000) or low precision (0.001) were specified to all prior distributions of the model coefficients as shown in Table 6.1. Sensitivity analysis was performed for the range of variance given by Equation 6.7.

$$\text{VARIANCE} = 10^{C} \tag{6.7}$$

where C = {-2, -1, 0, 1, 2, 3, 4}. The sensitivity of the posterior estimates for the axle loading model coefficient β_1 (DBM) and the maximum temperature coefficient β_6 (HRA) are depicted in Figure 6.31 and Figure 6.32 respectively. Horizontal solid line in each plot represents the posterior mean while the dotted lines are the 2.5% and 97.5% percentiles of the distribution. The results show that the posterior means are robust within the range of prior variance

investigated with the mean values ranging from 0.240 to 0.270 for β_1 (DBM) and from 0.024 to 0.025 for β_5 (HRA). Results for other model coefficients are depicted in Appendix C6.

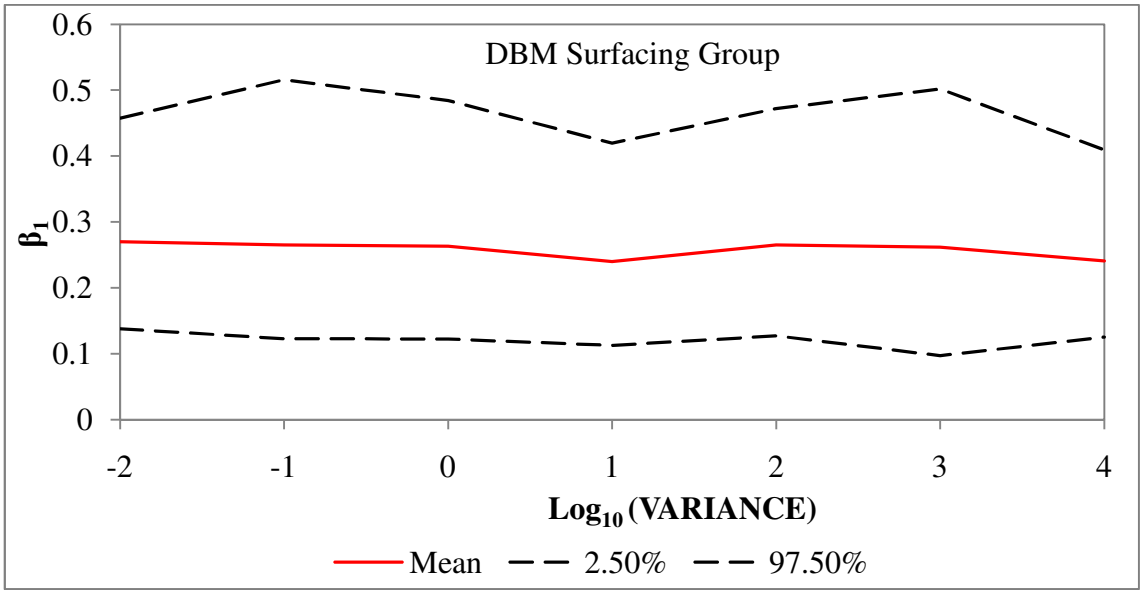

Figure 6.31: Sensitivity of Posterior Mean Axle Loading (YE4) Model Coefficient for DBM Surfacing Group to Variance of Prior Distribution.

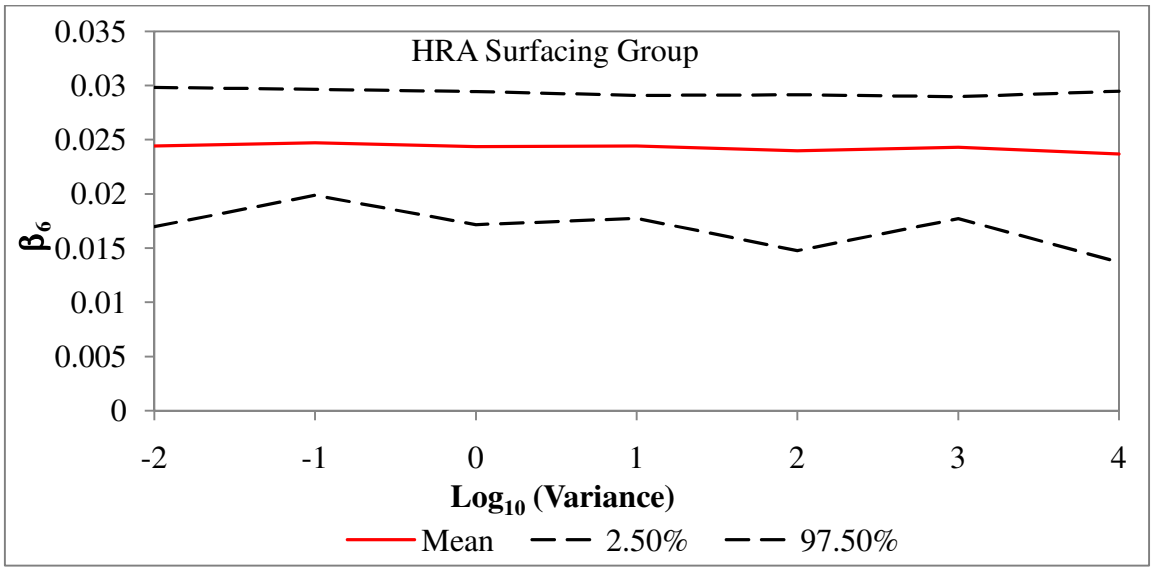

Figure 6.32: Sensitivity of Posterior Mean Maximum Temperature (TPmax) Model Coefficient for HRA Surfacing Group to Variance of Prior Distribution.

6.8 Effect Including Climate Variable

A key objective of this study was to develop improved annual incremental rut depth models which can be used for assessing the impact of future changes in climate on asphalt road networks. To that end, Model structures 1, 2 and 3 referred to in previous sections in this chapter and formulated in Chapter 4 includes a climate variable (TPmax) represented by the mean daily maximum summer temperature. This section is aimed at investigating whether including the climate variable (TPmax) in the model structure resulted in an improved model or not given the data used in the study.

The Deviance Information Criteria (DIC) was used to compare Model structure 1 which embodies the climate variable TPmax and is given below as Equation 6.8 with a modified structure without the climate variable (Equation 6.7).

Rut depth model structure 1 with climate variable is given as

$$\Delta RUT_{imt} = YE4_{imt}^{\beta_{1m}} \times sh_{im}^{\beta_{2m}} \times G_i^{\beta_{3m}} \times HS_{imt}^{\beta_{4m}} \times \left(\frac{VIM_{imt}}{SP_{imt}}\right)^{\beta_{5m}} \times [H_0 + \beta_{6m} \times TPmax_{it} \times H_1] + \varepsilon_{imt} \quad (6.8)$$

where ΔRUT_{imt}= annual incremental increase in deformation within the asphalt layers of the pavement, in mm for road section i during time period t; $YE4_{it}$= annual number of equivalent standard axles, in millions/lane on road section i during year t; sh_{it}= average speed of heavy vehicles on section i, in km/h during year t; G_i gradient of road section i; HS_{it}= thickness of asphalt layer on section i during year t, in mm; VIM_{imt} = Voids in Mix for road asphalt material type m on road section i during year t; SP_{imt}= Softening point of binder for road

section i with material type m during year t.; $TPmax_{imt}$ = Maximum Summer Temperature during hot dry summer year in ^{o}C; ε_{imt} = error term; β_{1m} to β_{6m} are model coefficients for surface material type m; Ho takes a value of 0 during hot and dry summer years and a value of 1 in other years; H1 takes on a value of 1 during hot dry summer years and a value of 0 otherwise.

The revised model structure without climate variable is given as

$$\Delta RUT_{imt} = YE4_{imt}^{\beta_{1m}} \times sh_{im}^{\beta_{2m}} \times G_{it}^{\beta_{3m}} \times HS_{imt}^{\beta_{4m}} \times \left(\frac{VIM_{imt}}{SP_{imt}}\right)^{\beta_{5m}} + \varepsilon_{imt} \quad (6.9)$$

The DIC for both model structures calculated using the WinBUGS software is given in Table 6.13. The model structure with the climate had a lower DIC value than the model structure without. This implies that the model structure 1 with climate variable provides a better fit to the data than the structure without the climate variable.

Table 6.13: Model Comparison using DIC

Model Structure	Dbar	Dhat	pD	DIC
With Climate Variable	5974.5	5984.15	-9.655	5964.84
Without Climate Variable	6371.08	6541.86	-170.778	6200.30

Note to Table 6.13

1. Dbar is the posterior mean of the deviance.
2. ϕ is a vector of the model coefficients for the annual incremental rut depth models.
3. Dhat is a point estimate of the deviance.
4. pD is the effective number of parameters, and is given by pD = Dbar - Dhat. Thus pD is the posterior mean of the deviance minus the deviance of the posterior means.

The distribution of the error term (ε) for model structures with and without climate variable is given in Figure 6.33. It is clear that including the climate variable results in an improved model since the distribution of the error term are scattered around zero for model structure with climate variable and away from zero for the model structure without climate variable.

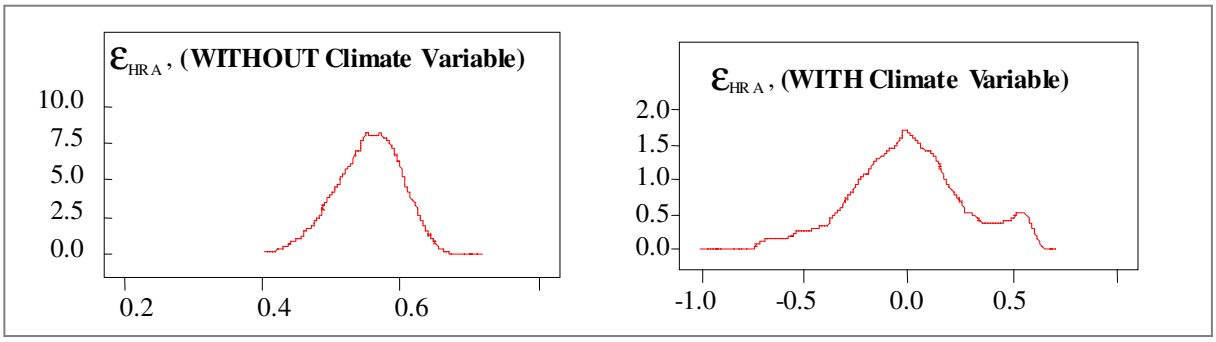

Figure 6.33: Posterior Distribution of the Error Term for HRA Surfacing Group for Model Structures WITHOUT and WITH Climate Variable.

6.9 Summary

This chapter presented the Bayesian estimation of model coefficients for the three improved annual incremental rut depth model structures proposed in Chapter 4 using the double exponential, lognormal, normal and student's t assumptions of the likelihood of the observed data. For each combination of model structure and likelihood assumptions the coefficients of the models were estimated for three asphalt surfacing groups (DBM, HRA and TSCS).

The importance of each explanatory variable given the model coefficients were assessed by examining the posterior distributions to establish whether they are scattered around zero or not. All six explanatory variables were found to be important for the prediction of annual incremental rut depth when Model Structures 1 (Equation 4.5) and 2 (Equation 4.6) were

used. For model structure 3 (Equation 4.7), material properties variable was the least important.

The association (whether positive, negative or other) were assessed by examining the signs of the posterior mean values of the model coefficients and probability that the posterior values of the model coefficients are greater than zero. Estimated model coefficients for model structure 1 were found to have associations that are mostly consistent with theory.

Comparison of model fit and complexity for the Bayesian models with associations that were consistent with theory was performed using the Deviance Information Criteria. Model structure 1 with lognormal likelihood was found to provide posterior estimates of model coefficients that would best fit and replicate the data used in the study. To that end model structure 1 and coefficients estimated under the lognormal likelihood assumption were selected for use in subsequent analysis in other Chapters.

CHAPTER 7 MODEL CHECKING AND VALIDATION

7.1 Introduction

Interpretation of the results of the estimation of model coefficients for the proposed rut depth model structures in section 6.6 suggested that the Bayesian model 1L with a lognormal likelihood and rut depth model structure 1 (Equation 4.5) was the most suitable out of the 12 possible Bayesian models described in section 6.4.1. This Chapter sets out model checks and validation performed to establish if the selected Bayesian model (Model 1L) and the estimated model coefficients are appropriate for use in performing predictions.

Section 7.2 of the chapter sets out the data used for checking and validating the model. Section 7.3 discusses results of the Bayesian predictive model checks. Section 7.4 provides time series comparison of observed rut depth for selected road sections with predictions made using developed rut depth model. Section 7.5 provides a framework which can be used to improve the estimation of the model coefficients when new data becomes available. Section 7.6 summarises the chapter.

7.2 Data for Model Checking and Validation

The types, sources, and accuracy of data used in the study are detailed in Chapter 5. Data was available for a total of 3,006 road sub-sections of which 1994 or 66% were used in the estimation of the model coefficients (model development) presented in Chapter 6 and the remaining 1,012 sub-sections or 34% were used for model checking and validation.

The data used for model validation were randomly sampled from the combined dataset without replacement thereby ensuring that a separate set of data was used for model development.

Table 7.1 summarises the data that was used for model checking and validation in the form of a matrix defined by the following headings:

- Three asphalt surfacing groups (Dense Bituminous Macadam (DBM), Hot Rolled Asphalt (HRA), and Thin Surface Course System (TSCS));
- Year (2002 to 2006) in which the data were observed;
- Number of road subsections in each surface group and year;
- The average (Ave.), minimum (Min.), and maximum (Max.) values of the data variables.
- Nine data variables including: annual incremental rut depth (ΔRUT), annual equivalent standard axle loading (YE4), speed of heavy vehicles (sh), absolute road section gradient (G), asphalt thickness (HS), voids in mix (VIM), asphalt surfacing age (AGE), binder softening point (SP), and maximum summer pavement temperature (TPmax).

Table 7.1: Summary of Data used for Model Checking and Validation

Asphalt Surfacing Group	Number of Sub-Sections	Year	Statistics	Length	Annual Incremental Rut Depth	Annual Axle Loading	Heavy Vehicle Speed	Gradient	Asphalt Thickness	Voids in Mix	Surfacing Age	Softening Point	Asphalt Temperature
				-	ΔRUT	YE4	sh	G	HS	VIM	AGE	SP	TPmax
				m	mm	msa	km/h	-	mm	%	Years	°C	°C
DBM	66	2002	Mean	98.3	1.5	0.7	78.7	1.1	215.2	1.4	17.7	75.1	38.2
			Min.	61.0	0.1	0.5	49.4	0.0	96.0	0.9	3.0	55.0	37.1
			Max.	100.0	7.0	1.3	93.5	3.3	388.0	5.4	35.8	78.0	38.6
	80	2003	Mean	99.3	3.5	0.8	77.8	1.2	264.3	1.2	18.7	75.0	39.7
			Min.	78.0	0.0	0.2	49.5	0.1	97.0	0.9	4.0	59.8	37.7
			Max.	100.0	13.6	1.9	102.7	4.7	561.0	3.0	36.8	78.0	40.7
	124	2004	Mean	99.7	0.7	1.0	78.9	1.4	249.5	1.3	22.4	75.7	38.5
			Min.	75.0	0.0	0.2	48.9	0.1	96.0	0.9	5.0	62.2	36.7
			Max.	100.0	4.3	2.0	98.6	4.7	534.0	3.9	37.8	78.0	39.3
	174	2005	Mean	98.6	0.8	0.8	73.8	1.3	236.7	1.2	22.3	76.3	37.7
			Min.	61.0	0.0	0.2	47.8	0.0	96.0	0.9	6.0	59.9	35.9
			Max.	100.0	4.4	1.4	95.5	4.7	561.0	2.9	38.8	78.0	38.7
	2	2006	Mean	100.0	0.9	1.6	102.9	0.8	414.0	1.3	12.3	72.9	39.4
			Min.	100.0	0.7	1.6	102.9	0.7	414.0	0.9	12.3	72.6	38.6
			Max.	100.0	1.0	1.6	102.9	0.8	414.0	1.7	12.3	73.3	40.2
HRA	43	2002	Mean	98.1	1.4	0.9	85.5	1.2	278.7	1.2	13.6	77.7	38.5
			Min.	51.0	0.0	0.5	49.4	0.0	150.0	0.9	9.5	75.2	38.1
			Max.	100.0	3.6	1.1	97.4	4.6	450.0	1.5	34.8	78.0	38.7
	48	2003	Mean	98.1	1.8	1.1	85.1	1.1	281.6	1.2	15.2	77.2	40.1
			Min.	63.0	0.0	0.4	41.5	0.0	113.0	0.9	4.7	64.8	38.3
			Max.	100.0	13.1	2.2	109.1	4.2	546.0	2.0	28.8	78.0	40.7
	226	2004	Mean	98.1	0.9	1.5	83.5	1.3	260.4	1.2	15.8	76.9	38.8
			Min.	100.0	50.0	0.0	0.5	18.0	0.0	100.0	0.9	5.1	36.7
			Max.	2300.0	100.0	5.0	2.8	106.7	6.4	546.0	1.8	36.8	39.3
	113	2005	Mean	98.0	0.7	0.8	80.6	1.3	256.0	1.2	19.4	77.9	37.8
			Min.	50.0	0.0	0.2	48.7	0.0	120.0	0.9	6.7	69.4	36.0
			Max.	100.0	4.0	1.2	98.1	5.4	450.0	1.5	37.8	78.0	38.8
	5	2006	Mean	100.0	2.1	1.6	97.6	1.3	406.0	1.1	12.3	77.4	40.3
			Min.	100.0	0.4	1.6	97.3	0.1	390.0	0.9	12.3	74.9	40.3
			Max.	100.0	3.4	1.6	98.0	2.4	420.0	1.3	12.3	78.0	40.3

Table 7.1: Summary of Data used for Model Checking and Validation (Continued)

Asphalt Surfacing Group	Number of Sub-Sections	Year	Statistics	Length	Annual Incremental Rut Depth	Annual Axle Loading	Heavy Vehicle Speed	Gradient	Asphalt Thickness	Voids in Mix	Surfacing Age	Softening Point	Asphalt Temperature
				-	ΔRUT	YE4	sh	G	HS	VIM	AGE	SP	TPmax
				m	mm	msa	km/h	-	mm	%	Years	°C	°C
TSCS	5	2002	Mean	100.0	2.0	1.1	76.6	0.8	214.4	3.4	4.0	66.0	38.0
			Min.	100.0	0.5	1.1	75.5	0.1	173.0	2.4	3.8	61.1	37.1
			Max.	100.0	3.1	1.3	80.8	1.6	250.0	3.9	4.9	80.0	38.3
	5	2003	Mean	100.0	5.4	0.6	57.2	1.6	242.2	4.0	4.3	66.9	38.9
			Min.	100.0	0.9	0.4	40.8	0.8	222.0	1.0	0.2	58.2	38.4
			Max.	100.0	8.5	1.1	95.0	2.2	275.0	6.4	15.3	80.0	39.3
	61	2004	Mean	98.8	0.7	1.5	82.9	1.2	217.0	3.7	4.4	66.5	38.8
			Min.	61.0	0.1	0.4	48.4	0.1	30.0	1.0	0.3	46.8	36.7
			Max.	100.0	1.8	2.2	98.9	4.4	609.0	6.8	31.8	80.0	39.3
	60	2005	Mean	99.3	0.5	0.9	84.7	1.0	235.0	3.4	4.5	66.8	38.1
			Min.	61.0	0.0	0.4	40.8	0.1	30.0	0.9	2.2	50.7	37.9
			Max.	100.0	2.1	1.2	96.3	3.2	609.0	5.7	38.8	80.0	38.1

7.3 Model Checking and Validation within Bayesian Framework

7.3.1 Concepts of Model Checking using Posterior Predictive Distribution

Prediction of future annual incremental rut depth ΔRUT_{imt}^{FUT} is possible in Bayesian theory using predictive distribution (Gelman et al., 2004) which, in the context of this study can be written as Equation 7.1.

$$f\left(\Delta RUT_{imt}^{FUT}/\Delta RUT_{imt}^{OBS}\right) = \int f\left(\Delta RUT_{imt}^{FUT}/\phi\right)\left(\phi/\Delta RUT_{imt}^{OBS}\right)d\phi \quad (7.1)$$

where $f\left(\Delta\mathrm{RUT}_{\mathrm{imt}}^{\mathrm{FUT}}/\Delta\mathrm{RUT}_{\mathrm{imt}}^{\mathrm{OBS}}\right)$ is the future prediction conditional on the observed data; $f\left(\Delta\mathrm{RUT}_{\mathrm{imt}}^{\mathrm{FUT}}/\phi\right)$ is the likelihood of future annual incremental rutting data given the

distribution of the model coefficients ϕ; $\phi = \{\beta_1, \beta_2, \beta_3, \beta_4, \beta_5, \beta_6\}^T$ is the transpose of the vector of the distribution of the model coefficients and $\left(\phi/\Delta RUT_{imt}^{OBS}\right)$ is the posterior distribution of the model coefficients given the observed incremental rutting data ΔRUT_{imt}^{OBS}.

According to Ntzoufras (2009) predictive distributions can be used to measure the probability of again observing in the future each annual incremental rut depth value used in the estimation of the model coefficients (ΔRUT_{imt}) assuming that the adopted model is true. It therefore follows that predictive distributions may be used not only to predict future observations but also to check the plausibility of the assumed Bayesian model. This is achieved using a Markov Chain Monte Carlo sampler such as that implemented in the Bayesian software WinBUGS to generate replicated values ΔRUT_{imt}^{REP} of the observed incremental rutting ΔRUT_{imt}^{OBS}. According to Meng (1996), the posterior distribution of these vectors of the form $D\left(\Delta RUT_{imt}^{REP}, \phi\right)$ and $D\left(\Delta RUT_{imt}^{OBS}, \phi\right)$ can be used to provide individual as well as overall goodness-of-fit diagnostics that can be presented graphically. Further discussions on the concepts of model checking using Bayesian posterior predictive distribution is given in Gelman et al. (2004).

The model checks and validation was performed using the WinBUGS software described in section 6.4. The results are discussed under two headings:

- Individual diagnostics; and
- Goodness-of-fit diagnostics.

7.3.2 Individual Diagnostics

Individual diagnostics were performed by comparing each individual predicted value of ΔRUT^{REP} with the observed annual incremental rut depth data ΔRUT^{OBS} described in section 7.2. This check is aimed at identifying outliers or surprising trends in the predictions.

Figure 7.1 compares the ordered mean predicted annual incremental rut depth (ΔRUT^{REP}) and 95% posterior credible intervals with the observed values. The dotted reference line $\Delta RUT^{REP} = \Delta RUT^{OBS}$ is enclosed by the 95% credible interval indicating that the model predictions are acceptable.

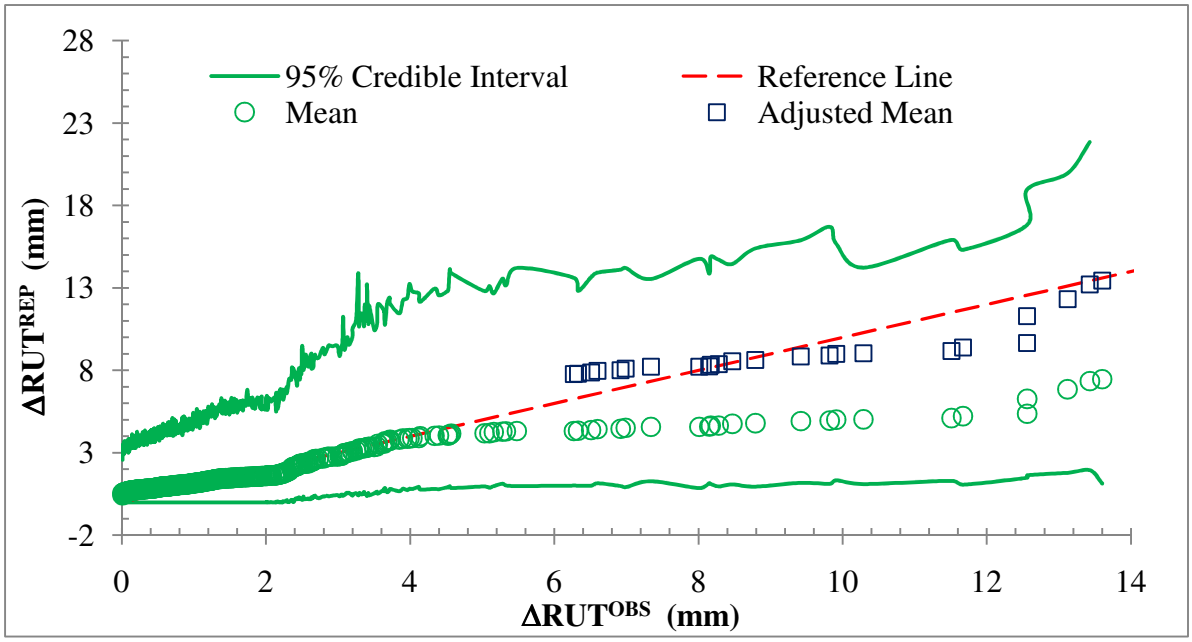

Figure 7.1: Posterior Predictive Mean and 95% Error Bars of ΔRUT^{REP} versus Observed Data ΔRUT^{OBS}

The predicted posterior 95% credible interval illustrated in Figure 7.1 increases with the magnitude of the observed rut depth indicating that greater uncertainty exists in the prediction of high values of annual incremental rut depth. Mean predictions (ΔRUT^{REP}) corresponding to

observed (ΔRUT^{OBS}) values greater than 5mm are generally lower but still acceptable since they fall within the 95% credible interval. Predictions of extreme mean values (greater than 6mm) can be improved by multiplying the predicted mean ΔRUT^{REP} by factor of 1.8. This adjustment to the predicted mean rut depth values is illustrated (using adjusted mean plots) in Figure 7.1.

When observed values greater than 5mm were removed, then by inspection, the plot of the mean prediction and the observed rut depth values were close to the reference line as depicted in Figure 7.2.

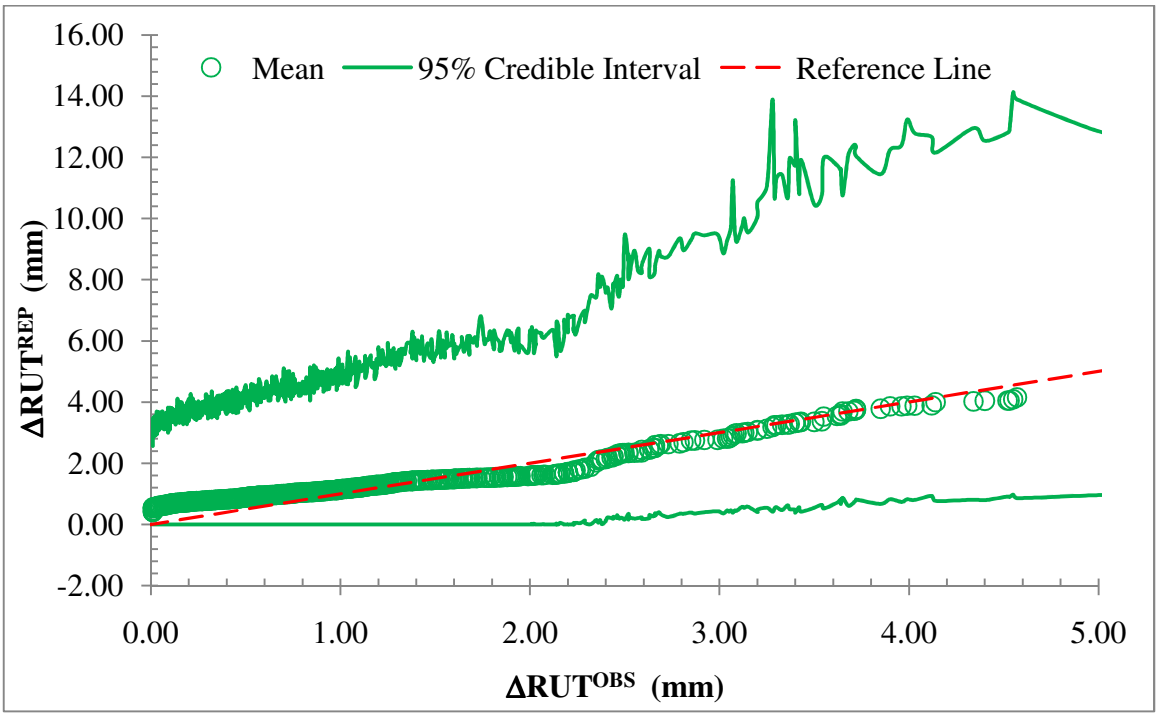

Figure 7.2: Posterior Predictive Mean and 95% Error Bars of ΔRUT^{REP} versus Observed Data ΔRUT^{OBS} less than 5mm.

A comparison of the predictive distribution of the Bayesian model with the distribution of the observed data was achieved by plotting the cumulative distributions of the predicted annual incremental rut depth (F^{REP}) and the observed annual incremental rut depth (F^{OBS}) against the

observed data (ΔRUT^{OBS}) as shown in Figure 7.3. It can be observed from Figure 7.3 that the assumed model provides an adequate fit to the observed validation data. The next section considers the goodness-of-fit of the assumed model.

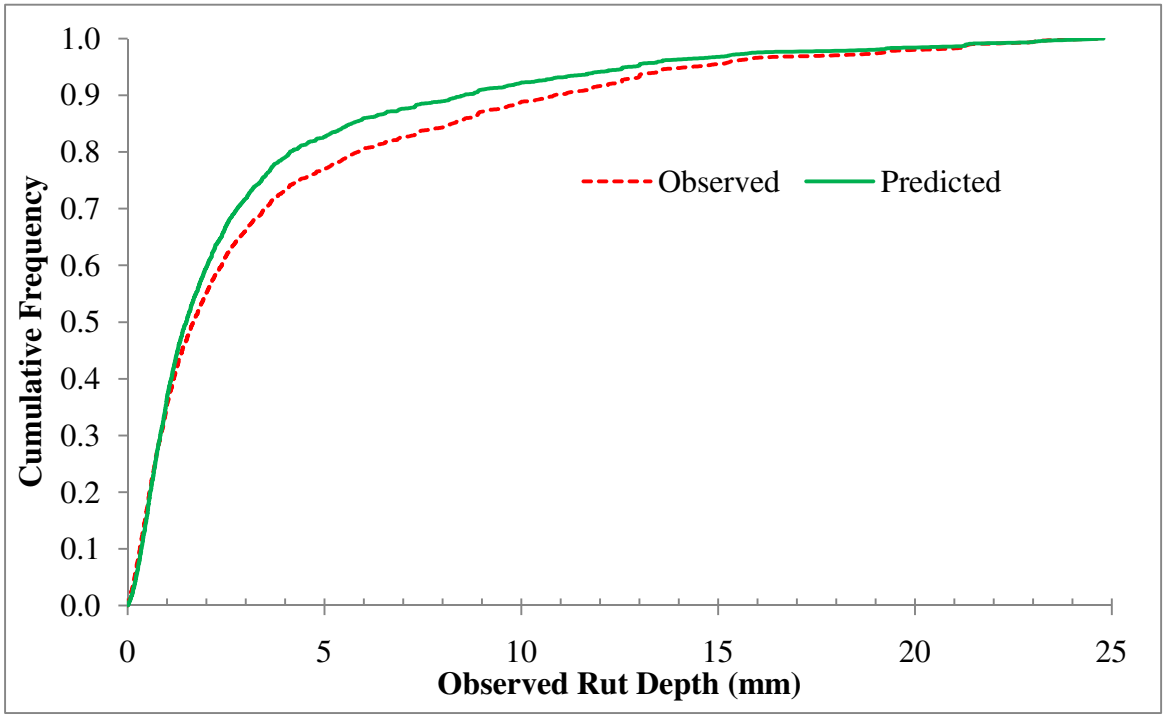

Figure 7.3: Cumulative Distribution for Observed and Predicted Data

7.3.3 Goodness-of-fit diagnostics

The overall goodness-of-fit of the model was assessed by calculating the Bayesian version R-squared statistic (R_B^2) in the WinBUGS software using Equation 7.2 which was adopted from Ntzoufras (2009).

$$R_B^2 = 1 - \frac{\tau^{-1}}{S_{\Delta RUT}^2} \tag{7.2}$$

Where τ is the precision of the Bayesian model and is defined as the reciprocal of the square of the standard deviation ($\tau^{-1} = \sigma^2$). A high precision indicates that the model is appropriate

for describing or predicting the annual incremental rut depth (ΔRUT). $S^2_{\Delta RUT}$ is the variance of the observed annual incremental rut depth.

The R^2_B statistic indicates the reduction in the error variance of the model as a result of the explanatory variables used in the model. Values of R^2_B close to 1 are preferred. Models with acceptable predictive ability are expected to have a R^2_B values greater than 0.7 (Ntzoufras 2009).

The R^2_B value for the assumed model calculated using the WinBUGS software is given in Table 7.2. The mean value of 0.96 is close to 1 indicating that the model is appropriate for performing future predictions.

Table 7.2: Summary Outputs for Calcuated R^2_B

Node	Mean	SD	MC Error	2.50%	Median	97.50%	Start	Sample
R^2_B	0.9624	0.001203	5.72E-06	0.96	0.9625	0.9647	50001	150000

7.4 Model Validation using Climate Impact and Adaptation Model

In section 7.3 model checks and validation were performed within a Bayesian framework using the WinBUGS software. This section is aimed at demonstrating the appropriateness of the developed rut depth model to perform time-series predictions. To that end, the Climate Impact and Adaptation model described in detail in Chapter 8 was used. The Climate Impact and Adaptation model was developed using the rut depth model structure in Equation 4.5 and the model coefficients given in section 6.5.

7.4.1 Observed Time-Series Data

Observed data for the two sections of road used to perform the time-series comparison are given in Table 7.3. These two sections of road were selected on the basis that for a given road sub-section the observed annual incremental rut depth derived using the process described in section 5.3.2.5 was available for a minimum of three consecutive years and the data were not used in the estimation of the coefficients of the rut depth model.

Table 7.3: Observed Road Section Data for Model Validation using Climate Impact and Adaptation Model

Section ID/ Name	Start (m)	End (m)	Surfacing Group	Year	ΔRUT (mm)	YE4 (msa)	sh (km/h)	G	HS (mm)	AGE (Years)	TPmax (^{o}C)
2600A11/111 (Section 1)	100	900	DBM	2003	3.03	1.32	85.2	3.962	184.4	14.34	40.04
			DBM	2004	0.43	1.34	88.1	4.56	170	15.34	38.84
			DBM	2005	0.93	1.37	82.1	3.962	184.4	16.34	38.40
2600A47/560 (Section 2)	0	491	HRA	2002	0.59	0.53	95.5	1.51	251	10.5	38.12
			HRA	2003	0.82	0.54	95.5	0.54	251	11.5	39.16
			HRA	2004	0.28	0.55	95.5	1.51	251	12.5	38.10
			HRA	2005	0.81	0.56	95.9	1.025	251	13.5	37.40

Notes to Table 7.3

1. ΔRUT = Annual Incremental Rut Depth
2. YE4 = Annual Equivalent Standard Axle Loading
3. sh = Average Speed of Heavy Vehicles
4. G = Average Absolute Road Section Gradient
5. AGE = Asphalt Surfacing Age
6. TPmax = Mean Daily Maximum Summer Temperature

7.4.2 Approach

A detailed description of the analysis process of the Climate Impact and Adaptation model is given in the next chapter (Chapter 8). An outline of the steps of analysis performed for the purpose of the time-series validation is given below:

(i) For the analysis year t =1 observed model input variables including traffic loading (YE4), heavy vehicle speeds (sh), road gradient (G), asphalt material properties, maximum summer temperature (TPmax) were defined in the Climate Impact and Adaptation model;

(ii) During the analysis year t = 1 a set of model coefficients were randomly sampled from the distribution of the model coefficient given in section 6.5.1.

(iii) The annual incremental rut depth for year t=1 and the set of stochastic random samples n=1 was calculated using Equation 4.5. This step was repeated for N sets of stochastic random variables.

(iv) Steps (i) to (iii) were repeated for each year for which predictions were performed on each road section to give distributions of annual incremental rut depth.

(v) The mean, 80^{th} percentile and 40^{th} percentiles of the distribution of the predicted annual incremental rut depth were graphically compared with the observed rut depth on each road section.

7.4.3 Time-series Comparison of Observed and Predicted Rut Depth

A comparison of predicted mean, 80th percentile and 40th percentile annual incremental rut depths for road section 1 with observed values over three consecutive annual periods is depicted in Figure 7.4. In Figure 7.5, the annual incremental rut depths shown in Figure 7.4 were cumulated from an observed initial rut depth of 2.3 mm. An inspection of Figure 7.5 suggests that the trend of the cumulative rut depth predicted by the model is similar to the observed trend.

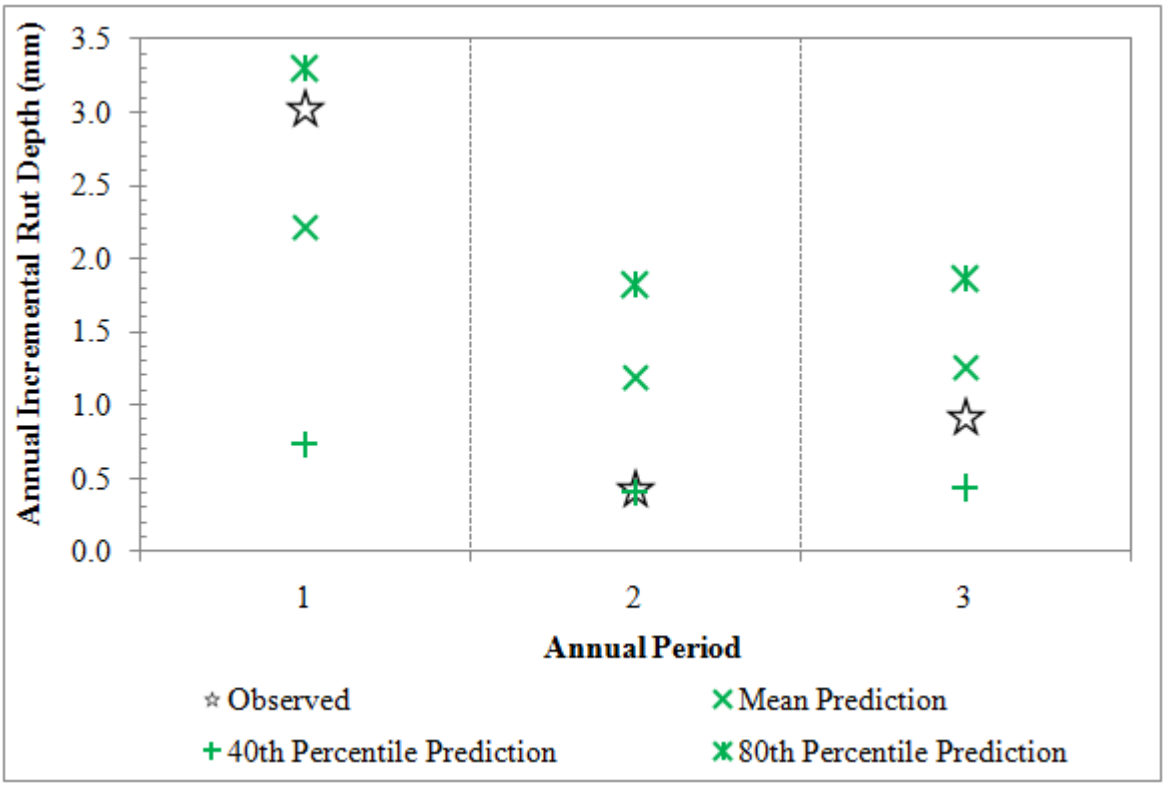

Figure 7.4: Predicted and Observed Annual Incremental Rut Depths for Road Section 1

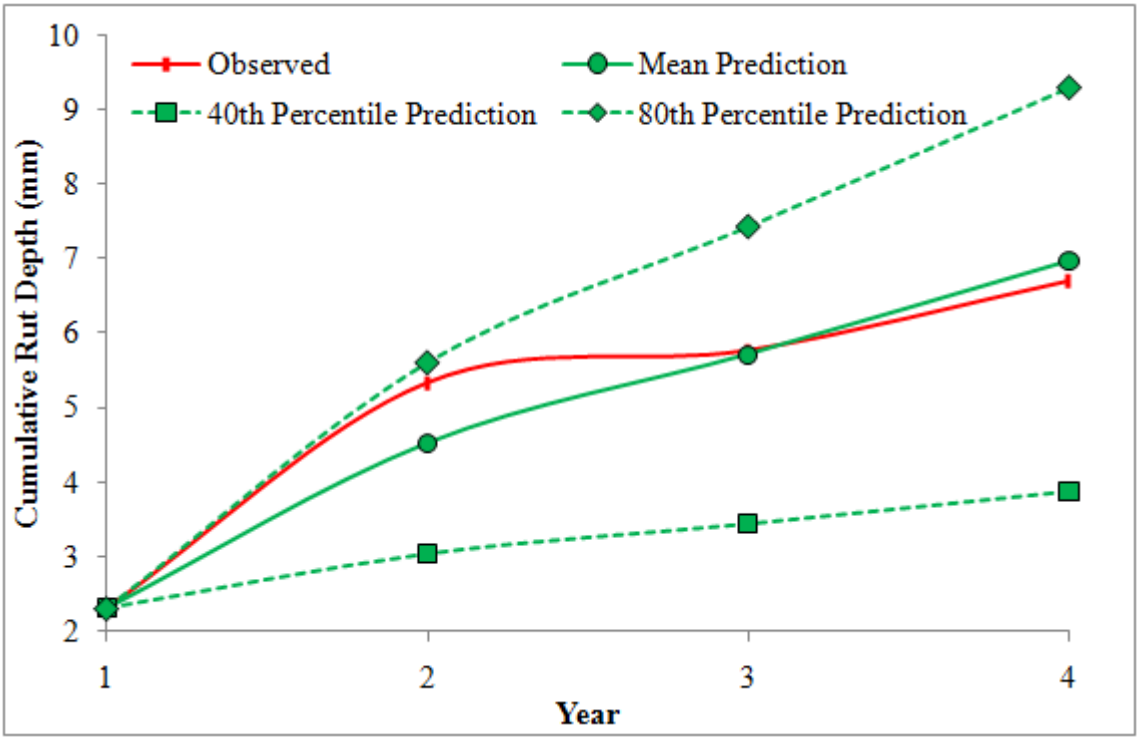

Figure 7.5: Observed and Predicted Cumulative Rut Depth for Road Section 1.

A comparison of predicted mean, 80th percentile and 40th percentile annual incremental rut depths for road section 2 with observed values over three consecutive annual periods is depicted in Figure 7.6. In Figure 7.7, the annual incremental rut depths shown in Figure 7.6 were cumulated from an observed initial rut depth of 3.1 mm. The predicted mean cumulative rut depth deterioration trend is close to the observed trend.

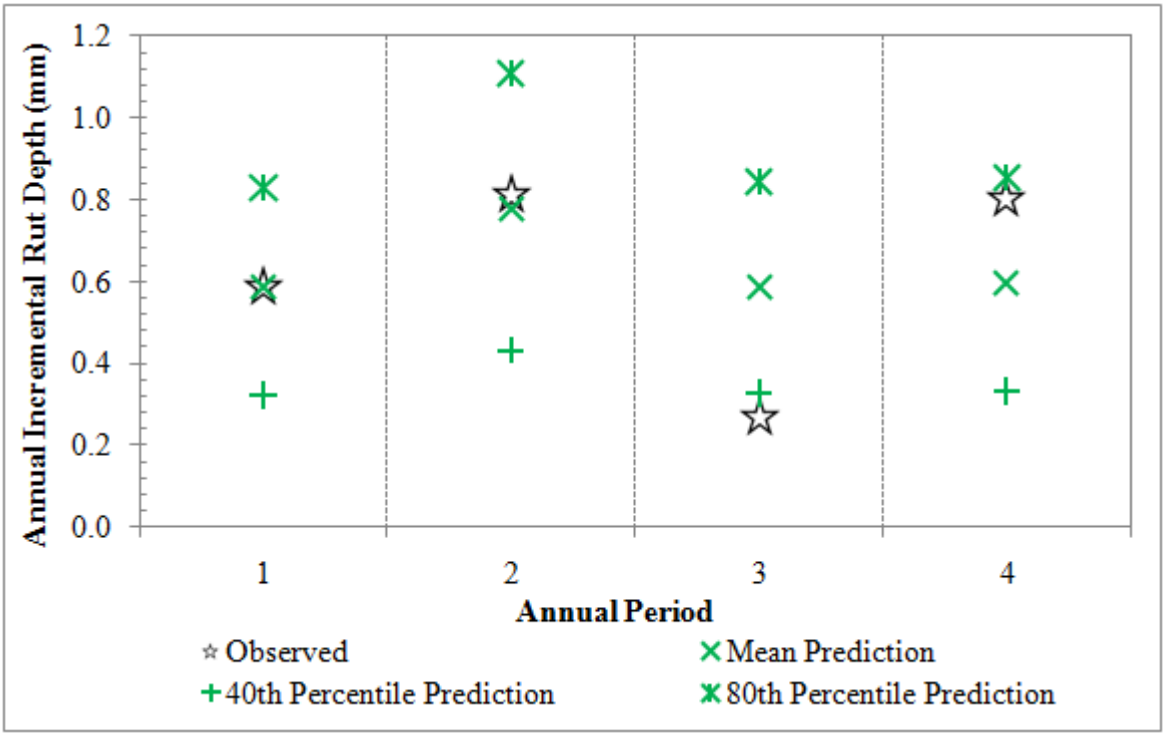

Figure 7.6: Predicted and Observed Annual Incremental Rut Depths for Road Section 2.

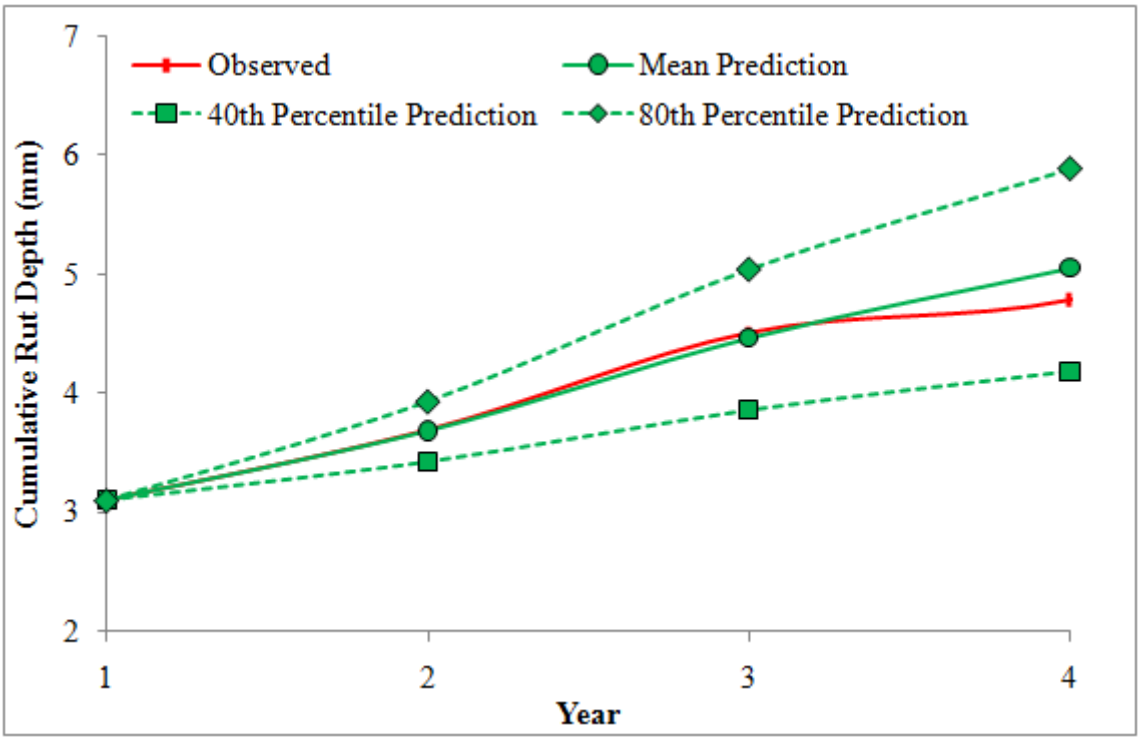

Figure 7.7: Observed and Predicted Cumulative Rut Depth for Road Section 2.

7.5 Framework for updating Model Coefficients

Although, the model validation and checks discussed in sections 7.3 and 7.4 showed that the developed rut depth model is appropriate for use in making predictions, it is possible to improve the model when new data is collected or new knowledge on the performance of the study roads becomes available.

Improvement to the rut depth model is possible by updating the model coefficients given in section 6.5 using the framework illustrated in Figure 7.8. With reference to Figure 7.8, the current model coefficients (given in section 6.5) augmented with expert knowledge or new research findings becomes the new prior distribution $P[\phi]$ in Bayes' theorem given in Equation 4.8. The likelihood of the observed data given the model coefficients $P[\Delta RUT / \phi]$ (in Equation 4.8) is derived from the newly collected data and combined with the new prior distribution to give the posterior distribution $P[\phi/\Delta RUT]$. The updated model coefficient is then derived using the methodology described in section 4.6.

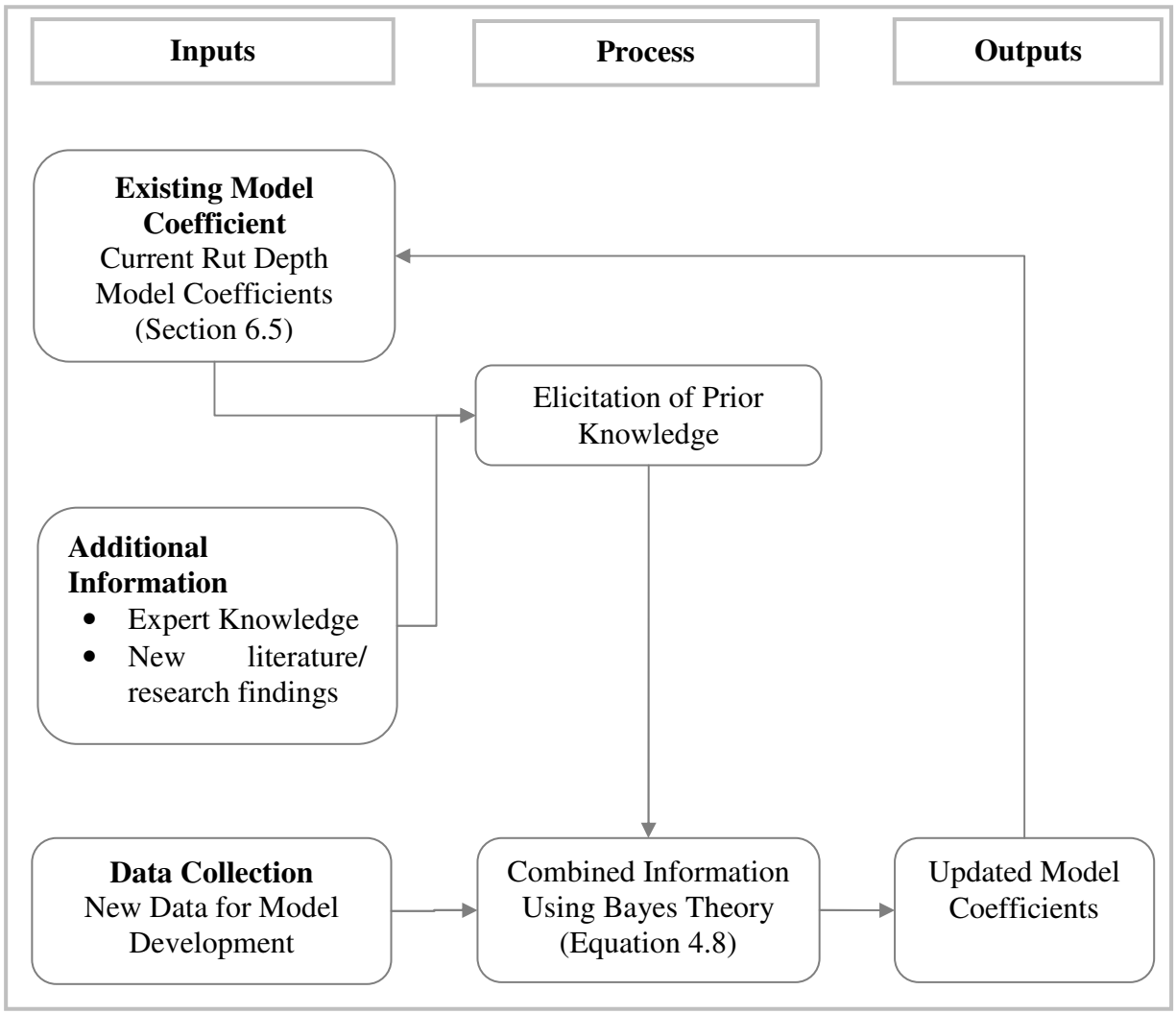

Figure 7.8: Framework for Updating Model Coefficients.

7.6 Summary

Model checks and validation were performed using observed data from 1,012 road sub-section which were not used in the estimation of the model coefficients. Validation was performed within the Bayesian framework as well as using the rut depth Climate Impact and Adaptation model given in Chapter 8.

The results of the validation showed that annual incremental rut depths below 5mm are predicted by the model with more accuracy. Predictions of observed annual incremental rut

depth greater than 5mm were still within the 95% posterior credible interval indicating that the model is appropriate for predicting such extreme values.

CHAPTER 8 CLIMATE IMPACT AND ADAPTATION MODEL

8.1 Introduction

This chapter provides a description of the analytical framework of the model developed for use in assessing the impact of future climate predictions on road pavement maintenance on the basis of asphalt pavement rut depth deterioration. The model calls on key findings, assumptions, and information detailed in previous chapters of this thesis including:

- The improved rut depth model structure given in Equation 4.5;
- Data types described in Chapter 5;
- Approach to definition of hot dry summer climate scenarios detailed in Section 5.4.3; and,
- The estimated rut depth model coefficients given in section 6.5.

Section 8.2 of this chapter sets out the overall structure of the analytical framework of the model while section 8.3 outlines the model input requirements. An illustration of the analysis process is given in section 8.4 followed by a step by step description of the components of the process. Section 8.5 describes the outputs that can be produced by the model while verification of the model is discussed in section 8.6. Section 8.7 provides a summary to the chapter.

8.2 Overall Model Structure

The overall structure of the model is shown in Figure 8.1. The components of the model structure are categorised into inputs, analysis and outputs. Discussions of the model components under each of these categories are provided in subsequent sections.

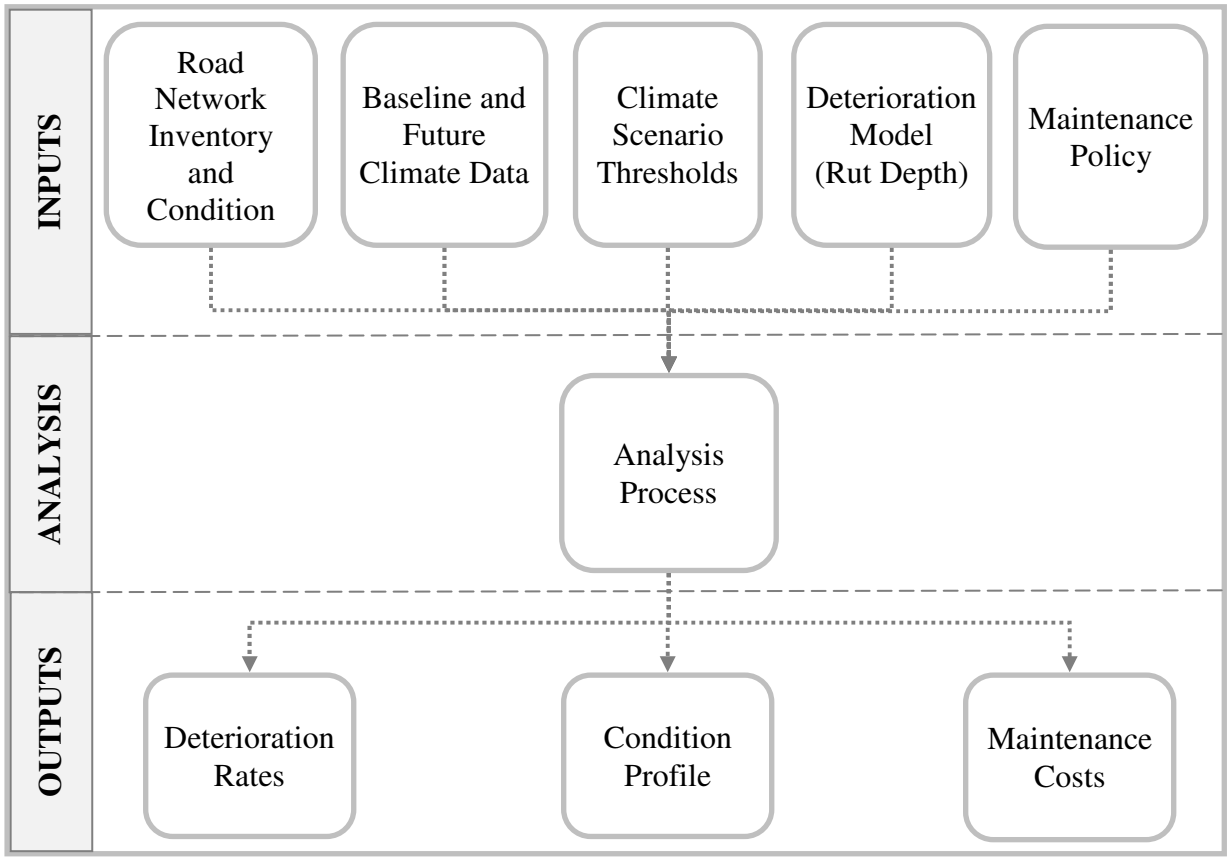

Figure 8.1: Structure of the Climate Impact and Adaptation Model

8.3 Model Inputs

The model inputs comprise lookup tables of values of road network inventory and condition, observed and predicted climate data, the rut depth model and materials properties model coefficients, treatment options, effects of treatments, unit cost of treatment works, and maintenance strategy. Each of these inputs is described further in Appendix D1.

8.4 Analysis Process

This section provides a step by step description of the analysis sequence of the climate impact model. The analysis process is shown in Figure 8.2. A step by step description is provided in subsequent sections.

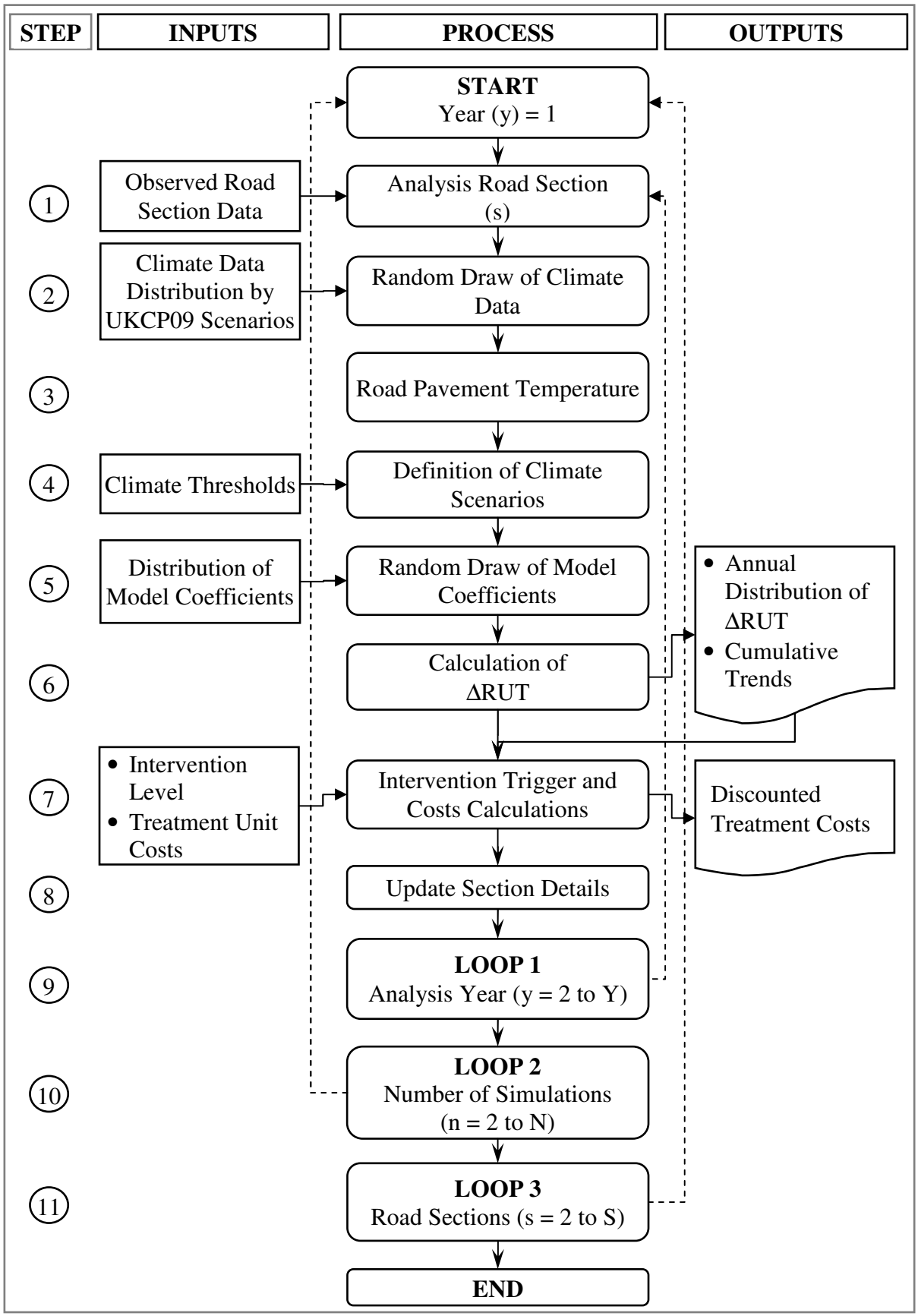

Figure 8.2: Climate Impact and Adaptation Model Analysis Process

8.4.1 Initial Values of Explanatory Variables (Step 1)

The first step is to input observed or initial values required as inputs to the model. These include:

- Number of equivalent standard axles in million standard axles per year;
- Speed of heavy vehicles in kilometres per hour;
- Absolute average gradient of the road section;
- Thickness of asphalt surfacing in millimetres;
- Binder softening point and voids in mix of the asphalt surfacing. Default estimates are provided by SP and VIM models incorporated in the Climate Impact and Adaptation model; and
- The geographical latitude of the road section. This is necessary for the calculation of pavement temperature in Step 3.

8.4.2 Associating Climate Data to Analysis Road Section (Step 2)

In Step 2, a random sample is generated from the distribution of change in mean maximum summer temperature and change in monthly summer precipitation for the UKCP09 scenario and time period selected for analysis. Climate data is used to estimate the pavement temperature variable of the rut depth model (Step 3) and to investigate hot dry climate scenario (Step 4).

8.4.3 Pavement Temperature Data (Step 3)

Equations 5.1 and 5.2 were then used to calculate the pavement temperature at 20mm below the asphalt surface, which is required as input for the model variable TPmax. Maximum air

temperature input required in Equation 5.1 was obtained by adding the change in maximum temperature in Step 2 to the absolute maximum summer temperature for the baseline period.

8.4.4 Annual Road Section Climate Scenario (Step 4)

In Step 4, user defined threshold values of maximum temperature and precipitation anomalies are compared with the road section climate data derived in Step 2 to investigate the climate scenario that should be associated to the road section in a given year.

Four possible climate scenarios that can be associated to a road section in an analysis year are illustrated in Figure 8.3 by quadrants delineated by the solid vertical and horizontal threshold lines. For example, if for a given road section and analysis year, the predicted temperature anomaly is greater than the defined threshold value and the precipitation anomaly is less than the rainfall threshold value, then a hot dry (HD) climate scenario is inferred.

When a hot dry climate is inferred, then constants H_0 and H_1 in the rut depth model structure given in Equation 4.5 are assigned values of 0 and 1 respectively, otherwise H_0 takes on a value of 1 and H_1 a value of 0.

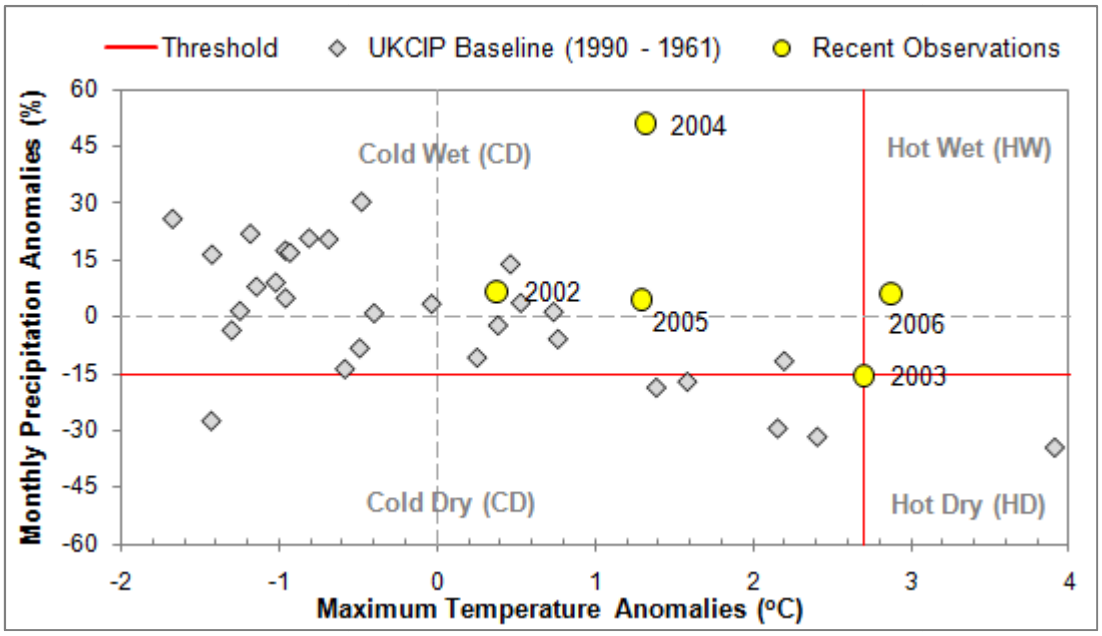

Figure 8.3: Definition of Climate Scenarios

8.4.5 Model Coefficients (Step 5)

In Step 5, a random but plausible set of model coefficients for all explanatory variables of the rut depth, binder softening point and voids in mix models are generated and associated to the road section being analysed.

8.4.6 Calculation of Annual Incremental Rut Depth (Step 6)

Annual incremental rut depth in analysis year (y) for the road section and the selected UKCP09 scenario is calculated using Equation 4.5 and model coefficients from Step 5. Cumulative rut depths are calculated by adding the estimated annual incremental rut depth for the analysis year to the total estimates in previous years.

8.4.7 Treatment Intervention and Costs (Step7)

Treatments are applied in a given analysis year when a specified rut depth intervention threshold is exceeded by the cumulative rut depth calculated in Step 6 as illustrated in Figure 8.4. A default treatment intervention threshold of 11mm was specified in the model so that road sections with moderate or severe rut depth deterioration as defined in Table 5.2 were treated. The assumption used in the model is that treatment works are applied at the end of the analysis year.

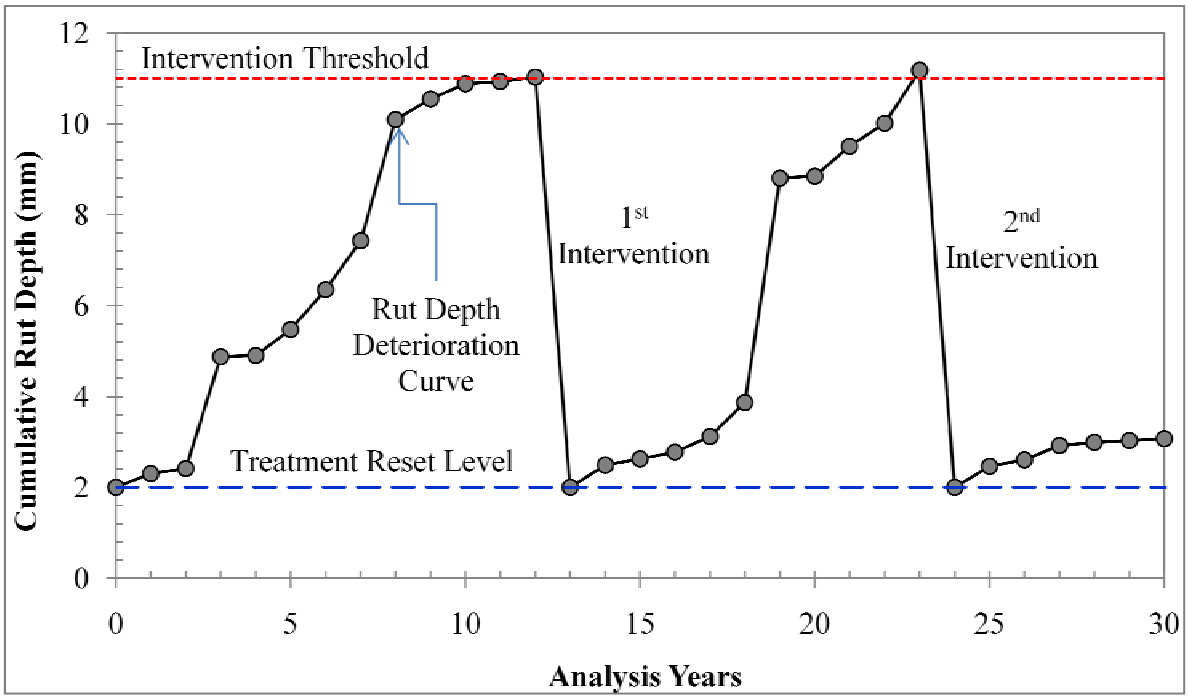

Figure 8.4: Illustration of Treatment Intervention and Effects

When treatment is applied in a given year (y), undiscounted costs of treatment (C_U) in that year is calculated by multiplying the treatment unit costs by the area of the road section treated. Discounted treatment costs (C_D) are calculated using Equation 8.1 for a user specified discount rate (r).

$$C_D = \frac{C_y}{(1+r)^y} \qquad 8.1$$

8.4.8 Updating Section Details (Step 8)

Once treatments that are appropriate for removing the rut depth deformation are applied in Step 8, the cumulative rut depth value is reset to 2mm as illustrated in Figure 8.4. The reset value of 2mm is typical of asphalt deformation that would usually occur within one year due to initial densification following the laying of a new asphalt surfacing layer. The value of 2mm was deemed representative since it is also used by UK Highways Agency in the Whole Life Cost Optimisation (WiLCO) decision support system to inform the Agency's strategic planning and investment decisions (Smith, 2011)

Values for explanatory variables required for the next analysis year are also updated in this step. Updates to values for binder softening point and voids in mix are performed using the models described in section 7 of Appendix D1. The next year values for other variables are derived externally using existing road decision support systems such as the Highway Development and Management system (HDM-4) and the National Transport Model (NTM).

8.4.9 Analysis Loop 1 (Step 9)

Steps 2 to 8 are repeated until the analysis year is equal to 30, which is the period synonymous to the duration over which UKCP09 climate data is provided.

8.4.10 Analysis Loop 2 (Step 10)

Steps 1 to 9 is repeated for all N number of simulations defined by the user to ensure the variability associated with the inputs to the analysis are sufficiently reflected in the outputs. An approach for estimating the number of simulations (N) performed in each road section is illustrated section 9.2.4.

8.4.11 Analysis Loop 3 (Step 11)

Steps 1 to 10 are repeated for all S sections being analysed.

8.5 Outputs

Outputs of the impact model comprise the following:

- Predicted annual rut depth deterioration rates for each maintenance scenario and climate scenario analysed;
- Predicted condition profile for each maintenance scenario and climate scenario;
- Discounted treatment costs for each maintenance scenario and climate change scenarios analysed.

The above outputs are illustrated in section 10.8. Other potential outputs that can be produced by the model are given in Appendix D2.

8.6 Comparison with HDM-4 Model

Verification was undertaken by comparing the Climate Impact and Adaptation Model (CIAM) described in the previous sections in this chapter with outputs derived from the Highway Development and Management System (HDM-4) asphalt surfacing rut depth model. The HDM-4 model was used because it is considered to be the de facto international standard decision support tool for road management (Kerali, 2001; Fletcher et al., 2006). Furthermore configuration parameters for the HDM-4 model were derived from a study undertaken by

Odoki et al. (2006) to configure and calibrate HDM-4 for the UK Department for Transport (DfT).

Data from the same road section was modelled in both the CIAM and HDM-4 model using the following UKCP09 climate datasets: 2020s (2010 – 2039) and the 2050s (2040 – 2079)

- Baseline (1961-1990) climate data;
- 2020s (2010 – 2039) medium emission scenario; and
- 2050s (2040 – 2079) medium emission scenario.

It is apparent from Figure 8.5 that the cumulative trend of the mean predictions using the CIAM model is similar to the trend of the cumulative rut depth predicted using HDM-4 when the baseline climate data was used. This suggests that the CIAM model can reasonably replicate predictions performed using HDM-4 when past data that excludes the effects the effects of future climate change are used.

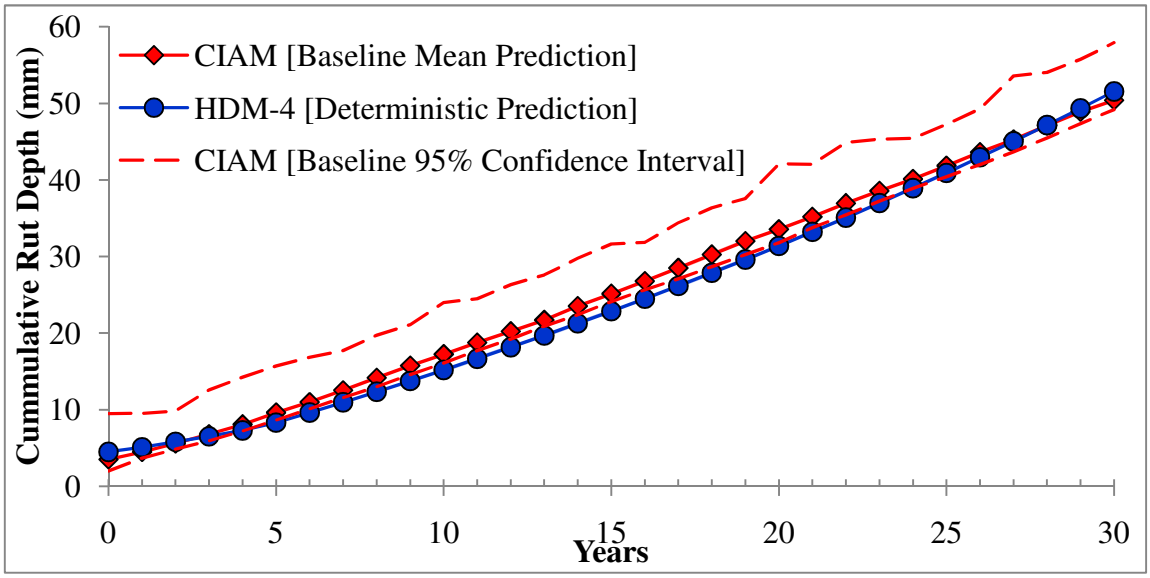

Figure 8.5: Comparison of Outputs from Climate Impact and Adaption Model with HDM-4 Outputs for the Baseline Climate Scenario

Cumulative rut depth trend predicted by the CIAM model using 2020s medium emission climate data is marginally higher than HDM-4 the HDM-4 trend as shown in Figure 8.6. Higher cumulative rut depths were however predicted by the CIAM model when future climate data for the 2050s medium emission scenarios was used as shown in Figure 8.6 and Figure 8.7 respectively. Discrepancies between the CIAM and HDM-4 predictions are apparent in Figures 8.6 and 8.7 because the structure of the HDM-4 asphalt surfacing rut depth model given in Equation 4.1 does not include a variable for accounting for the effects of future climate, hence the effects of future climate change on rut depth progression is not captured. The CIAM model structure given in Equation 4.5 however includes a variable to account for the effects of future climate changes.

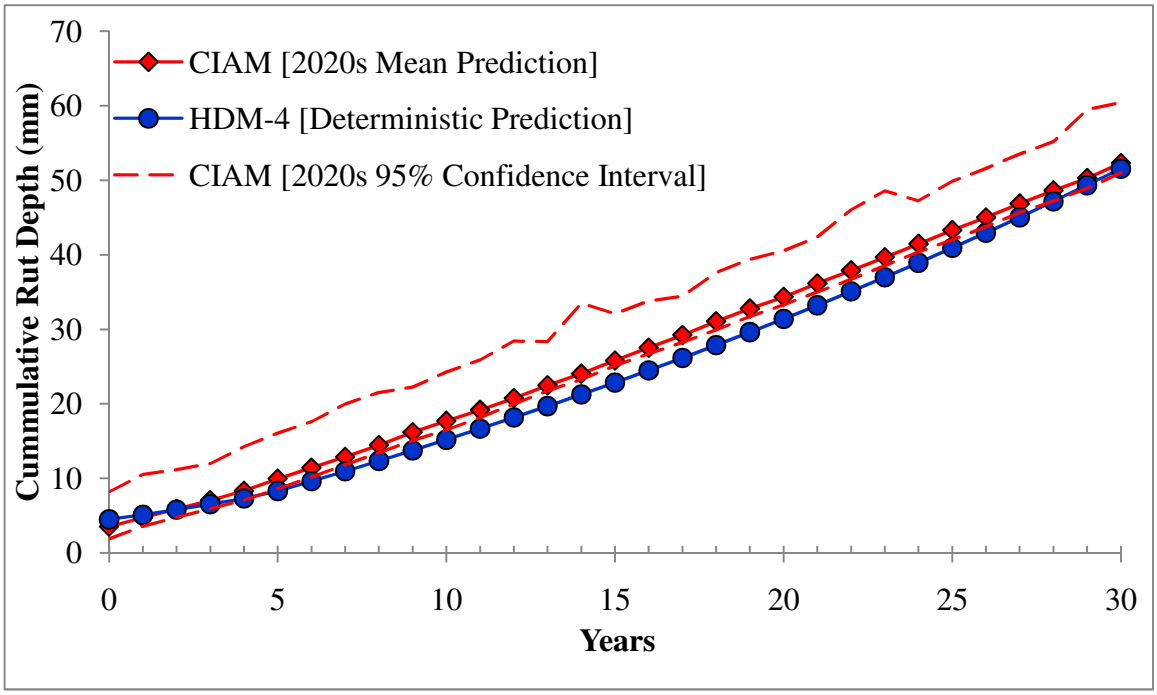

Figure 8.6: Comparison of Outputs from Climate Impact and Adaption Model with HDM-4 Outputs for the 2020s Climate Scenario

The marginal discrepancy between predicted trends of rutting by the CIAM and HDM-4 models over the 2020s compared to the 2050s is due to relatively lower predicted frequency of hot dry summers during the 2020s.

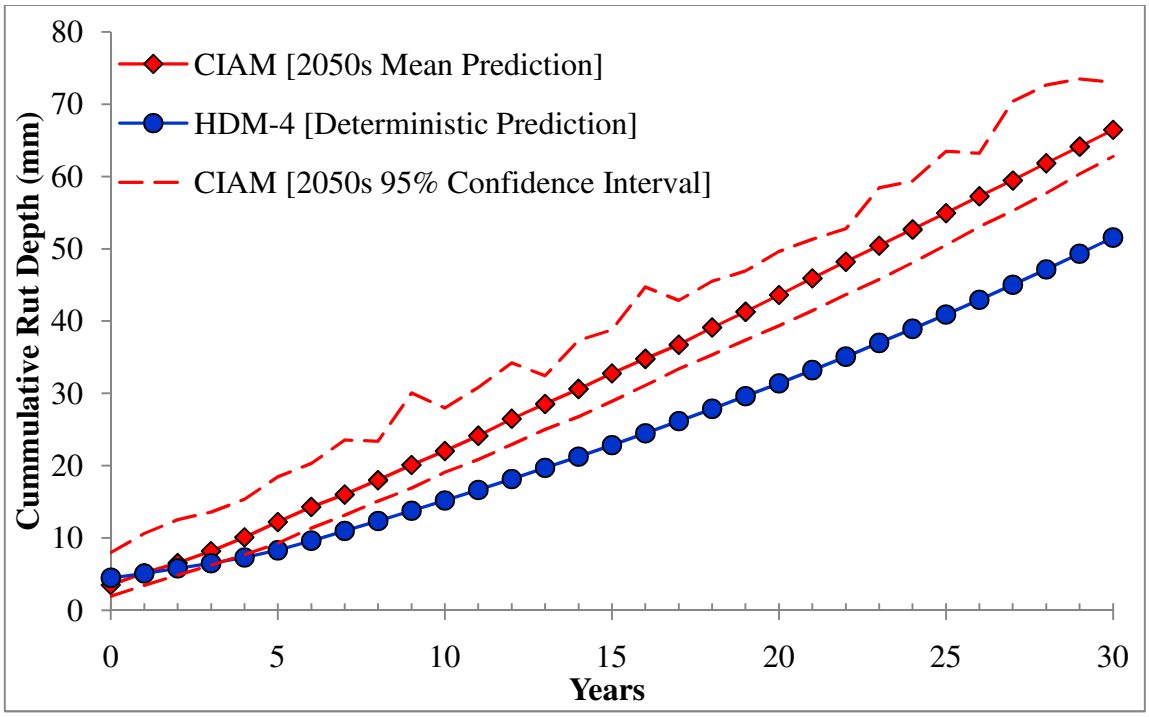

Figure 8.7: Comparison of Outputs from Climate Impact and Adaption Model with HDM-4 Outputs for the 2050s Climate Scenario

8.7 Summary

This chapter provided a description of the analytical framework of the Climate Impact and Adaptation model implemented in Microsoft Excel to demonstrate the application of the rut depth model developed in this study. The components of the structure of the model were categorised into inputs, outputs and analysis. Components categorised as inputs were: road section inventory data; climate data; definition of hot dry climate scenario threshold; rut depth deterioration model; and maintenance policy.

A step by step description of the analysis process of the model is provided in section 8.4. The outputs produced by the model include: Summary statistics and probability distribution of average rates of rut depth deterioration for predefined climate and road maintenance

scenarios; and summary statistics and probability distribution of discounted road maintenance costs for predefined climate and road maintenance scenarios.

The next chapter sets out a framework within which this model can be applied in the assessment of the impact of climate change.

CHAPTER 9 FRAMEWORK FOR QUANTIFICATION AND PROPAGATION OF UNCERTAINTIES

9.1 Introduction

This Chapter sets out a framework within which the Climate Impact and Adaptation model discussed in Chapter 8 may be applied in climate impact and adaptation studies related to road pavement maintenance management. The framework was formulated to guide the quantification and propagation of uncertainties inherent in future climate predictions, other inputs to the model and the coefficients of the model to the outputs of the analysis.

Section 9.2 of this chapter introduces the components of the framework followed by a step by step discussion of each of component. A summary to the chapter is provided in section 9.3.

9.2 Components of the Framework

A schematic outline for the framework for quantification and propagation of uncertainties associated with the assessment of the impacts of climate change on road maintenance is depicted in Figure 9.1. These components are discussed in sub-sequent sections.

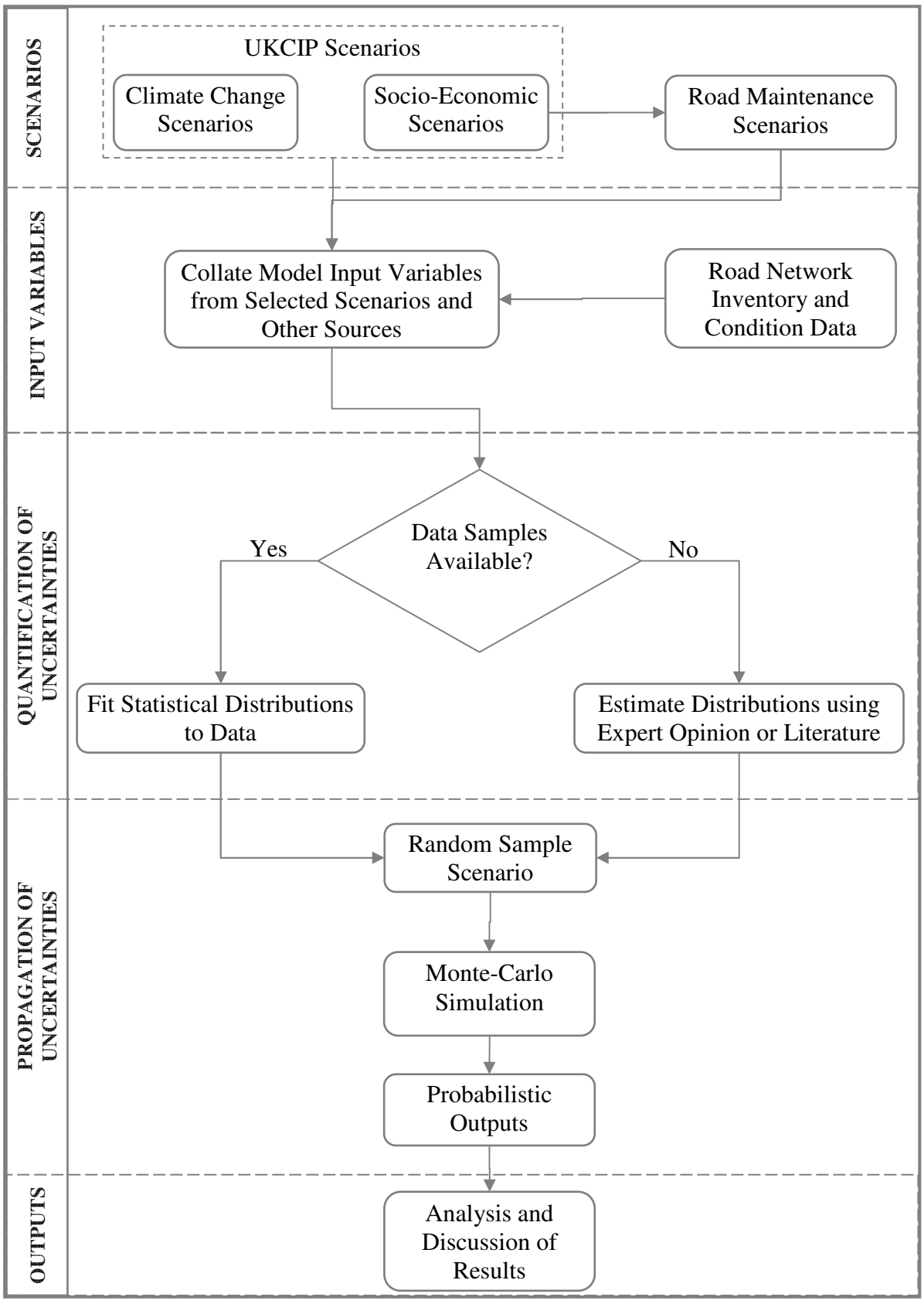

Figure 9.1: Framework for Quantification and Propagation of Uncertainties.

9.2.1 Socio-Economic, Climate Change and Road Maintenance Scenarios

9.2.1.1 Social Economic Scenarios

According to UKCIP (2000), future climate change is likely to take place in a world different from the current social and economic setting. Thus, climate impact assessment studies that assume a static society are conceptually flawed. The UK Climate Impacts Programme developed a Socio-Economic Scenario (UKCIP SES) framework which reflects possible alternative futures for use in climate change impact assessment (UKCIP, 2000). These scenarios reflect how society may change in the future based on policy decisions that may be made. Four scenarios have been developed within a global context for two time periods: 2020s (2010 – 2039) and the 2050s (2040 – 2079) and are referred to as:

- National Enterprise,
- Local Stewardship,
- World Markets and
- Global Sustainability

The above scenarios are defined based on the following four dimensions of change:

- Composition and rate of economic development;
- Rate and direction of technological change;
- The nature of governance; and
- Social and political values.

Figure 9.2 illustrates the framework within which the scenarios were formulated. Detailed description of these scenarios is provided in UKCIP (2000).

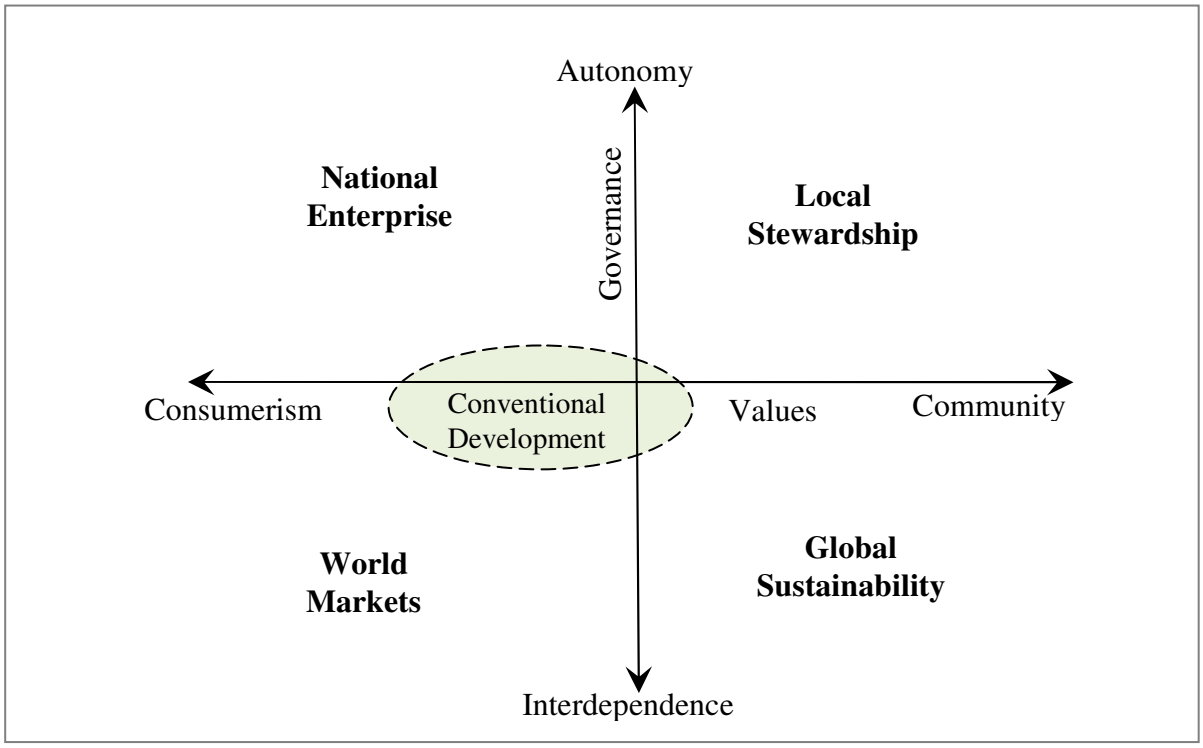

Figure 9.2: Illustration of the UKCIP SES framework. (UKCIP, 2000)

The underlying assumptions of the four scenarios relevant to road infrastructure maintenance and more specifically within the context of average Growth Domestic Product (GDP), regional economic growth, and transport operation and infrastructure are summarised in Table 9.1. These assumptions were elicited from guidance provided in UKCIP (2000).

The summary in Table 9.1 is used to inform the choice of socio-economic scenario(s) that are relevant to specific studies to which the Climate Impact and Adaptation model described in Chapter 8 is to be applied. Table 9.2 identifies the variables of the impact model that are relevant to socio-economic changes. The use of socio-economic scenarios in climate impact assessment using the impact model described in Chapter 8 is illustrated in section 10.3.1.

Table 9.1: Summary of UKCIP SES Assumptions Relevant to Road Management and Maintenance

UKCIP SES	Average GDP	Regional Economic Development Trends	Transport Infrastructure and Operations
National Enterprise	1.75%	• London and the South East experience high economic development • The rest of the UK experience relative under development	• The spread of car ownership is limited due to moderate GDP. • Slow growth of car fleets • Increased congestion and accidents on roads • Many roads operate at full capacity • No new developments of road system
Local Stewardship	1.25%	Economic growth is evenly spread	• Transportation sector affected by slowdown in growth of trade • Use of private car is dominant • Public road and rail structures are extended • Increase use of low emission technology in cars
World Markets	3%	All regions experience rapid economic growth	• New roads are built to meet increased demand for passenger transport • Traffic efficiently managed using new control systems • Quality of road infrastructure improved through high investment
Global Sustainability	2.25%	Regional development equally distributed	• New roads, rail and air infrastructure are developed but high priority given to minimising environmental impacts • Emphasis given to energy and resource efficient transport projects

Notes to Table 9.1

1. The summary in the table is adapted from UKCIP (2000)
2. UKCIP = UK Climate Impacts Programme
3. SES = Social Economic Scenarios
4. GDP = Growth Domestic Product

9.2.1.2 Climate Change Scenarios

The proposed framework utilises the 2009 climate projections for the United Kingdom (UKCP09) which is described in detail by Murphy et al. (2009). The projections were performed for low, medium, and high greenhouse gas (GHG) emission scenarios. These

scenarios represent possible future trends of GHG emissions in the UK and consequently future climate trend.

For each scenario, the change in climate variables including temperature and precipitation relative to the baseline period from 1961 to 1990 are available in a probabilistic format at 30 year temporal time scales for the periods listed in Table D1-2 in Appendix D1. The projections are available at 25km by 25km gridded spatial resolution. The probabilistic data captures uncertainties due to natural climate variability while the three climate scenarios accounts for uncertainties associated with anthropogenic climate change (Murphy et al., 2009).

Table 9.2 links relevant impact model variables to the climate change scenarios. An illustration of the choice and use of climate change scenarios for impact assessment using the model presented in Chapter 8 is provided in section 10.3.2.

9.2.1.3 Road Maintenance Scenarios

Road maintenance scenarios in the context of this study relates to key components necessary for long-term planning of road maintenance activities by authorities responsible for managing a road network. These components include the following:

- Asphalt pavement treatment options such as overlays and inlays;
- The effect of treatment works;
- Material types for asphalt pavement maintenance such as Dense Bituminous Macadam (DBM) or Hot Rolled Asphalt (HRA);
- Treatment intervention thresholds;

- The unit costs of treatment works;
- The condition to which the road network should be maintained in the long term;
- Traffic growth rates;
- Future predictions of vehicle speeds;
- Forecasts of heavy vehicle axle loading.

Whereas current maintenance scenarios are well defined in maintenance manuals and design standards such as the UK Highways Agency Design Manual for Roads and Bridges, uncertainties exist in choosing possible future scenarios. Information provided under each social-economic scenario in Table 9.1 are used where possible to define generic scenarios required as annual inputs for selected variables of the impact model identified in Table 9.2.

Annual forecasts of other model inputs can be derived from outputs of road decision support tools such as the National Transport Model (NTM) and the Highway Development and Management System (HDM-4). An illustration of the definition of road maintenance strategy is given in section 10.3.3.

9.2.2 Model Input Variables and Socio-Economic Scenarios

In this stage of the framework illustrated in Figure 9.1 scenarios described in the previous section are broken down into variables required as inputs to the impact model. These model variables are grouped under climate, traffic and maintenance standards as illustrated in Table 9.2.

Table 9.2: Summary Relating Model Variables to Scenarios

Scenarios	Groups	Impact Model Variables	Units
Climate Change	Climate	Mean Monthly Summer Precipitation	mm
		Mean Maximum Daily Summer Temperature (TPmax)	^{o}C
Socio-Economic	Traffic	Heavy vehicle speeds (sh)	km/h
		Number of Equivalent Standard Axles per Vehicle (YE4)	msa
Road Maintenance scenario	Maintenance Standards	Treatment options	-
		Intervention Thresholds	mm
		Unit costs of treatment works	£/m^2
		Target Aggregate Condition	-

Data for these model variables are inferred from the scenarios that would have been selected from section 9.2.1 for the purpose of performing the impact studies using the model described in Chapter 8. Road network condition and inventory data which are required as inputs to the impact model are normally available in databases such as the Highways Agency Pavement Management System (HAPMS).

9.2.3 Quantification of Uncertainty Using Probability Distribution

With reference to Figure 9.1, following the collection of data required as input to the impact model, this section discusses the quantification of uncertainties and variability inherent in this data using probability distributions. Probability distribution enables the full range of the values of the input variable to be described. In addition, the likelihood of the occurrence of the values of the variables is weighted accordingly.

9.2.3.1 Types of Distributions

Several types of probability distributions exist in literature. Some common types include the triangular, normal and uniform distributions. Figure 9.3 illustrates a normal distribution. The horizontal axis comprise a range of values of the variables to which the distribution refers while the vertical axis gives the relative weightings of the frequency of occurrence of specific values of the variable. This representation ensures that uncertainties and variability inherent in the values of the variables being modelled are encapsulated in the modelling process. Examples of other types of probability distributions used in this study are given in sections 6.2, 6.3 and Appendix D1.

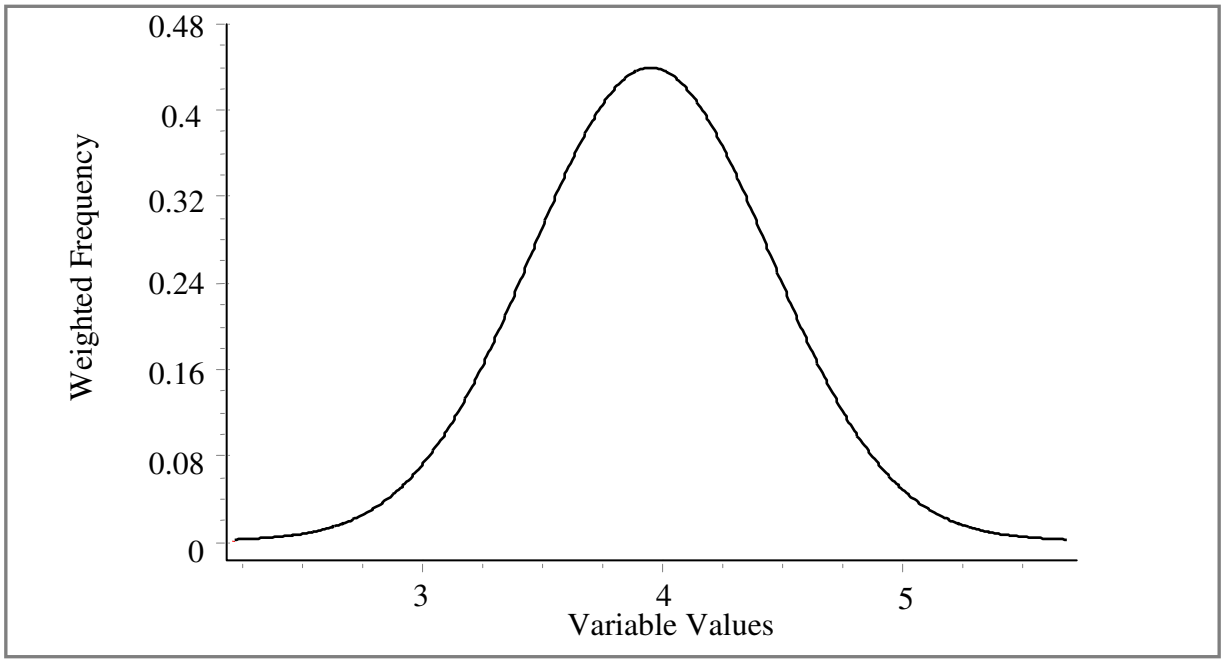

Figure 9.3: Illustration of a Normal Distribution

9.2.3.2 Developing Probability Distributions

When data is available then statistical software such as SPSS are used to fit the data to probability distributions that bests describe the variability of the data. Goodness of fit

indicators such as Kolmogorov–Smirnov (K-S) and the Anderson-Darling (A-D) are used to indicate how close the distributions fit to the data. Examples of such distribution fitting are given in section 10.5.

For model input variables with limited data, probability distributions can be developed through subjective approaches such as group interviews with a panel of experts or through literature review.

9.2.4 Propagation of Uncertainties

Monte-Carlo random sampling is the best known method for propagating the probability distribution of the model inputs through the impact model to derive a probabilistic representation of the output of the analysis (Luo et al., 2005). With reference to the framework illustrated in Figure 9.1, random values are selected from each input data distribution as well as the distribution of model coefficients given in section 6.5 to define a plausible scenario that is then input in the impact model to calculate output values. This approach is repeated N times to give N output values that characterize the uncertainty in the model prediction given the assumed uncertainty in the input variables. A detailed description of the analysis process of the model was provided in section 8.4.

The total number of number of model simulations is determined by comparing the mean and standard error of the mean of the output distribution with the cumulative number of model simulation as illustrated in Figure 9.4. For example, from Figure 9.4 both the standard error and the mean of the output the model appear stable by 4000 model iterations.

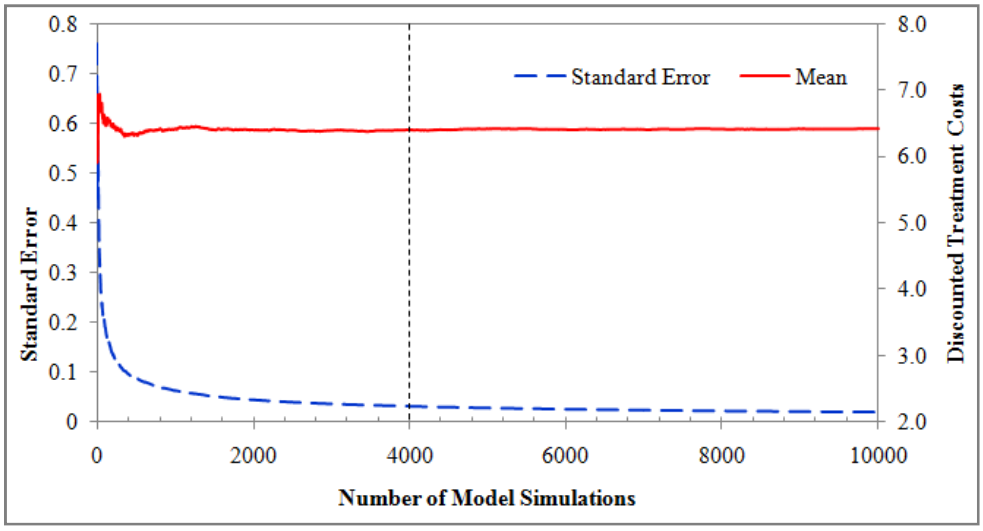

Figure 9.4: Comparison of Standard Error and Mean of Model Output with Number of Iterations.

9.2.5 Presentation and Interpretation of Outputs

The outputs of the analysis for each combination of climate and road maintenance scenario that are analysed are presented using probability distributions in the form of histograms such as that shown in Figure 9.5. The horizontal axis of the histogram shows the complete range of possible outcomes while the vertical axis provides the probability of each output occurring. The variability of the model output about the mean can be inferred from the width of the distribution such that distributions with larger width have greater variability.

An alternative representation of the analysis results for each combination of climate and road maintenance scenario is in the form of cumulative probability distribution depicted in Figure 9.6 the output value is represented on the horizontal axis. The vertical axis represents the probability that the output value of the model will be less than the corresponding value on the horizontal axis. For example, from Figure 9.6, there is a 60% probability that the treatment costs will be less than 6.6 million pounds.

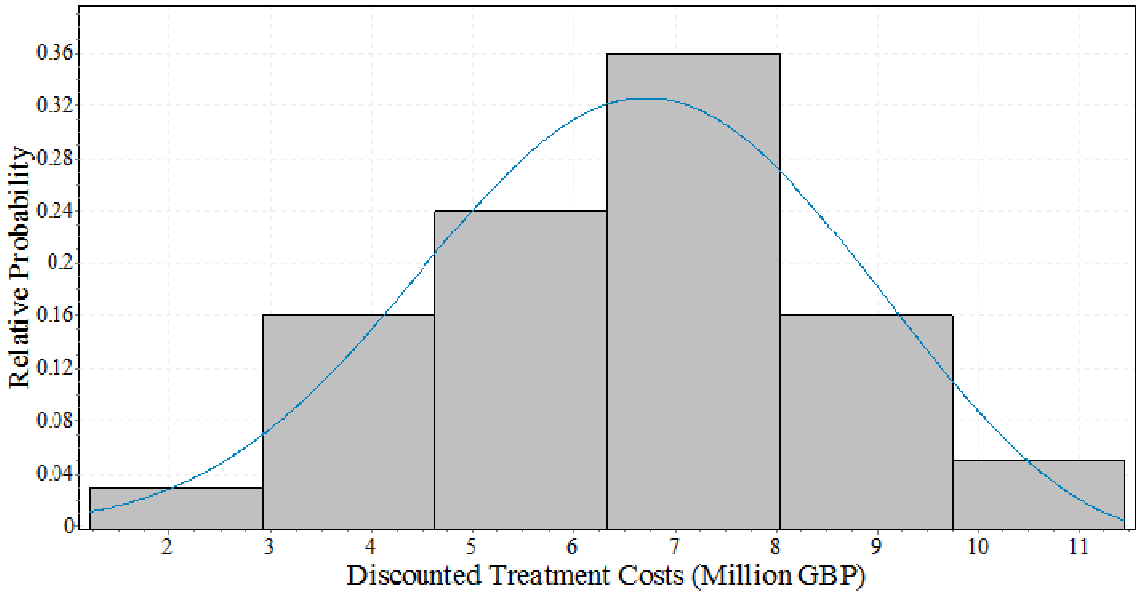

Figure 9.5: Distribution of Discounted Treatment Costs

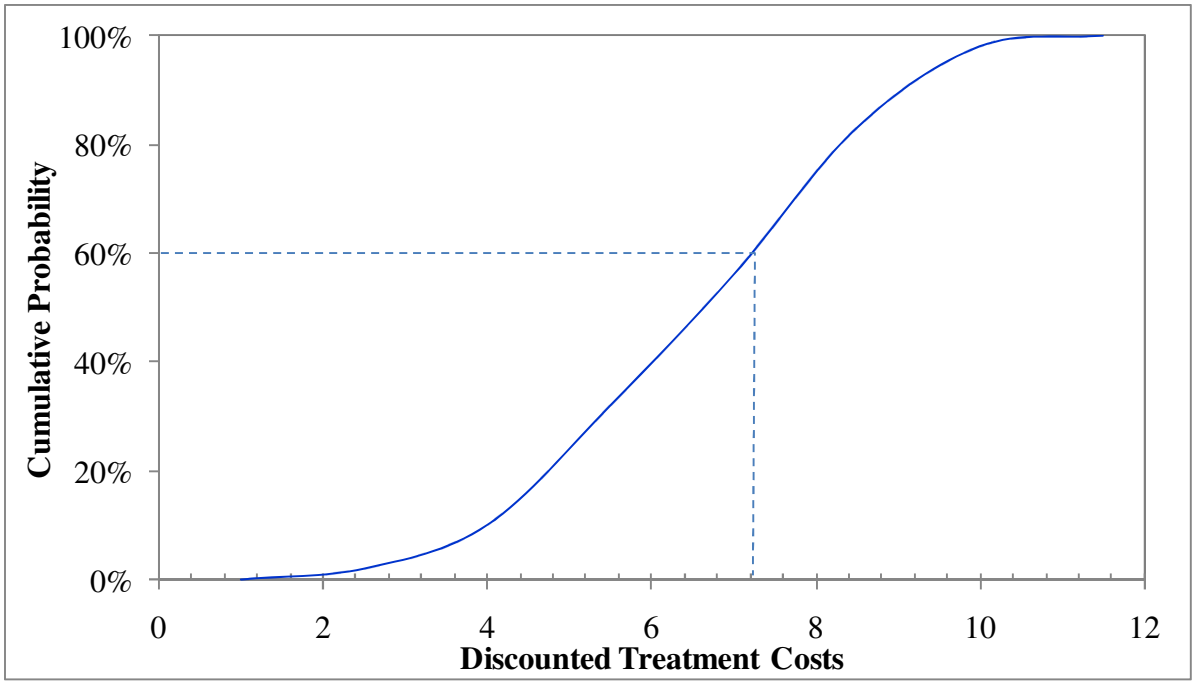

Figure 9.6: Cumulative Distribution of Discounted Treatment Costs

Results for each combination of climate change and road maintenance scenarios may also be presented using summary statistics including the minimum value, maximum value, mean, and

standard deviation as illustrated in section 10.8.2.3. Additional discussions on the presentation and interpretation of the results of the analysis are given in sections 10.8 and 10.9.

9.3 Summary

This chapter presented a framework within which the model described in Chapter 8 can be applied in the assessment of the impact of climate change on road maintenance. The framework is structured into the following components:

- Definition of plausible analysis scenarios;
- Collation of impact model input variables;
- Quantification of uncertainties and variability inherent in the inputs to the impact model;
- Propagation of uncertainties and variability in the inputs of the model to the output of the analysis; and,
- Representation and interpretation of the outputs.

The next chapter discusses a case study performed to assess the impact of climate change on road maintenance. The case study makes use the framework presented in this chapter and the model described in Chapter 8.

CHAPTER 10 ASSESSMENT OF THE IMPACT OF CLIMATE CHANGE ON ROAD MAINTENANCE

10.1 Introduction

This chapter is aimed at demonstrating the application of the Climate Impact and Adaptation model described in Chapter 8 and the framework presented in Chapter 9. These tools can be applied to several studies such as:

1. Investigating the relative difference in the predicted performance of asphalt pavements with respect to rut depth deterioration for pre-determined scenarios of observed and future climate for a given set of road maintenance policies;

2. Investigating the relative costs of road maintenance between predefined scenarios of climate change and the baseline climate from 1961 to 1990 for a given set of maintenance policy;

3. Investigating alternative road maintenance policies for adapting to the potential effects of climate change. Such policies may be characterised by one or a combination of the following:

   (i) the use of materials known to provide more resilience to the effects of predicted changes in climate;

   (ii) use of recycled materials for performing road maintenance with a view to encouraging a sustainable approach to exploitation of materials for road construction and maintenance;

(iii) projected reduction in traffic growth or advances in vehicle technology which would reduce the contribution of traffic loading and vehicle speed to road pavement deterioration with respect to rut depth;

4. Assessing the impacts that may be attributed to pre-determined scenarios of future climate on road user costs. This analysis can be performed by using the developed tools described in Chapters 8 and 9 together with an existing road management systems such as the Highway Development and Management System (HDM-4) or the Deighton Total Infrastructure Management System (dTIMS);

5. Investigating the impact of future socio-economic scenarios on road pavement performance and maintenance cost. This is based on the assumption that car ownership and consequently traffic growth are linked to socio-economic trends.

The case study presented in this chapter focuses on demonstrating the application of the model described in Chapter 8 together with the framework given in Chapter 9 in deriving the following outputs:

- Rut depth deterioration on the study road;
- Road condition over a 30 year analysis period; and
- Discounted costs of maintaining the study road pavement on the basis of rut depth deterioration.

These outputs are investigated using predefined socio-economic, climate change and road maintenance scenarios.

Section 10.2 of this chapter provides an introduction to the case study area, section 10.3 sets out plausible future socio-economic and climate change scenarios used in the case study. Section 10.4 outlines the data used, while section 10.5 is concerned with the representation of variability and uncertainty inherent in the input data. Section 10.6 discusses the setup and configuration of the model for each analysis scenario. Section 10.7 deals with the model analysis and sets out the basis for the convergence of the Monte-Carlo sampling. The outputs of the analysis are presented in section 10.8 while section 10.9 provides a discussion on the component of the cost of road maintenance that can be attributed to climate change. A summary to the chapter is provided in section 10.10.

10.2 The Case Study Area

The case study area comprised asphalt pavement sections on the southbound traffic flow direction of the M11 motorway between junctions 4 and 6. The location of the study road is depicted in Figure 10.1. This location was used because of availability of data and due to its close proximity to the study area (depicted in Figure 4.2).

Figure 10.1: Map of Case Study Road (adapted from Google maps)

10.3 Socio-Economic, Climate Change and Road Maintenance Scenarios

The socio-economic, climate and road maintenance scenarios that were investigated in this case study are described in subsequent sections.

10.3.1 Socio-Economic Scenarios

The application of the model described in Chapter 8 requires that future trends of traffic loading (YE4) and heavy vehicle speed (sh) are represented on an annual basis for each modelled road section. Future socio-economic trends were used as a basis for estimating values of these model variables. The socio-economic scenarios that were considered were those used to formulate the UKCP09 climate projections since the climate change data used in the study were based on UKCP09. UKCP09 projections were derived using four alternative

future socio economic scenarios (National Enterprise, Local Stewardship, World Markets, and Global Sustainability) which are briefly described in section 9.2.1.1 and detailed in UKCIP (2000).

This case study was limited to the World Markets scenario which relates more to the perception of conventional development or "business as usual" as illustrated in Figure 9.2. Furthermore the characteristics of the World Markets scenario described in Table 9.1 are consistent with the underlying assumptions of the UK Department for Transport (DfT) National Transport Model (NTM). To that end, forecasts of future annual equivalent standard axle load and change in vehicle speeds required for use in the analysis were derived from NTM results of traffic flow and heavy vehicle speed forecast for South East England (DfT, 2008; DfT, 2009).

10.3.2 Climate Change Scenarios

The climate projections used in the case study were limited to the UKCP09 Baseline (1961 – 1990) observation for the study area and the Medium Emission scenario for the 2020s (2010 – 2039), 2030s (2020 – 2049), 2040s (2030 – 2059) and 2050s (2040 – 2069). The Baseline and Medium Emission scenarios were selected because they are sufficient to demonstrate the relative differences in rut depth deterioration and road maintenance costs predicted using a static past climate (described by the Baseline scenario) and a projected future climate (described by the Medium Emission scenario and time periods). Furthermore, the World Markets socio-economic scenario selected in section 10.3.1 is consistent with the assumptions upon which the Medium Emissions climate projections were derived (UKCIP, 2000).

10.3.3 Road Maintenance Scenario

The road maintenance scenario used in the case study is described under the following headings:

- Treatment types;
- Intervention levels and treatment reset values; and
- Maintenance strategies.

10.3.3.1 Treatment Types

The treatment types used in the study are given in Table 10.1. The definition of each treatment type is provided in section 8.1 of Appendix D1. These treatments were selected because they are used in road pavement maintenance of trunk roads in the UK (Transport Scotland, 2008). Given that asphalt surface rutting is manifested as transverse deformation in the wheel paths, treatments such as surface dressing and application of high friction surfacing are not ideal because they do not remove the deformation and have not therefore been used.

Table 10.1: Description of Treatment Types

Group	Code	Type
Thin Treatment	THIN	Thin surfacing or inlay
		Thin overlay
Moderate Treatment	MOD	Moderate inlay
		Moderate overlay
Thick Treatment	THICK	Thick inlay
		Thick overlay
Reconstruction	RECON	Reconstruction

The treatment types and description were obtained from Transport Scotland (2008).

10.3.3.2 Intervention Levels and Treatment Reset Values

The asphalt rut depth threshold at which treatment works described in Table 10.1 were applied was 11mm and is illustrated in Figure 8.4. This rut depth intervention threshold was defined such that moderate or severe rut depth deterioration as defined in Table 5.2 were treated to give a road section with a mostly good and fair condition (in accordance with the definition in Table 10.8) over the 30-year analysis period.

Once treatments are applied, the cumulative rut depth value is reset to 2mm based on the rationale discussed in section 8.4.8.

10.3.3.3 Maintenance Strategies

Table 10.2 illustrates two road maintenance strategies that were analysed. The strategies were formulated using the treatment types described in section 10.3.3.1. These strategies are referred to as the Current Practice and Adaptation maintenance strategies and are described in subsequent sections.

Table 10.2: Summary of Maintenance Strategies

Maintenance Strategy	**Treatment Strategy Name**	**Initial Rut Depth**	**Intervention Sequence**			
			1st	**2nd**	**3nd**	**Subsequent**
Current Practice	Strategy 1	>11mm	RECON	THIN	MOD	MOD
	Strategy 2	6 – 11 mm	THICK	THIN	RECON	MOD
	Strategy 3	< 6mm	THIN	MOD	RECON	MOD
Adaptation	Strategy 1	All	RECON	THIN	MOD	MOD

Notes to Table 10.2:

1. RECON = Reconstruction
2. THIN = Thin Treatment
3. MOD = Moderate Treatment

10.3.3.3.1 Current Practice Strategy

The Current Practice strategy in Table 10.2 reflects a typical strategy currently used to maintain the case study road. It is characterised by the following three treatment strategies:

- Strategy 1, which is applicable to road sections with moderate (rut depth greater than 11mm and less or equal to 20mm) or severe (rut depth greater than 20mm) observed asphalt surface rutting. The severity of rut depth observed in such road sections suggests that their structural integrity may have been compromised. The strategy modelled (Strategy 1) therefore involves Reconstruction (RECON) of the asphalt layers at the first intervention, followed by renewal of the surface course using Thin Treatment (THIN). Moderate Treatment (MOD) is scheduled as the third and subsequent interventions as necessary.
- Strategy 2, which was associated to road sections categorised using the criteria given in Table 5.2 as showing some deterioration with initial rut depth between 6 and 11mm. Thick Treatment (THICK) is applied to these sections at the first intervention followed by Thin Treatment (THIN) as a second intervention to renew the surface course. The asphalt pavement is reconstructed at the third intervention and subsequently maintained using Moderate Treatment (MOD) whenever the set intervention threshold of 11mm is exceeded.
- Strategy 3, which is applied to sections with initial rut depth less than 6mm. Such sections are categorised in Table 5.2 as being sound with no visible deterioration.

Reconstruction (RECON) is consequently delayed until the third intervention when the pavement would be expected to be approaching the end of its design life. A Thin Treatment (THIN) is applied as the first intervention followed by Moderate Treatment (MOD) as the second intervention. Moderate Treatment is applied to any subsequent interventions after the third intervention.

10.3.3.3.2 Adaptation Strategy

The Adaptation Strategy illustrated in Table 10.2 is aimed at investigating the consequence of using asphalt materials that provides more resilience to the effects of climate change than that used in the Current Practice strategy. Thus, the treatment strategy used was to reconstruct the road in the first year of analysis irrespective of the initial condition followed by a series of maintenance interventions synonymous with those applied under treatment strategy 1 in the Current Practice strategy.

10.4 Model Input Data

Model input data used in the study are presented under climate data and road network data headings.

10.4.1 Climate Data

10.4.1.1 Baseline Climate Data

Gridded datasets of observed mean maximum daily summer temperature and average monthly summer precipitation for the baseline period (1961 – 1990) at 5km spatial resolution were obtained from UKCP09 gridded observation datasets (Met Office, 2009). The methodology

used to derive the gridded data set from a network of weather stations is detailed in Perry and Hollis (2005).

While the baseline climate data obtained was available at 5km grid boxes, the predicted data for the Medium Emission scenario are provided at 25km grids. The observed (baseline) data within the vicinity of the study area was therefore aggregated to 25km grid box illustrated in Figure 10.2 to achieve a consistent spatial resolution with the predicted climate data.

Observed average monthly precipitation during summer months and mean maximum daily temperature over summer months for each year over the baseline period from 1961 to 1990 are shown in Figure 10.3. The observed maximum temperature during summer months ranged from 19.6^{o}C and 25.1^{o}C with a mean of 21.2^{o}C. While the monthly summer precipitation ranged from 17.4mm to 82.2mm with an average value of 52mm.

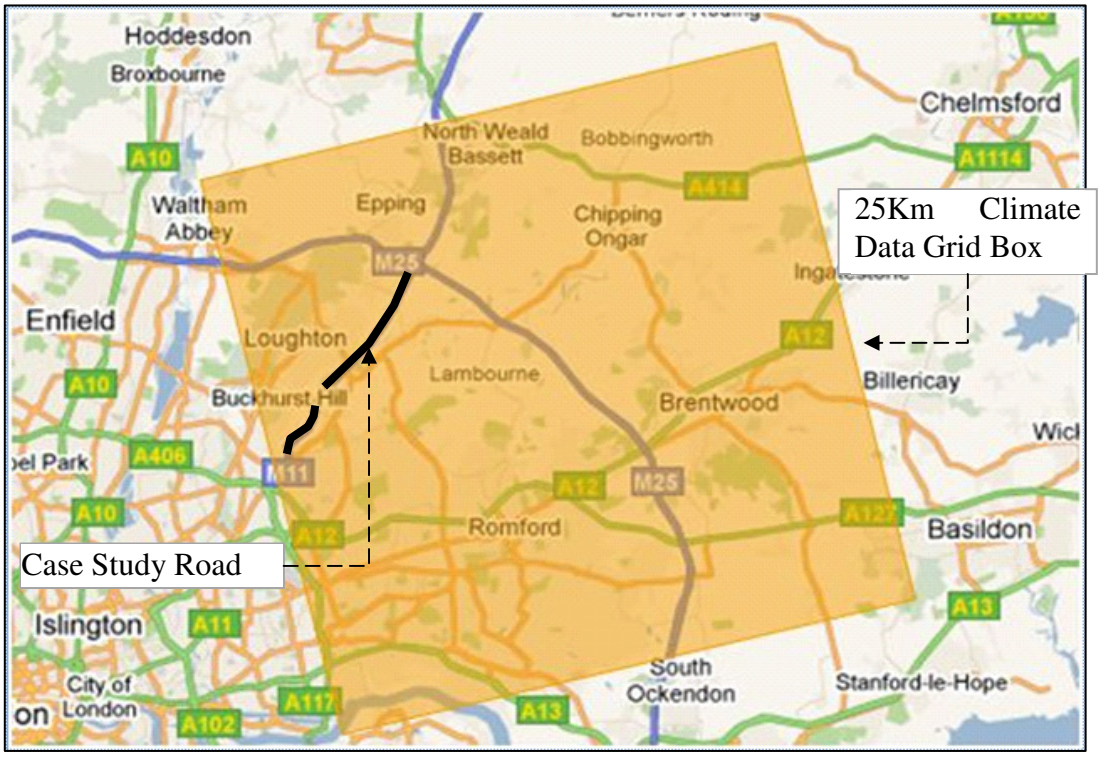

Figure 10.2: Location of UKCP09 Climate Data for the Case Study Road (Source, UKCP09 User Interface and Google Maps)

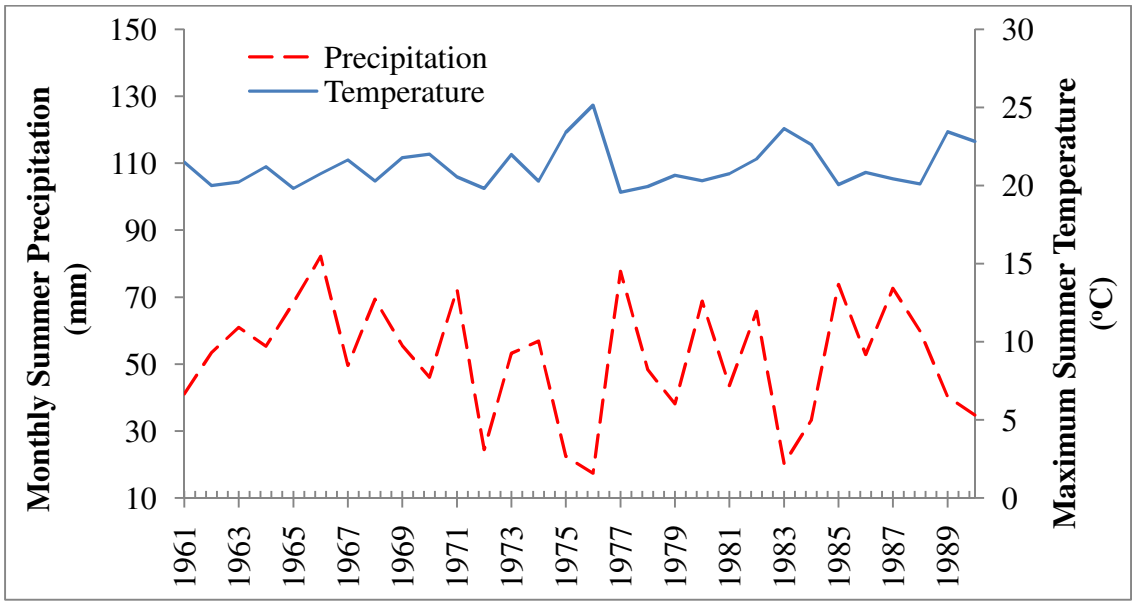

Figure 10.3: Location of UKCP09 Climate Data for the Case Study Road (Source, UKCP09 User Interface and Google Maps)

The average values of the precipitation and temperature data presented in Figure 10.3 were used as a baseline for comparison with the projected climate data.

10.4.1.2 Predicted Climate Data

Predicted climate data for the Medium Emission scenario for the 25 km grid box overlapping the study road (Figure 10.2) was sourced from UKCP09 climate projections (Murphy et al., 2009). Cumulative frequencies of predicted change in average maximum daily temperature in summer months relative to the baseline observation for the case study area are shown in Figure 10.4 for the Medium Emission scenario and the four 30-year time periods described in section 10.3.2. The vertical line in Figure 10.4 corresponds to the change in maximum summer temperature observed in the very hot summer of 2003 relative to the baseline period from 1961 to 1990. It is apparent from Figure 10.4 that summer temperatures are predicted to get hotter with time. During the 2020s (2010 – 2039) 18% of the years are predicted to have summers that are hotter than that observed in 2003, this proportion increases to 34% during the 2030s (2020 – 2049), 48% during the 2040s (2030 – 2059) and 60% during the 2050s (2040 – 2069).

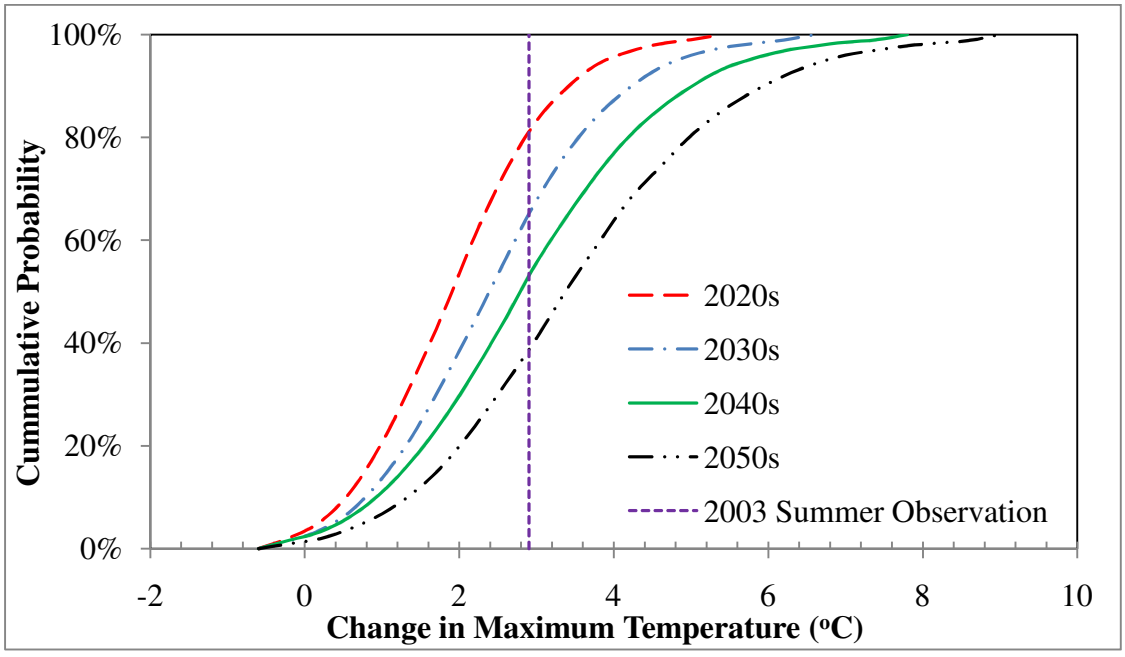

Figure 10.4: Cumulative Frequency of Predicted Change in Average Maximum Daily Summer Temperature for the Case Study Area

Cumulative frequencies of predicted change in average monthly precipitation during the summer relative to the baseline observation for the case study area are shown in Figure 10.5 for the Medium Emission scenario and the four 30-year time periods. The vertical line in Figure 10.5 corresponds to the observed change in monthly summer precipitation in 2003 relative to the baseline observation. From Figure 10.5, during the 2020s (2010 – 2039), 29% of the years are predicted to have summers that are drier than that observed in 2003, this proportion increases to 35% during the 2030s (2020 – 2049), 44% during the 2040s (2030 – 2059) and 56% during the 2050s (2040 – 2069).

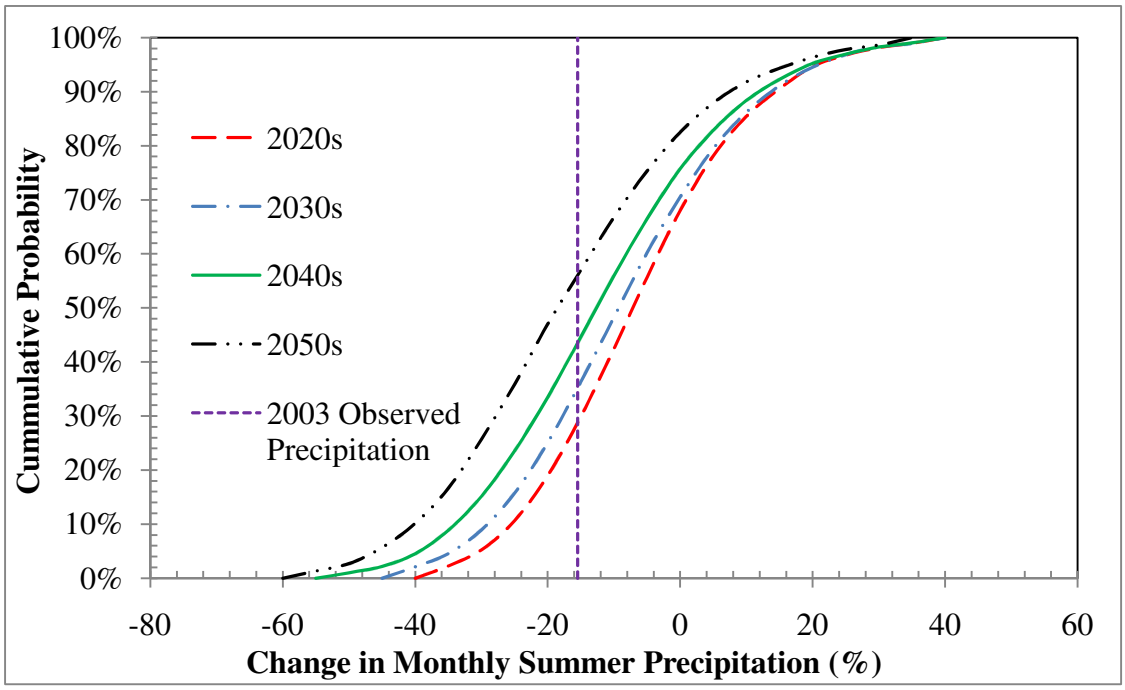

Figure 10.5: Cumulative Frequency of Predicted Change in Average Monthly Summer Precipitation for the Case Study Area

10.4.2 Road Network Data

Road network data required for the analysis included the following:

- Inventory and condition data; and,

- Treatment unit costs and discount rate.

10.4.2.1 Inventory and Condition Data

Inventory and condition data for the study road including road length and width, observed rut depth, asphalt thickness, asphalt surfacing age, and traffic data are shown in the strip maps in Appendix E1. The source of the data is shown on the strip maps. Data for gradient of the road were elicited from maps of the study road.

10.4.2.2 Treatment Unit Costs and Discount Rate

Typical treatment unit costs were collated from Management Agent Contractors responsible for maintaining trunks roads in the United Kingdom were used (Transport Scotland, 2008). Summary statistics of these costs including the mean, standard deviation, minimum value, maximum value and sample size are given in Table 10.3.

Table 10.3: Summary Statistics for Treatment Unit Costs by Treatment Group

Statistics	Thin Treatment (£/m^2)	Moderate Treatment (£/m^2)	Thick Treatment (£/m^2)	Reconstruction (£/m^2)
Mean	18.66	26.73	36.90	69.91
Standard Deviation	7.58	7.79	13.70	27.33
Minimum	8.77	18.68	22.32	43.75
Maximum	35.00	42.00	65.00	112.00
Sample Size	10	10	10	5

The rate at which the costs of treatment works were discounted to the start of the analysis period was 3.5% in line with advice given in the HM Treasury Green Book (HM Treasury, 2003).

10.5 Representation of Uncertainty and Variability in Input Data

Uncertainties and variability inherent in the climate and road network input data were included in the analysis by fitting statistical distributions to the collected data.

10.5.1 Climate Input Data

The baseline climate data presented in section 10.4.1.1 were used in the model as annual deterministic inputs since they are based on observed values. Future climate predictions for the Medium Emission scenario for each time period described in section 10.4.1.2 were represented using probability distributions. The Generalised Extreme Value (GEV) distribution was found to provide a good fit to 10,000 samples of climate data for each time period. The parameters of the distribution together with a summary of the Kolmogorov – Smirnov (K-S) goodness of fit statistics are given in Table 10.4.

The results of the K-S tests shows that the assumed distribution provides a good fit to the predicted climate data since the P-Value of the K-S tests statistic is higher than the 0.05 critical value.

Table 10.4: Probability of Distribution of Predicted Climate Data

Climate Variable	Time Period	Parameters			K-S Tests		
		shape	scale	location	Statistics	P-Value	Critical at 0.05 Level
Temperature Change (^{o}C)	2020s	-0.202	1.063	1.511	0.010	0.315	0.014
	2030s	-0.180	1.257	1.925	0.010	0.319	0.014
	2040s	-0.167	1.473	2.262	0.008	0.542	0.014
	2050s	-0.146	1.642	2.790	0.008	0.448	0.014
Precipitation	2020s	-0.185	14.434	-12.446	0.008	0.521	0.014

Change (%)	2030s	-0.194	15.683	-14.841	0.007	0.763	0.014
	2040s	-0.191	16.771	-18.680	0.007	0.723	0.014
	2050s	-0.17175	17.327	-24.641	0.00658	0.7767	0.014

10.5.1.1 Road Network Data

Selected road network related variables were represented using probability distributions based on availability of data. This approach ensures that the uncertainty and variability of the input value is captured in the modelling process, and propagated to the outputs of the analysis.

The road network data that were probabilistically represented included: road gradient, observed rut depth, surfacing age, and heavy vehicle speed. The distributions fitted to the data and summary of the K-S goodness of fit test is shown in Table 10.5. The fitted distributions are appropriate for describing the respective datasets since the P-Value of the test statistic are higher than the 0.05 rejection level.

Table 10.5: Distribution of Road Network Input Data

Variable	Units	Sample Size	Distribution	Parameters for Statistical Distributions				K-S Tests			
				Para1	Para2	Para3	Para4	Para5	Statistics	P-Value	Critical
Gradient	-	101	Normal (μ, σ)	-0.005	0.025	NA	NA	NA	0.117	0.116	0.135
Initial Rut Depth	mm	160	Burr (k, a, b,g)	0.252	24.294	9.567	-6.827	NA	0.074	0.333	0.107
Surfacing Age	Years	21	Beta (α_1, α_2, a, b)	0.076	0.083	0.852	21.011	NA	0.218	0.232	0.280
Speed	km/h	336	Wakeby (a, β, g, s, z)	1612.4	30.630	5.651	-0.566	40.392	0.071	0.066	0.074

1. NA = Not Applicable
2. Para1-5 = Parameters of the distribution
3. Normal (m, s) = Normal distribution with mean m and standard deviation s.
4. Burr (κ, α, β,γ) = Burr distribution with shape parameters κ and α , scale parameter β and location parameter γ
5. Beta (α_1, α_2, a, b) = Beta distribution with shape parameters α1 and α2 and boundary parameters a and b.
6. Wakeby (α, β, γ, σ, ζ) = Wakeby distribution with parameters α, β, γ, σ, and ζ

10.6 Model Configuration

This section describes the setup and configuration applied to the impact model to ensure that the assumptions associated with the Current Practice and Adaptation maintenance strategies are appropriately modelled.

10.6.1 Model Configuration for Current Practice Strategy

The analysis of Current Practice maintenance strategy utilised the rut depth model coefficient for the Dense Bituminous Macadam (DBM) surfacing group given in Figure 6.5 and summarised in Table 6.3. The treatment strategies used are given in Table 10.2.

10.6.2 Model Configuration for Adaptation Strategy

Analysis of the maintenance strategy for adaptation (Adaptation Strategy) assumed that the case study road is reconstructed in the first year with asphalt materials which offer higher resistance to surface rutting than Dense Bitumen Macadam (DBM). One such material is the high modulus Enrobe a Module Eleve (EME2) (Sanders and Nunn, 2005; Brennan et al., 2010). The Climate Impact and Adaptation model was configured prior to analysis by adjusting relevant model coefficients to reflect the observed performance and properties synonymous with EME2 asphalt material.

An EME2 type asphalt material was modelled by modifying selected rut depth model coefficients for DBM Surfacing Group using data from the full-scale wheel-tracking tests study reported by Sanders and Nunn (2005). The study compared the rutting resistance of EME2 to that of conventional Heavy Duty Macadam (HDM50) commonly used on trunk

roads in the United Kingdom (DMRB HD26/06, 2006). Measurement of rut depth development in accordance with wheel tracking tests stipulated in BSI BS598 (1998) indicated that the rate of rut depth development in EME2 was 29% slower than those observed in HDM50.

Since the performance of HDM50 and DBM50 materials are similar (DMRB HD26/06, 2006), and given that the study by Sanders and Nunn (2005) was performed under conditions that simulated a heavily trafficked trunk road on a hot summer day, the distribution of the DBM Surfacing Group rut depth model coefficient distribution for traffic loading variable (β_1) and hot dry summer (β_6) given in Figure 6.5 were calibrated by reducing their mean values and range by 29% to reflect improved resistance to asphalt surface rutting. This calibration process is illustrated in Figure 10.6 for the traffic loading model coefficient (β_1).

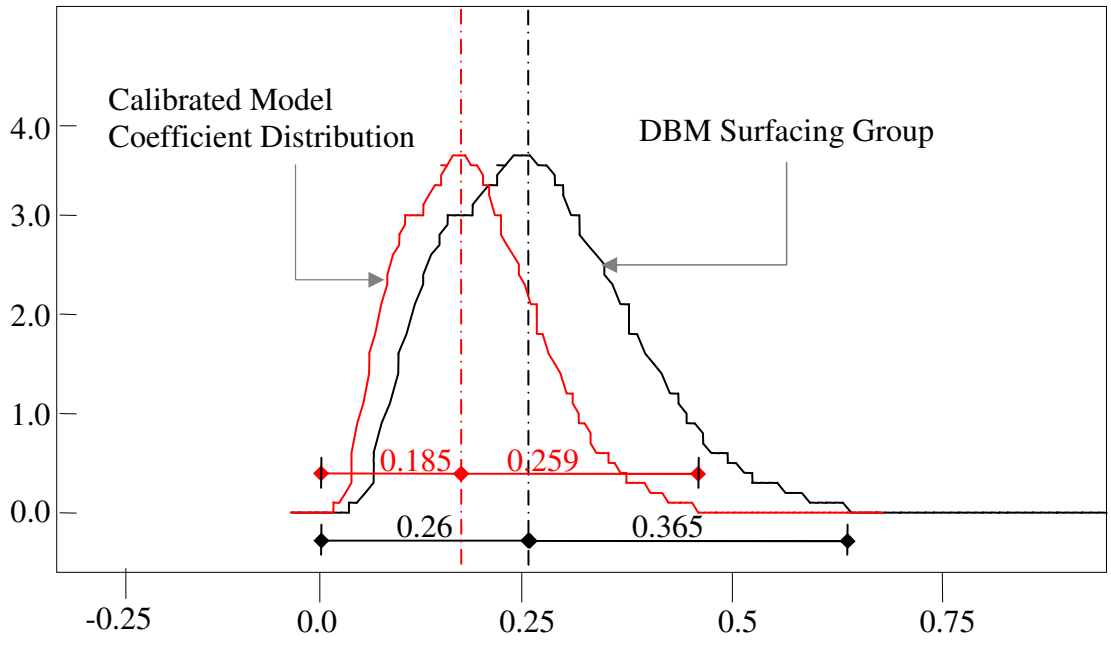

Figure 10.6: Calibration of Annual Equivalent Standard Axle Load Model Coefficient (β_1).

Furthermore, the Voids in Mix (VIM) and binder Softening Point (SP) models were calibrated by adjusting their model coefficients using the following properties of the EME2 samples taken from the full-scale tests by Sanders and Nunn (2005):

- Initial VIM of 5%;
- Initial binder SP of 66^{o}C; and
- Binder SP after ageing of 72^{o}C.

The distribution of the calibrated model coefficients are summarised in Table 10.6. Model coefficients for Heavy Vehicle Speed (β_2), Gradient (β_3) and Asphalt Thickness (β_4) were not adjusted since much is not known about them with respect to EME2 asphalt material.

Table 10.6: Distribution of Calibrated Model Coefficients

Variable Name	Units	Model Coefficient Notation	Distribution
Number of Annual Equivalent Standard Axle Load (YE4)	msa	β_1	Pert (0.18, 0, 0.444)
Average Maximum Daily Summer Temperature (TPmax)	^{o}C	β_6	Pert (0.0284, 0, 0.0639)
Softening Point (SP)	^{o}C	α_1	Normal (0.9, 0.2)
		α_2	Normal (70.3, 0.3)
Voids in Mix (VIM)	%	η_1	Normal (-0.4, 0.01)
		η_2	Normal (3.149, 0.01)

Notes to Table 10.6

1. Pert (m, a, b) = Pert Distribution with Mode m, Lower Boundary a, and Upper Boundary b.
2. Normal (μ, σ) = Normal Distribution with Mean μ and Standard Deviation σ.

10.7 Monte Carlo Analysis

Monte Carlo Sampling was used to draw random but plausible scenarios of input data and model coefficients for each run or iteration of the model. The number of iterations necessary to exhaust the sampling space of the distributions of the model inputs and the model coefficients was determined when the values of the standard error and mean of the discounted treatment costs were observed to be stable. This was achieved by monitoring the trend of the standard error and mean of the discounted costs maintenance treatment as illustrated in Figure 10.7.

From Figure 10.7, the trend of both the mean and standard deviation of the discounted costs of maintenance works were deemed to have stabilised after 20,000 models runs (iterations). Consequently, the analysis was performed with 20, 748 model runs.

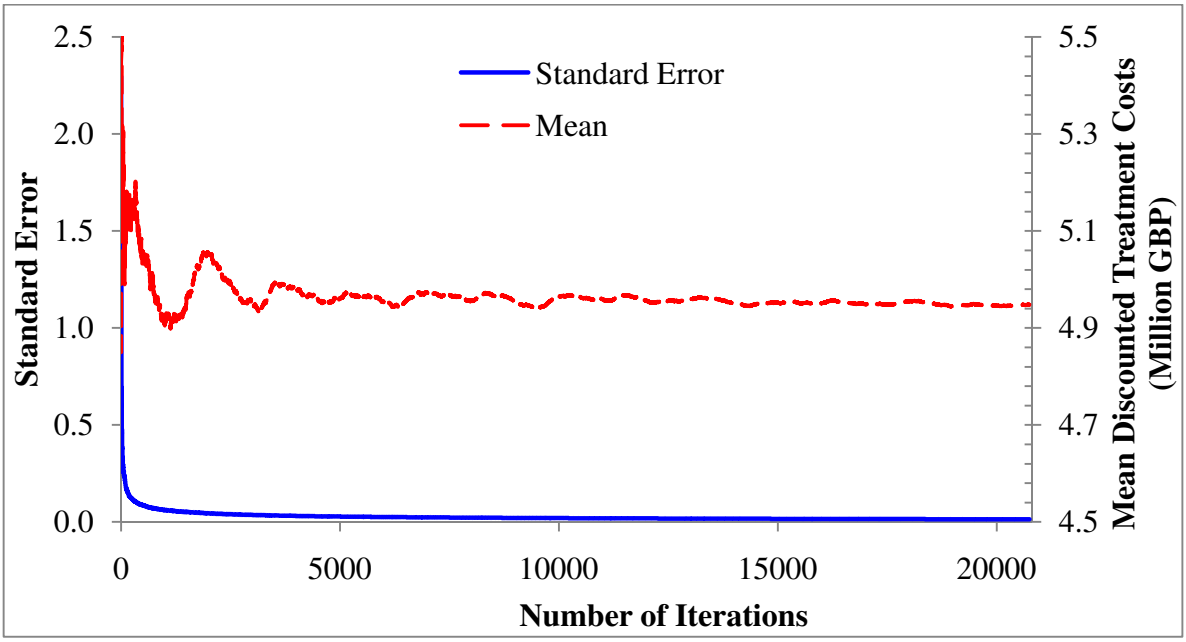

Figure 10.7: Comparison of Standard Error and Mean of Discounted Maintenance Costs with Number of Model Runs.

10.8 Analysis Results

The results of the analysis are presented under the following three sub-headings:

- Predicted rut depth deterioration rates under the Current Practice strategy and Adaptation strategy analyses;
- Predicted condition and discounted treatment costs for the Current Practice maintenance strategy;
- Predicted condition and discounted treatment costs for the Adaptation maintenance strategy.

10.8.1 Predicted Rut Depth Deterioration Rates

This section describes the predicted rut depth deterioration rates derived by running the model described in Chapter 8 using the configuration for the Current Practice and Adaptation maintenance strategies without applying any treatment works.

10.8.1.1 Deterioration Rates for Current Practice Strategy Model Configuration

Descriptive statistics of the average annual incremental rut depth when the model was run over the 30-year analysis period using assumptions stated in section 10.6.1 without applying treatment works is provided in Table 10.7.

Table 10.7: Summary Statistics of Predicted Annual Incremental Rut Depth under Current Practice Strategy

Description	Baseline (1961-1990)	2020 Medium Emission	2030 Medium Emission	2040 Medium Emission	2050 Medium Emission
Mean	1.329	1.404	1.487	1.593	1.768
Standard Error	0.003	0.003	0.003	0.003	0.004
Median	1.283	1.346	1.425	1.523	1.682
Standard Deviation	0.380	0.424	0.456	0.500	0.570
Range	3.405	4.362	4.228	5.921	6.709
Minimum	0.436	0.427	0.386	0.459	0.350
Maximum	3.842	4.789	4.614	6.380	7.060
Number of Iterations	20748	20748	20748	20748	20748

The predicted average annual rate of asphalt surfacing rutting was about 1.3 mm per year over the Baseline period (1961 – 1990). The average annual rut depth deterioration rate increases relative to the baseline deterioration rate by about 0.1mm per year over the 2020s, by about 0.2mm over the 2030s, by about 0.3mm per year over the 2040s and by about 0.5mm per year over the 2050s. The increase in average annual incremental rut depth relative to the baseline climate scenario represents the effect of increased frequency of 2003-type hot dry summers during the 2020s, 2030s, 2040s, and 2050s periods under the Medium Emission Scenario. Inference on the significance of these relative differences in rates of rut depth deterioration is made in section 10.9 by considering the cost of maintaining the road using the Current Practice maintenance strategy.

Cumulative probability plots of the predicted annual incremental rut depth are given in Figure 10.8. The maximum predicted annual incremental rut depth is 3.8mm for the baseline period, 4.8mm for the 2020s, 4.6mm for the 2030s, 6.4mm for the 2040s and 7.1mm for the 2050s.

However, considering 90% of the model outputs, the average annual incremental rut depth does not exceed 1.91mm for the baseline scenario, 1.99mm for the 2020s, 2.05mm for the 2030s, 2.12mm for the 2040s and 2.25mm for the 2050s. These suggest that extreme estimates of the average annual incremental rut depths are apparent in the remaining 10% of the model runs.

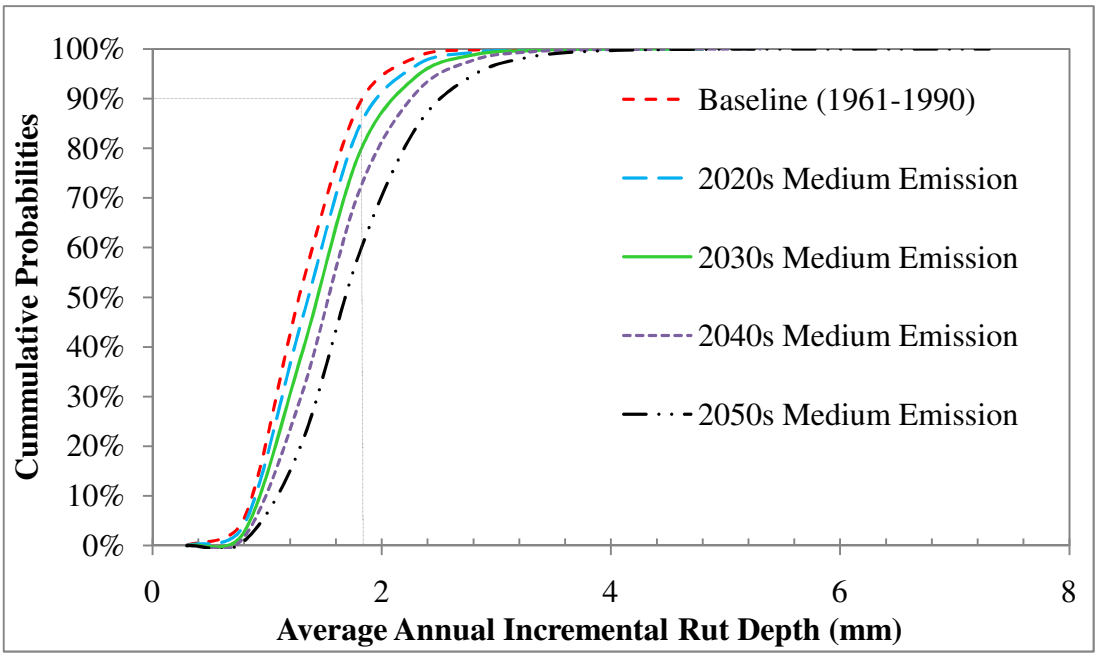

Figure 10.8: Cumulative Distribution of Predicted Annual Incremental Rut Depth for Current Practice Model Setup and Configuration without Treatment Works.

Figure 10.9 shows the cumulative progression of the mean annual incremental rut depth for a typical iteration of the model for each of the four climate periods. The cumulative rut depth trends are non-linear and differences between the predictions for each scenario and time periods are not obvious because annual climate data as well as other input data and model coefficients were obtained by drawing random samples from distributions of climate predictions available in 30-year periods. Figure 10.10 shows the average cumulative annual incremental rut depth predictions for 20,748 iterations of the model.

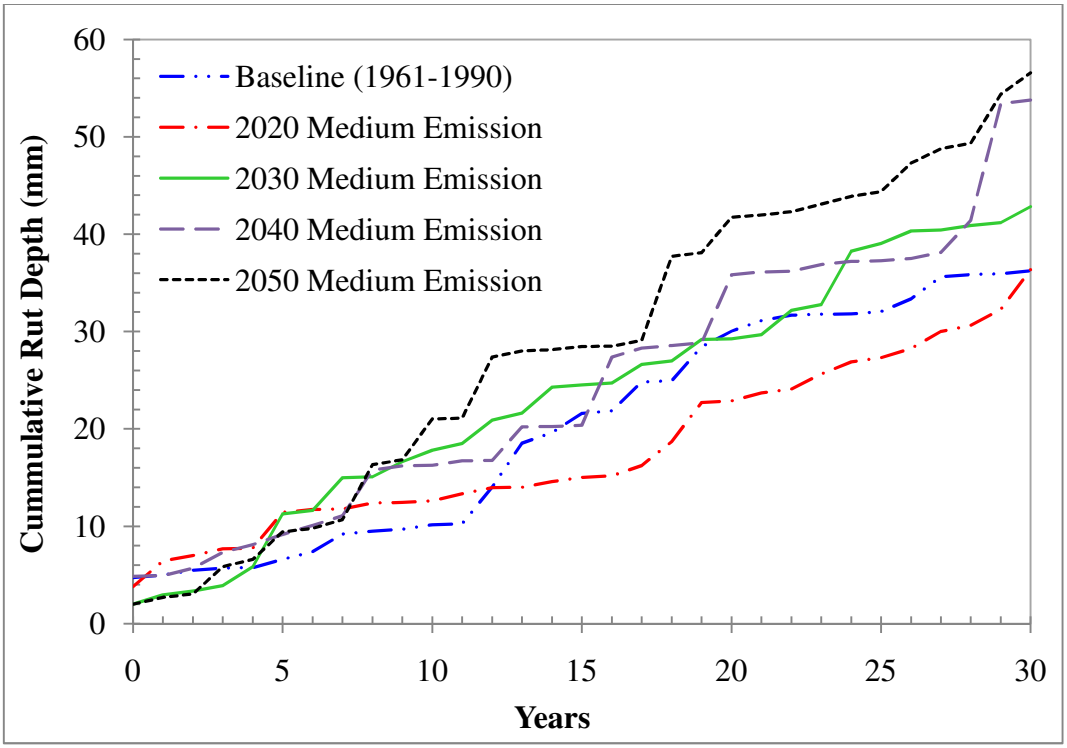

Figure 10.9: Average Cumulative Rut Depth Progression by Climate Scenario and Time Periods for a Single Model Simulation

The predicted average cumulative rut depth at the end of the 30-year analysis period (Figure 10.10) using the model configuration for the Current Practice maintenance strategy (section 10.6.1) was 57mm for the 2050s, 51mm for the 2040s, 48mm for the 2030s, 46mm for the 2020s, and 43mm for the Baseline period.

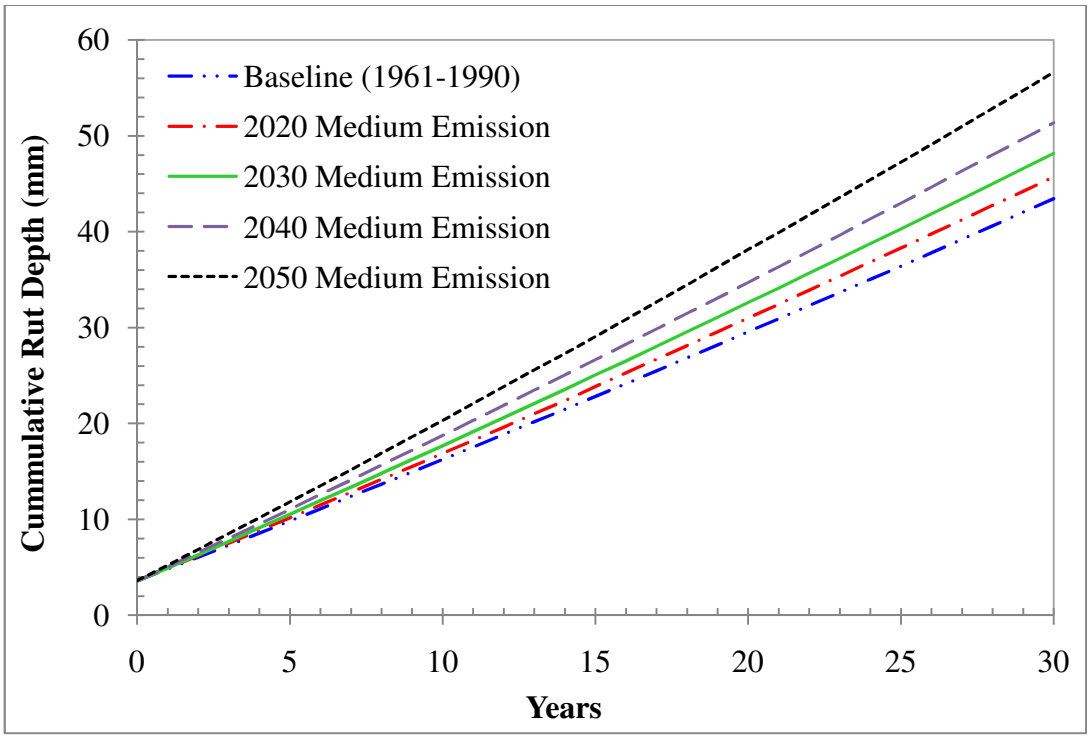

Figure 10.10: Average Cumulative Rut Depth Progression by Climate Scenario for 20,748 Simulations

Figure 10.11 illustrates the rut depth deterioration trend over the 30-year period for the 2020s Medium Emission Scenario represented as annual proportions of the number of model runs with cumulative rut depth categorised into four condition bands. The four conditions bands are defined in Table 10.8. The definition of the condition bands is consistent with the rut depth categorisation specified in Table 5.2 which in turn was obtained from the Highways Agency Design Manual for Roads and Bridges (DMRB) (HD29/08, 2008). Annual cumulative deterioration by condition bands for the Baseline scenario as well as the 2020s, 2030s, 2040s and 2050s Medium Emissions climate scenarios are tabulated in Appendix E2.

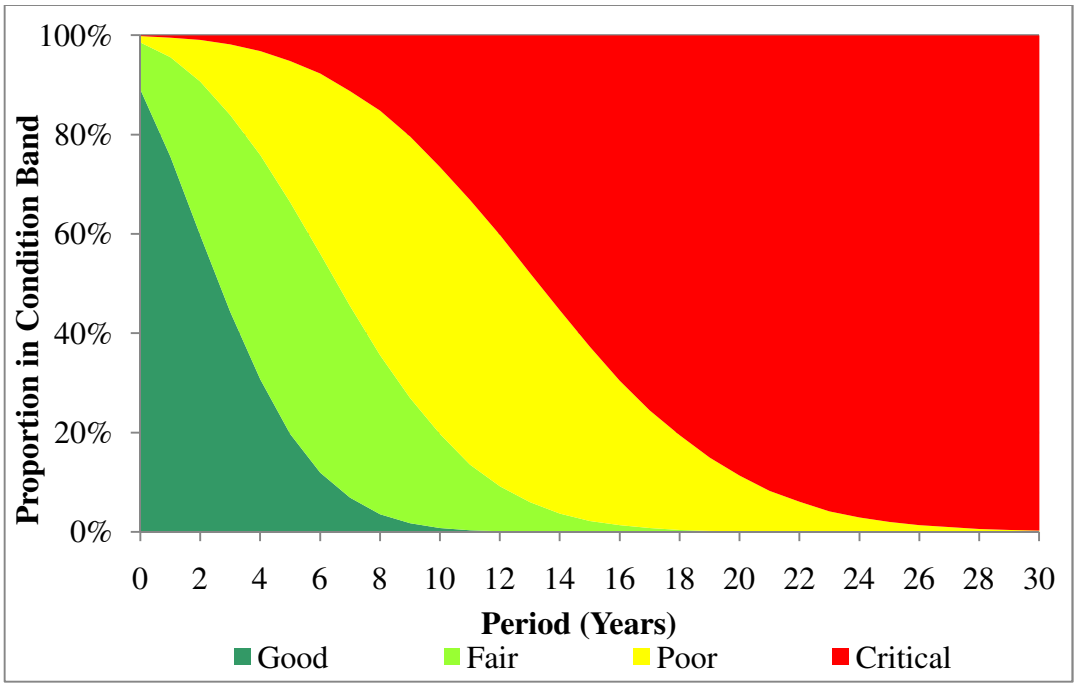

Figure 10.11: Cumulative Rut Depth Proportions without Treatment Works for 2020s Medium Emission Scenario using Current Practice Model Configuration

Table 10.8: Definition of Cumulative Rut Depth Condition Band

Rut Depth Range (mm)	Condition Band	Description
0 – 6	Good	No visible deterioration.
6.1 – 11	Fair	The deterioration is not serious and more detailed investigations are not needed.
11.1 – 20	Poor	The deterioration is becoming serious and needs to be investigated.
>20	Critical	Severe level of deterioration

10.8.1.2 Deterioration Rates for the Adaptation Strategy Model Configuration

Descriptive statistics of the average annual incremental rut depth when the model was run over the 30-year analysis period using assumptions described in section 10.6.2 without applying treatment works is provided in Table 10.9.

Table 10.9: Summary Statistics of Predicted Annual Incremental Rut Depth for Adaptation Model Setup

Description	Baseline (1961-1990)	2020s Medium Emission	2030s Medium Emission	2040s Medium Emission	2050s Medium Emission
Mean	1.231	1.258	1.289	1.324	1.390
Standard Error	0.002	0.003	0.003	0.003	0.003
Median	1.191	1.214	1.239	1.271	1.332
Standard Deviation	0.347	0.365	0.378	0.398	0.426
Range	3.069	2.954	3.690	4.775	4.205
Minimum	0.363	0.362	0.341	0.379	0.369
Maximum	3.432	3.316	4.031	5.154	4.574
Number of Iterations	20,748	20,748	20,748	20,748	20,748

The predicted average annual rate of asphalt surfacing rutting is 1.2 mm per year over the Baseline (1961 – 1990) period. The average annual rate of rut depth deterioration marginally increases relative to baseline estimate by about 0.03mm per year for predictions using the 2020s Medium Emission scenario, by about 0.06mm over the 2030s Medium Emission, by about 0.09mm per year over the 2040s Medium Emission and by about 0.16mm per year over the 2050s Medium Emission. These annualised rut depth deterioration rates are lower than those predicted using the Current Practice configuration of the model.

Cumulative probability plots of the predicted annual incremental rut depth are given in Figure 10.12. The plot shows that the maximum values of predicted annual incremental rut depth for the five climate periods range from 3.3mm to 4.6mm. However, for 90% of the model simulations (Figure 10.12), the average annual incremental rut depth does not exceed 1.70mm for the baseline scenario, 1.75mm for the 2020s, 1.79mm for the 2030s, 1.81mm for the 2040s and 1.91mm for the 2050s. This suggests that extreme estimates of the average annual incremental rut depths are apparent in the remaining 10% of the model runs.

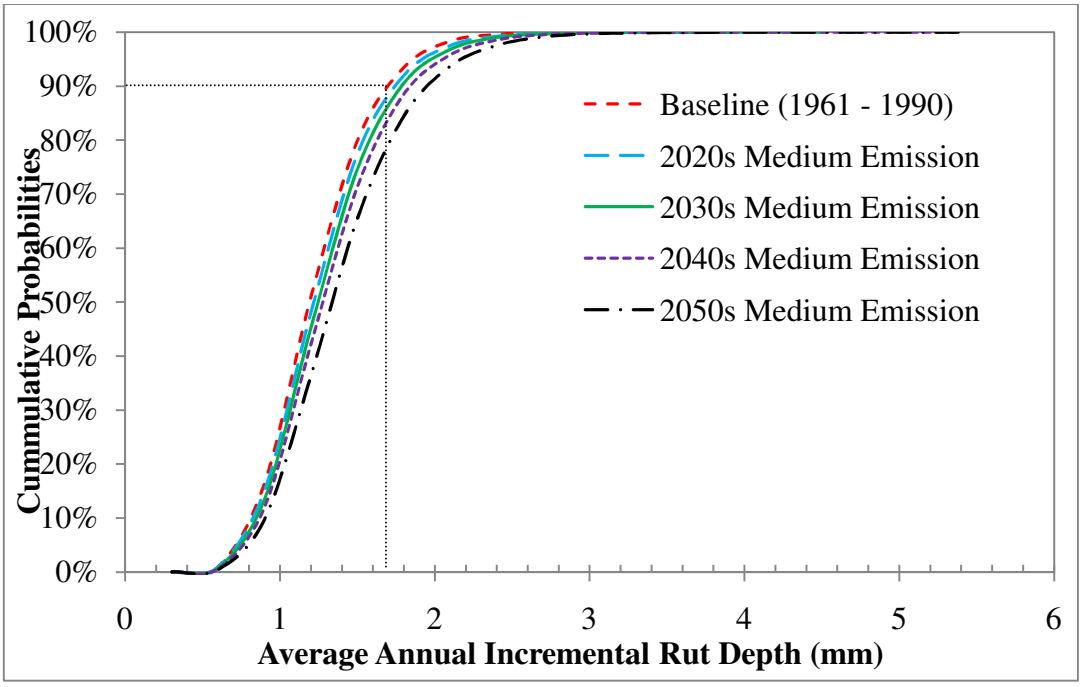

Figure 10.12: Cumulative Distribution of Predicted Annual Incremental Rut Depth for Adaptation Configuration of the Model without Treatment Works.

The predicted average cumulative rut depth at the end of the 30-year analysis period (Figure 10.13) using the Adaptation setup of the model was 46mm for the 2050s, 44mm for the 2040s, 43mm for the 2030s, 42mm for the 2020s, and 41mm for the Baseline period.

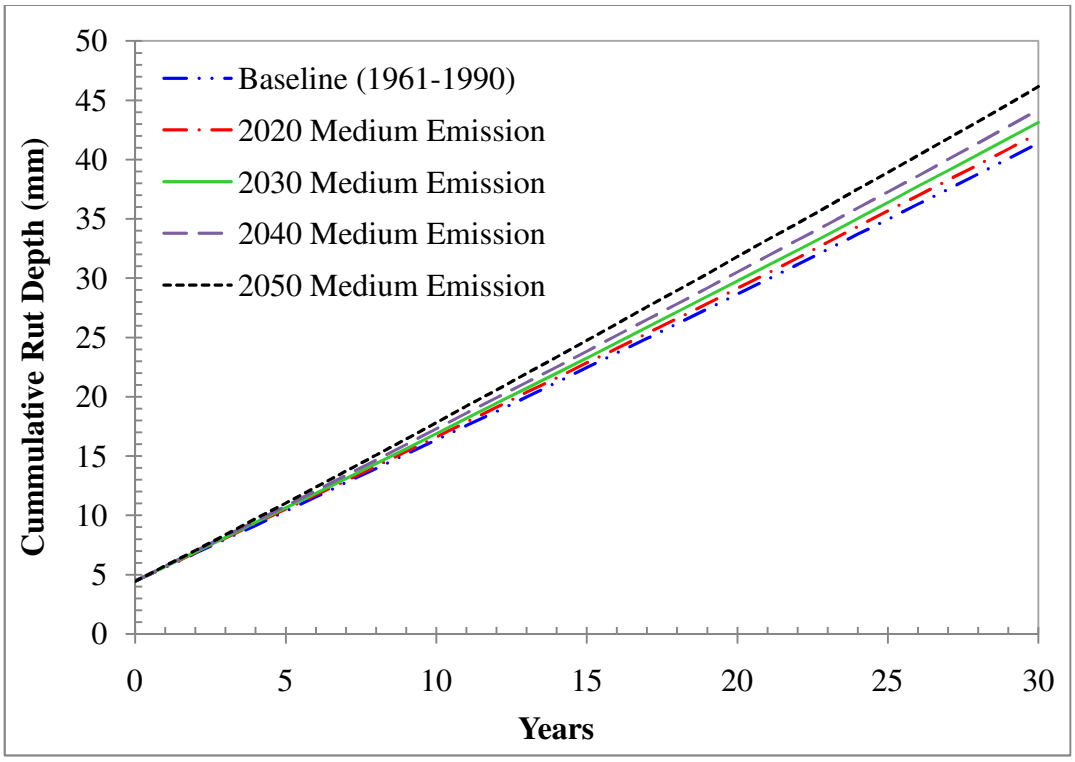

Figure 10.13: Average Cumulative Rut Depth Progression by Climate Scenario for 20,748 Simulations using the Adaptation Model Setup

Figure 10.14 illustrates the rut depth deterioration trend over the 30-year period for the 2020s Medium Emission Scenario using the Adaptation model configuration. The deterioration trend is represented as annual proportions of the number of model runs with cumulative rut depth categorised into the four condition bands defined in Table 10.8. The annual cumulative proportions in condition bands for all the scenarios and time periods analysed using the Adaptation model configuration are tabulated in Appendix E2.

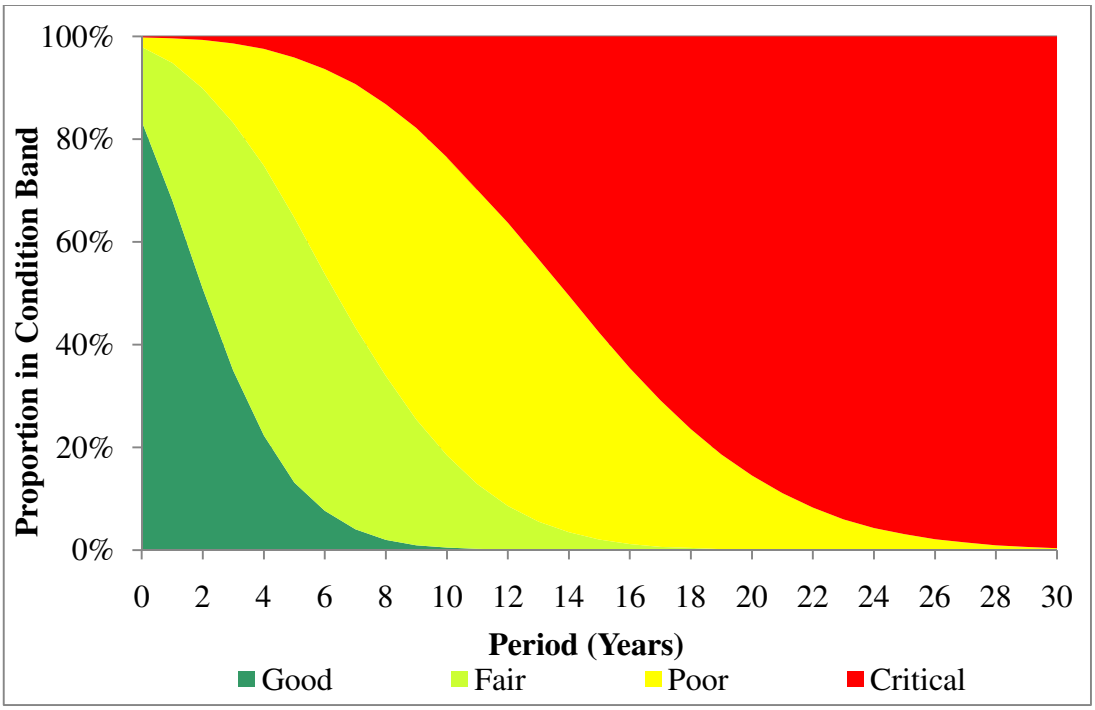

Figure 10.14: Cumulative Rut Depth Proportions without Treatment Works for 2020s Medium Emission Scenario using Adaptation Model Configuration

10.8.2 Analysis Results for Current Maintenance Practice Strategy

Analysis results for the Current Practice strategy described in section 10.3.3.3.1 are presented and discussed under the following headings:

- Predicted condition trend;
- Distribution of discounted treatment costs or road agency costs; and,
- Summary statistics of discounted treatment costs.

10.8.2.1 Predicted Condition Trend

Predicted annual condition profile for the 2050s Medium Emission scenario using the Current Practice maintenance strategy is given in Figure 10.15. Condition profiles for the Baseline period, 2020s Medium Emission, 2030s Medium Emission and 2040s Medium Emission are

provided in Appendix E3. The condition profiles shows that under both the Baseline climate scenario and the four 30-year time periods of the Medium Emission scenarios, the road would be largely maintained in a good to fair condition with total annual proportion in poor and critical condition not exceeding 13% in any year during the 30-year analysis period.

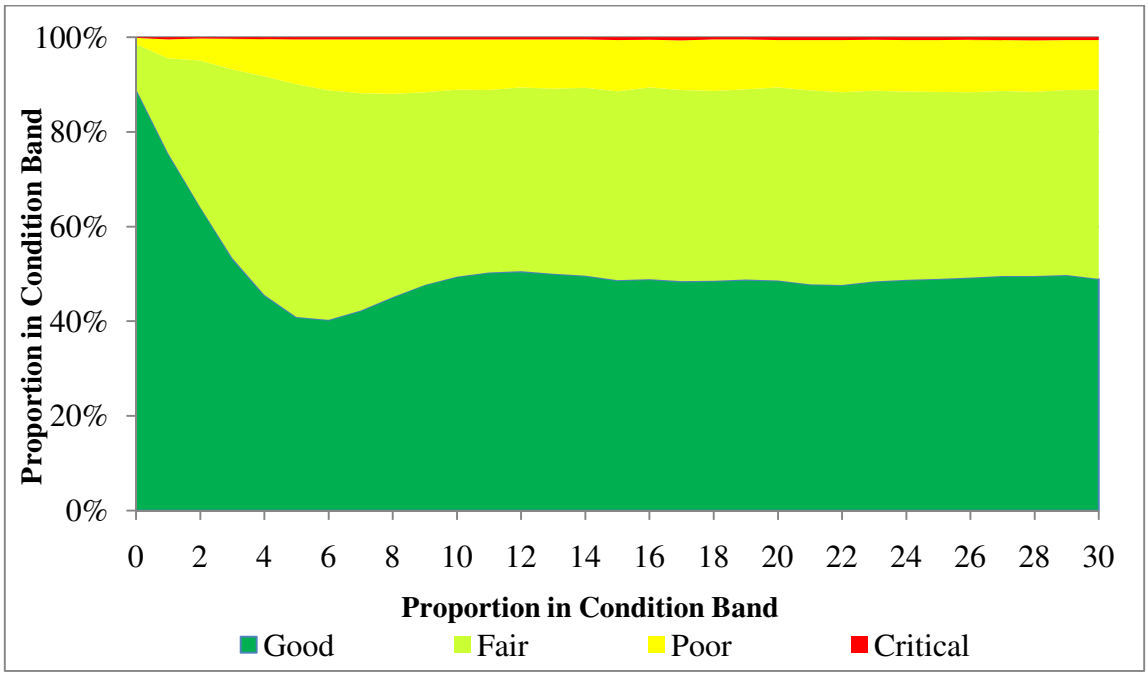

Figure 10.15: Cumulative Rut Depth Proportions with Treatment Works for 2050s Medium Emission Scenario and the Current Practice Maintenance Strategy

A summary of the proportions of model outputs in condition bands averaged over the 30-year analysis period for the Baseline period, 2020s, 2030s, 2040s and 2050s is given in Table 10.10. The proportion of predicted rut depth in condition bands are similar across the climate periods analysed because treatments are triggered when cumulative rut depth exceeds 1lmm across all climate scenarios and time periods that were analysed. The costs necessary to achieve this condition distribution are presented and in the next section.

Table 10.10: Summary of Average Proportion of Model Outputs in Condition Band for Current Practice Strategy

	Baseline (1961-1990)	**2020s**	**2030s**	**2040s**	**2050s**
Good	50.5%	50.8%	50.8%	51.0%	51.2%
Fair	39.6%	39.0%	38.5%	37.8%	36.9%
Poor	9.5%	9.7%	10.0%	10.4%	11.0%
Critical	0.4%	0.5%	0.6%	0.8%	1.0%

10.8.2.2 Distribution of Maintenance Costs for Current Practice Maintenance Strategy

The distribution of the discounted maintenance costs is shown in Figure 10.16 and Figure 10.17 for the Baseline climate scenario and the 2020s Medium Emission scenario. The distribution of maintenance costs for the 2030s Medium Emission, 2040s Medium Emission and 2050s Medium Emission are provided in Appendix E4. The distributions embody the uncertainties inherent in the input data and the coefficients of the model.

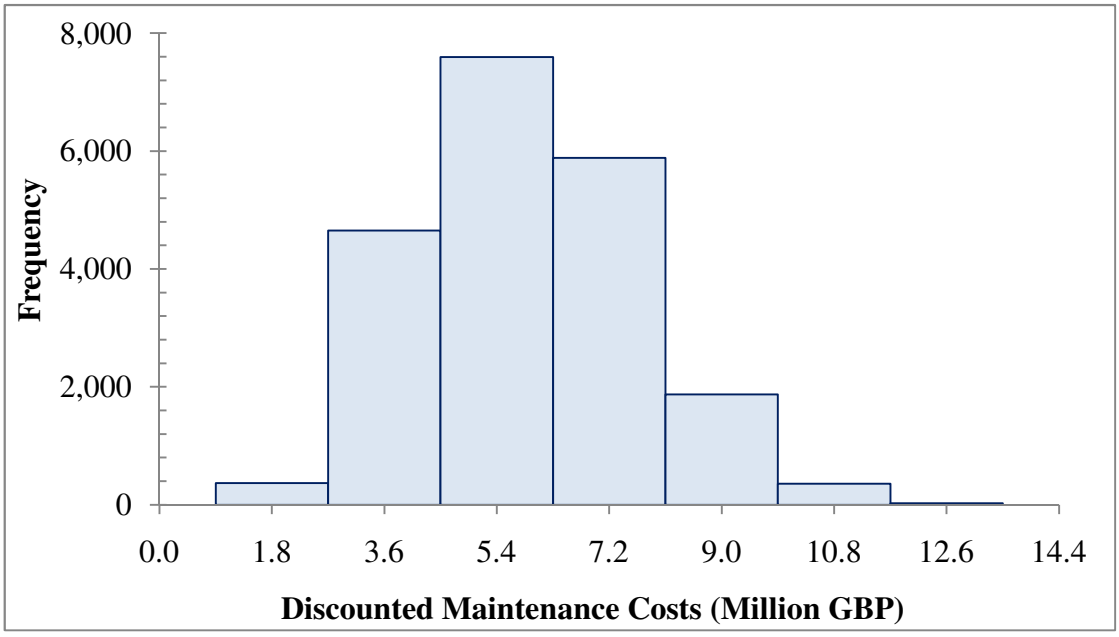

Figure 10.16: Distribution Discounted Maintenance Costs for the Baseline (1961 – 1990) Scenario for the Current Practice Maintenance Strategy

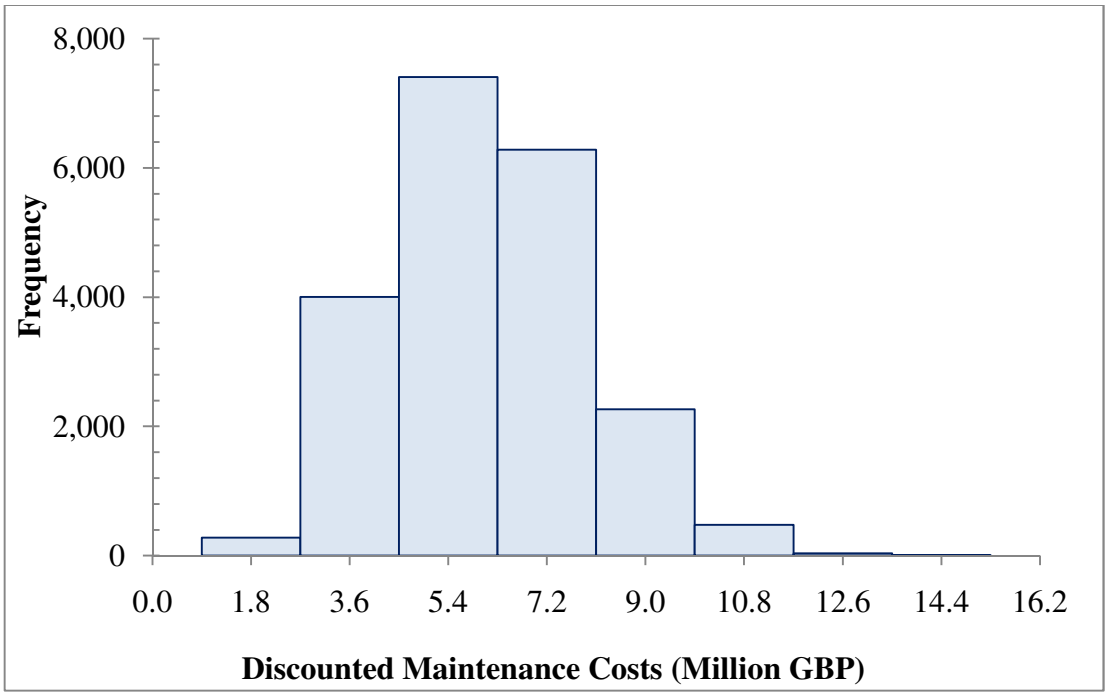

Figure 10.17: Distribution of Discounted Maintenance Costs for the 2020s Medium Emission Scenario for the Current Practice Maintenance Strategy

A comparison of the distribution of discounted treatment costs necessary to achieve the average condition given in Table 10.10 is illustrated in Figure 10.18 using cumulative distribution plots for each scenario and time periods analysed. It is apparent that higher investments in maintenance treatment would be required over the 2050s followed by the 2040s, 2030s, 2020s and the Baseline period. Comparison of summary statistics for the scenarios and time periods analysed is provided in the next section.

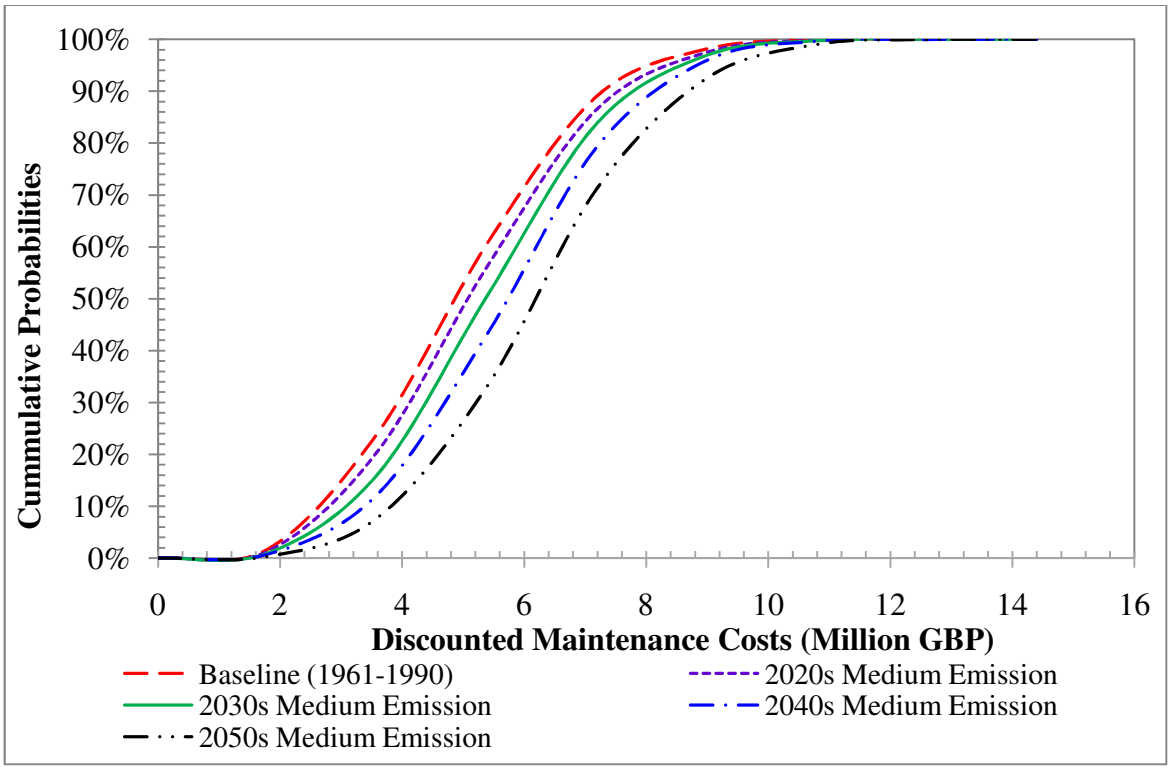

Figure 10.18: Cumulative Discounted Treatment Costs by Scenarios and Time Periods

10.8.2.3 Summary Statistics of Road Maintenance Costs for Current Practice Strategy

Descriptive statistics of the discounted treatment costs under the Current Practice maintenance strategy is given in Table 10.11 for the Baseline scenario and the Medium Emission scenarios for the 2020s, 2030s, 2040s and 2050s.

The estimated average cost of treatment works was lowest when the baseline climate data was used and progressively increased by about 5%, 10%, 16% and 26% relative to the baseline costs over the 2020s, 2030s, 2040s and 2050s respectively. This trend is consistent with the predicted rates of rut depth deterioration presented in section 10.8.1.1.

Table 10.11: Summary Statistics of Discounted Treatment Costs by Climate Scenario in Million GBP

Description	Baseline (1961-1990)	2020s Medium Emission	2030s Medium Emission	2040s Medium Emission	2050s Medium Emission
Mean	4.948	5.171	5.443	5.758	6.256
Standard Error	0.013	0.013	0.013	0.013	0.013
Median	5.040	5.177	5.380	5.722	6.278
Mode	2.244	2.132	2.283	2.283	2.131
Standard Deviation	1.925	1.929	1.908	1.881	1.901
Range	11.739	12.171	13.123	12.920	12.606
Minimum	0.676	0.700	0.700	0.676	0.700
Maximum	12.415	12.871	13.823	13.596	13.305
Number of Simulations	20,748	20,748	20,748	20,748	20,748

10.8.3 Adaptation Maintenance Strategy

10.8.3.1 Predicted Cumulative Condition Trend

The predicted condition profile for the Adaptation maintenance strategy is shown in Figure 10.19 for the 2020s Medium Emission scenario. Condition profile for the Baseline scenario, 2030s Medium Emission scenario, 2040s Medium Emission scenario and 2050s Medium Emission scenario are provided in Appendix E5. For all scenarios and time periods analysed, the proportions of outputs of the model simulations in critical condition are maintained to a minimum and the outputs of more than 90% of the model runs are categorised as Good or Fair.

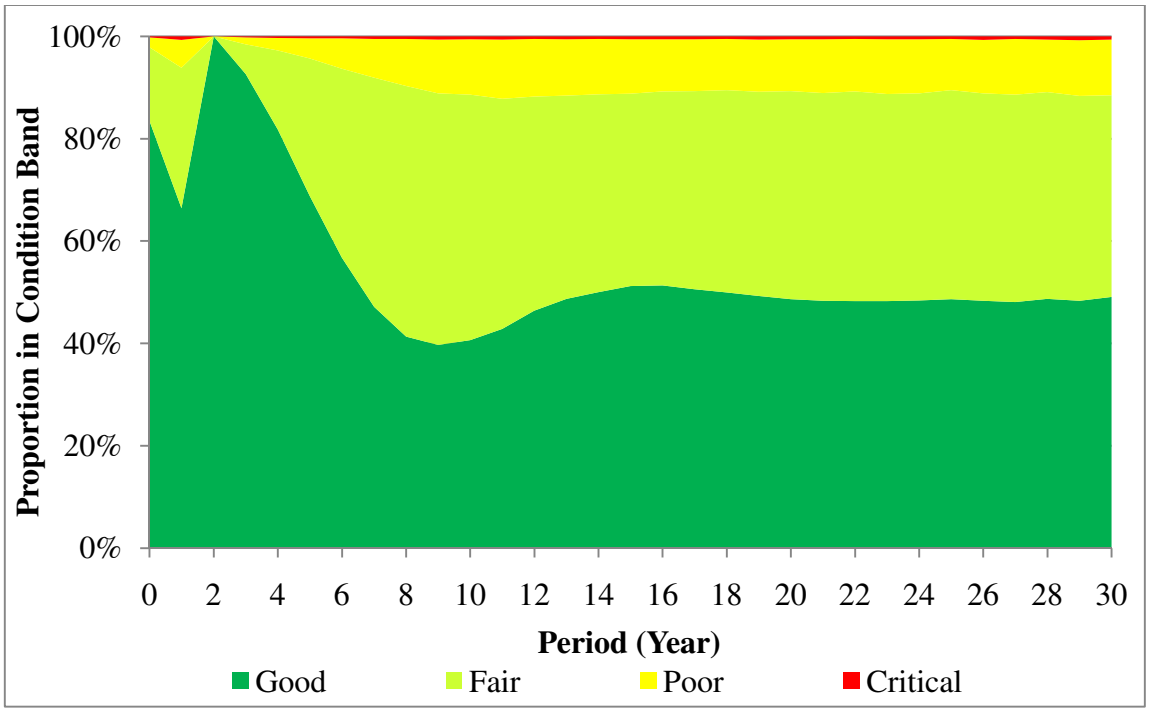

Figure 10.19: Cumulative Rut Depth Proportions with Treatment Works for 2020s Medium Emission Scenario for the Adaptation Maintenance Strategy

A summary of the proportions of model outputs in condition bands averaged over the 30-year analysis period for the climate scenarios analysed using the Adaptation maintenance strategy is given in Table 10.12. The proportions of the model outputs categorised in the good and fair condition bands under the Adaptation strategy are higher than estimates derived using the Current Practice maintenance strategy.

Table 10.12: Summary of Average Proportion of Model Outputs in Condition Band for Adaptation Maintenance Strategy

Condition Band	Baseline (1961-1990)	2020s	2030s	2040s	2050s
Good	54.5%	54.5%	54.6%	54.5%	54.6%
Fair	37.1%	36.9%	36.7%	36.9%	36.2%
Poor	8.2%	8.3%	8.4%	8.3%	8.7%
Critical	0.3%	0.3%	0.3%	0.3%	0.5%

The averaged proportion of predicted rut depth in condition bands given in Table 10.12 are similar across the climate periods analysed because treatments are triggered when cumulative rut depth exceeds 1lmm across all climate scenarios and time periods that were analysed. The costs necessary to achieve this condition distribution given the Adaptation maintenance strategy are presented and in the next section.

10.8.3.2 Distribution of Maintenance Costs for Adaptation Maintenance Strategy

The distribution of the costs of maintaining the road using the Adaptation maintenance strategy to conditions presented in section 10.8.3.1 are shown in Figure 10.20 and Figure 10.21 for the Baseline and 2020s Medium Emission scenarios. The maintenance costs were discounted to the start of the 30-year analysis period. Distributions of maintenance costs for the 2030s Medium Emission, 2040s Medium Emission and 2050s Medium Emission scenarios are provided in Appendix E6. The distributions embody the uncertainties inherent in the input data and model coefficients used in the analysis.

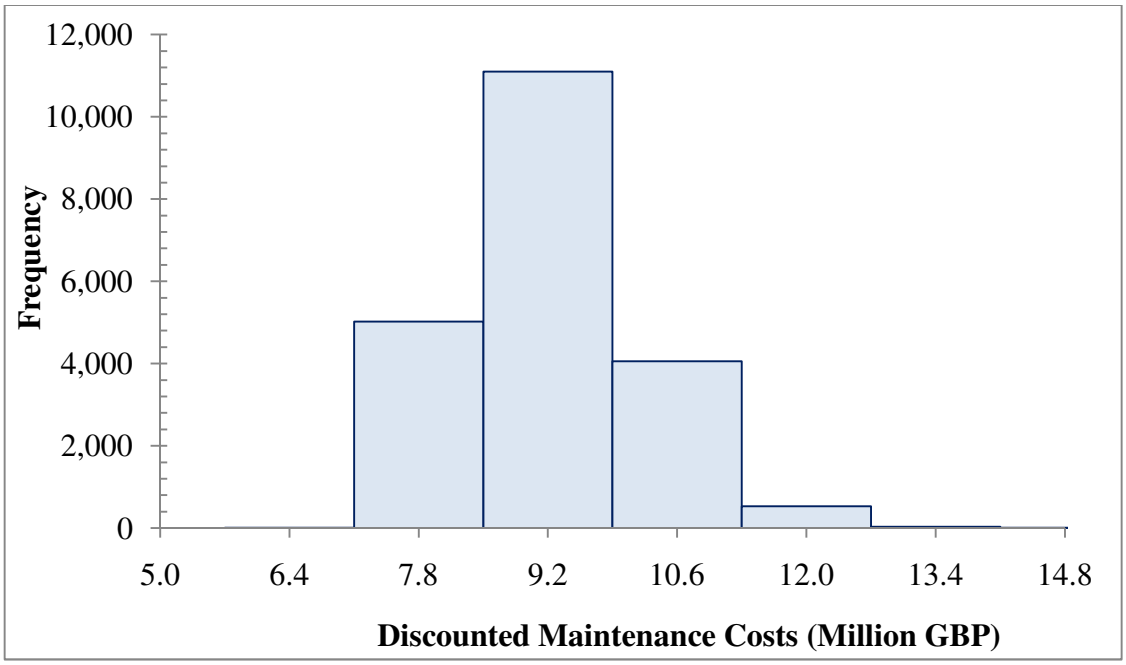

Figure 10.20: Distribution of Discounted Maintenance Costs for the Baseline (1961 – 1990) Scenario for the Adaptation Maintenance Strategy

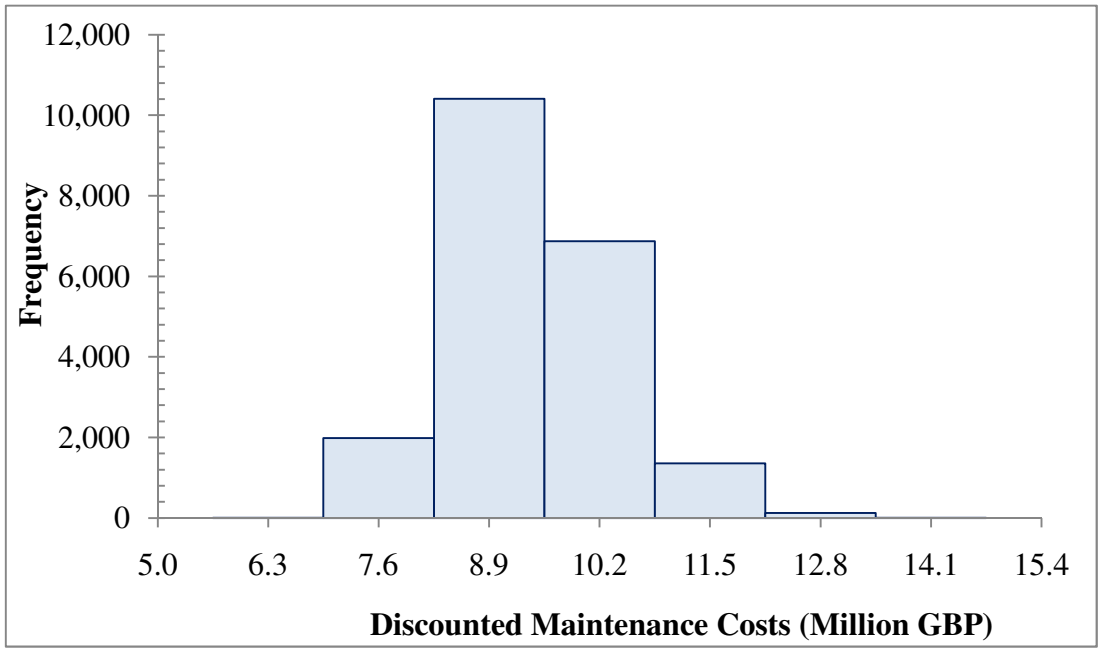

Figure 10.21: Distribution of Discounted Maintenance Costs for the 2020s Medium Emission Scenario for the Adaptation Maintenance Strategy

Cumulative distributions of the discounted treatment costs are depicted in Figure 10.22 for each climate scenario and time period analysed. It is clear from Figure 10.22 that marginally

higher investment would be required over the 2050s, followed by the 2040s, 2030s, 2020s and the Baseline period to maintain the road to the average condition given in Table 10.12.

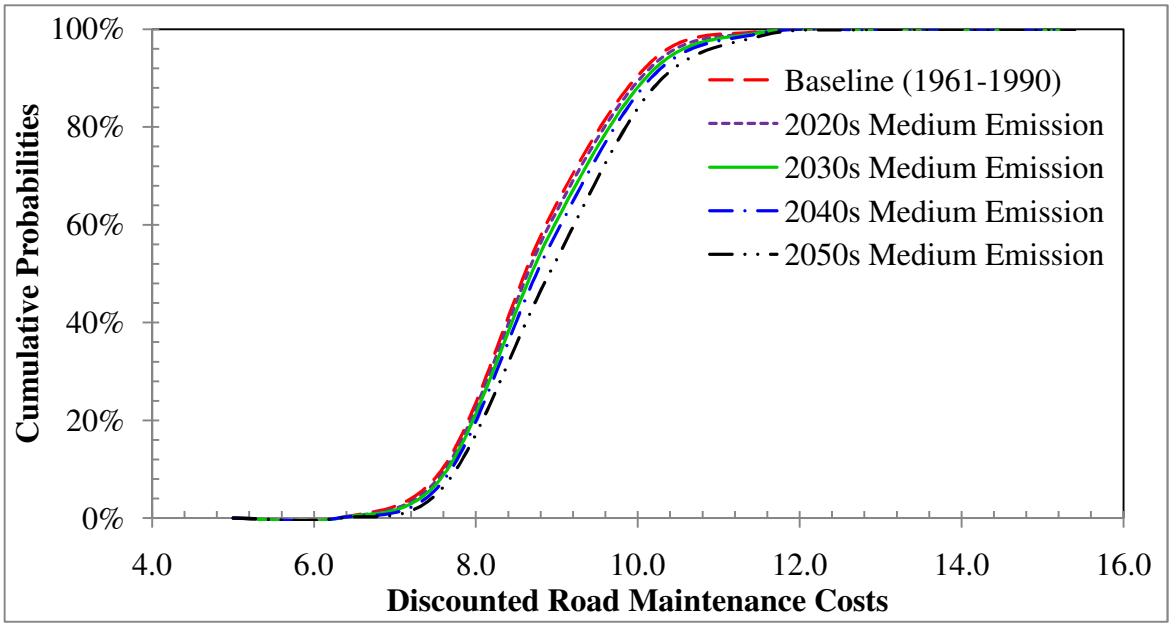

Figure 10.22: Cumulative Discounted Maintenance Costs by Scenarios and Time Periods

10.8.3.3 Summary Statistics of Road Maintenance Costs for Adaptation Strategy

Descriptive statistics of the discounted treatment costs under the Adaptation maintenance strategy is given in Table 10.13 for the Base climate scenario and the 2020s, 2030s, 2040s and 2050s Medium Emission climate scenarios.

The estimated average cost of treatment works was lowest when the baseline climate data was used and marginally increased by 0.7%, 1.3%, 2.1% and 3.6% relative to the baseline estimate over the 2020s, 2030s, 2040s and 2050s time periods. This trend is consistent with the predicted rates of rut depth deterioration presented in section 10.8.1.2.

Table 10.13: Summary Statistics of Road Agency Costs by Climate Scenario in Million GBP for Adaptation Strategy

Description	Baseline (1961-1990)	2020s Medium Emission	2030s Medium Emission	2040s Medium Emission	2050s Medium Emission
Mean	8.532	8.588	8.642	8.708	8.841
Standard Error	0.007	0.007	0.007	0.007	0.007
Median	8.448	8.646	8.731	8.791	8.903
Mode	7.807	7.842	7.843	7.878	7.915
Standard Deviation	0.958	0.984	0.993	1.016	1.042
Range	7.698	7.578	8.167	7.687	7.865
Minimum	6.373	5.783	6.353	6.415	6.373
Maximum	14.070	13.362	14.520	14.101	14.238
Sample Size	20748	20748	20748	20748	20748

The mean discounted treatment costs under this maintenance strategy (Adaptation) is higher than the values predicted under the Current Practice strategy because of the heavy investment necessary to reconstruct the road initially using a more climate resilient material as described in section 10.3.3.3.2. The use of a more climate resilient material however leads to a lower rate of rut depth deterioration under the Adaptation strategy compared to the rates estimate under the Current Practice strategy. These rates of deterioration are given in sections 10.8.1.1 and 10.8.1.2 respectively. The higher investment costs under the adaptation strategy would therefore be fully or partially offset by savings in road user costs resulting from the improved road condition (Robinson and Thagesen, 2004). These benefits include savings in road user costs components such as fuel consumption, vehicle parts consumption, lubricating oil consumption, tyre consumption, and less disruption to road users due to reduced frequency of road works and consequently road closures. According to Paterson (1987), for a given road maintenance strategy, the total Vehicle Operating Costs (VOC) typically outweigh the maintenance costs by significantly large factors in the order of 10 to 20. Therefore small improvements in road condition can yields high benefits relative to the cost of road improvement.

The quantification of savings in road user costs is possible by using the developed model together with existing decision support systems such as the HDM-4. Such an analysis is beyond the scope of this study. A comparison between the Current Practice and Adaptation maintenance strategies is however made in the next section by considering the additional costs necessary to maintain the road if future climate predictions are used instead of past (Baseline) observation.

10.9 The Impact of Climate Change on Maintenance Cost

The concept used to estimate the impact of climate change on maintenance costs from the results presented in sections 10.8.2.2 and 10.8.3.2 is illustrated in Figure 10.23. The difference between the predicted discounted maintenance costs derived using future climate predictions for the 2020s, 2030s, 2040s and 2050s Medium Emission Scenario (C_F) and the corresponding maintenance cost obtained using the observed climate over the baseline period (C_B) represents the impact of predicted climate change on the cost of maintaining the road (C_C) given the assumptions used in the modelling process.

The climate impact costs (C_C) was calculated for each of the 20,748 iterations of the model under the Current Practice and Adaptation maintenance strategies and are presented using the cumulative distribution plots in Figure 10.24.

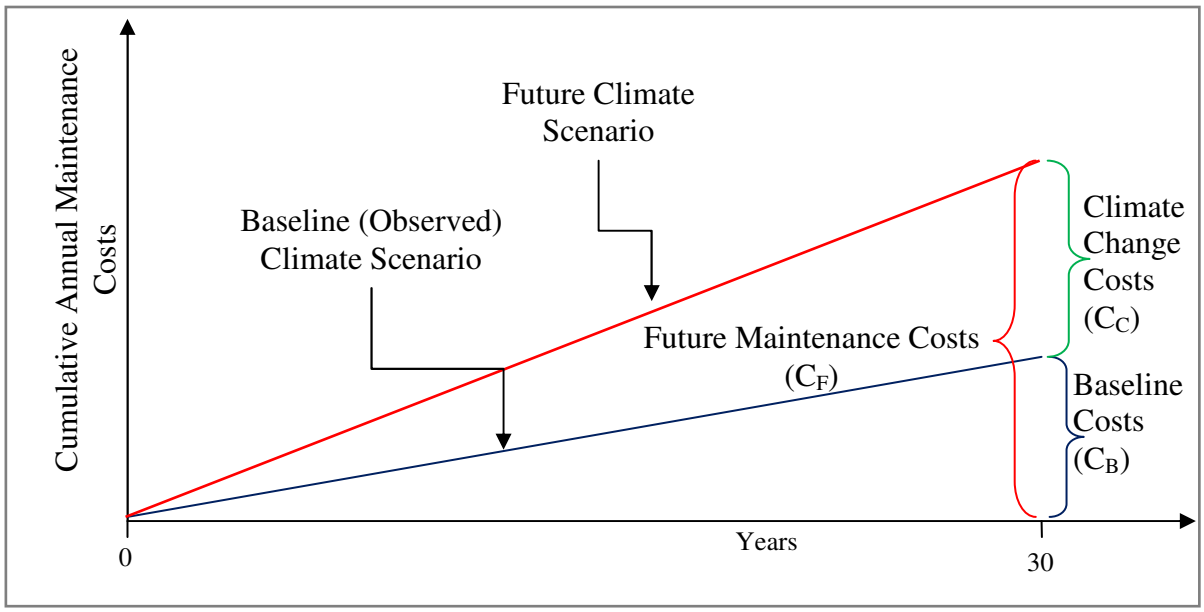

Figure 10.23: Illustration of the Costs of Climate Change on Maintenance Costs

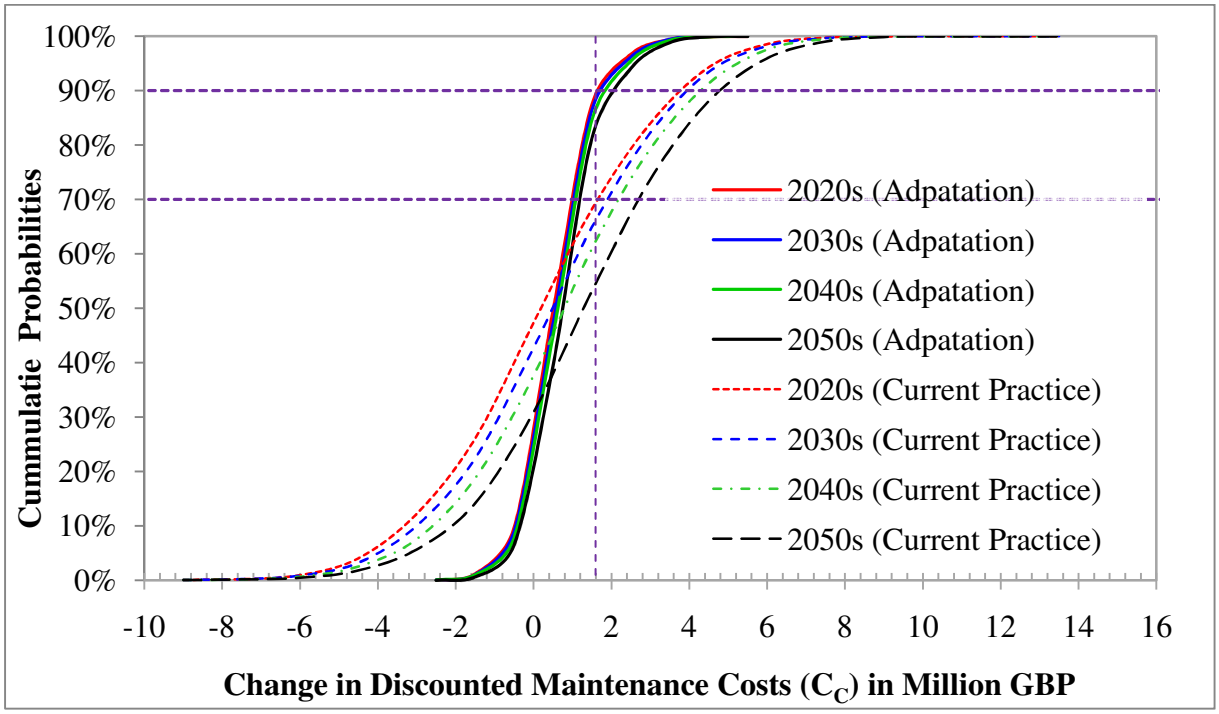

Figure 10.24: Cumulative Distribution of Climate Change Costs for Current Practice and Adaptation Maintenance Strategies

Considering Figure 10.24, for a given maintenance strategy and future climate scenario, the horizontal axis represents the maximum costs of climate change (C_C) that are not exceeded by the corresponding weighted cumulative frequency or cumulative probabilities (probability level) of the model iterations given on the vertical axis. This representation of the impact of climate change on the costs of maintaining the road network provides a decision making framework for use by Road Agencies responsible for managing and maintaining the road based on the Agency's tolerance for risk. For example, if the maximum cost of climate change on road maintenance that the Road Agency can tolerate over the 30-year analysis period during the 2020s (2010 – 2039) is 1.6 Million GBP, then from Figure 10.24 under the Current Practice maintenance strategy, 30% of the model simulations would be expected to result in climate change costs that exceed the 1.6 Million GBP limit. However, if the Adaptation strategy is used, then the proportion of the model simulation that would be expected to exceed the 1.6 Million GBP tolerance level reduces to only 10%. In other words, it may be inferred that the probability of exceeding the Agency's tolerance for risk limit of 1.6 Million GBP is only 10% for the Adaptation strategy but 30% for the Current Practice strategy.

An alternative representation of the cumulative distribution plots in Figure 10.24 is provided in Figure 10.25. The maximum level of contribution of climate change to road maintenance is provided in the horizontal axis while the vertical axis gives the probability of exceeding a given climate change costs threshold. With reference to the example in the previous paragraph, Figure 10.25 can be interpreted as follows:

- The probability that a climate change costs tolerance threshold of 1.6 Million GBP would be exceeded during the 2020s under the Current Practice strategy is 30%. This

probability reduces to 10% if the Adaptation maintenance strategy is used instead of the Current Practice strategy;

- A low climate change costs tolerance level (climate change costs threshold) results in a high probability that such a threshold would be exceeded for a given future climate period and road maintenance strategy. Conversely, a high climate change costs tolerance level results in a low probability that the limit will be exceeded.

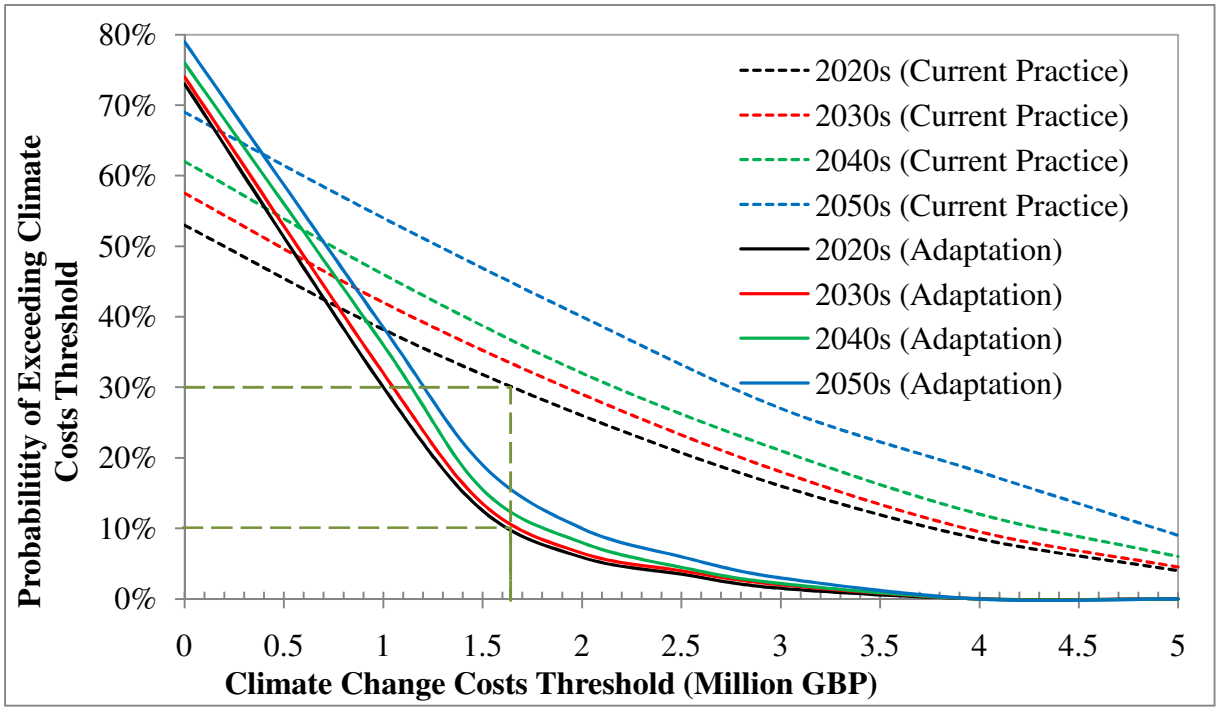

Figure 10.25: Change in Maintenance Costs by Future Climate Periods Relative to Baseline Costs.

10.10 Summary

This chapter discussed a case study aimed at demonstrating the application of the model described in Chapter 8 using the framework discussed in Chapter 9. The objective of the case study was to investigate the relative performance of the study road under the baseline and future climate scenarios and two road maintenance strategies. The costs of road maintenance

attributed to the impacts of future climate change under the two road maintenance scenarios were also investigated.

Two road maintenance scenarios were analysed: a Current Practice scenario and an Adaptation scenario which involved the use of an asphalt material known to provide better resilience to the impacts of the 2003-type hot dry summers. Model analysis was performed over a 30-year period in line with the duration over which UKCP09 climate data were provided. Uncertainties and variability inherent in the inputs to the model were represented using suitable statistical distributions. Monte-Carlo sampling was then used to derive distributions of the outputs of the model after 20,748 iterations.

The predicted average rate of rut depth deterioration under the current practice strategy ranged from 1.33 mm per year during the Baseline period to 1.77 mm per year during the 2050s. Under the Adaptation strategy, the average rate of rut depth deterioration ranged from 1.23 mm per year during the Baseline period to 1.39 mm per year during the 2050s. The predicted costs of climate change associated to each maintenance strategy and future climate periods are given in section 10.9.

CHAPTER 11 CONCLUSION

11.1 Conclusion

This study was concerned with the development of an improved rut depth model for use in the assessment of the impact of future changes in climate on road pavement maintenance need and consequently for informing decisions on appropriate adaptation strategies given the uncertainties that exist in the prediction of future climate, choice of future socio-economic scenarios, and road pavement performance. This section outlines the conclusion drawn from the findings of the study.

11.1.1 Rut Depth Model

1. Following statistical comparison of observed annual incremental rut depths derived from data collected from in-service road sections with climate data (discussed in section 5.4), it was concluded that evidence of the effects of hot dry summer recorded in 2003 was evident in the rut depth data. This is consistent with the risk of deformation of asphalt roads attributed in literature (presented in section 3.5.1) to increase in frequency and magnitude of high temperatures.
2. Comparison of the rut depth models developed using structures "with" and "without" the climate variable (discussed in section 6.8) showed that the model structure "with" the climate variable provided a better fit to the data used in the study. The inclusion of a climate variable therefore resulted in an improved rut depth model.
3. The Bayesian regression approach provides a good framework for the estimation of coefficients of the model. The estimated distribution of the model coefficients given in

section 6.5 embody uncertainties inherent in the data used. The estimated model coefficients were found to be robust to alternative assumptions of the prior distribution. Furthermore, the association of the model coefficients associated to each model variable (whether positive, negative or other) were consistent with literature as discussed in section 6.6.2.

4. The rut depth model variables that have important effects on asphalt surface rutting given the data used in the study included: traffic loading, heavy vehicle speed, asphalt thickness, material properties and maximum pavement temperature. Road section gradient had the least effect on asphalt rutting.

11.1.2 Climate Impact and Adaptation Model, Uncertainty Framework and Case Study

1. Outputs from the Climate Impact and Adaptation Model described in Chapter 8 can be presented using probability distributions. This was important for consideration of uncertainties associated with climate impact assessments.
2. Comparison of the outputs of the Climate Impact and Adaptation Model with the HDM-4 asphalt surfacing model (given in section 8.6) showed that the predictions using the Climate Impact and Adaptation model were responsive to changes in future temperature while the HDM-4 model was not.
3. Predictions based on a single iteration of the Climate Impact and Adaptation Model (Figure 10.9) resulted in outputs of cumulative rut depth that were non-linear with step-changes in rut depth deterioration trend. This reflects the uncertain nature of future climate in contrasts to predictions using the HDM-4 asphalt surfacing rut depth model which resulted in cumulative outputs that were non-linear but without any step-changes.

4. Following the case study, discounted road pavement maintenance costs attributed to climate change (presented in section 10.9) for each road maintenance strategy investigated were represented using cumulative probability plots for each 30-year period of observed and future climate. This representation of the impact of climate change on the costs of maintaining the road network provides a useful decision making framework for use by road managers and Engineers in comparing alternative road maintenance strategies for adapting to climate change based on the level of climate change risks that the organisation responsible for managing the road can tolerate.
5. It was concluded that the framework for quantification and propagation of uncertainties discussed in Chapter 9 provides a useful tool for use by road managers and Engineers in the evaluation of road pavement maintenance strategies for adapting to climate change. The framework ensures that uncertainties associated with future climate predictions, future socio-economic scenarios, components of road maintenance strategies, and road network inventory and condition data are embodied in the outputs of the analysis.

11.2 Summary of Contribution

The following are summaries of key contributions to knowledge of this study:

1. Development of an improved asphalt rut depth prediction model that includes a climate variable for considering the contribution of future climate to the progression of asphalt surface rutting.

2. Demonstrated the first use of Bayesian regression in the development of rut depth model for climate impact assessment using rut depth data collected from in-service road pavements located in the United Kingdom.
3. Developed a Microsoft Excel based tool for use in assessing the impact of climate change on asphalt road pavement maintenance and for investigating maintenance options for adapting to the impacts of climate change. Key features of the tool includes:
    - Representation of inputs for model variables using probability distributions thereby enabling uncertainties inherent in the inputs to the model to be included in the modelling process;
    - Definition of climate thresholds using temperature and precipitation anomalies;
    - Allowance for inputs for road pavement maintenance policies such as treatment types, discount rate, unit costs of treatments, maintenance intervention levels and the effects of treatments; and
    - Ability to generate probabilistic outputs through Monte-Carlo simulation.
4. Formulated a framework to guide the quantification and propagation of uncertainties inherent in future climate predictions, other inputs to the model and the coefficients of the model to the outputs of the analysis.

11.3 Future Research

Recommendations for future research are as follows:

1. The application of the tools developed in this study could be extended by implementing them in existing road management decision support systems such as the

Highway Development and Management tool (HDM-4). Such studies would need to correctly consider the interdependencies that exist between rut depths and other pavement distresses.

2. This study used data obtained from trunk road network located in the East of England. Bespoke rut depth models based on the approach used in this study could be developed for use on trunk roads located in other regions in the United Kingdom or in other countries in order to account for the spatial variability of climate, traffic and road pavement performance.
3. The current study focused on trunk roads in the United Kingdom which have thick asphalt surfacing. The approach used could be applied to develop rut depth models for local roads which may have thinner asphalt surfacing and consequently a different rut depth deterioration mechanism from trunk roads.
4. The approach used in this study could be applied in developing improved models for other types of pavement distresses such as cracking and ride quality.
5. The case study discussed in Chapter 10 was limited to the analysis of two maintenance strategies. Alternative adaptation strategies could also be investigated using the tools developed. For example, the adaptation strategy analysed in Chapter 10 assumed that the whole existing asphalt pavement would be replaced initially by a more climate resilient material. An alternative adaptation strategy could involve replacing the existing pavement sections with a more climate resilient material as and when the road condition on each section exceeds a predefined maintenance intervention threshold.

LIST OF REFERENCES

1. Allen, M. R. (2005) **The Spectre of Liability: Part 1—Attribution**. In The Finance of Climate Change: A Guide for Governments, Corporations, and Investors (K. Tang, ed.), Chapter 29, Risk Books, Haymarket, London.

2. Anyala, M., Odoki, J.B. and Baker, C. (2011). **Assessment of the Impact of Climate Change on Road Maintenance**. 2nd International Conference on Advances in Engineering and Technology (AET2011). Entebbe, Uganda.

3. Archilla, A.R. and Madanat, S. (2000) **Development of a Pavement Rutting Model from Experimental Data**, Journal of Transportation Engineering, American Society of Civil Engineers, July/August 2000, Vol. 126, No. 4, pp 291-299.

4. Archilla, A.R. and Madanat, S. (2001) **Development of Pavement Rutting Model by Combining Data from Different Experimental Sources**. Journal of Transportation Engineering. Volume 126, Issue 4.

5. Arkell, B.P. Darch, G.J.C. (2006) **Impact of Climate Change on London's Transport Network**. Proceedings of the Institution of Civil Engineers: Municipal Engineer, 159, 4, 2006, p 231-237.

6. Asphalt Institute (2003) **SP-I Performance Graded Asphalt Binder Specification and Testing**. Superpave Series No. 1. 3rd Edition.

7. Atkinson V.M., Merill D. and Thom N. (2006) **Pavement Wear Factors**. Published Project Report PPR066. TRL Limited.

8. Austroads (2004) **Impact of climate change on road infrastructure**. Austroads Publication No. AP-R243/04. Sydney: Austroads.

9. Bennett, C.R. and Paterson, W.D.O. (2000) **A guide to calibration and adaptation of HDM**. Volume 5, International Study of Highway Development and Management (ISOHDM). World Road Association (PIARC): Paris.

10. Box, G. E. P. and Cox, D. R. (1964) **An analysis of transformations**, Journal of the Royal Statistical Society, Series B, 26, 211-252.

11. Brennan M. J., Ardill O., Kavanagh A., Sheahan J., (2010) **A Comparison of the Laboratory Performance of EME2 and HDM50**. Asphalt Professional. Journal of the Institute of Asphalt Technology, Volume No. 42.

12. Brohan, P., Kennedy, J.J., Harris, I., Tett, S.F.B. and Jones, P.D., (2006) **Uncertainty Estimates in Regional and Global Observed Temperature Changes**: A New Dataset from 1850. J Geophys Res, 111, D12106.

13. BSI BS598 (1998) **Sampling and examination of bituminous mixtures for roads and other paved areas. Part 110: Methods of test for the determination of wheel tracking rate.** British Standard Institution. London.

14. Burton, I., Huq, S., Lim, B., Pilifosova, O., and Schipper, E.L., (2002) **From impacts assessment to adaptation priorities: the shaping of adaptation policy**. Climate Policy 2, 145–159.

15. Carter, T.R., Parry, M.L., Harasawa, H., Nishioka, S. (1994) **IPCC Technical Guidelines for Assessing Climate Change Impacts and Adaptations**. Part of the IPCC special report to the first session of the Conference of the Parties to the UN framework Convention on Climate Change, Department of Geography, University College London, London

16. Casella, G. and George, E. (1992) **Explaining the Gibbs sampler**. The American Statistician 46, 167-174.

17. Chaddock, B. and Pledge, K. (1994) **Accelerated and Field Curing of Bituminous Road Bases**. Project Report 87. Transport Research Laboratory. Crowthorne.

18. Climate East Midlands (2009) **NI 188 Risk Assessment Methodology**. East Midlands Planning to Adapt Project [online]. Available from: http://www.climate-

em.org.uk/images/uploads/NI_188_Risk_Assessment_Methodology_v12_110310.pdf. [Accessed on 01 April 2011].

19. Congdon, P. (2003) **Applied Bayesian Modelling**. John Wiley and Sons Limited. Chichester, England.

20. Costello, S. B., Snaith, M. S. and Kerali, H. G. R. et al. (2006) **Stochastic Model for Strategic Assessment of Road Maintenance**. Proceedings of Institution of Civil Engineers, Transport, Vol 158, Issue 4.

21. C-SHRP (1994) **Canadian Strategic Research Programme. C-SHRP Bayesian Modelling: A User's Guide** [online]. Available from: http://www.cshrp.org/products/bayesian/guide/gtoc.htm [Accessed on 27 March 2011]

22. Daines, M.E. (1992) **The Performance of Hot Rolled Asphalt Containing Crushed Rock Fines, A303 Mere**. Research Report 298. Transport Research Laboratory. Crowthorne.

23. Deighton Associates Limited (2011) **Data Sheet: Deighton's Total Infrastructure Management System (dTIMS)** [online]. Available from: http://www.deighton.com/data%20sheet%20dtims.pdf. [Accessed on 27 March 2011]

24. DelSole, T. (2007) **A Bayesian Framework for Multimodel Regression**. J. Climate, 20, 2810-2826

25. Department for Environment Food and Rural Affairs (Defra) (2009) **Adapting to climate change. UK Climate Projections** [online]. Available from: http://archive.defra.gov.uk/environment/climate/documents/interim2/climate-uk-projections.pdf. [Accessed on 10 April 2011].

26. Department for Transport (DfT) (2008) **Road Transport Forecasts for England 2008**. Results from the Department for Transport National Transport Model [online]. Available from: http://www.dft.gov.uk/pgr/economics/ntm/roadtransportforcasts08 [Accessed on 4 November 2010]

27. Department for Transport (DfT) (2009) **Road Transport Forecasts for England 2009**. Results from the Department for Transport National Transport Model [online]. Available from: http://www.dft.gov.uk/pgr/economics/ntm/forecasts2009/pdf [Accessed on 4 November 2010]

28. Department for Transport (DfT) (2010) **Climate Change Adaptation Plan for Transport**. Enhancing Resilience to Climate Change. DfT Publications, London.

29. Dessai, S. and Hulme, M. (2004) **Does climate adaptation policy need probabilities**? Climate Policy 4:107-128.

30. Dessai, S. and Van der Sluijs, J.P. (2007) **Uncertainty and Climate Change Adaptation - a Scoping Study**. Report NWS-E-2007-198, Department of Science Technology and Society, Copernicus Institute, Utrecht University. 95 pp.

31. Dft(2009) **Chapter 5 Technical Note: Road Condition and Maintenance Data**. Vehicle Licensing and Road Condition Statistics Branch, Department for Transport.

32. DMRB (TA 22/81). **Vehicle Speed Measurement on All Purpose Roads**.

33. DMRB HD 24/06 (2006) **Traffic Assessment**. Design Manual for Roads and Bridges. Volume 7, Section 2 [online]. Available from: http://www.dft.gov.uk/ha/standards/dmrb/vol7/section2/hd2406.pdf [Accessed on 10 April 2011].

34. DMRB HD26/06 (2006) **Pavement Design. Design Manual for Roads and Bridges**. Volume 7, Section 2, Part 3 [online]. Available from:

http://www.dft.gov.uk/ha/standards/dmrb/vol7/section2/ [Accessed on 20 March 2011]

35. DMRB HD29/08 (2008) **Data for Pavement Assessment**. Design Manual for Roads and Bridges. Volume 7, Section 3, Part 2 [online]. Available from: http://www.dft.gov.uk/ha/standards/dmrb/vol7/section3 [Accessed on 20 March 2011].

36. Energy Saving Trust (2011) **The Nottingham Declaration on Climate Change** [online]. Available from: http://www.energysavingtrust.org.uk/nottingham/Nottingham-Declaration/The-Declaration/About-the-Declaration. [Accessed on 01 April 2011].

37. ESRI (2009) **Arcgis version 9.3 software**. Redlands, California.

38. Fletcher, J.P., Baguley, C.J., Sexton, B. and Done, S. (2006) **Road Accident Modelling for Highway Development and Management in Developing Countries**. Trials in India and Tanzania.

39. Freeme, C. R, (1983) **Evaluation of Pavement Behaviour for Major Rehabilitation of Roads**. ITRR Technical Report RP/19/83. CSIR. South Africa.

40. Gelman, A., Carlin, J., Stem, H. and Rubin, D. (2004) **Bayesian Data Analysis**, Texts in Statistical Science, 2nd ed., Chapman & Hall, London.

41. Geman, S. and Geman, D. (1984) **Stochastic relaxation, Gibbs distributions and the Bayesian restoration of images**, IEEE Transactions on Pattern Analysis and Machine Intelligence 6,72 1-741.

42. Gilks, W., Richardson, S. and Spiegelhalter, D. (1996) **Markov Chain Monte Carlo in Practice**, Interdisciplinary Statistics, Chapman & Hall, Suffolk, UK.

43. Gillett, N. P., Zwiers F.L., Weaver, A.J., Hegerl, G.C., Allen, M.R., and Stott, P.A. (2002) **Detecting Anthropogenic Influence with a Multi-Model Ensemble**. Geophysical Research Letters, Vol. 29, No. 20, p. 1970.

44. Haas, R., Hudson, W.R. and Tighe, S. (2001) **Maximising Customer Benefits as the Ultimate Goal of Pavement Management**. National Academy Standard. 5th International Conference on Managing Pavements. Seatle Washington.

45. Haas, R., Hudson, W.R. and Zaniewski J.P. (1994) **Modern Pavement Management.** Krieger Publishing Company. Malabar, Florida.

46. Haider, S. W., Chatti, K. and Buch, N. et al. (2007) Statistical **Analysis of In-service Pavement Performance Data for LTTPP SPS-1 and SPS-2 Experiments**. Journal of Transportation Engineering-ASCE. Volume 133. Pages 378 – 388.

47. Halcrow (2005) **SCANNER Surveys for Local Roads**. Specification Volume 5. Further Technical Guidance [online]. Available from: http://www.ukpms.com/owner_forum/shared_files/Volume%205_Further%20Technical%20Guidance.PDF [Accessed on: 12 December 2010].

48. Harun M, H., and Morosuik G. (1995) **A Study of the Performance of Various Bituminous Surfacings for use on Climbing Lanes**. Proceedings of the Eighth REAA A Conference.

49. HATRIS. Highway Agency Traffic Information System [online]. Available from: http://www.hatris.co.uk/index.php. [Accessed on 02 March 2011].

50. Hegerl, G.C., Jones, P.D. and Barnett T.P. (2001) **Effect of Observational Sampling Error on the Detection and Attribution of Anthropogenic Climate Change**. Journal of Climate, Vol. 14, No. 2, pp. 198–207.

51. Hermansson, A. (2000) **A Simulation Model for the Calculation of Pavement Temperatures, including the Maximum Temperature**. Transportation Research Record 1699: 134 – 141.

52. Hermansson, A. (2001) **Mathematical Model for Calculation of Pavement Temperatures: Comparison of Calculated and Measured Temperatures**. Transportation Research Record 1764: 180 – 188.

53. Highways Agency (2007) **Annual report and accounts 2006 – 2007** [online]. Available from: http://www.highways.gov.uk/aboutus/documents/AnnualReport_2006-2007.pdf [Accessed May 20th 2008].

54. Highways Agency (2009) **Climate Change Adaptation Strategy and Framework** [online]. Available from: http://www.highways.gov.uk/aboutus/documents/CCAF-Strategy_and_Vol_1-Rev_B_Nov.pdf. [Accessed on 10 April 2011].

55. Highways Agency (2009) **Network Management Manual. Part 2: Asset Management Records**. Version 1, Amendment 8 [online]. Available from: www.dft.gov/ha/standards/nmm_rwsc/docs [Accessed on 24 March 2011].

56. HM Treasury (2003) **The Green Book**. Appraisal and Evaluation in Central Government.

57. Hong, F. and Prozzi, J. (2006) **Estimation of Pavement Performance Deterioration using Bayesian Approach**. Journal of Infrastructure Systems, Volume 12, No. 2.

58. Hong, F. and Prozzi, J.A. (2010) **Roughness Model Accounting for Heterogeneity Based on In-Service Pavement Performance Data**. Journal of Transportation Engineering. Vol. 136.

59. Hong, H. P. and Wang, S. S. (2003) Stochastic **Modelling of Pavement Performance**. International Journal of Pavement Engineering. Volume 4, Issue 4.

60. Hoque, Z., Martin, T. and Choummanivong, L. (2008) **Development of HDM-4 Road Deterioration (RD) Model Calibrations for Sealed Granular and Asphalt Roads.** Austroroads Technical Report. Project No. No. AT1064, Publication No. AP–T97/08. Sydney: Austroroads

61. Hulme, M., Jenkins, G.J. and Lu, X., et al. (2002) **Climate Change Scenarios for the United Kingdom: The UKCIP02 Scientific Report**. Tyndall Centre for Climate Change Research, School of Environmental Sciences. University of East Anglia, Norwich, England. 120 pp.

62. Hunter R, N. (1994) **Bituminous Mixtures in Road Construction**. Thomas Telford. London

63. Hunter R, N. (2000) **Asphalts in Road Construction**. Thomas Telford. London.

64. Infrastructure Canada (2006) **Adapting Infrastructure to Climate Change in Canada's Cities and Communities** [online]. Available from: http://cbtadaptation.squarespace.com/storage/CdnInfrastructureAdaptation-LiteratureReview.pdf [Accessed on 10 April 2011]

65. Intergovernmental Panel on Climate Change (2001) **Climate Change 2001: the Scientific Basis**. Summary for Policy Makers. Cambridge University Press: Cambridge.

66. IPCC (2007) **Summary for Policymakers. In Climate Change 2007: The Physical Science Basis**. Contribution of Working Group I to the Fourth Assessment Report of the Intergovernmental Panel on Climate Change (S. Solomon, D. Qin, M. Manning, Z. Chen, M. Marquis, K. B. Averyt, M. Tignor, and H. L. Miller, eds.), Cambridge University Press, Cambridge, United Kingdom, and New York.

67. Isaacson, D.L. and Madsen, R.W. (1976) **Markov chains: Theory and applications**. Wiley, New York.

68. Jiang, P.P., He, Z.Q., Kitchen, N.R. and Sudduth, K.A. (2009) **Bayesian Analysis of Within-field Variability of Corn Yield using a Spatial Hierarchical Model**. Journal of Precision Agriculture, Volume 10.

69. Karl, T. R., Hassol, S.J., Miller, C. and Murray, W. (2006) **Temperature Trends in the Lower Atmosphere: Understanding and Reconciling Differences**. U.S. Climate Change Science Program, Asheville, N.C.

70. Karoly, D. J. and Wu, Q. (2005) **Detection of Regional Surface Temperature Trends**. Journal of Climate, Vol. 18, pp. 4337–4343.

71. Kerali, H.R. (2001) **The Role of HDM-4 in Road Management**. The University of Birmingham, UK.

72. Kerali, H.R.G, Odoki, J.B. and Stannard, E.E. (2000) **Overview of HDM-4**. Volume 1, International Study of Highway Development and Management (ISOHDM). World Road Association (PIARC): Paris.

73. Li, N., Xie, W. and Haas, R. (1996) **Reliability-Based Processing of Markov Chains for Modeling Pavement Network Deterioration** . Transportation Research Record: Journal of the Transportation Research Board. Transportation Research Board of the National Academies

74. Lincolnshire County Council (2011). Potholes**: FAQs [online]**. Available from: www.lincolnshire.gov.uk/potholesFAQs. [Accessed on 10 May 2011]

75. Lloyd, S.M. and Ries, R. (2007) **Characterizing, propagating, and analyzing uncertainty in life-cycle assessment**: A survey of quantitative approaches, Journal of Industrial Ecology, 11 (1) 2007, 161-179

76. Lorraine, H. (2005) **UKCIP Costing Methodology Case Study: Highway Asset Management**. Metroeconomica Limited and Cambridgeshire County Council.

77. Lunn, D.J., Thomas, A., Best, N. and Spiegelhalter, D. (2000) **Winbugs – a Bayesian Modelling Framework: concepts, structure, and extensibility**. Statistics and Computing, 10:325 – 337.

78. Luo, Q., Jones, R.N., Williams, M., Bryan, B. and Bellotti, W. (2005) **Probabilistic distributions of regional climate change and their application in risk analysis of wheat production**. Climate Research. Vol. 29: 41–52, 2005.

79. Lytton, R. L. (1987) **Concepts of Pavement Performance Prediction and Modeling**. Proc., 2nd North American Conference on Managing Pavement,. Vol. 2.

80. MacDonald, J.H. (2009) **Handbook of Biological Statistics (2nd edition)**. Sparky House Publishing, Baltimore, Maryland.

81. Martin, T. and Hoque, Z. (2006) **Under-performing pavements, identification, classification, inspection and causes**. contact report REAT-1067, ARRB Group, Vermont South, Victoria.

82. McElvaney, J. and Snaith, M.S. (2002) **Analytical design of flexible pavements**. Highways, the location, design, construction and maintenance of pavements (Ed. C. A. O'Flaherty), Chapter 15 (Butterworth-Heine-mann, Oxford, U.K).

83. Meng, X.L. and Wong, W. (1996) **Simulating ratios of normalizing constants via a simple identity**: A theoretical exploration, Statistica Sinica 6 , 83 1-860.

84. Merrill, D., Van Dommelen, A. and Gáspár, L. (2006) **A review of practical experience throughout Europe on deterioration in fully-flexible and semi-rigid long-life pavements**. International Journal of Pavement Engineering, 1477-268X, Volume 7, Issue 2, 2006, Pages 101 – 109

85. Met Office (2009) **UKCP09: Gridded Observation Datasets** [online]. Available fromhttp://www.metoffice.gov.uk/climatechange/science/monitoring/ukcp09/index.html [Accessed 13 September 2009]

86. Metroeconomica (2004) **Costing the impacts of climate change in the UK. UKCIP Implementation Report**. UKCIP, Oxford.

87. Mills, B.N., Tighe, L. and Andrey, J. et al. (2007). **The road well travelled. Implication of climate change for pavement infrastructure in Southern Canada**. Final technical report.

88. Morosuik, G., Riley, M. and Odoki, J.B. (2004) **Modelling Road Deterioration and Works Effects**. Highway Development and Management. HDM-4 Series of Publications. Volume 6. World Bank, Washington DC, and PIARC, Paris, France.

89. Mott MacDonald (2006) **Using SCANNER Data for Maintenance Management on Local Roads**. Part 1 – Final Project Report, PPAD 9/100/92.

90. Murphy, J. M., Sexton, D. M. H. and Jenkins, G. J., et al., (2009) **UK Climate Projections Science Report: Climate change projections**. Met Office Hadley Centre, Exeter, UK.

91. National Research Council (2008) **Potential Impacts of Climate Change on U.S. Transportation**. Transportation Research Board Special Report 290.

92. NDLI (1995) **Modelling Road Deterioration and Maintenance Effects in HDM-4**. Final Report: Asian Development Bank Project RETA 5549. N.L. Lea International, Vancouver.

93. Nicholls, C. (1998) **Asphalt Surfacings**. A Guide to Asphalt Surfacings and Treatments Used for the Surface Course of Road Pavements. E&FN Spon, London.

94. Nicholls, J. C. and Carswell, I. (2004) **Durability of Thin Asphalt Surfacing Systems. Part 2: Findings after Three Years Monitoring**. TRL Report TRL606. Transport Research Laboratory. Crowthorne.

95. Nicholls, J. C., Carswell, I. and Langdale P, C. (2002) **Durability of Thin Asphalt Surfacing Systems. Part 1: Initial Findings**. TRL Report TRL557. Transport Research Laboratory. Crowthorne.

96. Nicholls, J. C., Carswell, I., Thomas C. and Walter L, K. (2007) **Durability of Thin Asphalt Surfacing Systems. Part 3: Findings after Six Years Monitoring**. TRL Report TRL660. Transport Research Laboratory. Crowthorne.

97. Ntzoufras, I. (2009) **Bayesian modelling Using WinBUGS**. John Wiley and Sons: Hoboken, New Jersey.

98. Nunn M, E., Brown A., Weston D. and Nicholls, J. C. (1997) **Design of Long-Life Flexible Pavements for Heavy Traffic. TRL Report 250**. Transport Research Laboratory. Crowthorne.

99. Odoki, J.B. and Kerali, H.R.G. (2000) **Analytical Framework and Model Descriptions. Highway Development and Management. HDM-4 Series of Publications**. Volume 4. World Bank, Washington DC, and PIARC, Paris, France.

100. Odoki, J.B., Stannard, E.E., Ourad, A. and Koranteng-Yorke, B. (2006) Development of HDM-4 at a Strategic Level for the Department for Transport, UK. **HDM-4 Configuration and Calibration**. The University of Birmingham, UK.

101. Ortiz-Garcia, J., Costello, S.B., Snaith, M.S. (2006) **Derivation of Transition Probability Matrices for Pavement Deterioration Modelling**. Journal of Transportation Engineering. Volume 132.

102. Osborne, J.W. (2010) **Improving your Data Transformations: Applying the Box – Cox transformation**. Practical Assessment, Research and Evaluation. Volume 15, Number 12.

103. Parry, M.L. and Carter, T.R. (1998) **Climate Impact and Adaptation Assessment**: A Guide to the IPCC Approach. Earthscan, London.

104. Paté-Cornell, M.E. (1996) **Uncertainties in risk analysis: six levels of treatment**. Reliability Engineering and System Safety 54, 95–111.

105. Paterson, W.D.O. (1987) **Road Deterioration and Maintenance Effects Models for Planning and Management**. The International Bank for Reconstruction and Development. Washington DC, USA.

106. Perry, M. C. and Hollis, D. M. (2005) **The generation of monthly gridded datasets for a range of climatic variables over the UK**. International Journal of Climatology 25: 1041 - 1054.

107. Pittock, A.B., Jones, R.N. and Mitchell, C.D. (2001) **Probabilities will help us plan for climate change**. Nature 413, 249. Pulwarty, R.S., Melis, T.S., 2001. Climate extremes and adaptive management on the Colorado River: lessons from the 1997–1998 ENSO event. Journal of Environmental Management 63, 307–324.

108. Powell, W.D., Potter, J.F., Mayhew, H.C. and Nunn, M.E. (1984) **The Structural Design of Bituminous Roads (LR1132)**. Transport Research Laboratory, Crowthorne Berkshire, UK.

109. Prozzi, J. and Madanat, S. (2000) **Analysis of Experimental Pavement Failure Data using Stochastic Duration Models**. Transportation Research Record 1699. Transportation Research Board. National Research Council, Washington, D.C.

110. Prozzi, J.A. and Madanat, S. (2001) **Nonlinear Model for Predicting Pavement Performance Before and After Rehabilitation**. Proceedings of the Second

International Symposium on Maintenance and Rehabilitation of Pavements and Technological Control, Auburn, AL.

111. Prozzi, J.A. and Madanat, S. (2004) **Development of Pavement Performance Models by Combining Experimental and Field Data**. Journal of Infrastructure Systems, American Society of Civil Engineers, Vol. 10, No. 1, pp. 9-22.

112. Read J. and Whiteoak, D. (2003) **The Shell Bitumen Handbook**. Fifth Edition. Thomas Telford. London.

113. Robinson, R. (1985). A **Model for Calculating Pavement Temperature from Metereological Data**. Transport and Road Research Laboratory, Crowthorne, Berkshire.

114. Robinson, R. and Thagesen, N. (2004) **Road Engineering for Development**. London: Spoon Press.

115. Robinson, R., Danielson, U. and Snaith, M.S. (1998) **Road Maintenance Management: Concepts and systems**. Macmillan Publishers Limited: Basingstoke, Hamshire.

116. Sanders, P. J. and Nunn, M. (2005) **The Application of Enrobe a Module Eleve in Felxible Pavements**. TRL Report 636. TRL Limited.

117. Scottish Executive (2005) **Scottish Road Network Climate Change Study** [online]. Available from: http://www.scotland.gov.uk/Publications/2005/06/13103859/39009 [Accessed on 31 March 2011]

118. Seyedshohadaie, R., Damnjanovic, I. and Butenko, S. (2010) **Risk-based Maintenance and Rehabilitation Decisions for Transportation Infrastructure Networks**. Transportation Research Part A: Policy and Practice. Volume 44, Issue 4.

119. Smith, A. and Roberts, G. (1993) **Bayesian computation via the Gibbs sampler and related Markov chain Monte Carlo methods**. Journal of the Royal Statistical Society B **55,** 3-23.

120. Smith, D. (2011) **Pavements Model: Work Package 3.** A Report for the Highways Agency. WiLCO Model Build. Seams Limited.

121. Solaimanian, M. and Kennedy T.W. (1993) **Predicting Maximum Pavement Surface Temperature Using Maximum Air Temperature and Hourly Solar Radiation**. Transportation Research record 1417: 1 – 11.

122. Solomon, S., Qin, D. and Manning, et al. (2007) **Climate change 2007: The physical sciences basis**: Contribution of Working Group I to the Fourth Assessment Report of the Intergovernmental Panel on Climate Change. Cambridge University Press, Cambridge, UK.

123. Sousa, J.B., Craus, J. and Monismith, C.L. (1991). **Summary Report o Permanent Deformation in Asphalt Concrete**. SHRP – A/IR – 91 – 104. National Research Council.

124. Spiegelhalter, D., Thomas, A., Best, N. and Lunn, D. (2003). **WinBUGS user Manual**. Version 1.4.

125. Stone, D. A. and Allen, M.R. (2005) **Attribution of Global Surface Warming Without Dynamical Models**. Geophysical Research Letters, Vol. 32, No. 18, L18711.

126. Stott, P. A., Tett, S.F.B., Jones, G.S., Allen, M.R., Ingram, W.J. and Mitchell, J.F.B. (2001) **Attribution of Twentieth Century Temperature Change to Natural and Anthropogenic Causes**. Climate Dynamics, Vol. 17, pp. 1–21.

127. Stott, P.A., Tett, S.F.B., Jones, G.S., Allen, M.R., Mitchell, J.F.B. and Jenkins, G.J., (2000) **External Control of Twentieth Century Temperature by Natural and Anthropogenic Forcing**. Science, 15, 2133-2137.

128. Tett, S. F. B., Jones, G.S. and, Stott, P.A., et al. (2002) **Estimation of Natural and Anthropogenic Contributions to Twentieth Century Temperature Change**. Journal of Geophysical Research, Vol. 107, No. D16, 4306.

129. The National Archives (2008) **Climate Change Act 2008** [online]. Accessed from: http://www.legislation.gov.uk/ukpga/2008/27 [Accessed on 31 March 2011].

130. Transport Research Laboratory (TRL) (1993) **Overseas Road Note 31. A Guide to the Structural Design of Bitumen-Surfaced Roads in Tropical and Sub-tropical Countries**. Overseas Centre. TRL, Crowthorne, Berkshire.

131. Transport Scotland (2008) **Work Package 6: Lifecycle Planning Analytical Framework and Model Description. Asset Management Improvement Programme**. Project Report Produced by Atkins.

132. TRL (1998) **Overseas Road Note 15**. Guideline for the Design and Operations of Road Management Systems. Transport Research Laboratory. Crowthorne, Berkshire.

133. UK Climate Impacts Programme (UKCIP) (2000) **Socio-economic Scenarios for Climate Change Impact Assessment**: A Guide to their use in the UK Climate Impacts Programme. UKCIP, Oxford.

134. UKCIP (2009) UK **Climate Projections User Interface** [online]. Available from: http://ukclimateprojections-ui.defra.gov.uk/ui/admin/login.php [Accessed on: 12 January 2011]

135. US Department of Transportation (2011) **Long-Term Pavement Performance Program. Accomplishments and Benefits 1989 – 2009**. Federal Highways Administration.

136. Weston, D.J., Nunn, M.E. and Brown, A.J. et al. (2001). **Development of a Performance-based Surfacing Specification for High Performance Asphalt Pavements**. TRL Report 456, Crowthorne: TRL.

137. Willows, R.I. and R.K. Connell, eds. (2003) **Climate adaptation: Risk, uncertainty and decision-making**. UKCIP Technical Report. Oxford : UKCIP.

138. Willway T., Reeves S. and Baldachin L. (2008) **Maintaining Pavements in a Changing Climate**. A Study Commissioned by the Department for Transport. Transport Research Laboratory.

139. Yang, J., Lu, J. J., Dietrich, B. (2006) **Modelling Crack Deterioration of Flexible Pavements: Comparison of Recurrent Markov Chains and Artificial Neural Networks**. Transportation Research Record: Journal of the Transportation Research Board. Volume 1974.

140. Zhang, X., Zwiersm F.W. and Stott. P.A. (2006) **Multi-Model Multi-Signal Climate Change Detection at Regional Scale**. Journal of Climate, Vol. 19, pp. 4294–4307.

141. Zwiers, F.W. and Zhang, X. (2003) **Toward Regional Scale Climate Change Detection**. Journal of Climate, Vol. 16, pp. 793–797.

BIBLIOGRAPHY

1. Attoh-Okine, N.O. (2005). **Modelling Incremental Pavement Roughness Using Functional Network**. Canadian Journal of Civil Engineering, Volume 32, No. 5, Pages 899 – 905. NRC Research Press.

2. Bennet, C.R. and Greenwoood, I.D. (2003) **Highway management and development, Volume 7**: Modelling road user and environmental effects in HDM-4.

3. Black, W.P.M. and Lister, N.W. (1979) **The strength of clay fill subgrades: its prediction in relation to road performance**. Department of the Environment Department of Transoport, TRRL Report LR 889. Crowthorne.

4. Cambridgeshire County Council (2004). **Highway maintenance network management policies and standards.** [online] http://www.cambridgeshire.gov.uk/NR/rdonlyres/813B089E-824C-4C3E-9C1F-37AA58954125/0/nmsp.pdf [Accessed March 20th 2008].

5. Darter, M.I. and Hudson, W.R. (1973) **Probabilistic Design Concepts Applied to Flexible Pavement System Design**. Austin Texas: Centre for Highway Research.

6. Department for Transport (2005) **The changing climate: its impact on the Department for Transport** [online]. http://www.dft.gov.uk/pgr/scienceresearch/key/ [Accessed May 19th 2008].

7. Department for Transport (2007) **Further Guidance for Surveys for BV223 and BV224 (a) in 2007/08**. [online] http://www.dft.gov.uk/pgr/roads/network/local/servicelevels/surveysbv223224a [Accessed April 5th 2008].

8. HD29/94 (2001) **Design manual for roads and bridges. Structural assessment method. Volume 7, Part 2.** [online]. http://www.standardsforhighways.co.uk/dmrb/vol7/section3/hd2994.pdf [Accessed March 8th 2008]

9. Interim Advice Note 42/05 (2005) **Traffic-speed condition surveys (TRACS): Revised assessment criteria**. Highways Agency, England.

10. Interim Advice Note 73/06 (2006) **Design guidance for road pavement foundations. Highways Agency**, England.

11. Kandhal, P. S. And Rickards, I. J. (2001) Premature failure of asphalt overlays from stripping: Case histories**. Paper presented at the annual meeting of the Association of Asphalt Paving Technologiest held in Clear Water, Florida**. National Center for Asphalt Technology. Auburn University, Alabama.

12. Kerali, H. R., Lawrance, A. J. and Awad, K. R. (1996) **Data Analysis Procedures for Long-Term Pavement Performance Prediction**. Transportation Research Record: Journal of the Transportation Research Board. Volume 1524. Transportation Research Board of National Academies

13. Kilsby, C.G., Jones, P.D., Burton, A., ford, A.C., Fowler, H.J., Harpham, C., James, P., Smith, A. and Wilby, R.L. (2007) **A daily weather generator for use in climate change studies**. Environmental modelling and software, 22, 1705-1719.

14. Kinsella Y. and Mcguire F. (2005) **Climate change uncertainty and the state highway network: a moving target**. New Zealand Institute of Highway Technology and Transit New Zealand Symposium: Wellignton, New Zealand.

15. Martin slavik and Strauss, P. (2006). **Quantifying uncertainty in road pavement design by simulation**. Proceedings of the 25th Southern African Transport Conference (SATC 2006).

16. Mcrobbie S, Wright M.A. and Willet M. (2002) **The effect of Road Geometry on the interpretation of Longitudinal Profile**. TRL Published Report PR/CSN/08/02.

17. Odoki J.B., Stannard E.E., Ourad A. and Koranteng-Yorke, B. (2006) **Development of HDM-4 at a strategic level of the Department for Transport, UK**. HDM-4

configuration and calibration. Draft final report. Part 3: The University of Birmingham.

18. Published Document (PD) 6692 (2006) **Asphalt - Guidance on the use of BS EN 12697 bituminous mixtures**. British standards institute.

19. Senzoz, B. and Agar, E. (2007) **Effect of asphalt film thickness on the moisture sensitivity characteristics of hot-mix asphalt**. Journal of Building and Environment. Vol 42, Pages 3621 – 3628.d

20. Shaw, R., Colley, M., and Connell, R. (2007) **Climate change adaptation by design:a guide for sustainable communities**. TCPA, London

21. Tsunokawa, K. and Ul-Islam, R. (2007) Pitfalls of HDM-4 strategy analysis. **International Journal of pavement Engineering**. Vol. 8 No. 1 Page 67 – 77.

22. UK Roads board (2007) **SCANNER surveys for local roads. Draft user guided and specification** volume 1. Introduction to SCANNER surveys.

APPENDIX A PEER REVIEWED PAPER

This appendix includes a copy of the following peer reviewed paper:

Anyala, M., Odoki, J.B. and Baker, C. (2011). **Assessment of the Impact of Climate Change on Road Maintenance**. 2nd International Conference on Advances in Engineering and Technology (AET2011). Entebbe, Uganda.

AET2011(066)
Assessment of the Impact of Climate Change on Road Maintenance

Michael Anyala[1], Jennaro B Odoki[2], Chris Baker[3]

[1]PhD Reasearch Student, Department of Civil Engineering, University of Birmingham UK, B15 2TT.
Corresponding author email: mxa361@bham.ac.uk
[2]Senior Lecturer, Department of Civil Engineering, University of Birmingham UK, B15 2TT
[3]Professor of Environmental Fluid Mechanics, Department of Civil Engineering, University of Birmingham UK, B15 2TT.

ABSTRACT

Climate affects road deterioration, vehicle operating costs, road safety and the environment. Current and past pavement design guides and engineering models assume a static climate whose variability can be determined from past data. This fixed climate assumptions is often used in road management decision support models such as the Highway Development and Management system (HDM-4) to simulate future behaviour of road sections and consequently inform long-term road maintenance strategies and policies. Contrary to the assumption of a static climate in road management approaches, observations over the last 40 or 50 years show increasing trend in global warming. This raises the possibility that the severity and frequency of pavement defects may be altered leading to premature pavement deterioration and increased costs of managing and using roads. As a consequence, current road management strategies and policies may not offer sufficient resilience to increased frequency of future extreme climate events. A study was undertaken at the University of Birmingham to develop improved deterioration model for asphalt rut depth prediction. The approach used entailed the application of Bayesian Monte Carlo analysis. The output of the study will be used to improve existing road management systems such as HDM-4 and to consequently facilitate the investigation of strategies for adapting to future changes in climate.

Keywords: Deterioration Models, Rut Depth, Climate Change, HDM-4, Bayesian Models

1.0 INTRODUCTION

Pavement deterioration prediction models used to simulate the initiation and progression of key defects such as rutting and cracking are important components of road decision support systems such as the World Bank's Highway Development and Management System (HDM-4). Such systems are used by road authorities and general practitioners at the planning, programming and project levels of road management to investigate road improvement and maintenance policies, develop work programmes under budget constraints, compare road improvement and maintenance alternatives, evaluate appropriate standards for various classes of roads, and to determine the implication of marginal increase or decrease in funding levels on the road authority as well as road users. An important requirement of these models is that they must correctly consider all important factors that have significant impacts on pavement deterioration including but not limited to, traffic loading, road geometry, pavement material properties, and climate (Paterson, 1987). Climate and consequently climate change affects road deterioration, vehicle operating costs, road safety and the environment. There is a concern that the structure and model coefficients of existing deterioration models such as that implemented in HDM-4 do not properly account for predicted change in climate. This study is focused on asphalt rut depth deterioration prediction.

2.0 THE PROBLEM

The structure of current and past pavement deterioration models assume a static climate whose variability can be determined from past data over often not more than 30 years. This static climate assumption is often used as inputs into road management decision support models to simulate the long-term performance of road systems. The recently observed hot and dry summer of 2003 caused significant damage to road systems in the United Kingdom. Figure 1 shows plots of annual rates of rutting observed on trunk road sections located in East England against maximum summer temperatures in each road section by year from 2002 to 2005. Higher rates of rutting were observed in 2003 compared to other years. A similar trend to that shown in Figure 1 could not be replicated when other climate variables such as rainfall intensity and the number of days with snow lying were used instead of maximum summer temperature.

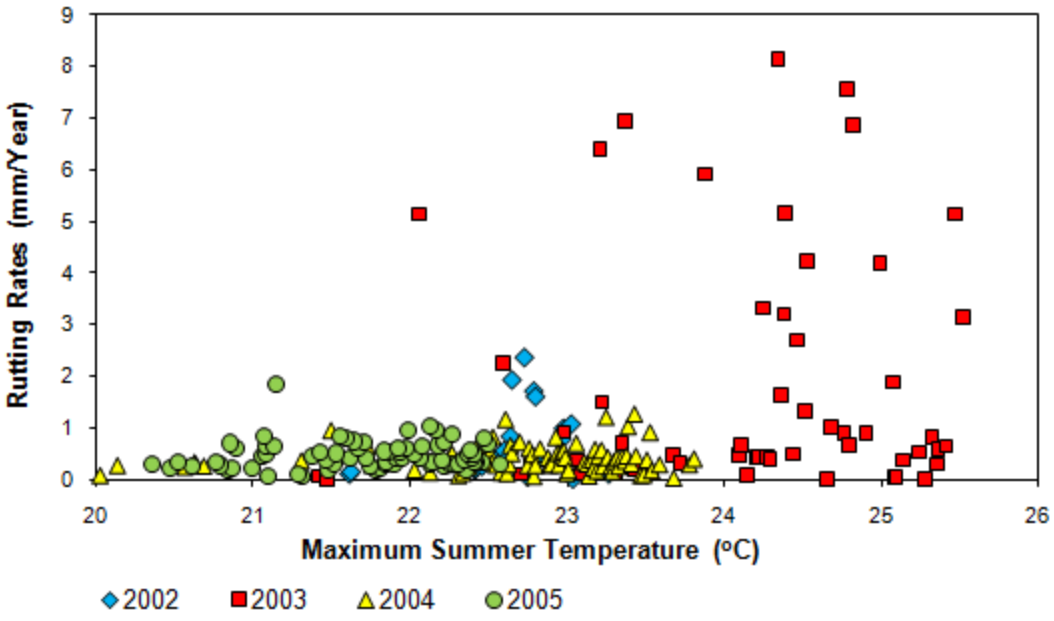

Figure 1: Annual Rutting and Corresponding Summer Temperature for Each Road Sections on Trunk Roads in East of England

According to information from the UK Climate Impacts Programme, in the East of England 5 percent of the years within the baseline period (1960 – 1990) had a 2003-type hot dry summer. The frequency of this climate event is predicted to significantly increase as summarised in Table 1. Table 1 summarises the predicted frequency of 2003-type hot dry summers in East England over 30 year periods or time for three green house gas emission scenarios. This raises the possibility that the severity and frequency of pavement defects and in particular asphalt rut depths on trunk roads in the UK may be altered leading to premature pavement deterioration and increased costs of managing and using roads. Road maintenance policies derived using deterioration prediction models or methodologies that assume a static climate and do not properly take into account other causes of deterioration are likely to underestimate the risks of increased frequency and severity of impacts associated future climate.

Table 1: Observed and Predicted Frequency of 2003-Type Hot and Dry Summers in East England

Time Slice	Green House Gas Emission Scenario	Percentage of 2003-type Summers
Baseline (1960 - 1990)	-	5
2020s [2011 - 2040]	Low	14
	Medium	15
	High	16
2050s [2041 - 2070]	Low	24
	Medium	30
	High	38
2080s [2071 - 2100]	Low	34
	Medium	49
	High	67

Source (UK Climate Impacts Programme)

3.0 MODEL STRUCTURE

A study by Nunn et al. (1997), found that rutting on UK asphalt trunk roads is restricted to the top 100mm of the asphalt layer. This finding suggests that the problem of pavement deformation on UK asphalt trunk roads is that of surface deformation rather than structural deformation. The model structure adopted therefore considers variables that are deemed important for the performance of the pavement asphalt surfacing layers. A multiplicative model structure was used because the effects of variables that contribute to rut depth progression such as traffic loading, climate, and properties of asphalt surfacing materials is synergetic.

3.1 Existing Model Structure

The existing model structure given in Equation 1 is that implemented in the Highway Development and Management system (HDM-4).

$$\Delta \mathrm{RUT}_{\mathrm{mt}} = \alpha_0 \times \mathrm{CDS}_{\mathrm{m}}^{\alpha_1} \times \mathrm{YE4}_{\mathrm{mt}} \times \mathrm{Sh}_{\mathrm{mt}}^{\alpha_2} \times \mathrm{HS}_{\mathrm{m}}{}^{\alpha_3} \quad (1)$$

Where $\Delta \mathrm{RUT}_{\mathrm{mt}}$ is the annual incremental change in plastic deformation within the asphalt layers of the pavement, in mm for road sections with surfacing material *m* during time period *t*; CDS_m is a continuous variable ranging in value between 0.5 and 1.5 and used as an indicator of the general level of binder content and stiffness relative to the optimal material design for specified asphalt surfacing mixes. $YE4_{mt}$ is the annual number of equivalent standard axles, in millions/lane on sections with surfacing material *m* during time period *t*; Sh_{mt} is the average speed of heavy vehicles on sections

with surfacing material *m*, in km/h during period *t*; HS_m is thickness of bituminous layer on sections with surfacing *m*, in mm; and α_0 to α_3 are model coefficients given in Morosuik et al. (2001).

This model structure (Equation 1) does not include climate variables necessary for accounting for the impacts of future extreme climate events such as the 2003-type summers.

3.2 Improved Model Structure

The Improved model structure inlcudes additional variables deemed important for prediction of asphalt surface rutting that were not properly accounted for in the existing model structure. These additional variables inlcude road Gradient (G), asphalt binder Softening Point (SP), asphalt surfacing Voids in Mix (VIM), asphalt surfacing age (AGE) and climate variable $f(\mathrm{Cmax}_{\mathrm{imt}})$. The improved model structure is given in Equation 2.

$$\Delta \mathrm{RUT}_{\mathrm{imt}} = \mathrm{YE4}_{\mathrm{imt}}^{\beta_{1\mathrm{m}}} \times \mathrm{Sh}_{\mathrm{im}}^{\beta_{2m}} \times \mathrm{G}_{\mathrm{im}}^{\beta_{3\mathrm{m}}} \times \mathrm{HS}_{\mathrm{imt}}^{\beta_{4\mathrm{m}}} \times \left(\frac{\mathrm{SP}_{\mathrm{im}}}{\mathrm{VIM}_{\mathrm{im}}} \times \left(\mathrm{AGE}_{\mathrm{imt}} + 1^{-4} \right) \right)_{imt}^{\beta_{5\mathrm{m}}} \times f(\mathrm{Cmax}_{\mathrm{imt}}) \qquad (2)$$

Where $\mathrm{SP}_{\mathrm{im}}$ is the initial softening point of the asphalt binder of road section i for material type m, $\mathrm{VIM}_{\mathrm{im}}$ is the Voids in Mix for road section i with asphalt surfacing material m. $\mathrm{AGE}_{\mathrm{imt}}$ is the age of the most recent surfacing material on road section i with material type i during year t. The number $1\mathrm{x}10^{-4}$ is used to avoid numerical overflow.

The multiplicative function $f(\mathrm{Cmax}_{\mathrm{imt}})$ given in Equation 3 is a function of hot dry climate variable such as maximum summer temperature at road section i with material type m and during time period t derived from 5km gridded climate dataset for England.

$$f(\mathrm{Cmax}_{\mathrm{imt}}) = \left(1 + \left(\frac{\theta_{1m}}{1 + \exp(\theta_{2m} + \theta_{3m} \mathrm{Cmax}_{\mathrm{imt}})} \right) \times \mathrm{T}_{\mathrm{HOLD}} \right) \qquad (3)$$

The function is assumed logistic in nature and is formulated to simulate the increase in rut depth during 2003-type hot dry summer climate scenario. It is expected that at low air temperature rutting is mainly governed by the compaction effect of traffic loading on the pavement asphalt material using Equation 2. As temperature in combination with other factors increases, the asphalt in the mix becomes less viscous resulting in increased rates of rutting and Equation 2 would be adjusted using the logistic component in Equation 3. After the hot period, it is assumed that the bituminous mix will not change significantly hence Equation 2 would still be applicable.

A parameter $\mathrm{T}_{\mathrm{HOLD}}$ that takes binary numbers of 1 or 0 was adopted as an "on/off" switch for the logistic function given in Equation 3. $\mathrm{T}_{\mathrm{HOLD}}$ is assigned a value of 1 during hot dry summer years and a value of 0 otherwise. The completed improved asphalt surface rutting model is given in Equation 4.

$$\Delta \mathrm{RUT}_{\mathrm{imt}} = \mathrm{YE4}_{\mathrm{imt}}^{\beta_{1\mathrm{m}}} \times \mathrm{Sh}_{\mathrm{im}}^{\beta_{2m}} \times \mathrm{G}_{\mathrm{im}}^{\beta_{3\mathrm{m}}} \times \mathrm{HS}_{\mathrm{imt}}^{\beta_{4\mathrm{m}}} \times \left(\frac{\mathrm{SP}_{\mathrm{im}}}{\mathrm{VIM}_{\mathrm{im}}} \times \mathrm{AGE}_{\mathrm{imt}} \right)_{imt}^{\beta_{5\mathrm{m}}} \times \left(1 + \left(\frac{\theta_{1m}}{1 + \exp(\theta_{2m} + \theta_{3m} \mathrm{Cmax}_{\mathrm{imt}})} \right) \times \mathrm{T}_{\mathrm{HOLD}} \right) + \varepsilon_{\mathrm{imt}} \qquad (4)$$

Where ε_{imt} is the error term; β_{1m} to β_{5m}, and θ_{1m} to θ_{3m} are model coefficients to be estimated for each surfacing material type.

4.0 BAYESIAN ESTIMATION OF MODEL COEFFICIENTS

Bayesian inference combines information from observed data with prior knowledge about the model coefficients (referred to as priors) to give updated distribution of the model coefficients (referred to as posterior), which is described using Bayes theory as:

$$p(\beta, \theta/X, \Delta RUT) = \frac{p(X, \Delta RUT/\beta, \theta)p(\beta, \theta)}{\int p(X, \Delta RUT/\beta, \theta)P(\beta, \theta)d(\beta, \theta)} \quad (5)$$

$P(\beta, \theta/ X, \Delta RUT)$ = posterior distribution of elements of the vector β or θ given observed data including explanatory or independent variables (X) and dependent variables (ΔRUT); $P(X, \Delta RUT/ \beta, \theta)$ = the likelihood of the observed data given the model coefficients β or θ; and, $P(\beta, \theta)$ = prior distribution of the model coefficients sets of β and θ.

The main difference between estimation of model coefficients using ordinary least square and Bayesian approach is that the latter associates a probability distribution with model coefficients β and θ. This probability distribution known as *prior* distribution $p(\beta)$ or $p(\theta)$ quantifies uncertainties in model parameters before data becomes available (Desole, 2007).

4.1 Definition of Prior Probabilities

The prior distribution of the model coefficients were assumed to be normally distributed with mean μ and precision τ which can be denoted as $N(\mu,\tau)$. The precision τ is defined as the reciprocal of the variance. The means μ of the prior distribution were largely based on the existing model coefficients specified in HDM-4 documentation (Morosuik et al, 2001). Non-informative or vague priors with mean of 0 and precision of 0.001 were assumed for model coefficients of additional variables included in the improved model structure. The assumed prior distribution is given in Table 2.

Table 2: Summary of Prior Distribution of Model Coefficients

Variables	Model Coefficients	Prior Distribution	Data Source
Traffic Loading (YE4)	β_1	N(1, 0.001)	Morosuik (et al., 2001)
Heavy Vehicle Speed (Sh)	β_2	N(-0.78, 0.001)	Morosuik (et al., 2001)
Road Gradient (G)	β_3	N(0, 0.001)	Vague prior
Asphalt Surfacing Thickness (HS)	β_4	N(0.71, 0.001)	Morosuik (et al., 2001)
Asphalt Surfacing Properties (SP*AGE/VIM)	β_5	N(0, 0.001)	Vague prior
Climate Variables	θ_1, θ_2, θ_3	N(0, 0.001)	Vague prior

4.2 Likelihood Specification

In Bayesian analysis likelihood specification refers to the assumption of the underlying distribution of the observed response variable. The observed incremental rut depth data which was assumed to be independent and identically distributed was stochastically represented as

$$\Delta \mathrm{RUT}_{\mathrm{imt}} \sim N[W(x)]$$

Where W(x) is a deterministic function given in Equation 4 comprising explanatory variables and model coefficients. N is the underlying statistical distribution of the data which was assumed to be normally distributed.

4.3 Estimation of Model Coefficients

The Windows version of Bayesian Updating using Gibbs Sampler (WinBUGS) was used to derive the marginal distribution of the model coefficients. The marginal distributions were achieved after a large number of iterations and when the Markov chain converges to a target distribution. The convergence is required for the sampled value to represent a random draw from the marginal distribution. This was achieved by simultaneously running three Markov chains. The first 10,000 iterations of each chain deemed to include the random draws before convergence or "burn-in" were discarded. Convergence was considered achieved when the traces of the chains were found to be overlapping. The estimated model coefficients are presented in the next section.

4.4 Estimated Model Coefficients

Model coefficients were estimated for asphalt road sections with Dense Bituminous Macadam surfacing. The estimated posterior distribution of the model coefficients are presented in Figure 3. Model variables such as traffic loading, vehicle speed, and hot dry climate with posterior model coefficients clustered away from zero are considered important for the prediction of annual incremental rut depth. Variables with coefficients scattered around zero are less important. In addition the sign (negative or positive) associated with the mean values of the estimated model coefficients given in Figure 3 are consistent with theory. For example the mean model coefficient for traffic loading ($\beta 1$) has a positive association which is consistent with the fact that as traffic loading increases asphalt surface rutting is expected to increase. Similarly the model coefficient for heavy vehicle speed ($\beta 2$) has a negative association which suggests that as heavy vehicle speeds decreases the asphalt surfacing is expected to become more susceptible to rutting due to increased stresses associated with increased heavy loading time on the road pavement.

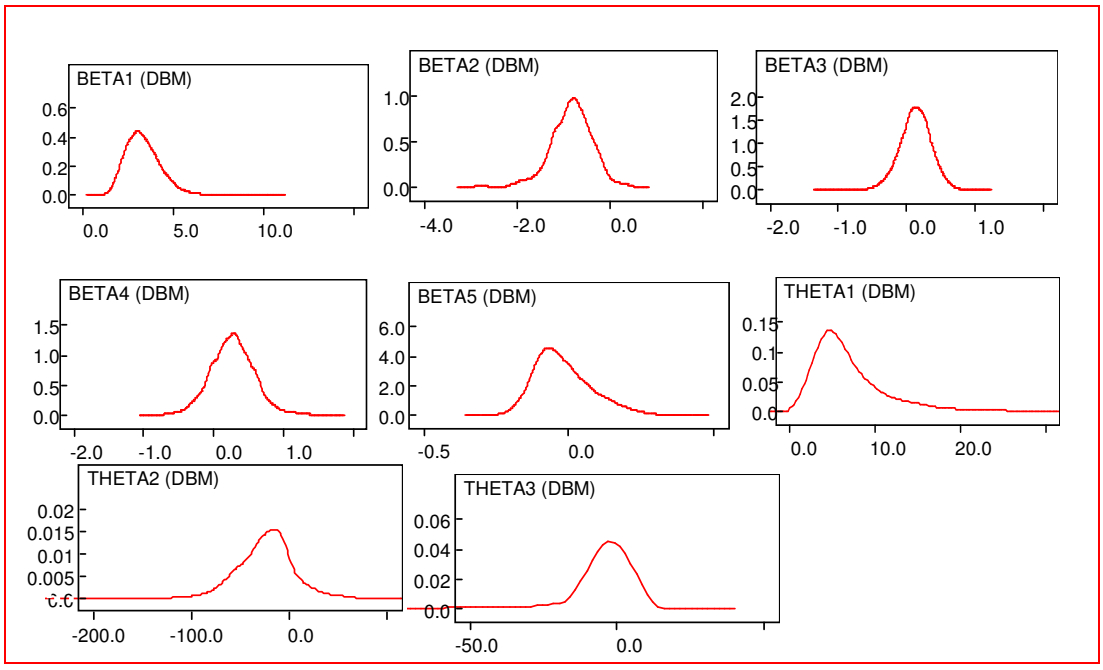

Figure 3: Posterior Distribution of Model Coefficients

5.0 CASE STUDY

A case study was undertaken using data obtained from the UK Highways Agency and the UK Climate Impacts Programme. Climate predictions used in the case study was provided for the low, medium and high green house gas emission scenarios. For each of these emission scenarios future climate data was available in the form of probability distributions for four 30 year time slices denoted as 2020s (2011 to 2040), 2030s (2021 to 2050), 2040s (2031 to 2060) and 2050s (2041 to 2070). The results reported in this paper are for the medium emission scenario only.

The following approach was followed:

1. For the analysis year t =1 deterministic input variables comprising traffic loading, heavy vehicle speeds, and road gradient, asphalt material surfacing and material properties were defined in bespoke prototype model.
2. During the analysis year t = 1 a set of stochastic input variables n=1 comprising model coefficients given in Figure 3 and climate data were randomly sampled.
3. The annual incremental rut depth for year t=1 and the set of stochastic random samples n=1 was calculated using Equation 4. This step is repeated for 5000 sets of stochastic random variables.
4. Steps 1 to 3 were repeated for each year t=2 to 30 for each time slice for which climate data was available.

The output of the analysis was a distribution of incremental rut depths in each year. The mean predicted cumulative rut depths for the four time slices are given in Figure 4. The results of the case study suggest that the future prediction of rut depths is highly sensitive to future climate predictions.

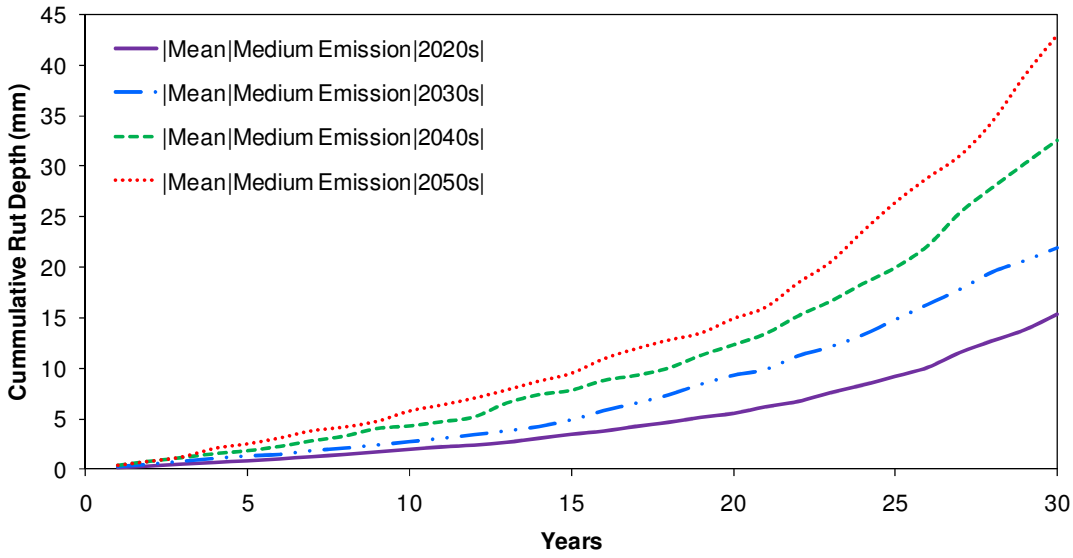

Figure 4: Mean Cumulative Rut Depth Prediction for Medium Emission Scenario for four Time Slices

6.0 CONCLUSION

This study has demonstrated the need for pavement deterioration models used in decision support systems such as HDM-4 to be improved to allow the impact of future climate events to be accounted for in road performance modelling. Model coefficients for an improved rut depth prediction model were estimated using a Bayesian approach. The approach associates probability distribution to estimated model coefficients thereby ensuring that uncertainties inherent in the observed data are reflected in the predicted model coefficients. The study methodology can be applied in any climatic zone or country provided appropriate data are available. Work is continuing towards linking the developed model with HDM-4 decision support tool. This will provide authorities and general practitioners with the capabilities to investigate the impact of various future climate scenarios on road agency as well as road user costs thereby facilitating improved choices necessary to adapt to the inevitable impacts of climate change.

1.6 REFERENCES

DelSole, T., 2007: *A Bayesian Framework for Multimodel Regression*. J. Climate, 20, 2810-2826. (Boston: American Meteorological Society).

Morosuik, G., Riley, M and Odoki, J.B (2001). *Modelling Road Deterioration and Works Effects*. Highway Development and Management. HDM-4 Series of Publications. Volume 6. (World Bank, Washington DC, and PIARC, Paris, France).

Nunn, M.E., Brown, A., Weston, D. And Nicholls, J.C. (1997) *Design of long-life flexible pavements for heavy traffic*. TRL report 250. (Crowthorne, Berkshire: The Transport Research Laboratory).

Paterson W.D.O (1987). *Road Deterioration and Maintenance Effects. Models for Planning and Management*. The Johns Hopkins University Press Baltimore and London

APPENDIX B DATA SUMMARY

This appendix includes the following:

Appendix B1	Rut Depth GIS Maps
Appendix B2	Rut Depth Sample Summary Statistics by Study Road
Appendix B3	Summary of Climate Data by Year
Appendix B4	Maps of Annual Heavy Vehicle Speed
Appendix B5	Transformed Heavy Vehicle Speeds Data
Appendix B6	Summary of Annual Equivalent Standard Axle Load
Appendix B7	Asphalt Material Properties Data
Appendix B8	Calculations for one-way RM-ANOVA

Appendix B1 Rut Depth GIS Maps

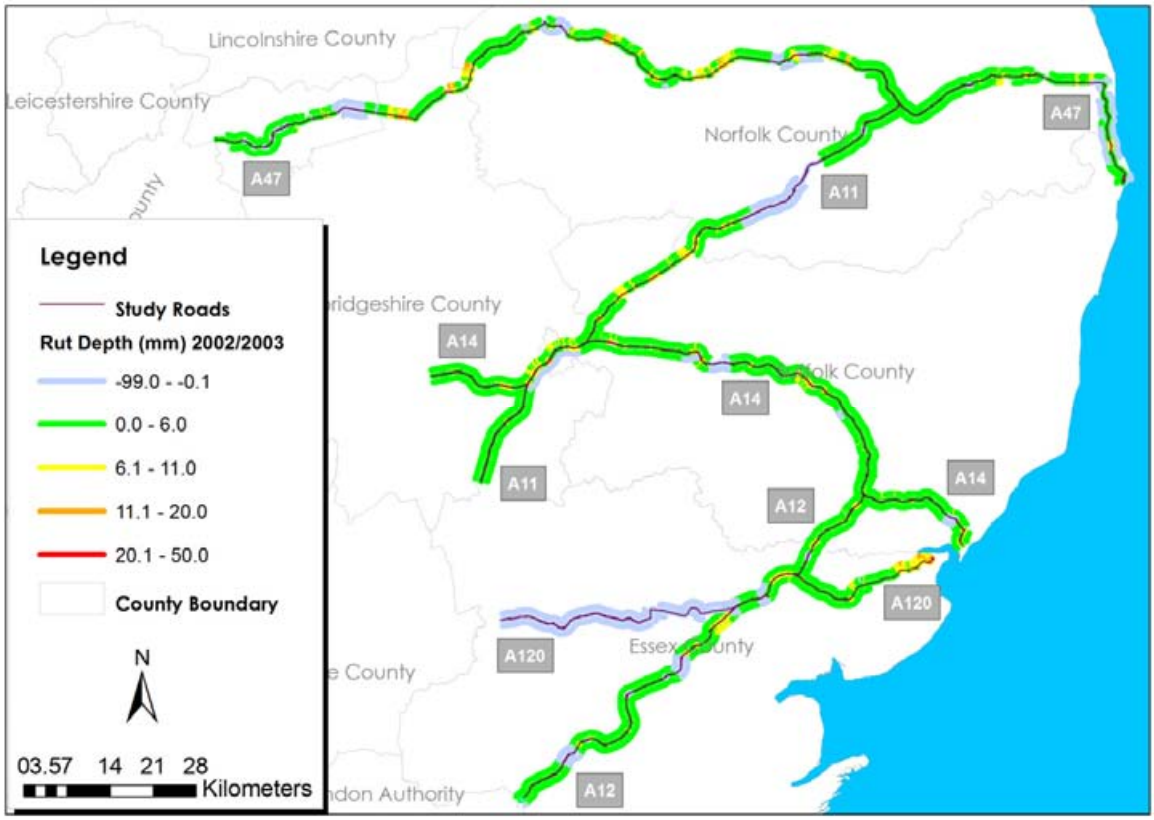

Figure B1-1: Spatial Representation of Sampled Rut Depth Measured in 2002/2003.

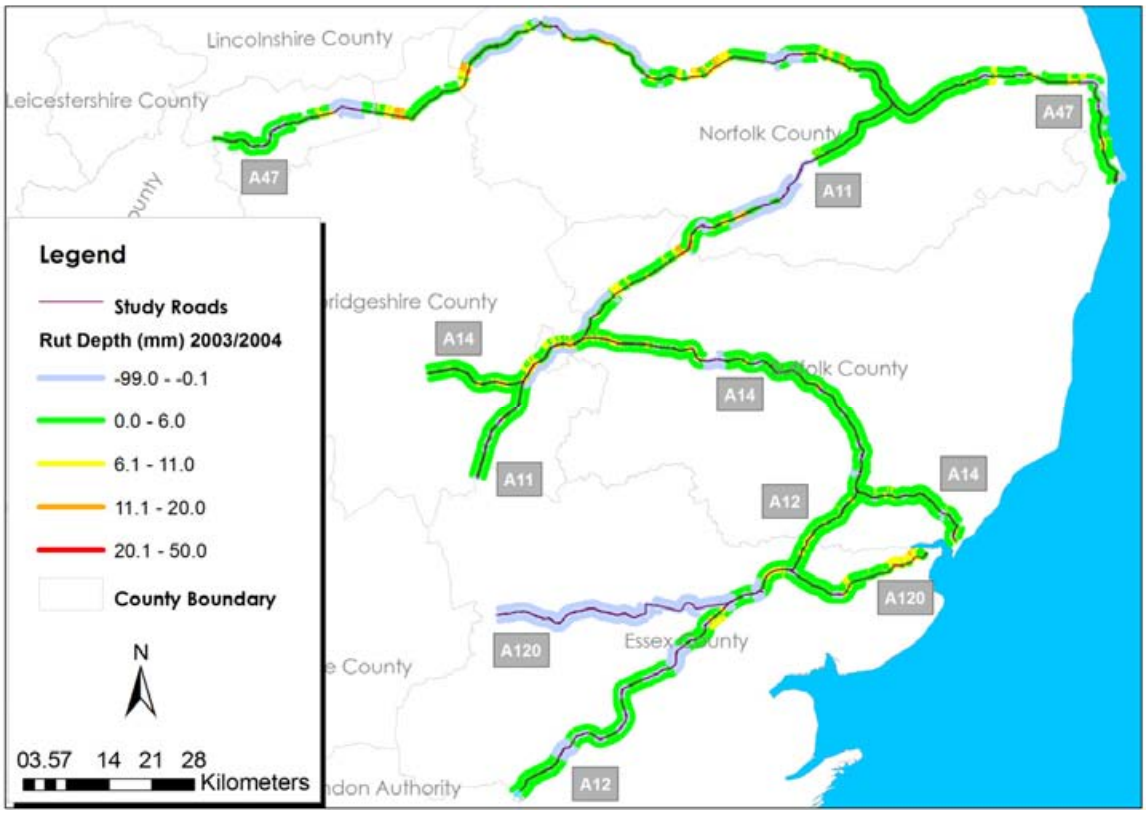

Figure B1-2: Spatial Representation of Sampled Rut Depth Measured in 2003/2004.

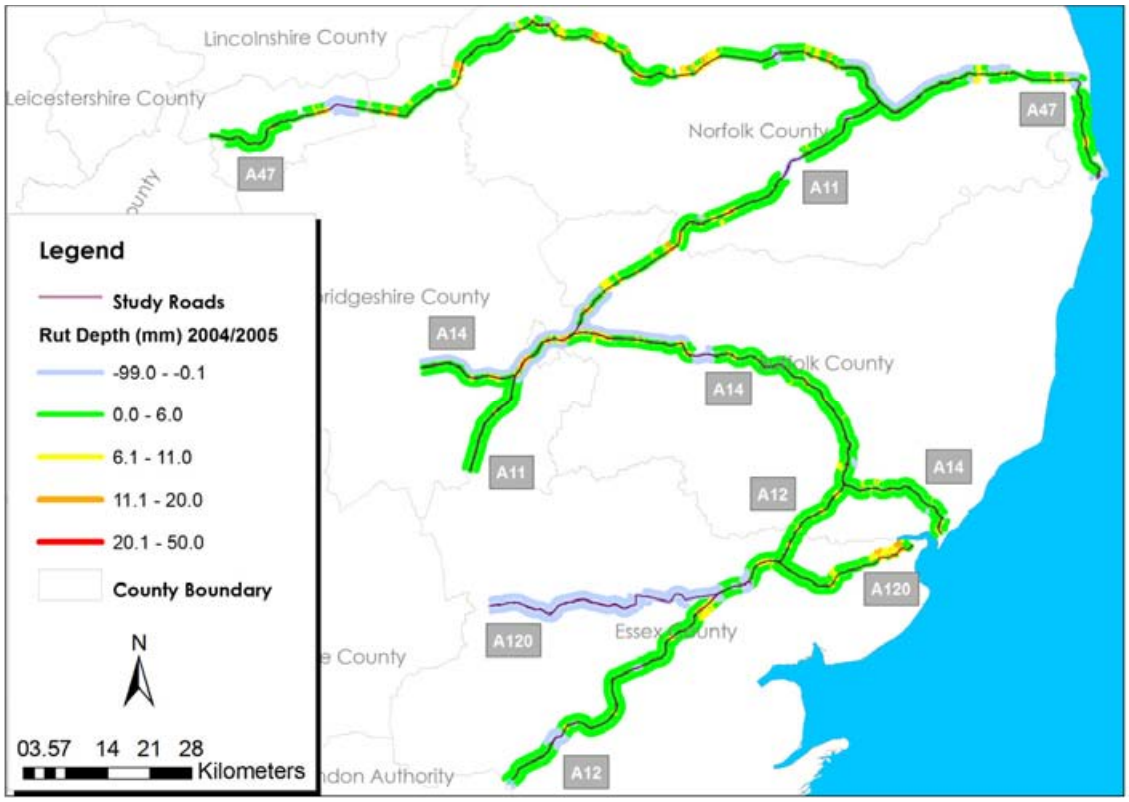

Figure B1-3: Spatial Representation of Sampled Rut Depth Measured in 2004/2005.

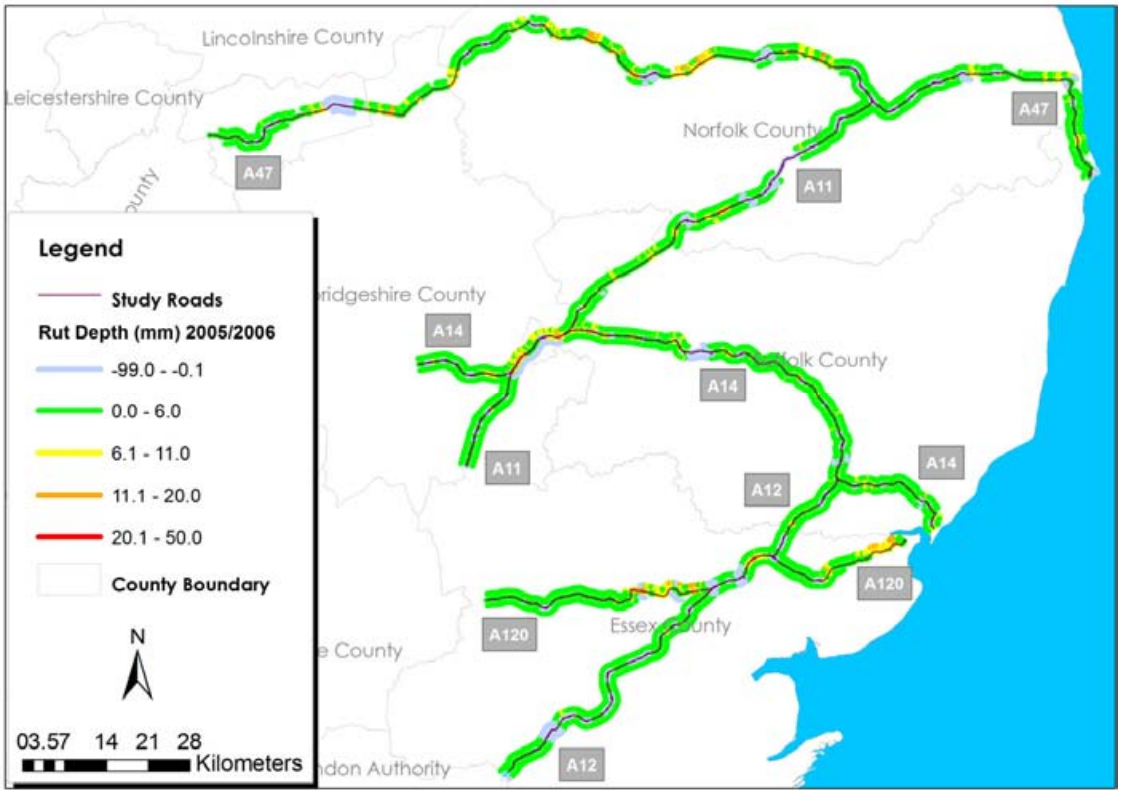

Figure B1-4: Spatial Representation of Sampled Rut Depth Measured in 2005/2006.

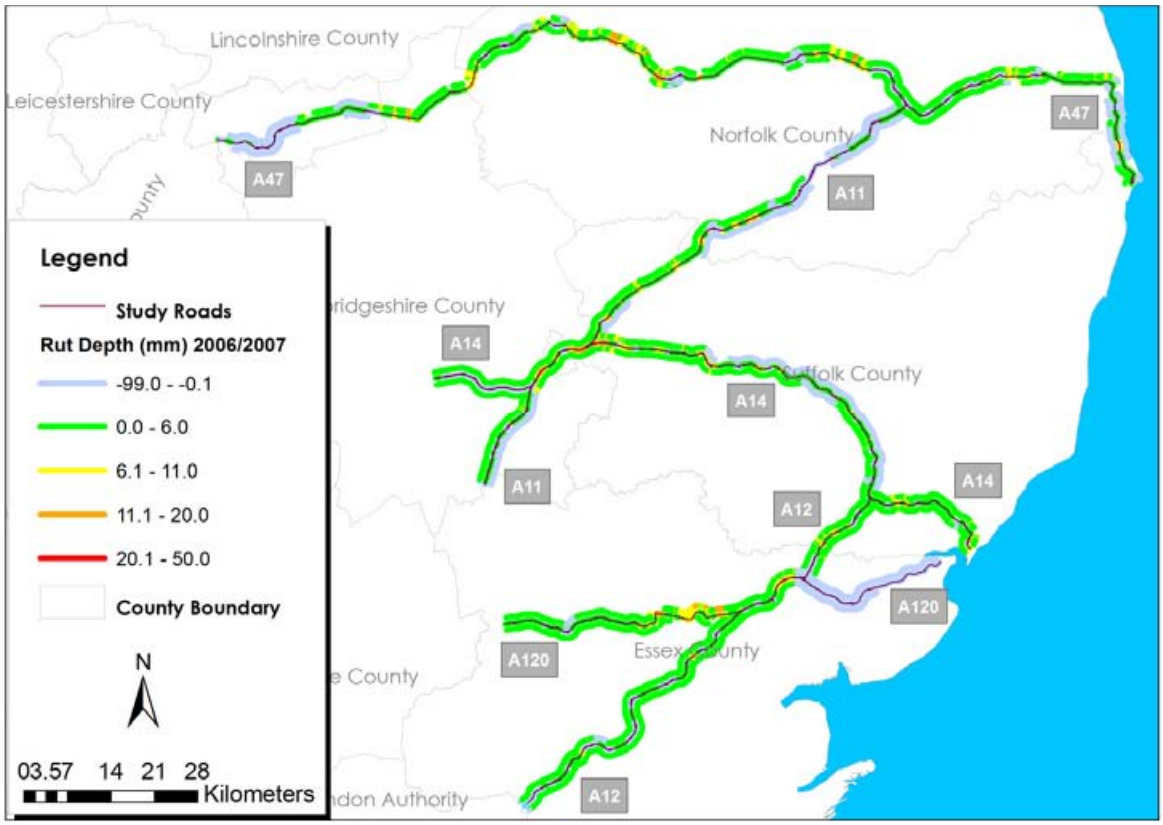

Figure B1-5: Spatial Representation of Sampled Rut Depth Measured in 2006/2007.

Appendix B2 Rut Depth Sample Summary Statistics by Study Road

Table B2-1: Summary Statistics for Rut Depth Sample by Study Roads and Survey Period

Road	Statistics	2001/ 2002	2002/ 2003	2003/ 2004	2004/ 2005	2005/ 2006	2006/ 2007	2007/ 2008
A11	Sample Size	2,823	2,964	2,878	3,265	3,193	2,286	1,904
	Mean	3.948	3.411	3.570	3.413	3.299	3.996	4.015
	Standard Error	0.045	0.040	0.044	0.041	0.035	0.049	0.053
	Median	3.197	2.731	2.803	2.688	2.716	3.260	3.245
	Mode	2.370	1.927	2.300	2.681	2.151	3.260	2.637
	Standard Deviation	2.374	2.198	2.343	2.329	1.976	2.346	2.316
	Sample Variance	5.636	4.829	5.490	5.424	3.904	5.502	5.362
	Kurtosis	5.636	8.541	8.436	9.443	9.692	6.789	3.774
	Skewness	1.996	2.453	2.460	2.605	2.511	2.258	1.828
	Range	20.015	21.999	21.624	22.915	20.290	19.673	16.973
	Minimum	0.000	0.487	0.639	0.551	0.572	1.038	1.027
	Maximum	20.015	22.486	22.263	23.466	20.862	20.711	18.000
	Confidence Level (95.0%)	0.088	0.079	0.086	0.080	0.069	0.096	0.104
A12	Sample Size	4,068	3,952	3,751	4,228	3,877	3,707	2,451
	Mean	3.884	3.409	3.340	3.323	3.042	3.623	3.852
	Standard Error	0.035	0.034	0.038	0.035	0.028	0.033	0.041
	Median	3.319	2.912	2.714	2.726	2.601	3.165	3.298
	Mode	0.000	2.372	1.816	3.443	1.593	2.100	2.800
	Standard Deviation	2.216	2.138	2.334	2.246	1.757	1.989	2.012
	Sample Variance	4.911	4.571	5.449	5.044	3.087	3.958	4.046
	Kurtosis	6.943	6.820	9.227	9.932	8.957	8.381	5.694
	Skewness	2.171	2.196	2.513	2.596	2.348	2.392	2.091
	Range	20.075	18.862	21.353	20.861	19.820	17.776	14.859
	Minimum	0.000	0.545	0.725	0.537	0.505	0.796	0.862
	Maximum	20.075	19.407	22.078	21.398	20.325	18.572	15.721
	Confidence Level(95.0%)	0.068	0.067	0.075	0.068	0.055	0.064	0.080
A120	Sample Size	836	881	842	885	2,274	1,162	1,526
	Mean	4.304	4.082	3.517	3.786	3.988	4.246	4.247
	Standard Error	0.102	0.100	0.096	0.102	0.065	0.097	0.076
	Median	3.334	3.156	2.166	2.394	2.725	2.885	3.033
	Mode	2.285	1.517	1.805	1.261	2.676	2.634	3.106
	Standard Deviation	2.946	2.963	2.798	3.030	3.089	3.305	2.960
	Sample Variance	8.676	8.781	7.828	9.182	9.540	10.925	8.763
	Kurtosis	1.843	3.094	2.157	2.661	2.946	2.599	2.002
	Skewness	1.409	1.639	1.591	1.739	1.821	1.792	1.668
	Range	16.162	18.184	17.224	18.378	19.585	20.599	15.241
	Minimum	1.135	0.600	0.548	0.881	0.780	0.818	1.307
	Maximum	17.297	18.784	17.772	19.259	20.365	21.417	16.548
	Confidence Level(95.0%)	0.200	0.196	0.189	0.200	0.127	0.190	0.149

Table B2-1: Summary Statistics for Rut Depth Sample by Study Roads and Survey Period (Continued)

Road	Statistics	2001/ 2002	2002/ 2003	2003/ 2004	2004/ 2005	2005/ 2006	2006/ 2007	2007/ 2008
A14	Sample Size	4,798	5,085	4,987	4,081	4,626	4,202	3,258
	Mean	4.250	3.802	3.745	4.089	4.167	4.574	4.218
	Standard Error	0.031	0.031	0.033	0.042	0.039	0.043	0.042
	Median	3.792	3.416	3.192	3.413	3.484	3.813	3.666
	Mode	2.488	2.914	2.939	3.243	2.227	3.919	2.190
	Standard Deviation	2.180	2.198	2.336	2.679	2.649	2.814	2.395
	Sample Variance	4.752	4.829	5.457	7.177	7.015	7.918	5.734
	Kurtosis	5.529	6.101	4.498	4.512	4.894	4.910	4.254
	Skewness	1.861	1.843	1.819	1.881	1.946	2.028	1.828
	Range	21.276	22.122	19.080	21.158	22.651	21.931	19.209
	Minimum	0.380	0.327	0.297	0.545	0.370	1.161	0.627
	Maximum	21.656	22.449	19.377	21.703	23.021	23.092	19.836
	Confidence Level(95.0%)	0.062	0.060	0.065	0.082	0.076	0.085	0.082
A47	Sample Size	5,059	4,922	4,576	4,851	4,894	4,479	4,046
	Mean	4.614	3.873	4.191	4.142	4.357	4.254	4.028
	Standard Error	0.037	0.034	0.037	0.038	0.038	0.038	0.034
	Median	3.850	3.206	3.530	3.391	3.659	3.650	3.613
	Mode	3.406	3.381	3.170	2.141	2.179	3.268	2.802
	Standard Deviation	2.615	2.396	2.491	2.644	2.652	2.562	2.156
	Sample Variance	6.838	5.742	6.203	6.988	7.032	6.566	4.649
	Kurtosis	4.514	5.863	5.731	6.069	6.012	7.972	6.068
	Skewness	1.899	2.158	2.121	2.177	2.129	2.363	2.021
	Range	24.147	17.783	18.440	19.266	20.825	22.321	16.292
	Minimum	0.000	0.536	0.605	0.609	0.493	0.794	0.798
	Maximum	24.147	18.319	19.045	19.875	21.318	23.115	17.090
	Confidence Level(95.0%)	0.072	0.067	0.072	0.074	0.074	0.075	0.066

Appendix B3 Summary of Climate Data by Year

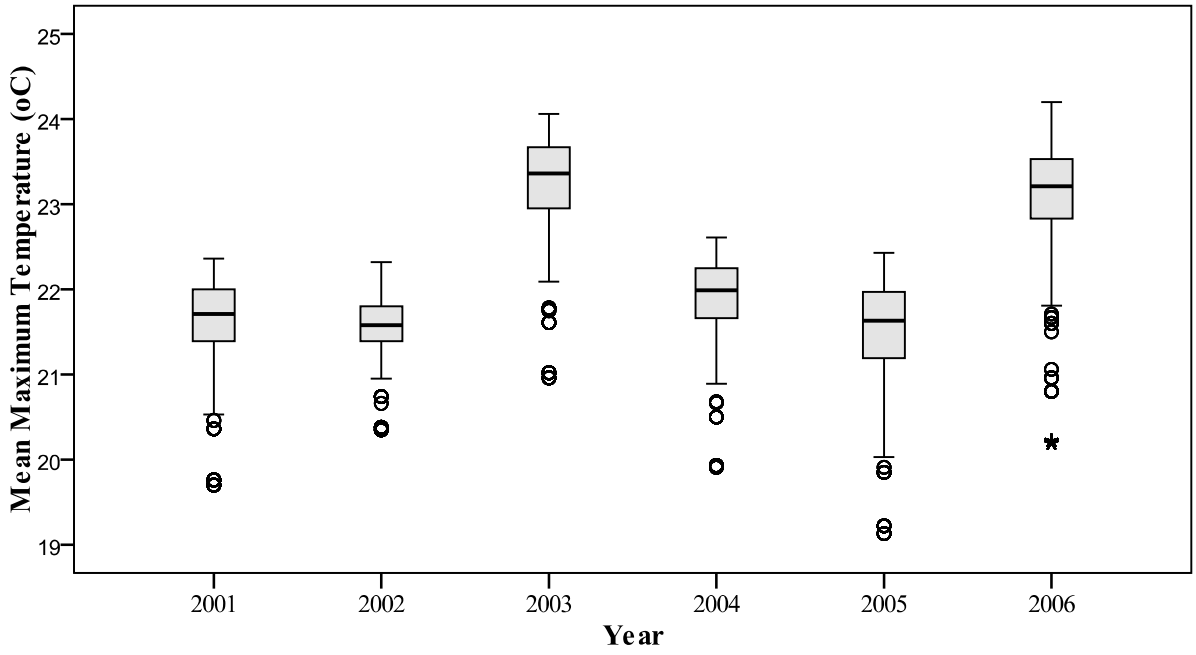

Figure B3-1: Mean Monthly Summer Days with Rainfall Greater Than 10mm

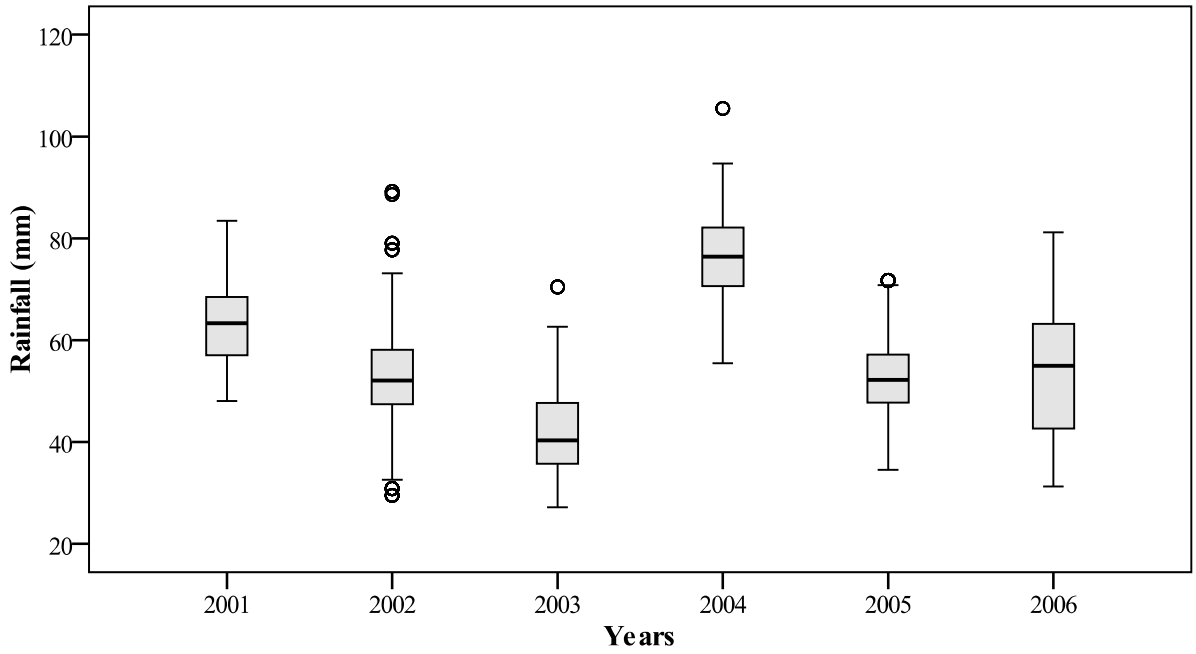

Figure B3-2: Mean Total Monthly Summer Precipitation (mm)

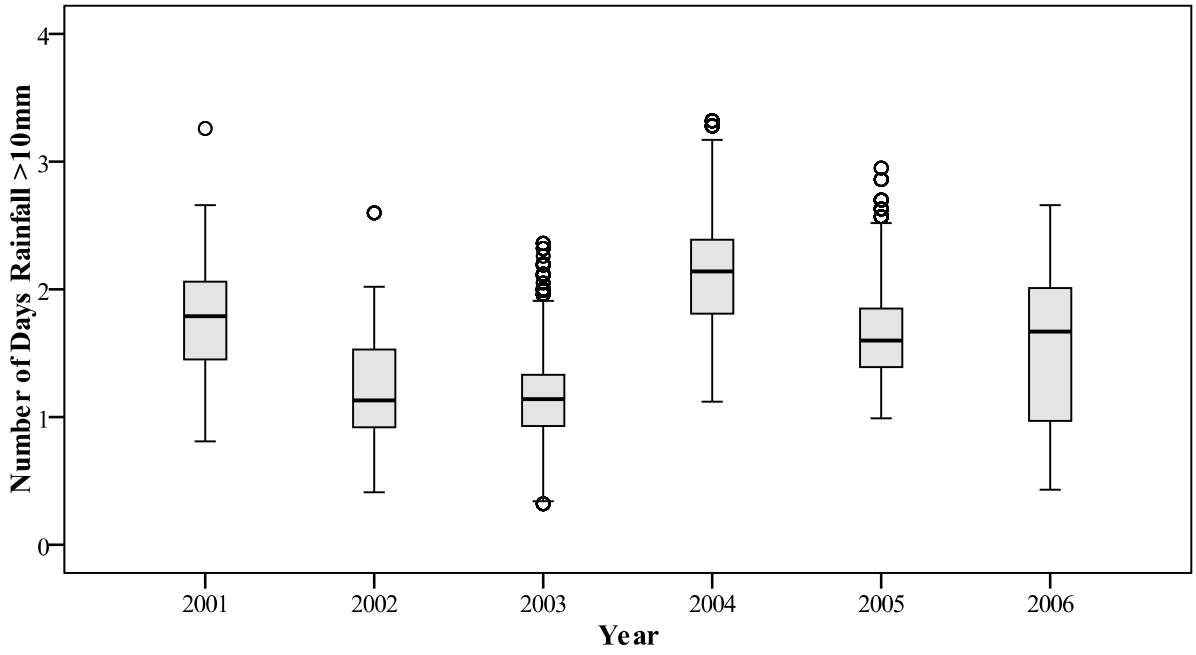

Figure B3-3: Mean Number of Days during the Summer with Precipitation greater than 10mm

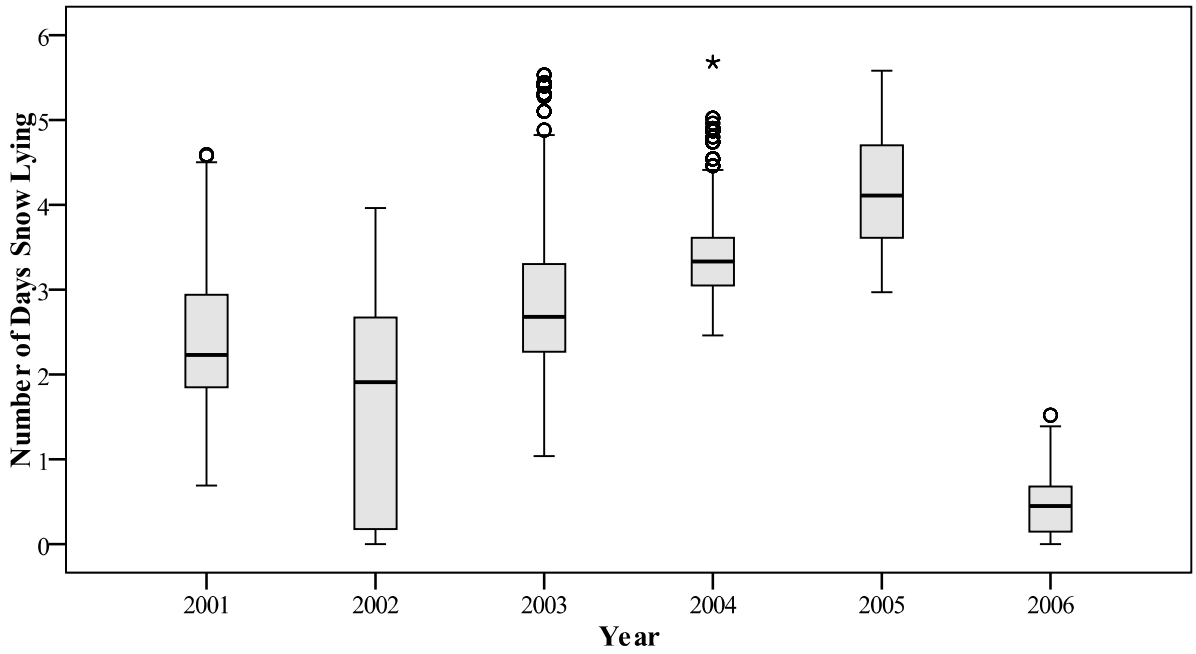

Figure B3-4: Maximum Annual Number of Days with Snow Lying

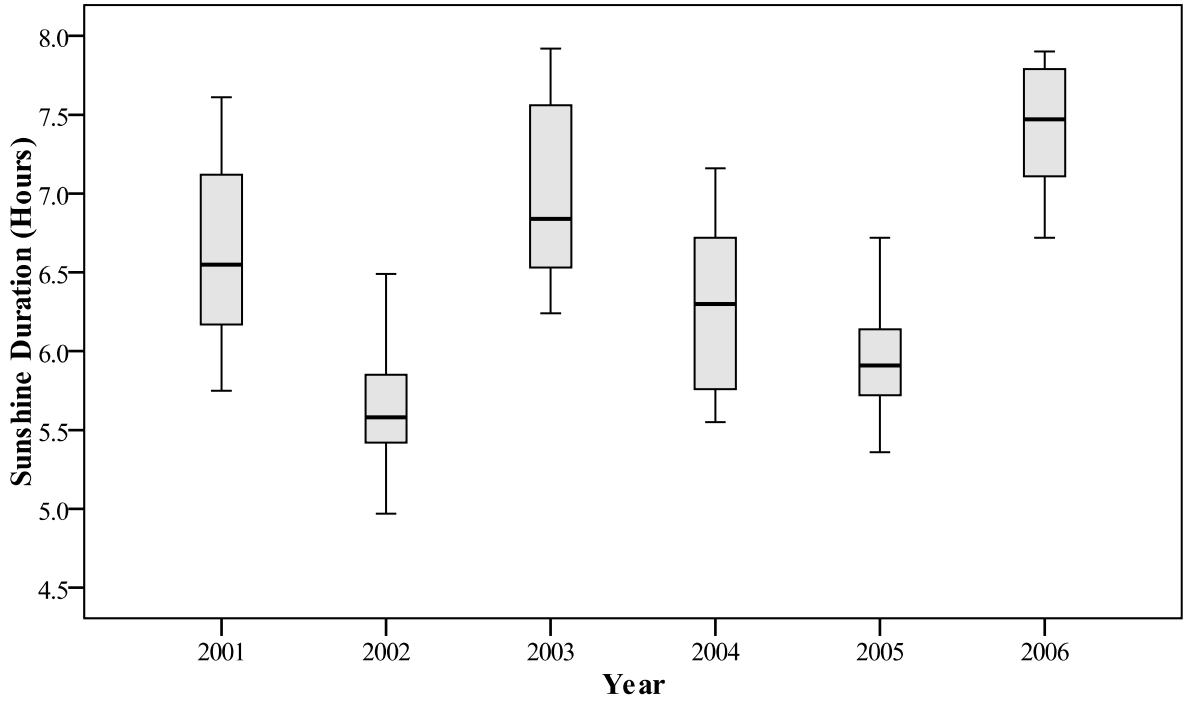

Figure B3-5: Mean Maximum Monthly Sunshine Duration in Hours per Day

Table B3-1: Summary Statistics for Average Monthly Maximum Summer Temperature

Parameter	2001	2002	2003	2004	2005	2006
Mean	21.625	21.578	23.224	21.887	21.486	23.043
Standard Error	0.009	0.006	0.011	0.009	0.012	0.013
Median	21.710	21.577	23.363	21.987	21.627	23.207
Mode	21.430	21.703	22.603	22.273	20.807	23.073
Standard Deviation	0.493	0.326	0.592	0.486	0.635	0.720
Sample Variance	0.243	0.106	0.351	0.236	0.403	0.518
Kurtosis	2.670	2.482	2.527	3.859	1.937	3.977
Skewness	-1.404	-1.065	-1.449	-1.674	-1.299	-1.782
Range	2.660	1.963	3.097	2.700	3.293	4.003
Minimum	19.703	20.353	20.960	19.910	19.133	20.193
Maximum	22.363	22.317	24.057	22.610	22.427	24.197
Sample Size	2970	2970	2970	2970	2970	2970

Table B3-2: Mean Monthly Summer Days with Rainfall Greater Than 10mm in mm

Parameter	2001	2002	2003	2004	2005	2006
Mean	1.749	1.203	1.182	2.136	1.647	1.574
Standard Error	0.008	0.007	0.008	0.009	0.008	0.011
Median	1.787	1.133	1.140	2.140	1.600	1.670
Mode	1.037	1.013	1.297	2.060	1.070	0.793
Standard Deviation	0.455	0.399	0.431	0.472	0.412	0.604
Sample Variance	0.207	0.159	0.186	0.223	0.170	0.365
Kurtosis	-0.460	-0.409	0.034	0.011	0.312	-1.174
Skewness	-0.301	0.282	0.425	0.227	0.656	-0.222
Range	2.450	2.190	2.040	2.197	1.957	2.230
Minimum	0.810	0.410	0.323	1.123	0.993	0.427
Maximum	3.260	2.600	2.363	3.320	2.950	2.657
Sample Size	2970	2970	2970	2970	2970	2970

Table B3-3: Mean Total Summer Precipitation in mm

Parameter	2001	2002	2003	2004	2005	2006
Mean	63.044	53.112	42.519	75.665	52.550	53.431
Standard Error	0.133	0.177	0.155	0.172	0.140	0.222
Median	63.353	52.100	40.300	76.783	52.187	55.003
Mode	76.267	68.663	53.343	70.883	63.583	67.120
Standard Deviation	7.247	9.636	8.443	9.348	7.652	12.087
Sample Variance	52.523	92.848	71.280	87.387	58.555	146.085
Kurtosis	-0.874	0.462	-0.250	-0.204	0.221	-1.069
Skewness	-0.079	0.283	0.773	-0.163	0.037	-0.180
Range	35.397	59.660	43.260	50.020	37.213	49.927
Minimum	48.027	29.533	27.200	55.480	34.517	31.283
Maximum	83.423	89.193	70.460	105.500	71.730	81.210
Sample Size	2970	2970	2970	2970	2970	2970

Table B3-4: Maximum Annual Number of Days with Snow Lying

Parameter	2001	2002	2003	2004	2005	2006
Mean	2.441	1.547	2.904	3.405	4.151	0.470
Standard Error	0.017	0.023	0.017	0.010	0.012	0.007
Median	2.230	1.910	2.680	3.330	4.110	0.450
Mode	3.910	0.180	3.090	3.610	3.970	0.000
Standard Deviation	0.900	1.257	0.940	0.568	0.640	0.354
Sample Variance	0.810	1.579	0.883	0.322	0.409	0.126
Kurtosis	-0.563	-1.557	0.821	0.944	-1.022	-0.465
Skewness	0.552	0.089	1.019	0.926	-0.001	0.546
Range	3.900	3.960	4.490	3.220	2.610	1.520
Minimum	0.690	0.000	1.040	2.460	2.970	0.000
Maximum	4.590	3.960	5.530	5.680	5.580	1.520
Sample Size	2970	2970	2970	2970	2970	2970

Table B3-5: Mean Maximum Monthly Summer Sunshine Duration in Hours per Day

Parameter	2001	2002	2003	2004	2005	2006
Mean	6.619	5.622	7.008	6.251	5.946	7.421
Standard Error	0.009	0.005	0.009	0.009	0.006	0.007
Median	6.547	5.580	6.843	6.300	5.907	7.470
Mode	7.143	5.797	6.500	5.623	5.767	7.837
Standard Deviation	0.493	0.273	0.511	0.472	0.310	0.363
Sample Variance	0.243	0.075	0.261	0.222	0.096	0.132
Kurtosis	-1.507	-0.427	-1.526	-1.549	-0.696	-1.350
Skewness	0.081	0.021	0.214	0.041	0.365	-0.319
Range	1.863	1.520	1.683	1.610	1.363	1.173
Minimum	5.747	4.973	6.237	5.547	5.360	6.723
Maximum	7.610	6.493	7.920	7.157	6.723	7.897
Sample Size	2970	2970	2970	2970	2970	2970

Appendix B4 Maps of Annual Heavy Vehicle Speed

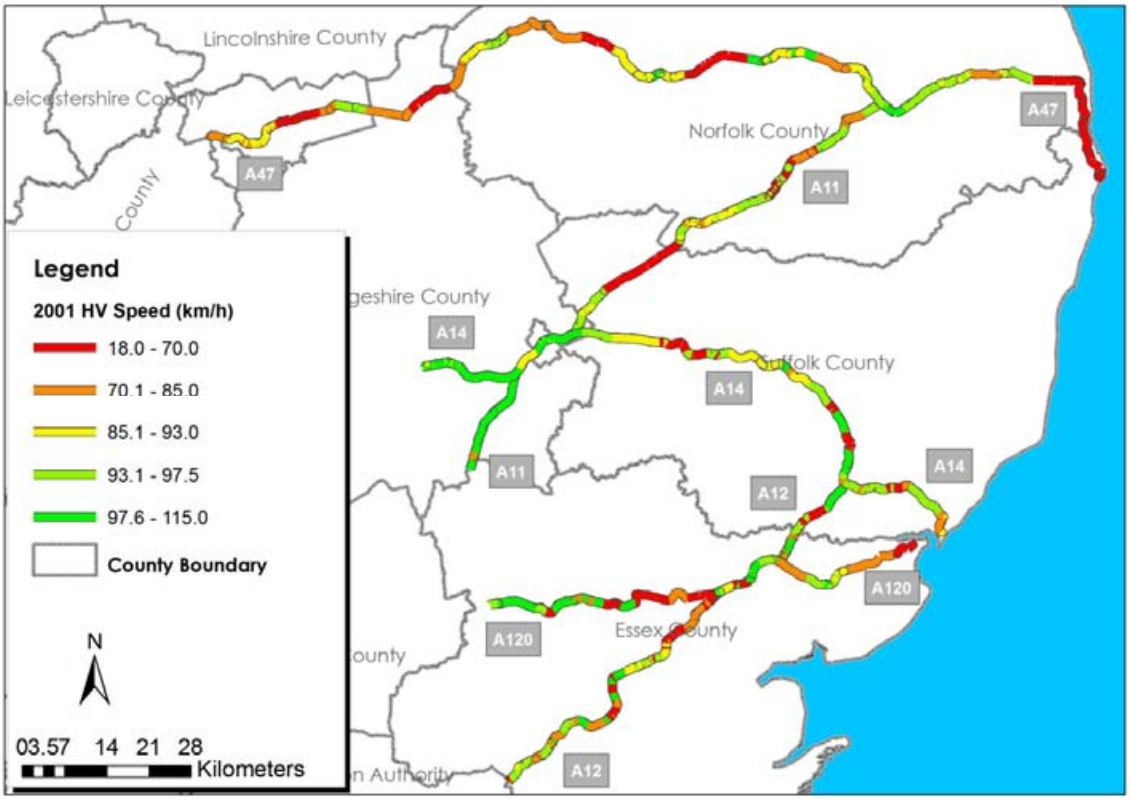

Figure B4-1: Heavy Vehicle Speeds in 2001 on the Study Road Network

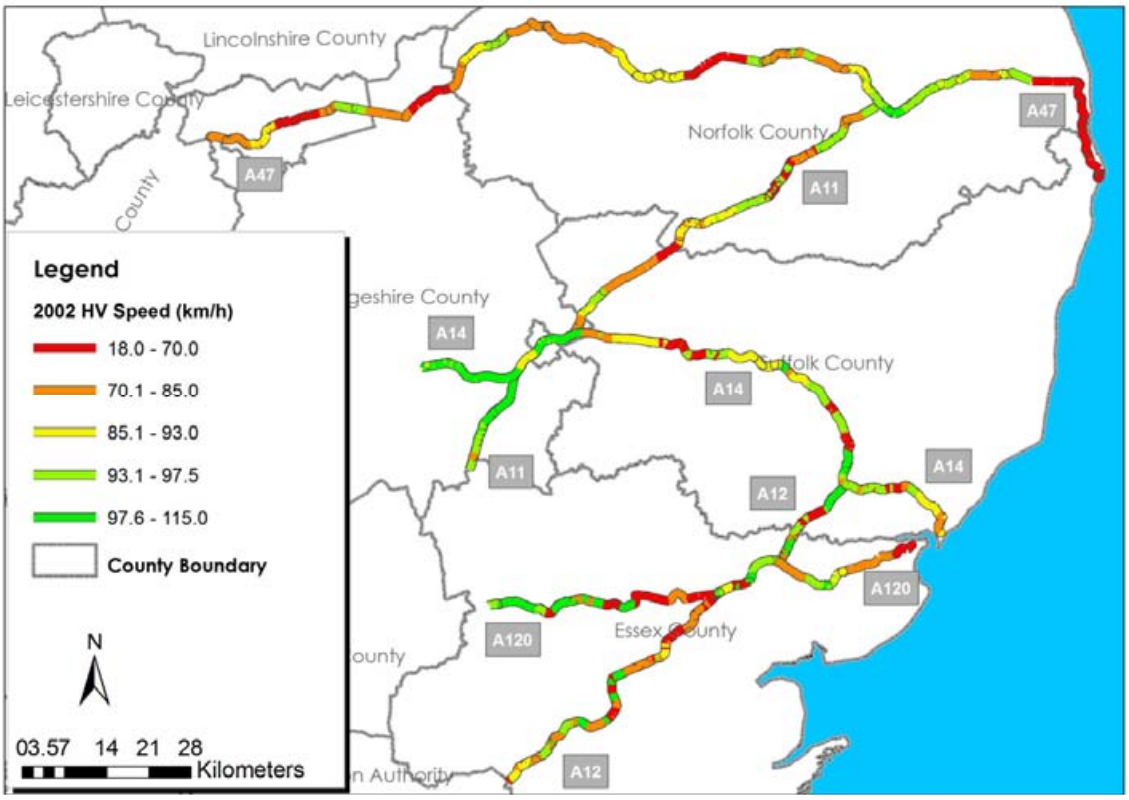

Figure B4-2: Heavy Vehicle Speeds in 2002 on the Study Road Network

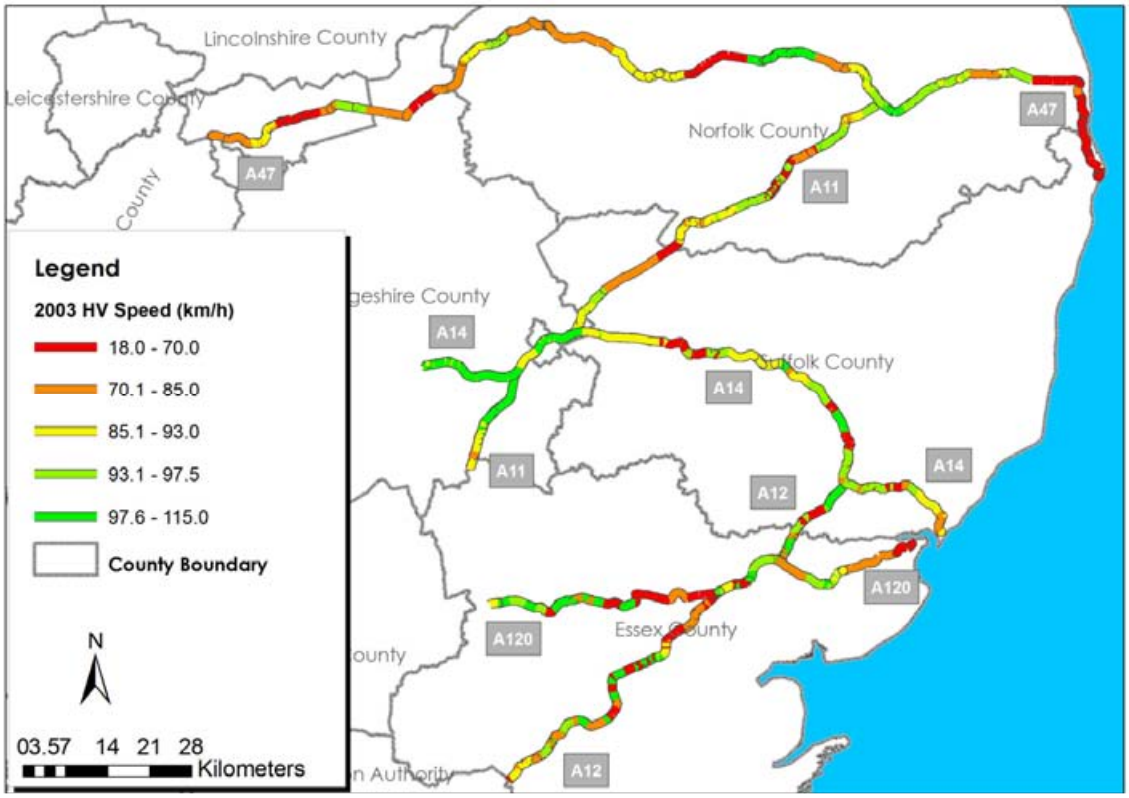

Figure B4-3: Heavy Vehicle Speeds in 2003 on the Study Road Network

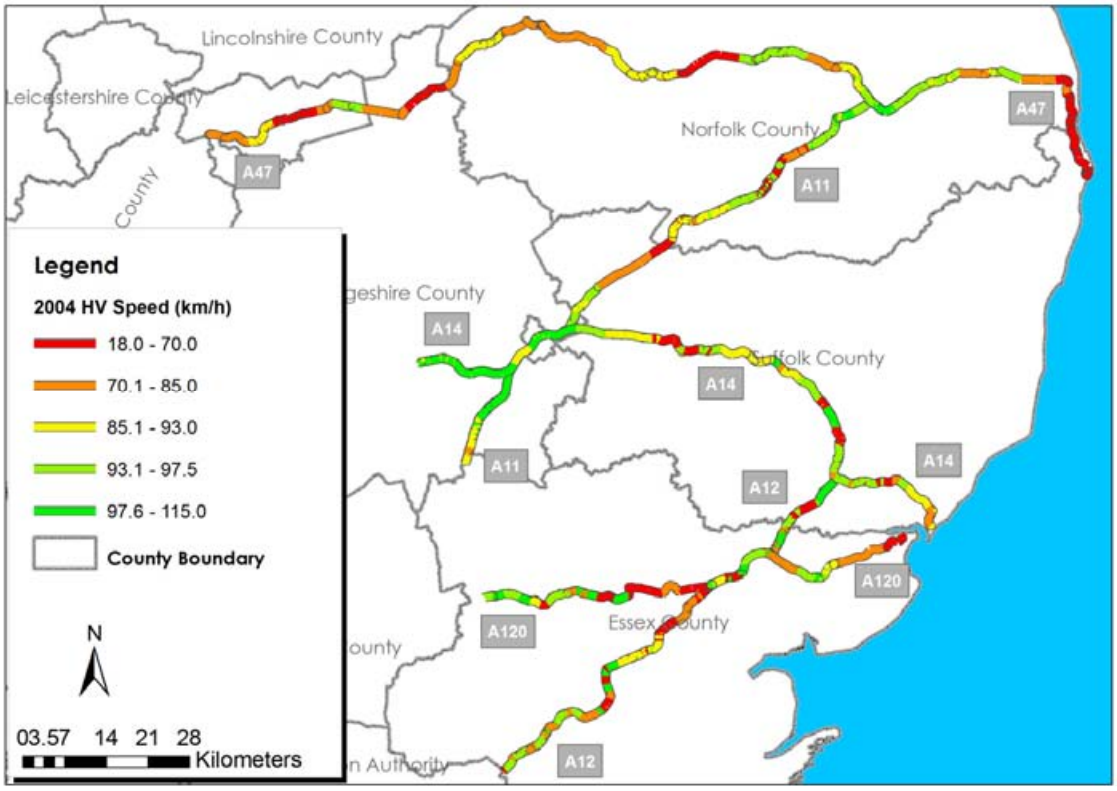

Figure B4-4: Heavy Vehicle Speeds in 2004 on the Study Road Network

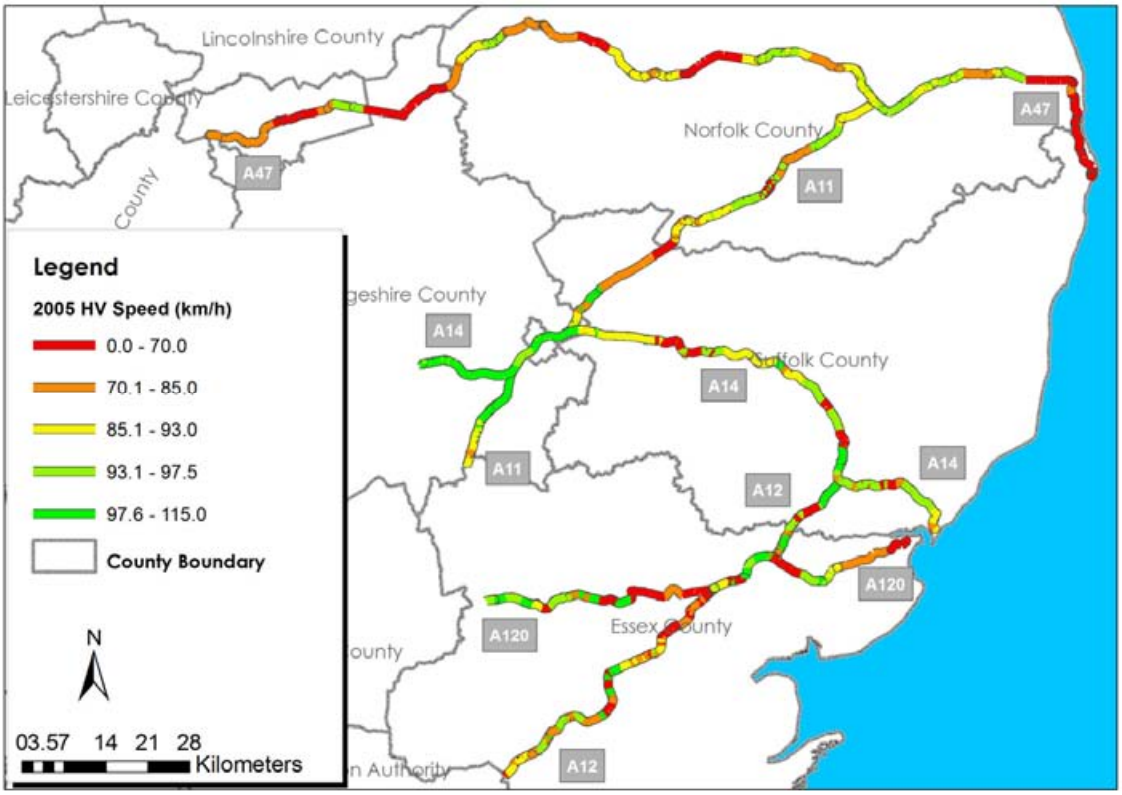

Figure B4-5: Heavy Vehicle Speeds in 2005 on the Study Road Network

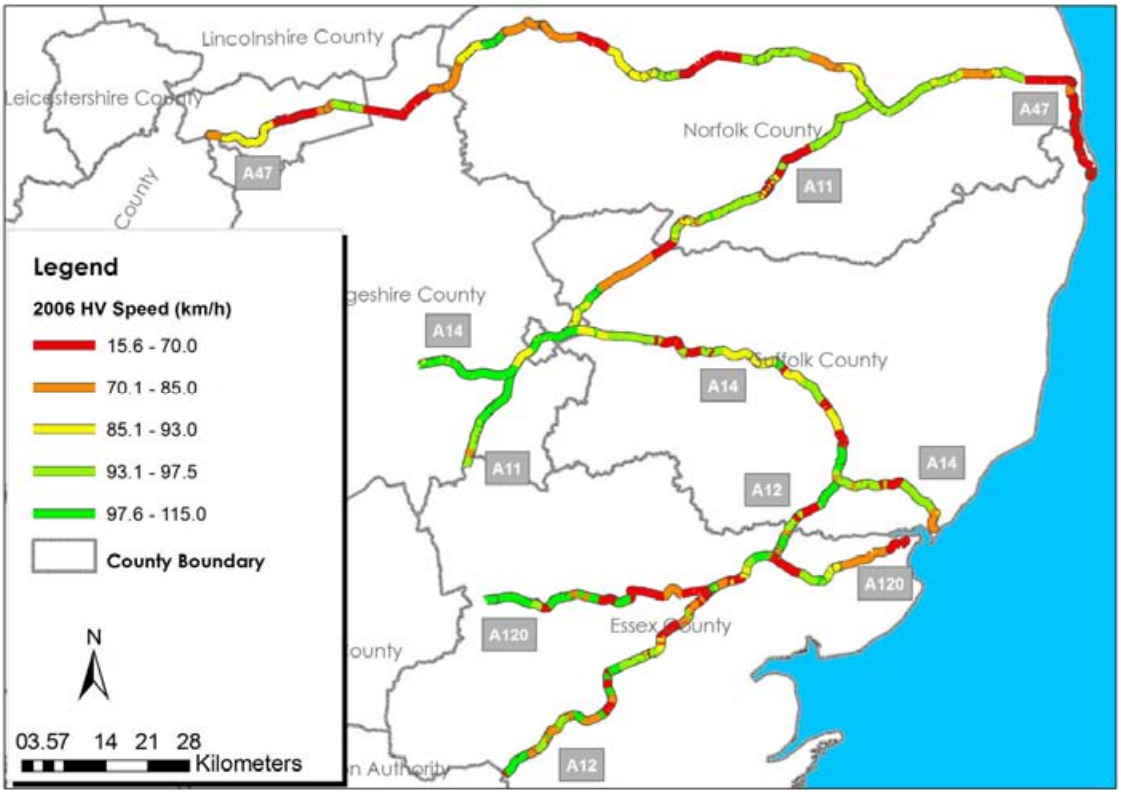

Figure B4-6: Heavy Vehicle Speeds in 2006 on the Study Road Network

Appendix B5 Transformed Heavy Vehicle Speeds Data

Table B5-1: Parameters for Box Cox Transformation Algorithm for Heavy Vehicle Speed Data

Transformation Parameters	Road				
	A11	A12	A120	A14	A47
Geometric Mean (GM)	80.941	74.242	83.884	81.621	79.70457
λ	3.799	1.985	2.512	3.355	1.0795

Table B5-2: Summary Statistics for Transformed Vehicle Speeds

Road	Year	Statistics				
		Mean	Sample Variance	Kurtosis	Skewness	Sample Size
A11	2001	29.367	212.037	-1.130	-0.551	34
	2002	31.053	211.317	-1.002	-0.395	34
	2003	29.138	199.531	-0.977	-0.498	34
	2004	27.924	195.599	-0.991	-0.632	34
	2005	28.385	180.158	-0.897	-0.484	34
	2006	29.348	230.432	-1.096	-0.649	34
A12	2001	49.225	372.324	-0.687	-0.455	65
	2002	50.034	359.961	-0.415	-0.397	65
	2003	49.861	366.848	-0.572	-0.462	65
	2004	47.864	342.471	-0.583	-0.525	65
	2005	46.949	377.112	-0.530	-0.543	65
	2006	48.692	368.457	-0.727	-0.491	65
A120	2001	38.898	228.001	-1.135	-0.323	53
	2002	38.955	228.929	-1.128	-0.321	53
	2003	38.599	222.333	-1.084	-0.297	53
	2004	38.213	209.238	-0.972	-0.331	53
	2005	38.383	216.467	-1.044	-0.329	53
	2006	39.194	242.350	-1.231	-0.261	53
A14	2001	31.906	219.650	-0.833	-0.370	64
	2002	31.091	208.623	-0.999	-0.433	64
	2003	31.032	206.575	-0.864	-0.395	64
	2004	30.857	205.535	-0.910	-0.383	64
	2005	31.475	213.754	-1.032	-0.439	64
	2006	32.491	238.895	-1.151	-0.468	64
A47	2001	73.918	198.777	-0.524	-0.274	65
	2002	73.234	179.666	-0.337	-0.313	65
	2003	74.223	198.541	-0.258	-0.233	65
	2004	73.507	183.568	-0.402	-0.353	65
	2005	73.380	176.089	-0.329	-0.295	65
	2006	73.825	196.208	-0.592	-0.298	65

Appendix B6 Summary of Annual Equivalent Standard Axle Load

Table B6-1: Summary Statistics for Annual Equivalent Standard Axle Loads

Road	Year	Mean	Variance	Minimum	Maximum	Number of Road Sections
A11	2001	0.78	0.24	0.05	2.30	312
	2002	0.79	0.25	0.05	2.34	312
	2003	0.80	0.26	0.05	2.38	312
	2004	0.82	0.27	0.05	2.43	312
	2005	0.84	0.28	0.05	2.48	312
	2006	0.85	0.29	0.05	2.53	312
A12	2001	1.06	0.51	0.05	2.66	371
	2002	1.07	0.53	0.05	2.70	371
	2003	1.10	0.55	0.05	2.76	371
	2004	1.12	0.57	0.05	2.81	371
	2005	1.14	0.59	0.05	2.87	371
	2006	1.16	0.62	0.05	2.92	371
A120	2001	0.56	0.10	0.05	1.52	178
	2002	0.57	0.10	0.05	1.55	178
	2003	0.58	0.11	0.05	1.58	178
	2004	0.59	0.11	0.05	1.61	178
	2005	0.61	0.12	0.05	1.64	178
	2006	0.62	0.12	0.05	1.67	178
A14	2001	1.34	0.72	0.09	5.80	383
	2002	1.36	0.74	0.09	5.89	383
	2003	1.39	0.77	0.10	6.01	383
	2004	1.41	0.80	0.10	6.13	383
	2005	1.44	0.83	0.10	6.25	383
	2006	1.47	0.86	0.10	6.37	383
A47	2001	0.65	0.14	0.05	1.67	555
	2002	0.66	0.15	0.05	1.70	555
	2003	0.67	0.15	0.05	1.74	555
	2004	0.69	0.16	0.05	1.77	555
	2005	0.70	0.17	0.05	1.81	555
	2006	0.71	0.17	0.05	1.84	555

Appendix B7 Asphalt Material Properties Data

Table B7-1: Summary of Binder Softening Point for In-service TSCS Road Sections

Site	Initial SP	Year Laid	SP of Recovered Binder in ^{o}C	Year SP Recovered	Surface Age in Years	Increase in SP in ^{o}C	Annual Increase in SP in ^{o}C
MS1	55	1999	75.2	2004	5	20.20	4.04
MS1	55	1999	71	2005	6	16.00	2.67
MS1	55	1999	73	2006	7	18.00	2.57
MS2	55	2000	65.2	2004	4	10.20	2.55
MS2	55	2000	74.8	2005	5	19.80	3.96
MS2	55	2000	77	2006	6	22.00	3.67
PLSD10	46	1995	63.2	2001	6	17.20	2.87
PLSD10	46	1995	59.4	2002	7	13.40	1.91
PLSD10	46	1995	58.8	2003	8	12.80	1.60
PLSD10	46	1995	55.6	2006	11	9.60	0.87
PLSD11	46	1995	61.6	2001	6	15.60	2.60
PLSD11	46	1995	61.6	2002	7	15.60	2.23
PLSD11	46	1995	60	2003	8	14.00	1.75
PLSD7a	46	1993	73.4	2001	8	27.40	3.43
PLSD7b	46	1993	73.8	2002	9	27.80	3.09
PLSD7b	46	1993	73.6	2003	10	27.60	2.76
PLSD7b	46	1993	70.4	2004	11	24.40	2.22
PLSD7b	46	1993	79.8	2005	12	33.80	2.82
PLSD7b	46	1993	74	2006	13	28.00	2.15
TAC1a	56	1992	60.4	2002	10	4.40	0.44
TAC1a	56	1992	73.8	2003	11	17.80	1.62
TAC1a	56	1992	61.8	2004	12	5.80	0.48
TAC1a	56	1992	64	2005	13	8.00	0.62
TAC1a	56	1992	73.8	2006	14	17.80	1.27
TAC2	56	1995	61.4	2001	6	5.40	0.90
TAC2	56	1995	66.8	2002	7	10.80	1.54
TAC2	56	1995	64.8	2003	8	8.80	1.10
TAC2	56	1995	72.6	2006	11	16.60	1.51
TAC3	58	1995	55.7	2001	6	-2.30	-0.38
TAC3	58	1995	65.5	2002	7	7.50	1.07
TAC3	58	1995	62	2003	8	4.00	0.50
TAC5	49	1996	60.7	2001	5	11.70	2.34
TAC5	49	1996	63	2002	6	14.00	2.33
TAC5	49	1996	63.8	2003	7	14.80	2.11
TAC5	49	1996	64.6	2004	8	15.60	1.95

Table B7-1: Summary of Binder Softening Point for In-service TSCS Road Sections (Continued)

Site	Initial SP	Year Laid	SP of Recovered Binder in ^{o}C	Year SP Recovered	Surface Age in Years	Increase in SP in ^{o}C	Annual Increase in SP in ^{o}C
TAC5	49	1996	68.6	2005	9	19.60	2.18
TAClb	56	1992	57.4	2002	10	1.40	0.14
TAClb	56	1992	58.2	2003	11	2.20	0.20
TAClb	56	1992	66.4	2004	12	10.40	0.87
TAClb	56	1992	66.6	2005	13	10.60	0.82
TAClb	56	1992	68.2	2006	14	12.20	0.87
TSMA10	52.5	1996	57	2004	8	4.50	0.56
TSMA10	52.5	1996	57.8	2005	9	5.30	0.59
TSMA10	52.5	1996	60.8	2006	10	8.30	0.83
TSMA15	52.5	1998	65.6	2001	3	13.10	4.37
TSMA15	52.5	1998	61	2002	4	8.50	2.13
TSMA15	52.5	1998	64.4	2003	5	11.90	2.38
TSMA15	52.5	1998	68.4	2006	8	15.90	1.99
TSMA17	52.5	1998	65.2	2006	8	12.70	1.59
TSMA4	51	1995	61	2004	9	10.00	1.11
TSMA4	51	1995	67.8	2005	10	16.80	1.68
TSMA5	51	1995	66.2	2004	9	15.20	1.69
TSMA5	51	1995	67.4	2005	10	16.40	1.64
TSMA5	51	1995	60.4	2006	11	9.40	0.85
TSMA6	51	1995	62.3	2001	6	11.30	1.88
TSMA6	51	1995	64.2	2002	7	13.20	1.89
TSMA6	51	1995	64.4	2003	8	13.40	1.68
TSMA7	52.5	1995	62.5	2001	6	10.00	1.67
TSMA7	52.5	1995	61.7	2002	7	9.20	1.31
TSMA7	52.5	1995	62.2	2003	8	9.70	1.21
TSMA8	52.5	1995	63.9	2001	6	11.40	1.90
TSMA8	52.5	1995	63.6	2003	8	11.10	1.39
TSMA8	52.5	1995	67.8	2006	11	15.30	1.39

Where PLSD = Paved laid surface dressing
TAC = Thin Asphalt Concrete
TSMA = Thin Stone Mastic Asphalt
MSA = Micro-surfacing.

Table B7-2: In-Service Asphalt (DBM and HRA) Binder Softening Point

Site/Sample Reference	Initial Softening Point (^oC)	Surfacing Age (Years)	Recovered Softening Point (^oC)	Annual Increase in Softening Point (^oC) Relative to Initial Value	Data Source
TP7/M/H	51.02	0.47	53.44	5.21	Chaddock and Pledge (1994)
TP7/M/L	51.02	0.47	53.44	5.21	
TP7/N/H	45.95	0.47	45.95	0.00	
TP7/N/L	45.95	0.47	45.95	0.00	
TP1/A/L	43.52	0.99	48.79	5.34	
TP1/B/L	42.60	0.99	47.57	5.04	
TP6/A/H	48.79	1.08	58.40	8.85	
TP6/A/L	48.79	1.08	58.40	8.85	
TP6/B/H	49.48	1.08	54.47	4.60	
TP6/B/L	49.48	1.08	54.47	4.60	
TP6/C/H	49.97	1.08	55.56	5.16	
TP6/C/L	49.97	1.08	55.56	5.16	
TP6/D/H	48.79	1.08	58.83	9.26	
TP6/D/L	48.79	1.08	58.83	9.26	
TP6/E/H	52.48	1.08	58.83	5.85	
TP6/E/L	52.48	1.08	58.83	5.85	
TP6/F/H	52.48	1.08	55.56	2.84	
TP6/F/L	52.48	1.08	55.56	2.84	
TP6/G/H	59.73	1.08	63.16	3.16	
TP6/G/L	59.73	1.08	63.16	3.16	
TP2/E/L	49.01	2.05	61.15	5.93	
TP2/G/L	48.36	2.05	59.73	5.56	
TP2/E/H	49.01	2.06	61.15	5.90	
TP2/G/H	48.36	2.06	59.73	5.53	
TP3/H/H	39.28	2.24	47.57	3.70	
TPS/H/L	39.28	2.24	47.57	3.70	
TP3/J/H	44.34	2.24	54.12	4.37	
TP3/J/L	44.34	2.24	54.12	4.37	
TP3/K/H	55.19	2.24	64.22	4.03	
TP3/K/L	55.19	2.24	64.22	4.03	
TP1/A/H	42.18	3.08	56.73	4.72	
TP1/B/H	47.21	3.08	56.73	3.09	
TP1/C/H	42.09	3.08	57.55	5.01	
TP1/C/L	40.86	3.08	57.55	5.41	

Table B7-3: In-Service Asphalt (DBM and HRA) Binder Softening Point (Continued)

Site/Sample Reference	Initial Softening Point (^oC)	Surfacing Age (Years)	Recovered Softening Point (^oC)	Annual Increase in Softening Point (^oC) Relative to Initial Value	Data Source
1N	38	6.5	45.1	1.09	Daines (1992)
1S	38	6.5	50.9	1.98	
2N	38	6.5	42.5	0.69	
2S	38	6.5	42.7	0.72	
3N	38	6.5	39.5	0.23	
3S	38	6.5	37.9	-0.02	
4N	45	6.5	58.1	2.02	
4S	45	6.5	61.5	2.54	
5N	45	6.5	60	2.31	
5S	45	6.5	55.9	1.68	
6N	45	6.5	53.1	1.25	
6S	45	6.5	52.5	1.15	
7N	45	6.5	48.1	0.48	
7S	45	6.5	48.9	0.60	
8N	45	6.5	46.3	0.20	
8S	45	6.5	45.8	0.12	
9N	45	6.5	45.5	0.08	
9S	45	6.5	46.7	0.26	
10N	54	6.5	72.2	2.80	
10S	54	6.5	71.9	2.75	
11N	54	6.5	71	2.62	
11S	54	6.5	64.4	1.60	
12N	54	6.5	63.1	1.40	
12S	54	6.5	66.6	1.94	
N1	44.02	1	49.24	5.22	Nunn et al. (1997)
N2	44.02	1	46.54	2.52	
N3	44.02	1	46.87	2.85	
N4	44.02	1	47.21	3.19	
N5	44.02	1	47.96	3.94	
N6	44.02	1	48.79	4.77	
N7	44.02	1	50.02	6.00	
N8	44.02	1	51.30	7.28	
N9	44.02	1	51.88	7.86	
N10	44.02	1	52.48	8.46	
N11	44.02	1	54.05	10.03	
N12	44.02	1	44.42	0.40	
N13	44.02	1	45.79	1.77	

Table B7-3: In-Service Asphalt (DBM and HRA) Binder Softening Point (Continued)

Site/Sample Reference	Initial Softening Point (^{o}C)	Surfacing Age (Years)	Recovered Softening Point (^{o}C)	Annual Increase in Softening Point (^{o}C) Relative to Initial Value	Data Source
N14	44.02	1	47.21	3.19	Nunn et al. (1997)
N15	44.02	1.8	50.43	3.56	
N16	44.02	1.9	47.96	2.07	
N17	44.02	1.9	54.47	5.50	
N18	44.02	2.5	56.73	5.08	
N19	44.02	3.1	54.76	3.46	
N20	44.02	3.1	54.47	3.37	
N21	44.02	3.8	58.40	3.78	
N22	44.02	4.3	58.40	3.34	
N23	44.02	4.5	54.05	2.23	
N24	44.02	4.5	55.19	2.48	
N25	44.02	4.5	56.57	2.79	
N26	44.02	4.9	56.57	2.56	
N27	44.02	4.9	66.22	4.53	
N28	44.02	5	54.05	2.01	
N29	44.02	5.5	62.34	3.33	
N30	44.02	5.9	50.43	1.09	
N31	44.02	5.9	47.96	0.67	
N32	44.02	6	55.95	1.99	
N33	44.02	6.1	51.07	1.16	
N34	44.02	6.1	62.34	3.00	
N35	44.02	6.2	48.79	0.77	
N36	44.02	6.2	46.87	0.46	
N37	44.02	10	59.28	1.53	
N38	44.02	13.5	64.87	1.54	
N39	44.02	14.2	63.16	1.35	
N40	44.02	14.2	65.32	1.50	
N41	44.02	14.2	66.45	1.58	
N42	44.02	15	58.40	0.96	
N43	44.02	15	63.16	1.28	
N44	44.02	16	56.73	0.79	
N45	44.02	17.3	63.79	1.14	
N46	44.02	17.3	71.39	1.58	
N47	44.02	19	57.55	0.71	
N48	44.02	19	59.28	0.80	
N49	44.02	19	70.61	1.40	
N50	44.02	23	65.32	0.93	
N51	44.02	24	67.63	0.98	
N52	44.02	35	66.45	0.64	

Appendix B8 Calculations for one-way RM-ANOVA

The concept of one-way RM-ANOVA is based on the calculation of the F statistics given as:

$$F = \frac{MSC}{MSE_{ad}}$$

MSC is the systematic variance in annual incremental rut depth between the measurements undertaken in 2003, 2004 and 2005 divided by MSE_{ad} the unsystematic variance or random variance present in each year that cannot be explained by the differences in annual incremental rut depths between the 177 road sub-sections. The approach to the calculation is categorised into 9 stages as illustrated in Figure B8-1.

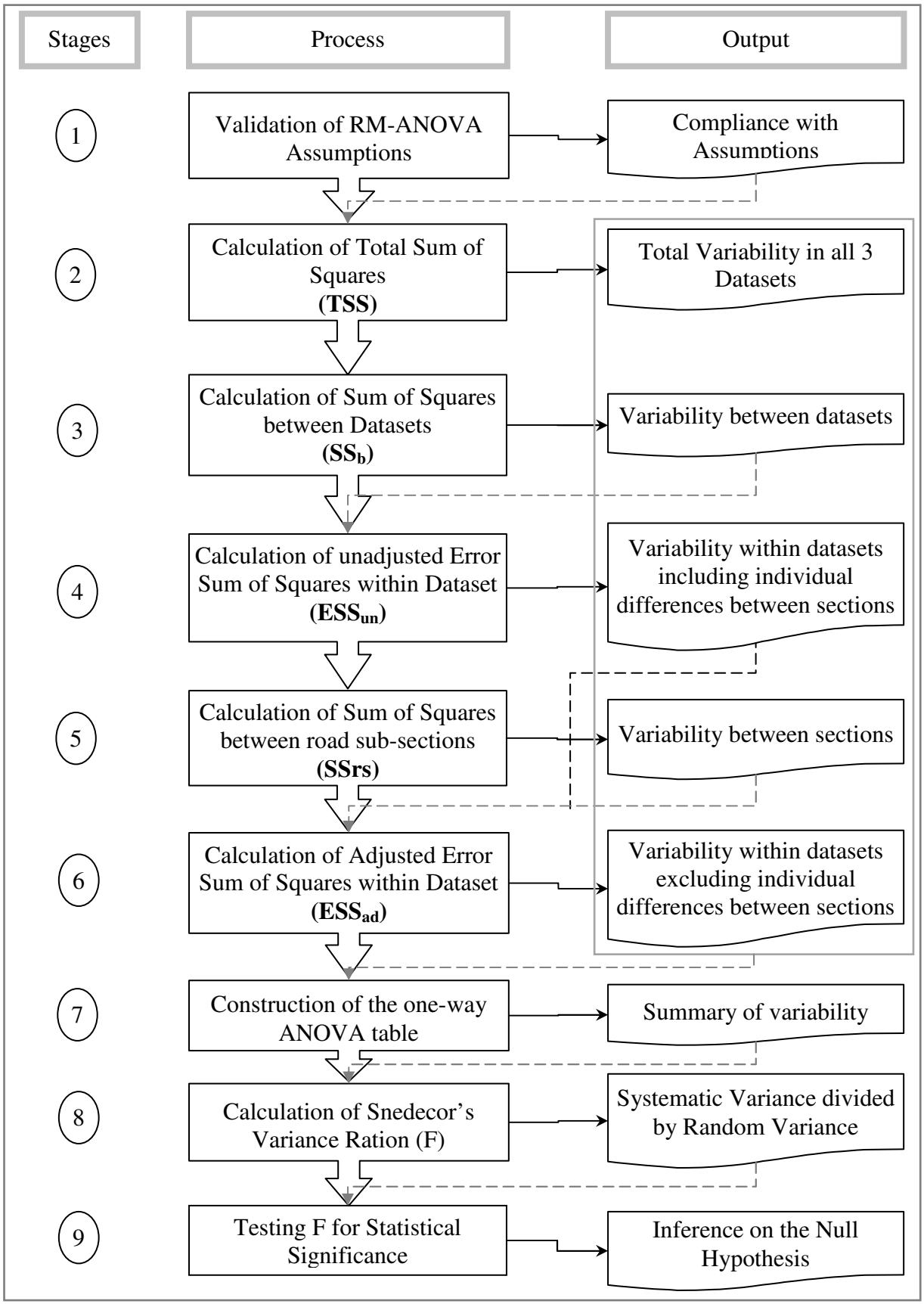

Figure B8-1: RM-ANOVA Calculation Stages

STAGE 1: Validation of Assumption of RM-ANOVA

Hypothesis tests using RM-ANOVA are based on the following assumptions: normality of the data samples, and sphericity which is the assumption that the differences between observations in each pair of samples have equal variances.

Considering the assumption of normality, it is apparent from the summary statistics given in Table 5.19 that the data sample is skewed with high excess kurtosis. To achieve normality the data set summarised in Table 5.19 was transformed using the Box Cox power transformation (Box and Cox, 1964 and Osborne, 2010) of the form

$$\Delta\mathrm{RUT}(\lambda) = \begin{cases} \frac{\Delta\mathrm{RUT}^{\lambda}-1}{\lambda * \mathrm{GM}^{\lambda-1}}; \text{if } \lambda \neq 0 \\ \mathrm{GM} * \mathrm{LOG}(\Delta\mathrm{RUT}); \text{if } \lambda = 0 \end{cases}$$

where ΔRUT is the annual incremental rut depth, GM is the geometric mean of the data sample and λ is the transformation variable that minimises the sum of squares of residuals. The values of λ and GM were determined for each of the three data samples and are given in Appendix B8. Summary statistics for the transformed data including skewness and excess kurtosis for the transformed data are given in Table B8-1.

Table B8-1: Descriptive Statistics for Normalised Data Samples

Statistics	2005 [1°C, 4%]	2004 [1.3°C, 51%]	2003 [2.7°C, -15%]
Mean	3.244	3.220	4.769
Median	3.274	3.233	4.950
Mode	3.126	2.958	2.574
Kurtosis	-0.381	-0.006	-0.932
Skewness	-0.076	-0.018	-0.151
Minimum	2.317	2.382	0.035
Maximum	4.265	4.196	9.073
Sample Size	177	177	177

The sphericity of the data which is the assumption that the variances of the differences between the samples are equal was investigated using Mauchly's test performed using SPSS software. The result of the test is shown in Table B8-2. Mauchly's test showed that the assumption of sphericity has been violated (Chi-Square = 390.458, $p < 0.001$) since significance of Mauchly's W is less than 0.05.

Table B8-2: Results of Mauchly's test for Sphericity

Mauchly's W	Approx. Chi-Square	Degrees of Freedom (DF)	Significance of Mauchly's W	Greenhouse-Geisser Epsilon[1]
0.107	390.458	2	<0.001	0.528

Note to Table B8-2

1. Greehouse Geisser Epsilon is used to adjust the degrees of freedom if sphericity is not satisfied.

Since the assumption of sphericity was violated, the number of degrees of freedom for determining the critical value of F (calculation Stage 8, see Figure B8-1) was adjusted by applying the Greenhouse Geisser Epsilon correction factor given in Table B8-2. The results of these adjustments are shown in Stage 7 of the calculation.

STAGE 2: Calculation of Total Sum of Squares (TSS)

The total sum of squares (TSS) represents the total variability present in the three samples (2005 [1^{o}C, 4%], 2004 [1.3^{o}C, 51%], 2003 [2.7^{o}C, -15%]). In calculating the TSS, the difference between each observation and the overall mean was computed. These differences were then squared and added together to give TSS value of 1207.921.

STAGE 3: Calculation of Sum of Squares between Samples (SSb)

The Sum of Squares between Samples (SS_b) was obtained by computing the difference between each sample mean and the overall mean. The differences were then squared, multiplied by the number o observations in each sample (177) and then added together to give a SS_b value of 278.702.

STAGE 4: Calculation of the Unadjusted Error Sum of Squares (ESSun)

The Unadjusted Error Sum of Squares (ESSun) represents random error including the individual difference that may exist between road sub-sections. Within the context of this study, individual differences between road sub-sections may have arisen due to differences in the susceptibility to asphalt surface rutting of each road sub-section. These differences in susceptibility may be because of factors other than hot and dry climate. Such factors could include the geometry of the road section, the speed of heavy vehicles on the road section, the type of asphalt material specific to the section of road, and the traffic loading on the road section.

The ESS_{un} was obtained by computing the difference between each observation and its respective sample mean. The differences were then squared and added together to give a ESS_{un} value of 929.218.

STAGE 5: Calculation of Sum of Squares between Road Sub-sections (SSrs)

The Sum of Squares between Road Sub-sections (SS_{rs}) represents the variability in annual incremental rut depths amongst the 177 road sub-sections. This variability is due to individual differences between road sub-sections. SS_{rs} was calculated by computing the difference between the mean incremental annual rut depth at a particular road sub-section and the overall mean. This difference was then squared and multiplied by three which is the number of times that measurements were taken at that site. The process is repeated for the 177 road sub-sections and the results for all the sub-sections added together to give a SS_{rs} value of 363.520.

STAGE 6: Calculation of the Adjusted Error Sum of Squares (ESSad)

The process of the computing the adjusted Error Sum of Squares (ESS_{ad}) removes the individual differences associated with some road sections being more susceptible to rutting than other sections. This ensures that the comparison of the three data samples is based on the annual systematic differences associated with annual climate variability and random errors associated with sampling at the three different years. ESS_{ad} is computed as follows:

$$ESS_{ad} = ESS_{un} - SS_{rs}$$

This gives an ESS_{ad} value of 565.698. About 39% (363.520 units out of 929.218 units) of the variance within each sample (error variance) reflects the fact that in a given year some road sub-sections in the study area are more susceptible to asphalt surface rutting than others. About 61% (363.520 units out of 929.218 units) is due to the random variations attributable to sampling at the three different periods (2005, 2004, and 2003).

STAGE 7: Analysis of Variance Table

The ANOVA Table B8-2 summarises the information on the variability present in the three samples. The adjusted degrees of freedom were obtained by multiplying the unadjusted degrees of freedom using the Greenhouse Geisser factor (0.528) derived in Stage 1. The adjustment to the degrees of freedom was necessary to correct for violation of the assumption of sphericity.

Table B8-2: Summary of Sources of Variability

Source of Variation	DF (Unadjusted)[a]	DF (Adjusted)	Sum of Squares	Mean Sum of Squares (Variance)
Between Samples (**SS_b**)	2[b]	1.056	278.702	263.922[g]
Within Samples-Unadjusted (**ESS_{un}**)	528[c]	-	929.218	-
Between Sub-sections (**SS_{rs}**)	176[d]	-	363.520	-
Within Samples-Adjusted (**ESS_{ad}**)	352[e]	185.856	565.698	3.044[h]
Total Variance (**TSS**)	530[f]	-	1207.921	-

Notes

a. DF is Degrees of Freedom
b. Unadjusted DF for between samples variability given as the number of samples minus 1.
c. Unadjusted DF for unadjusted within samples variability given as the number of observations minus the number of samples

d. Unadjusted DF for between sub-section variability calculated as the number of road sub-sections minus 1.
e. Unadjusted DF for the adjusted within samples variability given as the number of samples minus 1 multiplied by the number of sub-sections minus 1
f. Unadjusted DF for the total variance calculated as the total number of observations minus 1.
g. Systematic variance in annual incremental rut depths between the three years in which data was recorded
h. Unsystematic variance or random error present in each year

STAGE 8: Calculation of Snedecor's Variance Ratio F

Within the context of this study, the F ratio reflects the systematic variance (MSC) in annual incremental rut depths between the three years divided by the unsystematic variance or random error (MSE_{ad}) present in each year which cannot be explained by differences in annual incremental rut depths between the 177 road sub-sections.

F = (MSC/MSEad) = (263.922/3.044) = 86.702

STAGE 9: Testing F for Statistical Significance

At the 0.05 level the critical F(1.056, 185.856) = 3.891. The calculated F(86.702) is however greater than the Critical F and falls within the rejection region as illustrated in Figure , hence there is a significant difference in annual incremental rut depths recorded in the three years (2005 [1^{o}C, 4%], 2004 [1.3^{o}C, 51%], 2003 [2.7^{o}C, -15%]).

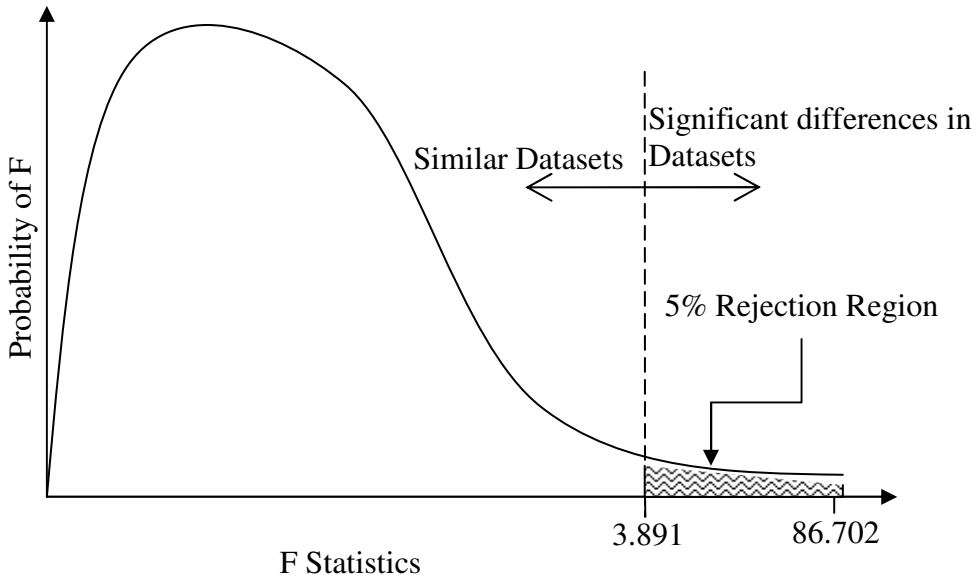

Figure B8-2: Plots of differences between samples

Whilst the findings confirm significant difference between the three data samples, the specific aim is to determine the source of this difference. A multiple paired samples Student's t test was undertaken using SPSS. The results are reported in B8-3. The test is used to investigate if the difference in means between pairs of data is equal to zero or not by determining the probability of the corresponding t statistics. For a given pair of data if the probability (p) is greater than significance level, then it can be inferred that data pair are similar and if the probability (p) is less than the significant level, then the data pair are significantly different.

Table B8-3: Multiple Paired Samples Student's t Tests

Paired Samples	**Paired Differences**					**t**	**DF**	**P-value**
	Mean	**Std. Deviation**	**Std. Error Mean**	**95% Confidence Interval of the Difference**				
				Lower	**Upper**			
Pair 1 2005 – 2004	0.024	0.422	0.032	-0.038	0.087	0.764	176	0.446
Pair 2 2005 – 2003	-1.525	2.183	0.164	-1.848	-1.201	-9.292	176	<0.001
Pair 3 2004 – 2003	-1.549	2.168	0.163	-1.870	-1.227	-9.505	176	<0.001

To that end, assuming a 0.05 significance level, there are significant differences between paired samples 2005-2003 (Pair 2) and 2004-2003 (Pair 3); that is, the most significant difference is between 2003 annual incremental rut depth samples and the other two samples. The null hypothesis Ho for the RM-ANOVA is therefore rejected in favour of the alternative hypothesis Ha that the mean of annual incremental rut depths observed in 2004 and 2005 differ from that recorded in 2003 due to the hot dry summer recorded in that year.

APPENDIX C ESTIMATED MODEL COEFFICIENTS

This appendix includes the following:

Appendix C1 WinBUGS Model Code in BUGS Language for Bayesian Model 1N

```
Model{

    # LEVEL 1 MODEL FOR THE LIKELIHOOD.
    For (k in 1:1994) {# Loop over each k observation on each road sub-section, asphalt surfacing
                       type and year.

                       # Stochastic models for Softening Point (SP), Voids in Mix (VIM), and
                       Annual Incremental Rut Depth (dRUT).
                       SP[k] ~ dnorm(mu.SP[k], tau.SP)
                       VIM[k] ~ dnorm(mu.VIM[k], tau.VIM)
                       dRUT[k] ~ dnorm(mu.dRUT[k], tau)

                       mu.SP[k] <- Alpha[1, SURID[k]]*log(AGE[k]+0.001) + Alpha[2, SURID[k]]
                       # Equation 4.2 in Chapter 4.

                       mu.VIM[k] <- Eta[1, SURID[k]]*log(AGE[k]+0.001) + Eta[2, SURID[k]] #
                       Equation 4.3 in Chapter 4.

                       mu.dRUT[k] <- pow(YE4[k], Beta[1, SURID[k]])*pow(sh[k], Beta[2,
                       SURID[k]]) * pow( G[k], Beta[ 3 , SURID[k]] ) * pow( HS[k], Beta[ 4,
                       SURID[k]]) *pow( (VIM[k]/SP[k]), Beta[5, SURID[k]])* (H0[k]  + Beta[6,
                       SURID[k]]*TPmax[SURID[k]]*H1[k])+ b[SURID[k]] # Equation 4.5 in
                       Chapter 4.
    }
    #END OF LEVEL 1 MODEL

    # LEVEL 2 MODEL FOR HYPER PARAMETERS
    for ( j in 1:3 )  { # Loop over each asphalt surfacing material type

                        #Equation 4.17 in Chapter 4
                        Beta[ 1, j ] ~ dnorm( Beta.mu1, Beta.tau1 )
                        Beta[ 2, j ] ~ dnorm( Beta.mu2, Beta.tau2 )
                        Beta[ 3, j ] ~ dnorm( Beta.mu3, Beta.tau3 )
                        Beta[ 4, j ] ~ dnorm( Beta.mu4, Beta.tau4 )
                        Beta[ 5, j ] ~ dnorm( Beta.mu5, Beta.tau5 )
                        Beta[ 6, j ] ~ dnorm( Beta.mu6, Beta.tau6 )
                        Alpha[1, j] ~ dnorm( Alpha.mu1, Alpha.tau1 )
                        Alpha[2, j] ~ dnorm( Alpha.mu2, Alpha.tau2 )
                        Eta[1, j] ~ dnorm( Eta.mu1, Eta.tau1 )
                        Eta[2, j] ~ dnorm( Eta.mu2, Eta.tau2 )

                        # Equation 6.1 stochastic representation of the error term.
                        b[j] ~ dnorm(0, tau.b)
    }
    #END OF LEVEL 2 MODEL

    # PRIOR DISTRIBUTIONS [Given in Table 6.1 of this Chapter ( Chapter  6)]
    #Prior Distribution of Model Coefficients
    Beta.mu1 ~ dnorm(1, 0.001)
    Beta.mu2 ~ dnorm(-0.78, 0.001)
    Beta.mu3 ~ dnorm(0.5, 0.001)
    Beta.mu4 ~ dnorm(0.71, 0.001)
    Beta.mu5 ~ dnorm(0, 0.001)
    Beta.mu6 ~ dnorm(0, 0.001 )
```

```
 Alpha.mu1 ~ dnorm(2.7, 0.01)
 Alpha.mu2 ~ dnorm(60, 0.01)
 Eta.mu1 ~ dnorm(-0.6, 0.01)
 Eta.mu2 ~ dnorm(6.8, 0.01)

  #Prior Distribution of Precision Parameters
Beta.tau1 ~ dgamma(0.1, 0.1)
Beta.tau2 ~ dgamma(0.1, 0.1)
Beta.tau3 ~ dgamma(0.1, 0.1)
Beta.tau4 ~ dgamma(0.1, 0.1)
Beta.tau5 ~ dgamma(0.1, 0.1)
Beta.tau6 ~ dgamma(0.1, 0.1)
Alpha.tau1 ~ dgamma(0.1, 0.1)
Alpha.tau2 ~ dgamma(0.1, 0.1)
Eta.tau1 ~ dgamma(0.1, 0.1)
Eta.tau2 ~ dgamma(0.1, 0.1)
tau ~ dgamma(0.001, 0.001)
tau.b ~ dgamma(0.001, 0.001)
tau.SP ~ dgamma(0.1, 0.1)
tau.VIM ~ dgamma(0.1, 0.1)
# END OF DEFINITION OF PRIOR DISTRIBUTIONS

# DEFINITION OF VARIANCE, STANDARD DEVIATION AND CORRELATION

S2 <- 1/tau       #Overall variance
S2.b <- 1/tau.b #Variance between surfacing samples (S2.b)

#Calculation of Total Variability
TS2 <- (S2 + S2.b)

S <- sqrt( S2)
S.b <- sqrt( S2.b)

#Calculation of Within Sub-section Correlation
R.Y <- (S2.b)/TS2

#CALCULATION OF SAMPLE VARIANCE AND BAYESIAN VERSION R-SQUARED
for ( i in 1:1994)   { #loop over each observation on each road section on each year
                        VdRUT[i] <- dRUT[i] - mean(dRUT[])
}
SdRUT <- inprod( VdRUT[ ], VdRUT[ ] )/(1994-1)

R2B < - 1 - (S2) / (SdRUT)

# CALCULATION OF POSTERIOR PROBABILITIES OF POSITIVE MODEL
COEFFICIENTS
for (j in 1:3) { #loop over each Surface Material Type
                    P.Beta[ 1, j] <- step(Beta[ 1, j])
                    P.Beta[ 2, j] <- step(Beta[ 2, j])
                    P.Beta[ 3, j] <- step(Beta[ 3, j])
                    P.Beta[ 4, j] <- step(Beta[ 4, j])
                    P.Beta[ 5, j] <- step(Beta[ 5, j])
```

```
                    P.Beta[ 6, j] <- step(Beta[ 6, j])
                    P.Alpha[ 1, j] <- step(Alpha[ 1, j])
                    P.Alpha[ 2, j] <- step(Alpha[ 2, j])
                    P.Eta[ 1, j] <- step(Eta[ 1, j])
                    P.Eta[ 2, j] <- step(Eta[ 2, j])
    }
}
#END OF MODEL CODE
```

DATA
#DEFINITION OF OBSERVED DATA SAMPLE

#The data matrix below gives a random sample of 12 observations out of 1994 observations used in the modelling.

OBSNO[ ]	SECID[ ]	SURID[ ]	YEAR[ ]	H0[ ]	H1[ ]	dRUT[ ]	YE4[ ]	sh[ ]	G[ ]	HS[ ]	VIM[ ]	AGE[ ]	SP[ ]	TPmax[ ]
1	351	1	1	1	0	3.0	1.3	80.8	0.1	194.0	3.8	3.7	52.6	56.3
2	357	1	1	1	0	2.8	1.3	80.8	0.9	232.0	1.4	13.3	77.1	56.3
172	2053	1	2	0	1	1.7	1.1	73.5	0.9	202.0	1.1	36.8	78.0	57.7
440	2083	1	3	1	0	0.5	1.1	73.0	2.2	218.0	1.2	37.8	78.0	56.4
881	3294	2	1	1	0	0.8	1.1	89.2	0.2	206.0	1.5	11.8	76.5	56.5
1027	7172	2	2	0	1	4.3	0.6	59.0	0.6	385.0	1.2	12.6	78.0	56.8
1271	3786	2	3	1	0	1.4	1.4	84.2	0.2	270.0	1.0	7.3	75.0	55.7
1365	4761	2	3	1	0	0.5	0.8	75.3	0.5	299.0	1.2	20.8	78.0	56.3
1561	3210	2	4	1	0	2.6	0.7	84.4	1.8	215.0	1.1	24.8	78.0	55.4
1712	4535	2	5	1	0	1.3	1.6	98.0	0.2	420.0	1.5	12.3	78.0	58.0
1782	6235	3	3	1	0	2.8	1.9	81.4	1.4	180.0	5.4	2.5	66.4	57.1
1811	6446	3	3	1	0	1.0	1.9	81.4	1.7	150.0	5.2	2.5	66.7	57.1
1994	7363	3	4	1	0	2.1	1.2	72.1	1.3	225.0	4.2	2.4	69.1	56.0

END
#END OF DATA DEFININATION

INITS
#DEFINITION OF INITIAL VARIABLES FOR MULTIPLE (3) CHAINS

#Initial Values for Chain 1
list(tau = 1, tau.b = 1.1, tau.SP = 1.2, tau.VIM = 1.3, Beta.mu1 = 2, Beta.mu2 = -1, Beta.mu3 = 0.1 Beta.mu4 = 0.1, Beta.mu5 = 0.1, Alpha.mu1 = 2, Alpha.mu2 = 50, Eta.mu1 = -0.5, Eta.mu2 = 6, Beta.tau1 = 1, Beta.tau2 = 1, Beta.tau3 = 1, Beta.tau4 = 1, Beta.tau5 = 1, Theta.mu1 = 5, Theta.tau1 = 1.4, Alpha.tau1 = 1.6, Alpha.tau2 = 1.7, Eta.tau1 = 1.8, Eta.tau2 = 1.9)

#Initial Values for Chain 2
list(tau = 2, tau.b = 1.5, tau.SP = 1.1, tau.VIM = 1.3, Beta.mu1 = 3, Beta.mu2 = -4, Beta.mu3 = 0.5 Beta.mu4 = 0.7, Beta.mu5 = 0.4, Beta.mu6 = 0.4, Alpha.mu1 = 2.3, Alpha.mu2 = 53, Eta.mu1 = -0.6, Eta.mu2 = 9, Beta.tau1 = 1.3, Beta.tau2 = 1.6, Beta.tau3 = 4, Beta.tau4 = 2, Beta.tau5 = 3, Theta.mu1 = 1.2, Theta.tau1 = 1.4, Alpha.tau1 = 1.6, Alpha.tau2 = 1.7, Eta.tau1 = 1.8, Eta.tau2 = 1.9)

#Initial Values for Chain 3
list(tau = 1, tau.b = 1.1, tau.SP = 1.2, tau.VIM = 1.3, Beta.mu1 = 2, Beta.mu2 = -1, Beta.mu3 = 0.1 Beta.mu4 = 0.1, Beta.mu5 = 0.1, Alpha.mu1 = 2, Alpha.mu2 = 50, Eta.mu1 = -0.5, Eta.mu2 = 6,

```
Beta.tau1 = 1, Beta.tau2 = 1, Beta.tau3 = 1, Beta.tau4 = 1, Beta.tau5 = 1, Theta.mu1 = 4,
Theta.tau1 = 1.4, Alpha.tau1 = 1.6, Alpha.tau2 = 1.7, Eta.tau1 = 1.8, Eta.tau2 = 1.9)
```

Appendix C2 Estimated Model Coefficients for Model Structure 1

Table C2-1: Summary Statistics for Estimated Model Coefficient for Model 1D (Model Structure 1 and Double Exponential Likelihood)

Surfacing Group	Nodes	Mean	SD	MC Error	2.50%	Median	97.50%	P0	Start	Sample
DBM	β_1	0.7	0.142	2.80E-03	0.394	0.669	0.961	1.0	50,001	150,000
	β_2	-2.2	0.364	1.40E-02	-2.83	-2.182	-1.475	0.0	50,001	150,000
	β_3	0.2	0.076	1.50E-03	0.074	0.197	0.37	1.0	50,001	150,000
	β_4	1.5	0.245	9.30E-03	0.984	1.462	1.905	1.0	50,001	150,000
	β_5	0.1	0.195	7.20E-03	-0.309	0.094	0.466	0.7	50,001	150,000
	β_6	0.5	0.342	1.10E-02	0.158	0.432	1.381	1.0	50,001	150,000
HRA	β_1	6.6	1.962	7.40E-02	3.751	6.282	11.31	1.0	50,001	150,000
	β_2	-1.3	0.667	2.50E-02	-2.866	-1.25	-0.246	0.0	50,001	150,000
	β_3	0.1	0.058	8.20E-04	0.002	0.043	0.215	1.0	50,001	150,000
	β_4	0.8	0.298	1.10E-02	0.188	0.797	1.364	1.0	50,001	150,000
	β_5	0.9	0.373	1.40E-02	0.171	0.933	1.594	1.0	50,001	150,000
	β_6	0	0.014	1.50E-04	-0.016	0.007	0.039	0.8	50,001	150,000
TSCS	β_1	2.1	0.721	1.90E-02	0.699	2.106	3.565	1.0	50,001	150,000
	β_2	-1.5	0.419	1.50E-02	-2.408	-1.421	-0.746	0.0	50,001	150,000
	β_3	0.2	0.254	4.10E-03	-0.123	0.197	0.871	0.9	50,001	150,000
	β_4	1.3	0.295	1.10E-02	0.768	1.325	1.929	1.0	50,001	150,000
	β_5	1.1	0.277	8.90E-03	0.572	1.132	1.647	1.0	50,001	150,000
	β_6	2.4	2.982	7.80E-02	0.375	1.513	10.16	1.0	50,001	150,000

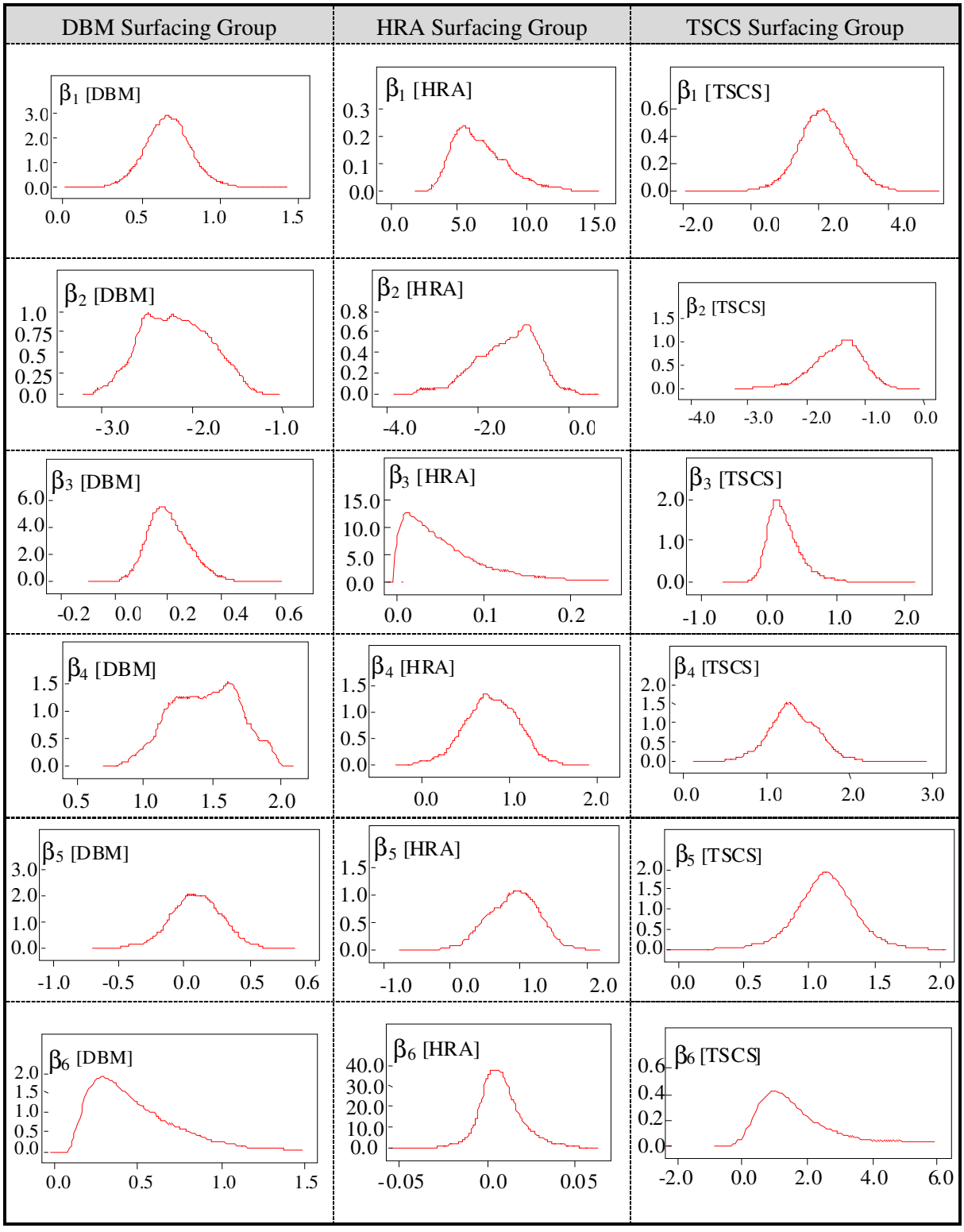

Figure C2-1: Estimated Distribution of Model Coefficients for Model 1D (Model Structure 1 and Double Exponential Likelihood)

Table C2-2: Summary Statistics for Estimated Model Coefficient for Model 1N (Model Structure 1 and Normal Likelihood)

Surfacing Group	Nodes	Mean	SD	MC Error	2.50%	Median	97.50%	P0	Start	Sample
DBM	β_1	0.6	0.096	2.60E-03	0.388	0.557	0.764	1.0	50,001	150,000
	β_2	-0.9	0.211	8.00E-03	-1.388	-0.93	-0.575	0.0	50,001	150,000
	β_3	0	0.03	2.00E-04	-0.051	0.006	0.066	0.6	50,001	150,000
	β_4	0.7	0.102	3.80E-03	0.554	0.741	0.949	1.0	50,001	150,000
	β_5	0	0.09	3.20E-03	-0.22	-0.03	0.125	0.4	50,001	150,000
	β_6	0.1	0.036	1.20E-03	0.063	0.1	0.196	1.0	50,001	150,000
HRA	β_1	3.8	0.833	2.90E-02	2.669	3.662	5.586	1.0	50,001	150,000
	β_2	0.5	0.5	1.90E-02	-0.35	0.487	1.636	0.9	50,001	150,000
	β_3	0.1	0.056	6.10E-04	0.003	0.062	0.208	1.0	50,001	150,000
	β_4	0.3	0.228	8.50E-03	-0.157	0.29	0.708	0.9	50,001	150,000
	β_5	1.5	0.475	1.80E-02	0.722	1.477	2.581	1.0	50,001	150,000
	β_6	0	0.008	1.30E-04	-0.008	0.009	0.023	0.9	50,001	150,000
TSCS	β_1	0.8	1.516	4.60E-02	-3.43	1.105	3.012	0.8	50,001	150,000
	β_2	-1.4	0.865	3.20E-02	-3.781	-1.164	-0.189	0.0	50,001	150,000
	β_3	0.3	0.478	1.00E-02	-0.337	0.172	1.512	0.7	50,001	150,000
	β_4	1.1	0.555	2.10E-02	0.366	0.986	2.694	1.0	50,001	150,000
	β_5	1	0.516	1.70E-02	0.157	0.942	2.306	1.0	50,001	150,000
	β_6	1.9	5.001	9.80E-02	0.189	0.897	9.918	1.0	50,001	150,000

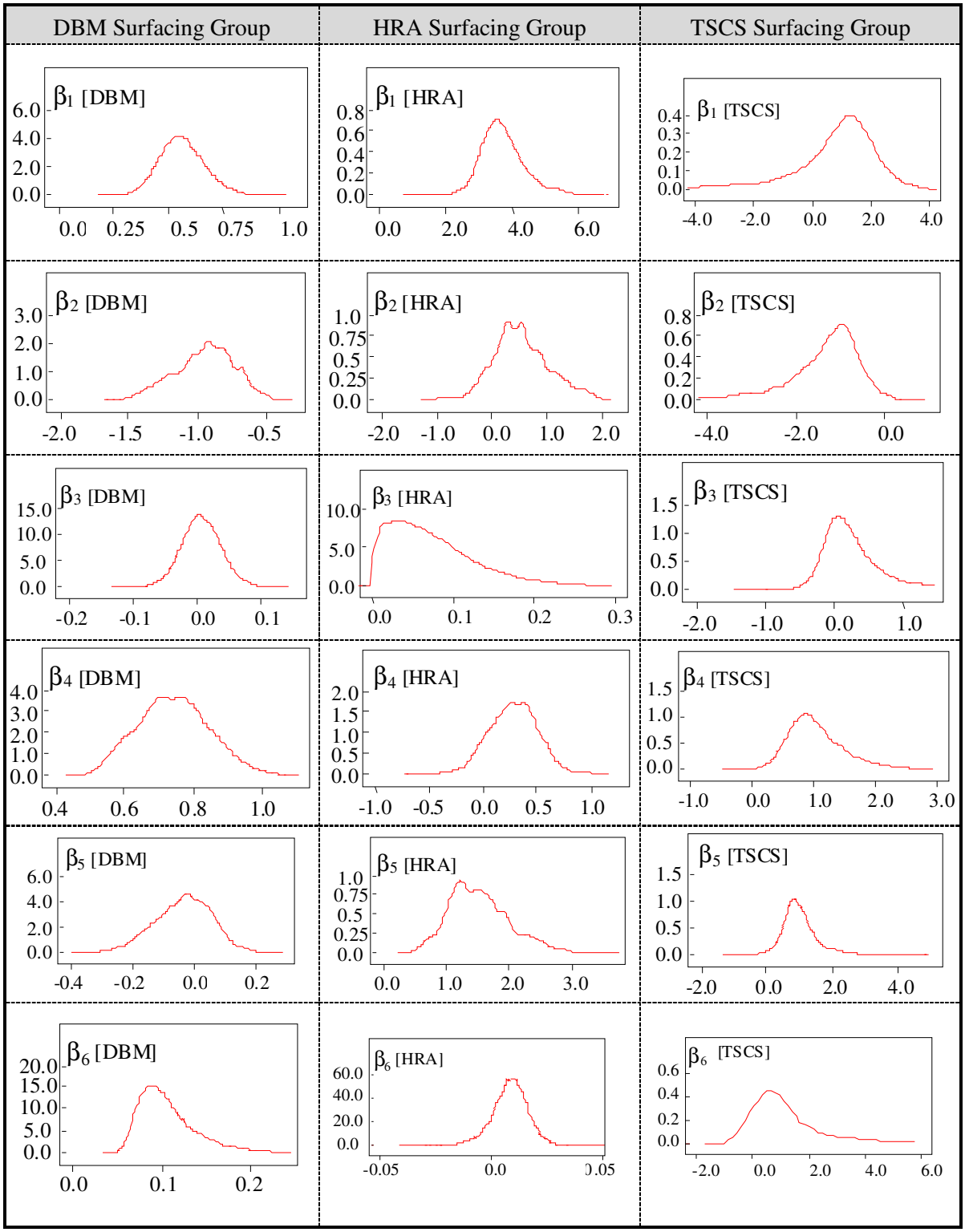

Figure C2-2: Estimated Distribution of Model Coefficients for Model 1N (Model Structure 1 and Normal Likelihood)

Table C2-3: Summary Statistics for Estimated Model Coefficient for Model 1S (Model Structure 1 and Students t Likelihood)

Surfacing Group	Nodes	Mean	SD	MC Error	2.50%	Median	97.50%	P0	Start	Sample
DBM	β_1	3.6	0.817	3.80E-02	1.291	3.783	4.68	1.0	210,001	170,000
	β_2	-4.8	0.825	4.10E-02	-5.848	-4.868	-2.483	0.0	210,001	170,000
	β_3	0.8	0.29	1.20E-02	0.163	0.851	1.384	1.0	210,001	170,000
	β_4	3.2	0.722	3.60E-02	0.591	3.304	3.814	1.0	210,001	170,000
	β_5	0.9	0.377	1.80E-02	-0.301	0.91	1.34	0.9	210,001	170,000
	β_6	40.2	41.47	2.00E+00	4.969	24.34	162.3	1.0	210,001	170,000
HRA	β_1	2.1	0.334	1.20E-02	1.481	2.071	2.795	1.0	210,001	170,000
	β_2	-5.4	0.567	2.70E-02	-6.56	-5.351	-4.313	0.0	210,001	170,000
	β_3	0.1	0.069	5.90E-04	0.004	0.076	0.26	1.0	210,001	170,000
	β_4	3.4	0.33	1.60E-02	2.71	3.398	4.031	1.0	210,001	170,000
	β_5	1	0.311	1.50E-02	0.399	0.918	1.631	1.0	210,001	170,000
	β_6	30.4	28.41	1.20E+00	6.088	22.04	108.8	1.0	210,001	170,000
TSCS	β_1	2.3	1.024	4.50E-02	0.3	2.267	4.215	1.0	210,001	170,000
	β_2	-4.7	1.04	5.10E-02	-6.034	-5.027	-1.604	0.0	210,001	170,000
	β_3	0.7	0.592	2.30E-02	-0.231	0.567	2.197	0.9	210,001	170,000
	β_4	3	0.537	2.60E-02	1.489	3.15	3.717	1.0	210,001	170,000
	β_5	1.1	0.26	1.10E-02	0.581	1.054	1.582	1.0	210,001	170,000
	β_6	51.2	87.03	3.40E+00	4.267	22.57	289.7	1.0	210,001	170,000

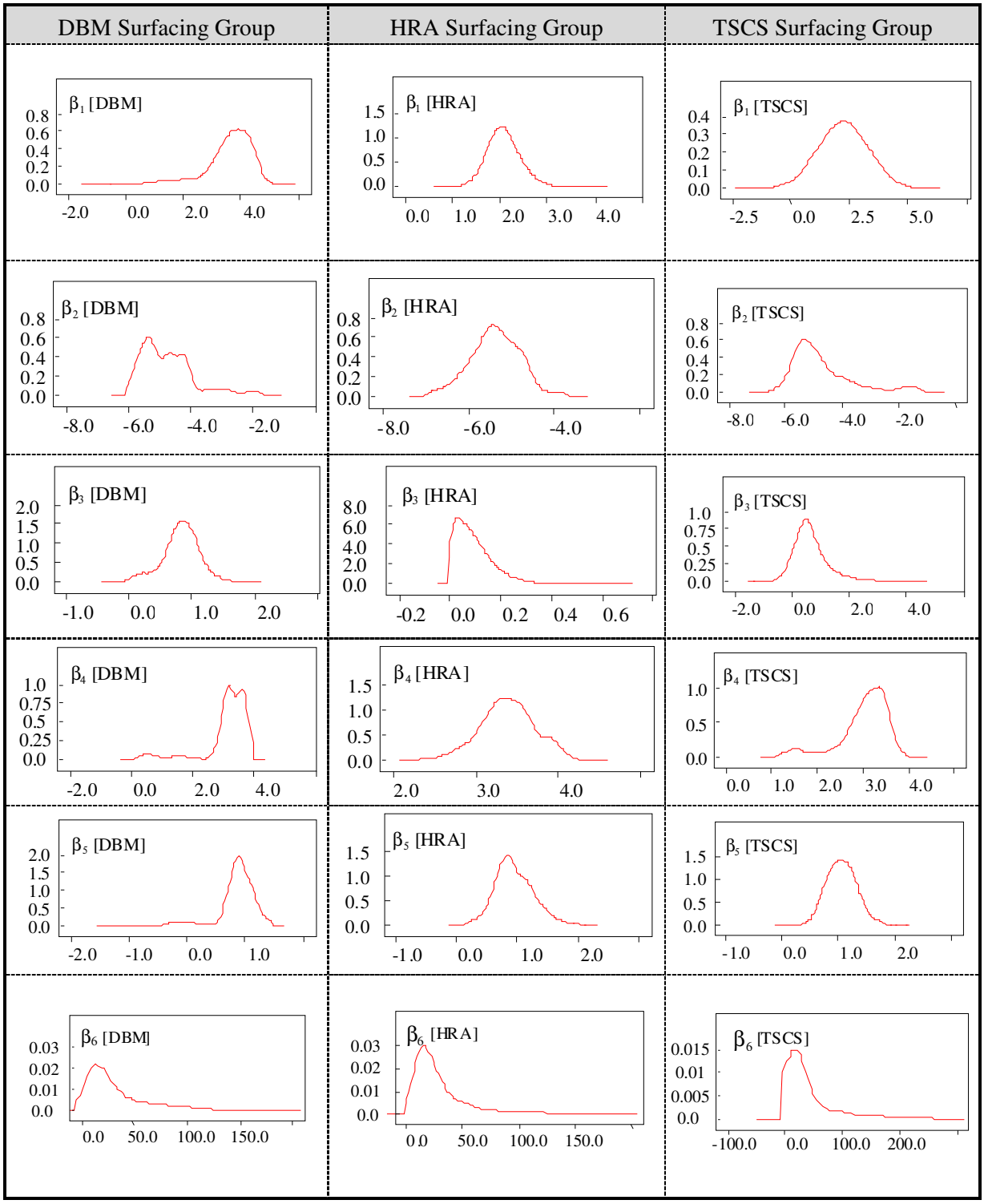

Figure C2-3: Estimated Distribution of Model Coefficients for Model 1S (Model Structure 1 and Students t Likelihood)

Appendix C3 Estimated Model Coefficients for Model Structure 2

Table C3-1: Summary Statistics for Estimated Model Coefficient for Model 2D (Model Structure 2 and Double Exponential Likelihood)

Surfacing Group	Nodes	Mean	SD	MC Error	2.50%	Median	97.50%	P0	Start	Sample
DBM	β_1	0.6	0.148	3.40E-03	0.343	0.636	0.925	1.0	100,001	150,000
	β_2	-2	0.416	1.60E-02	-2.804	-2.039	-1.228	0.0	100,001	150,000
	β_3	0.2	0.073	1.50E-03	0.061	0.181	0.349	1.0	100,001	150,000
	β_4	1.3	0.263	1.00E-02	0.839	1.37	1.837	1.0	100,001	150,000
	β_5	0	0.178	6.50E-03	-0.319	0.027	0.371	0.6	100,001	150,000
	β_6	0.7	0.137	4.90E-03	0.477	0.716	1.024	1.0	100,001	150,000
HRA	β_1	7.6	2.326	8.90E-02	3.855	7.471	12.24	1.0	100,001	150,000
	β_2	-1.7	0.808	3.10E-02	-3.356	-1.66	-0.371	0.0	100,001	150,000
	β_3	0.1	0.059	7.60E-04	0.002	0.043	0.216	1.0	100,001	150,000
	β_4	0.8	0.308	1.20E-02	0.229	0.837	1.417	1.0	100,001	150,000
	β_5	0.8	0.33	1.20E-02	0.117	0.756	1.474	1.0	100,001	150,000
	β_6	-3.1	5.491	1.80E-01	-15.21	-1.159	0.093	0.1	100,001	150,000
TSCS	β_1	2.9	1.401	5.00E-02	0.647	2.694	6.5	1.0	100,001	150,000
	β_2	-1.6	0.525	2.00E-02	-2.927	-1.494	-0.778	0.0	100,001	150,000
	β_3	0.2	0.273	5.30E-03	-0.192	0.16	0.867	0.8	100,001	150,000
	β_4	1.3	0.327	1.20E-02	0.783	1.323	2.063	1.0	100,001	150,000
	β_5	1.2	0.278	9.10E-03	0.578	1.193	1.725	1.0	100,001	150,000
	β_6	1.4	0.465	1.70E-02	0.746	1.297	2.67	1.0	100,001	150,000

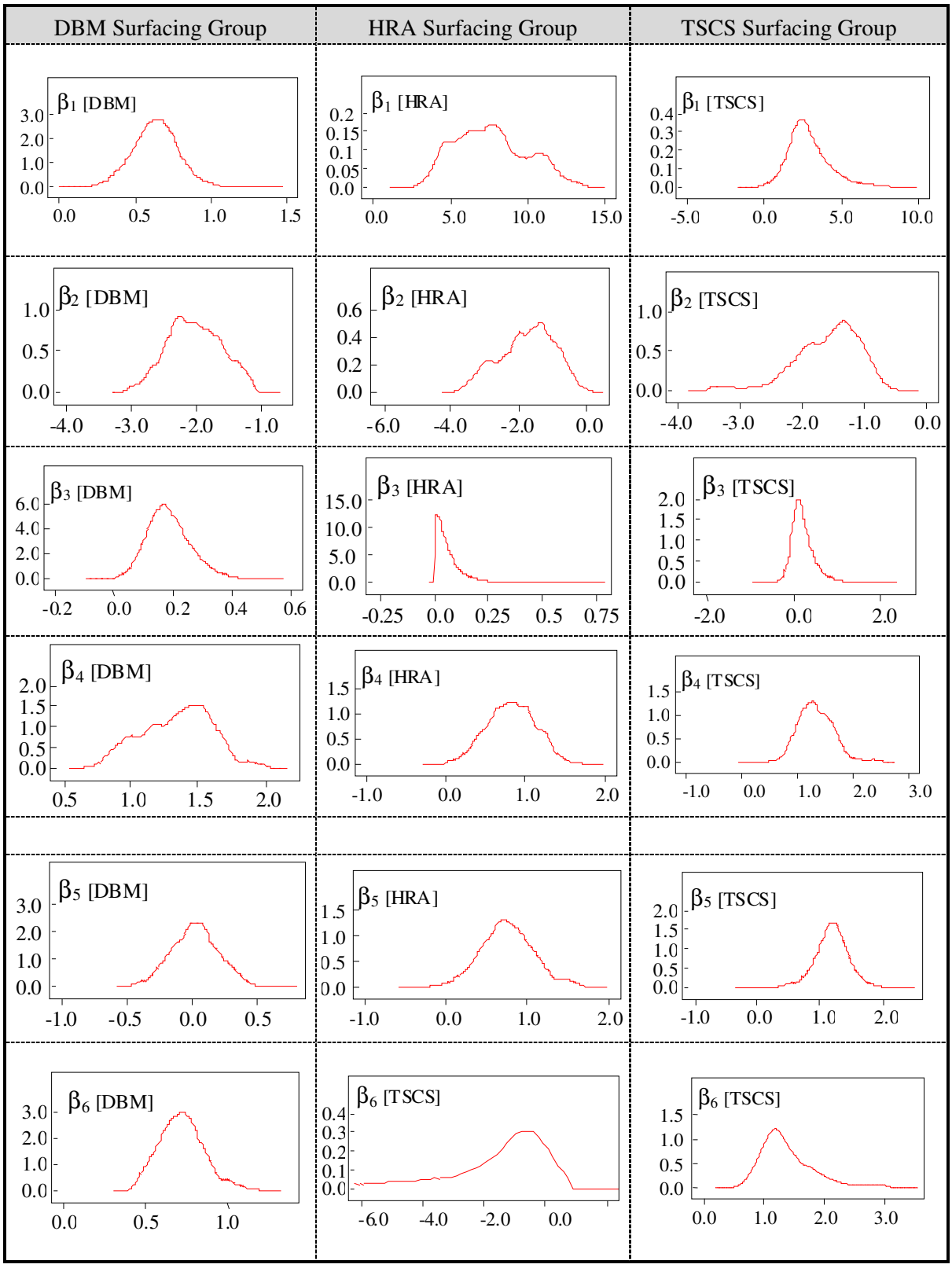

Figure C3-1: Estimated Distribution of Model Coefficients for Model 2D (Model Structure 2 and Double Exponential Likelihood)

Table C3-2: Summary Statistics for Estimated Model Coefficient for Model 2L (Model Structure 2 and Lognormal Likelihood)

Surfacing Group	Nodes	Mean	SD	MC Error	2.50%	Median	97.50%	P0	Start	Sample
DBM	β_1	0.245	0.092	3.10E-03	0.106	0.232	0.45	1.0	100,001	150,000
	β_2	-0.436	0.219	8.40E-03	-0.89	-0.405	-0.098	0.0	100,001	150,000
	β_3	0.040	0.023	4.20E-04	0.002	0.038	0.093	1.0	100,001	150,000
	β_4	0.273	0.101	3.90E-03	0.127	0.251	0.495	1.0	100,001	150,000
	β_5	-0.050	0.059	2.10E-03	-0.171	-0.048	0.065	0.2	100,001	150,000
	β_6	0.198	0.06	2.20E-03	0.104	0.191	0.332	1.0	100,001	150,000
HRA	β_1	0.520	0.237	8.40E-03	0.281	0.473	1.151	1.0	100,001	150,000
	β_2	-0.045	0.058	2.10E-03	-0.167	-0.04	0.064	0.2	100,001	150,000
	β_3	0.010	0.01	1.60E-04	0	0.007	0.036	1.0	100,001	150,000
	β_4	0.057	0.049	1.80E-03	-0.033	0.056	0.161	0.9	100,001	150,000
	β_5	0.111	0.1	3.80E-03	-0.038	0.095	0.385	0.9	100,001	150,000
	β_6	0.079	0.019	4.20E-04	0.045	0.078	0.117	1.0	100,001	150,000
TSCS	β_1	0.940	0.476	1.20E-02	0.288	0.853	2.08	1.0	100,001	150,000
	β_2	-0.676	0.266	9.50E-03	-1.332	-0.633	-0.282	0.0	100,001	150,000
	β_3	0.034	0.138	1.50E-03	-0.199	0.02	0.354	0.6	100,001	150,000
	β_4	0.334	0.198	7.10E-03	0.017	0.304	0.792	1.0	100,001	150,000
	β_5	0.140	0.216	7.20E-03	-0.227	0.118	0.604	0.7	100,001	150,000
	β_6	0.490	0.184	5.40E-03	0.211	0.467	0.903	1.0	100,001	150,000

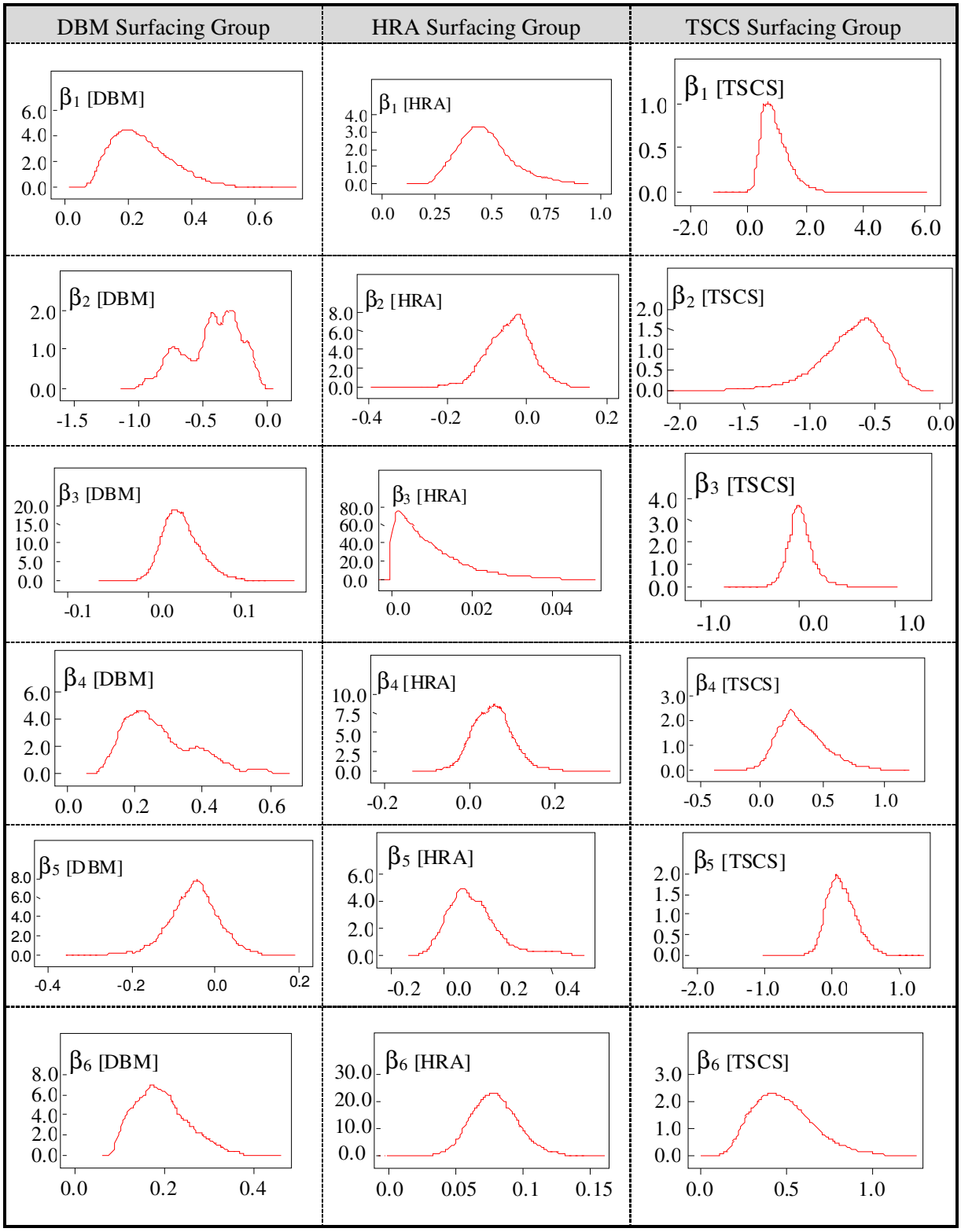

Figure C3-2: Estimated Distribution of Model Coefficients for Model 2L (Model Structure 2 and Lognormal Likelihood)

Table C3-3: Summary Statistics for Estimated Model Coefficient for Model 2N (Model Structure 2 and Normal Likelihood)

Surfacing Group	Nodes	Mean	SD	MC Error	2.50%	Median	97.50%	P0	Start	Sample
DBM	β_1	0.536	0.104	3.10E-03	0.343	0.532	0.75	1.0	100,001	150,000
	β_2	-0.884	0.244	9.30E-03	-1.358	-0.868	-0.426	0.0	100,001	150,000
	β_3	0.006	0.028	2.10E-04	-0.049	0.005	0.063	0.6	100,001	150,000
	β_4	0.711	0.125	4.80E-03	0.484	0.703	0.963	1.0	100,001	150,000
	β_5	-0.043	0.089	3.20E-03	-0.225	-0.044	0.124	0.3	100,001	150,000
	β_6	0.407	0.075	2.70E-03	0.272	0.401	0.566	1.0	100,001	150,000
HRA	β_1	3.881	0.618	2.00E-02	2.825	3.821	5.285	1.0	100,001	150,000
	β_2	0.763	0.613	2.30E-02	-0.242	0.704	2.117	0.9	100,001	150,000
	β_3	0.079	0.058	6.40E-04	0.004	0.068	0.219	1.0	100,001	150,000
	β_4	0.227	0.241	9.00E-03	-0.3	0.239	0.651	0.8	100,001	150,000
	β_5	1.736	0.608	2.30E-02	0.696	1.697	2.935	1.0	100,001	150,000
	β_6	-2.685	5.229	1.80E-01	-21.09	-0.676	0.007	0.0	100,001	150,000
TSCS	β_1	1.300	2.212	7.50E-02	-3.95	1.466	5.209	0.8	100,001	150,000
	β_2	-1.700	1.122	4.20E-02	-4.449	-1.478	-0.14	0.0	100,001	150,000
	β_3	0.200	0.565	1.20E-02	-0.597	0.147	1.632	0.7	100,001	150,000
	β_4	1.100	0.67	2.50E-02	-0.017	0.994	2.753	1.0	100,001	150,000
	β_5	1.300	0.964	3.50E-02	-0.049	1.084	3.723	1.0	100,001	150,000
	β_6	1.600	0.842	3.10E-02	0.564	1.415	3.868	1.0	100,001	150,000

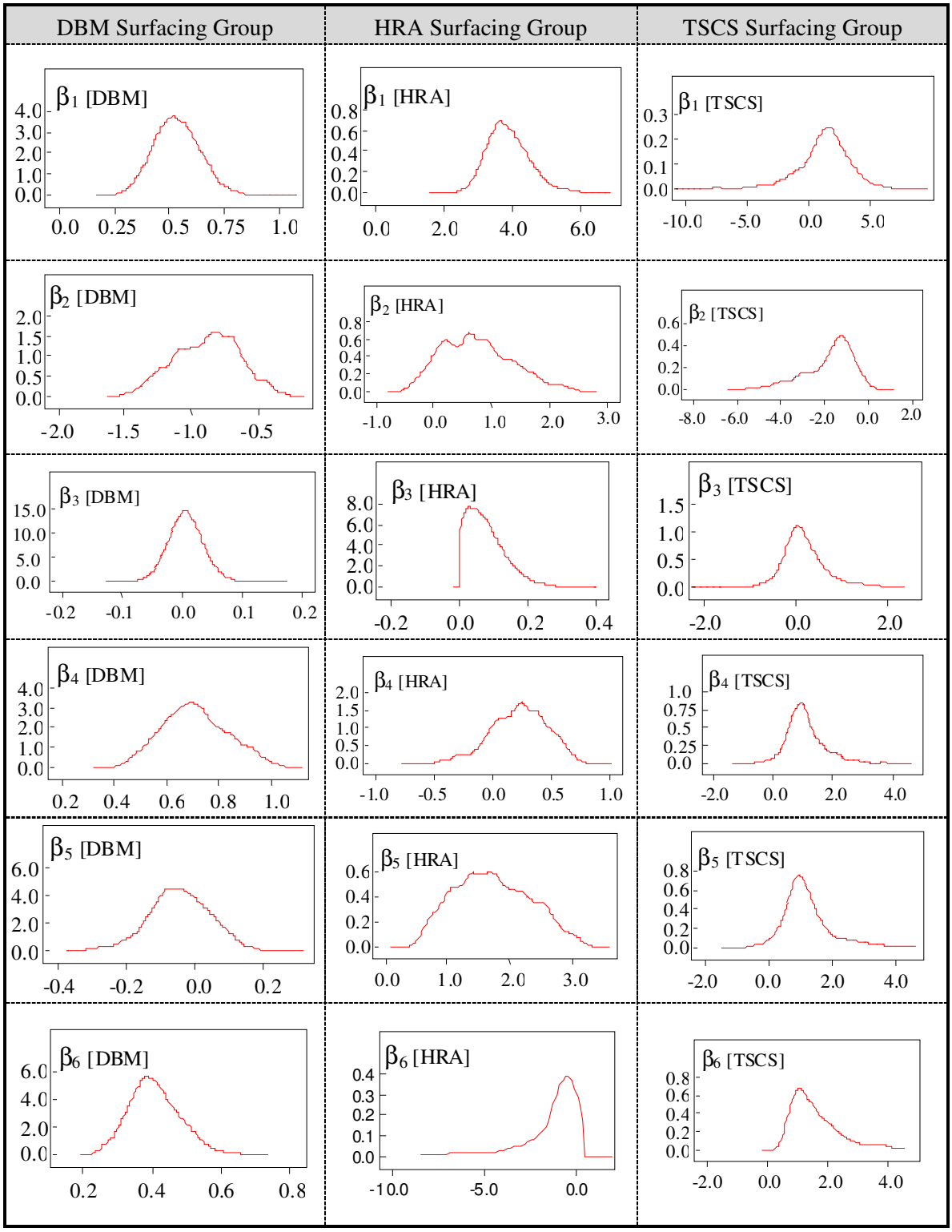

Figure C3-3: Estimated Distribution of Model Coefficients for Model 2N (Model Structure 2 and Normal Likelihood)

Table C3-4: Summary Statistics for Estimated Model Coefficient for Model 2S (Model Structure 2 and Students t Likelihood)

Surfacing Group	Nodes	Mean	SD	MC Error	2.50%	Median	97.50%	P0	Start	Sample
DBM	β_1	0.391	0.296	1.10E-02	0.022	0.321	1.154	1.0	40,001	170,000
	β_2	-0.762	0.422	2.10E-02	-1.773	-0.73	-0.102	0.0	40,001	170,000
	β_3	0.182	0.091	2.80E-03	0.047	0.17	0.393	1.0	40,001	170,000
	β_4	0.306	0.159	7.60E-03	0.056	0.29	0.646	1.0	40,001	170,000
	β_5	-0.188	0.176	8.30E-03	-0.638	-0.171	0.123	0.1	40,001	170,000
	β_6	0.340	0.153	7.10E-03	0.133	0.311	0.74	1.0	40,001	170,000
HRA	β_1	1.989	0.501	2.20E-02	0.947	1.989	3.061	1.0	40,001	170,000
	β_2	-5.131	1.21	5.90E-02	-7.8	-5.215	-2.286	0.0	40,001	170,000
	β_3	0.083	0.066	6.80E-04	0.003	0.069	0.245	1.0	40,001	170,000
	β_4	3.134	0.675	3.30E-02	1.594	3.174	4.688	1.0	40,001	170,000
	β_5	0.742	0.36	1.70E-02	-0.057	0.752	1.387	1.0	40,001	170,000
	β_6	1.709	0.38	1.80E-02	0.81	1.731	2.534	1.0	40,001	170,000
TSCS	β_1	2.676	0.922	4.20E-02	1.053	2.579	4.789	1.0	40,001	170,000
	β_2	-1.572	0.393	1.90E-02	-2.492	-1.536	-0.913	0.0	40,001	170,000
	β_3	0.246	0.271	7.80E-03	-0.109	0.178	0.933	0.9	40,001	170,000
	β_4	1.410	0.25	1.20E-02	0.94	1.41	1.915	1.0	40,001	170,000
	β_5	1.255	0.207	8.70E-03	0.856	1.251	1.664	1.0	40,001	170,000
	β_6	1.321	0.285	1.30E-02	0.874	1.275	2.009	1.0	40,001	170,000

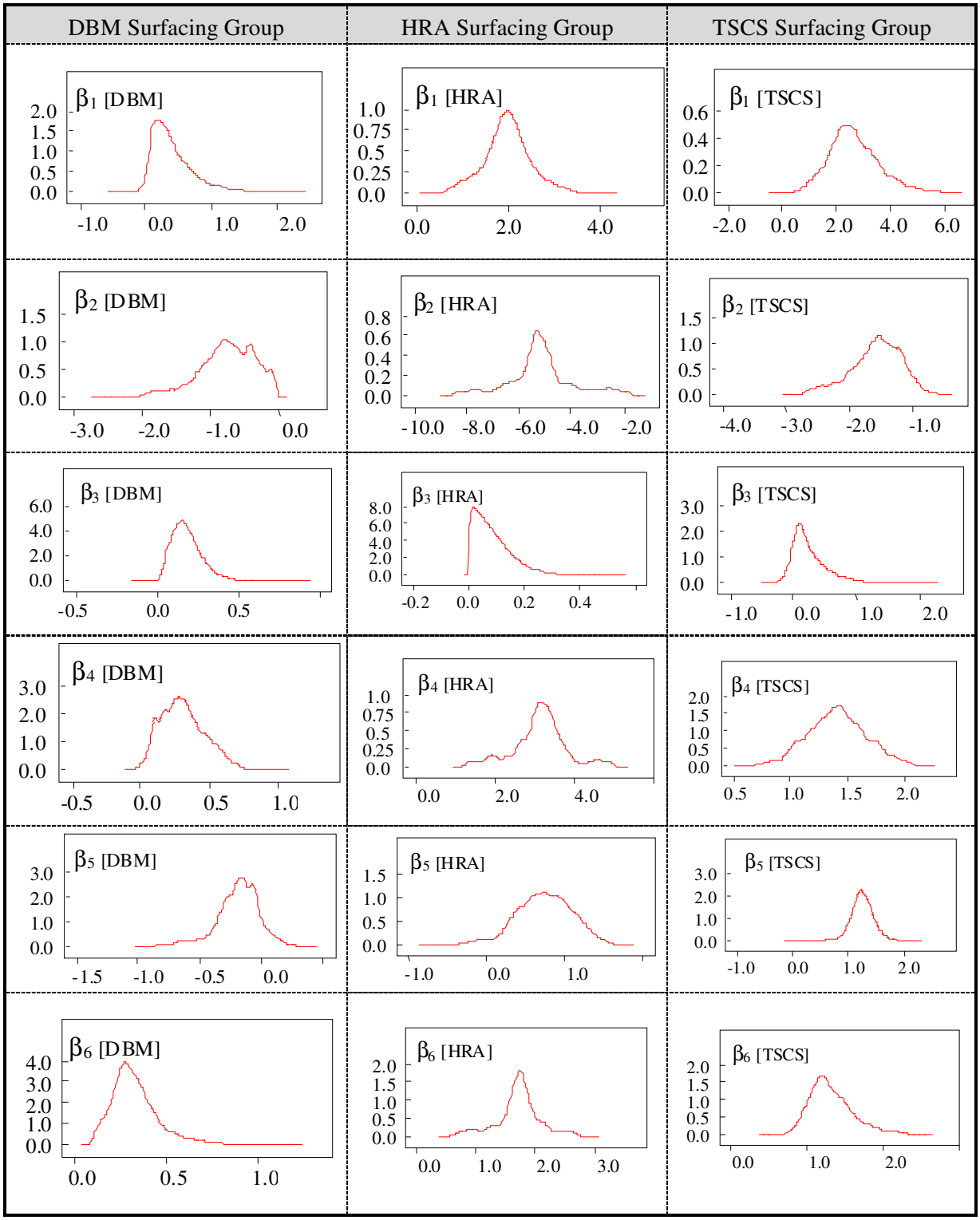

Figure C3-4: Estimated Distribution of Model Coefficients for Model 2S (Model Structure 2 and Student t Likelihood)

Appendix C4 Estimated Model Coefficients for Model Structure 3

Table C4-1: Summary Statistics for Estimated Model Coefficient for Model 3D (Model Structure 3 and Double Exponential Likelihood)

Surfacing Group	Nodes	Mean	SD	MC Error	2.50%	Median	97.50%	P0	Start	Sample
DBM	β_0	0.438	0.7	2.90E-02	-1.452	0.509	1.664	0.8	50,001	90,000
	β_1	0.264	0.109	1.30E-03	0.053	0.263	0.479	1.0	50,001	90,000
	β_2	-4.40E-03	0.003	7.60E-05	-0.01	-0.004	0.001	0.1	50,001	90,000
	β_3	0.069	0.049	3.40E-04	-0.023	0.068	0.167	0.9	50,001	90,000
	β_4	0.001	0.001	7.30E-06	0	0.001	0.002	1.0	50,001	90,000
	β_5	-0.57	2.2	3.00E-02	-6.217	-0.069	2.569	0.5	50,001	90,000
	β_6	0.047	0.004	1.70E-05	0.039	0.047	0.055	1.0	50,001	90,000
HRA	β_0	0.184	0.856	3.60E-02	-2.376	0.314	1.457	0.7	50,001	90,000
	β_1	0.674	0.084	9.20E-04	0.513	0.674	0.84	1.0	50,001	90,000
	β_2	-4.10E-03	0.002	3.30E-05	-0.008	-0.004	0	0.0	50,001	90,000
	β_3	-0.013	0.036	2.90E-04	-0.082	-0.013	0.058	0.4	50,001	90,000
	β_4	0.001	0	4.80E-06	0	0.001	0.001	1.0	50,001	90,000
	β_5	0.773	2.796	3.80E-02	-4.531	0.669	7.145	0.7	50,001	90,000
	β_6	0.016	0.003	1.20E-05	0.01	0.016	0.022	1.0	50,001	90,000
TSCS	β_0	0.984	1.127	4.70E-02	-1.908	1.151	2.62	0.9	50,001	90,000
	β_1	0.391	0.127	1.50E-03	0.143	0.39	0.646	1.0	50,001	90,000
	β_2	-0.019	0.005	1.50E-04	-0.03	-0.019	-0.009	0.0	50,001	90,000
	β_3	0.112	0.074	6.00E-04	-0.041	0.115	0.248	0.9	50,001	90,000
	β_4	0.001	0.001	7.00E-06	-0.001	0.001	0.002	0.9	50,001	90,000
	β_5	1.161	1.506	2.20E-02	-1.652	1.032	4.542	0.8	50,001	90,000
	β_6	0.022	0.013	7.60E-05	0.001	0.021	0.05	1.0	50,001	90,000

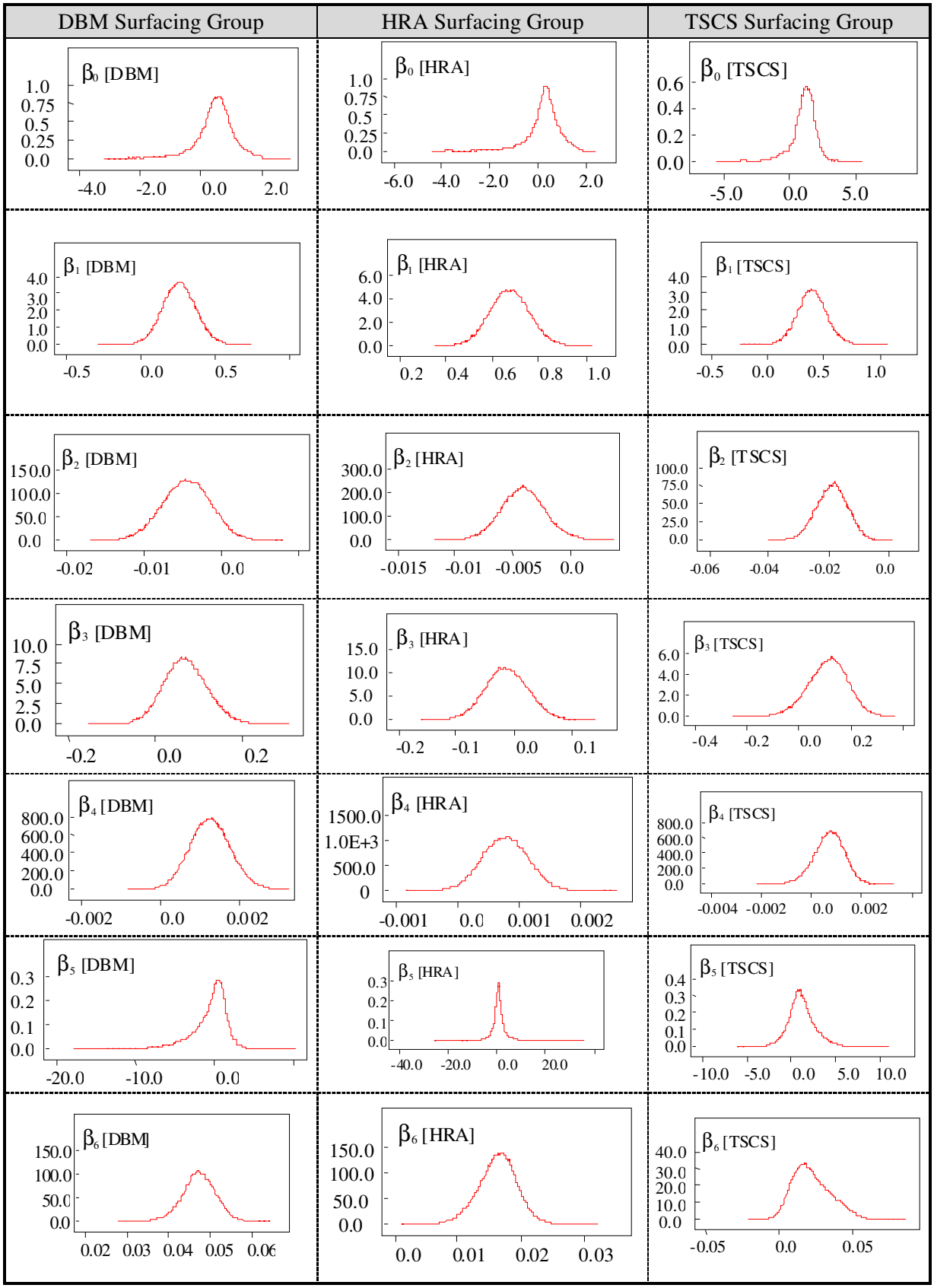

Figure C4-1: Estimated Distribution of Model Coefficients for Model 3D (Model Structure 3 and Double Exponential Likelihood)

Table C4-2: Summary Statistics for Estimated Model Coefficient for Model 3L (Model Structure 3 and Lognormal Likelihood)

Surfacing Group	Nodes	Mean	SD	MC Error	2.50%	Median	97.50%	P0	Start	Sample
DBM	β_0	0.221	0.048	5.60E-04	0.126	0.221	0.315	1.0	40,001	80,000
	β_1	0.324	0.406	1.90E-02	-0.758	0.348	1.076	0.9	40,001	80,000
	β_2	-1.5E-03	0.001	4.10E-05	-0.004	-0.002	0.001	0.2	40,001	80,000
	β_3	0.035	0.022	1.60E-04	-0.008	0.035	0.078	0.9	40,001	80,000
	β_4	9.2E-04	0	2.80E-06	0.001	0.001	0.001	1.0	40,001	80,000
	β_5	-1.434	1.958	2.90E-02	-5.999	-1.002	1.295	0.3	40,001	80,000
	β_6	0.016	0.001	3.50E-06	0.014	0.016	0.017	1.0	40,001	80,000
HRA	β_0	0.363	0.031	3.20E-04	0.302	0.363	0.425	1.0	40,001	80,000
	β_1	0.275	0.431	2.10E-02	-0.91	0.284	1.105	0.8	40,001	80,000
	β_2	1.4E-05	0.001	2.00E-05	-0.002	0	0.002	0.5	40,001	80,000
	β_3	-0.017	0.017	1.30E-04	-0.05	-0.017	0.016	0.2	40,001	80,000
	β_4	2.7E-04	0	2.40E-06	0	0	0.001	0.9	40,001	80,000
	β_5	0.234	2.133	3.10E-02	-4.596	0.326	4.698	0.6	40,001	80,000
	β_6	6.9E-03	0.001	4.20E-06	0.005	0.007	0.009	1.0	40,001	80,000
TSCS	β_0	0.236	0.068	1.10E-03	0.102	0.236	0.369	1.0	40,001	80,000
	β_1	0.783	0.492	2.20E-02	-0.661	0.848	1.582	0.9	40,001	80,000
	β_2	-9.4E-03	0.002	6.10E-05	-0.014	-0.009	-0.005	0.0	40,001	80,000
	β_3	9.7E-03	0.037	2.70E-04	-0.063	0.01	0.082	0.6	40,001	80,000
	β_4	1.5E-04	0	4.90E-06	0	0	0.001	0.7	40,001	80,000
	β_5	0.951	0.993	1.20E-02	-0.854	0.873	3.093	0.8	40,001	80,000
	β_6	0.011	0.003	2.80E-05	0.005	0.011	0.018	1.0	40,001	80,000

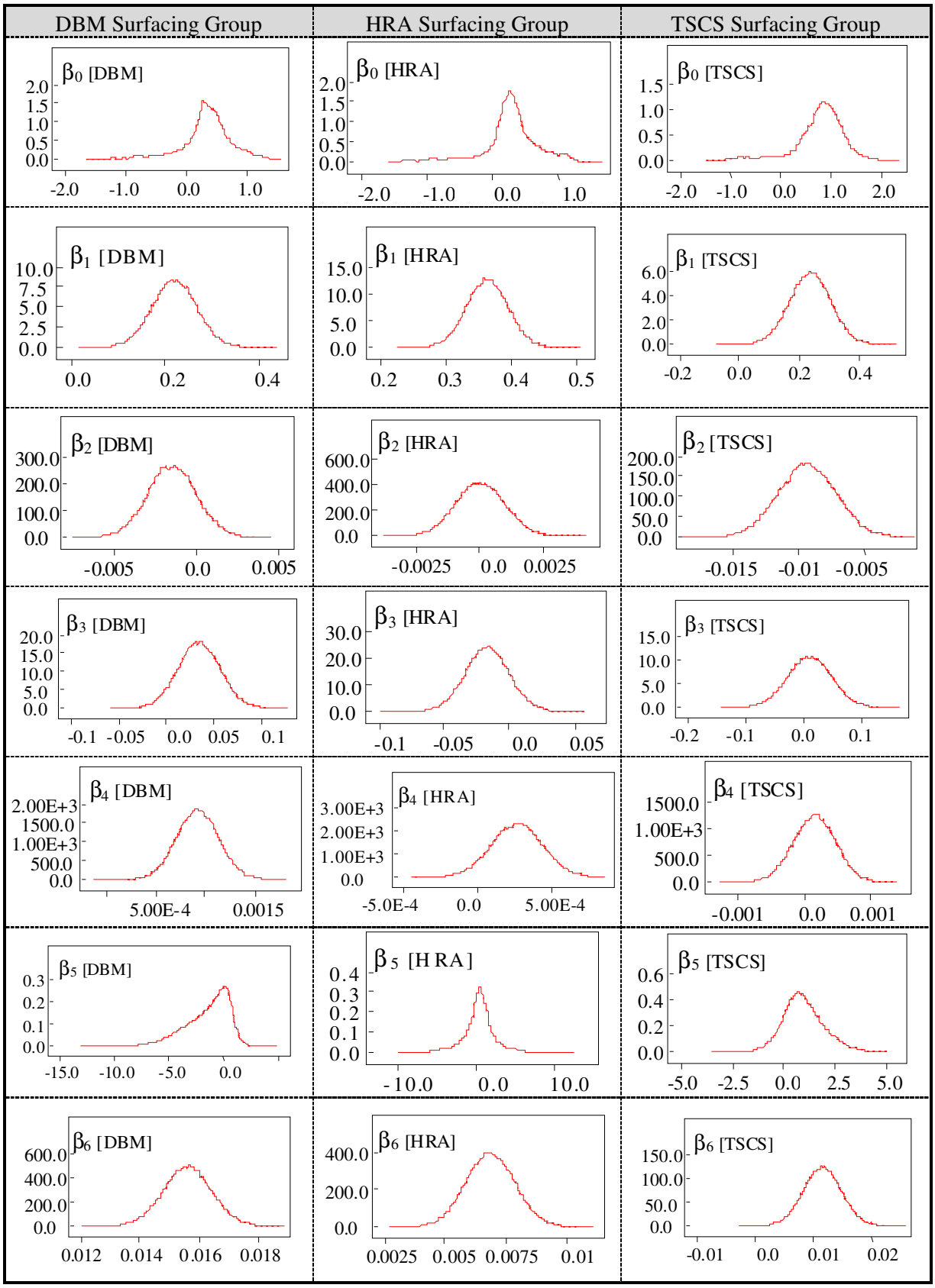

Figure C4-2: Estimated Distribution of Model Coefficients for Model 3L (Model Structure 3 and Lognormal Likelihood)

Table C4-3: Summary Statistics for Estimated Model Coefficient for Model 3N (Model Structure 3 and Normal Likelihood)

Surfacing Group	Nodes	Mean	SD	MC Error	2.50%	Median	97.50%	P0	Start	Sample
DBM	β_0	-0.497	1.465	3.60E-02	-3.07	-0.586	3.061	0.3	40,001	600,000
	β_1	0.928	0.203	8.40E-04	0.527	0.929	1.326	1.0	40,001	600,000
	β_2	0.002	0.007	7.10E-05	-0.011	0.002	0.015	0.6	40,001	600,000
	β_3	-0.061	0.097	2.50E-04	-0.251	-0.061	0.129	0.3	40,001	600,000
	β_4	0.005	0.001	4.80E-06	0.003	0.005	0.007	1.0	40,001	600,000
	β_5	-5.742	7.903	5.70E-02	-25.63	-2.668	3.473	0.2	40,001	600,000
	β_6	0.078	0.004	5.80E-06	0.071	0.078	0.085	1.0	40,001	600,000
HRA	β_0	-0.292	1.504	3.80E-02	-3.146	-0.359	3.361	0.3	40,001	600,000
	β_1	1.250	0.138	5.30E-04	0.981	1.249	1.521	1.0	40,001	600,000
	β_2	0.003	0.004	3.20E-05	-0.006	0.003	0.011	0.7	40,001	600,000
	β_3	-0.083	0.074	2.00E-04	-0.227	-0.082	0.062	0.1	40,001	600,000
	β_4	1.2E-03	0.001	3.50E-06	0	0.001	0.003	0.9	40,001	600,000
	β_5	1.810	8.522	5.50E-02	-13	0.42	24.34	0.6	40,001	600,000
	β_6	0.031	0.005	6.40E-06	0.022	0.031	0.04	1.0	40,001	600,000
TSCS	β_0	0.909	1.695	3.60E-02	-2.564	0.911	3.974	0.8	40,001	600,000
	β_1	0.715	0.291	2.00E-03	0.123	0.723	1.262	1.0	40,001	600,000
	β_2	-0.019	0.01	1.30E-04	-0.04	-0.019	0	0.0	40,001	600,000
	β_3	9.7E-04	0.155	4.50E-04	-0.303	0	0.307	0.5	40,001	600,000
	β_4	7.7E-04	0.001	9.70E-06	-0.002	0.001	0.004	0.7	40,001	600,000
	β_5	2.428	4.268	2.80E-02	-4.322	1.42	12.73	0.7	40,001	600,000
	β_6	0.051	0.015	5.50E-05	0.022	0.051	0.079	1.0	40,001	600,000

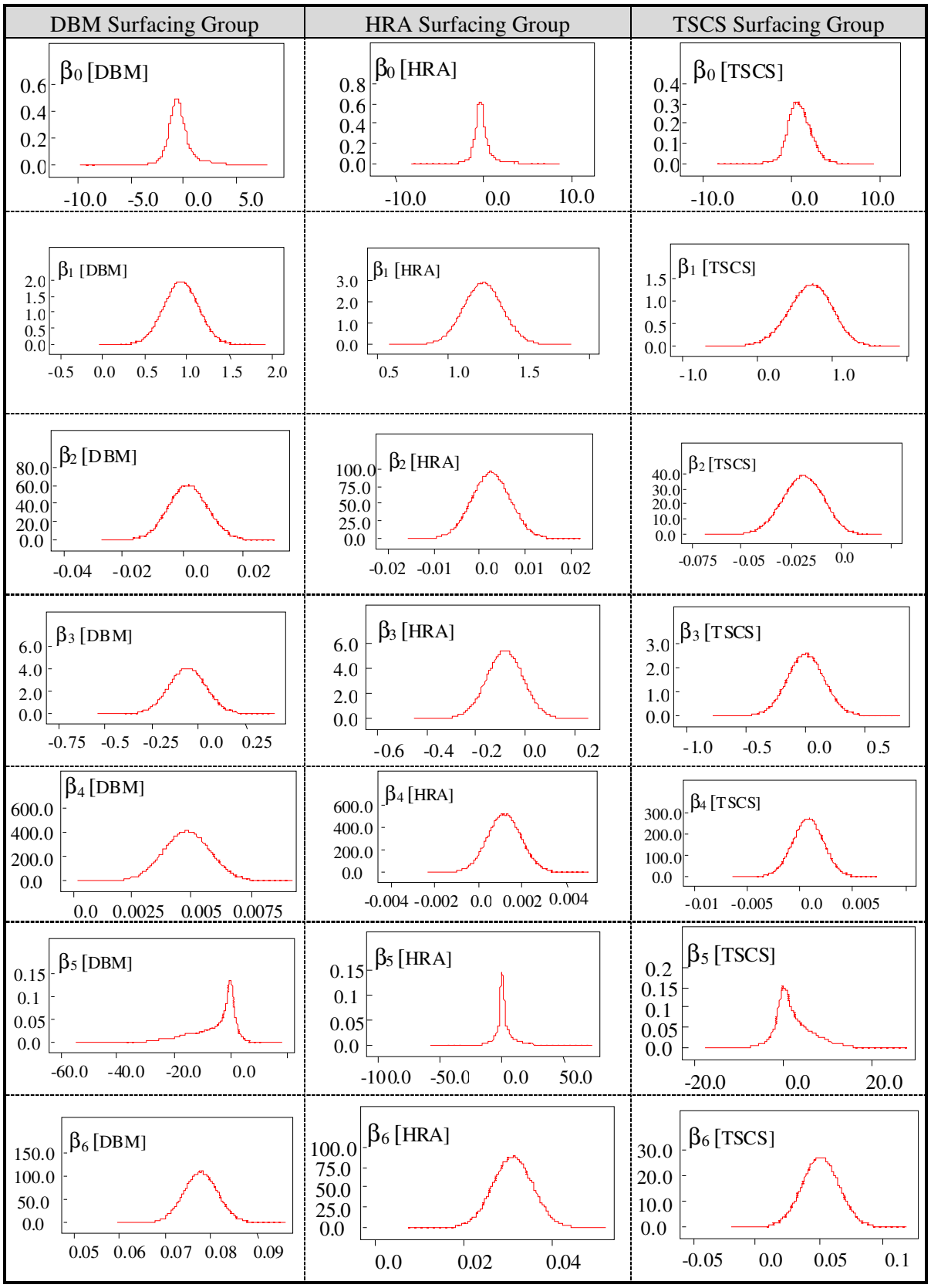

Figure C4-3: Estimated Distribution of Model Coefficients for Model 3N (Model Structure 3 and Normal Likelihood)

Table C4-4: Summary Statistics for Estimated Model Coefficient for Model 3S (Model Structure 3 and Students t Likelihood)

Surfacing Group	Nodes	Mean	SD	MC Error	2.50%	Median	97.50%	P0	Start	Sample
DBM	β_0	0.630	0.68	2.70E-02	-1.055	0.691	1.936	0.9	120,001	120,000
	β_1	0.172	0.079	9.80E-04	0.019	0.171	0.327	1.0	120,001	120,000
	β_2	-0.004	0.002	6.40E-05	-0.009	-0.004	0	0.0	120,001	120,000
	β_3	0.101	0.035	2.70E-04	0.033	0.101	0.17	1.0	120,001	120,000
	β_4	0.001	0	5.00E-06	0	0.001	0.001	1.0	120,001	120,000
	β_5	-1.319	2.444	3.70E-02	-7.209	-0.74	2.031	0.4	120,001	120,000
	β_6	0.020	0.002	1.60E-05	0.015	0.02	0.024	1.0	120,001	120,000
HRA	β_0	0.444	0.589	2.30E-02	-0.844	0.494	1.529	0.8	120,001	120,000
	β_1	0.402	0.063	8.00E-04	0.28	0.401	0.528	1.0	120,001	120,000
	β_2	-0.003	0.002	3.10E-05	-0.006	-0.003	0	0.0	120,001	120,000
	β_3	-0.006	0.028	2.30E-04	-0.06	-0.006	0.049	0.4	120,001	120,000
	β_4	4.6E-04	0	4.20E-06	0	0	0.001	0.9	120,001	120,000
	β_5	1.301	3.188	4.60E-02	-4.338	0.943	9.304	0.7	120,001	120,000
	β_6	6.7E-03	0.003	1.90E-05	0.002	0.007	0.012	1.0	120,001	120,000
TSCS	β_0	1.055	0.847	3.30E-02	-1.233	1.206	2.344	0.9	120,001	120,000
	β_1	0.388	0.11	1.50E-03	0.174	0.387	0.606	1.0	120,001	120,000
	β_2	-0.017	0.004	1.10E-04	-0.025	-0.017	-0.009	0.0	120,001	120,000
	β_3	0.064	0.055	4.30E-04	-0.045	0.064	0.172	0.9	120,001	120,000
	β_4	3.7E-04	0	6.10E-06	-0.001	0	0.001	0.8	120,001	120,000
	β_5	1.729	1.511	2.10E-02	-0.861	1.53	5.143	0.9	120,001	120,000
	β_6	0.012	0.008	5.50E-05	-0.002	0.011	0.029	1.0	120,001	120,000

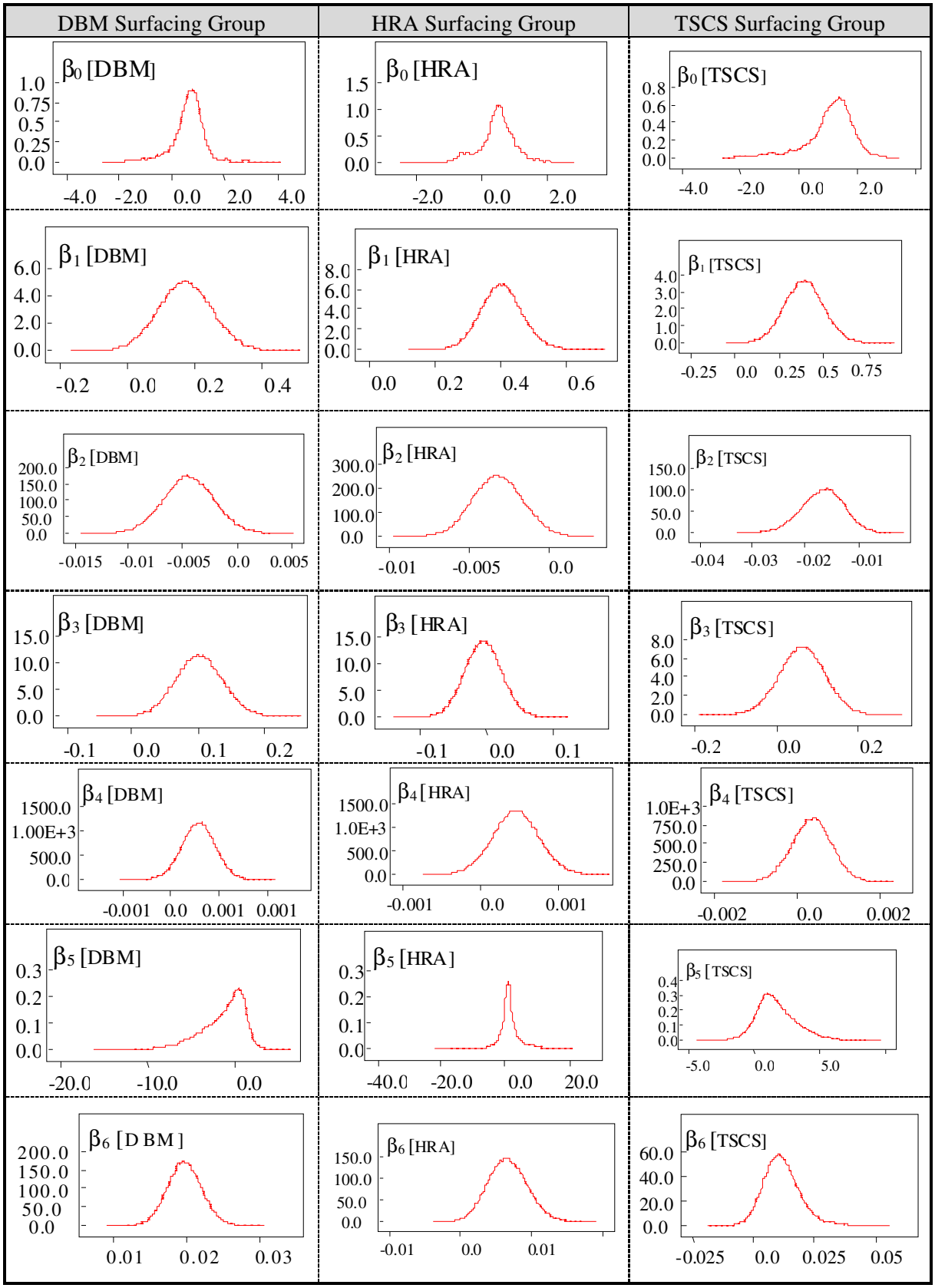

Figure C4-4: Estimated Distribution of Model Coefficients for Model 3S (Model Structure 3 and Students t Likelihood)

Appendix C5 Relative Magnitude of the Effect of Explanatory Variables

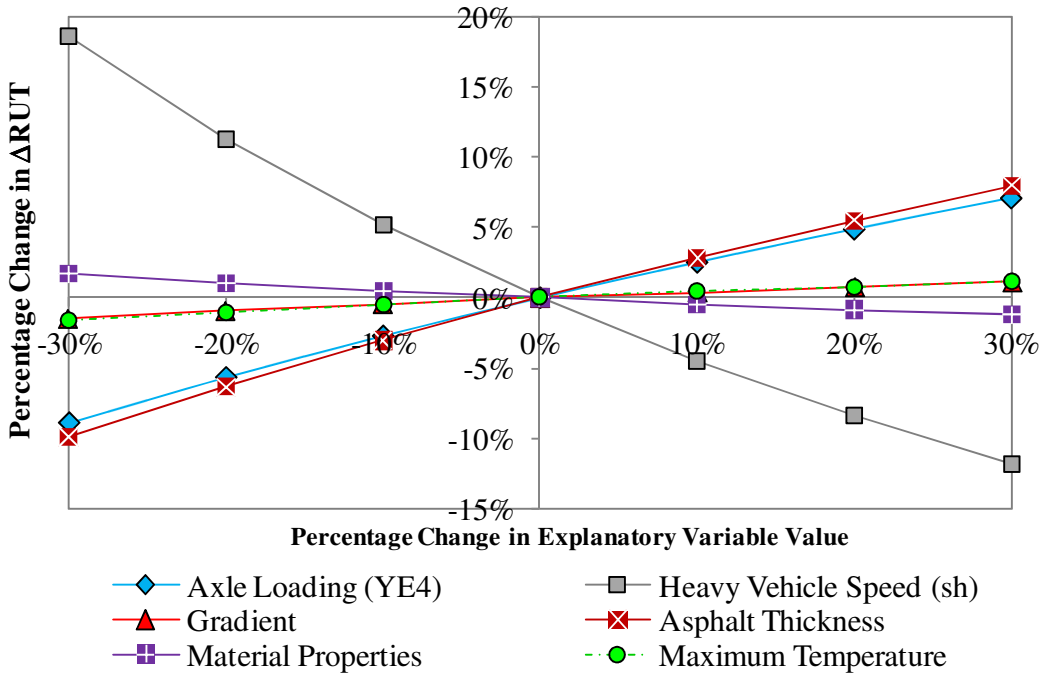

Figure C5-1: Relative Magnitude of the Effect of Explanatory Variables for DBM Surfacing Group

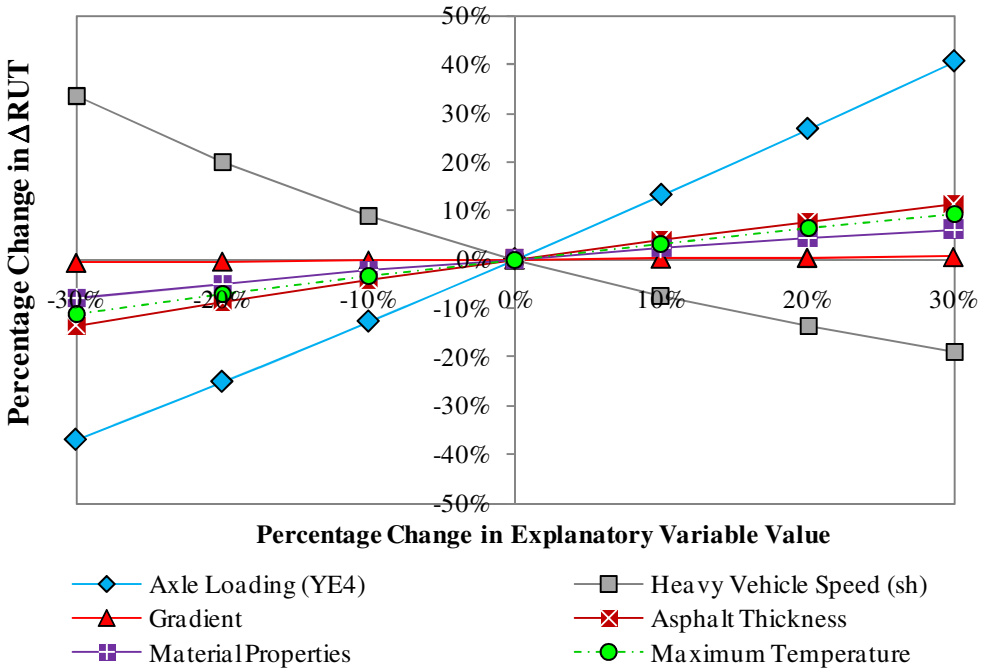

Figure C5-2: Relative Magnitude of the Effect of Explanatory Variables for TSCS Surfacing Group

Appendix C6 Results for Sensitivity of the Structure of Prior Distributions

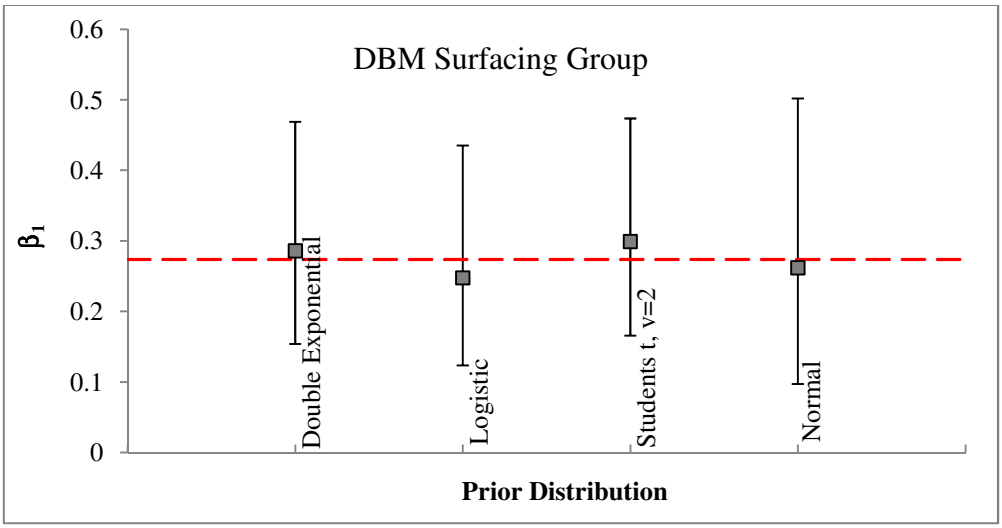

Figure C6-1: Sensitivity of DBM Model Coefficient β_1 to Structure of Prior Distribution.

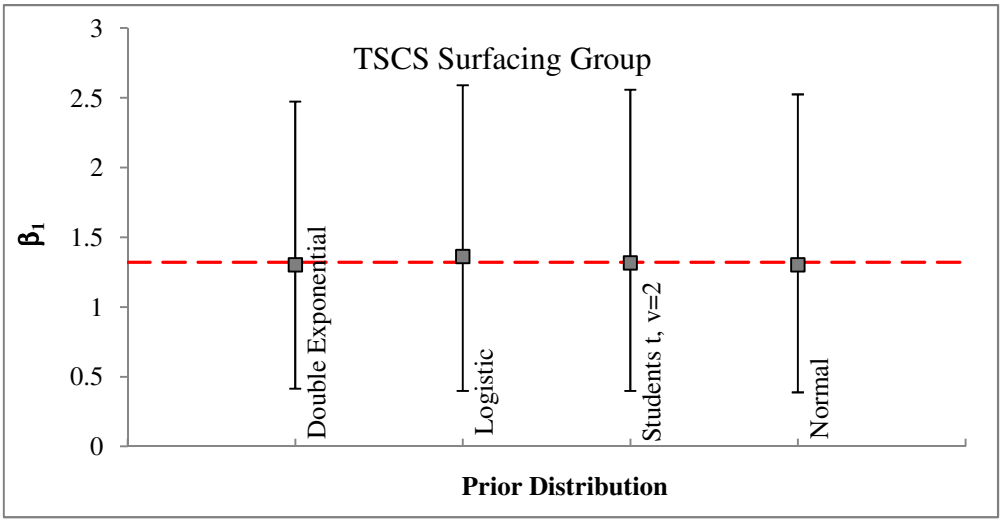

Figure C6-2: Sensitivity of TSCS Model Coefficient β_1 to Structure of Prior Distribution.

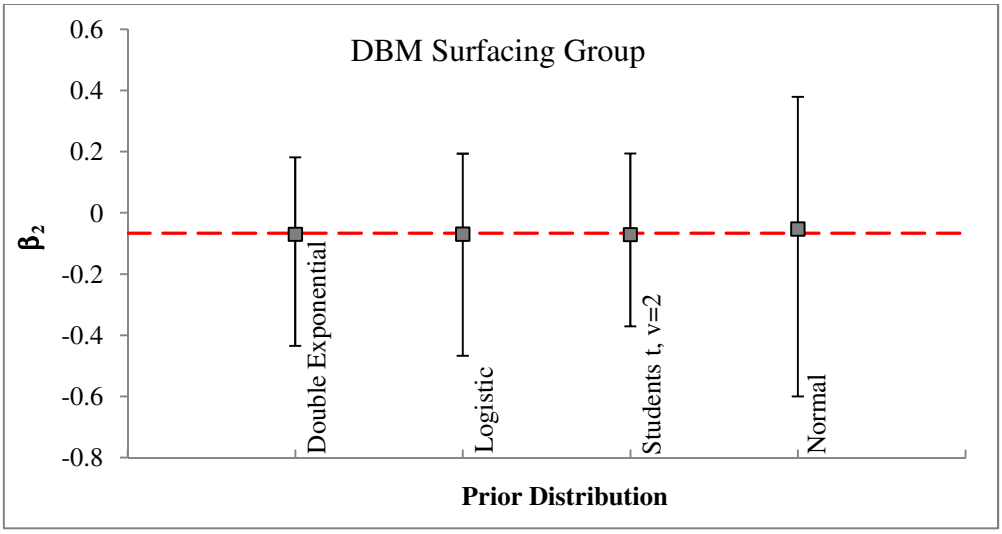

Figure C6-3: Sensitivity of DBM Model Coefficient β_2 to Structure of Prior Distribution.

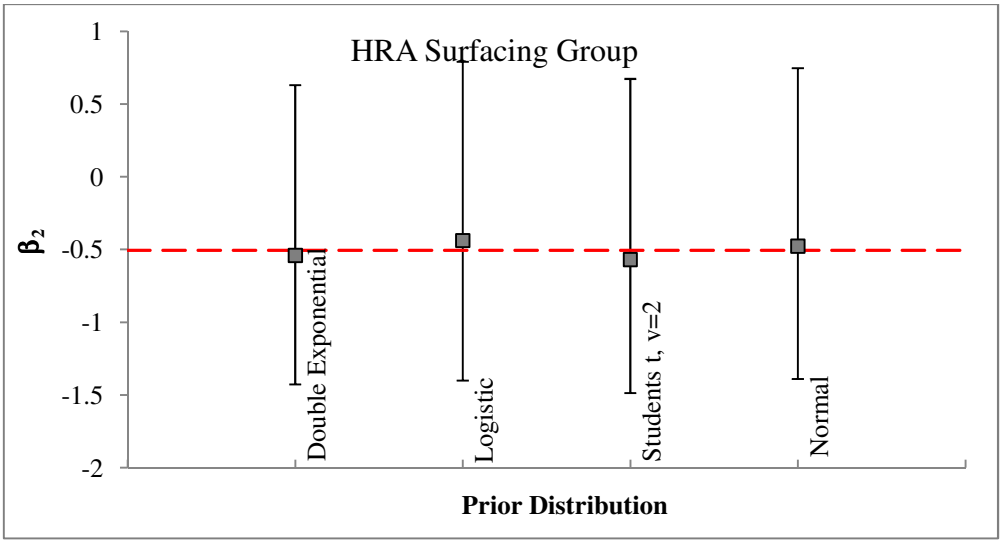

Figure C6-4: Sensitivity of HRA Model Coefficient β_2 to Structure of Prior Distribution.

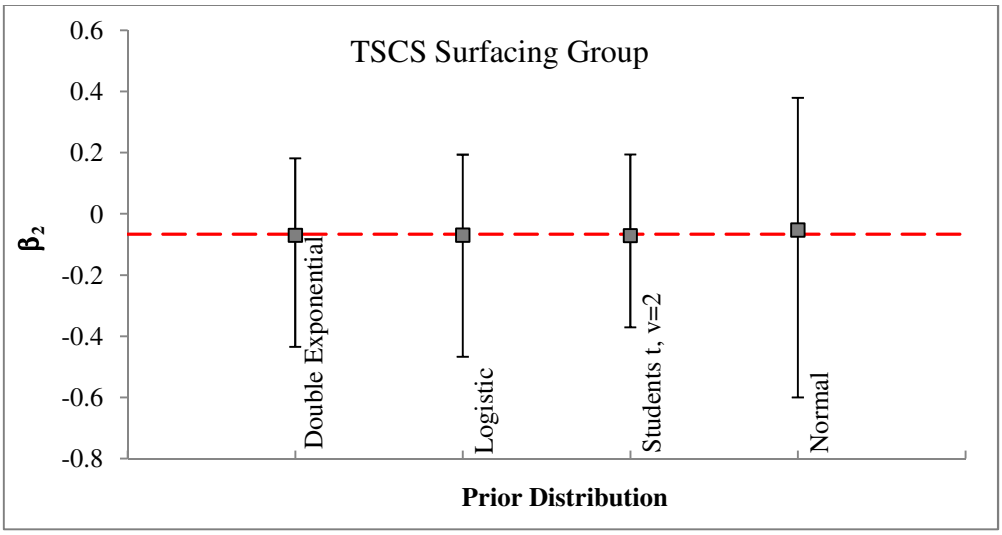

Figure C6-5: Sensitivity of TSCS Model Coefficient β_2 to Structure of Prior Distribution.

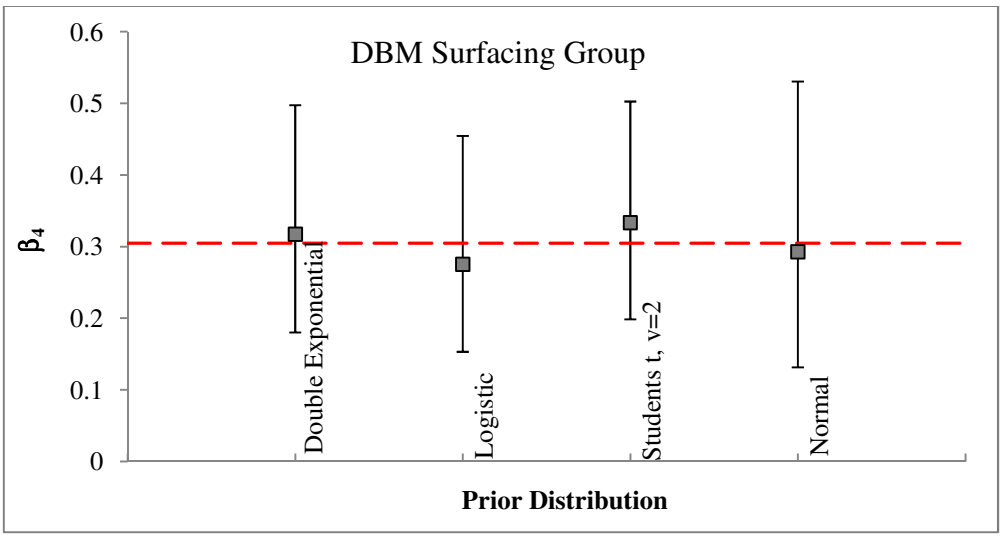

Figure C6-6: Sensitivity of DBM Model Coefficient β_4 to Structure of Prior Distribution.

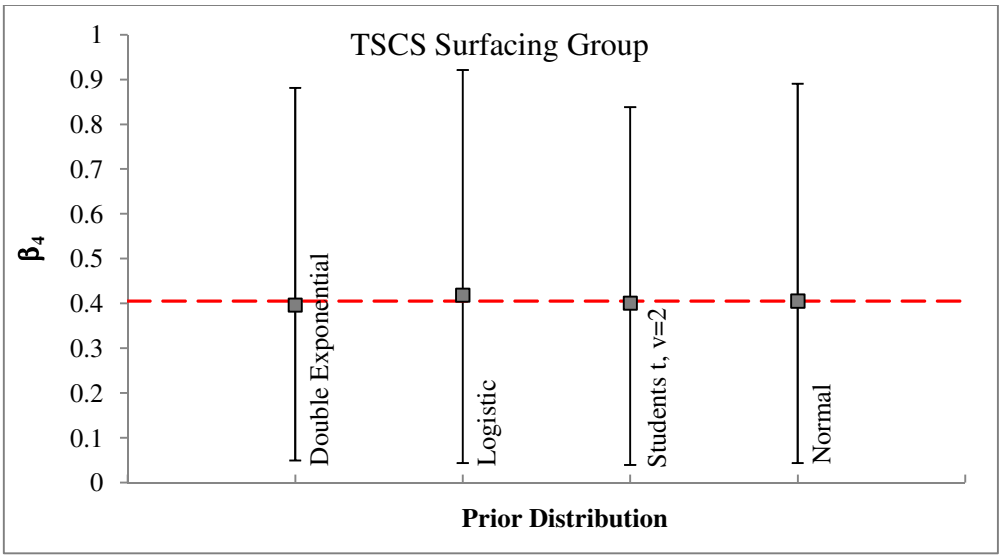

Figure C6-7: Sensitivity of TSCS Model Coefficient β_4 to Structure of Prior Distribution.

Appendix C8 Results for Sensitivity of Variance of Prior Distributions

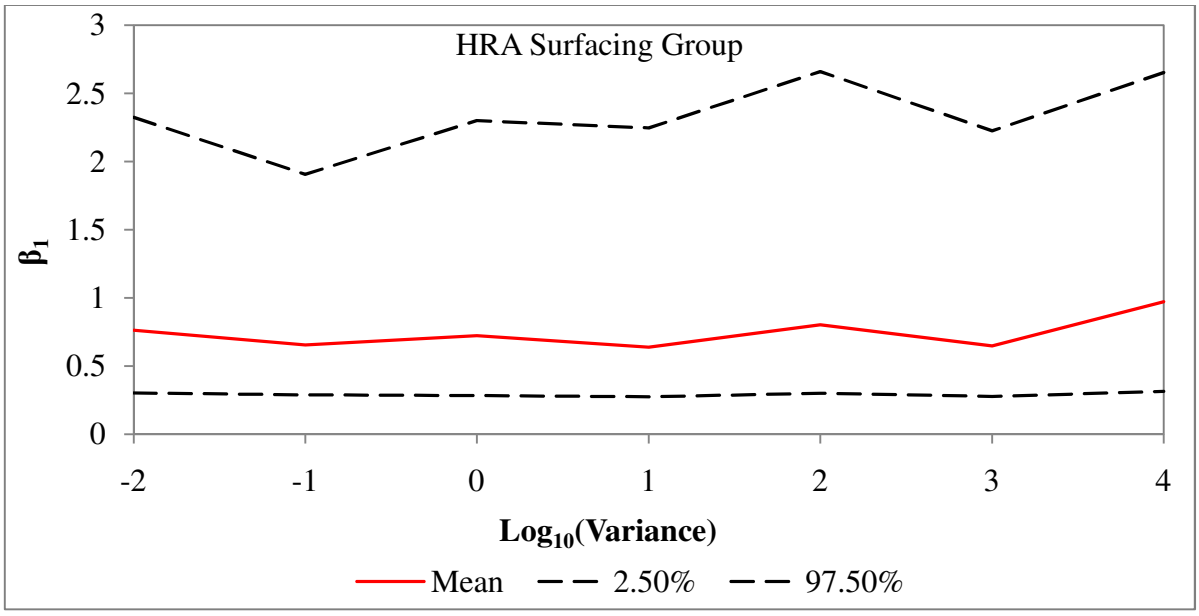

Figure C8-1: Sensitivity of Posterior Mean of Axle Loading (YE4) Model Coefficient for HRA Surfacing Group to Variance of Prior Distribution.

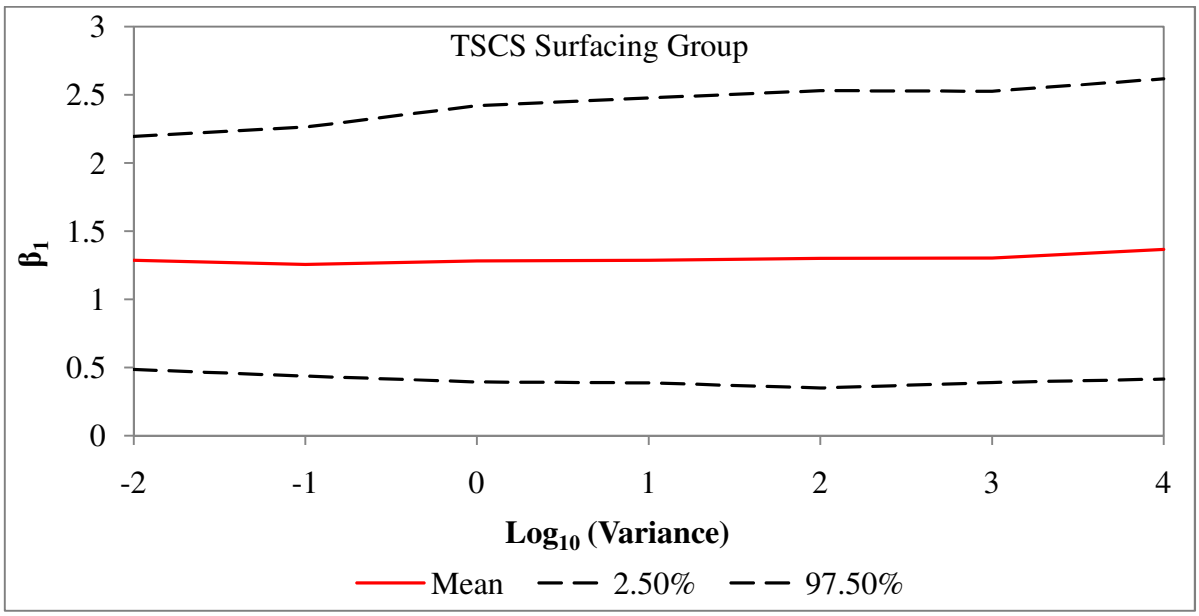

Figure C8-2: Sensitivity of Posterior Mean of Axle Loading (YE4) Model Coefficient for TSCS Surfacing Group to Variance of Prior Distribution.

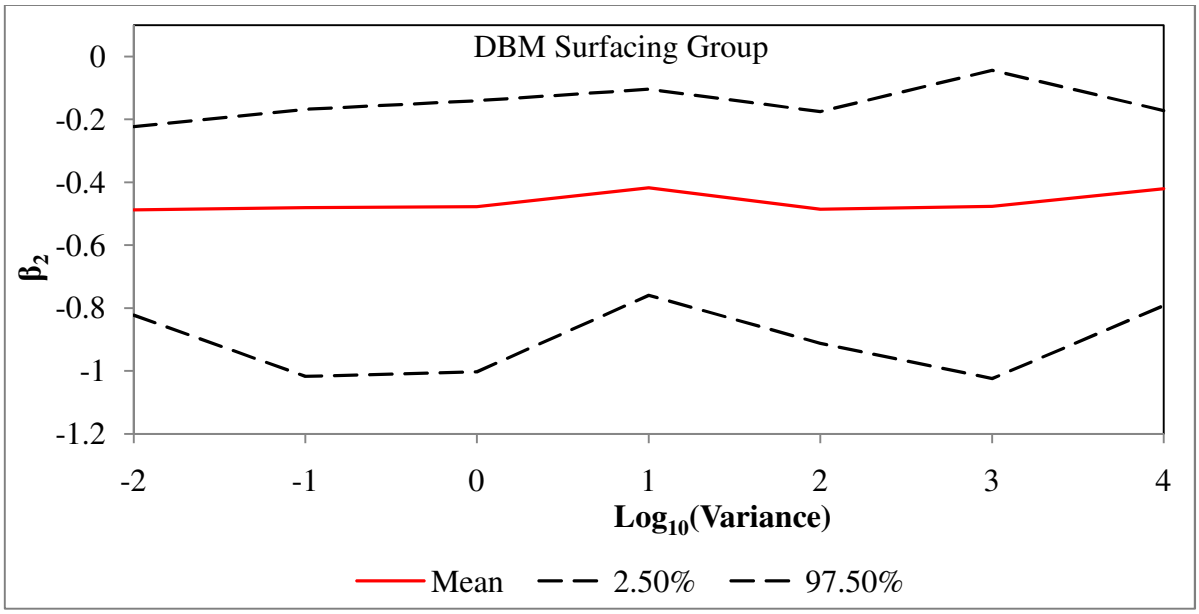

Figure C8-3: Sensitivity of Posterior Mean of Heavy Vehicle Speed (sh) Model Coefficient for DBM Surfacing Group to Variance of Prior Distribution.

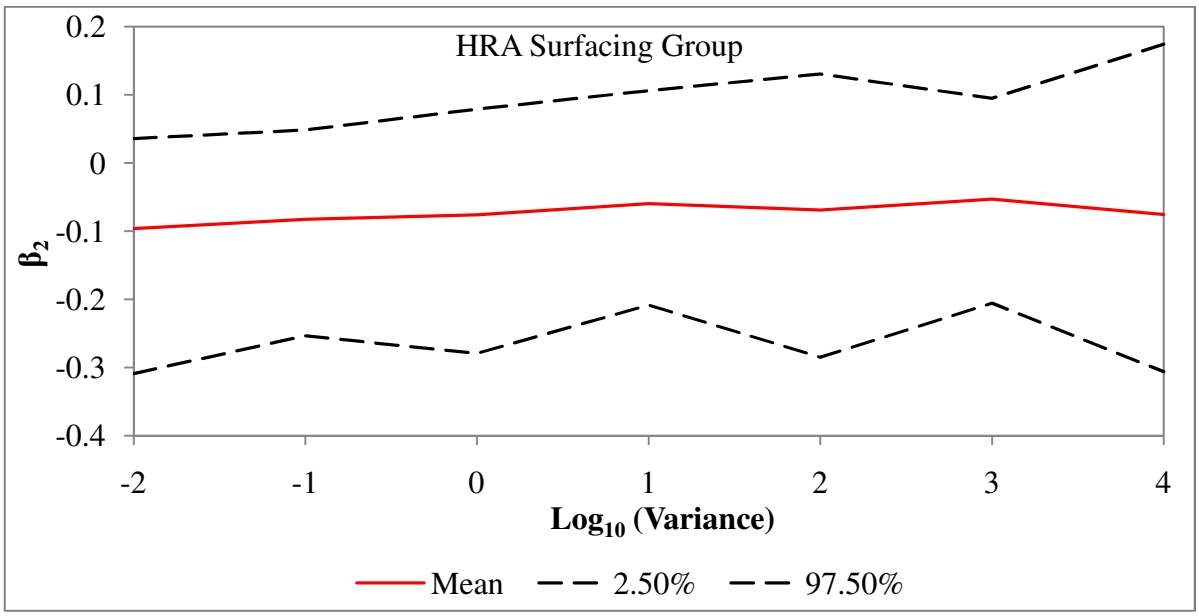

Figure C8-4: Sensitivity of Posterior Mean of Heavy Vehicle Speed (sh) Model Coefficient for HRA Surfacing Group to Variance of Prior Distribution.

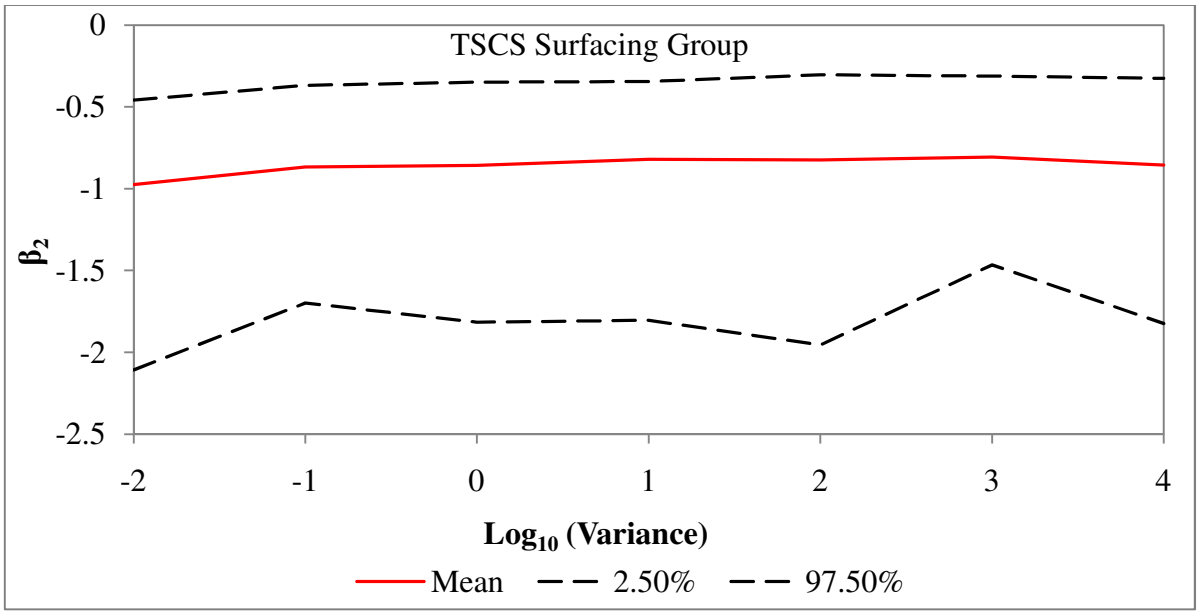

Figure C8-5: Sensitivity of Posterior Mean of Heavy Vehicle Speed (sh) Model Coefficient for TSCS Surfacing Group to Variance of Prior Distribution.

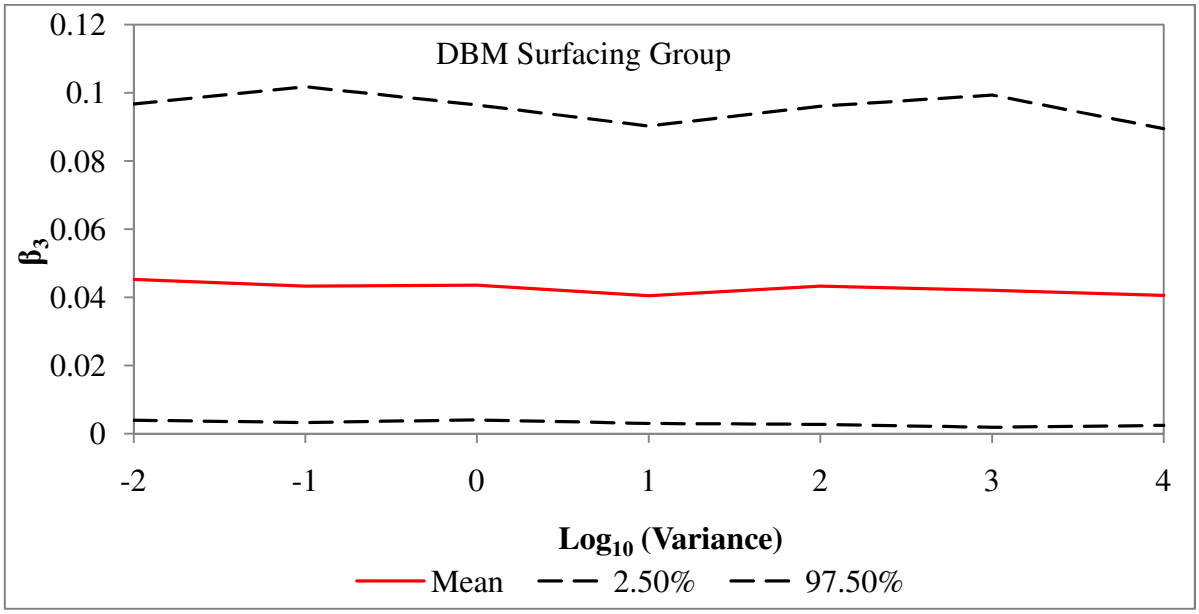

Figure C8-6: Sensitivity of Posterior Mean of Gradient (G) Model Coefficient for DBM Surfacing Group to Variance of Prior Distribution.

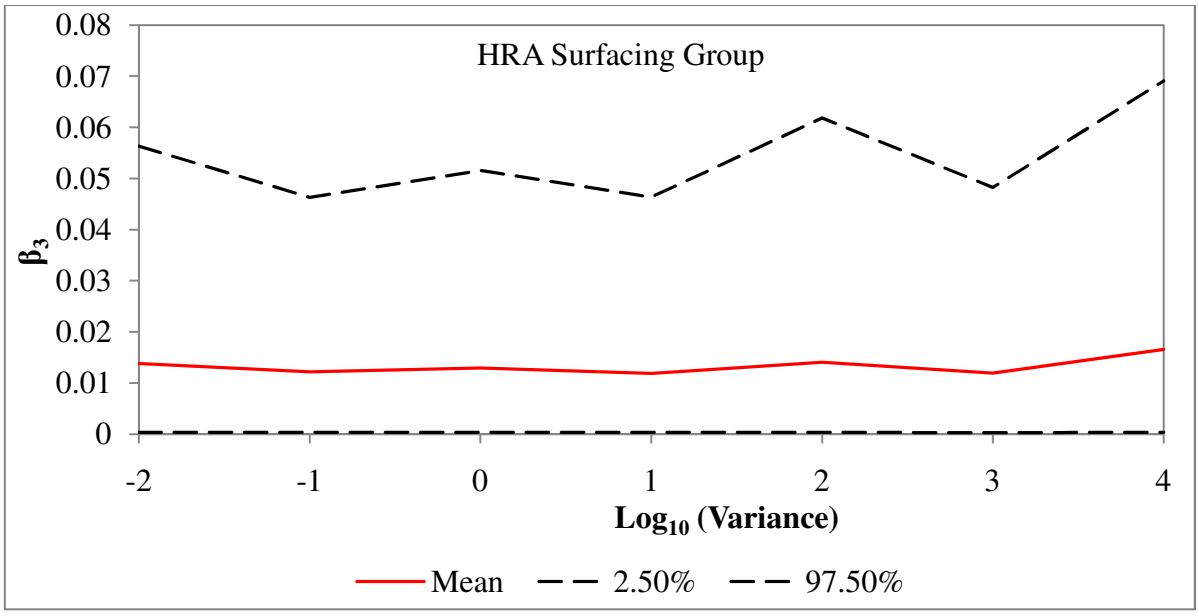

Figure C8-7: Sensitivity of Posterior Mean of Gradient (G) Model Coefficient for HRA Surfacing Group to Variance of Prior Distribution.

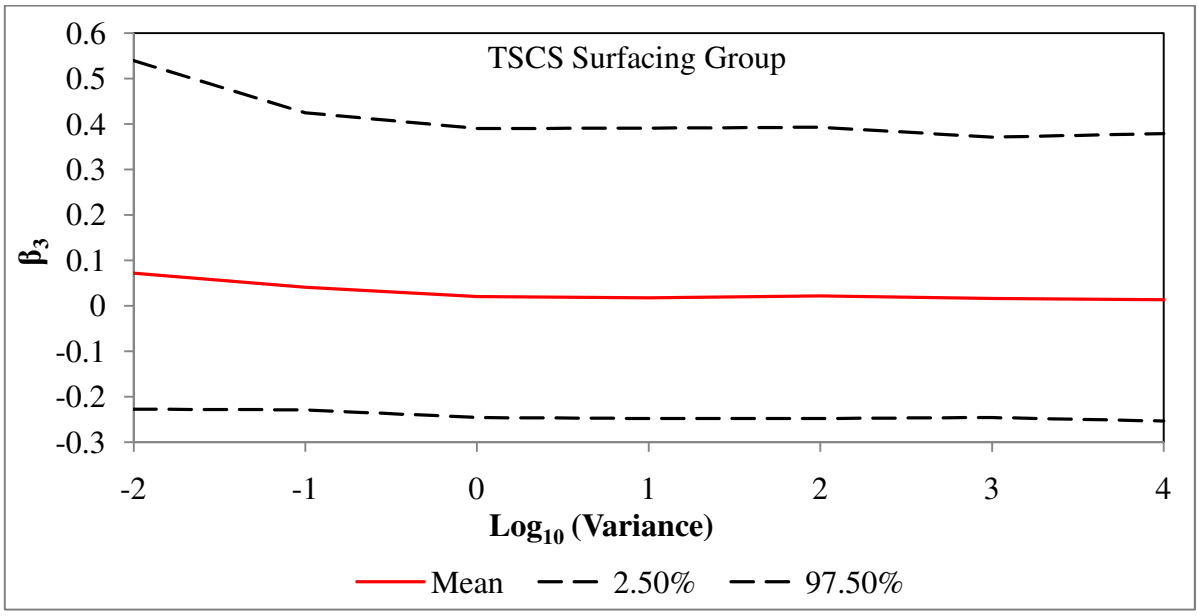

Figure C8-8: Sensitivity of Posterior Mean of Gradient (G) Model Coefficient for TSCS Surfacing Group to Variance of Prior Distribution.

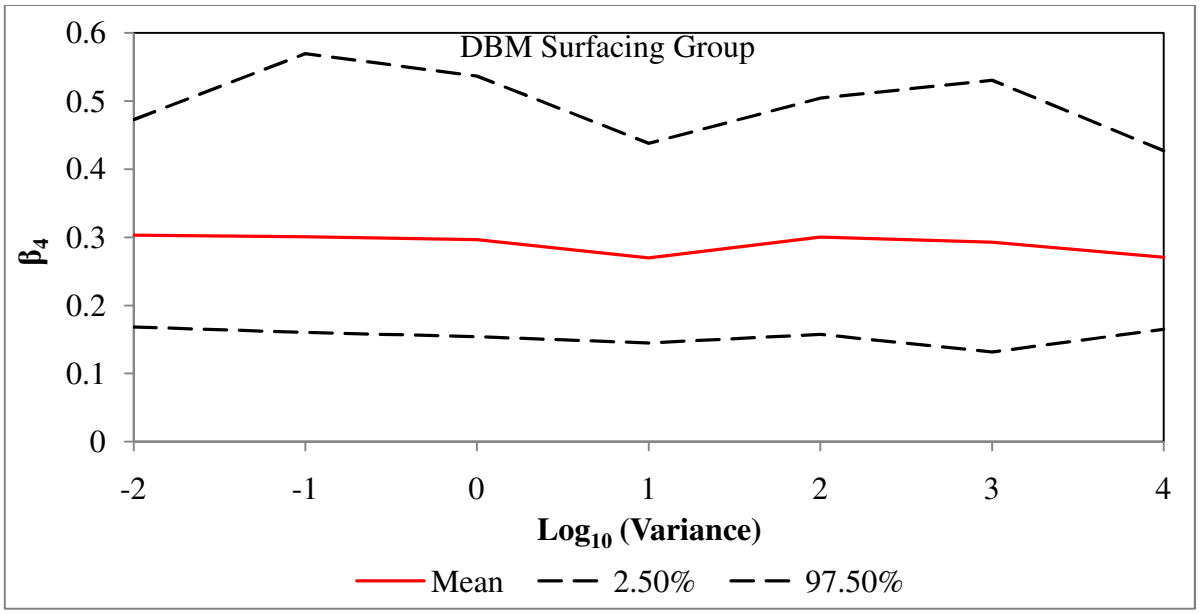

Figure C8-9: Sensitivity of Posterior Mean of Asphalt Thickness (HS) Model Coefficient for DBM Surfacing Group to Variance of Prior Distribution.

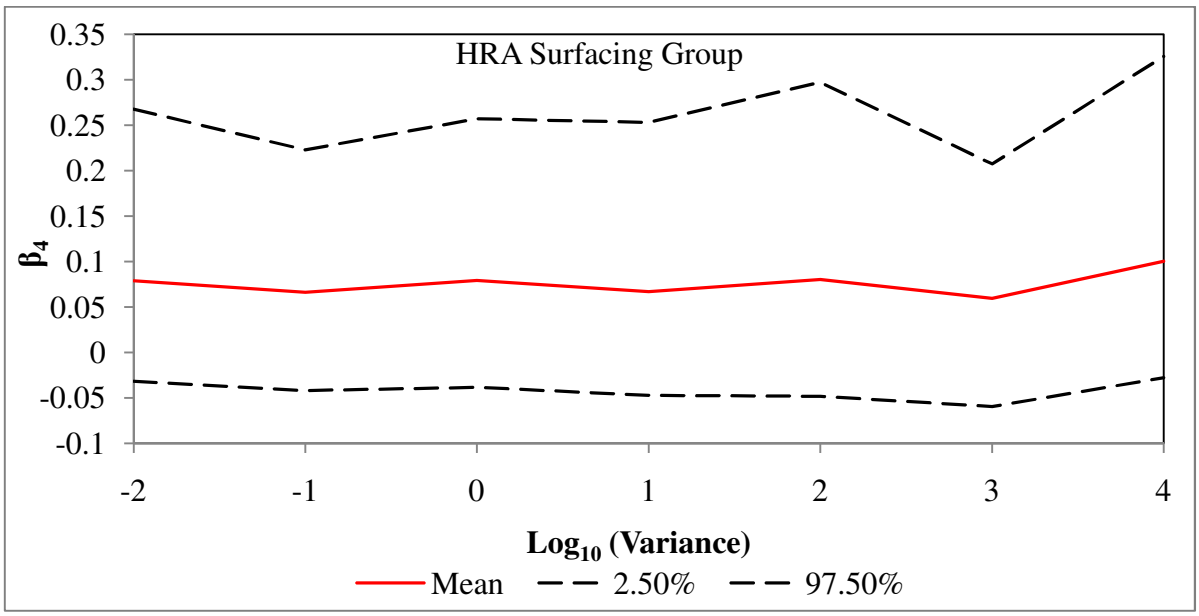

Figure C8-10: Sensitivity of Posterior Mean of Asphalt Thickness (HS) Model Coefficient for HRA Surfacing Group to Variance of Prior Distribution.

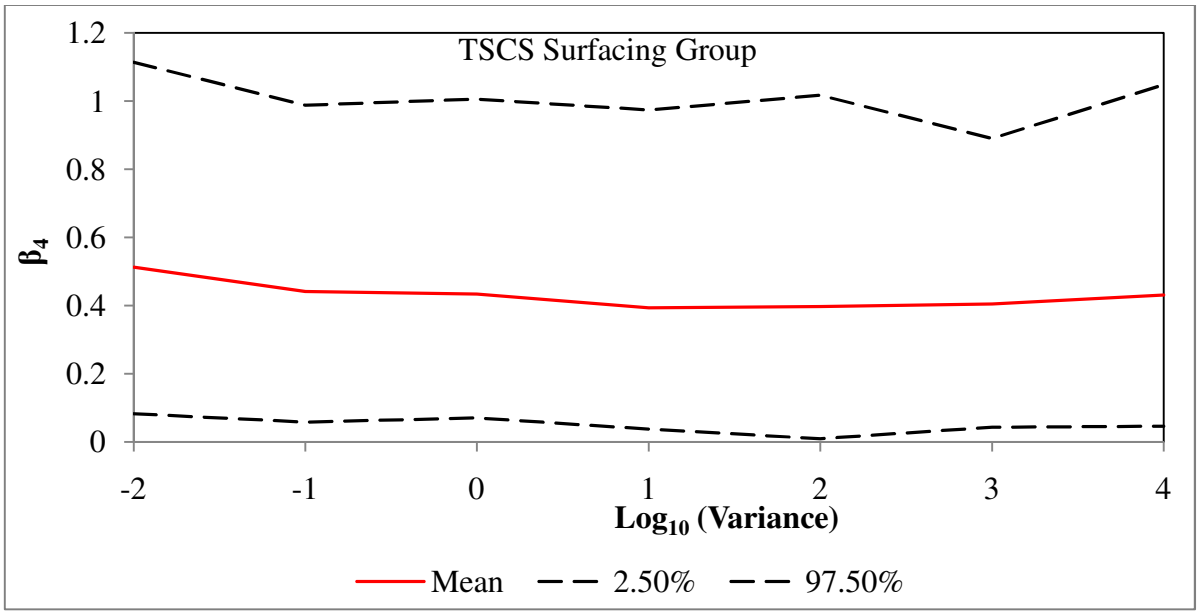

Figure C8-11: Sensitivity of Posterior Mean of Asphalt Thickness (HS) Model Coefficient for TSCS Surfacing Group to Variance of Prior Distribution.

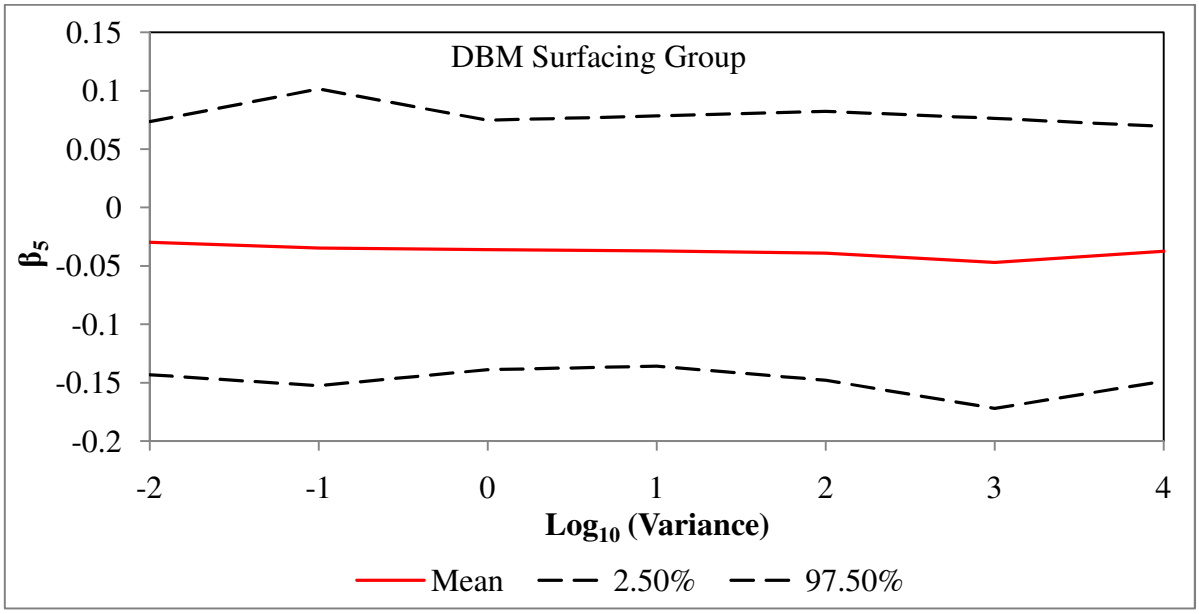

Figure C8-12: Sensitivity of Posterior Mean of Asphalt Material Properties (VIM/SP) Model Coefficient for DBM Surfacing Group to Variance of Prior Distribution.

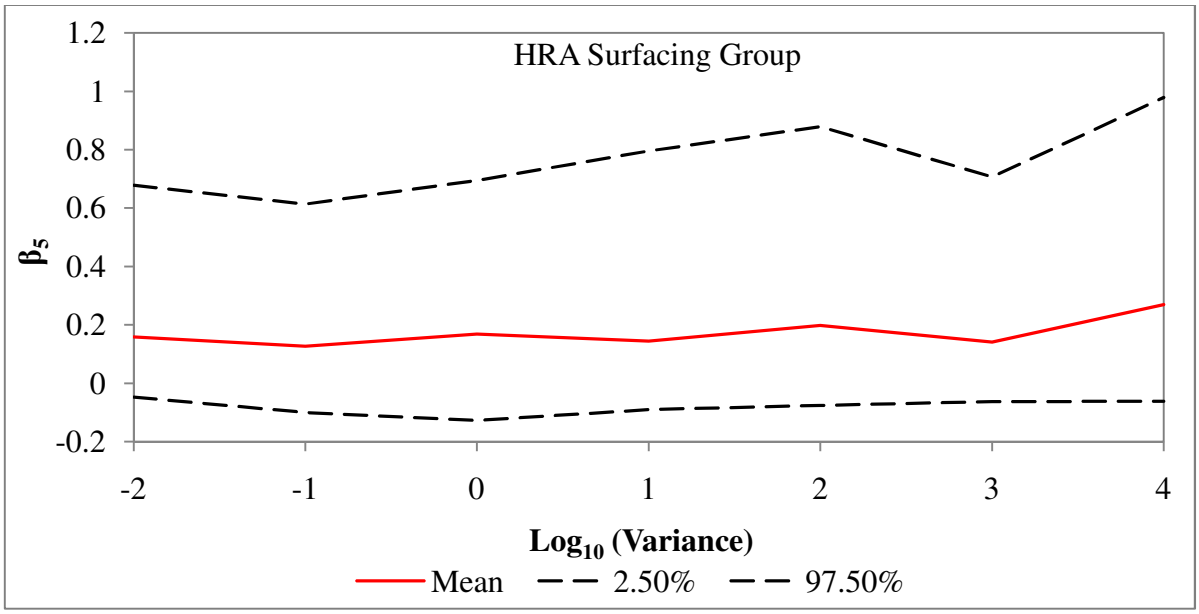

Figure C8-13: Sensitivity of Posterior Mean of Asphalt Material Properties (VIM/SP) Model Coefficient for HRA Surfacing Group to Variance of Prior Distribution.

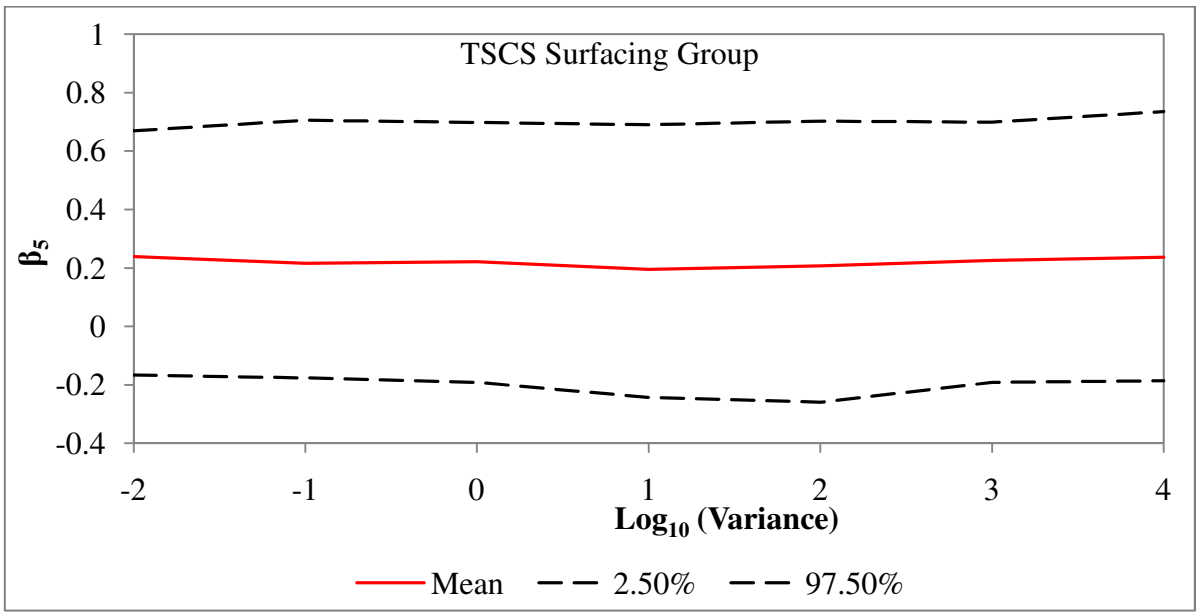

Figure C8-14: Sensitivity of Posterior Mean of Asphalt Material Properties (VIM/SP) Model Coefficient for TSCS Surfacing Group to Variance of Prior Distribution.

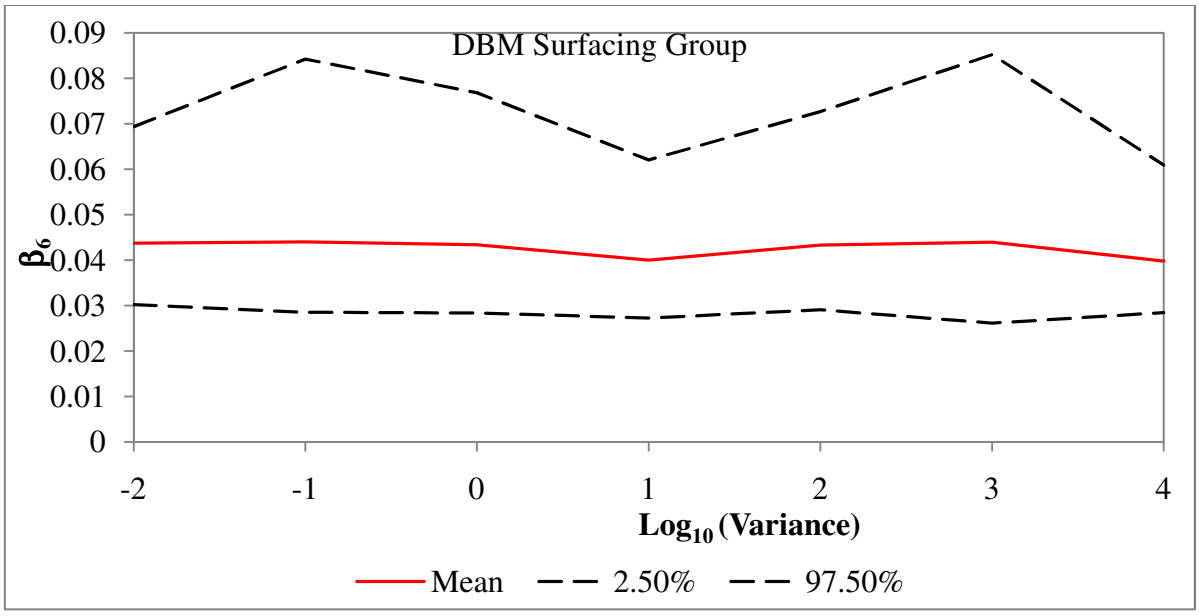

Figure C8-15: Sensitivity of Posterior Mean of Maximum Temperature (TPmax) Model Coefficient for DBM Surfacing Group to Variance of Prior Distribution.

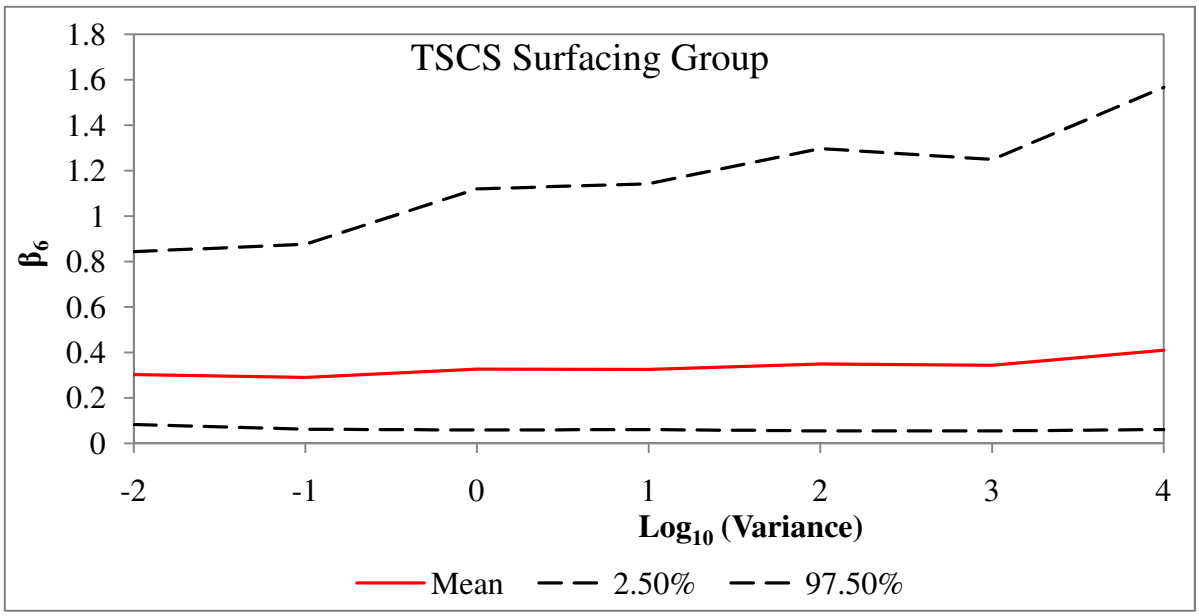

Figure C8-16: Sensitivity of Posterior Mean of Maximum Temperature (TPmax) Model Coefficient for TSCS Surfacing Group to Variance of Prior Distribution.

APPENDIX D Climate Impact and Adaptation Model

This appendix includes the following:

Appendix D1 Inputs to Climate Impact and Adaptation

1. General

The model inputs comprise lookup tables of values of road network inventory and condition, observed and predicted climate data, the rut depth model and materials properties model coefficients, treatment options, effects of treatments, unit cost of treatment works, and maintenance strategy. These inputs are described in subsequent sections.

2. Road Network Inventory and Condition

Road network data inputs illustrated in Figure D1-1 refer to records of observed or measured data for each modelled road section. The group column (in Figure D1-1) is used to group sections for purposes of probabilistic modelling. For each road section the data described in Table D1-1 are required.

ROAD NETWORK INVENTORY DATA															
ID	HOMOGENEOUS GROUP	DESCRIPTION	LATITUDE	YEAR	Material	Axle Load	Speed	Gradient	Asphalt Thickness	Softening Point (Initial)	Voids in Mix (Intial)	Surfacing Age	Observed Rut Depth	Length	Width
						YE4	sh	G	HS	SP	VIM	AGE	-	L	W
			Degress			(msa/Year/Lane)	(km/h)	-	(mm)	(oC)	(%)	(Years)	(mm)	(m)	(m)
1	1	2600A11/111	52.41	2002	DBM	1.32	85.20	3.96	184.40	72.27	1.23	14.34	2.00	400.00	3.65
2	1	2600A11/111	52.41	2002	DBM	1.32	85.20	3.96	184.40	72.90	1.39	14.34	2.00	400.00	3.65
3	1	2600A11/111	52.41	2002	DBM	1.32	85.20	3.96	184.40	74.34	1.49	14.34	2.00	400.00	3.65
4	1	2600A11/111	52.41	2002	DBM	1.32	85.20	3.96	184.40	74.28	1.26	14.34	2.00	400.00	3.65
5	1	2600A11/111	52.41	2002	DBM	1.32	85.20	3.96	184.40	74.01	1.33	14.34	2.00	400.00	3.65
6	1	2600A11/111	52.41	2002	DBM	1.32	85.20	3.96	184.40	74.39	1.65	14.34	2.00	400.00	3.65
7	1	2600A11/111	52.41	2002	DBM	1.32	85.20	3.96	184.40	74.02	1.50	14.34	2.00	400.00	3.65
8	1	2600A11/111	52.41	2002	DBM	1.32	85.20	3.96	184.40	74.67	1.53	14.34	2.00	400.00	3.65
9	1	2600A11/111	52.41	2002	DBM	1.32	85.20	3.96	184.40	73.62	1.58	14.34	2.00	400.00	3.65
10	1	2600A11/111	52.41	2002	DBM	1.32	85.20	3.96	184.40	73.95	1.50	14.34	2.00	400.00	3.65
11	1	2600A11/111	52.41	2002	DBM	1.32	85.20	3.96	184.40	72.68	1.37	14.34	2.00	400.00	3.65
12	1	2600A11/111	52.41	2002	DBM	1.32	85.20	3.96	184.40	73.59	1.37	14.34	2.00	400.00	3.65
13	1	2600A11/111	52.41	2002	DBM	1.32	85.20	3.96	184.40	74.51	1.62	14.34	2.00	400.00	3.65
14	1	2600A11/111	52.41	2002	DBM	1.32	85.20	3.96	184.40	73.54	1.44	14.34	2.00	400.00	3.65
15	1	2600A11/111	52.41	2002	DBM	1.32	85.20	3.96	184.40	73.73	1.45	14.34	2.00	400.00	3.65
16	1	2600A11/111	52.41	2002	DBM	1.32	85.20	3.96	184.40	75.77	1.35	14.34	2.00	400.00	3.65

Figure D1-1: Road Section Data

Table 10D-1: Road Network Inventory and Condition Input Data

Description	Units
Year in which data was collected;	Year
The geographical latitude in degrees of the road section;	Degrees
Asphalt surfacing type associated to the road section;	-
Average number of equivalent standard axle load	Million standard axles per year
Average absolute gradient of the road section	-
Average total asphalt thickness	Millimetres
Age of asphalt surfacing	Years
Softening Point (SP) of the binder for the in-service asphalt surfacing	Degrees Celsius
Voids in Mix (VIM) of the asphalt surfacing	Percentage
Observed rut depth on the road section	Millimetres
The length and width of the road section	Metres

To account for the fact that SP and VIM values for in-service pavements are rarely collected, default initial values were estimated within the model using SP and VIM models structures given in Section 4.4.3.2.

3. Climate Data Inputs

Climate data inputs to the model were aligned to the 2009 version of the UK Climate Projections (UKCP09). UKCP09 probabilistic projections are available for three green house gas emission scenarios of low, medium and high and seven 30-year time periods over which the data is averaged. Climate inputs to the model are described in Table D1-2.

Table D1-2: Climate Input Data

Description	Units	Time Period
Absolute mean daily maximum summer temperature in each year averaged over the baseline climate period	Degrees Celsius	Baseline (1961 – 1990)
Absolute average monthly precipitation during summer months for the baseline climate period	Millimetres	
Probability distribution of projected change in 30-year average of maximum daily summer air temperature at 1.5m above ground level	Degrees Celsius	2020s, (2010 to 2039) 2030s, (2020 to 2049) 2040s, (2030 to 2059) 2050s, (2040 to 2069) 2060s, (2050 to 2079) 2070s, (2060 to 2089) 2080s, (2070 to 2099)
Probability distribution of projected change in 30-year monthly summer precipitation	Millimetres	

Probability distribution of the predicted change in temperature and precipitation for a spatial location within which a study road section is located were derived by generating 10,000 random samples of data for given scenario and period from the UKCP09 User Interface tool (UKCIP, 2009). Statistical models of best fit are used to represent the data in the impact model as illustrated in Figure D1-2. The column labelled “distribution” (in Figure D1-2) is used to indicate the name of the statistical distribution that best fits the data. Considering the illustration in Figure D1-2, the distribution that best described the change in maximum summer temperature data within the study area was the generalized extreme value distribution. The distribution is defined by the shape, scale and location parameters denoted by Para. 1, Para. 2 and Para. 3 respectively.

Change in Maximum Summer Temperature (oC)							
Emission Scenario	Time Slice	Scenario Code	Distribution	Parameters			
				Para. 1	Para. 2	Para.3	Para. 4
High	2020s	|High|2020s|	Gen. Extreme Value	-0.175	1.019	1.490	-
Medium	2020s	|Medium|2020s|	Gen. Extreme Value	-0.202	1.063	1.511	-
Low	2020s	|Low|2020s|	Gen. Extreme Value	-0.187	1.014	1.616	-
High	2030s	|High|2030s|	Gen. Extreme Value	-0.146	1.191	2.091	-
Medium	2030s	|Medium|2030s|	Gen. Extreme Value	-0.180	1.257	1.925	-
Low	2030s	|Low|2030s|	Gen. Extreme Value	-0.187	1.261	1.955	-
High	2040s	|High|2040s|	Gen. Extreme Value	-0.135	1.430	2.561	-
Medium	2040s	|Medium|2040s|	Gen. Extreme Value	-0.167	1.473	2.262	-
Low	2040s	|Low|2040s|	Gen. Extreme Value	-0.177	1.435	2.330	-
High	2050s	|High|2050s|	Gen. Extreme Value	-0.145	1.810	3.249	-
Medium	2050s	|Medium|2050s|	Gen. Extreme Value	-0.146	1.642	2.790	-
Low	2050s	|Low|2050s|	Gen. Extreme Value	-0.167	1.593	2.569	-

Figure D1-2: Representation of Probabilistic Climate Data

Annualised climate data are associated to road sections by generating annual random samples from the probability distribution of the climate variable for each emission scenario and time period. Figure D1-3 depicts absolute maximum summer temperature by road section obtained by adding the predicted change in temperature to the corresponding averaged observed mean daily maximum summer temperature over the baseline period.

UKCP09 Summer Temperature Predictions by Emissions Scenario											
ID	Section Name	UKCIP09 Scenarios	Year								
			1	2	3	4	5	6	7	8	9
1	A14 NB C0:500	|Low|2020s|	23.06	23.46	23.12	22.03	23.52	24.25	23.52	24.27	23.07
2	A14 NB C0:500	|Low|2020s|	23.45	23.40	25.25	23.74	25.16	23.04	21.12	22.76	23.21
3	A14 NB C0:500	|Low|2020s|	22.88	24.50	22.10	24.53	23.08	23.34	24.29	23.07	24.58
4	A14 NB C0:500	|Low|2020s|	23.59	23.44	21.67	24.33	24.89	21.39	22.54	22.07	24.29
5	A14 NB C0:	|Low|2020s|	22.81	23.47	23.97	22.76	23.09	24.26	24.57	23.63	23.59
6	A14 SB C0:	|High|2030s|	23.95	23.90	24.40	24.52	21.95	24.65	23.44	23.06	22.81
7	A14 SB C0:	|Medium|2030s|	23.00	24.97	24.89	23.07	22.88	23.70	23.69	22.45	22.10
8	A14 SB C0:	|Low|2030s|	23.39	24.28	21.84	24.36	21.74	22.69	24.23	25.72	25.40
9	A14 SB C0:	|High|2040s|	23.31	22.28	24.36	24.31	22.97	23.29	22.90	25.24	21.68
10	A14 SB C0:	|Medium|2040s|	23.24	22.54	24.78	22.23	23.84	22.14	26.38	22.43	22.45
11	A14 NB C501:1000	|Low|2020s|	24.21	23.68	23.88	23.54	24.77	22.93	22.76	25.33	24.30

\|Low\|2020s\|
\|High\|2030s\|
\|Medium\|2030s\|
\|Low\|2030s\|
\|High\|2040s\|
\|Medium\|2040s\|
\|Low\|2040s\|
\|High\|2050s\|

Figure D1-3: Representation of Climate Data by Road Section

4. Definition of Climate Threshold

The occurrence of hot dry summers within the climate dataset associated to the road sections is determined using user defined threshold values of mean maximum summer anomaly in degrees Celsius and monthly summer precipitation anomaly expressed in percentages. Anomalies are defined as the difference between the maximum summer temperature or monthly summer precipitation in a given year and the average value of the same climate variable over the 30-year UKCIP baseline period from 1961 to 1990. The use of anomalies in defining thresholds was adopted because it provides a consistent basis for comparing future climate predictions with recent observations or past climate. The definition of the climate threshold values is depicted in Figure D1-4.

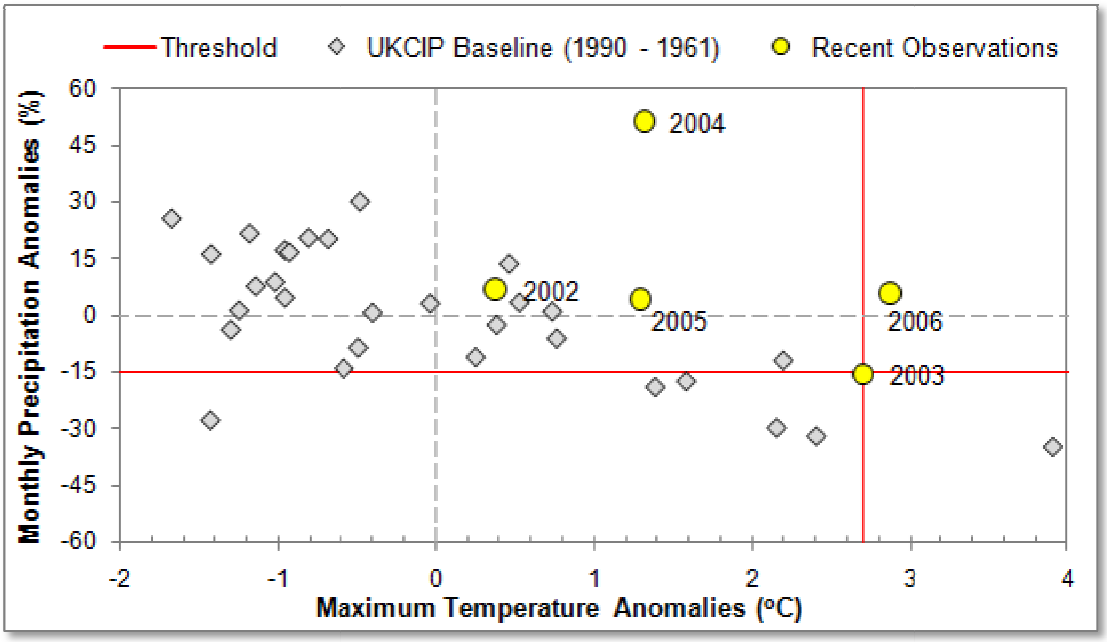

Figure D1-4: Definition of Climate Threshold Values

Plots of user defined threshold values which are shown as solid vertical and horizontal lines in Figure D1-4 are compared with baseline summer temperature and precipitation anomalies for the study area and anomalies for recent observations (2002 to 2006). For example, if it is

required to investigate the impact of 2003-type hot dry summers, then temperature and precipitation anomaly thresholds would be defined to correspond to 2003 observations as 2.7^{o}C and -15% respectively.

5. Rut Depth Deterioration Model

The rut depth deterioration model structure that was implemented in the climate impact model is given in Equation 4.5. Model structures for Void in Mix (VIM) and binder Softening Point (SP) are given in Equations 4.2 and 4.3 respectively.

6. Definition of Model Coefficients for Rut Depth Model

Distribution of rut depth model coefficients given in section 6.5.1 are implemented in the impact model using statistical distributions of best fit. The parameters of the statistical model were then used to describe the distribution of each model coefficient as illustrated in Figure D1-5.

Parameters of Best-fit Statistical Models of Model Coefficients

Description	Notation	Model Coefficient	PERT			TRIANGULAR			NORMAL	
			Mode	Lower Bound	Upper Bound	Mode	Lowew Bound	Upper Bound	Mean	Standard Deviation
Dense Bitumen Macadam (DBM)										
Axle Loading	YE4	β_1	0.2600	0.0000	0.6250					
Heavy Vehicle Speeds	sh	β_2	-0.4800	-1.5000	0.0000					
Gradient	G	β_3	0.0400	0.0000	0.1300					
Asphalt Thickness	HS	β_4	0.2900	0.08000	0.6000					
Material Properties	(SP/VIM)	β_5							-0.0500	0.0600
Pavement Temperature	Cmax	β_6	0.0400	0.0250	0.0900					
Error Distribution	ε	-							0.0000	0.1670
Hot Rolled Asphalt (HRA)										
Axle Loading	YE4	β_1							0.65000	0.11700
Heavy Vehicle Speeds	sh	β_2	-0.05	-0.30	0.00					
Gradient	G	β_3	0.01000	0.00000	0.04000					
Asphalt Thickness	HS	β_4	0.0600	0.0000	0.2500					
Material Properties	(SP/VIM)	β_5							0.1400	0.1900
Pavement Temperature	Cmax	β_6							0.02	0.00261
Error Distribution	ε	-				0.00	-0.75	0.75		
Thin Surface Course System (TSCS)										
Axle Loading	YE4	β_1							0.35000	1.30000
Heavy Vehicle Speeds	sh	β_2	-0.81	-1.80	-0.10					
Gradient	G	β_3	0.02000	0.00000	0.50000					
Asphalt Thickness	HS	β_4	0.4100	0.0000	1.0000					
Material Properties	(SP/VIM)	β_5							0.2300	0.2300
Pavement Temperature	Cmax	β_6	0.34	0.00	1.00					
Error Distribution	ε	-							0.3910	0.1062

Figure D1-5: Definition of Distribution of Model Coefficients

7. Definition of Model Coefficients for Asphalt Material Models

Model coefficients were developed for three asphalt surfacing groups including: Dense Bituminous Macadam (DBM), Hot Rolled Asphalt (HRA) and Thin Surface Course System (TSCS). The estimated model coefficients are given in section 6.5.2. Model inputs of the

distribution of the model coefficients for SP and VIM models are illustrated in Figure D1-6 and Figure D1-7 respectively.

$$SP = \alpha_{1m} \times LN(AGE_{imt}) + \alpha_{2m}$$

Description	Surfacing Type	Model Code	Distribution Properties				
			Type	Mean	SD	Min.	Max.
Factor for incremental effect of Ageing on binder softening point	DBM	$\alpha_{1[DBM]}$	Normal	6.310	0.220	-	-
	HRA	$\alpha_{1[HRA]}$	Normal	2.520	0.190	-	-
	TSCS	$\alpha_{1[TSCS]}$	Normal	5.060	0.220	-	-
	NEW	$\alpha_{1[OTHER]}$	Normal	4.000	0.200	-	-
Softening Point (°C) after year 1 of laying the bitumen	DBM	$\alpha_{2[DBM]}$	Normal	57.150	0.640	-	-
	HRA	$\alpha_{2[HRA]}$	Normal	70.500	0.500	-	-
	TSCS	$\alpha_{2[TSCS]}$	Normal	61.490	0.300	-	-
	NEW	$\alpha_{2OTHER]}$	Normal	68.000	0.300	-	-

Figure D1-6: Representation of Model Coefficients for Binder Softening Point Model

$$VIM = \eta_{1m} \times LN(AGE_{imt}) + \eta_{2m}$$

	Surfacing Type	Model Code	Distribution Properties				
			Type	Mean	SD	Min.	Max.
Factor for incremental change in VIM with time	DBM	$\eta_{1[DBM]}$	Normal	-0.52000	0.03000	-	-
	HRA	$\eta_{1[HRA]}$	Normal	-0.07000	0.03000	-	-
	TSCS	$\eta_{1[TSCS]}$	Normal	-1.30000	0.03000	-	-
	NEW	$\eta_{1[OTHER]}$	Normal	-1.00000	0.01000	-	-
Voids in Mix (%) after year 1 of surfacing	DBM	$\eta_{2[DBM]}$	Normal	2.8300	0.1000	-	-
	HRA	$\eta_{2[HRA]}$	Normal	1.3900	0.0700	-	-
	TSCS	$\eta_{2[TSCS]}$	Normal	5.110	0.050	-	-
	NEW	$\eta_{2[OTHER]}$	Normal	7.000	0.010	-	-

Figure D1-7: Representation of Model Coefficients for Voids in Mix Model

The input templates illustrated in Figure D1-6 and Figure D1-7 also allow for input of the distribution of model coefficients for alternative or new asphalt surfacing types other than DBM, HRA or TSCS.

Predicted trends of mean SP and VIM for each surfacing type with age given the defined model coefficients are visualised using plots illustrated in Figure D1-8.

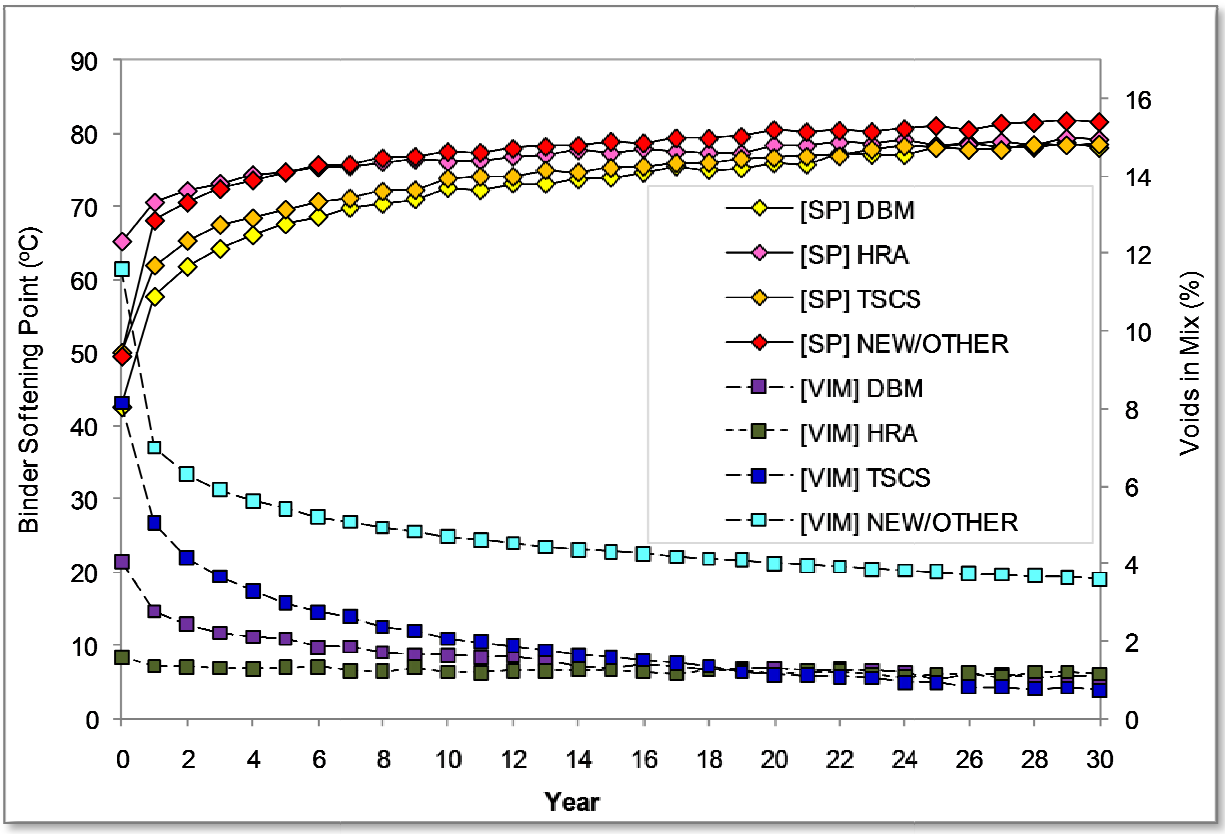

Figure D1-8: Mean SP and VIM with Surfacing Age in Years

8. Maintenance Policy

Road pavement maintenance scenario with respect to rut depth deterioration is defined by the following components:

- Treatment Options;
- Treatment intervention Threshold and Treatment Effects;
- Unit costs of treatments per square metres; and,

- Maintenance strategy.

8.1. Treatment Options

Asphalt surface rutting is manifested as transverse deformation in the wheel paths, treatments such as surface dressing and application of high friction surfacing are not ideal because they do not remove the deformation (Transport Scotland, 2008). Therefore, treatments groups defined in Table D1-3 were incorporated in the model as defaults. Alternative treatment types may be specified by the user.

Table D1-3: Description of Treatment Types

Group	Code	Type	Description
Thin Treatment	THIN	Thin surfacing or inlay	Mill and replace 30 to 45mm surface course
		Thin overlay	Mill 30 to 45mm and replace with 50mm of binder course and 30mm of surface course.
Moderate Treatment	MOD	Moderate inlay	Mill and replace the surface course (30 mm), and binder course (55mm)
		Moderate overlay	Mill 30 to 45mm and replace with 100mm of binder course and 30mm of surface course.
Thick Treatment	THICK	Thick inlay	Mill and replace the surface course (45mm), binder course (55mm) and base course (50mm)
		Thick overlay	Mill 30 to 45mm and replace with 150mm of binder course and 30mm of surface course.
Reconstruction	RECON	Reconstruction	Complete reconstruction of pavement layers

The treatment types and description were obtained from Transport Scotland (2008).

8.2. Treatment Intervention Threshold and Treatment Effects

Treatment intervention threshold refer to a fixed absolute rut depth threshold which if exceeded then treatment works described in section 9 of this appendix would be applied. The intervention threshold for a specific analysis is defined by the user. A default threshold of 11mm was specified in the model so that road sections with moderate or severe rut depth deterioration as defined in Table 5.2 were treated.

Once treatments that are appropriate for removing the rut depth deformation are applied, the cumulative rut depth value is reset to 2mm. The reset value of 2mm is typical of asphalt deformation that would usually occur within one year due to initial densification following the laying of a new asphalt surfacing layer. The value of 2mm was deemed representative since it is also used by UK Highways Agency in the Whole Life Cost Optimisation (WiLCO) decision support system to inform the Agency's strategic planning and investment decisions (Smith, 2011).

8.3. Treatment Unit Costs

Treatment unit costs per square metres are defined by the user. Typical unit costs for treatment types were provided in Table 10.3.

8.4. Maintenance Strategy

Maintenance strategies are defined by specifying the treatments that should be applied by the model as the first, second, third and subsequent interventions. The timing of these interventions is dependent upon the rate of rut depth deterioration predicted by the model.

When the cumulative rut depth deterioration predicted by the model exceeds a user defined threshold then a treatments are applied.

An example of the definition of maintenance strategies is illustrated in Figure D1-9. Strategy A is designed for maintaining road sections with initial rut depth categorised in poor condition. Strategy B is applicable to roads with initial rut depth in fair condition and Strategy C is applicable to roads which are initially classified to be in good condition. Further discussions on these maintenance strategies are provided in section 10.3.3.3.

Name	Initial Condition	1st Intervention	2nd Intervention	3nd Intervention	Subsequent
Strategy A	Poor (Rut Depth>= 11mm)	RECON	THIN	MOD	MOD
Strategy B	Fair (6mm<= Rut Depth < 11mm)	THICK	THIN	RECON	MOD
Strategy C	Good (Rut Depth < 6mm)	THIN	MOD	RECON	MOD

Figure D1-9: Illustration of Maintenance Strategies

Notes to Figure D1-9:

- RECON = Reconstruction
- THICK = Thick Treatment
- THIN = Thin Treatment
- MOD = Moderate Treatment

Appendix D2 Outputs from Climate Impact and Adaptation

1. Primary Model Outputs

Outputs of the impact model comprise the following:

- Predicted annual rut depth deterioration rates for each maintenance scenario and climate scenario analysed;
- Predicted condition profile for each maintenance scenario and climate scenario;
- Discounted treatment costs for each maintenance scenario and climate change scenarios analysed.

The above outputs are illustrated in section 10.8. The outputs generated by the model can be analysed externally to provide inference on:

- The impact of climate change associated with future climate scenarios relative to the baseline climate scenario for a given pavement maintenance policy; and,
- The costs of climate change that can be attributed to different sets of maintenance strategies for a given climate scenario.

Typical results of such an analysis are presented in section 10.9 following the case study to demonstrate the application of the model.

2. Additional Model Outputs

The model presented can potentially be used together with existing road decision support tools such as HDM-4 to derive the following additional outputs:

- Road user costs for a given set of climate change and road maintenance scenarios;
- Road works programme for a given set of climate change and road maintenance scenarios;
- Optimum road maintenance standards or maintenance scenarios for adapting to the impacts of climate change.

Analysis necessary to produce these additional outputs is outside the scope of this study.

APPENDIX E CASE STUDY INPUTS AND OUTPUTS

This appendix includes the following:

Appendix E1 Case Study Road Network Data

1 Asphalt Road Section Inventory

(Source: Highways Agency Pavement Management System (HAPMS))

JUNCTION 6

Section Label	1500M11/103												1500M11/105											1500M11/107			
Section Chainage (m)	0	100	200	300	400	500	600	700	800	900	1000	1093	100	200	300	400	500	600	700	800	900	1000	1080	100	200	300	400
Lane 1 Width (m)	3.25	3.25	3.25	3.25	3.25	3.25	3.25	3.25	3.25	3.25	3.25	3.25	3.25	3.25	3.25	3.25	3.25	3.25	3.25	3.25	3.25	3.25	3.25	3.25	3.25	3.25	3.25
Lane 2 Width (m)	3.25	3.25	3.25	3.25	3.25	3.25	3.25	3.25	3.25	3.25	3.25	3.25	3.25	3.25	3.25	3.25	3.25	3.25	3.25	3.25	3.25	3.25	3.25	3.25	3.25	3.25	3.25
Lane 3 Width (m)													3.25	3.25	3.25	3.25	3.25	3.25	3.25	3.25	3.25	3.25	3.25	3.25	3.25	3.25	3.25
Lane 4 Width (m)																											
Chainage (km)	**0**	**0.10**	**0.20**	**0.30**	**0.40**	**0.50**	**0.60**	**0.70**	**0.80**	**0.90**	**1.00**	**1.09**	**1.19**	**1.29**	**1.39**	**1.49**	**1.59**	**1.69**	**1.79**	**1.89**	**1.99**	**2.09**	**2.17**	**2.27**	**2.37**	**2.47**	**2.57**

2 Average Rut Depth (mm)

(Source: Highways Agency Pavement Management System (HAPMS))

Rut Depth Condition Bands

Sound
Some Deterioration
Moderate Deterioration
Severe Deterioration

Lane 1	14	10.6	3.2	3.1	2.9	2.7	3	3	4	5.2	5	4.1	3.2	2.6	2.9	4	4.9	6.9	4.2	6.4	17.2	16.8	9.4	9	10.3	9.2
Lane 2	7.1	6.6	4.1	3.6	5.3	3.8	3.1	3.1	4.2	4.3	5.6	1.2	1.2	1	3	4.2	4.5	5.2	5	6.1	8.2	5.5	3.5	4.7	5	4.2

3 Total Asphalt Thickness (mm)

(Source: Highways Agency Pavement Management System (HAPMS))

Thickness (mm)	280	280	150	150	150	290	290	290	290	290	290	490	490	490	490	490	490	490	490	150	280	280	480	480	480	480

4 Surfacing Age (Years)

(Source: Highways Agency Pavement Management System (HAPMS))

AGE (Years)	21	21	2.92	2.92	2.92	2.92	2.92	2.92	2.92	21	21	21	21	21	21	21	21	21	21	21	21	21	0.87	0.86	0.86	0.86

5 Traffic Flow Data

(Source: Highways Agency Traffic Information System (HATRIS))

Year	2010
Average Annual Daily Traffic (AADT)	35583
Percentage of Heavy Vehicles (% HGV)	14.8

Figure E1-1: Road Network Data

1 Asphalt Road Section Inventory

Section Label	1500M11/109																1500M11/113														1500M11/115					
Section Chainage (m)	500	600	700	715	100	200	300	400	500	600	700	800	900	1000	1056	100	200	300	400	500	600	700	741	100	200	300	400	411								
Lane 1 Width (m)	3.25	3.25	3.25	3.25	3.25	3.25	3.25	3.25	3.25	3.25	3.25	3.25	3.25	3.25	3.25	3.25	3.25	3.25	3.25	3.25	3.25	3.25	3.25	3.25	3.25	3.25	3.25	3.25								
Lane 2 Width (m)	3.25	3.25	3.25	3.25	3.25	3.25	3.25	3.25	3.25	3.25	3.25	3.25	3.25	3.25	3.25	3.25	3.25	3.25	3.25	3.25	3.25	3.25	3.25	3.25	3.25	3.25	3.25	3.25								
Lane 3 Width (m)	3.25	3.25	3.25	3.25	3.25	3.25	3.25	3.25	3.25	3.25	3.25	3.25	3.25	3.25	3.25	3.25	3.25	3.25	3.25	3.25	3.25	3.25	3.25	3.25	3.25	3.25	3.25	3.25								
Lane 4 Width (m)																																				
Chainage (km)	0	2.67	2.77	2.87	2.89	2.99	3.09	3.19	3.29	3.39	3.49	3.59	3.69	3.79	3.89	3.94	4.04	4.14	4.24	4.34	4.44	4.54	4.64	4.69	4.79	4.89	4.99	5.09	5.10							

2 Average Rut Depth (mm)

Rut Depth Condition Bands

Sound
Some Deterioration
Moderate Deterioration
Severe Deterioration

Lane 1	5.6	5.7	5.5	5.4	7.1	3.7	5.7	3	4	3	3.5	2.9	3.1	6.7	10.2	2.8	2.3	2.2	2.5	3.4	3.3	3.1	3.6	3.2	2.8	3.5	3.1	3.3								
Lane 2	4.1	1.8	2.1	1.7	4.8	4.7	5	4.3	3.5	3.4	3.3	3.3	2.3	3	2.8	5.6	6.7	5.9	2.7	7.3	7.7	8	7.6	7.3	3.1	1.7	4.4	5								

3 Total Asphalt Thickness (mm)

Thickness (mm)	480	480	490	490	470	470	470	470	470	470	470	470	470	470	470	480	480	480	480	480	480	480	480	90	90	90	480	480								

4 Surfacing Age (Years)

AGE (Years)	0.85	0.85	6.09	6.08	1.07	1.07	1.07	21	21	21	21	21	21	21	21	6.25	6.25	6.25	6.25	6.25	6.25	6.25	6.25	21	21	21	21	21								

5 Traffic Flow Data

Year	2010
Average Annual Daily Traffic (AADT)	35583
Percentage of Heavy Vehicles (% HGV)	14.8

Figure E1-2: Road Network Data (Continued)

1 Asphalt Road Section Inventory

JUNCTION 5 → JUNCTION 4

Section Label	1500M11/117																			1500M11/127			1500M11/129						
Section Chainage (m)	100	200	300	400	500	600	700	800	900	1000	1100	1200	1300	1400	1500	1600	1700	1800	1885	100	200	279	100	200	300	400	500	582
Lane 1 Width (m)	3.25	3.25	3.25	3.25	3.25	3.25	3.25	3.25	3.25	3.25	3.25	3.25	3.25	3.25	3.25	3.25	3.25	3.25	3.25	3.25	3.25	3.25	3.25	3.25	3.25	3.25	3.25	3.25
Lane 2 Width (m)	3.25	3.25	3.25	3.25	3.25	3.25	3.25	3.25	3.25	3.25	3.25	3.25	3.25	3.25	3.25	3.25	3.25	3.25	3.25	3.25	3.25	3.25	3.25	3.25	3.25	3.25	3.25	3.25
Lane 3 Width (m)	3.25	3.25	3.25	3.25	3.25	3.25	3.25	3.25	3.25	3.25	3.25	3.25	3.25	3.25	3.25	3.25	3.25	3.25	3.25									
Lane 4 Width (m)	3.25	3.25	3.25	3.25	3.25	3.25	3.25	3.25	3.25	3.25	3.25	3.25	3.25	3.25	3.25	3.25	3.25	3.25	3.25									
Chainage (km)	0	5.20	5.30	5.40	5.50	5.60	5.70	5.80	5.90	6.00	6.10	6.20	6.30	6.40	6.50	6.60	6.70	6.80	6.90	6.98	7.08	7.18	7.26	7.36	7.46	7.56	7.66	7.76	7.84

2 Average Rut Depth (mm)

Rut Depth Condition Bands

Sound
Some Deterioration
Moderate Deterioration
Severe Deterioration

Lane 1	NA	NA	3.4	3.8	3.6	3.1	3.6	3.4	3.2	3.6	3.5	3.6	2.9	2.5	2.6	2.6	3.1	2.9	3.5	3.5	3.5	3.2	4.3	3.9	3.4	3.6	3.1	3.1
Lane 2	NA	NA	4.6	5.3	5.2	5	5.2	5.1	5.8	4.3	4.5	5.6	6.2	5.9	5.2	5.3	4.9	4.5	4.3	2.8	2.8	3	2.9	2.6	2.7	2.6	2.4	2.4

3 Total Asphalt Thickness (mm)

Thickness (mm)	475	475	475	475	475	475	475	475	470	470	470	470	470	470	470	470	470	470	470	160	160	160	160	160	160	160	160	160

4 Surfacing Age (Years)

AGE (Years)	1.44	1.44	1.44	6.09	6.09	6.09	6.09	6.09	6.09	6.09	6.09	6.09	6.09	6.09	6.09	6.09	6.09	6.09	6.09	4.75	4.75	4.75	4.75	4.75	4.75	4.75	4.75	4.75

5 Traffic Flow Data

Year	2010
Average Annual Daily Traffic (AADT)	41796
Percentage of Heavy Vehicles (% HGV)	15.1

Figure E1-3: Road Network Data (Continued)

Appendix E2 Cumulative Rut Depth Deterioration in Condition Bands for Current Practice and Adaptation Strategies

Figure E2-1: Cumulative Rut Depth Proportions without Applying Treatment Works for Current Practice Strategy.

Year	Baseline (1961 - 1990)				2020s				2030s				2040s				2050s			
	Good	Fair	Poor	Critical	Good	Fair	Poor	Critical	Good	Fair	Poor	Critical	Good	Fair	Poor	Critical	Good	Fair	Poor	Critical
0	89%	9%	1%	0%	89%	9%	1%	0%	89%	9%	1%	0%	89%	9%	1%	0%	89%	9%	1%	0%
1	76%	20%	4%	0%	76%	20%	4%	0%	75%	20%	4%	0%	74%	21%	4%	1%	72%	22%	5%	1%
2	61%	30%	8%	1%	60%	31%	8%	1%	59%	31%	8%	1%	56%	33%	9%	1%	54%	32%	11%	2%
3	46%	40%	13%	1%	44%	40%	14%	2%	43%	40%	15%	2%	40%	41%	16%	3%	38%	40%	19%	4%
4	32%	45%	20%	3%	31%	45%	21%	3%	29%	45%	22%	4%	27%	45%	24%	4%	24%	43%	27%	6%
5	21%	48%	27%	4%	20%	47%	28%	5%	18%	45%	30%	6%	16%	44%	32%	7%	14%	41%	34%	10%
6	13%	46%	35%	7%	12%	44%	36%	8%	11%	42%	38%	9%	9%	39%	40%	11%	8%	36%	41%	15%
7	7%	41%	42%	10%	7%	39%	43%	11%	6%	36%	45%	13%	5%	33%	46%	16%	4%	30%	46%	20%
8	4%	34%	49%	13%	4%	32%	49%	15%	3%	30%	49%	18%	2%	26%	50%	22%	2%	22%	48%	27%
9	2%	27%	53%	18%	2%	25%	53%	20%	1%	23%	52%	24%	1%	20%	51%	28%	1%	16%	48%	35%
10	1%	21%	54%	24%	1%	19%	54%	27%	1%	16%	53%	30%	1%	14%	50%	35%	0%	11%	46%	43%
11	0%	15%	54%	30%	0%	13%	53%	33%	0%	11%	51%	37%	0%	10%	47%	43%	0%	7%	43%	50%
12	0%	10%	52%	37%	0%	9%	51%	40%	0%	8%	47%	45%	0%	6%	43%	51%	0%	4%	37%	58%
13	0%	7%	48%	45%	0%	6%	46%	48%	0%	5%	42%	53%	0%	4%	38%	58%	0%	3%	32%	66%
14	0%	4%	44%	52%	0%	4%	41%	55%	0%	3%	37%	60%	0%	2%	32%	66%	0%	2%	26%	72%
15	0%	3%	38%	59%	0%	2%	35%	63%	0%	2%	31%	67%	0%	1%	26%	72%	0%	1%	21%	78%

Figure E2-1: Cumulative Rut Depth Proportions without Applying Treatment Works for Current Practice Strategy (Continued).

Year	Baseline (1961 - 1990)				2020s				2030s				2040s				2050s			
	Good	Fair	Poor	Critical	Good	Fair	Poor	Critical	Good	Fair	Poor	Critical	Good	Fair	Poor	Critical	Good	Fair	Poor	Critical
16	0%	1%	33%	66%	0%	1%	29%	70%	0%	1%	26%	73%	0%	1%	21%	78%	0%	0%	16%	84%
17	0%	1%	27%	72%	0%	1%	24%	76%	0%	1%	20%	79%	0%	0%	17%	83%	0%	0%	12%	88%
18	0%	1%	22%	78%	0%	0%	19%	81%	0%	0%	16%	84%	0%	0%	13%	87%	0%	0%	8%	91%
19	0%	0%	17%	82%	0%	0%	15%	85%	0%	0%	12%	88%	0%	0%	9%	91%	0%	0%	6%	94%
20	0%	0%	14%	86%	0%	0%	11%	89%	0%	0%	9%	91%	0%	0%	7%	93%	0%	0%	4%	96%
21	0%	0%	10%	90%	0%	0%	8%	92%	0%	0%	6%	93%	0%	0%	5%	95%	0%	0%	3%	97%
22	0%	0%	8%	92%	0%	0%	6%	94%	0%	0%	5%	95%	0%	0%	4%	96%	0%	0%	2%	98%
23	0%	0%	6%	94%	0%	0%	4%	96%	0%	0%	3%	97%	0%	0%	2%	98%	0%	0%	1%	99%
24	0%	0%	4%	96%	0%	0%	3%	97%	0%	0%	2%	98%	0%	0%	1%	99%	0%	0%	1%	99%
25	0%	0%	3%	97%	0%	0%	2%	98%	0%	0%	1%	99%	0%	0%	1%	99%	0%	0%	1%	99%
26	0%	0%	2%	98%	0%	0%	1%	99%	0%	0%	1%	99%	0%	0%	1%	99%	0%	0%	0%	100%
27	0%	0%	1%	99%	0%	0%	1%	99%	0%	0%	1%	99%	0%	0%	0%	100%	0%	0%	0%	100%
28	0%	0%	1%	99%	0%	0%	1%	99%	0%	0%	0%	100%	0%	0%	0%	100%	0%	0%	0%	100%
29	0%	0%	1%	99%	0%	0%	0%	100%	0%	0%	0%	100%	0%	0%	0%	100%	0%	0%	0%	100%
30	0%	0%	0%	100%	0%	0%	0%	100%	0%	0%	0%	100%	0%	0%	0%	100%	0%	0%	0%	100%
Average	11%	13%	22%	53%	11%	13%	21%	55%	11%	12%	20%	57%	10%	11%	19%	59%	10%	10%	17%	62%

Figure E2-2: Cumulative Rut Depth Proportions without Applying Treatment Works for Adaptation Strategy.

Year	Baseline (1961 - 1990)				2020s				2030s				2040s				2050s			
	Good	Fair	Poor	Critical	Good	Fair	Poor	Critical	Good	Fair	Poor	Critical	Good	Fair	Poor	Critical	Good	Fair	Poor	Critical
0	84%	14%	2%	0%	83%	14%	2%	0%	83%	14%	2%	0%	84%	14%	2%	0%	83%	14%	2%	0%
1	68%	27%	5%	0%	68%	27%	5%	0%	67%	27%	5%	0%	67%	27%	5%	1%	66%	27%	5%	1%
2	51%	39%	9%	1%	51%	39%	10%	1%	50%	39%	10%	1%	49%	39%	10%	1%	49%	39%	11%	1%
3	35%	48%	15%	1%	35%	47%	16%	2%	35%	47%	17%	2%	33%	48%	17%	2%	33%	46%	18%	2%
4	22%	53%	23%	2%	22%	51%	24%	3%	22%	51%	24%	3%	21%	51%	24%	3%	21%	49%	25%	4%
5	13%	52%	31%	4%	14%	50%	32%	5%	13%	50%	32%	5%	13%	49%	33%	6%	12%	47%	34%	7%
6	8%	46%	40%	6%	8%	45%	40%	7%	7%	45%	40%	8%	7%	44%	41%	8%	7%	42%	41%	10%
7	4%	39%	47%	9%	4%	39%	47%	10%	4%	38%	47%	11%	4%	37%	48%	12%	4%	35%	47%	14%
8	2%	32%	53%	13%	2%	32%	53%	14%	2%	31%	52%	15%	2%	29%	53%	16%	2%	28%	52%	19%
9	1%	24%	57%	18%	1%	24%	56%	19%	1%	24%	55%	20%	1%	22%	55%	22%	1%	21%	54%	24%
10	0%	18%	58%	24%	0%	18%	57%	25%	0%	17%	56%	26%	0%	16%	56%	28%	0%	15%	54%	31%
11	0%	13%	57%	30%	0%	12%	56%	31%	0%	12%	55%	33%	0%	11%	54%	35%	0%	10%	52%	38%
12	0%	8%	55%	36%	0%	8%	53%	38%	0%	8%	53%	40%	0%	7%	51%	42%	0%	7%	48%	45%
13	0%	5%	51%	43%	0%	5%	49%	45%	0%	5%	48%	47%	0%	5%	46%	49%	0%	4%	43%	52%
14	0%	3%	46%	50%	0%	3%	44%	52%	0%	3%	43%	54%	0%	3%	41%	56%	0%	3%	38%	60%
15	0%	2%	40%	58%	0%	2%	39%	59%	0%	2%	37%	61%	0%	2%	35%	63%	0%	2%	32%	66%

Figure E2-2: Cumulative Rut Depth Proportions without Applying Treatment Works for Adaptation Strategy (Continued).

Year	Baseline (1961 - 1990)				2020s				2030s				2040s				2050s			
	Good	Fair	Poor	Critical	Good	Fair	Poor	Critical	Good	Fair	Poor	Critical	Good	Fair	Poor	Critical	Good	Fair	Poor	Critical
16	0%	1%	34%	65%	0%	1%	33%	66%	0%	1%	31%	67%	0%	1%	29%	70%	0%	1%	26%	73%
17	0%	1%	29%	71%	0%	1%	27%	72%	0%	1%	26%	73%	0%	1%	24%	76%	0%	0%	21%	78%
18	0%	0%	23%	76%	0%	0%	22%	78%	0%	0%	21%	79%	0%	0%	19%	81%	0%	0%	16%	83%
19	0%	0%	18%	81%	0%	0%	17%	82%	0%	0%	16%	83%	0%	0%	15%	85%	0%	0%	13%	87%
20	0%	0%	14%	85%	0%	0%	13%	86%	0%	0%	12%	87%	0%	0%	11%	89%	0%	0%	9%	91%
21	0%	0%	11%	89%	0%	0%	10%	90%	0%	0%	9%	91%	0%	0%	8%	92%	0%	0%	7%	93%
22	0%	0%	8%	92%	0%	0%	8%	92%	0%	0%	7%	93%	0%	0%	6%	94%	0%	0%	5%	95%
23	0%	0%	6%	94%	0%	0%	6%	94%	0%	0%	5%	95%	0%	0%	4%	96%	0%	0%	3%	97%
24	0%	0%	4%	96%	0%	0%	4%	96%	0%	0%	3%	97%	0%	0%	3%	97%	0%	0%	2%	98%
25	0%	0%	3%	97%	0%	0%	3%	97%	0%	0%	2%	98%	0%	0%	2%	98%	0%	0%	2%	98%
26	0%	0%	2%	98%	0%	0%	2%	98%	0%	0%	2%	98%	0%	0%	1%	99%	0%	0%	1%	99%
27	0%	0%	1%	99%	0%	0%	1%	99%	0%	0%	1%	99%	0%	0%	1%	99%	0%	0%	1%	99%
28	0%	0%	1%	99%	0%	0%	1%	99%	0%	0%	1%	99%	0%	0%	1%	99%	0%	0%	0%	100%
29	0%	0%	1%	99%	0%	0%	1%	99%	0%	0%	1%	99%	0%	0%	0%	100%	0%	0%	0%	100%
30	0%	0%	0%	100%	0%	0%	0%	100%	0%	0%	0%	100%	0%	0%	0%	100%	0%	0%	0%	100%
Average	7%	14%	25%	55%	7%	14%	24%	55%	7%	13%	24%	56%	7%	13%	23%	57%	7%	13%	22%	59%

Appendix E3 Predicted Condition Profiles for Current Practice Strategy

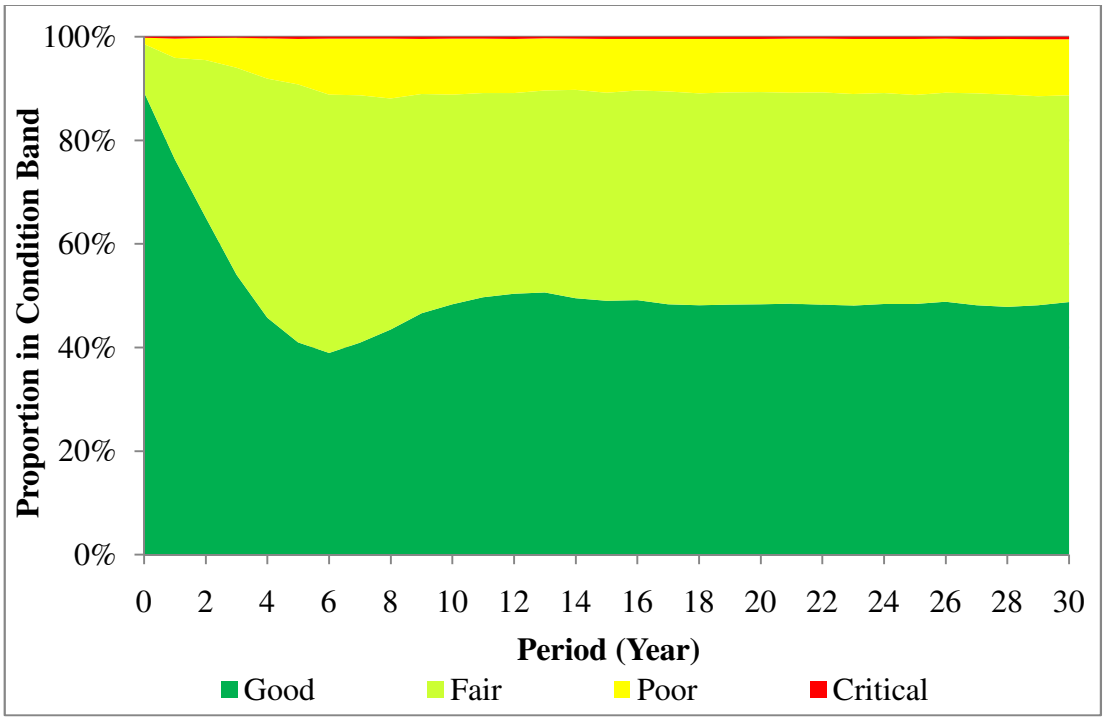

Figure E3-1: Cumulative Rut Depth Proportions with Treatment Works for the Baseline Scenario

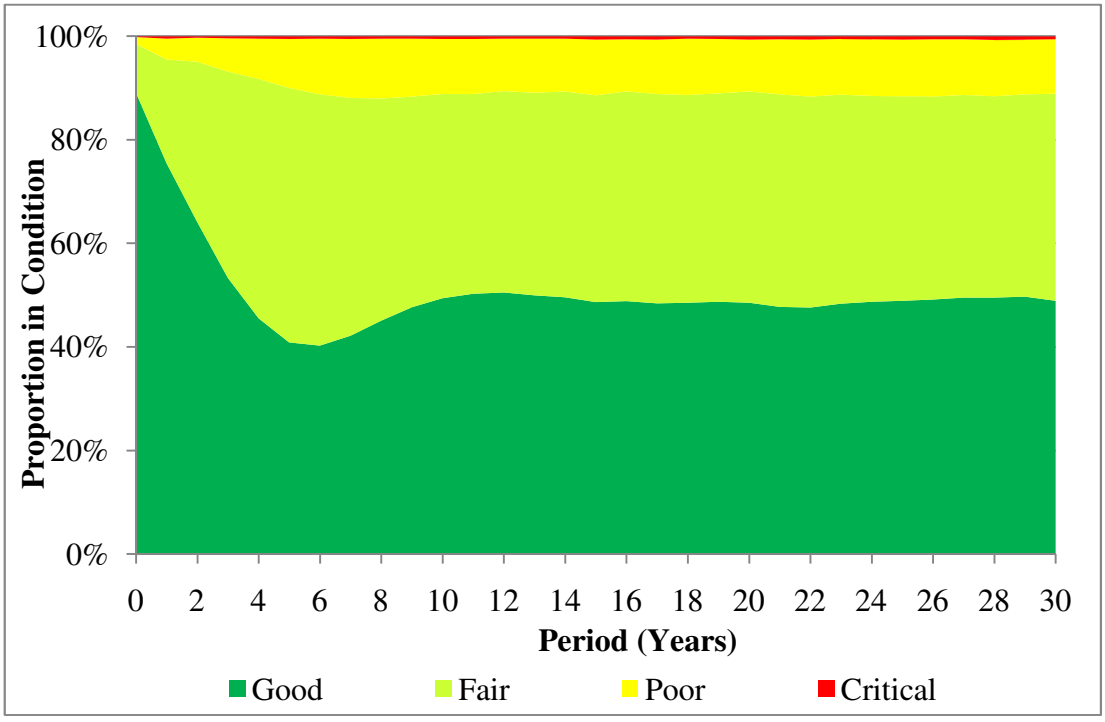

Figure E3-2: Cumulative Rut Depth Proportions with Treatment Works for the 2020s Medium Emission Scenario

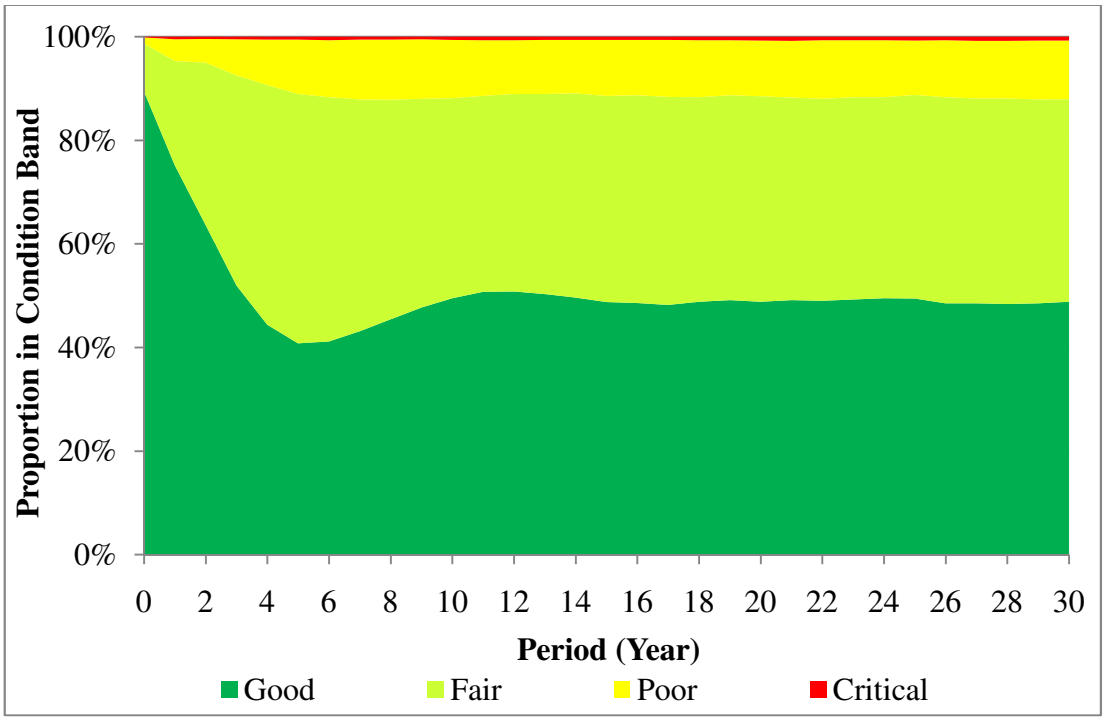

Figure E3-3: Cumulative Rut Depth Proportions with Treatment Works for the 2030s Medium Emission Scenario

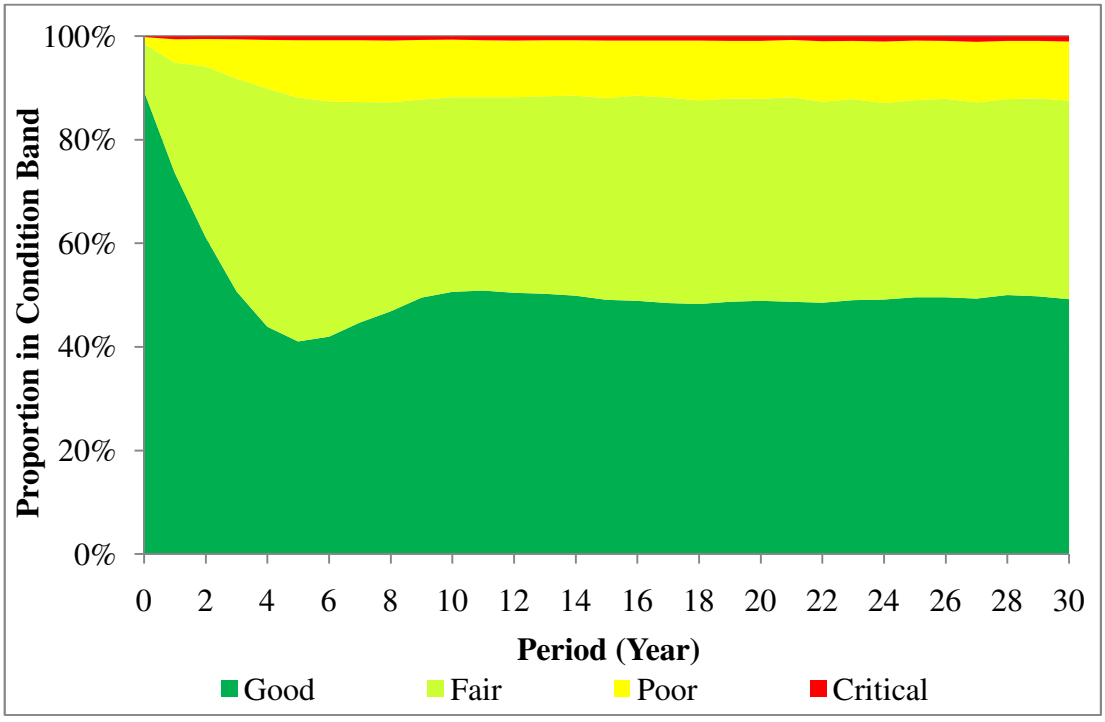

Figure E3-4: Cumulative Rut Depth Proportions with Treatment Works for the 2040s Medium Emission Scenario

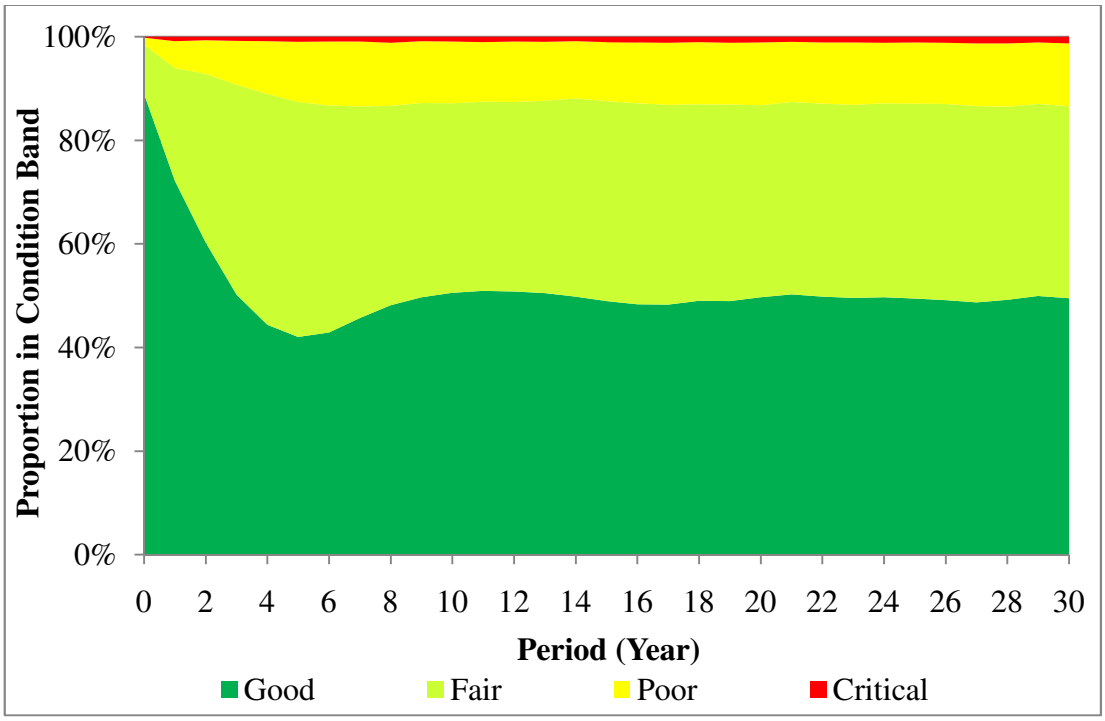

Figure E3-5: Cumulative Rut Depth Proportions with Treatment Works for the 2050s Medium Emission Scenario

Appendix E4 Distribution of Discounted Maintenance Costs for Current Practice Maintenance Strategy

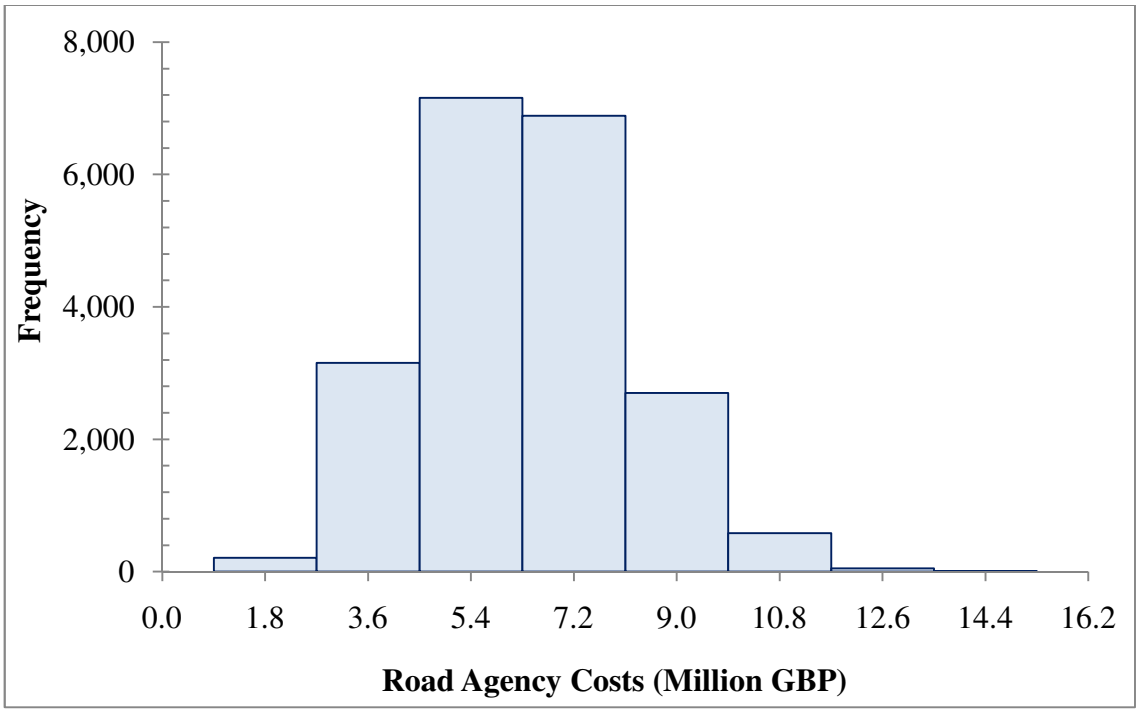

Figure E4-1: Distribution of Discounted Maintenance Costs for the 2030s Medium Emission Scenario for the Current Practice Maintenance Strategy

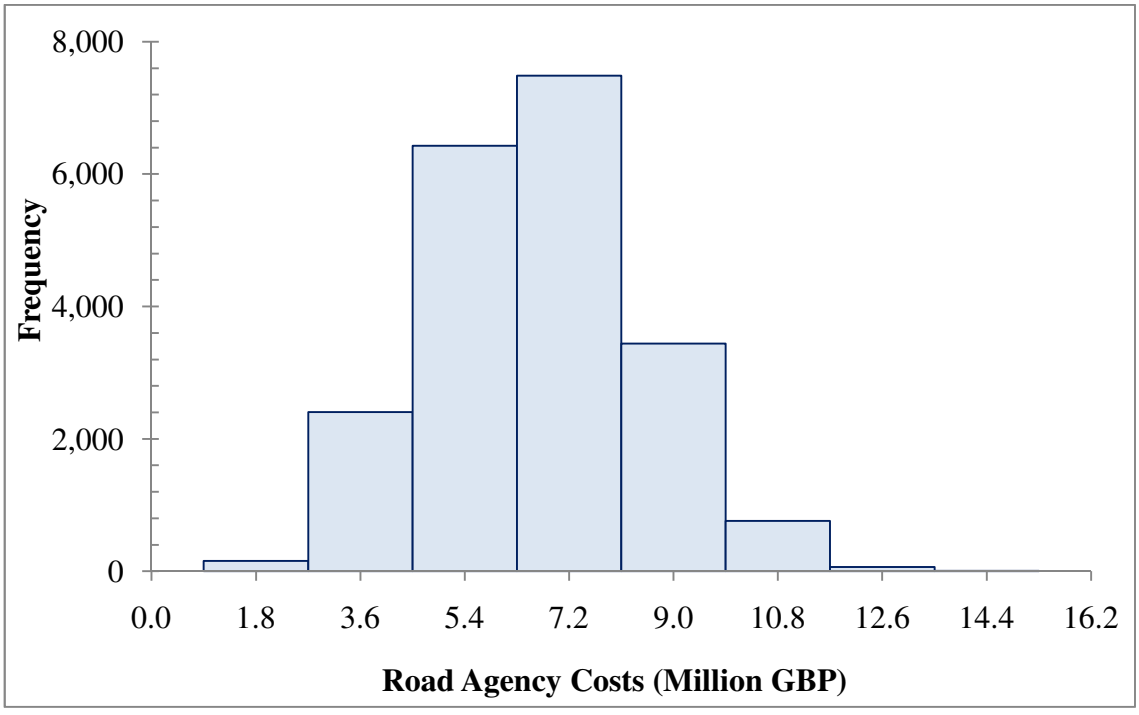

Figure E4-2: Distribution of Discounted Maintenance Costs for the 2040s Medium Emission Scenario for the Current Practice Maintenance Strategy

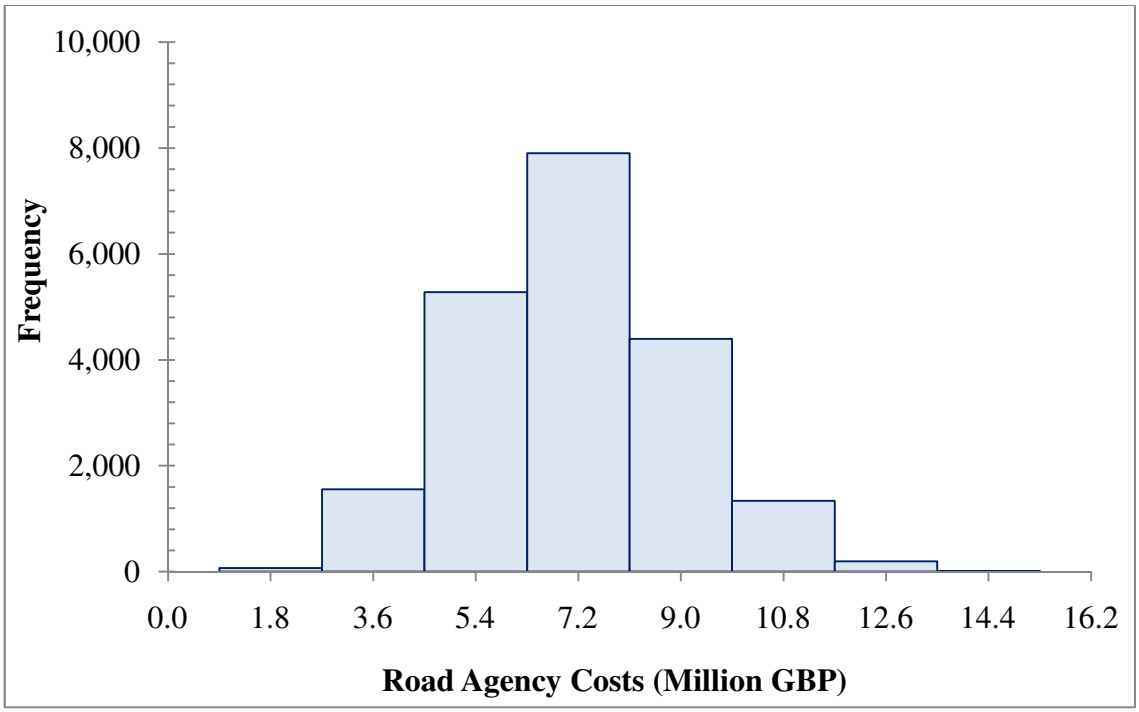

Figure E4-3: Distribution of Discounted Maintenance Costs for the 2050s Medium Emission Scenario for the Current Practice Maintenance Strategy

Appendix E5 Predicted Condition Profiles for Adaptation Maintenance Strategy

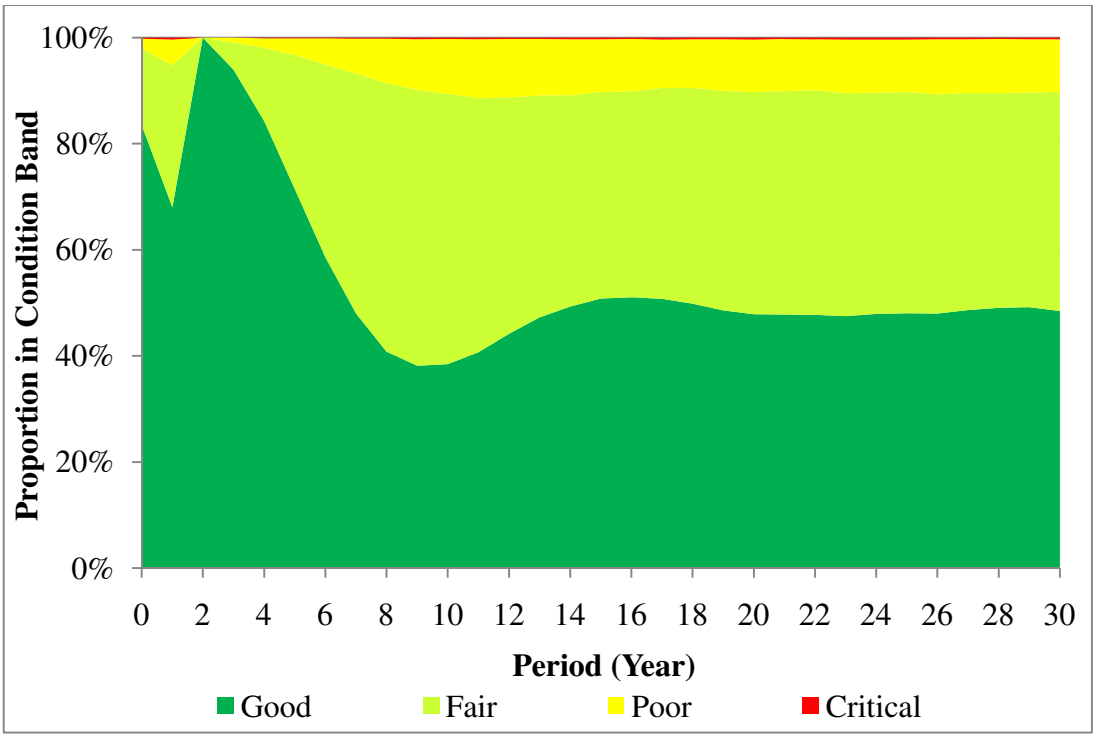

Figure E5-1: Adaptation Cumulative Rut Depth Proportions with Treatment Works for the Baseline Scenario

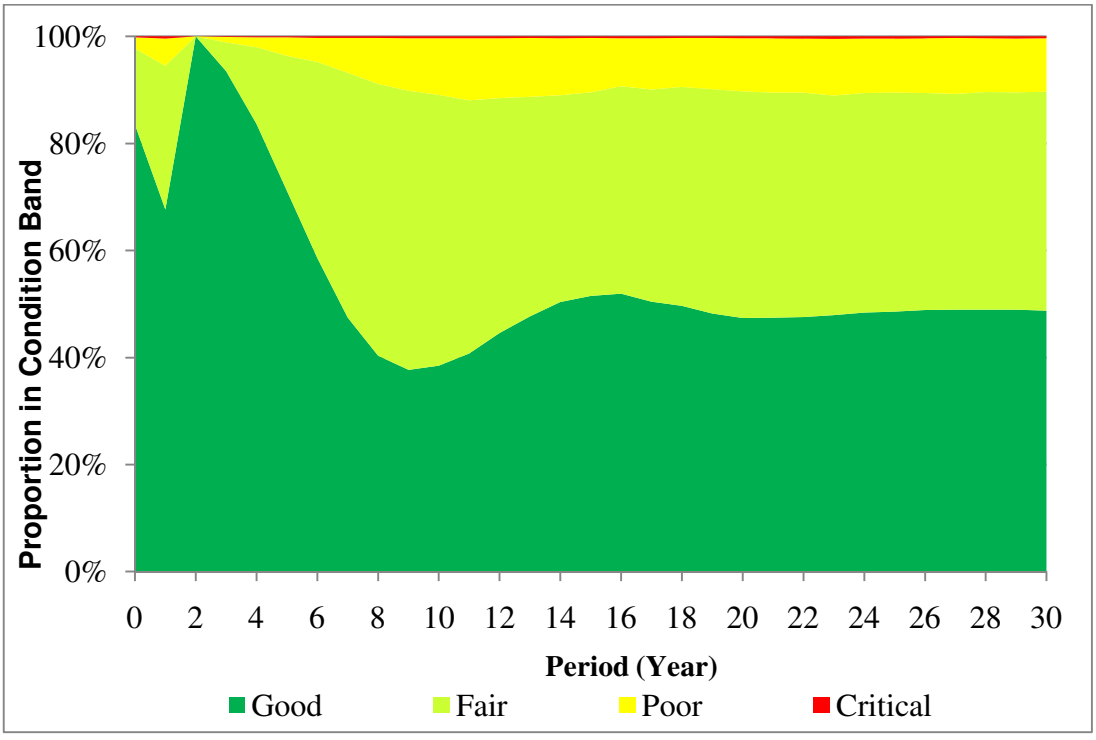

Figure E5-2: Adaptation Cumulative Rut Depth Proportions with Treatment Works for the 2020s Medium Emission Scenario

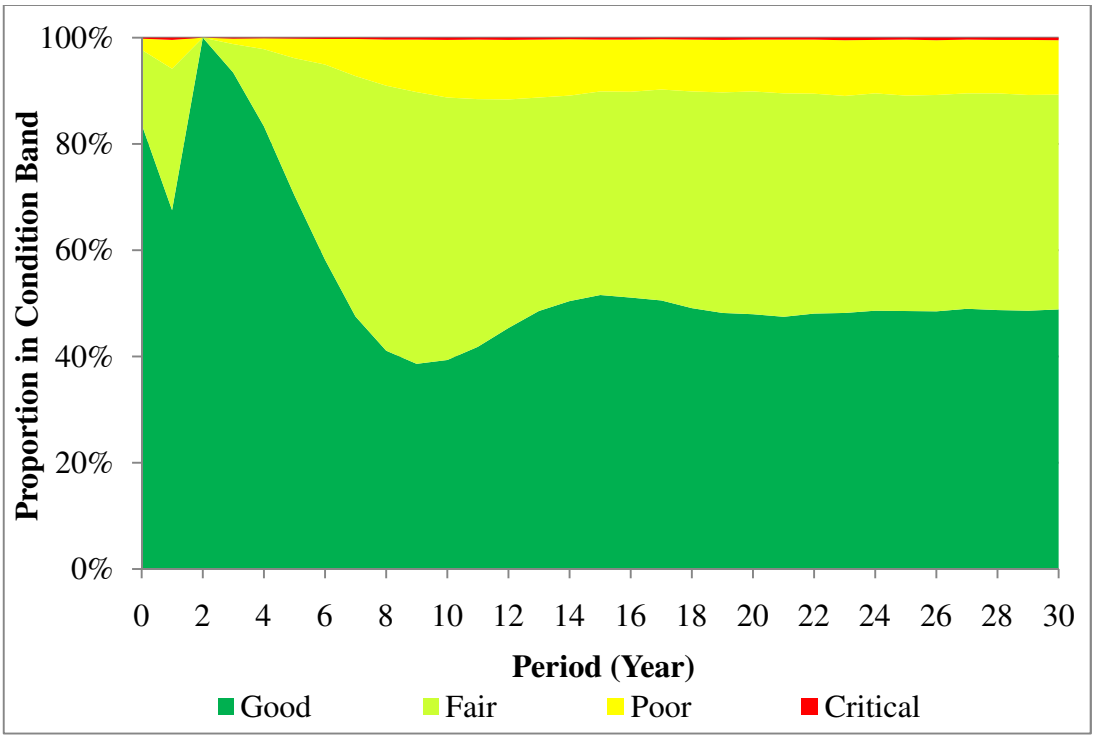

Figure E5-3: Adaptation Cumulative Rut Depth Proportions with Treatment Works for the 2030s Medium Emission Scenario

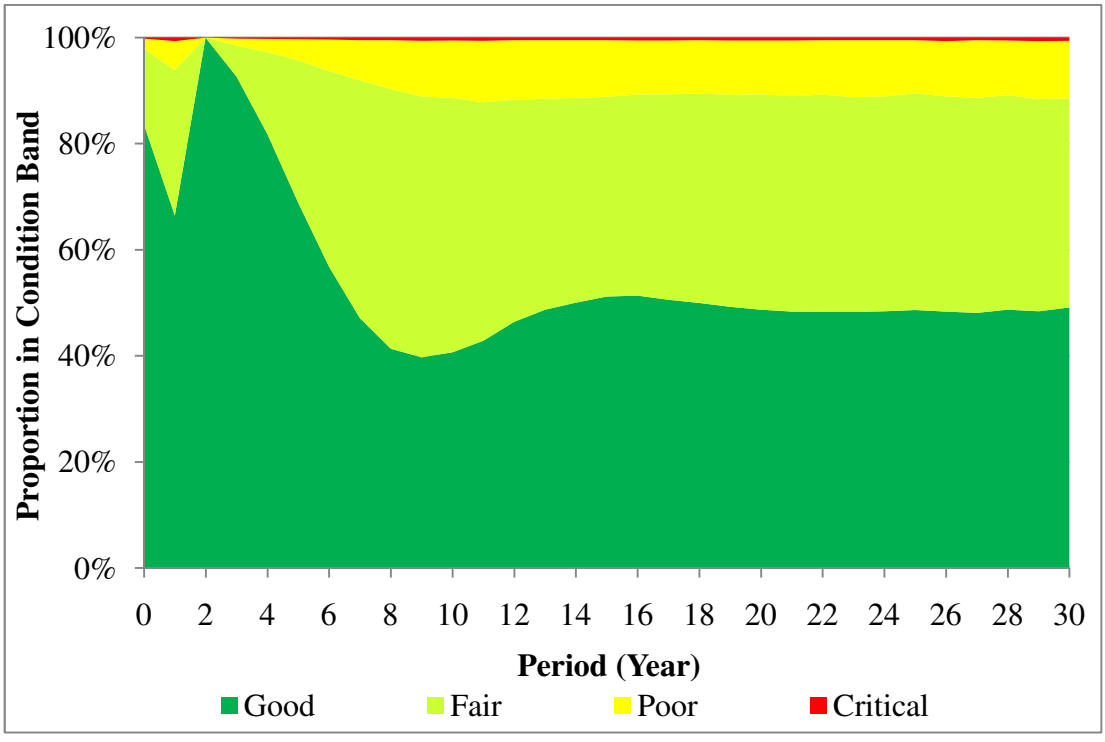

Figure E5-4: Adaptation Cumulative Rut Depth Proportions with Treatment Works for the 2040s Medium Emission Scenario

Appendix E6 Distribution of Discounted Cost for Current Practice Maintenance Strategy

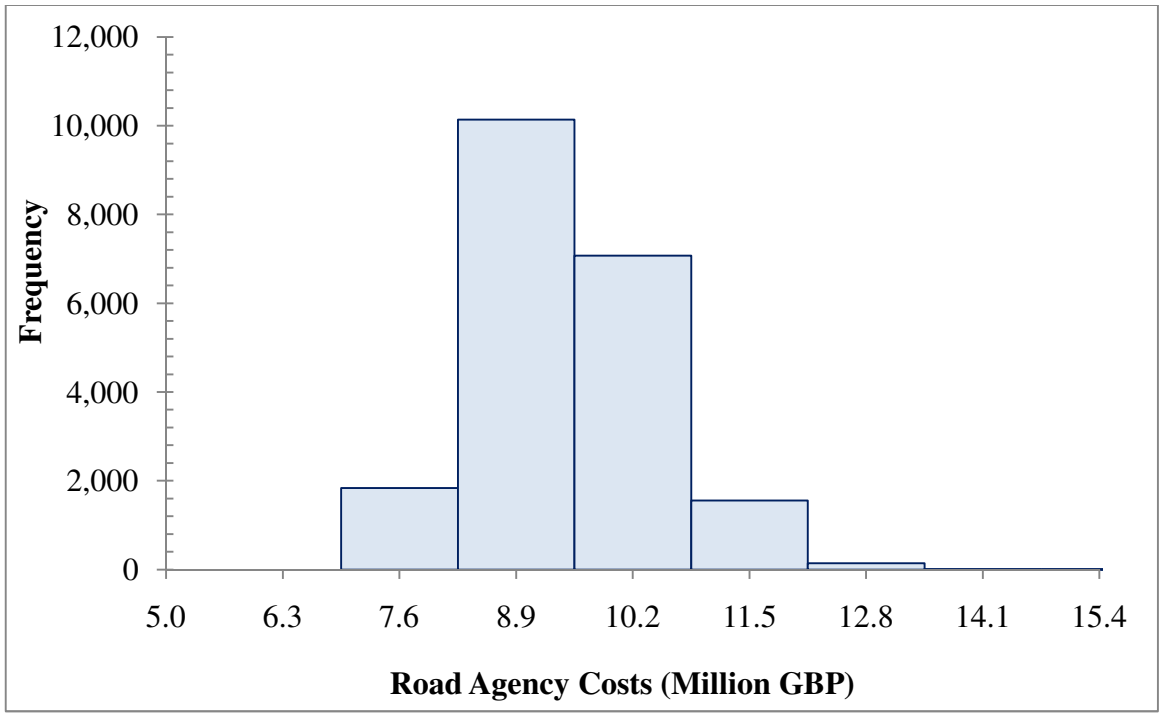

Figure E6-1: Distribution of Discounted Costs for the 2030s Medium Emission Scenario for the Adaptation Maintenance Strategy

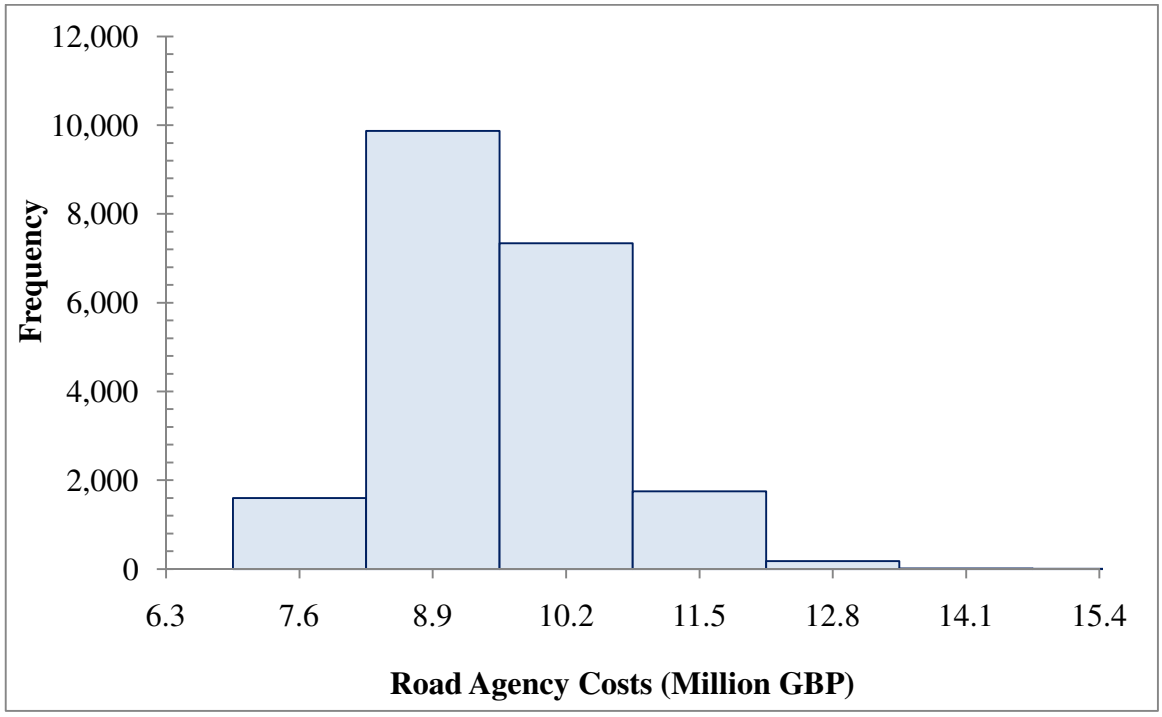

Figure E6-2: Distribution of Discounted Costs for the 2040s Medium Emission Scenario for the Adaptation Maintenance Strategy

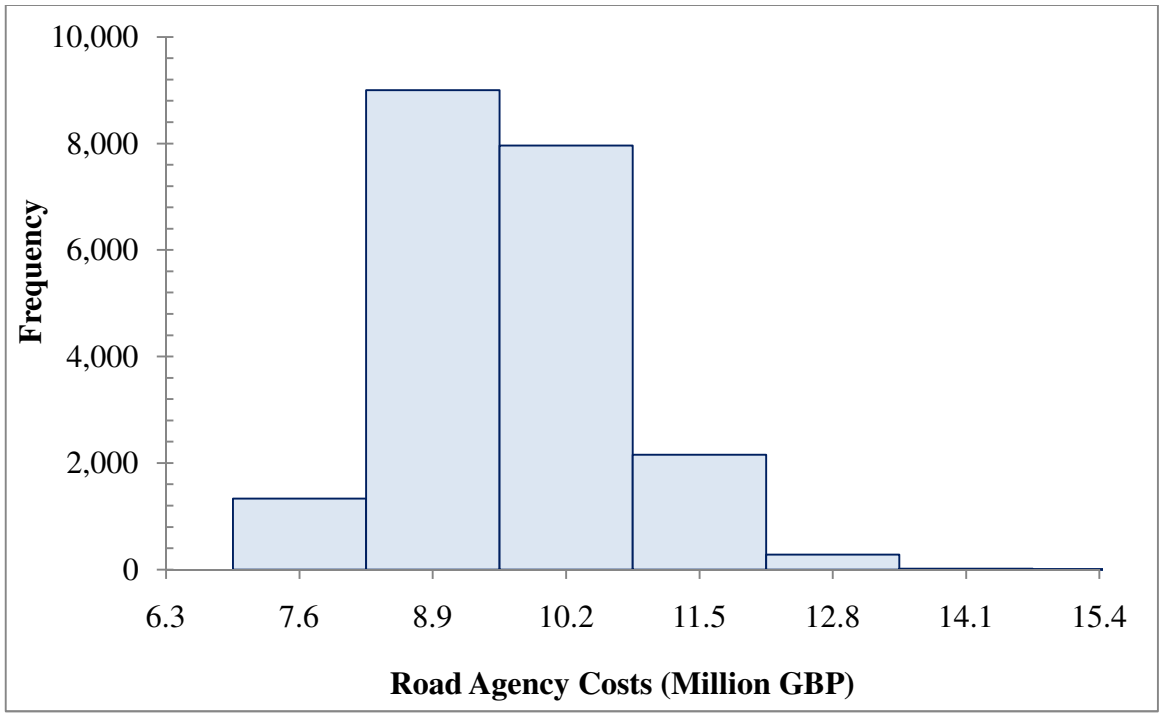

Figure E6-3: Distribution of Discounted Costs for the 2050s Medium Emission Scenario for the Adaptation Maintenance Strategy